

FIG 1A

2/385

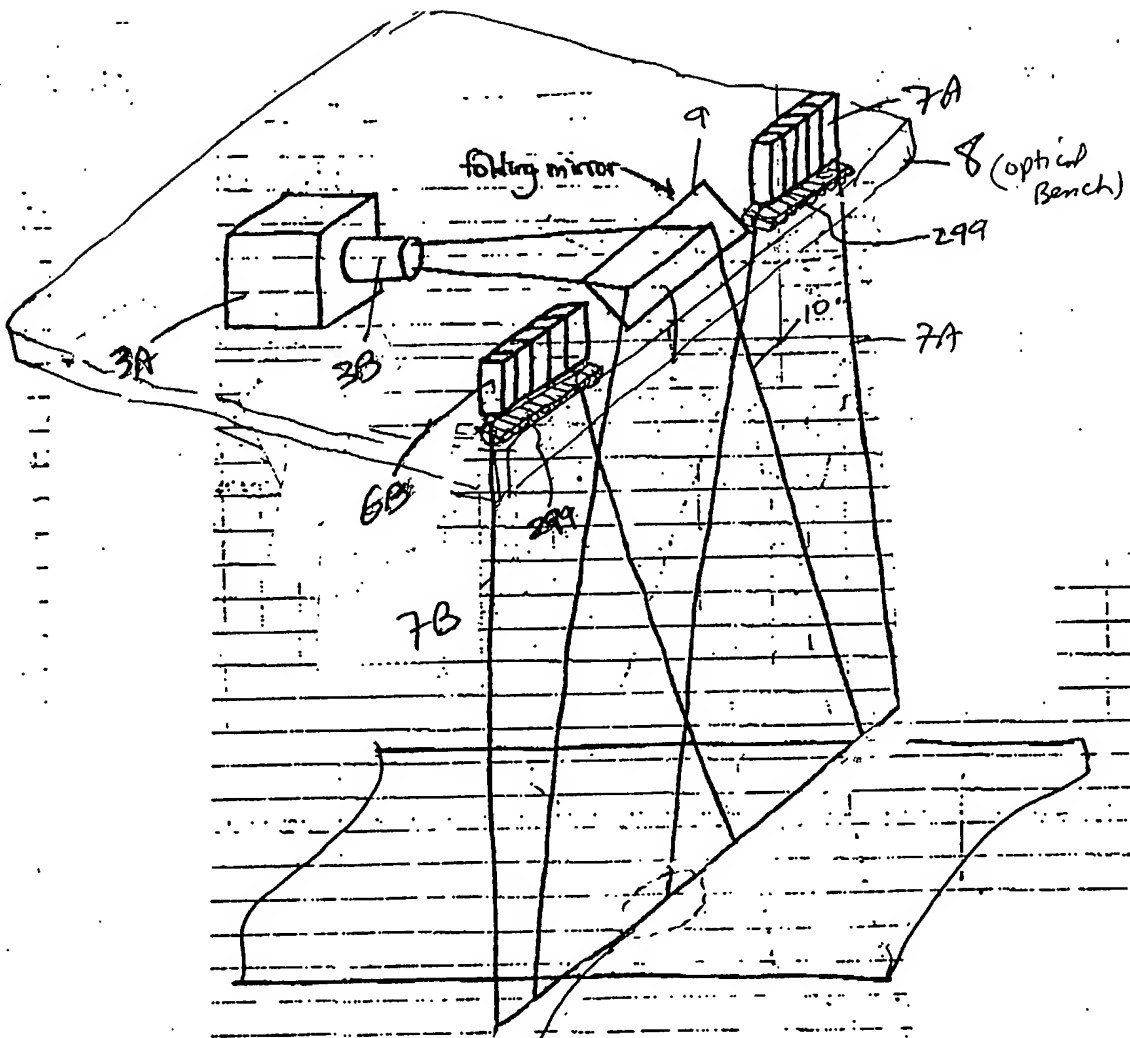


FIG 1B1

1A

Magnified Field of View of
CCD sensor element on
object
width of projected
Planar laser illumination
Beam on
object

FIG 1B3

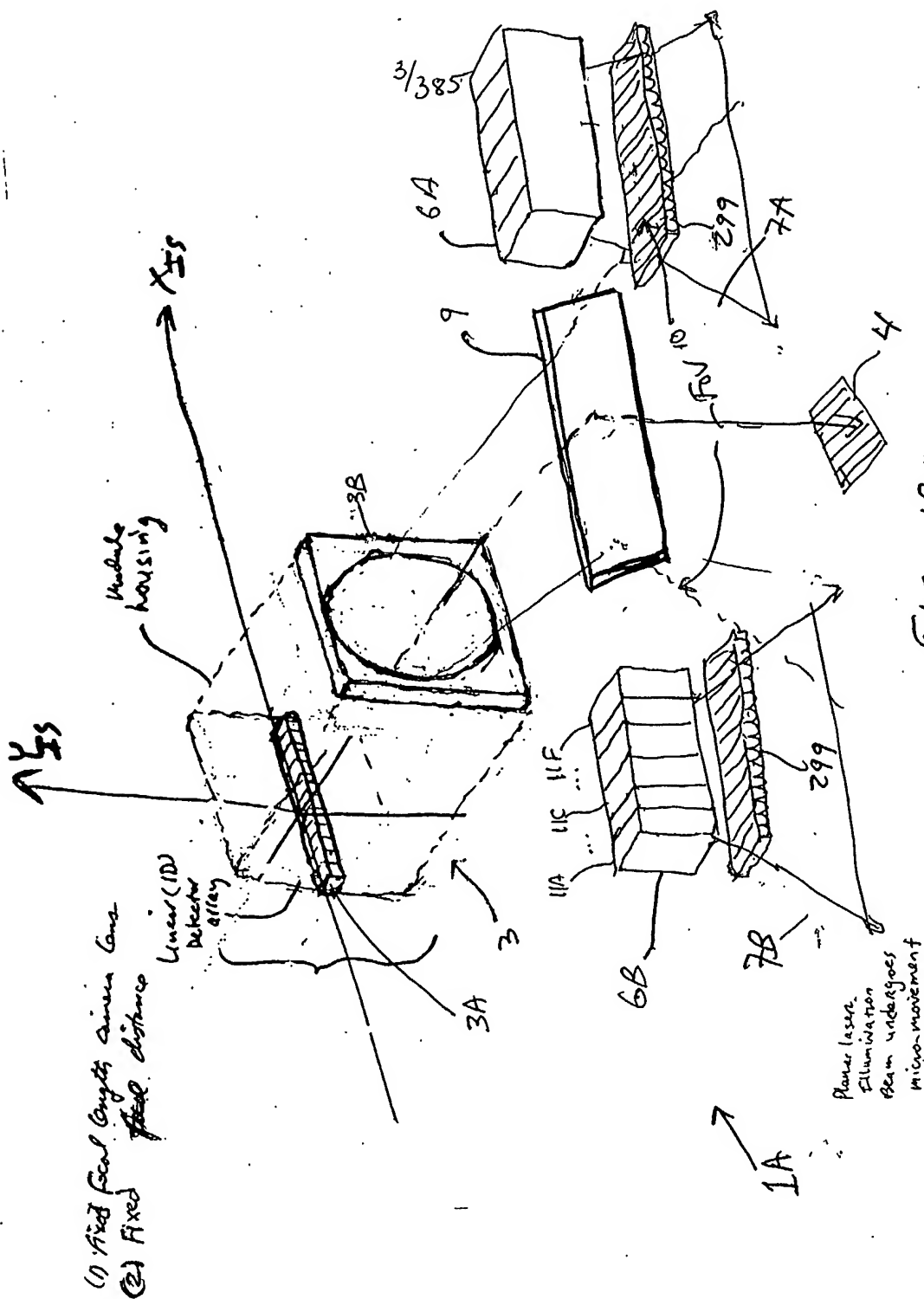
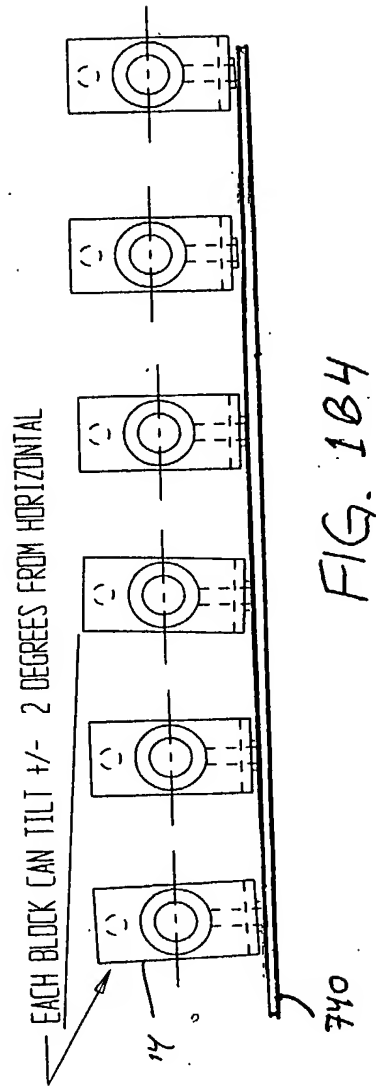
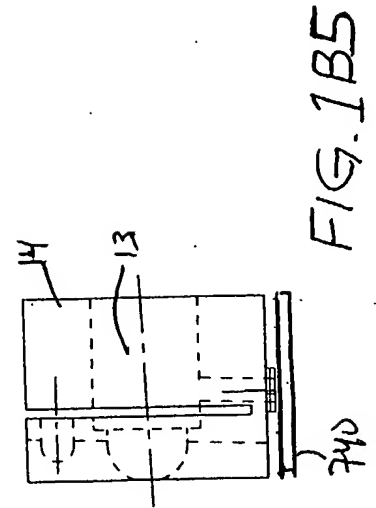


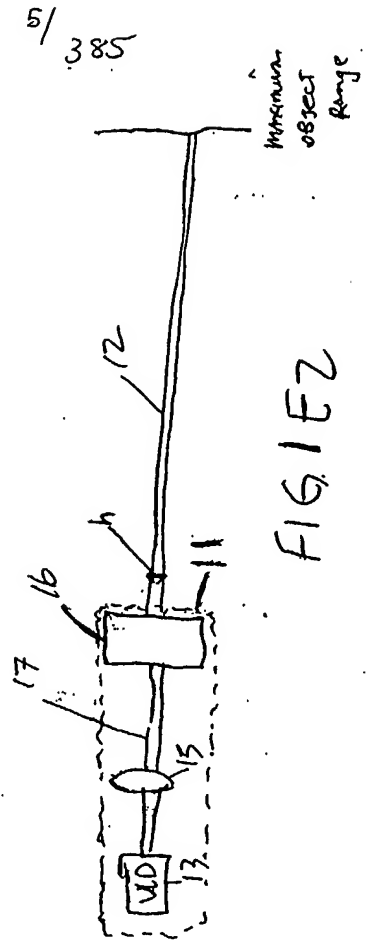
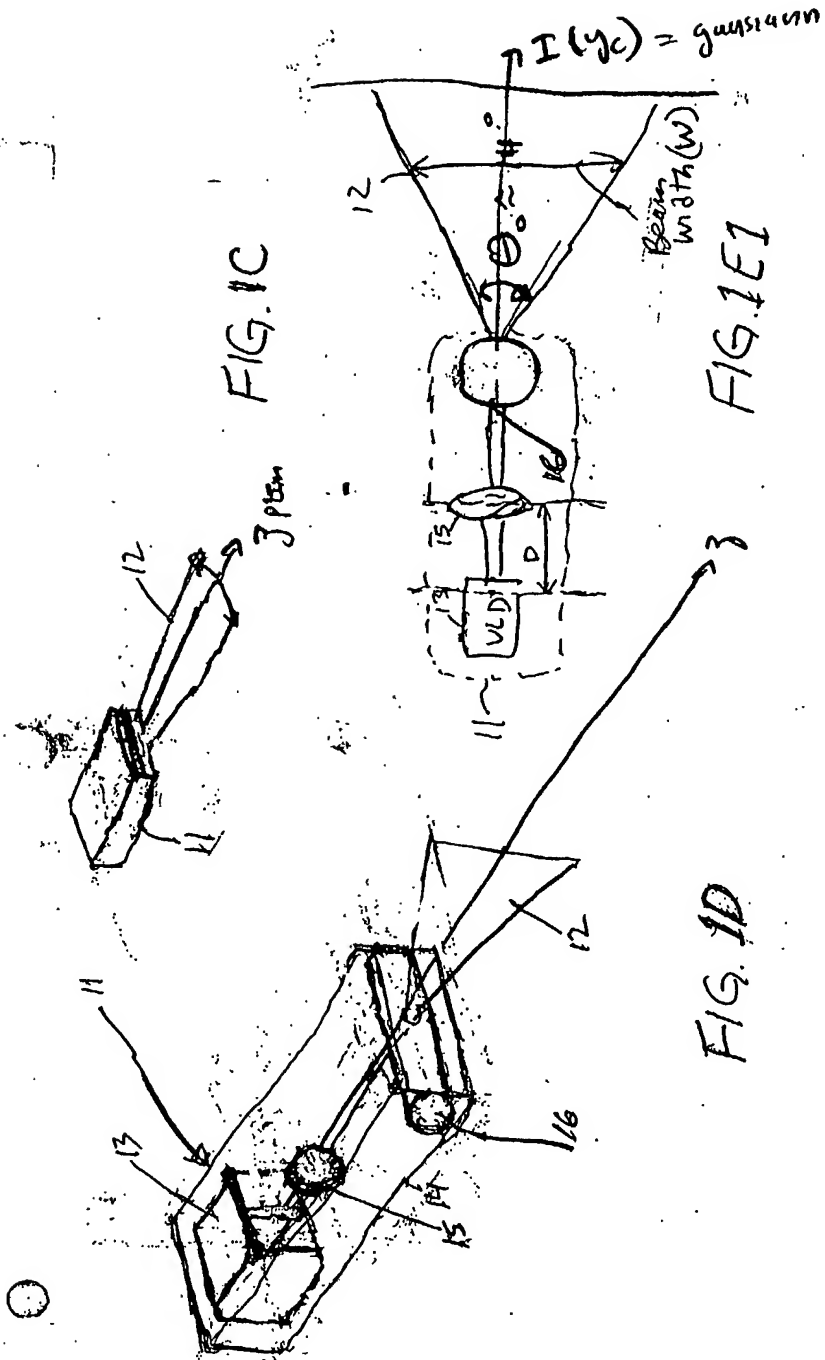
FIG. 1B2

4/385

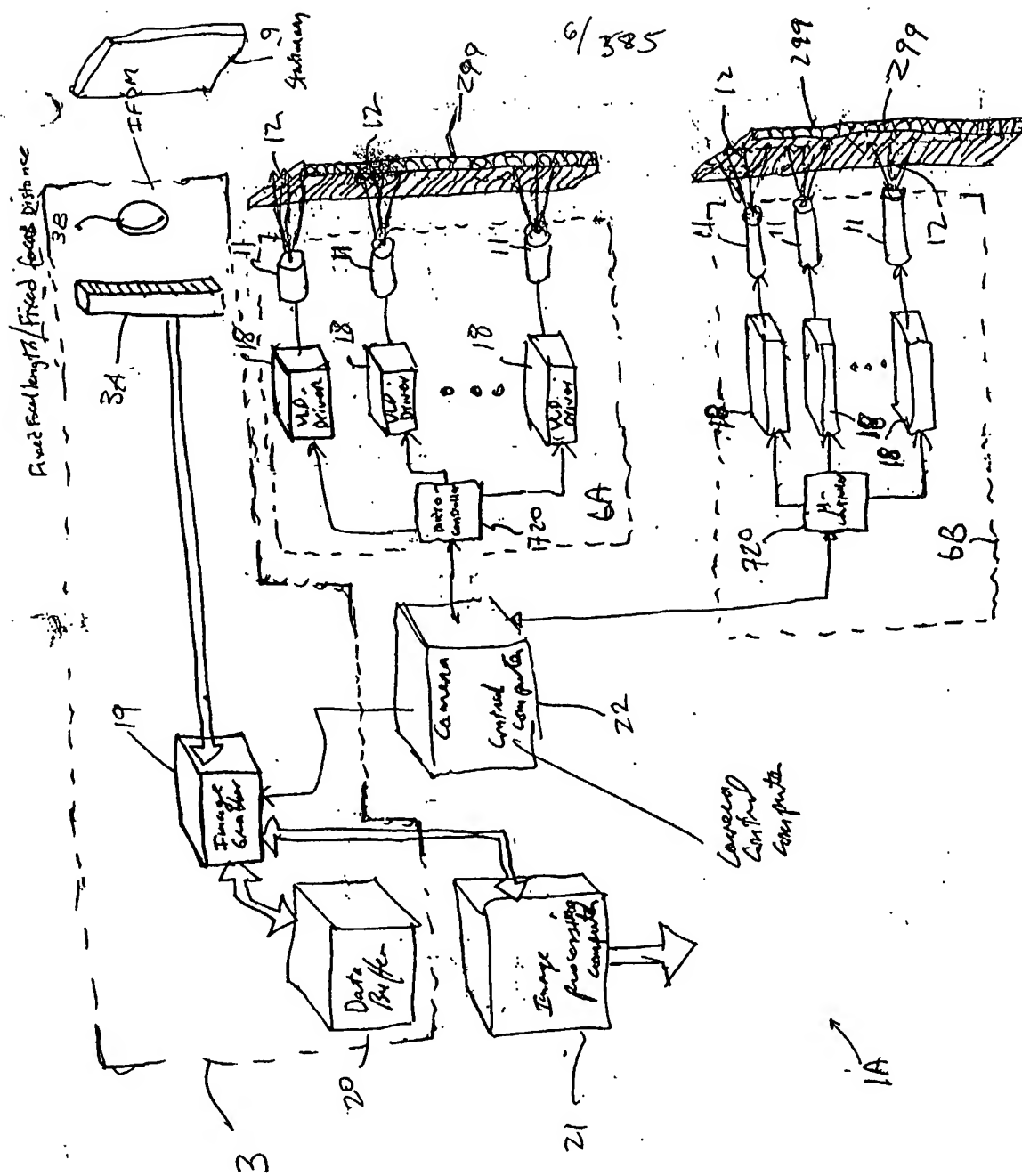


VLD BLOCK CAN PITCH FORWARD FOR ALIGNMENT WITH OTHER VLD BEAMS

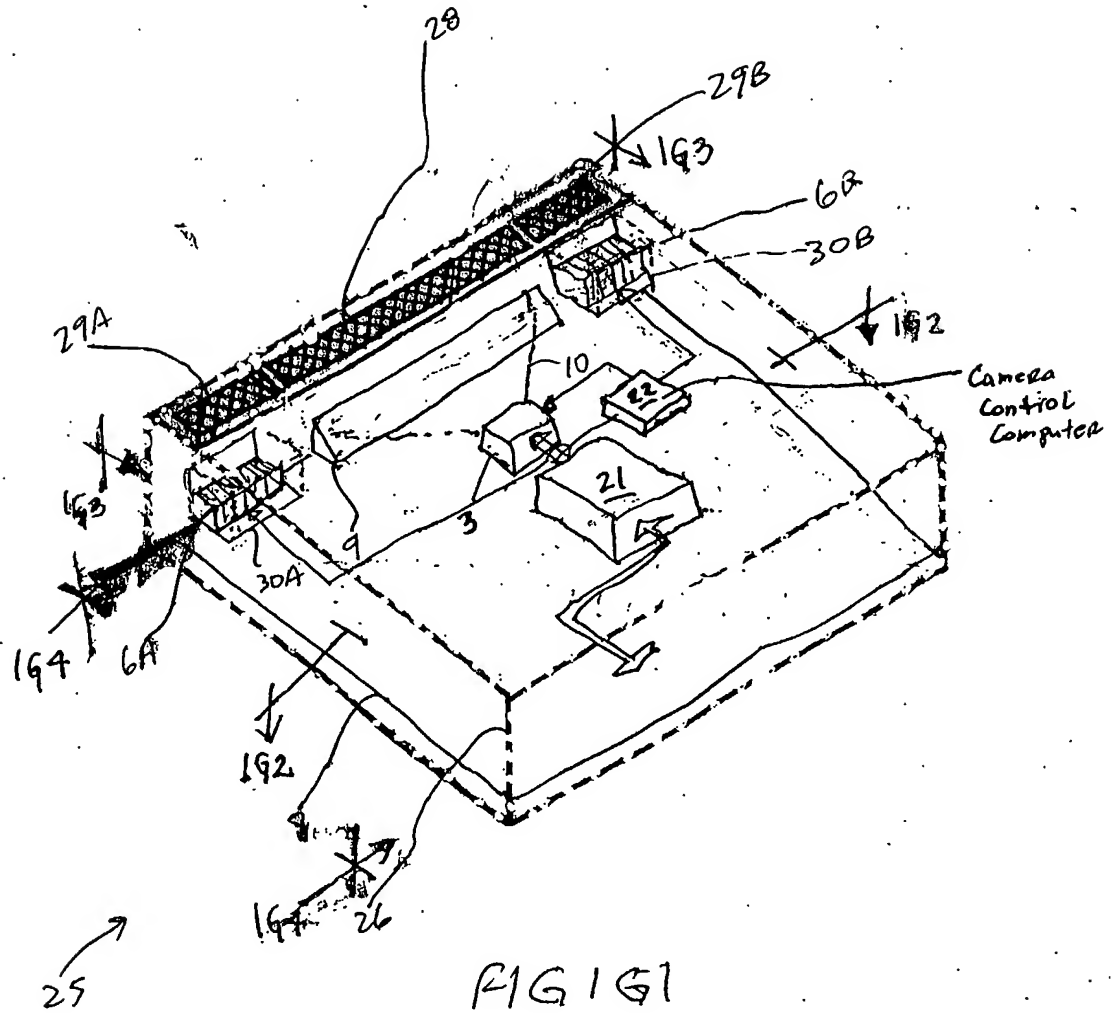




5/385



7/385



8/385

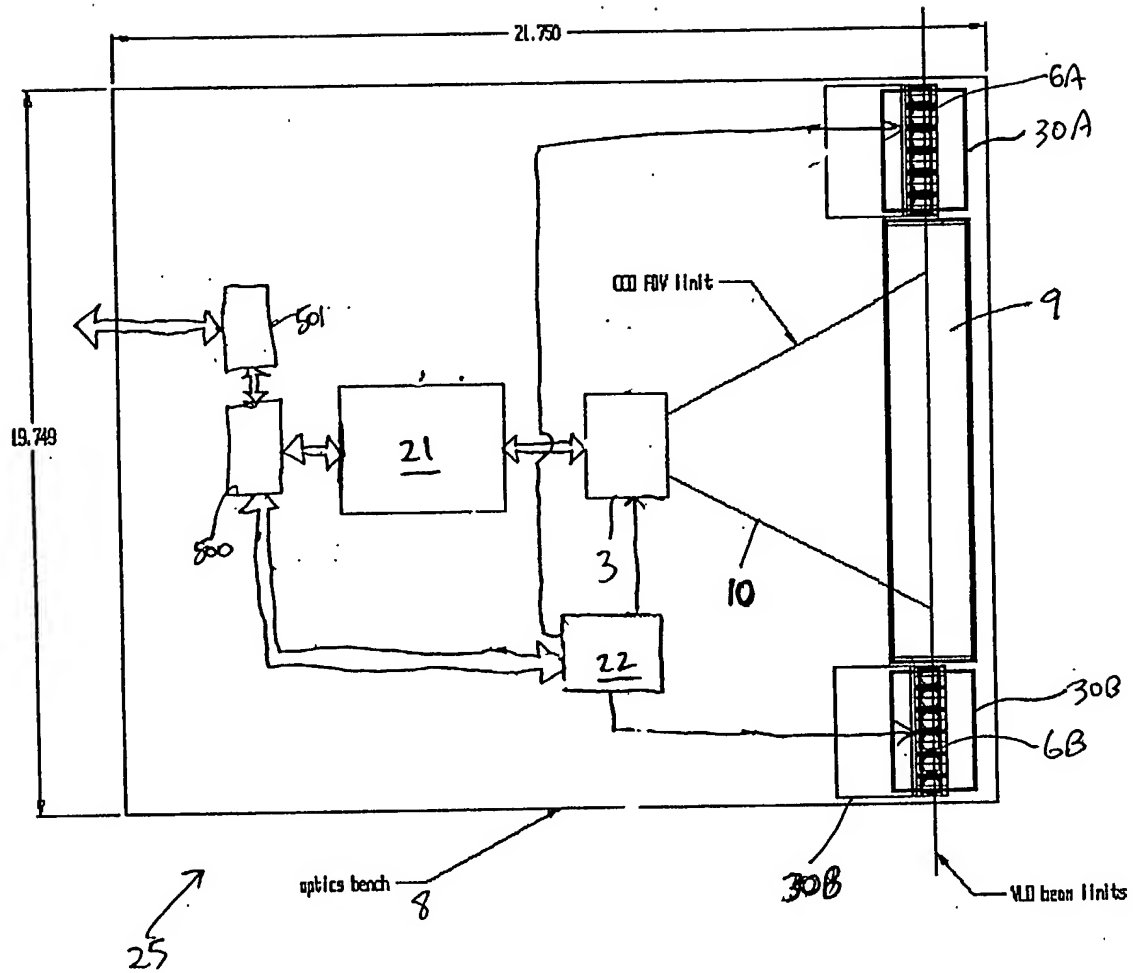


FIG. 142

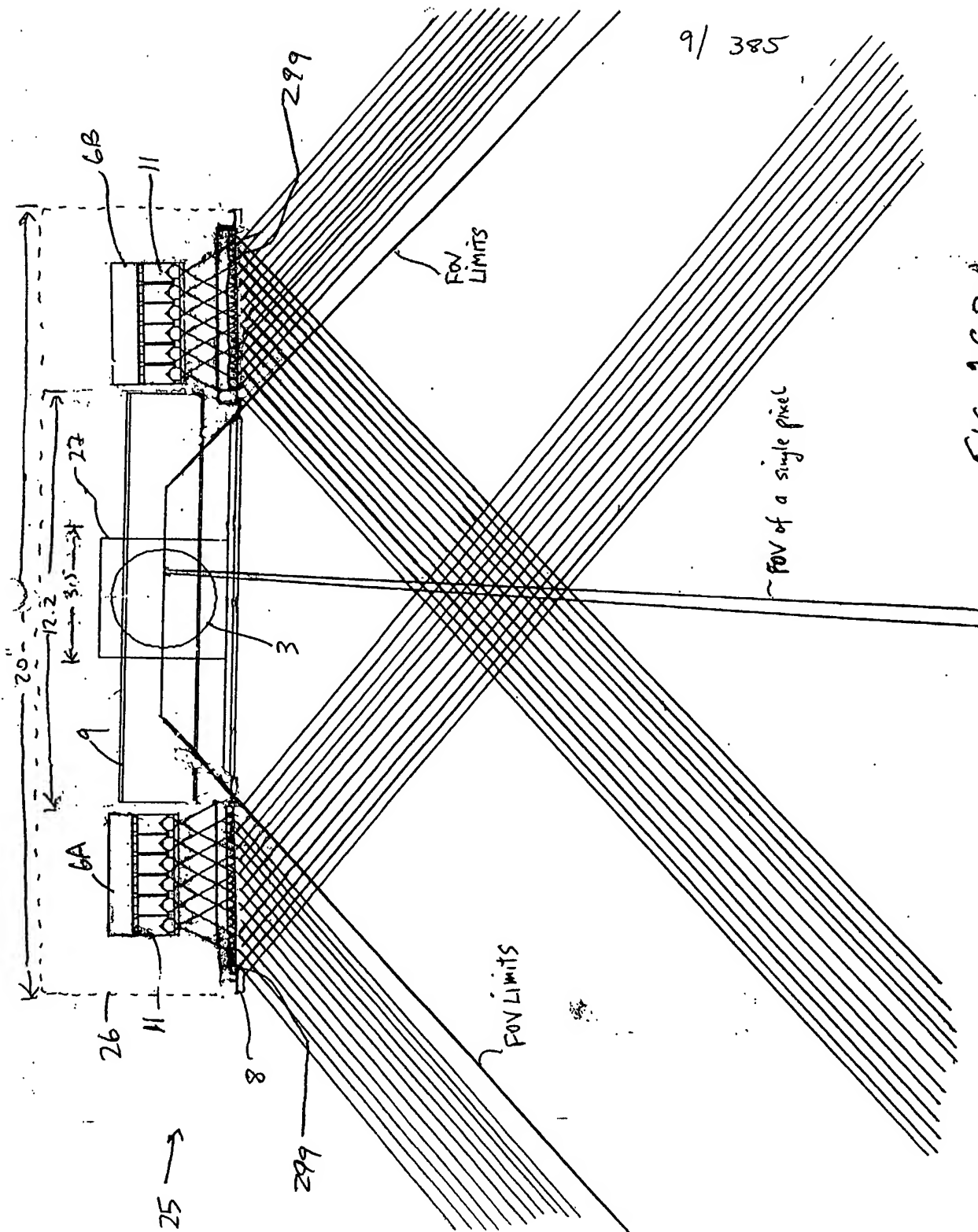


FIG. 1G3

10/385

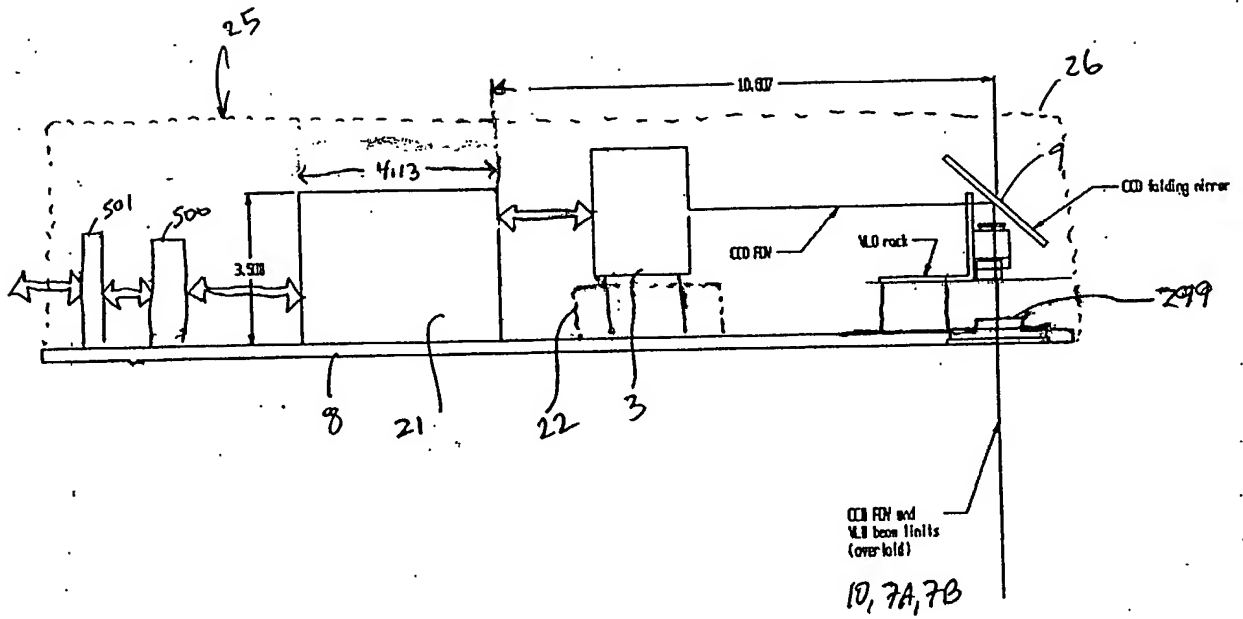


FIG. 164

11/385

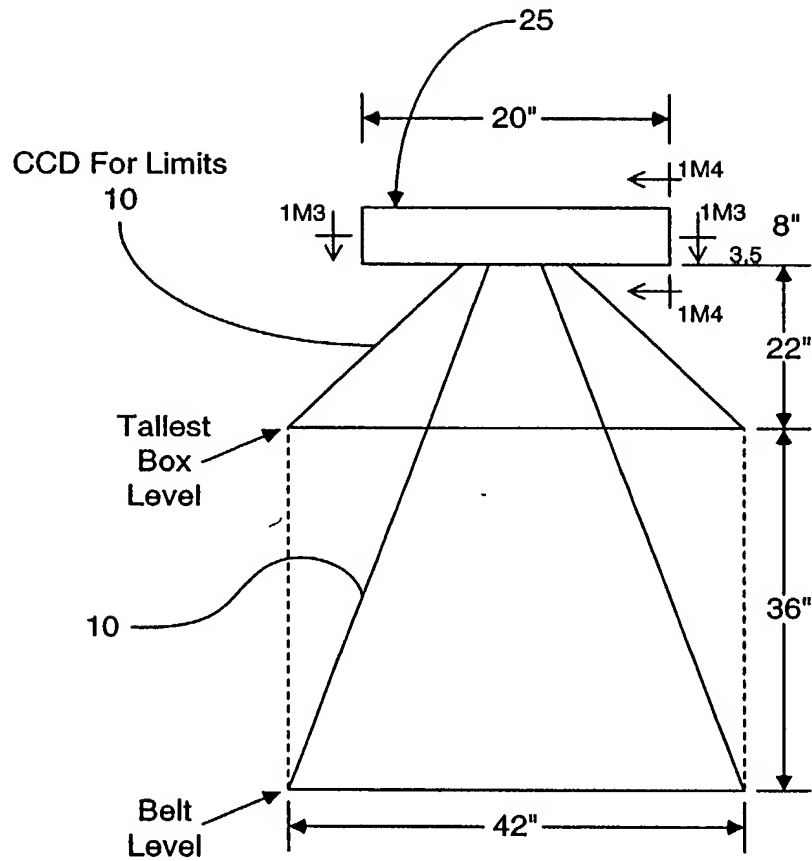
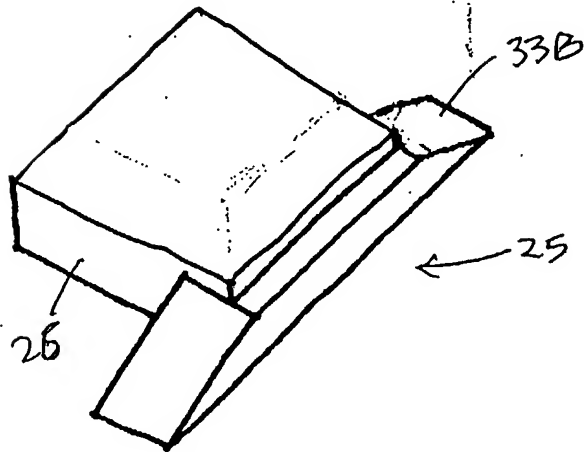
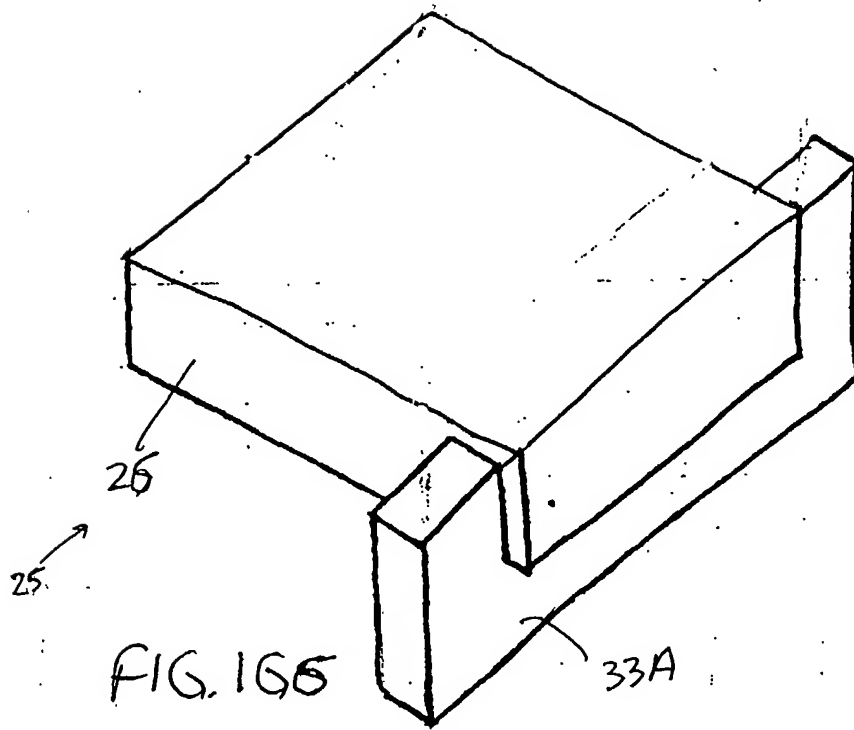


FIG. 1G5

12/385



13/385

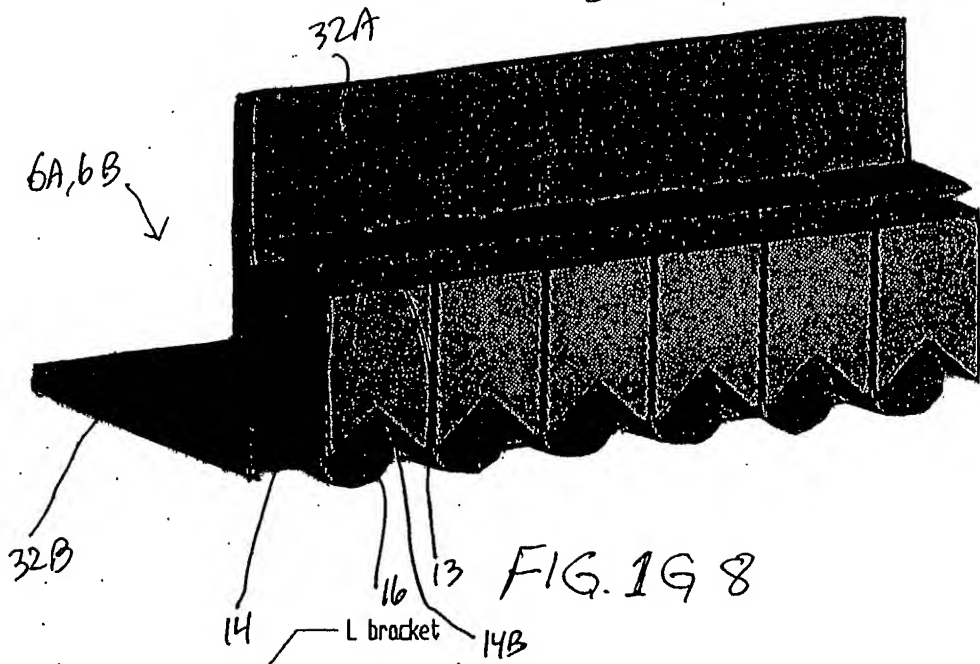


FIG. 1G 8

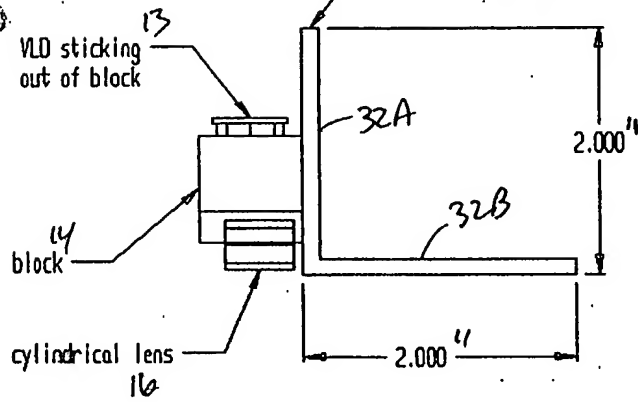


FIG. 1G.9

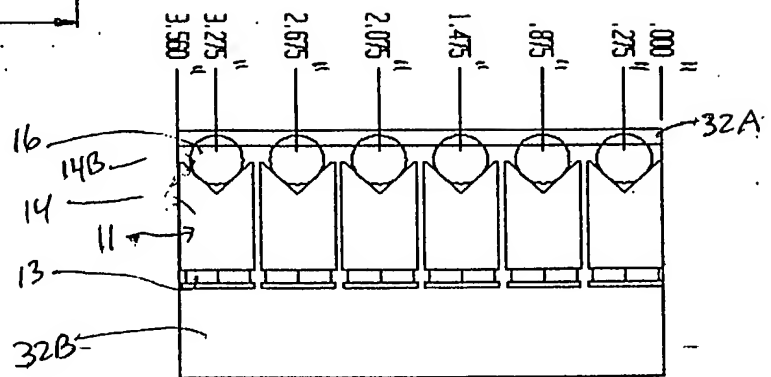


FIG. 1G 10

14/385

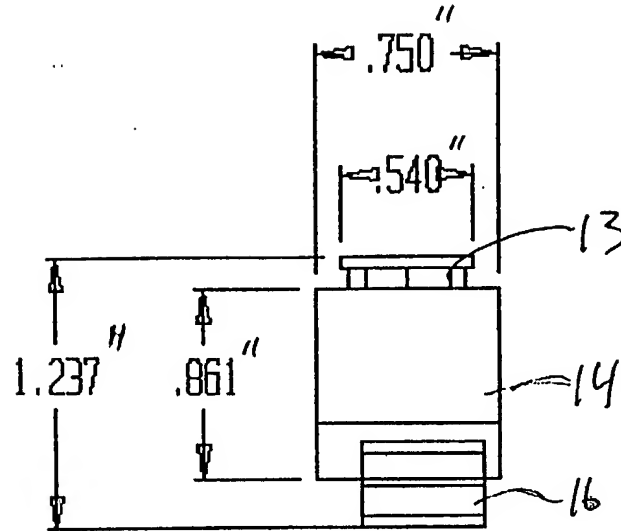


FIG. 1611

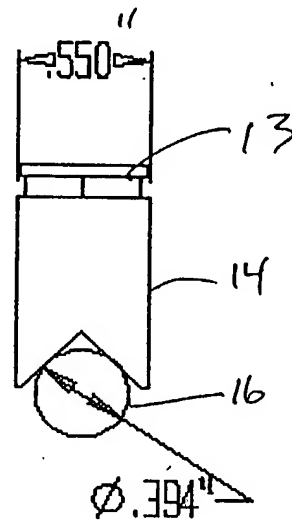


FIG. 1612

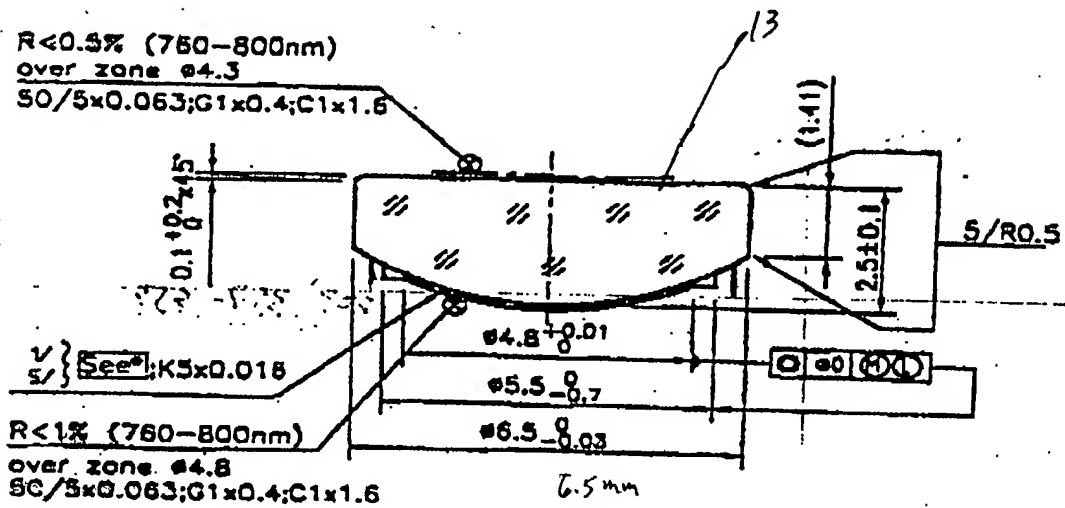
15/
385

FIG. 1G13

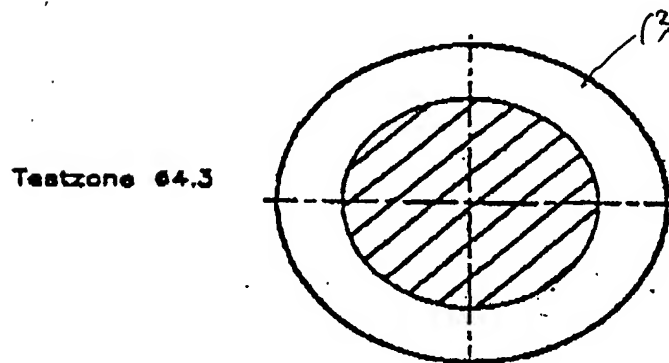


FIG. 1G14

16/385

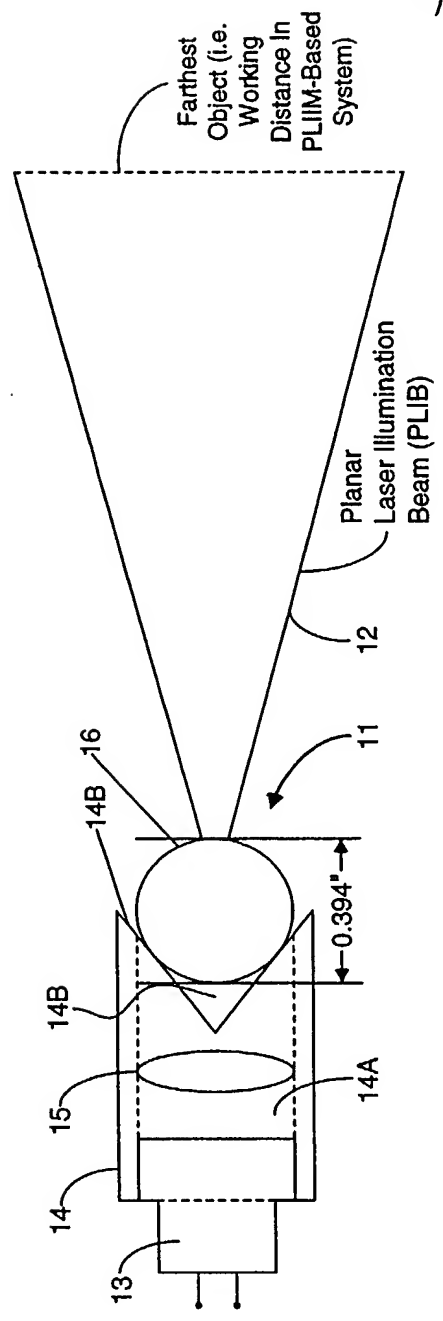


FIG. 1G15A

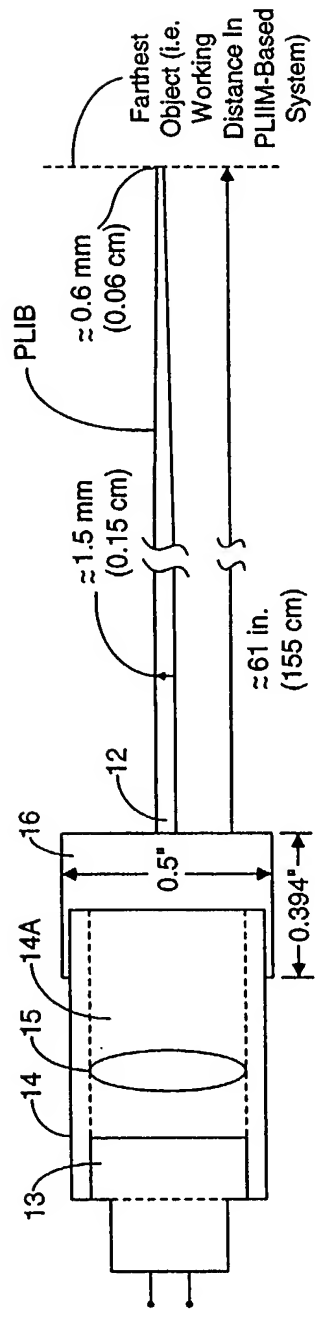


FIG. 1G15B

17/385

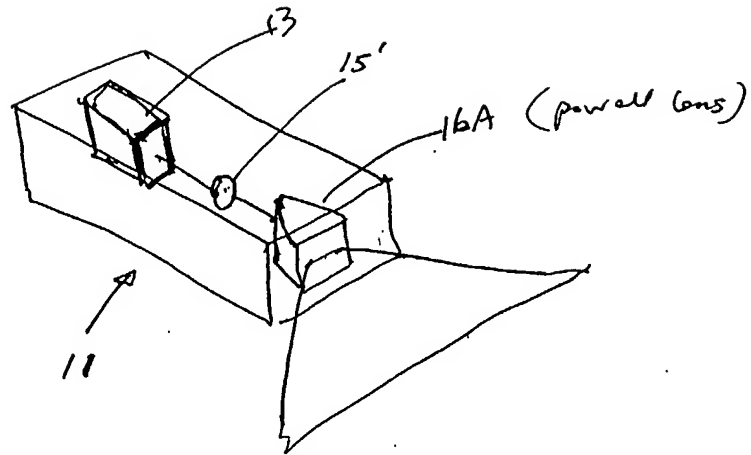


FIG. 1G.16A

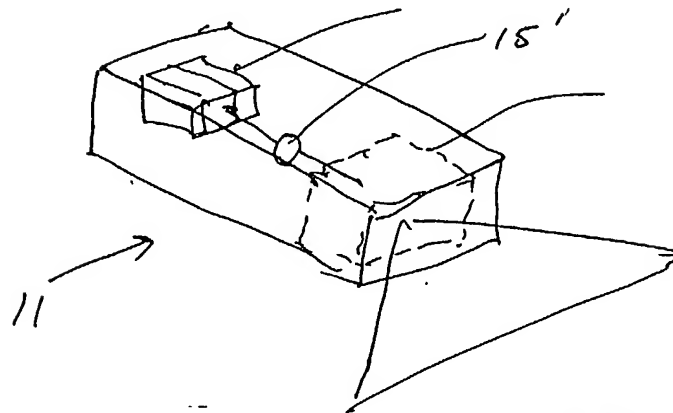


FIG. 1G.16B

- PLIM w/
powell lens

10/385

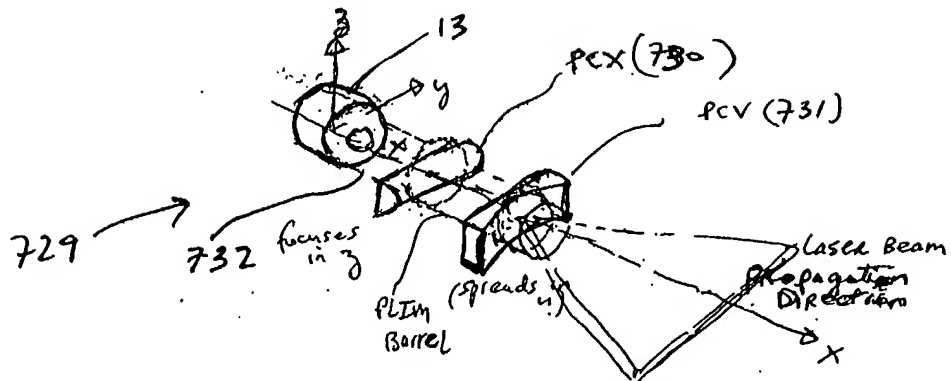


FIG. 16.17A

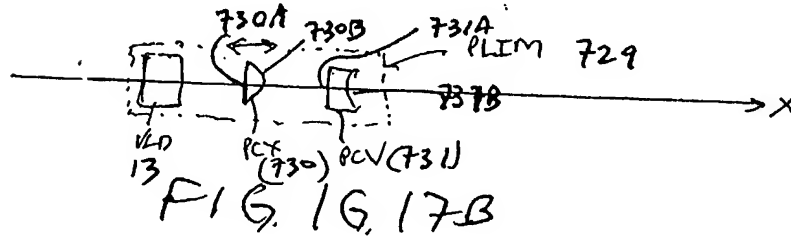


FIG. 16.17B

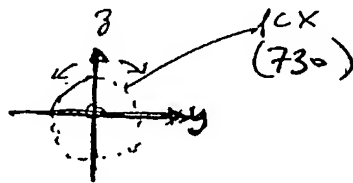


FIG. 16.17C

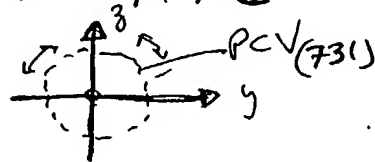


FIG. 16.17D



FIG. 16.17E

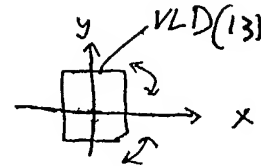


FIG. 16.17F

19/385

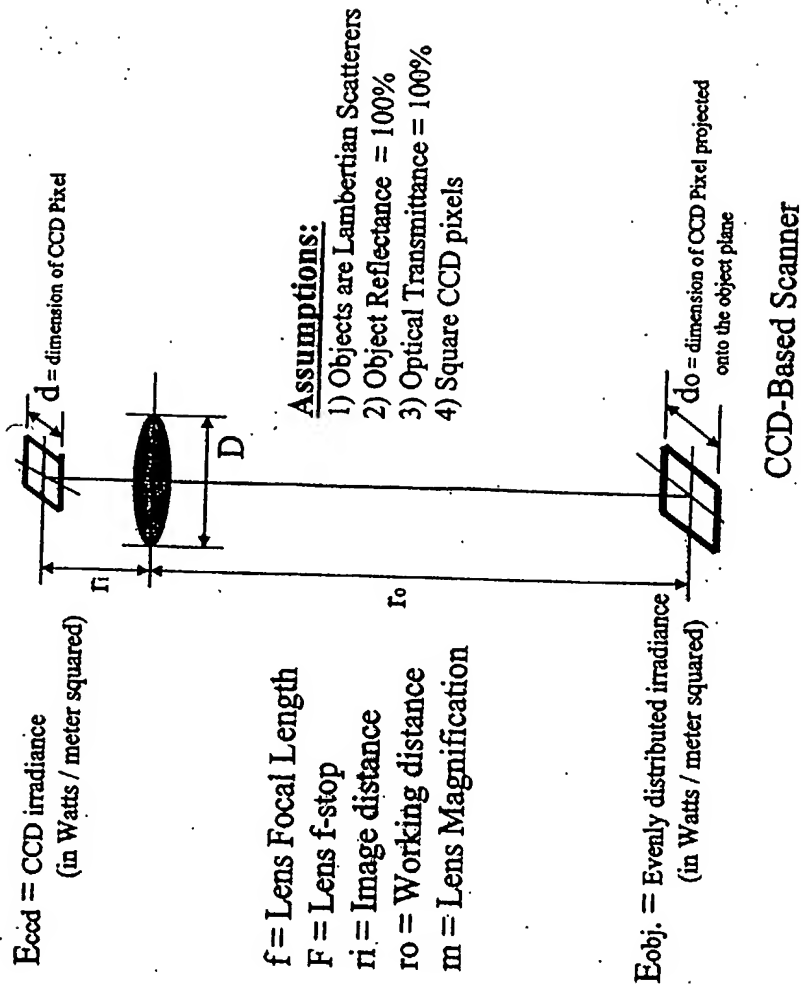


FIG. 146

FIRST GENERALIZED METHOD
of Reducing Speckle-Noise
PATTERNS AT IMAGE
DETECTION ARRAY OF THE
SPM SYSTEM (3)

20/ 385

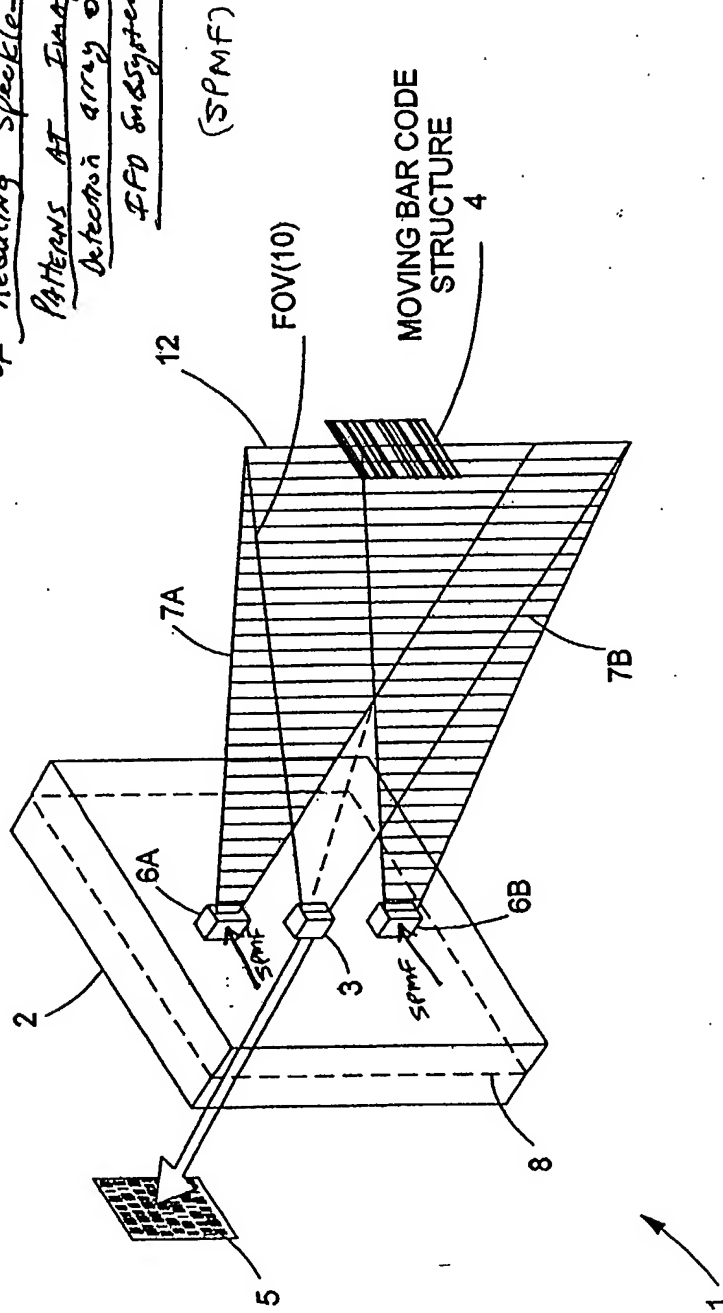
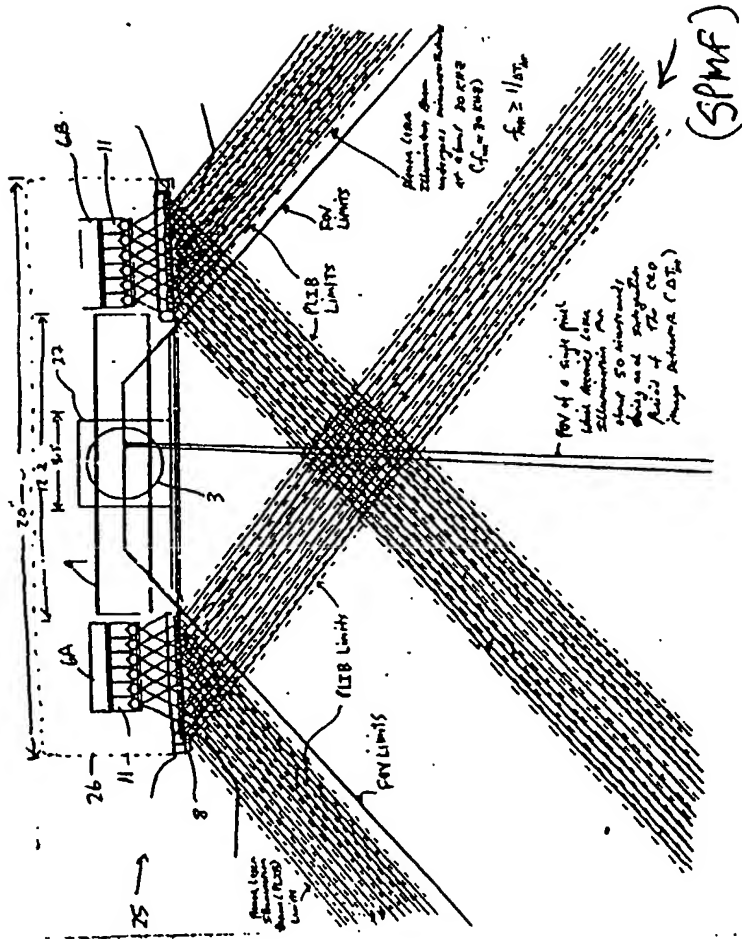


FIG. 1I1

21/385



Prior to object illumination

FIG. 112A

22/ 385

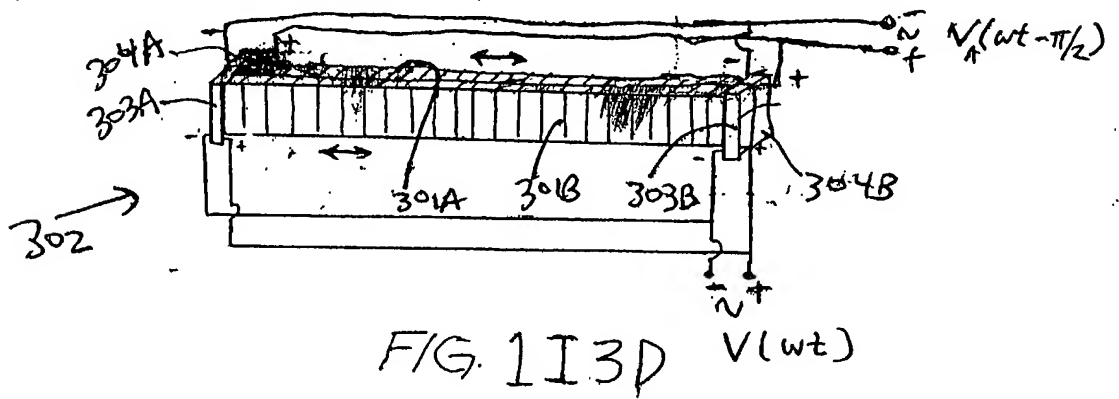
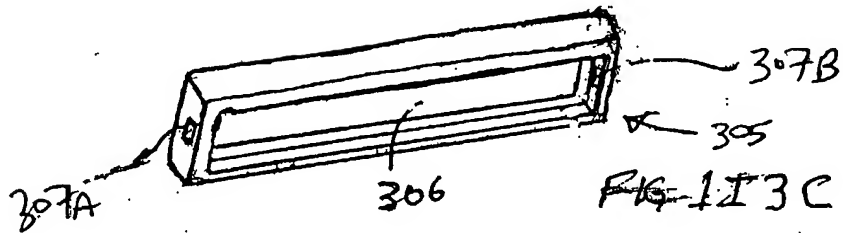
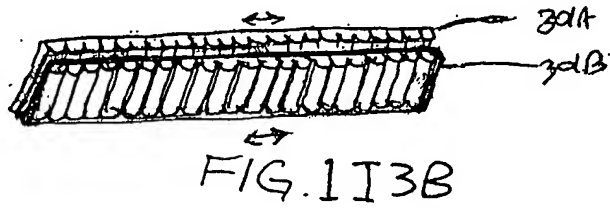
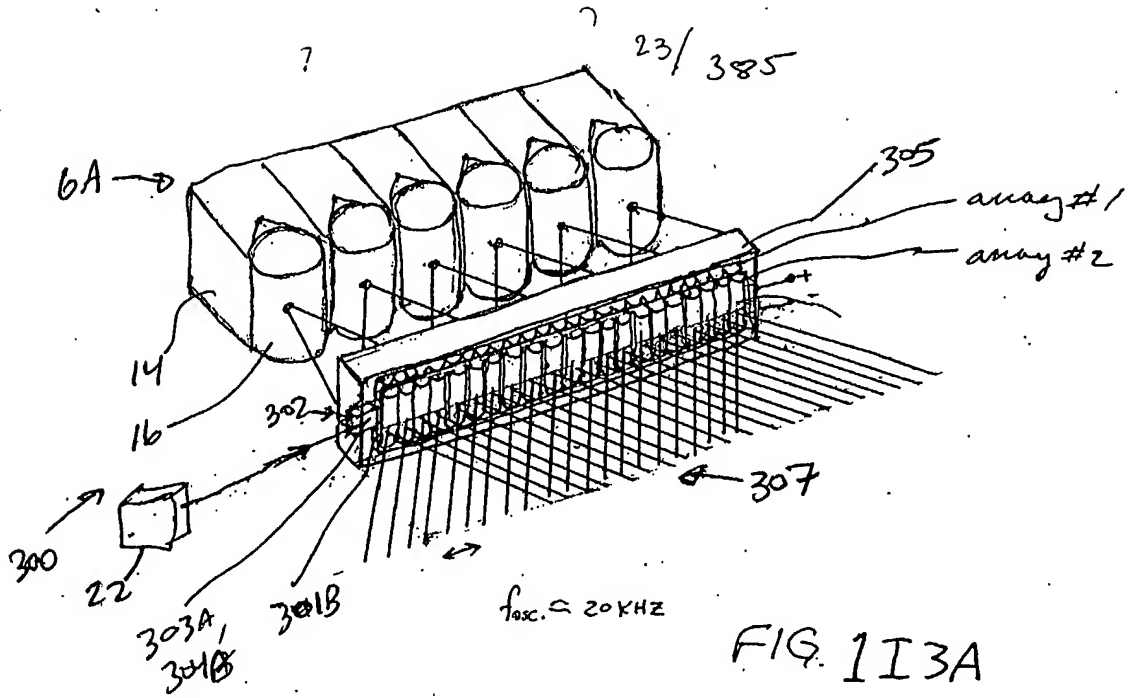
The First Generalized Speckle-Noise Pattern Reduction Method
Of The Present Invention

Prior to illumination of the target with the planar laser illumination beam (PLIB), modulate the spatial phase of the transmitted PLIB along the planar extent thereof according to a spatial phase modulation function (SPMF) so as to

produce numerous substantially different time-varying speckle-noise patterns at the image detection array of the IFD Subsystem during the photo-integration time period thereof.

Temporally average the numerous substantially different time-varying speckle-noise patterns produced at the image detection array in the IFD Subsystem during the photo-integration time period thereof, so as to thereby reduce the power of the speckle-noise pattern observed at the image detection array.

FIG. 1I2B



24/ 385

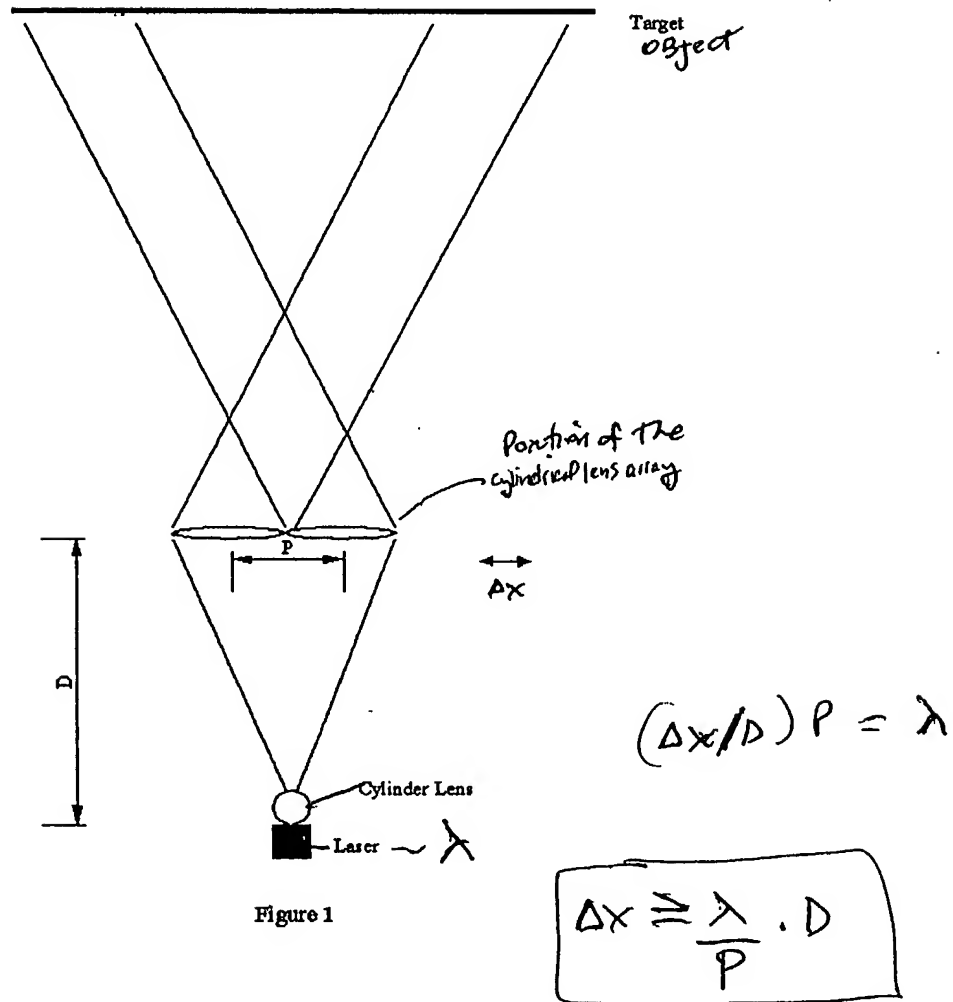


FIG. 1I3E

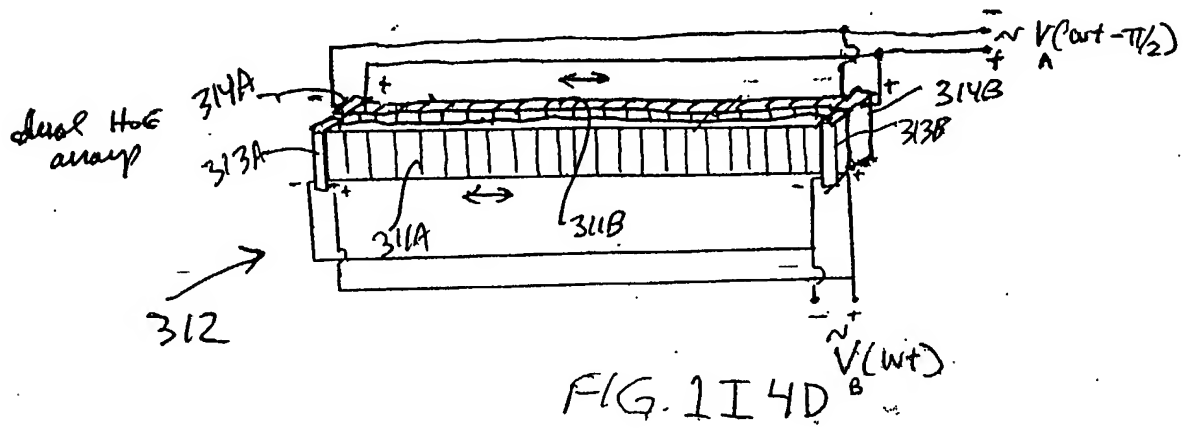
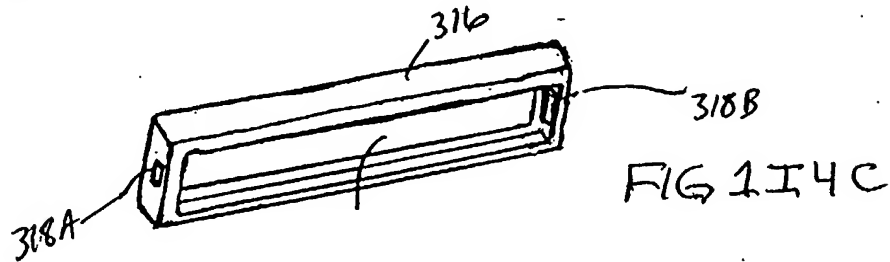
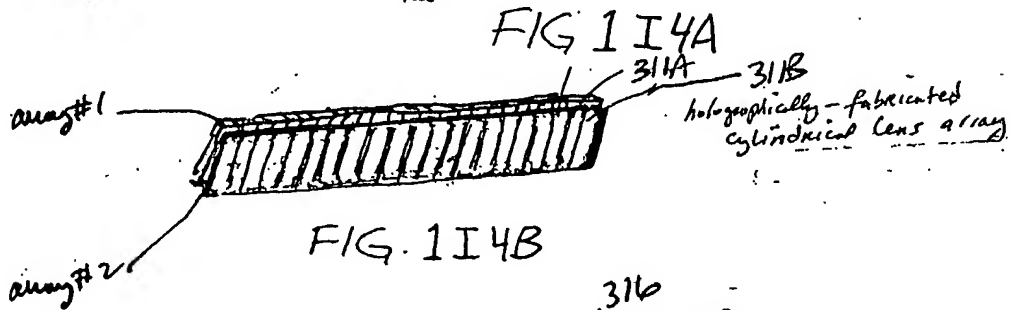
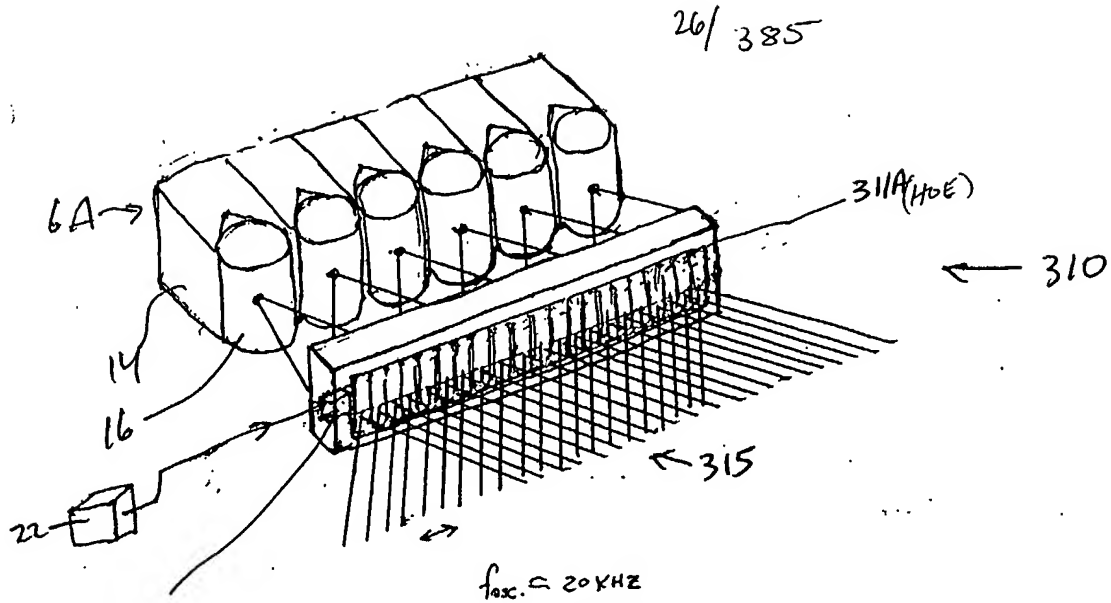
25/ 385

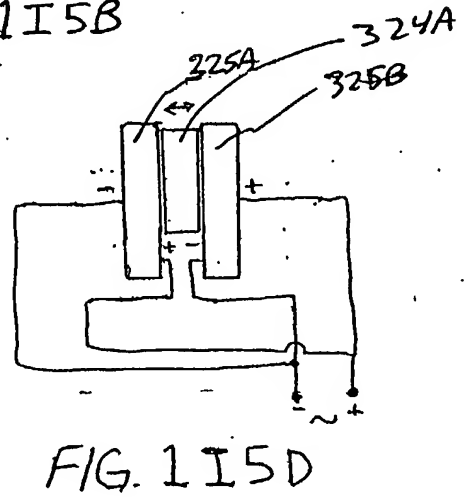
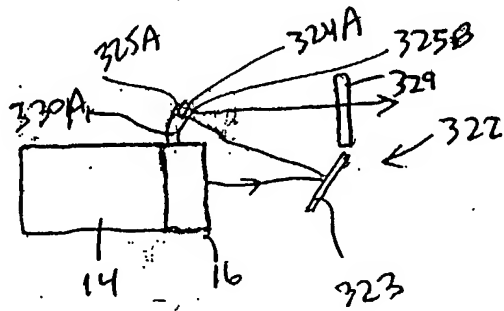
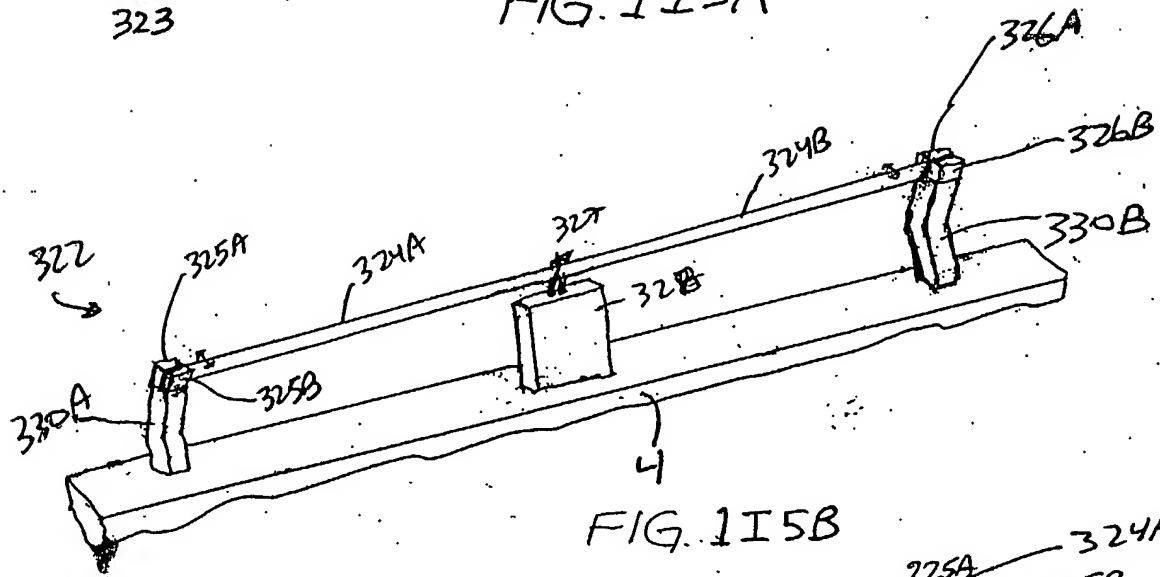
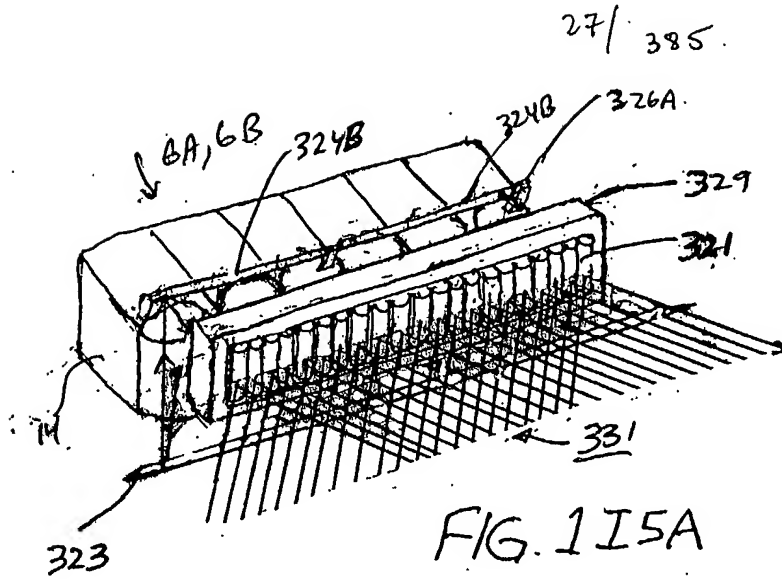


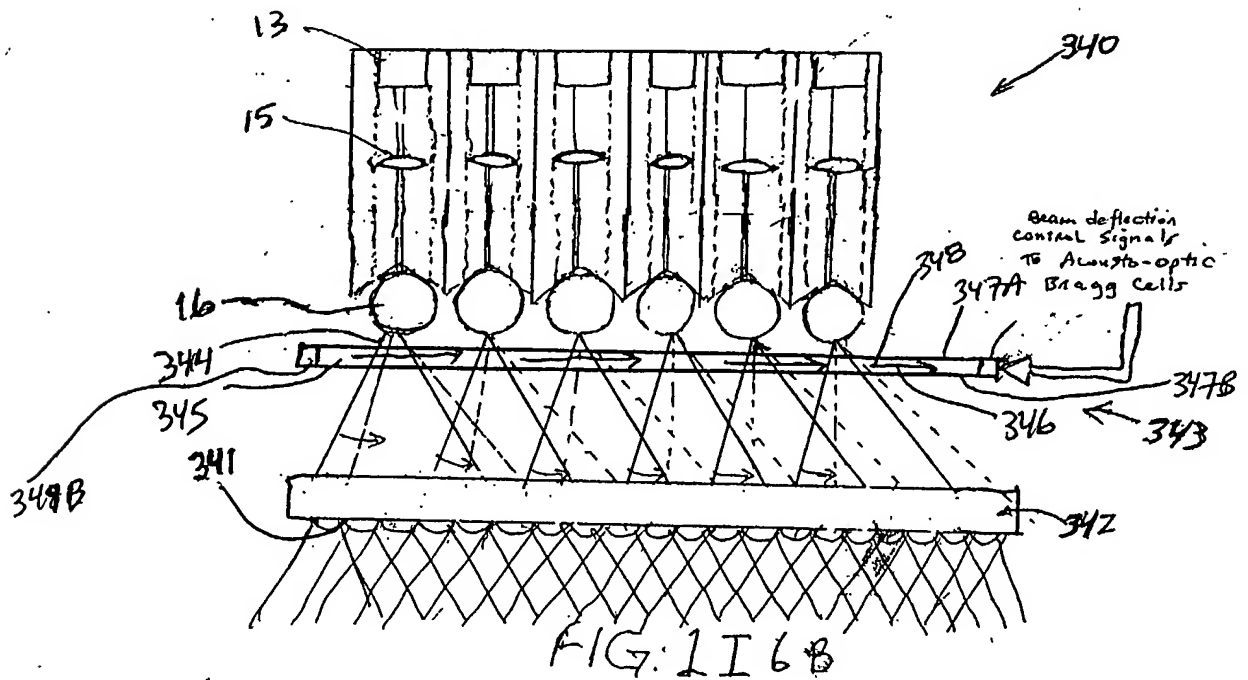
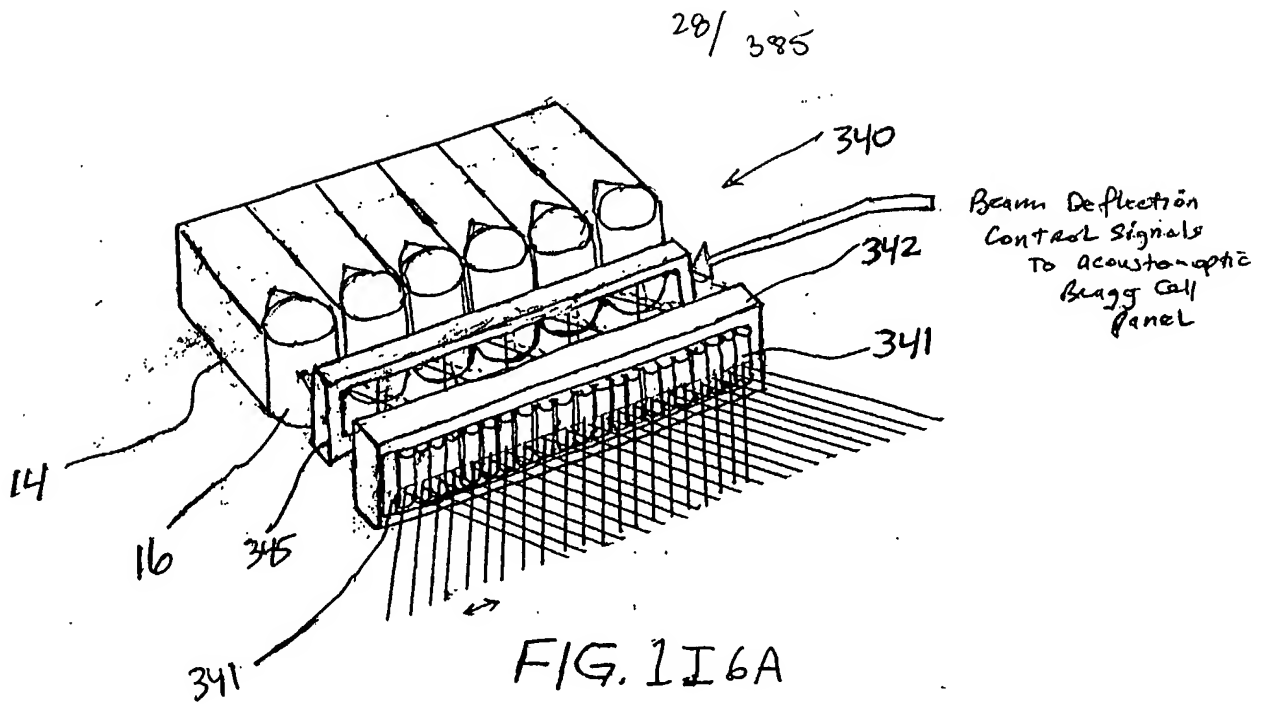
FIG. 1I3F



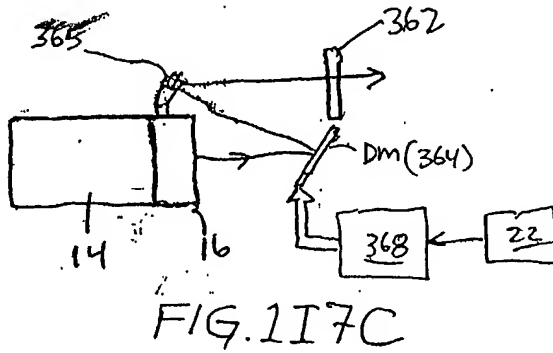
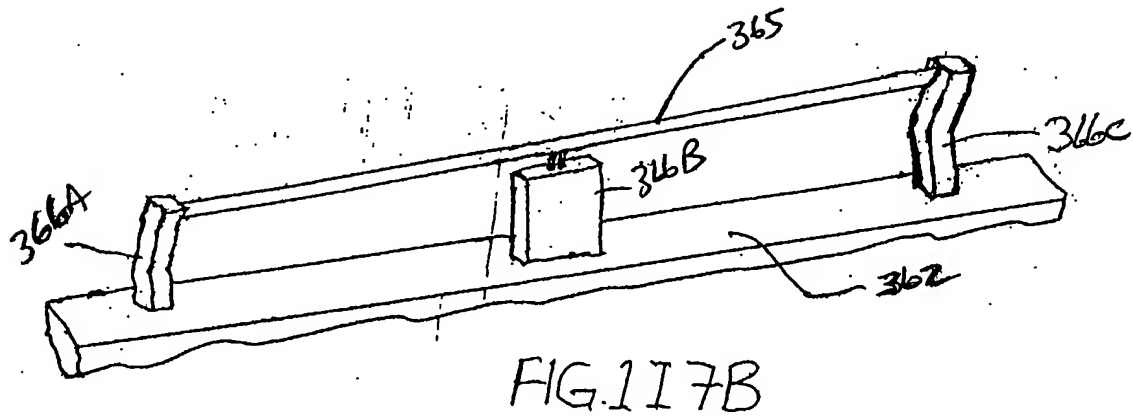
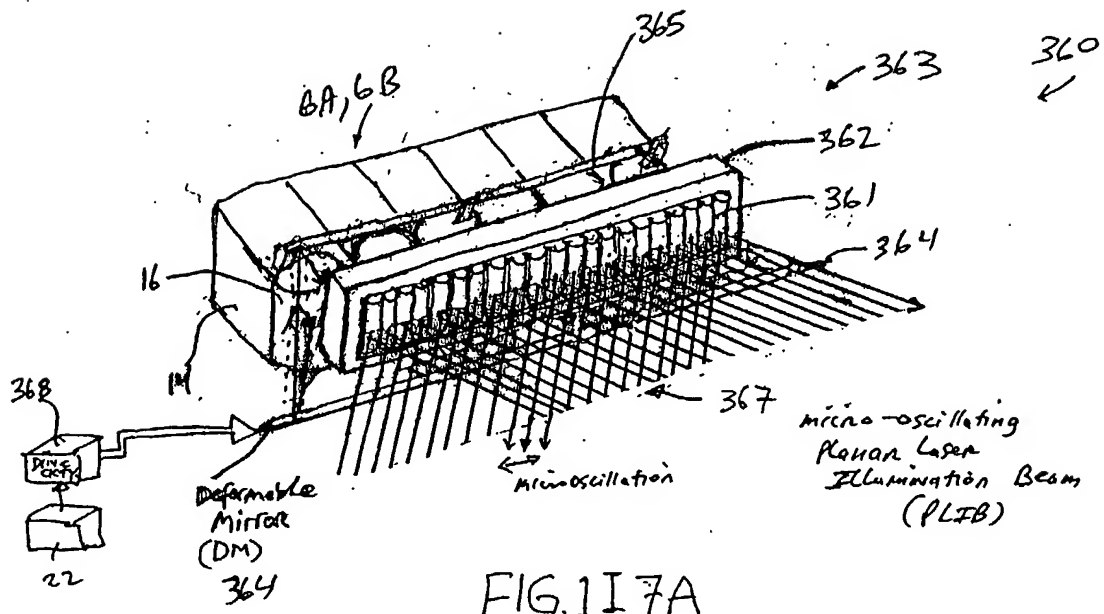
FIG 1I3G

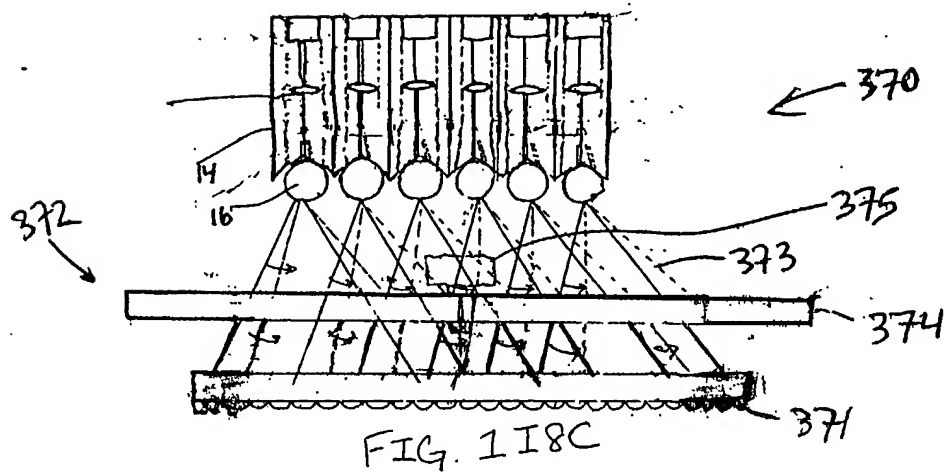
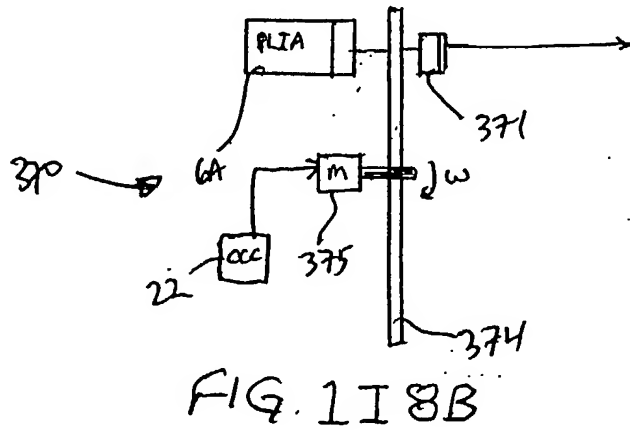
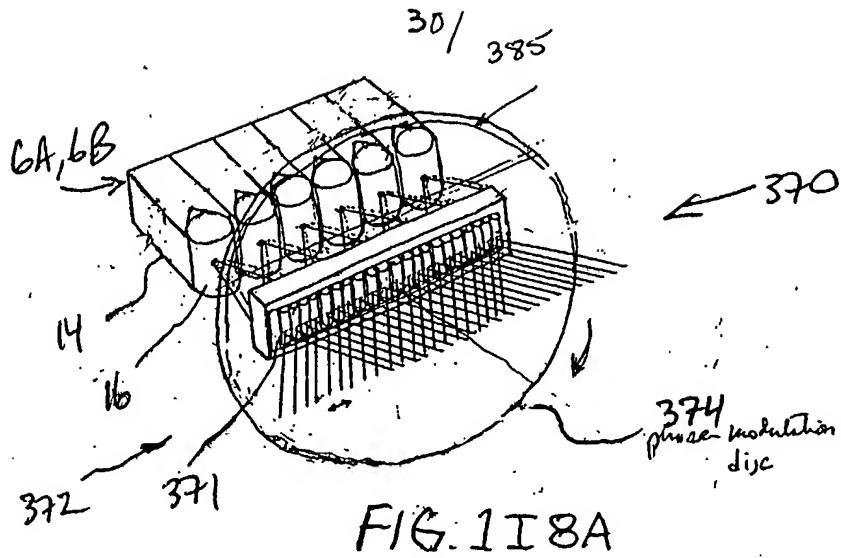




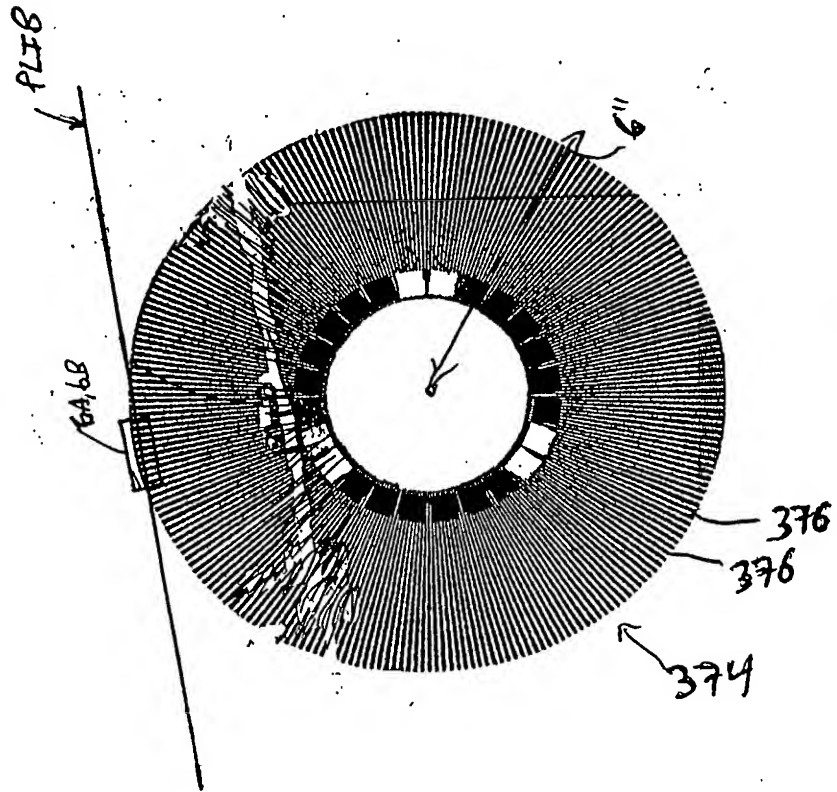
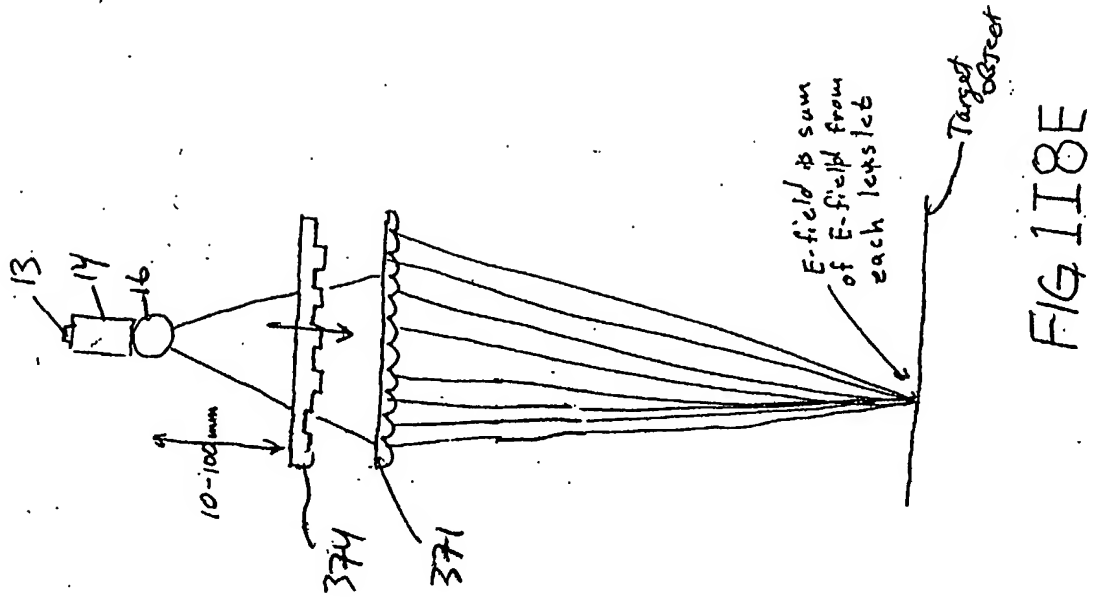


29/ 385

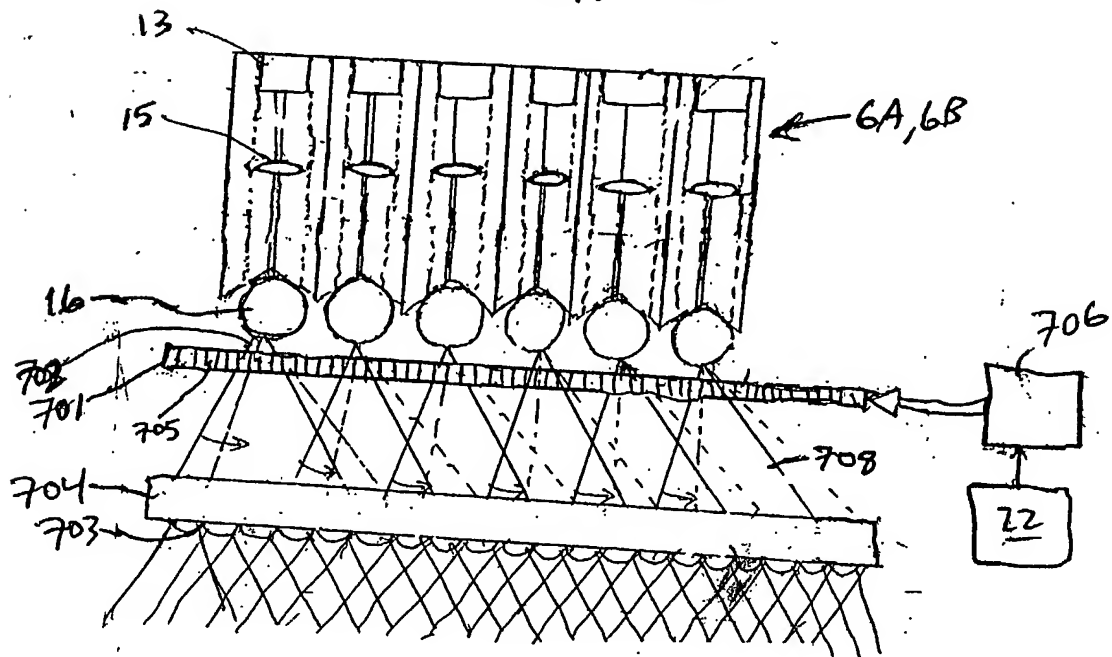
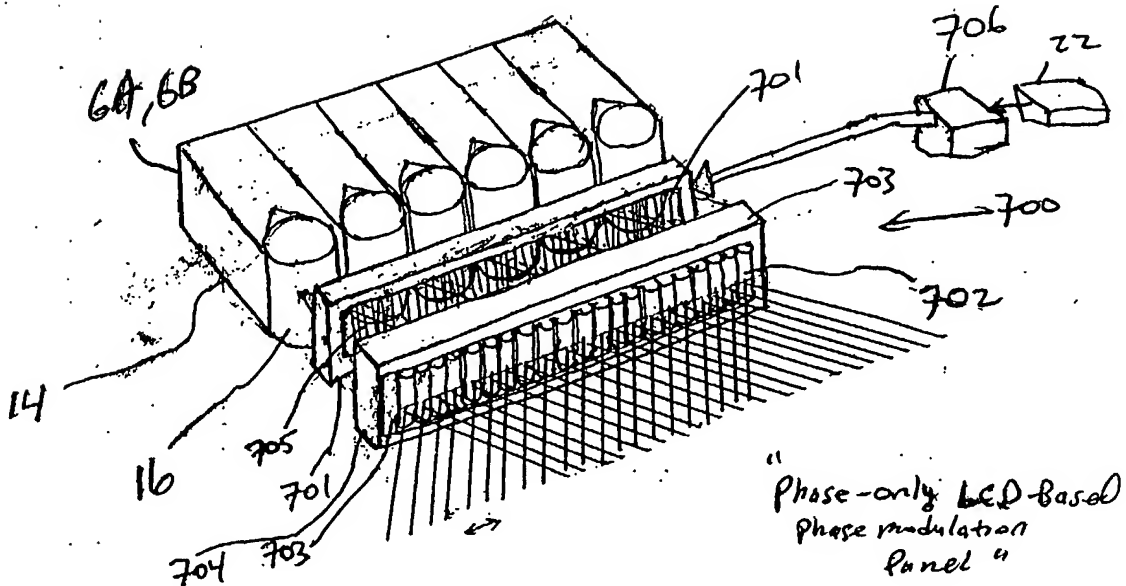




31 / 385



32/ 385



33/ 385

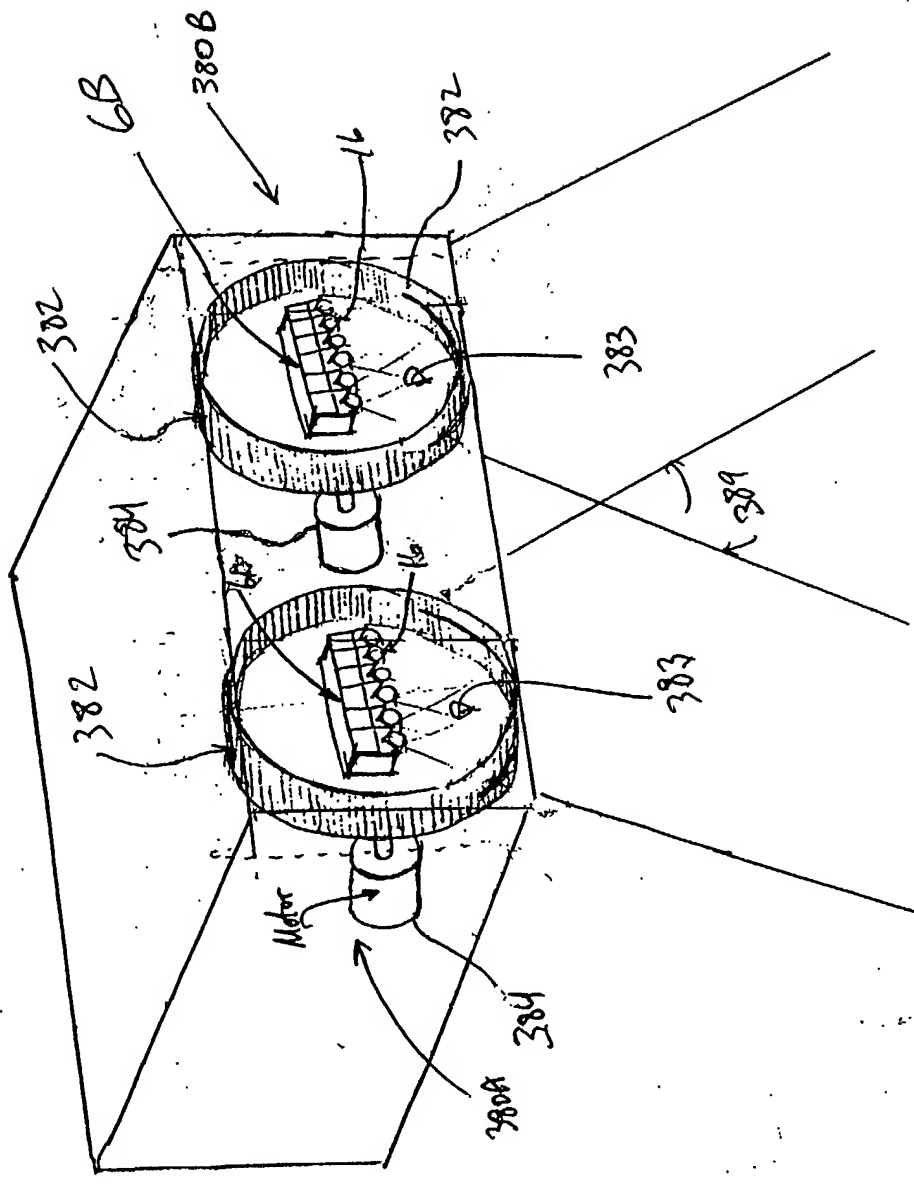
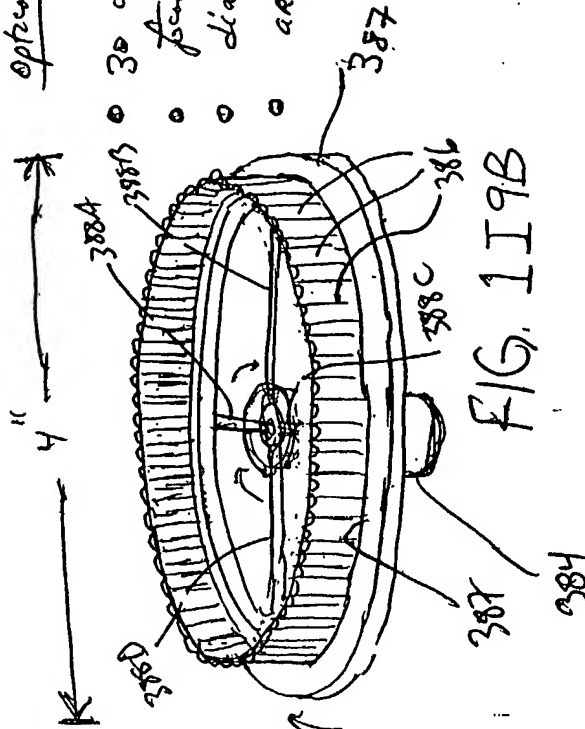


FIG. 11 9A

34/ 385

Optical specifications:

- 30 cylindrical lens (lens) per linear inch
- focal length ≈ 2.0 millimeters
- diameter of lens ≈ 4 inches
- acrylic material



35/ 385

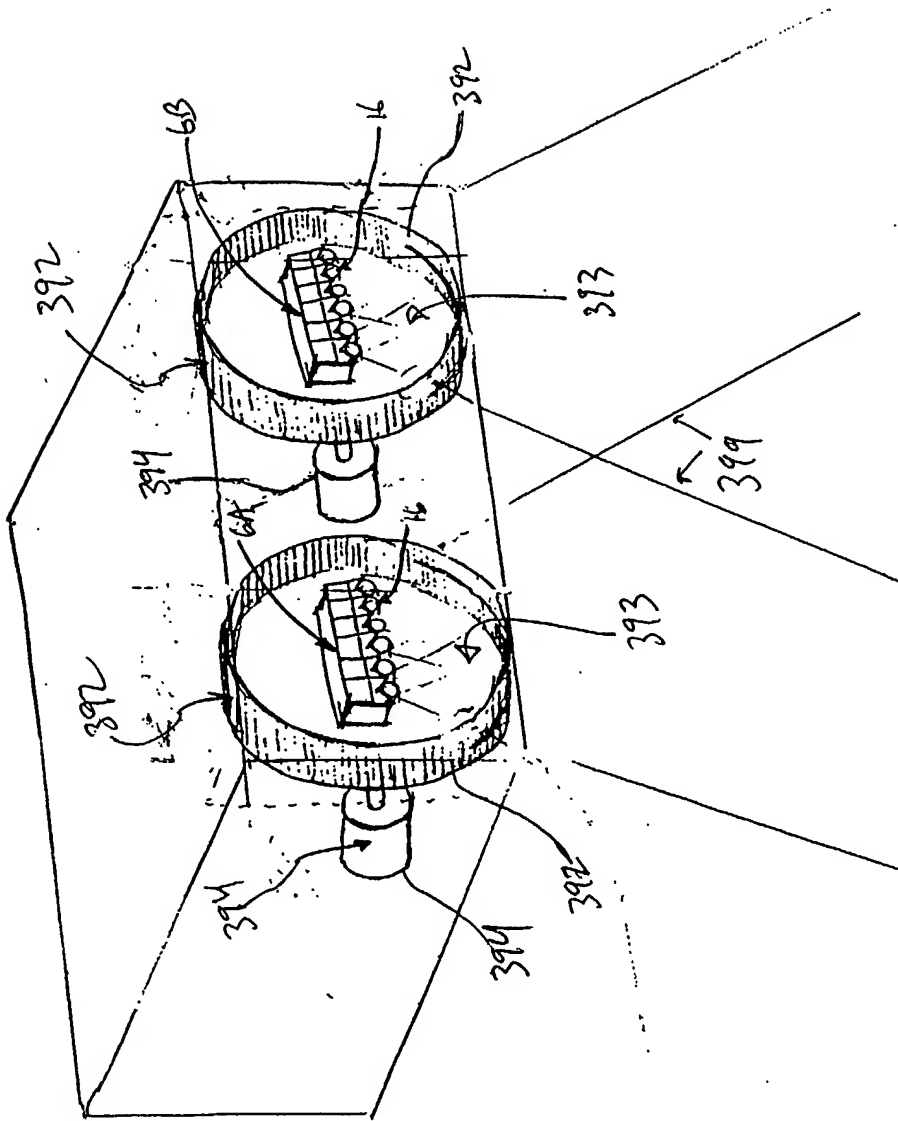


FIG. 1I10A

36/ 385

Optical specifications:

- 30 upturned lens (lens) per linear inch
- total length \approx 2.0 millimeters
- diameter of lens \approx 0.1 inches

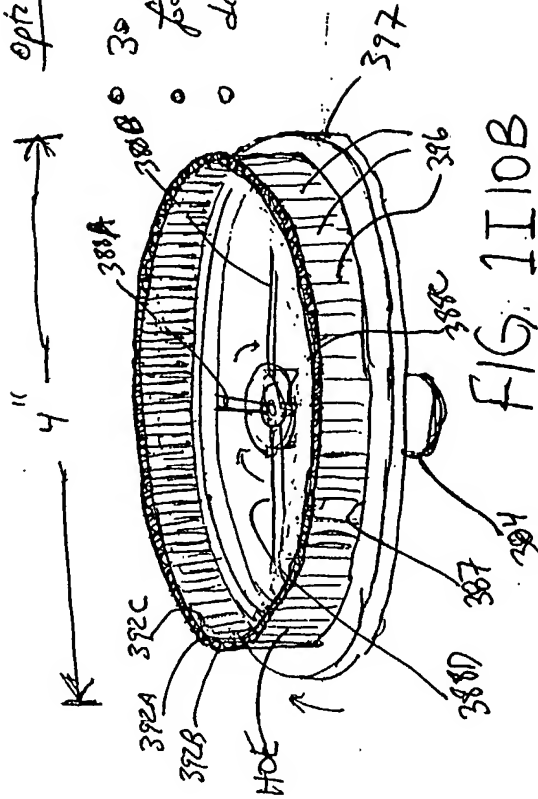


FIG. 1110B

37/ 385

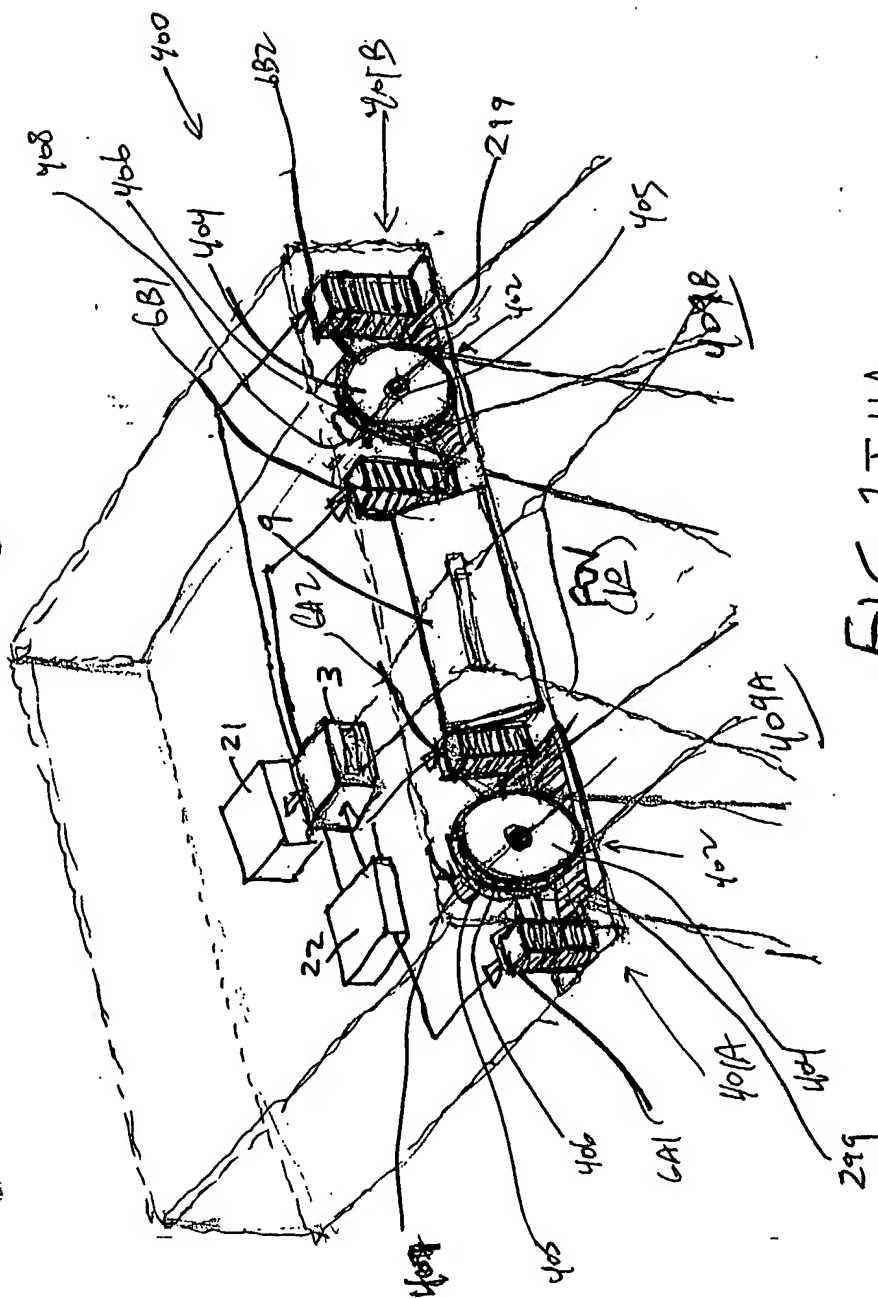


FIG. 111A

30/ 385

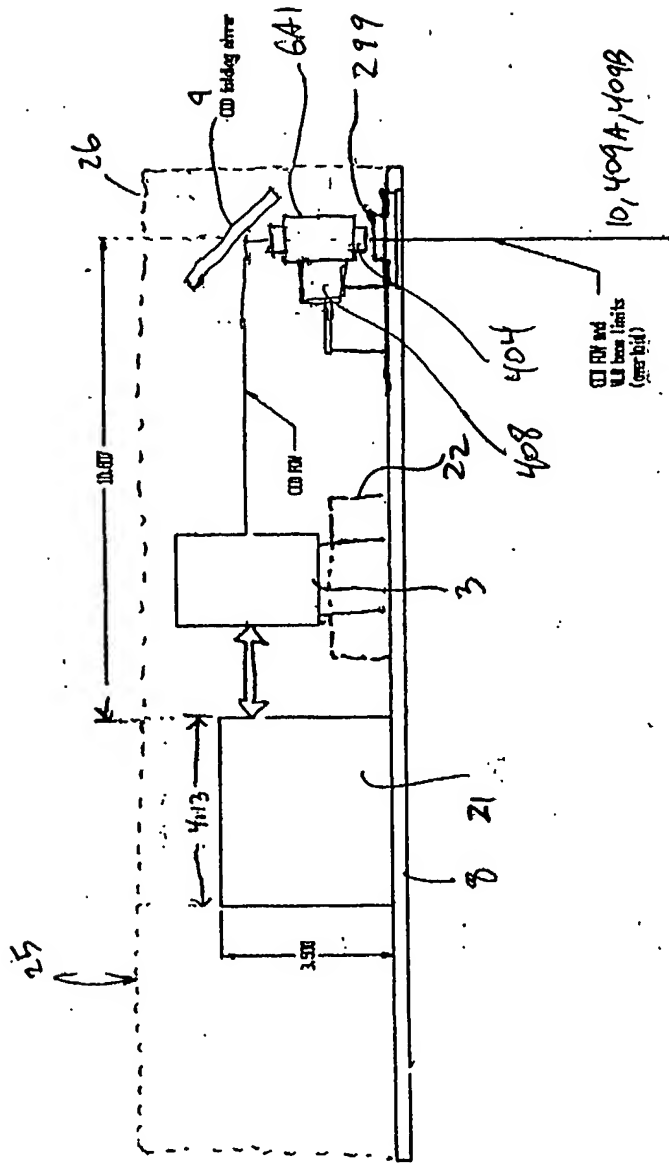
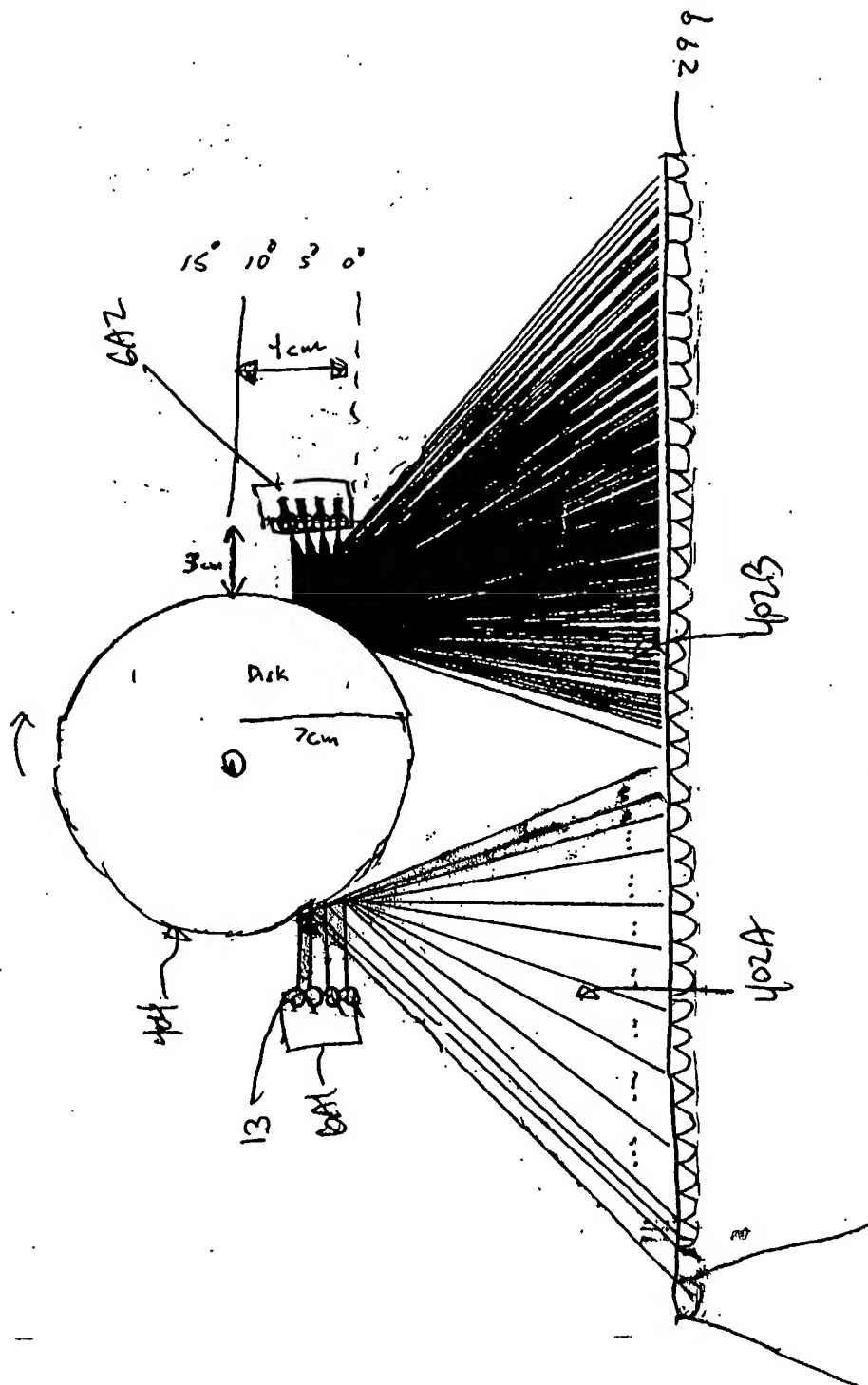


FIG 1I11B

39/ 385



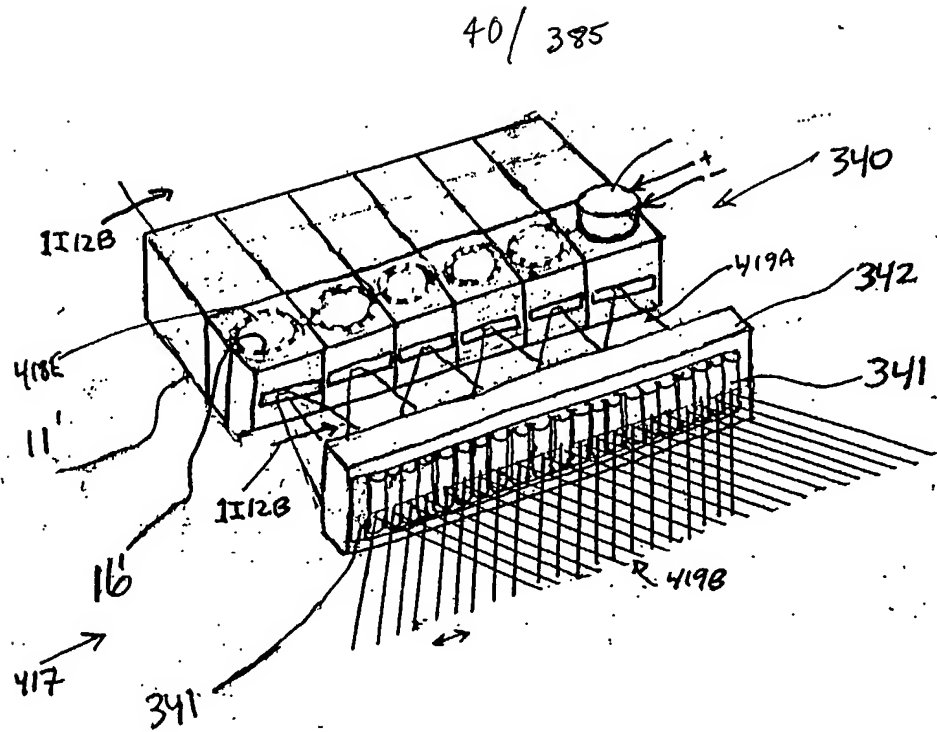


FIG. 1I12A

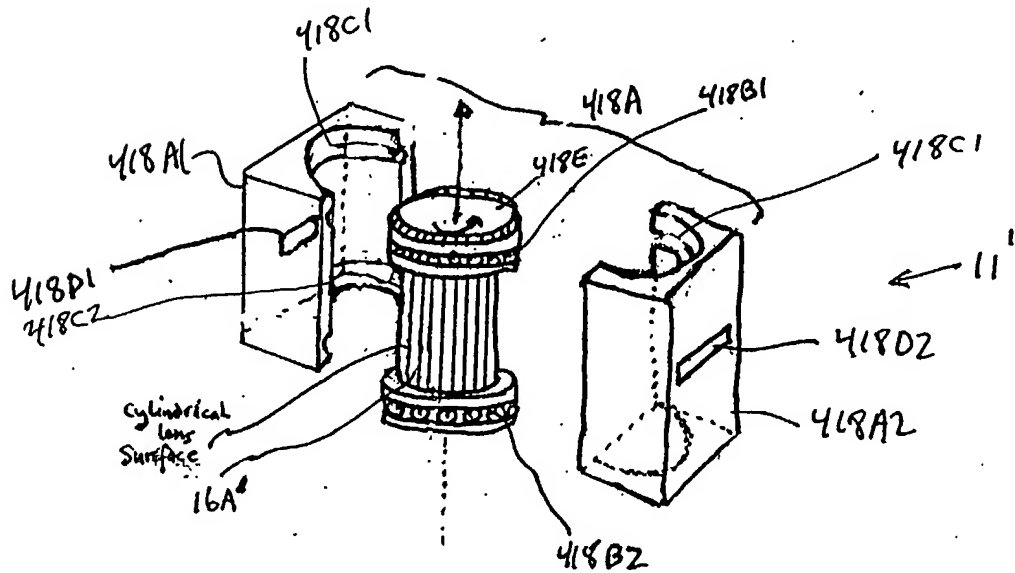


FIG. 1I12B

41/ 385

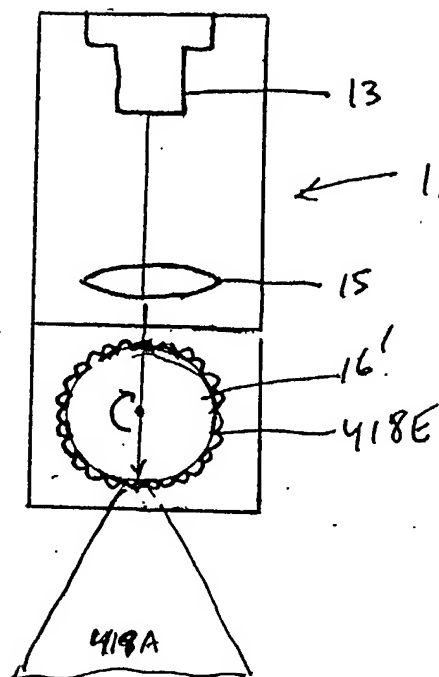


FIG. 1I12C

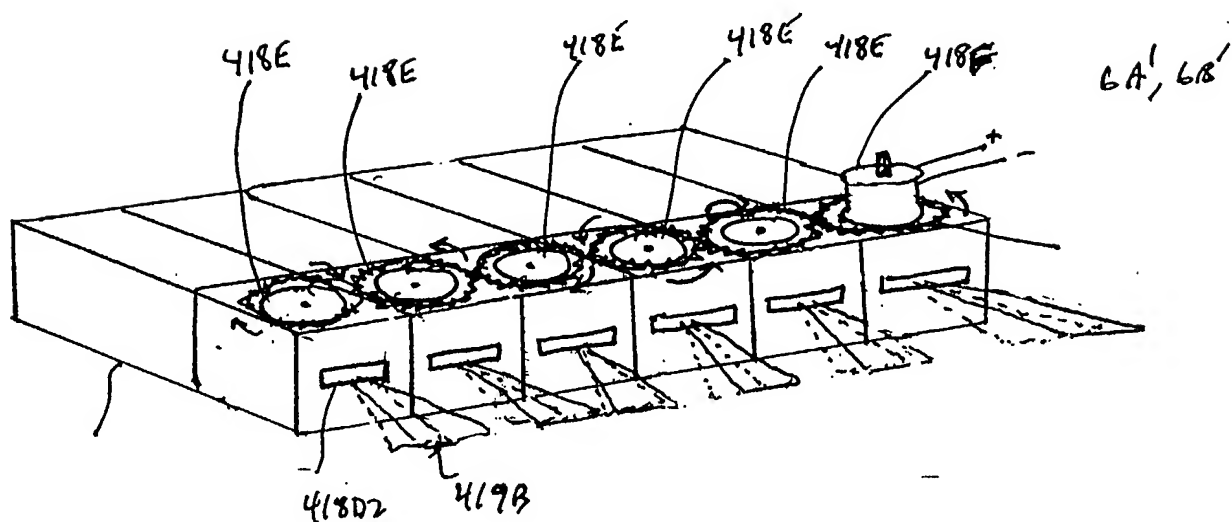


FIG. 1I12D

42/ 385

Second Generalized Method of
Reducing Speckle-Noise Patterns
at Image Detection Array
of FLD FFD Subsystem (3)

(TIME)

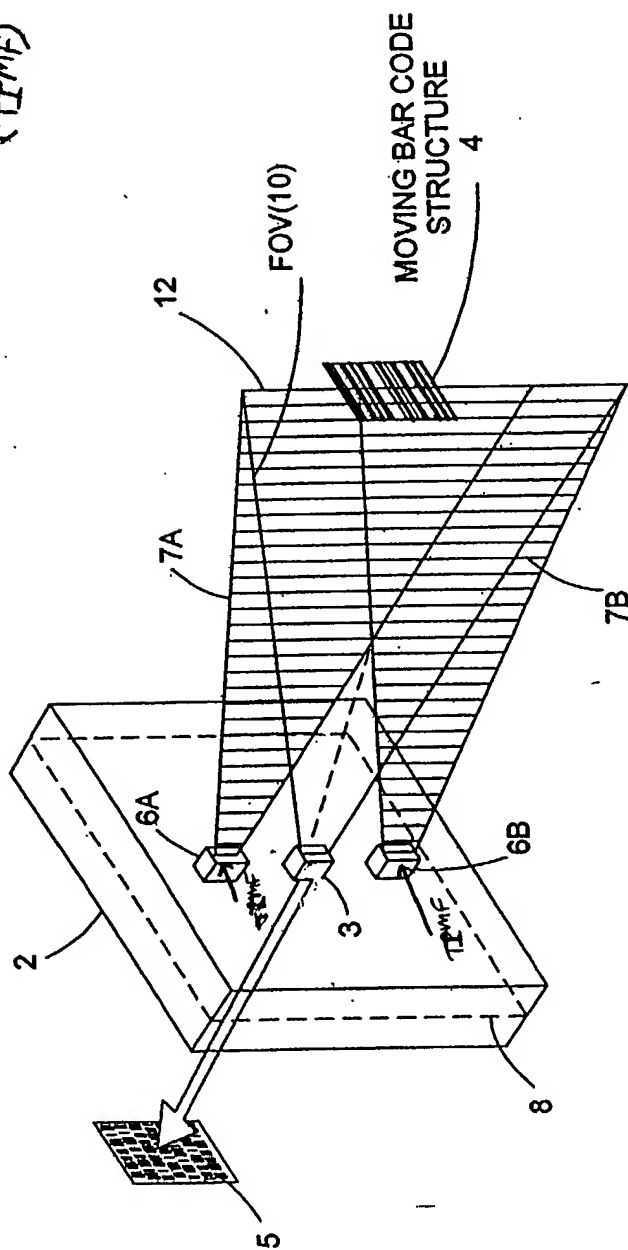


FIG. 1113

43/ 385

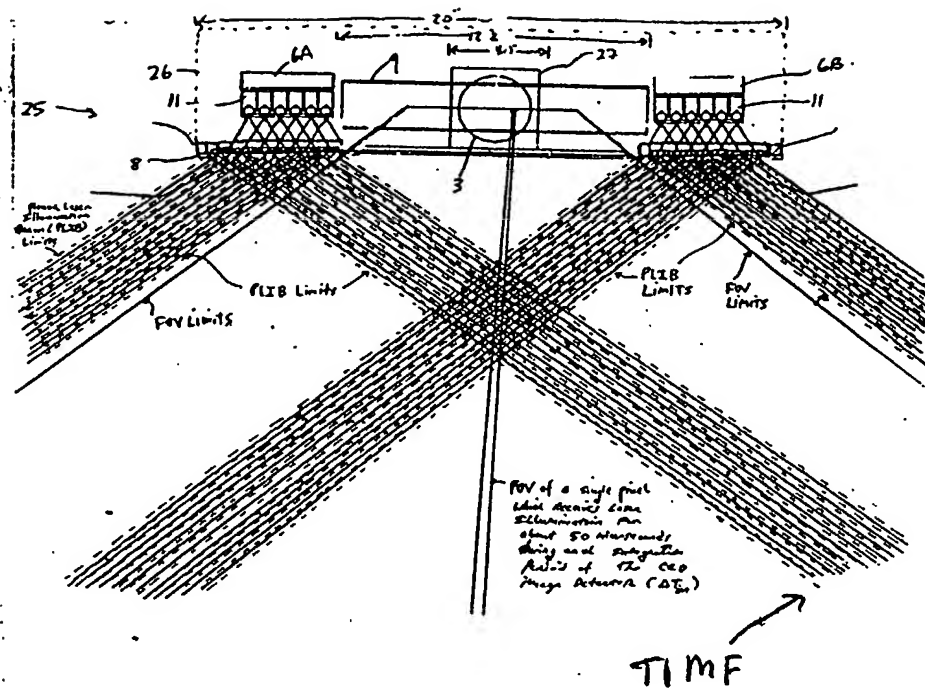


FIG. 1 I 13A

44/ 385

The Second Generalized Speckle-Noise Pattern Reduction Method
Of The Present Invention

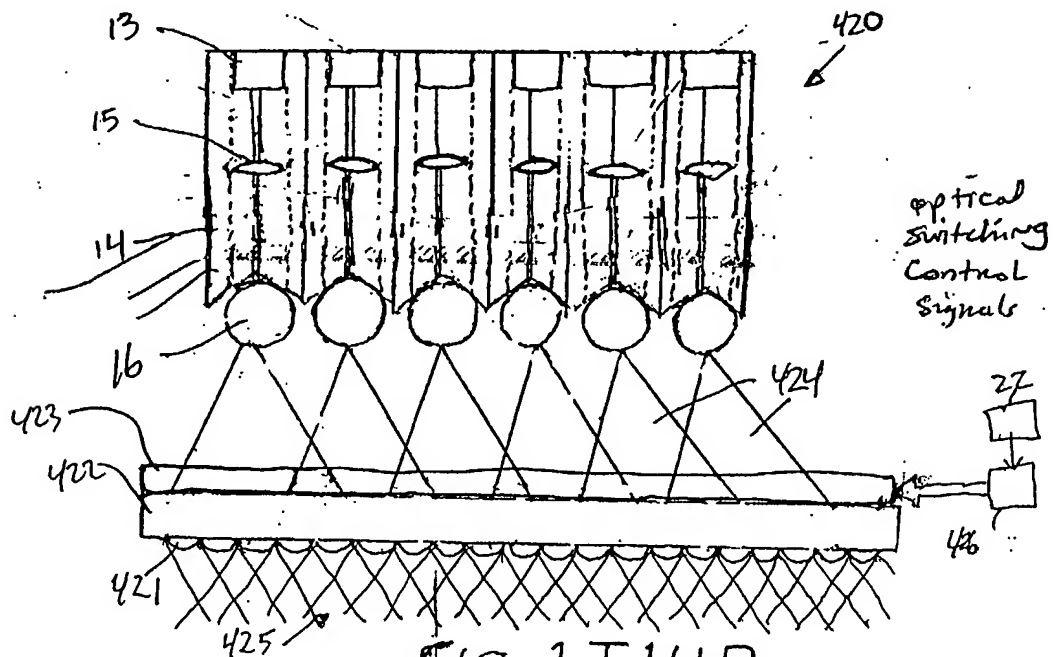
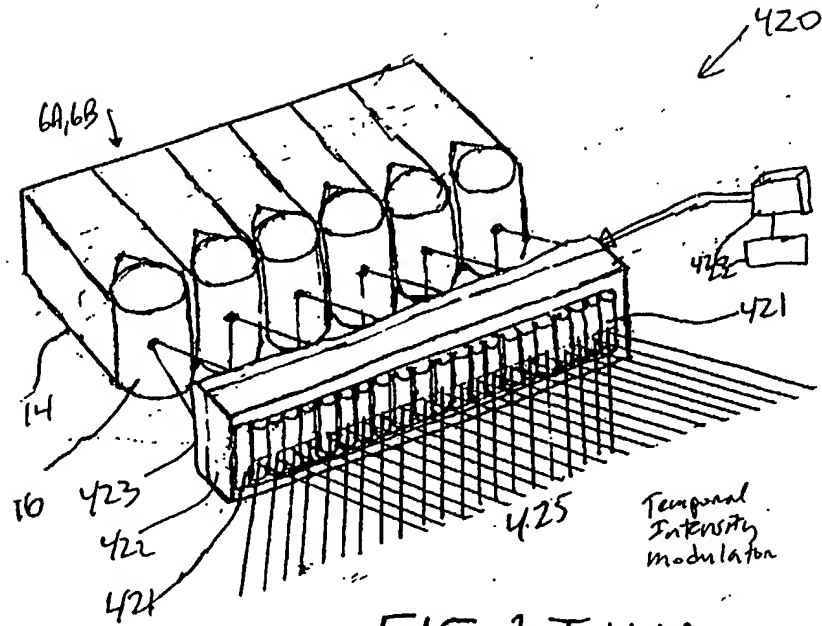
Prior to illumination of the target with the planar laser illumination beam (PLIB), modulate the temporal intensity of the transmitted PLIB along the planar extent thereof according to a temporal intensity modulation function (TIMF) so as to

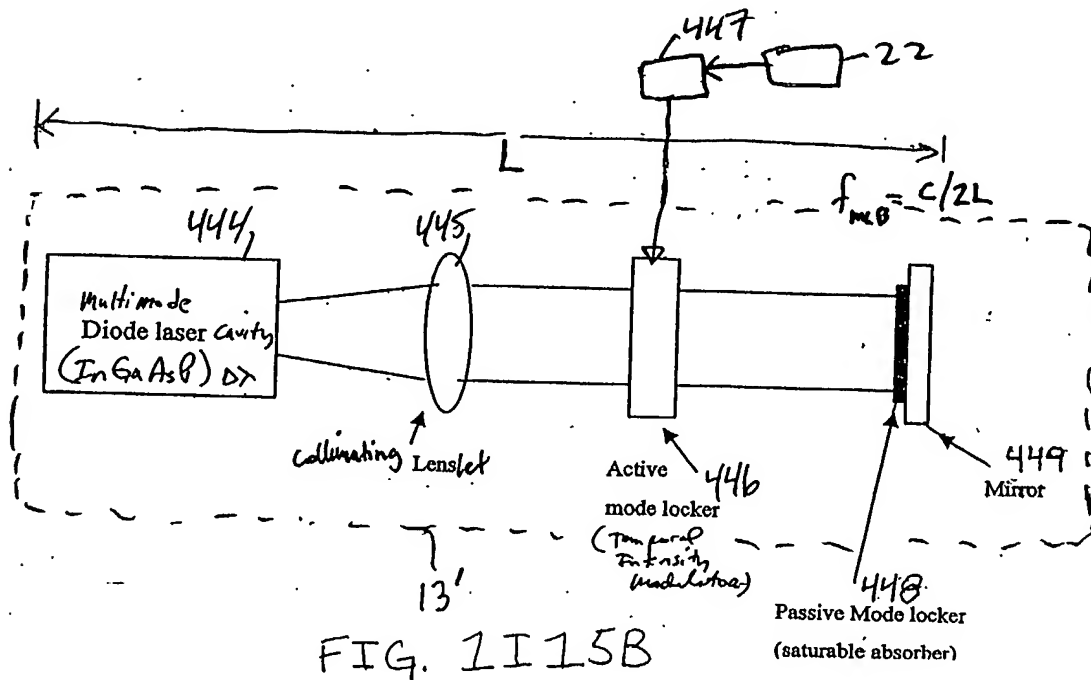
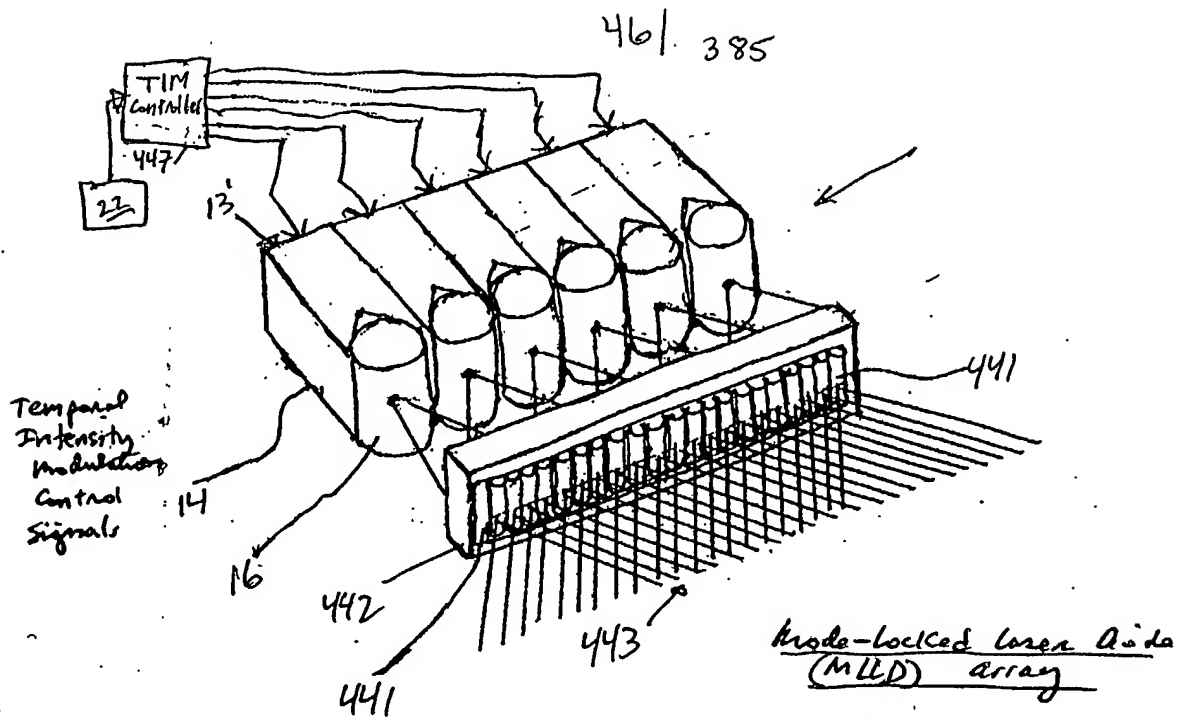
produce numerous substantially different time-varying speckle-noise patterns at the image detection array of the IFD Subsystem during the photo-integration time period thereof.

Temporally average the numerous substantially different time-varying speckle-noise patterns produced at the image detection array in the IFD Subsystem during the photo-integration time period thereof, so as to thereby reduce power of the speckle-noise pattern observed at the image detection array.

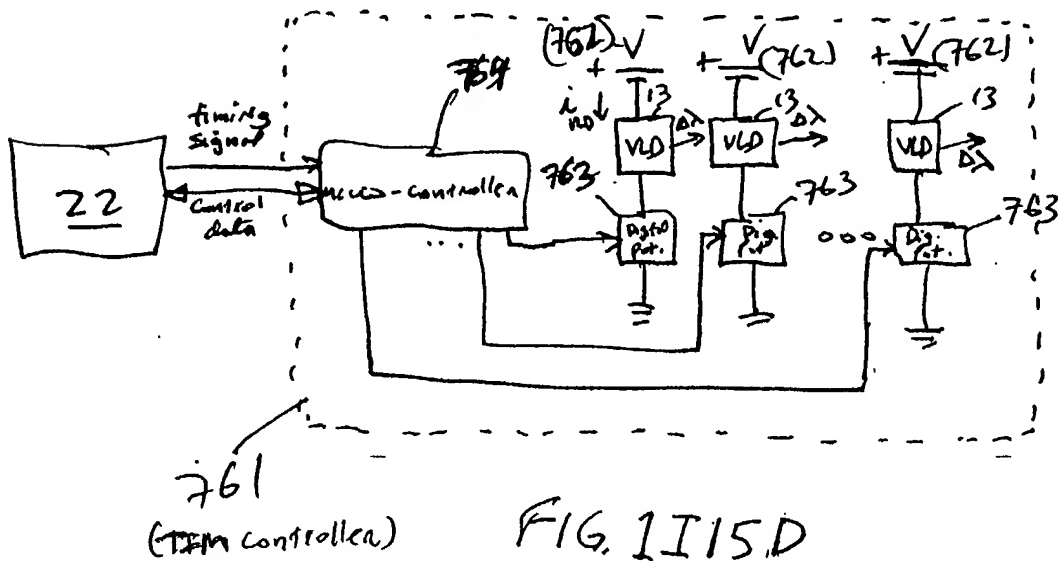
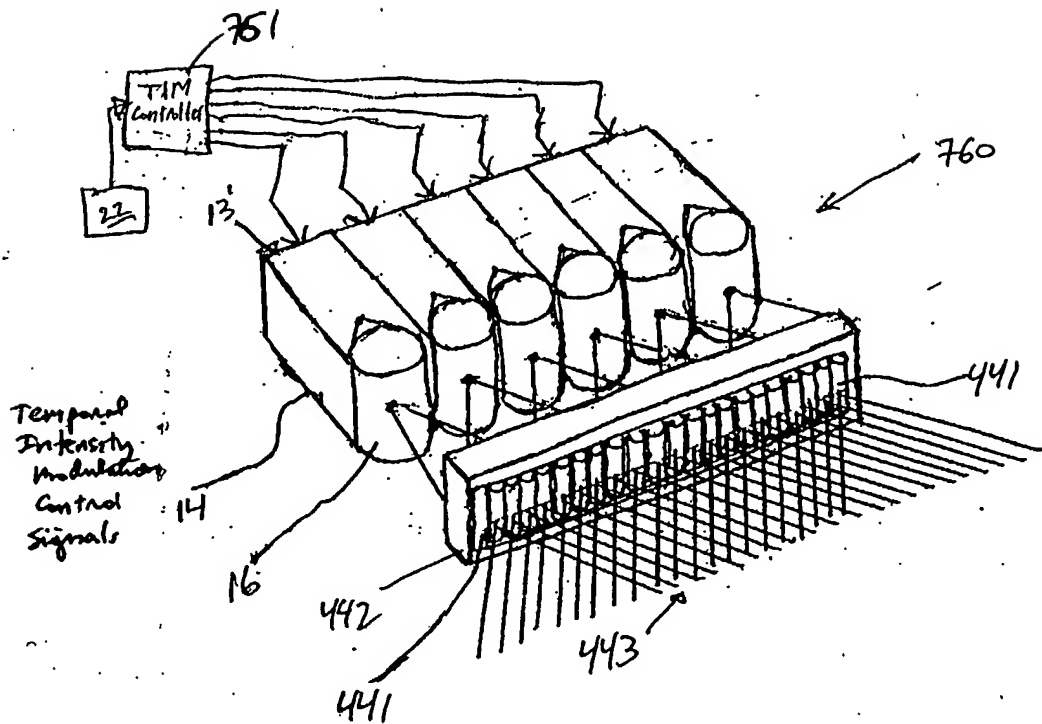
FIG. 1I13B

45/ 385





47 | 385



48/ 385

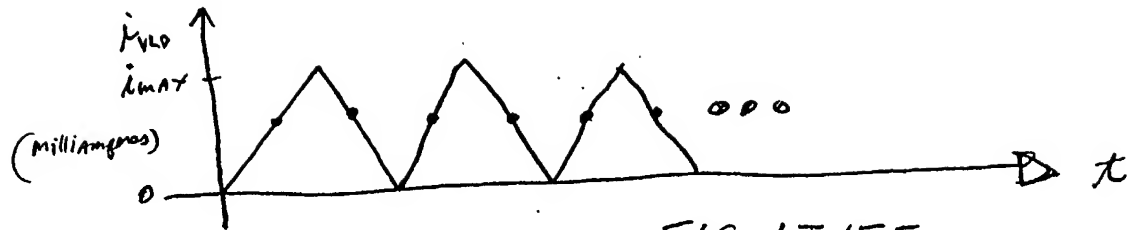


FIG. 1I15E

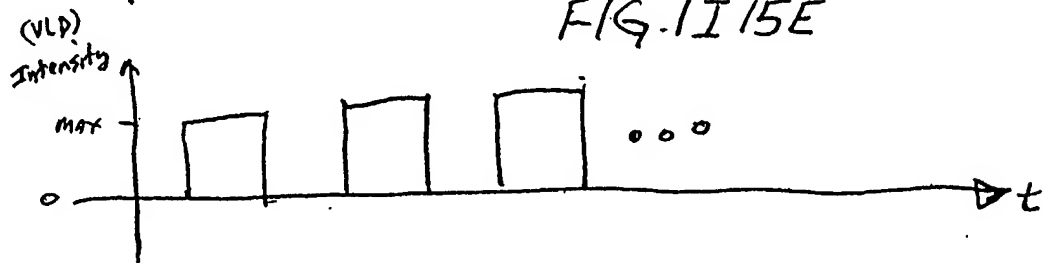


FIG. 1I15E

49/ 385

Third Generalized Method of
Reducing Spoke-Nose Patterns
at Image Detection Array
of the FFD Subsystem (3)

(TIME)

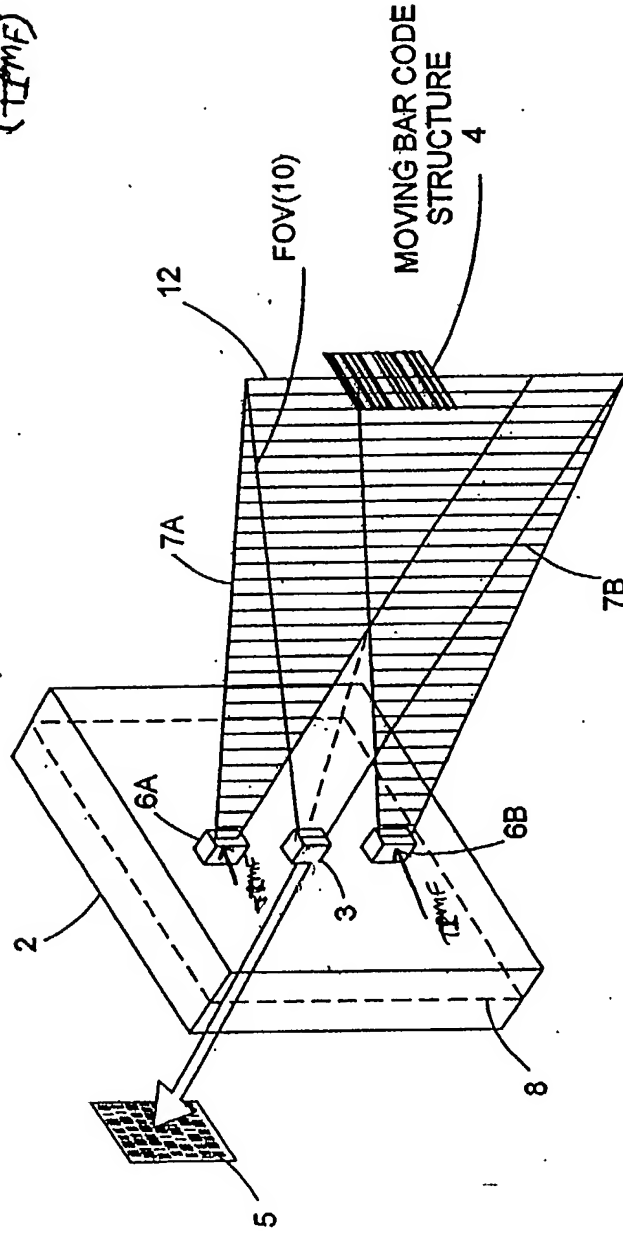


FIG. 1116

50/ 385

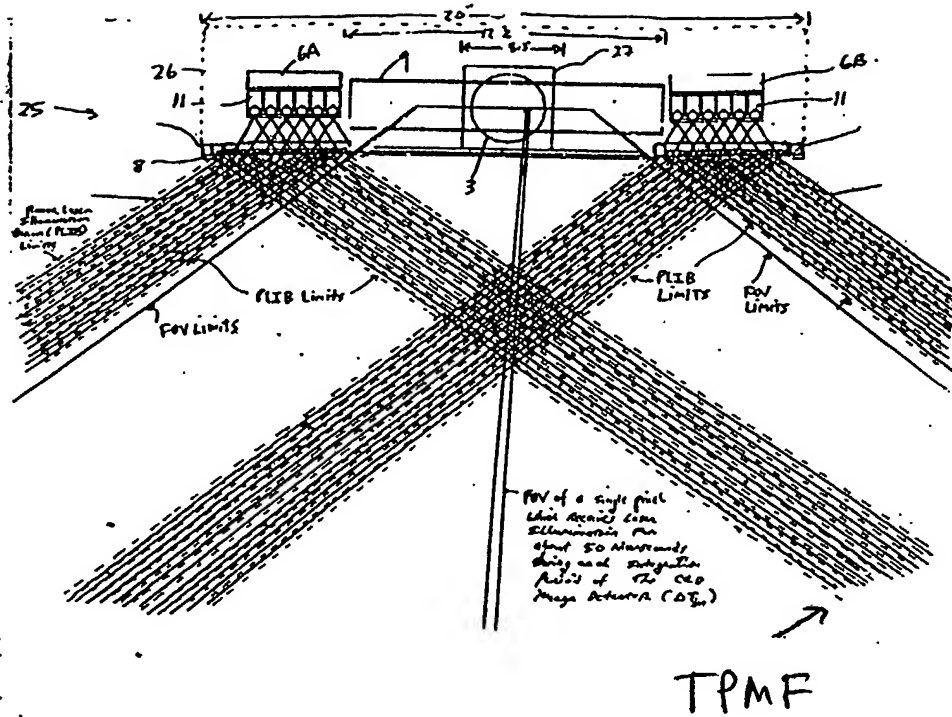


FIG. 1 I 16A

51/ 385

Third Generalized Speckle-Noise Pattern Reduction Method
Of The Present Invention

Prior to illumination of the target with the planar laser illumination beam (PLIB), modulate the temporal *phase* of the transmitted PLIB ~~along the planar extent thereof~~ according to a *temporal phase* modulation function (TPMF) so as to:

produce numerous substantially different time-varying speckle-noise patterns at the image detection array of the IFD Subsystem during the photo-integration time period thereof.

↓

Temporally average the numerous substantially different time-varying speckle-noise patterns produced at the image detection array in the IFD Subsystem during the photo-integration time period thereof, so as to thereby reduce power of the speckle-noise pattern observed at the image detection array.

FIG. 1I 16B

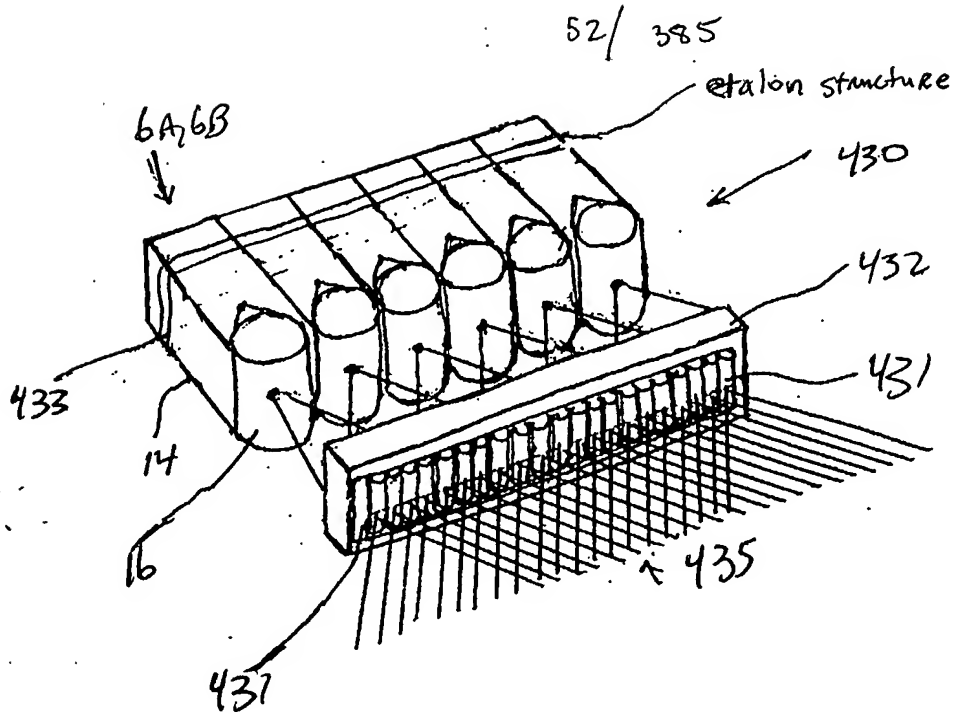


FIG. 1I17A

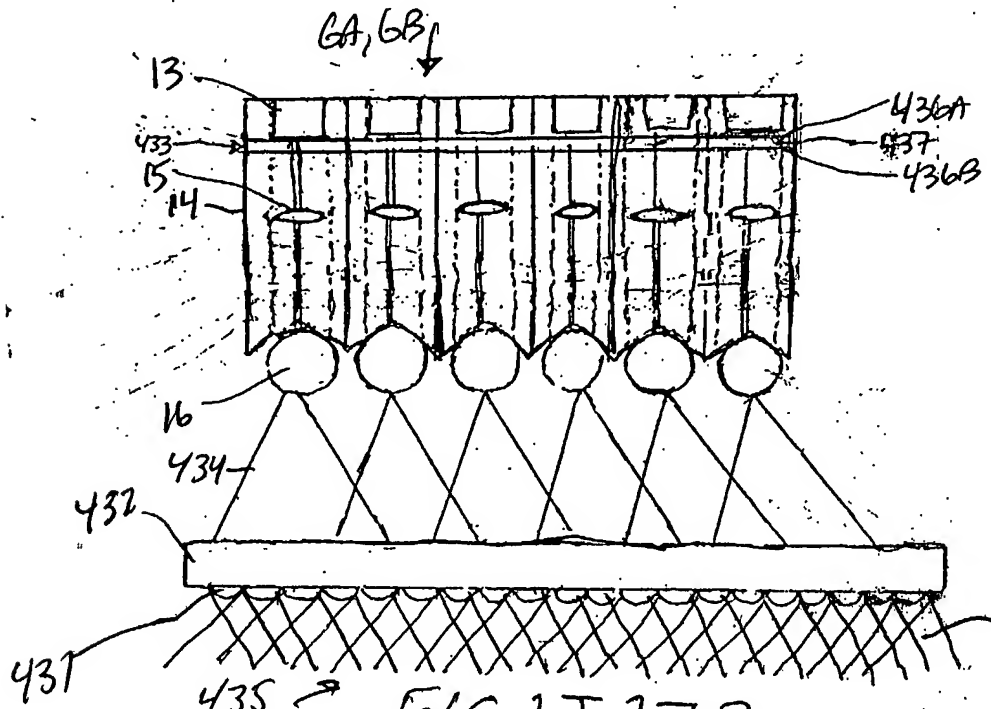


FIG. 1I17B

53/ 385

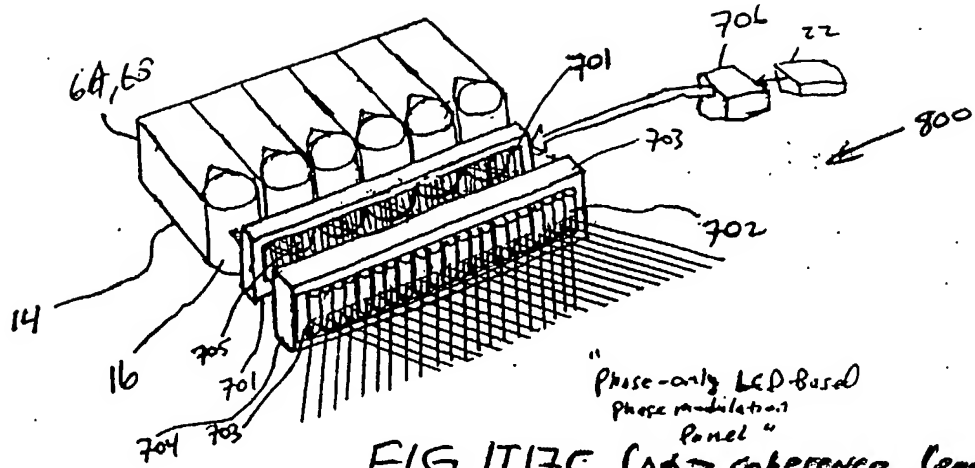


FIG. 1I17C ($\Delta\phi >$ coherence length
of VLD)

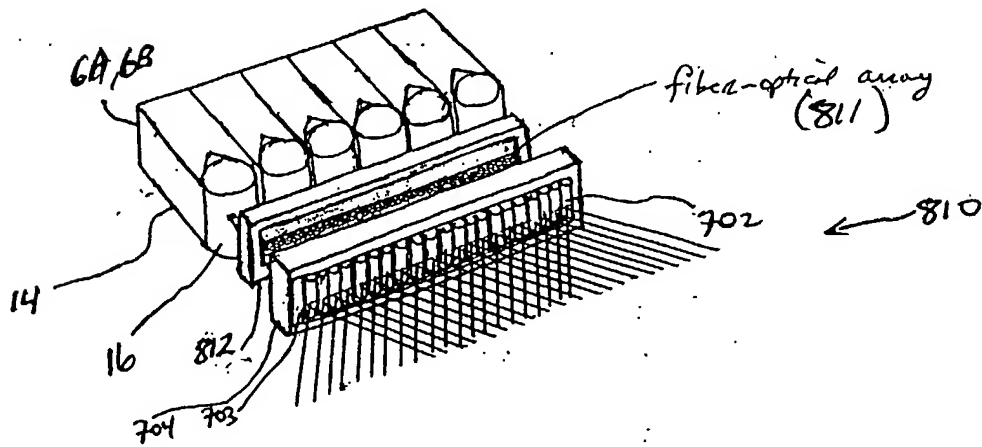


FIG. 1I17D

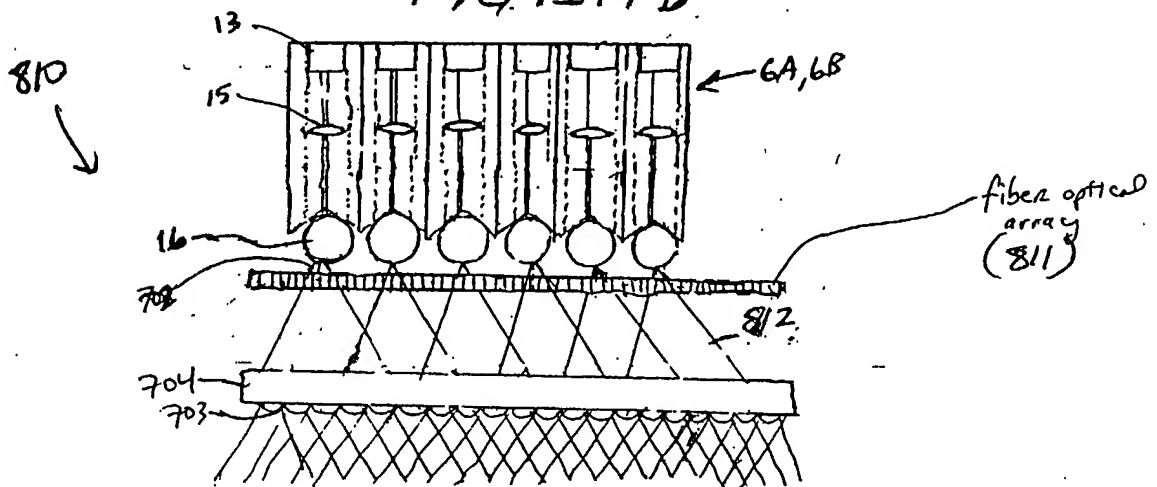


FIG. 1I17E

54/ 385

Fourth Generalized Method of
Reducing Salt-and-Pepper Noise Patterns
at Image Detection Array
of the FPD Subsystem (3)

(TFmp)

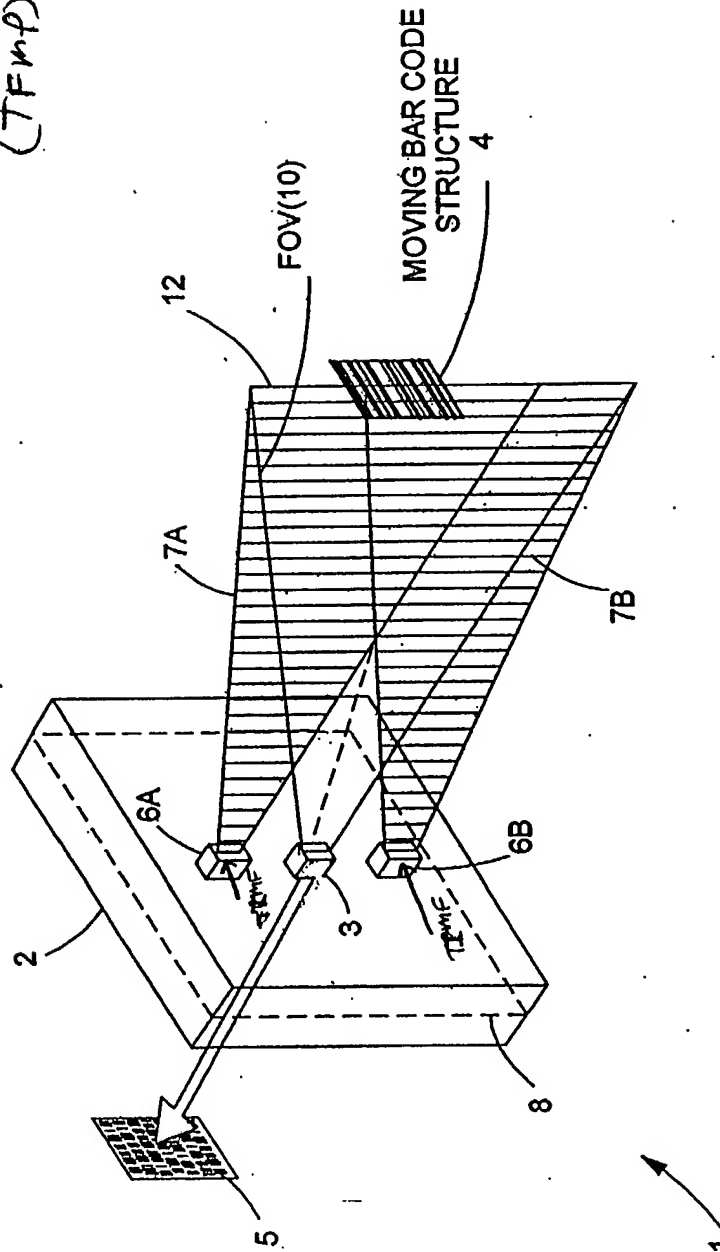


FIG. 11B

55/ 385

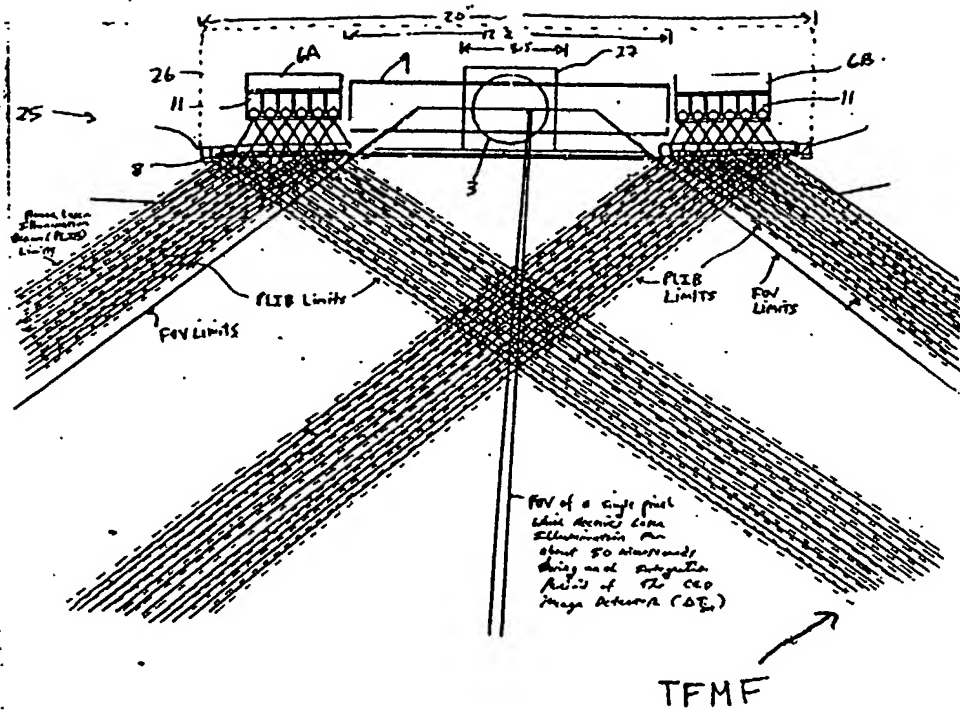


FIG. 1 I 18A

56/ 385

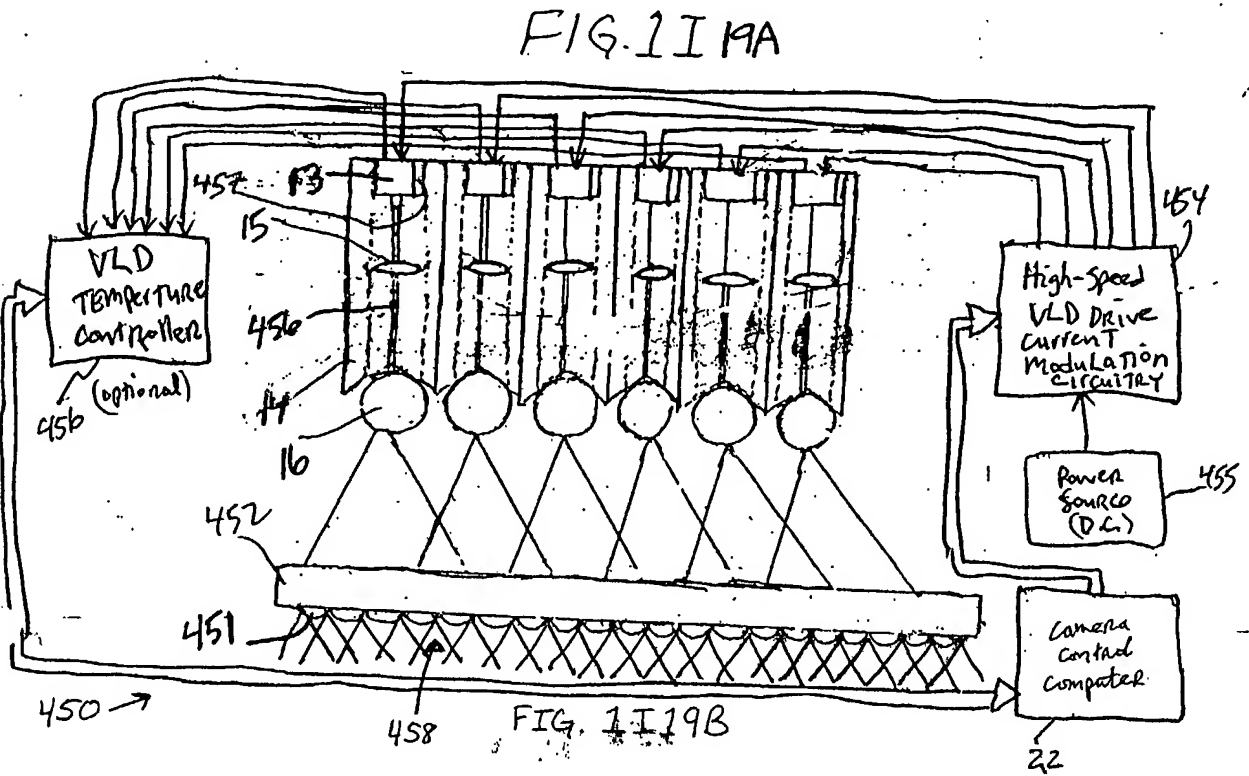
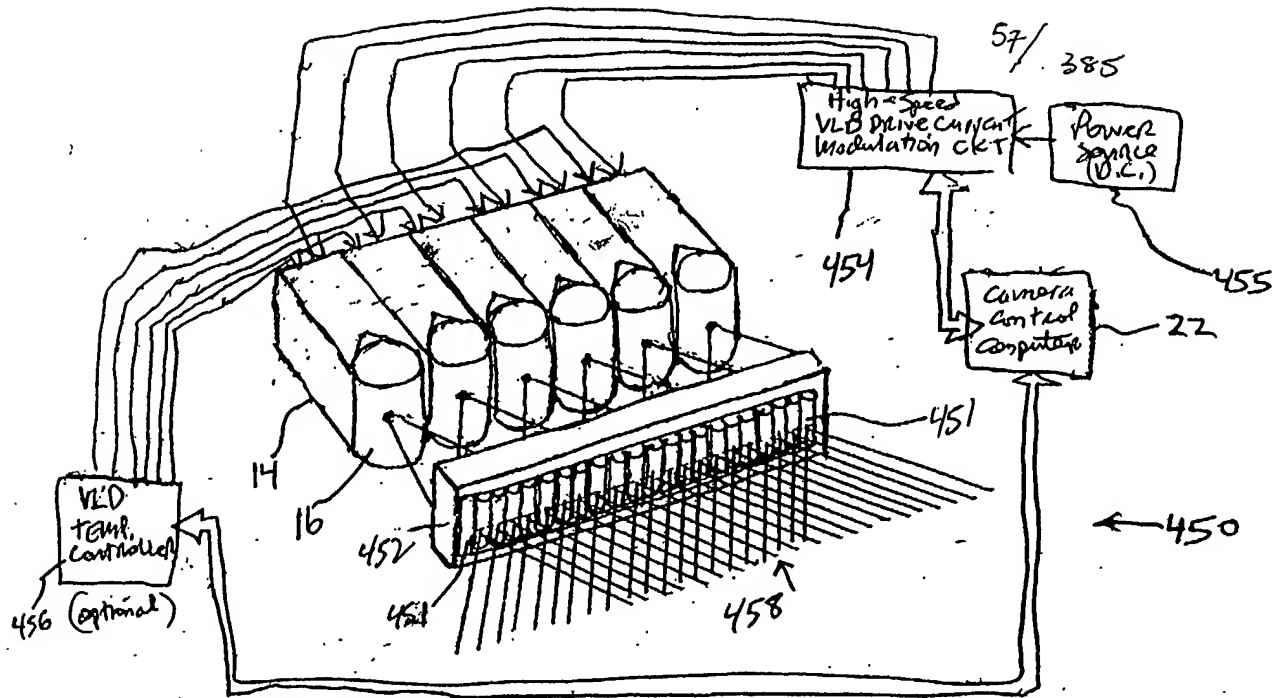
Fourth Generalized Speckle-Noise Pattern Reduction Method
Of The Present Invention

Prior to illumination of the target with the planar laser illumination beam (PLIB), modulate the temporal frequency of the transmitted PLIB according to a temporal intensity modulation function (T IMF) so as to

produce numerous substantially different time-varying speckle-noise patterns at the image detection array of the IFD Subsystem during the photo-integration time period thereof.

Temporally average the numerous substantially different time-varying speckle-noise patterns produced at the image detection array in the IFD Subsystem during the photo-integration time period thereof, so as to thereby reduce power of the speckle-noise pattern observed at the image detection array.

FIG. 1118B



58/385

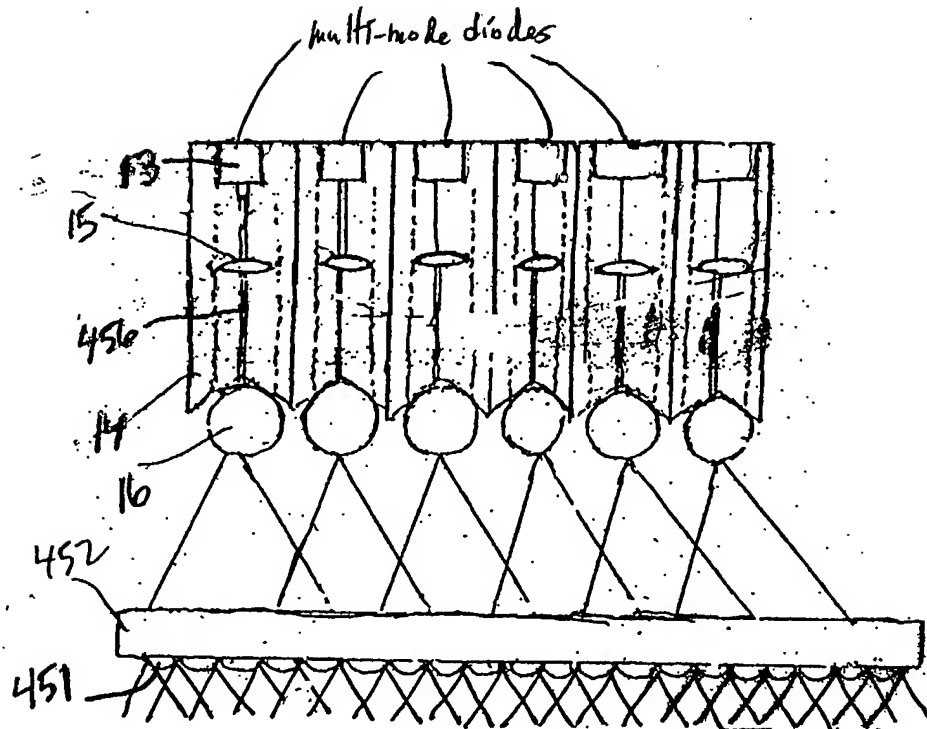


FIG 1I19C

59/ 385

Fifth Generalized Method
of Reducing Speckle-Noise
Patterns At Image
Detection array of the
IPD subsystem (3)

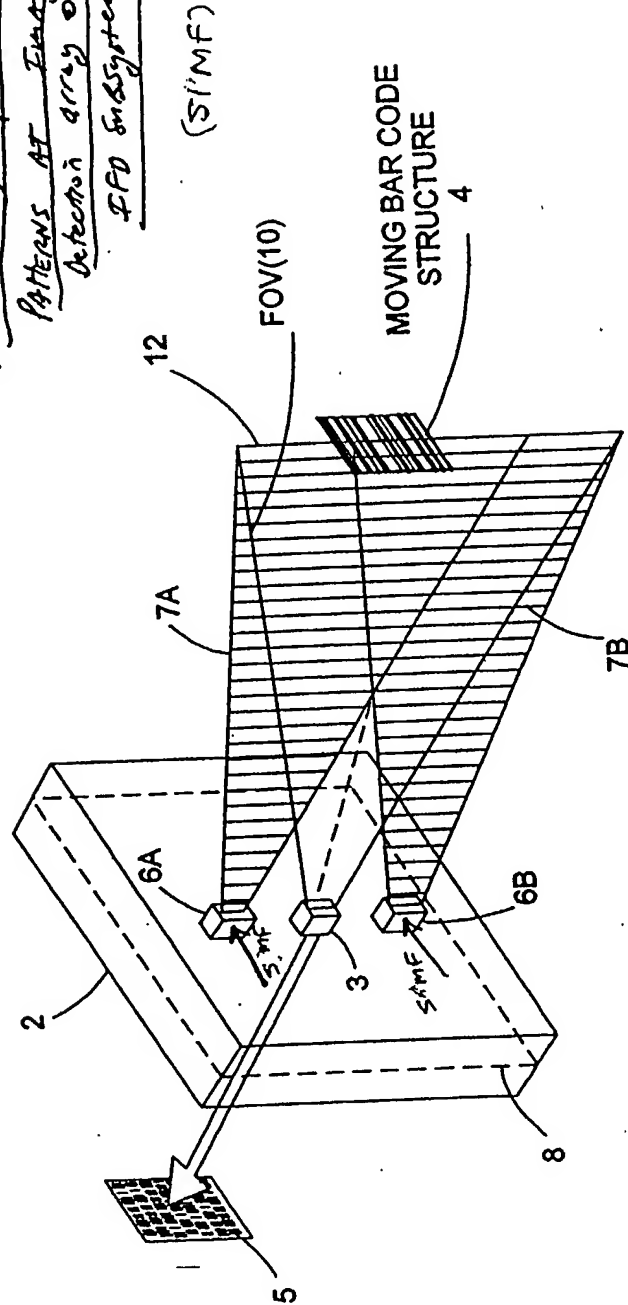
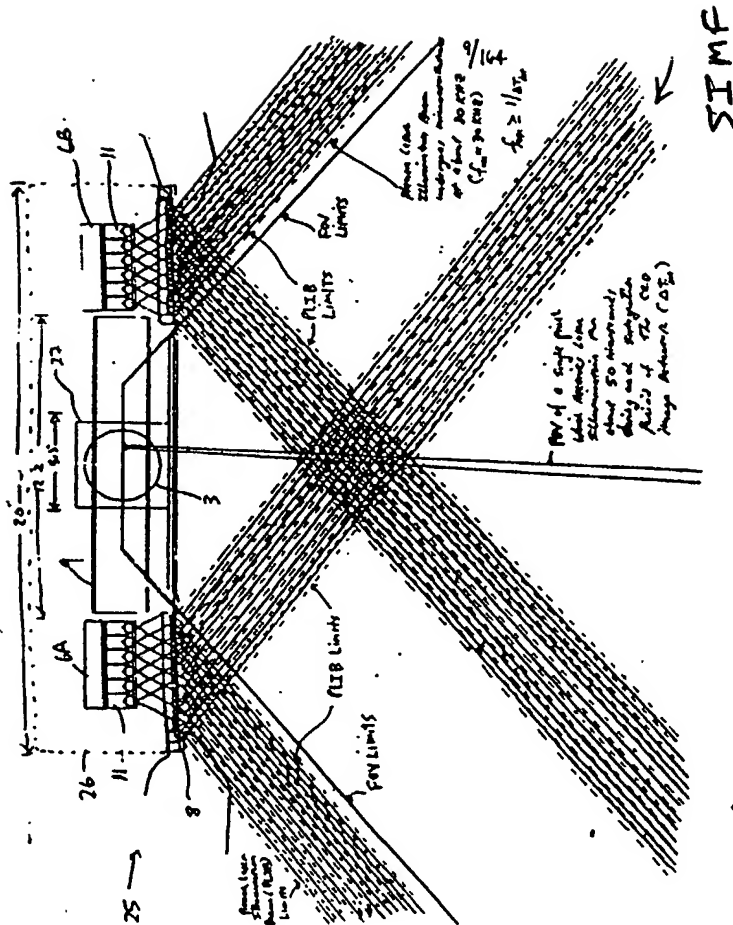


FIGURE 20

60 / 385



Ratio to object illumination

61/ 385

Fifth Generalized Speckle-Noise Pattern Reduction Method
Of The Present Invention

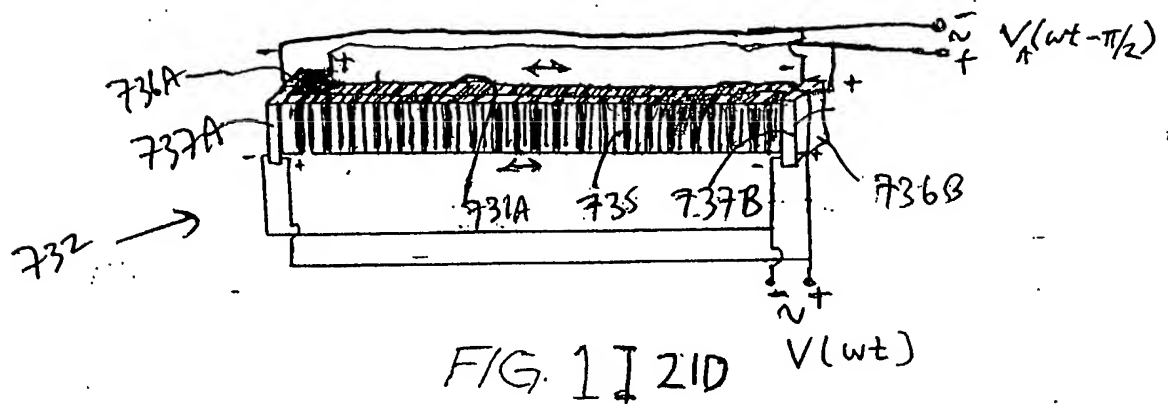
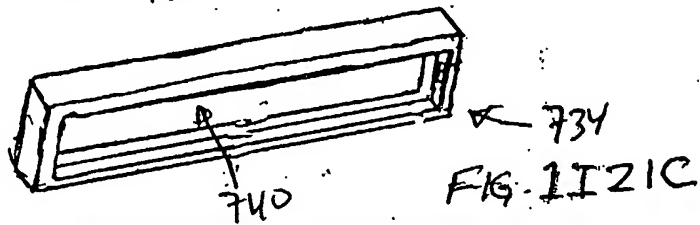
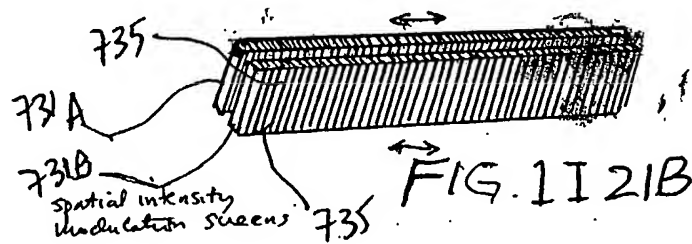
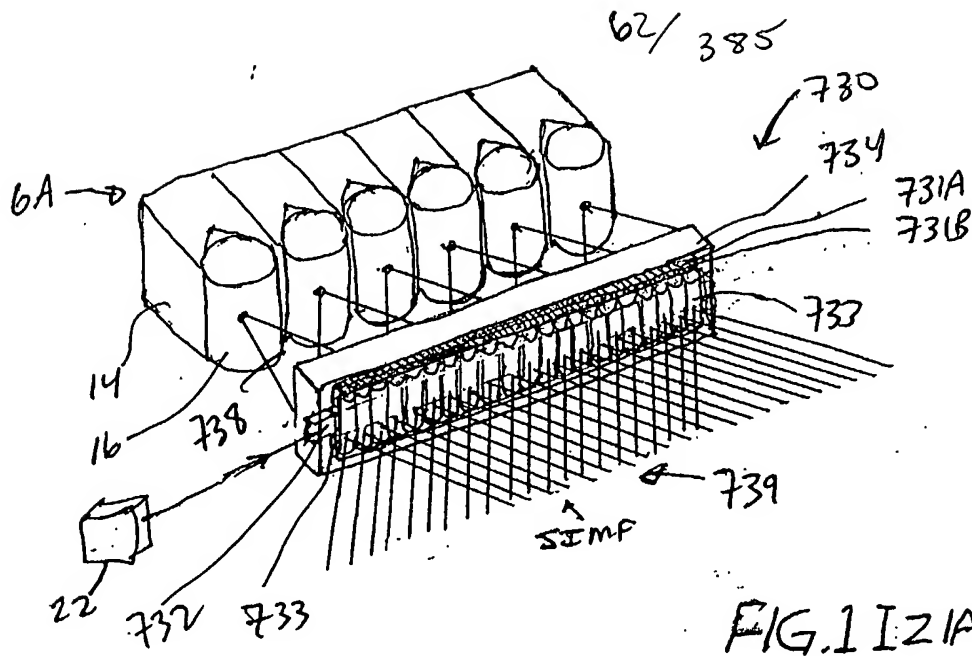
Prior to illumination of the target with the planar laser illumination beam (PLIB), modulate the spatial intensity of the transmitted PLIB along the planar extent thereof according to a spatial intensity modulation function (SIMF) so as to .

produce numerous substantially different time-varying speckle-noise patterns at the image detection array of the IFD Subsystem during the photo-integration time period thereof.

↓

Temporally average the numerous substantially different time-varying speckle-noise patterns produced at the image detection array in the IFD Subsystem during the photo-integration time period thereof, so as to thereby reduce power of the speckle-noise pattern observed at the image detection array.

FIG. 1I20B



Generalized Method of
Reducing Speckle-Noise Patterns
at Image Detection Array
of the IFD Subsystem

(SIMF)

63/ 385

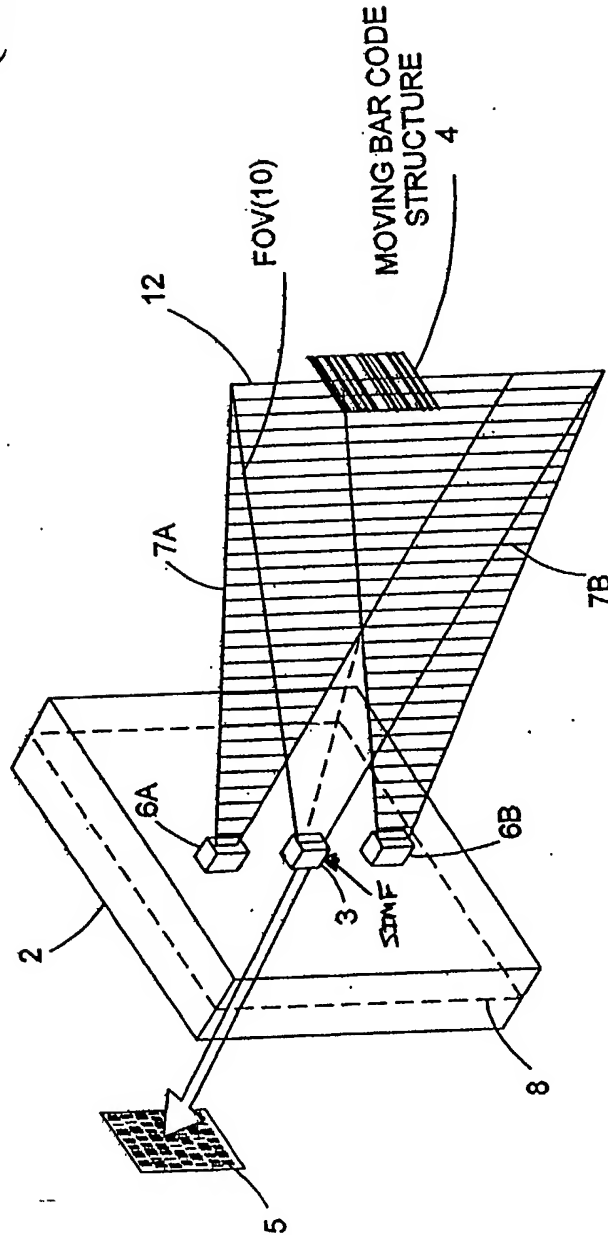


FIG. 11 22

64/385

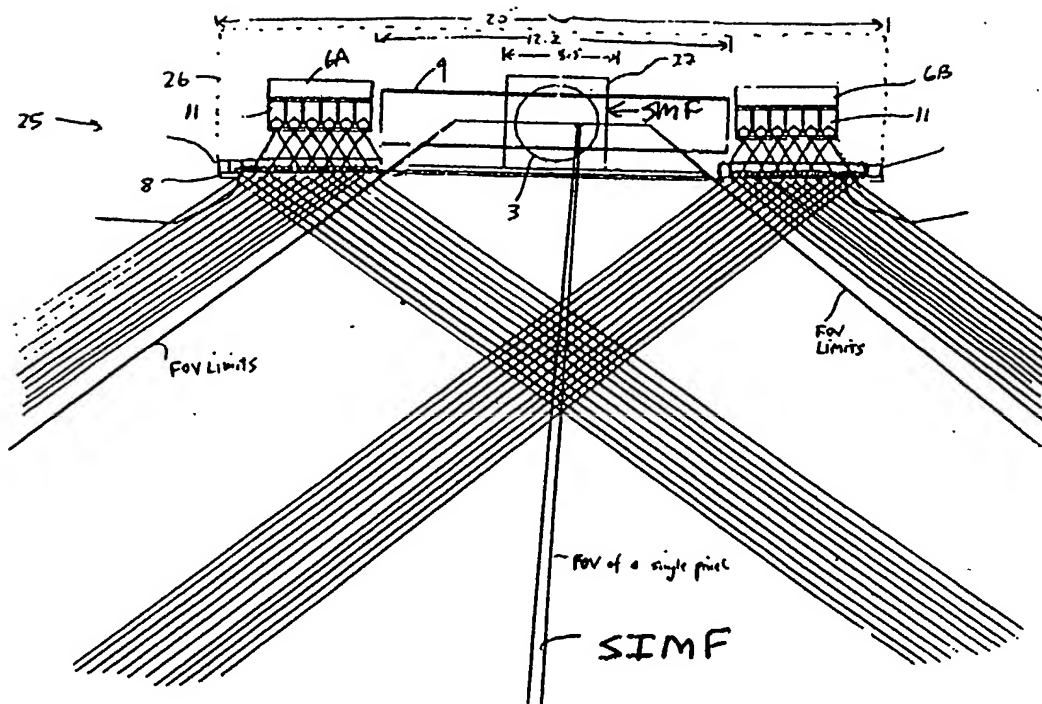


FIG. 1122A

65/385

Sixth Generalized Speckle-Noise Pattern Reduction Method
Of The Present Invention

After illumination of the target with the planar laser illumination beam (PLIB), modulate the spatial intensity of the reflected/scattered (i.e. received) PLIB along the planar extent thereof according to a spatial intensity modulation function (SIMF) so as to :

produce numerous substantially different time-varying speckle-noise patterns at the image detection array of the IFD Subsystem during the photo-integration time period thereof.

Temporally average the many substantially different time-varying speckle-noise patterns produced at the image detection array in the IFD Subsystem during the photo-integration time period thereof, so as to thereby reduce the speckle-noise pattern observed at the image detection array.

FIG. 1I 22B

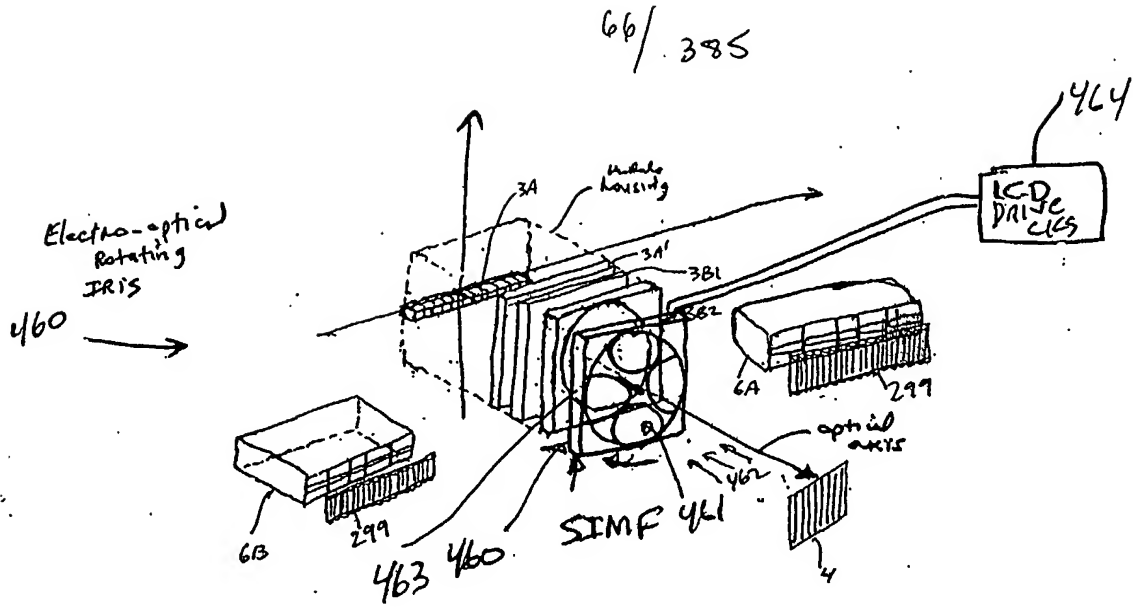


FIG. 1I 23A

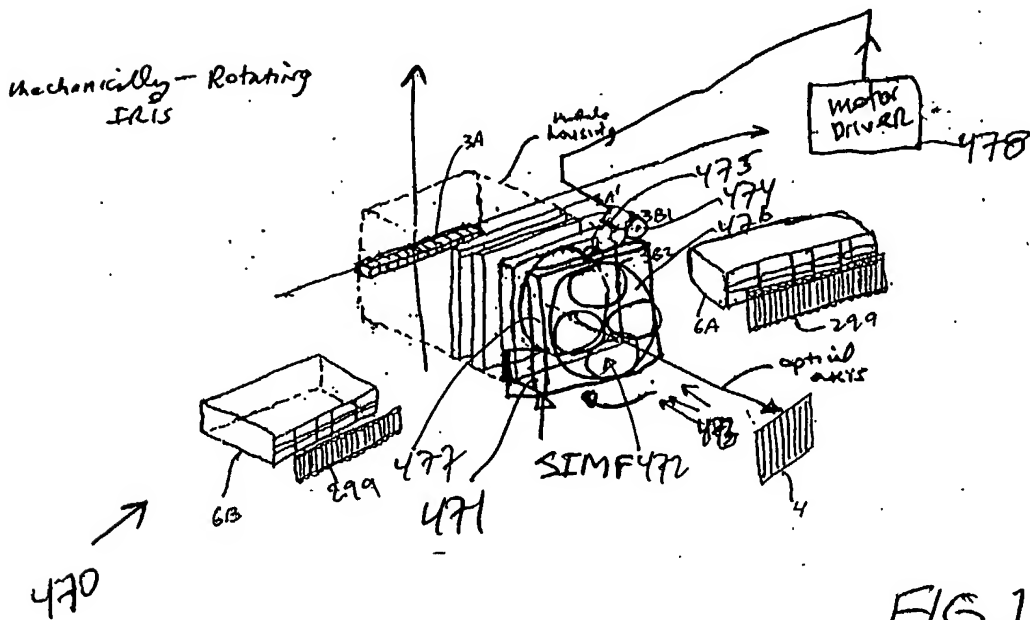


FIG. 1I 23B

Seventh Generalized Method of
Reducing Speckle-Noise Patterns
at Image Detection Array
of the IFD Subsystem

67/ 385

(TIME)

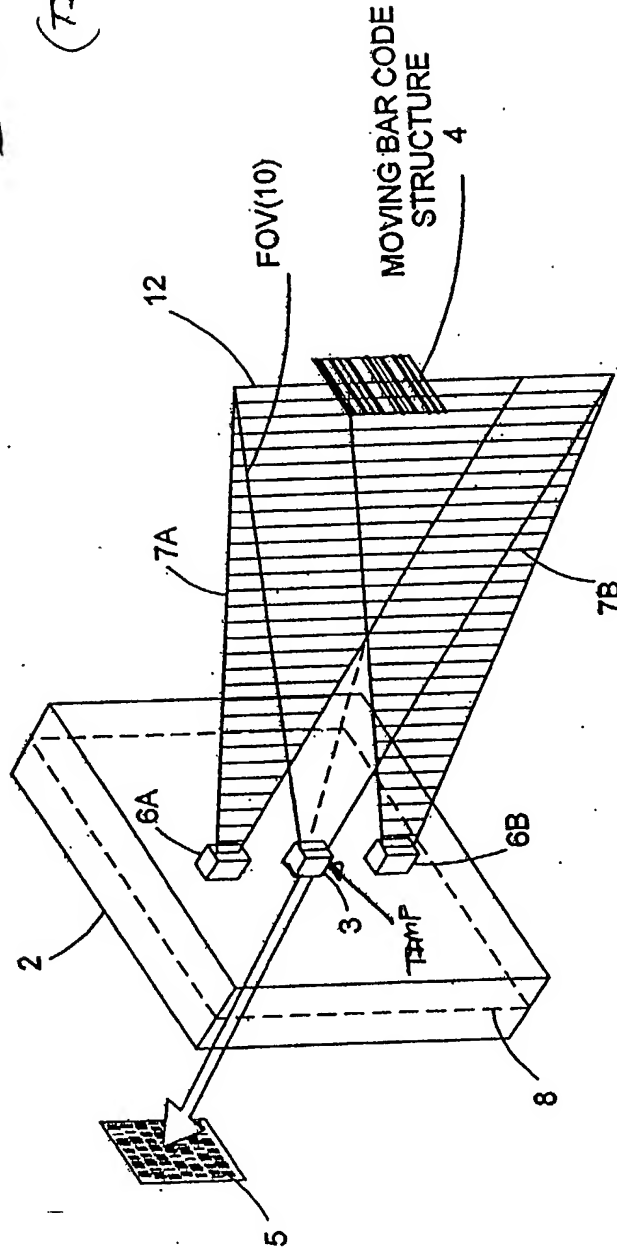


FIG. 11.24

68/ 385

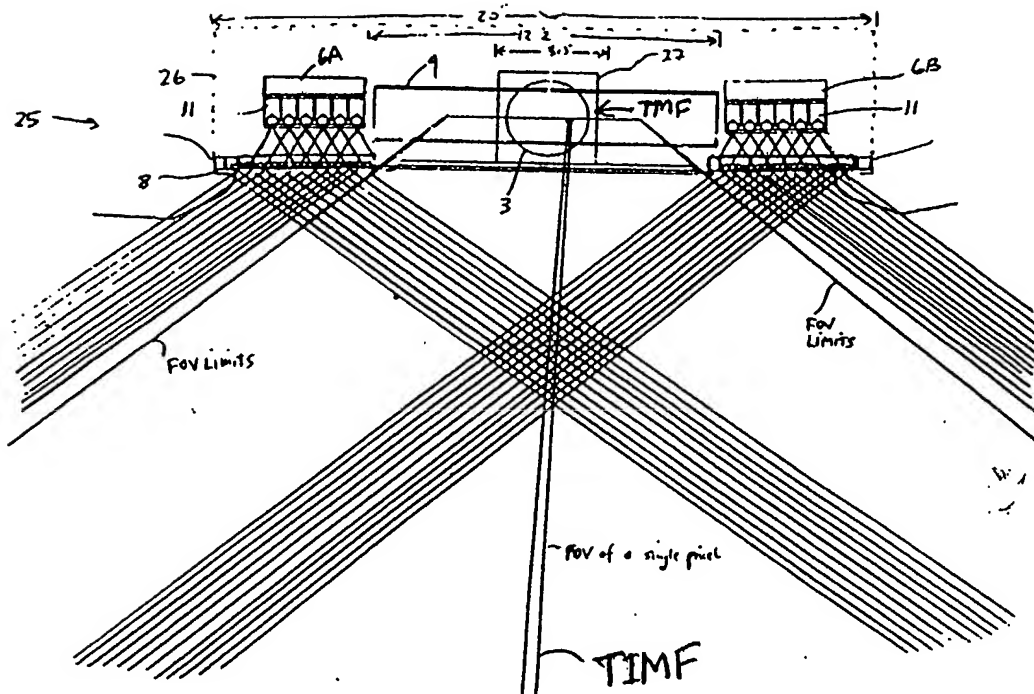


FIG. 1I24A

69/ 375

Seventh Generalized Speckle-Noise Pattern Reduction Method
Of The Present Invention

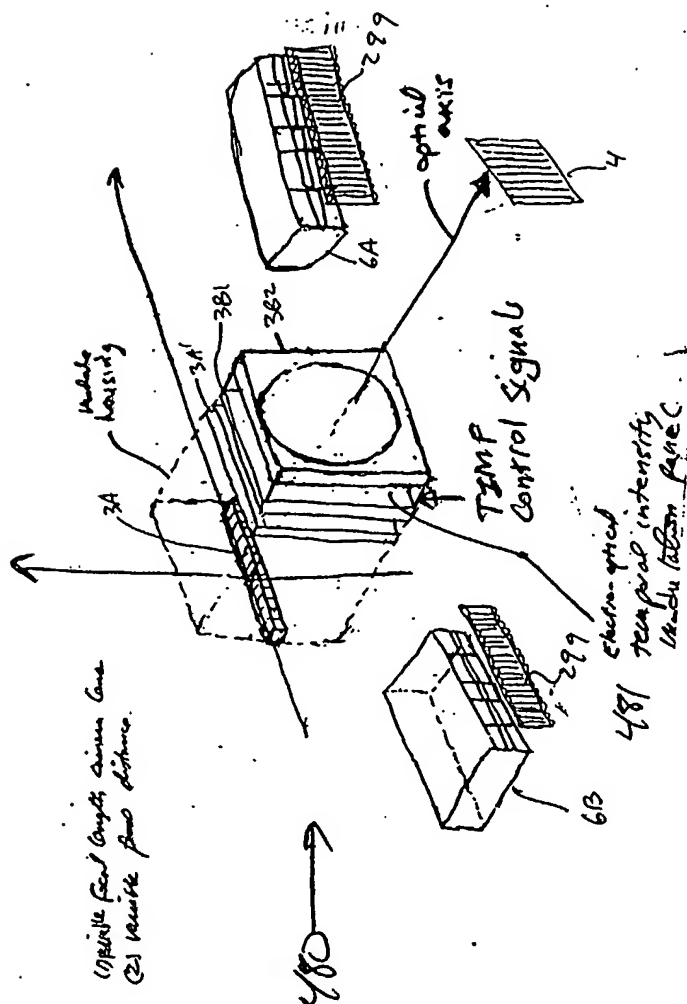
After illumination of the target with the planar laser illumination beam (PLIB), modulate the temporal intensity of the reflected/scattered (i.e. received) PLIB along the planar extent thereof according to a temporal intensity modulation function (TIMF) so as to .

produce many substantially different time-varying speckle-noise patterns at the image detection array of the IFD Subsystem during the photo-integration time period thereof.

Temporally average the many substantially different time-varying speckle-noise patterns produced at the image detection array in the IFD Subsystem during the photo-integration time period thereof, so as to thereby reduce the speckle-noise pattern observed at the image detection array.

FIG. 1I 24B

70/ 385



AG 1I 24C

7/1/85

EIGHT GENERALIZED METHOD OF REDUCING THE SPECKLE PATTERN
NOISE OBSERVED IN PLIIM-BASED IMAGING SYSTEMS

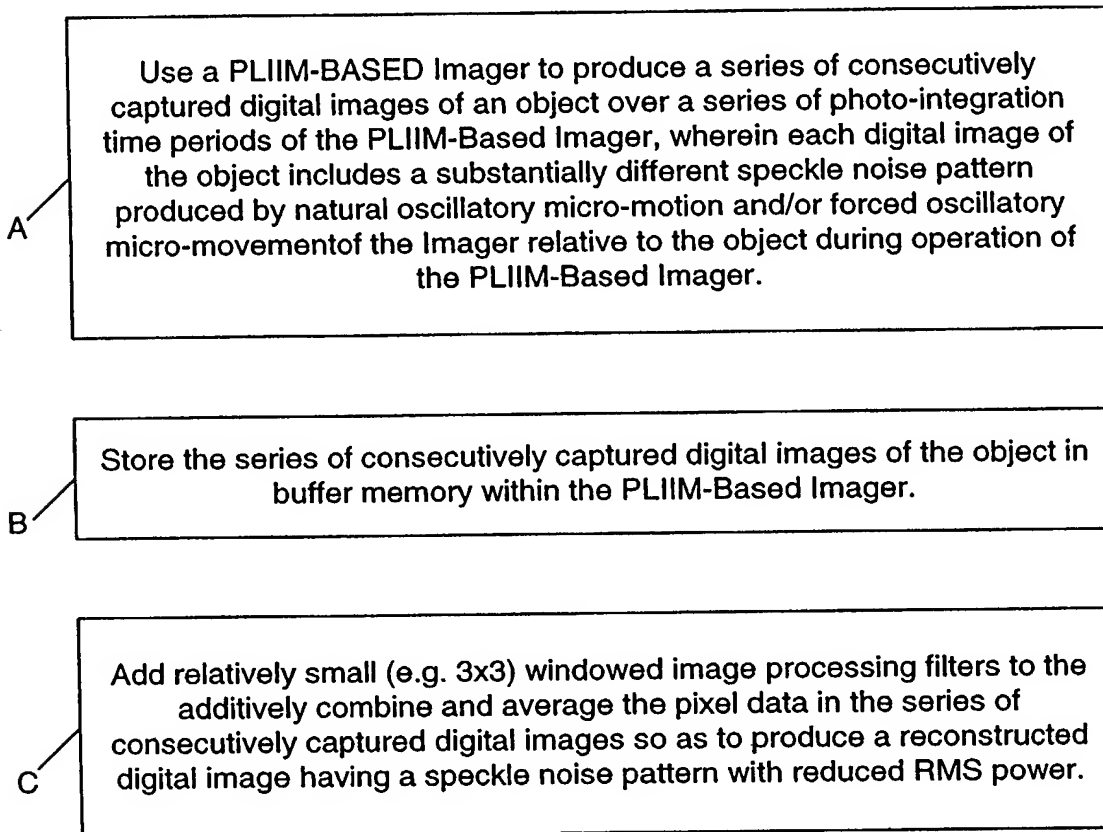


FIG. 1124D

72/385

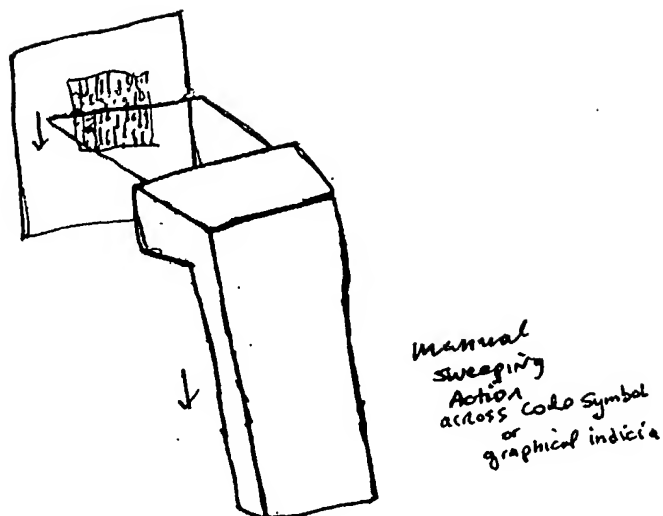
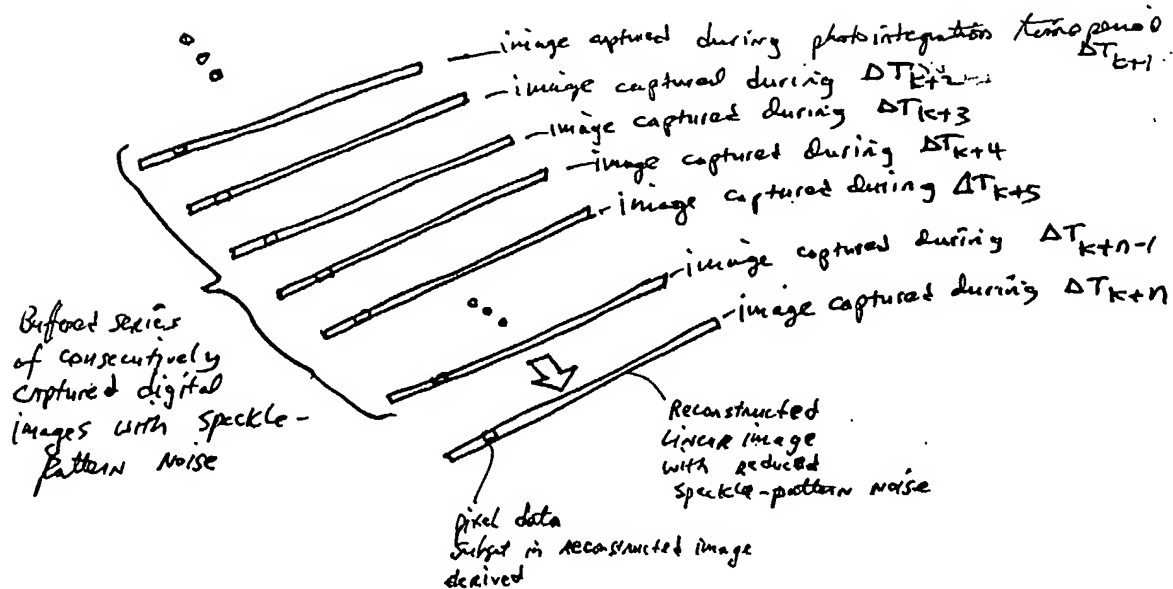


FIG. 1124E



Case: Linear image

FIG. 1124F

73/ 385

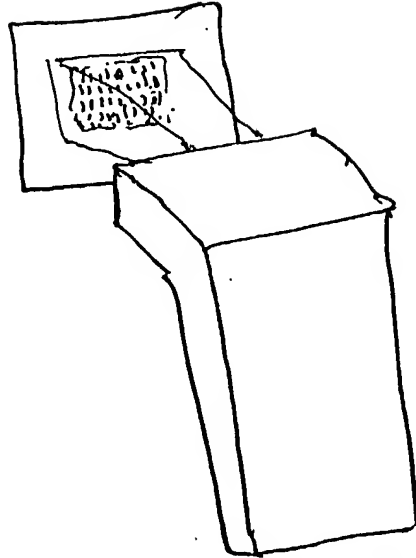


FIG. 1I24G

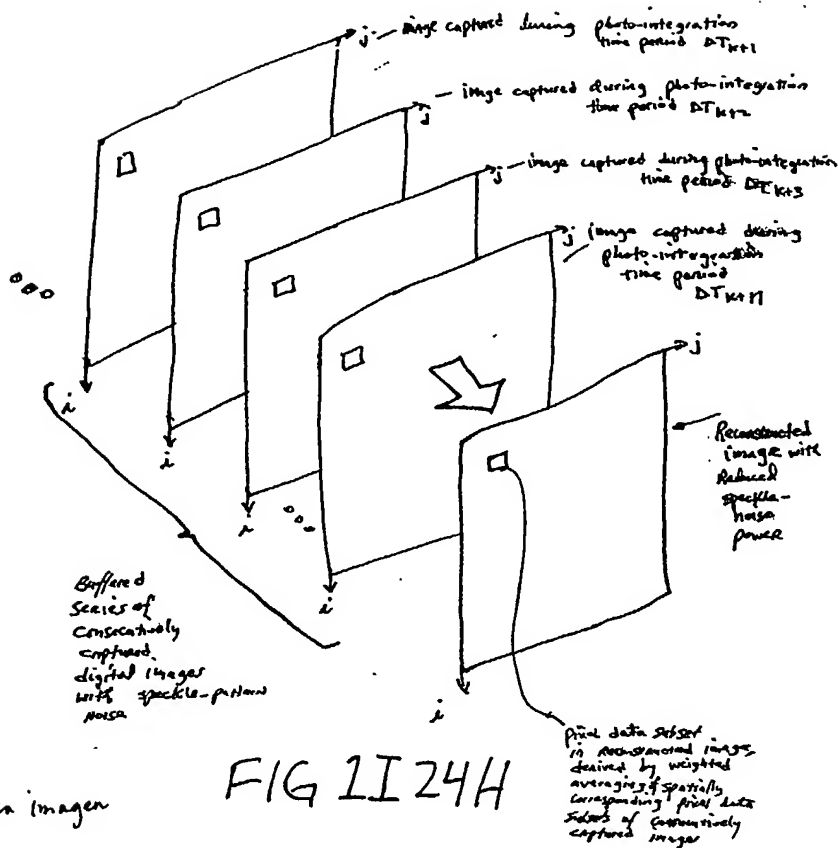


FIG 1I24H

Case: 2D Area Imager

74/385

NINTH GENERALIZED METHOD OF REDUCING SPECKLE PATTERN
NOISE IN PLIM-BASED IMAGING SYSTEMS

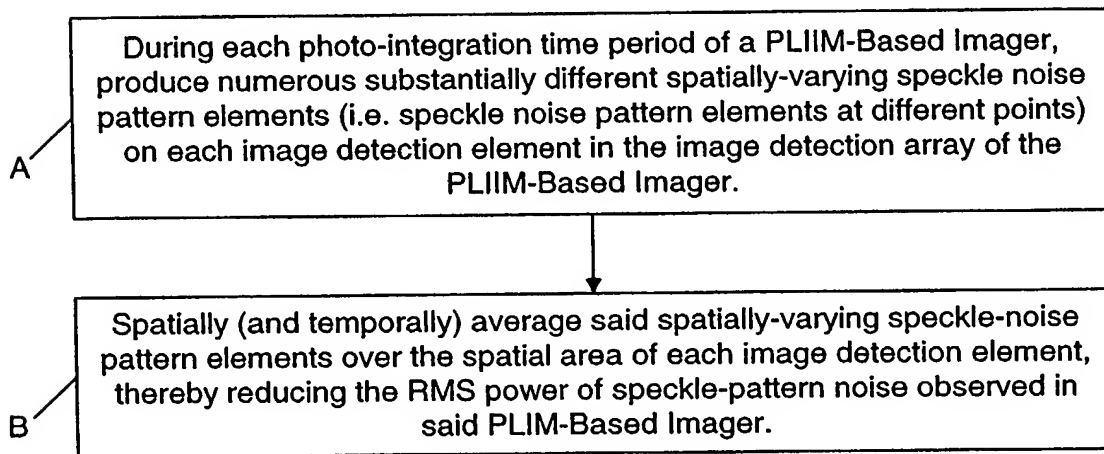
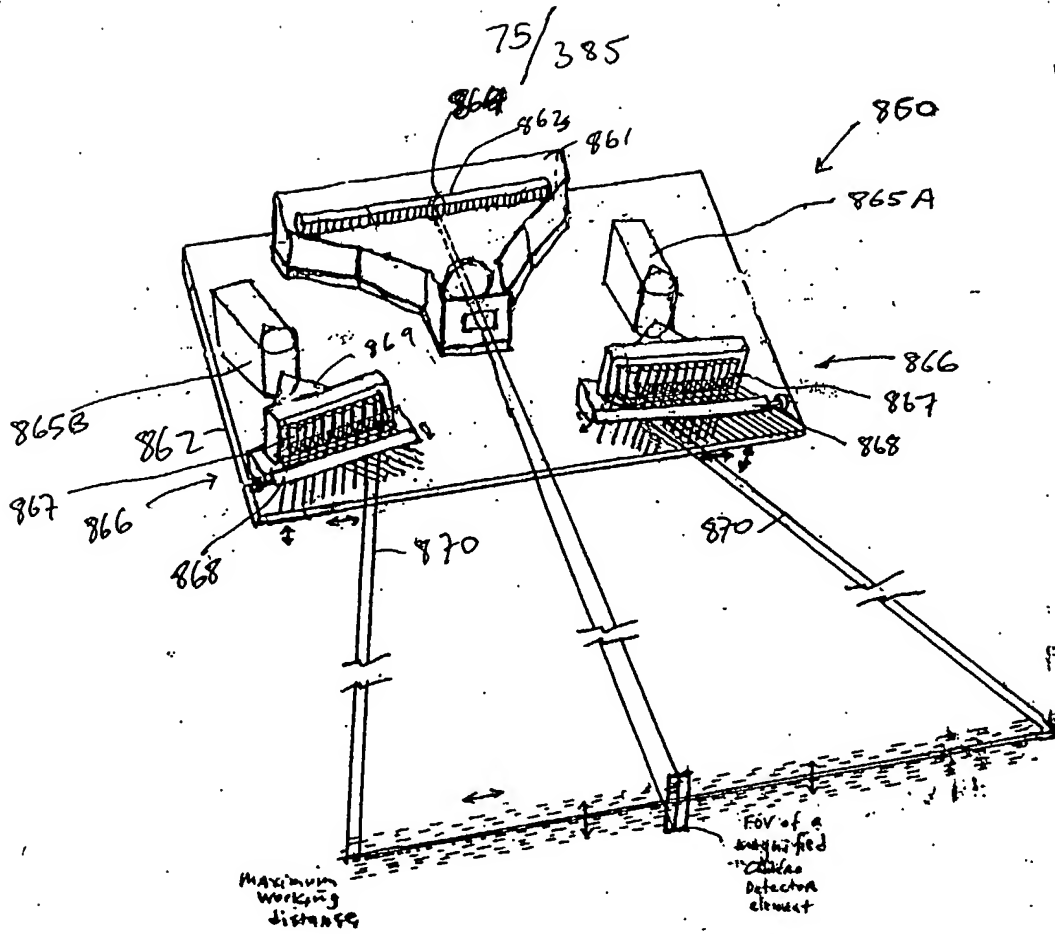


FIG. 1124I



* Lateral and Transverse Misalignment of PLIB

FIG. 1I25A1

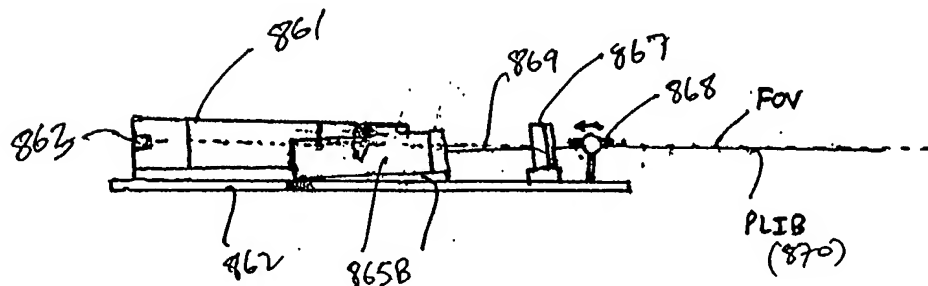
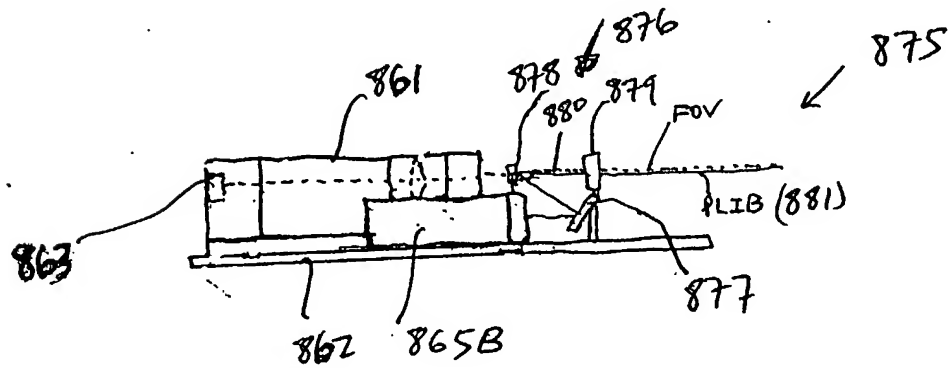
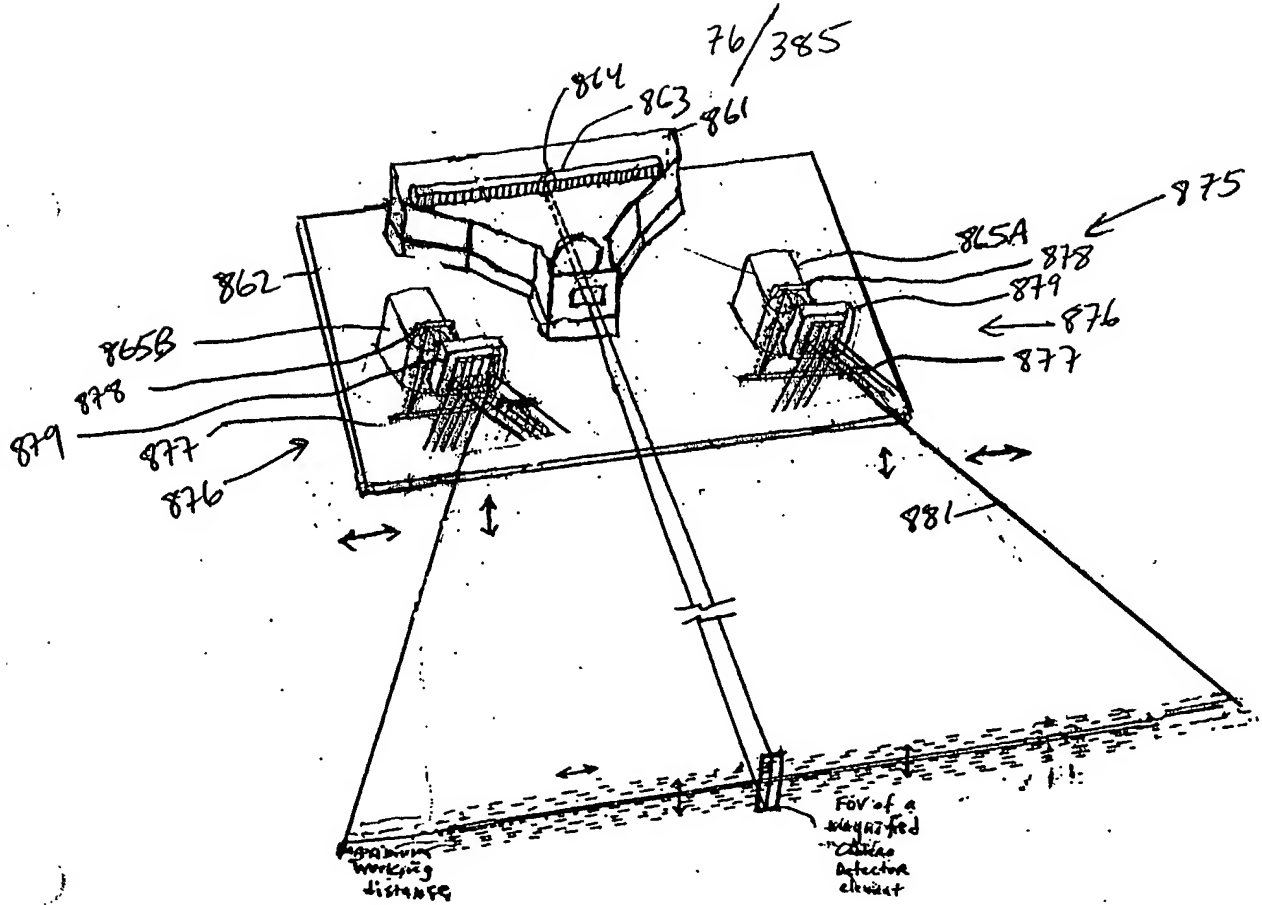
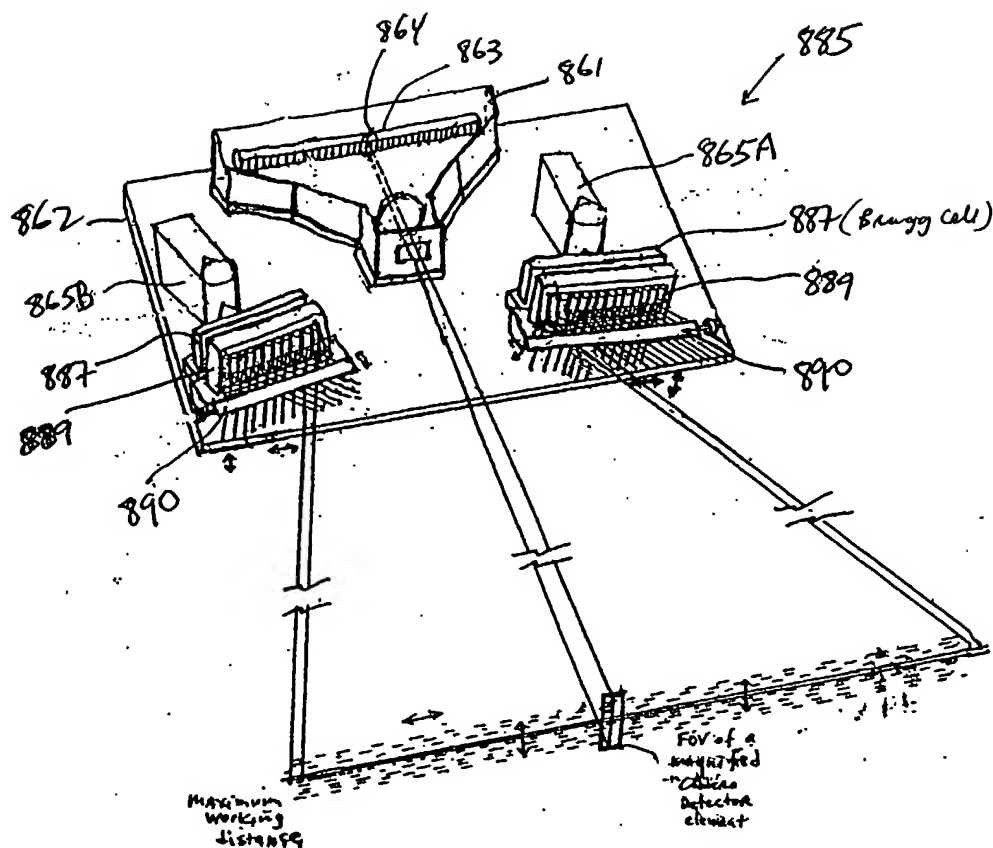


FIG. 1I25A2



77/385



* Lateral and Transverse Misalignment of PLIB

FIG. 1I25C1

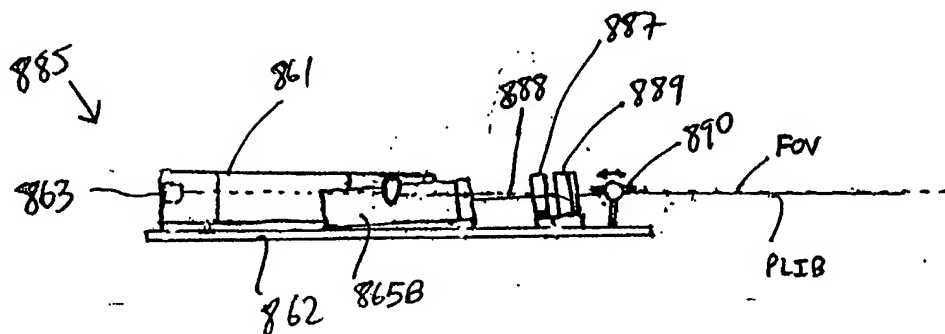


FIG. 1I25C2

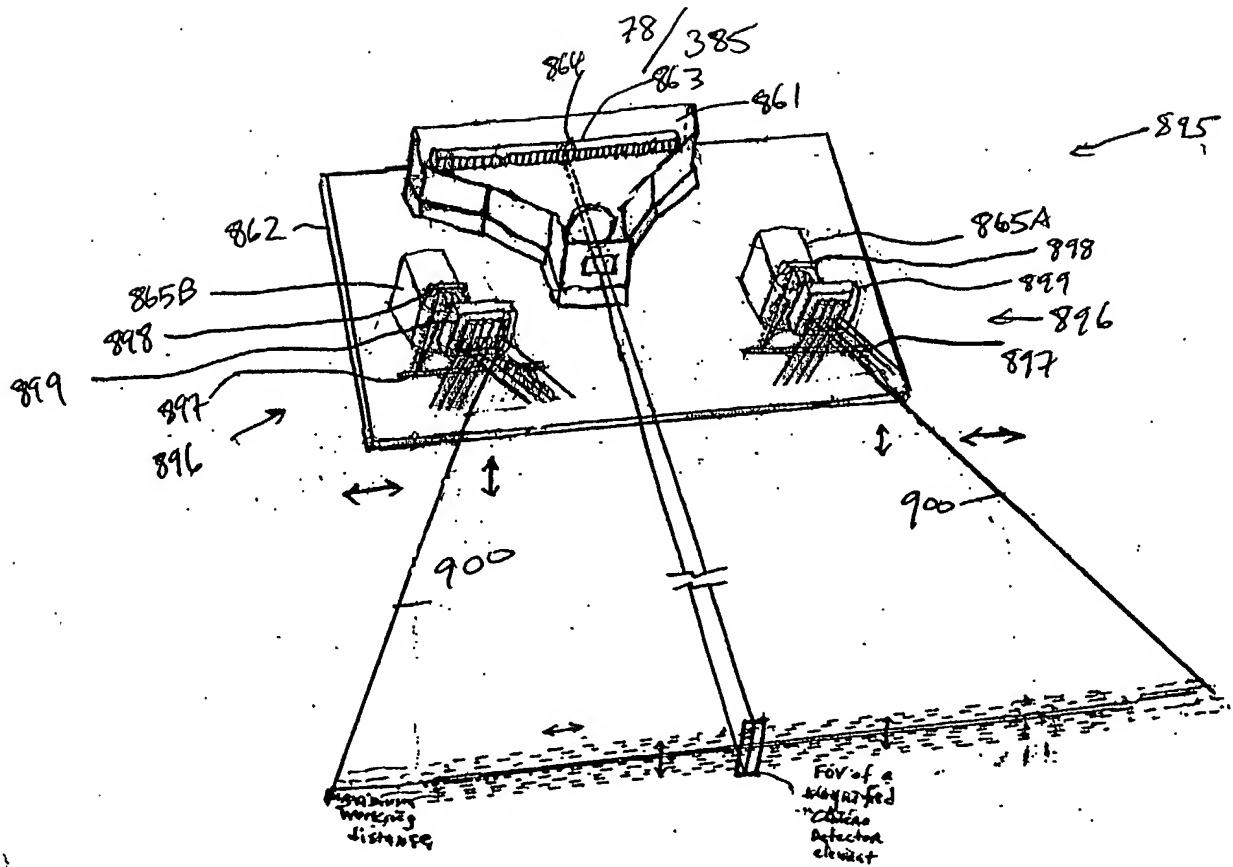


FIG. 1I25D1

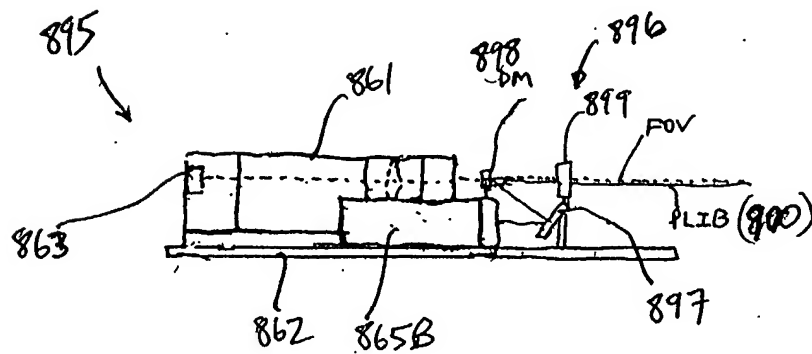
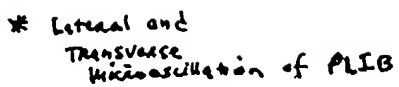


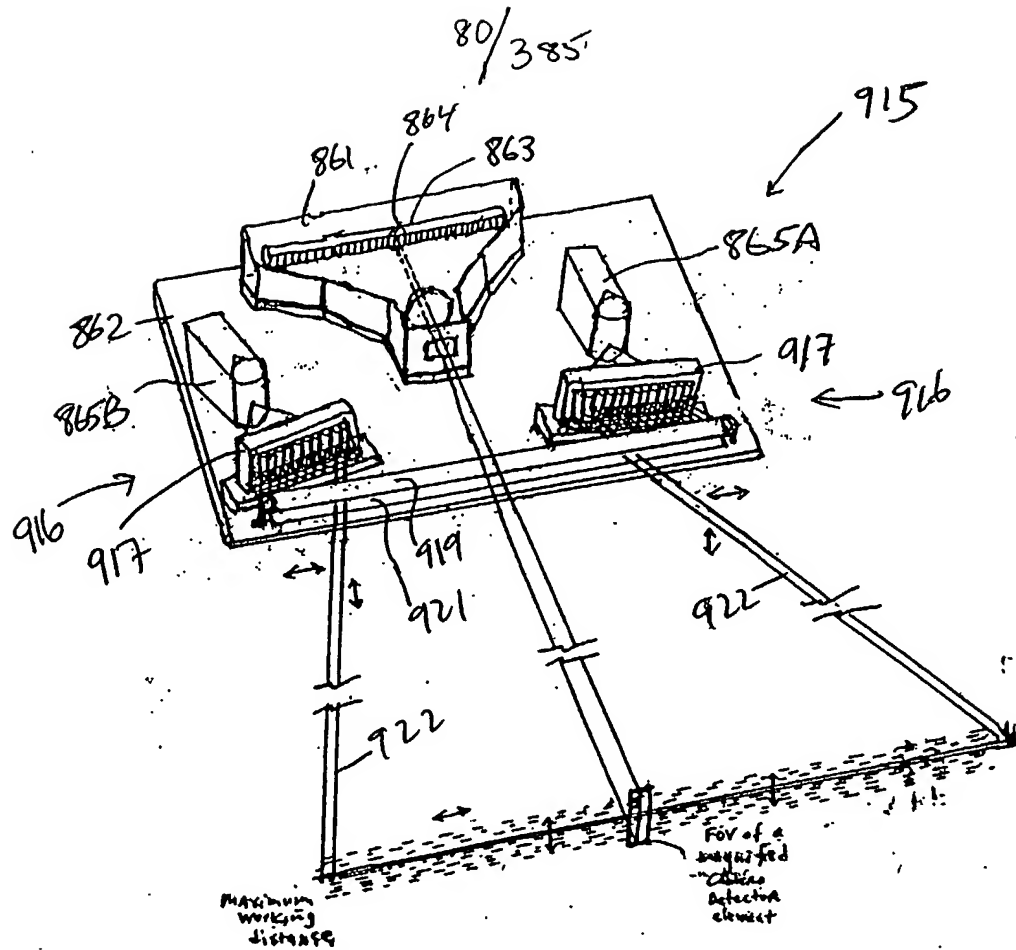
FIG. 1I25D2



905

[illegible]

FIG. 1I 25E2



* Lateral and Transverse Misalignment of PLIB

FIG. 1I25F1

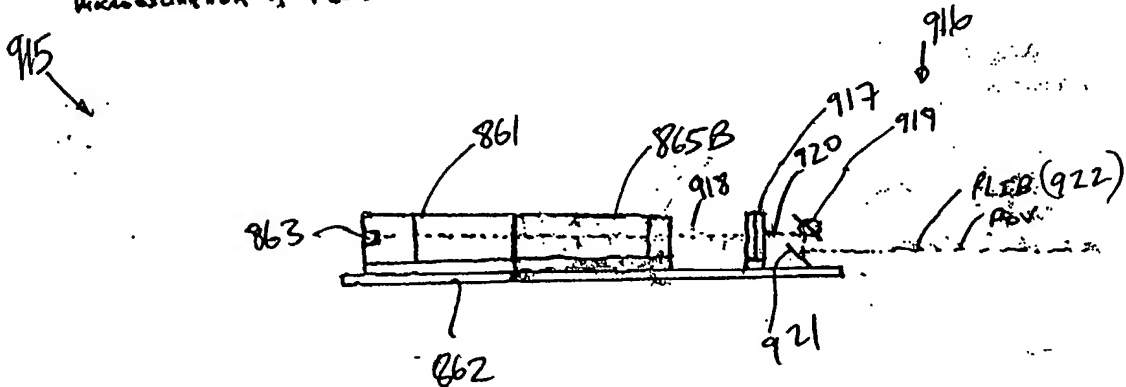
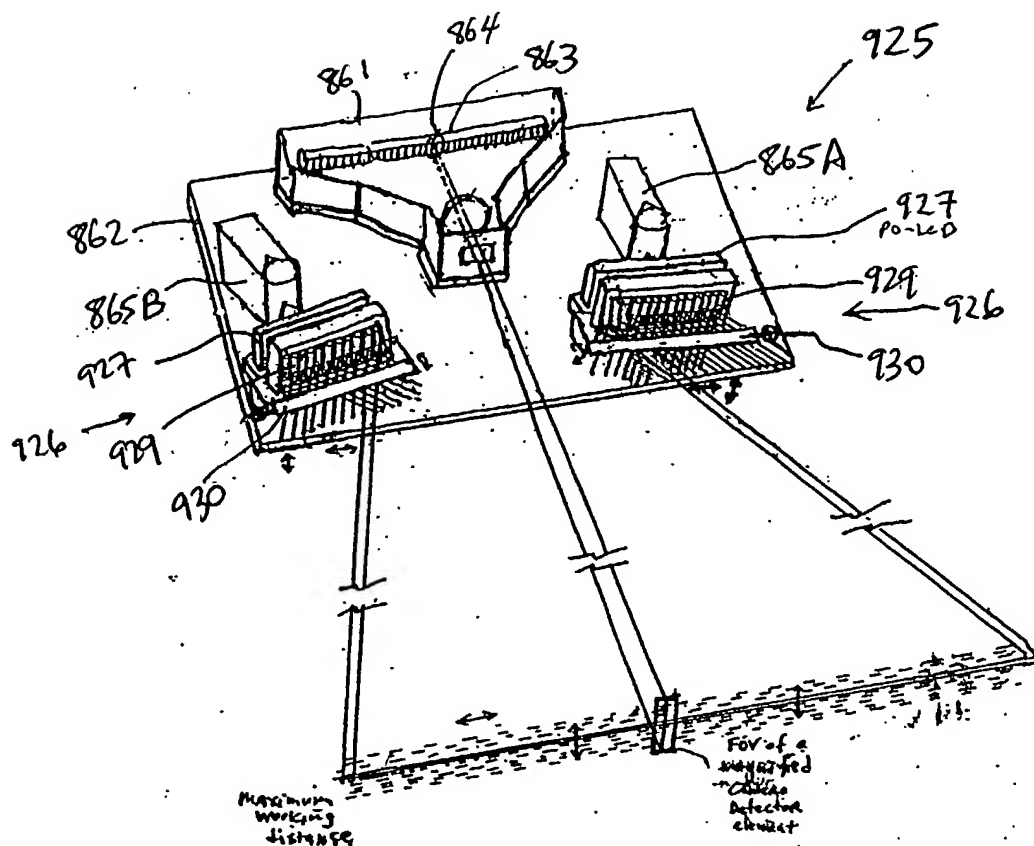


FIG. 1I25F2

81/385



- * Lateral and Transverse Macroadenoma of Pituitary

925

FIG. 1I 25G1

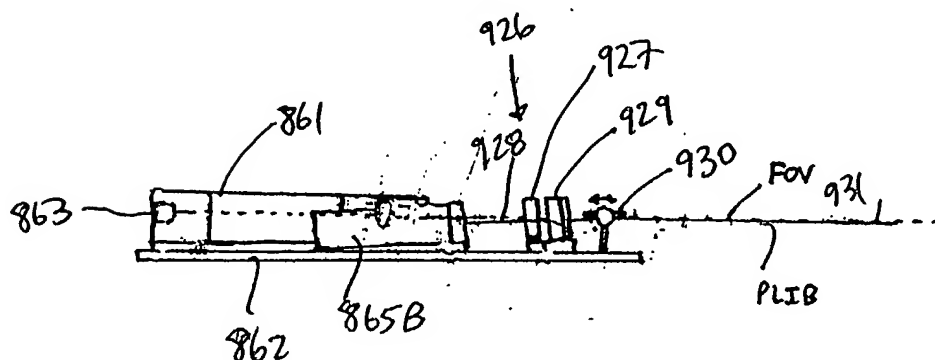
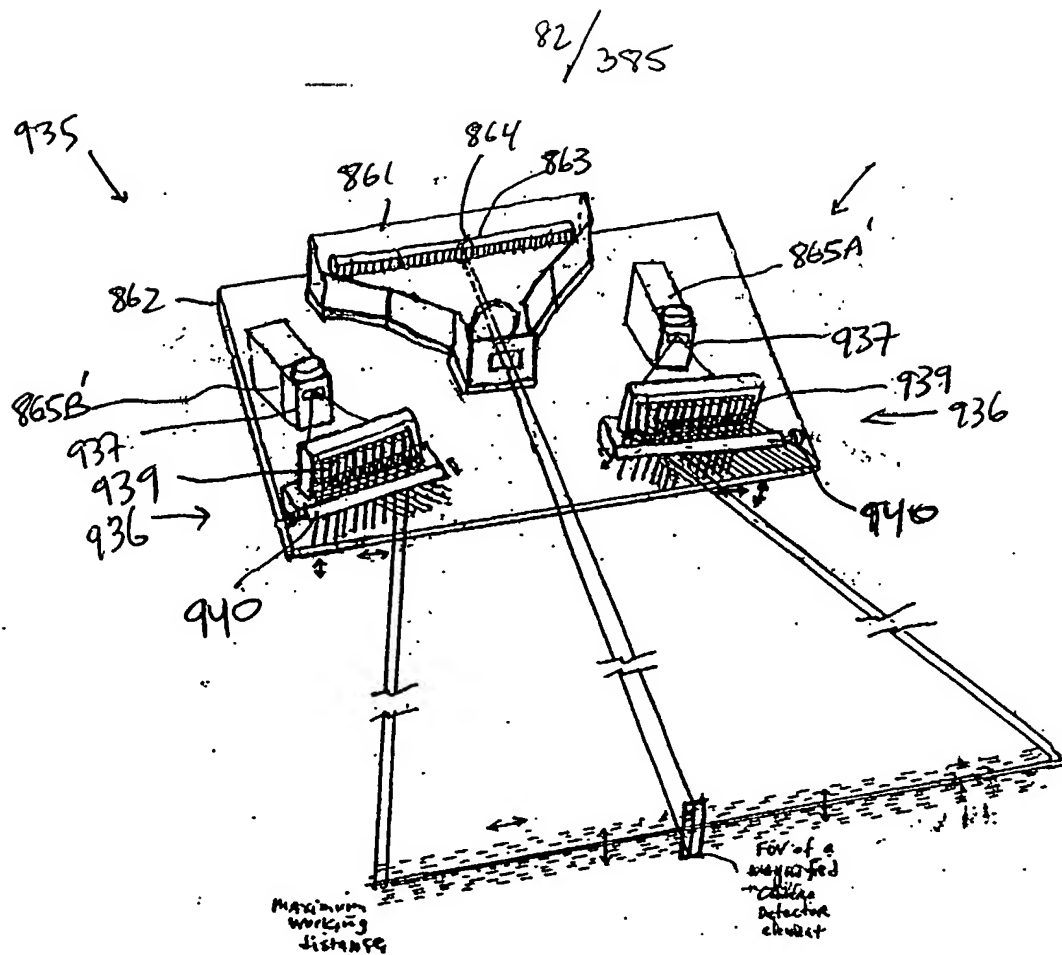


FIG. 1I25G2



* Lateral and Transverse Misalignment of PLIB

FIG 1I25H1

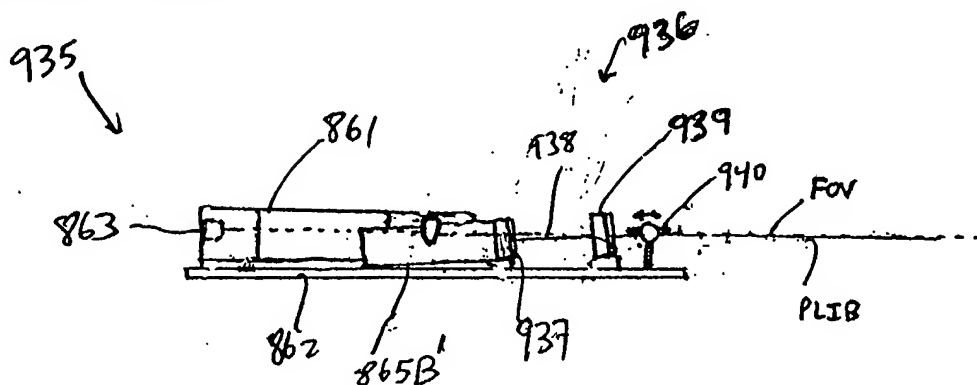
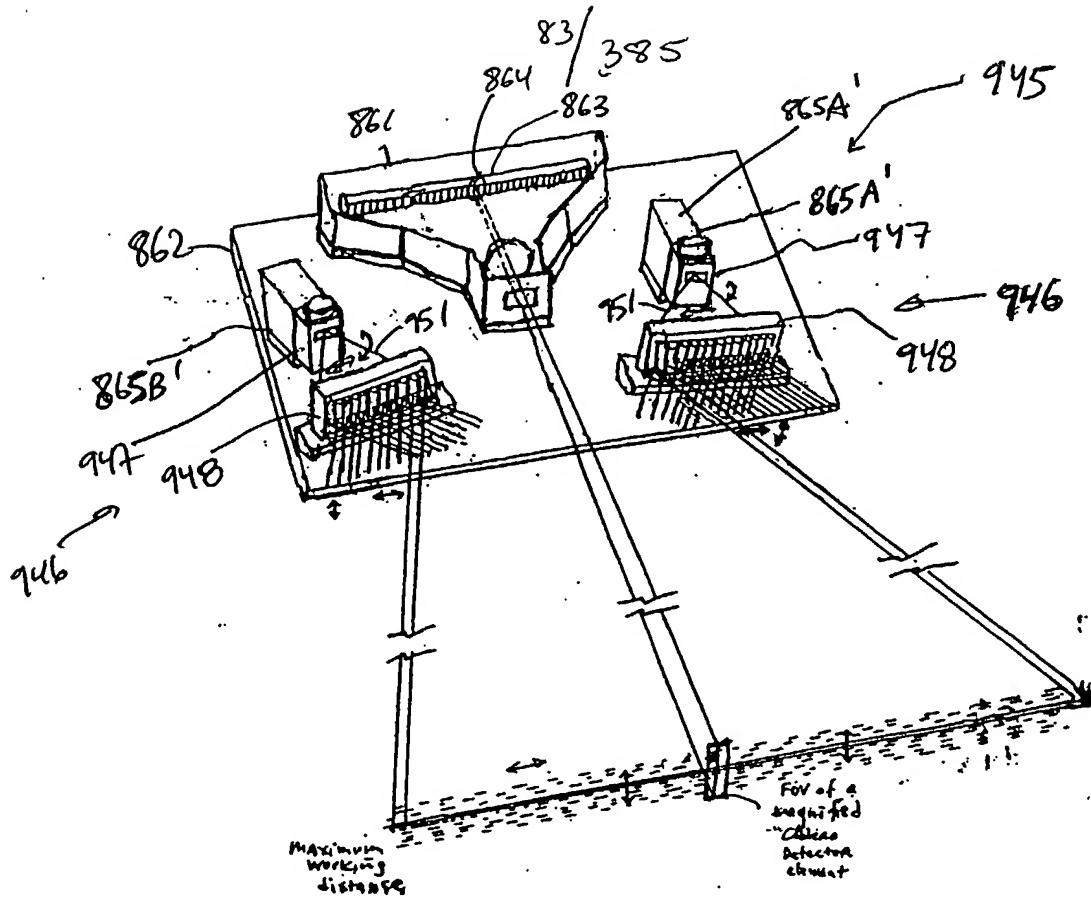


FIG 1I25H2



Lateral and Transverse Misalignment of ALB

FIG. 1I25I1

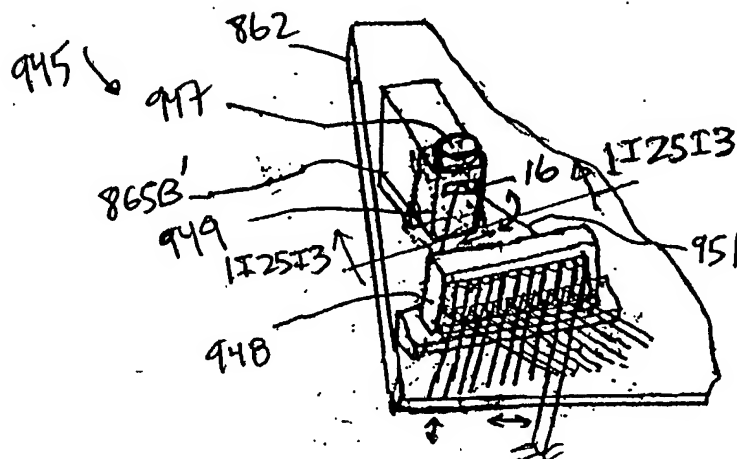


FIG. 1I25I2

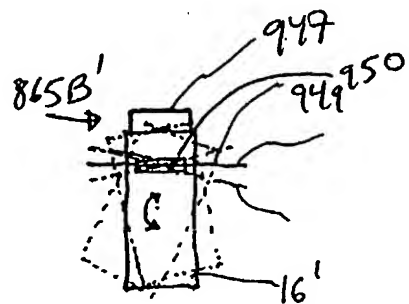


FIG. 1I25I3

84/385

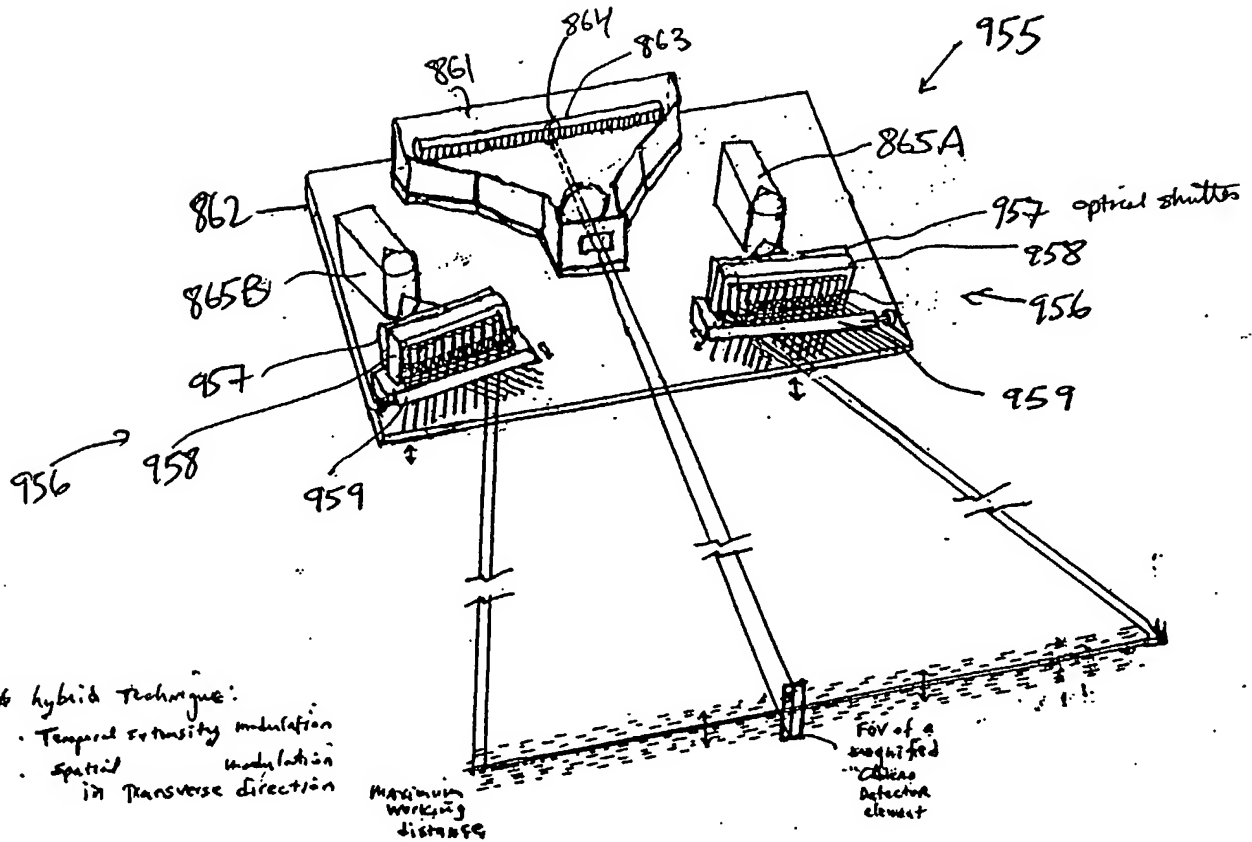


FIG. 1I25J1

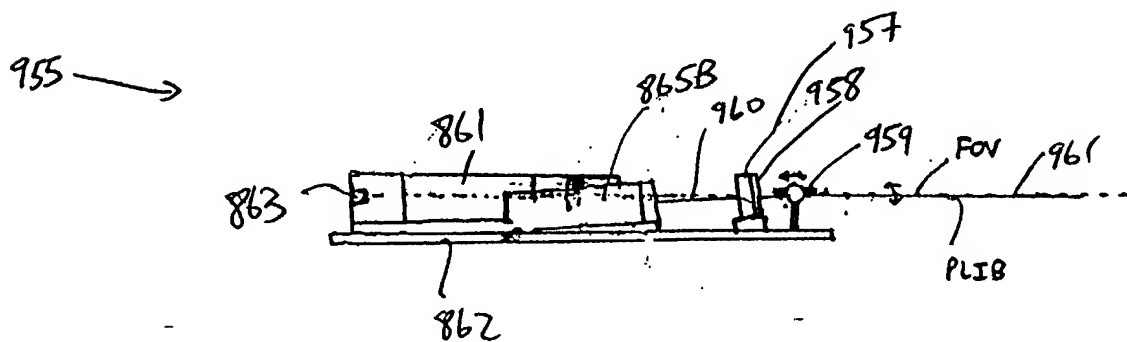
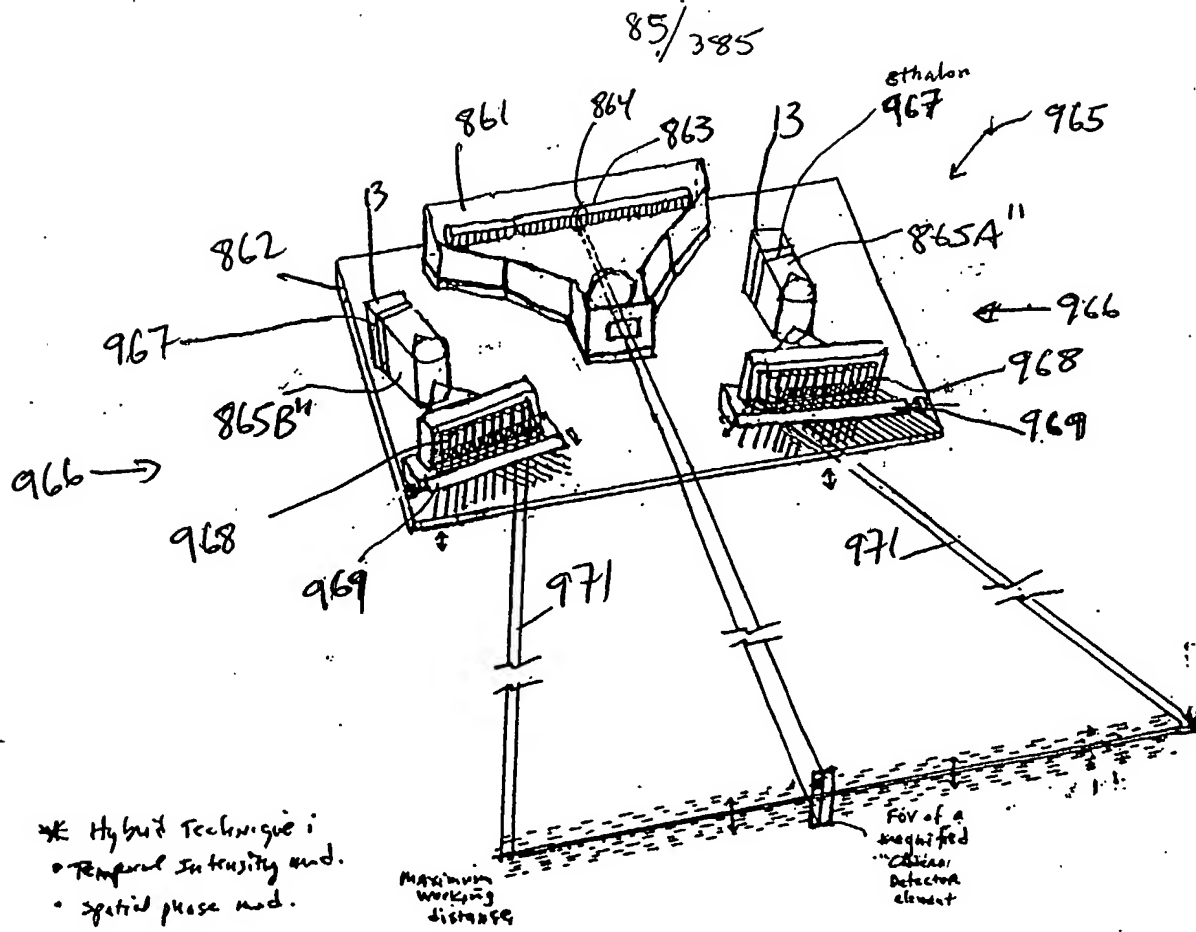


FIG. 1I25J2



* Transverse
 Modulation of PLIB
 965

FIG. 1I25K1

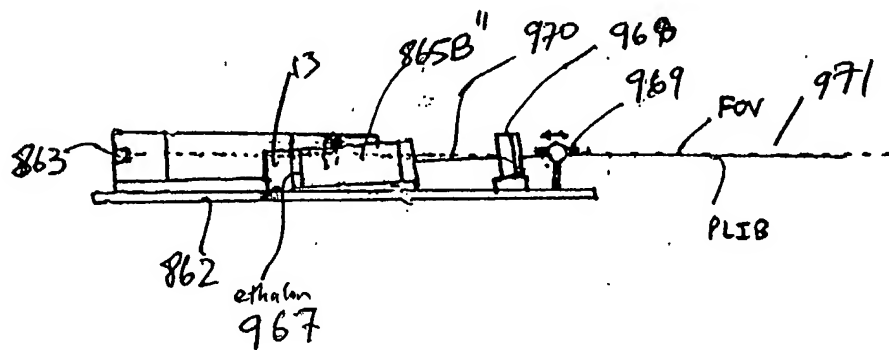
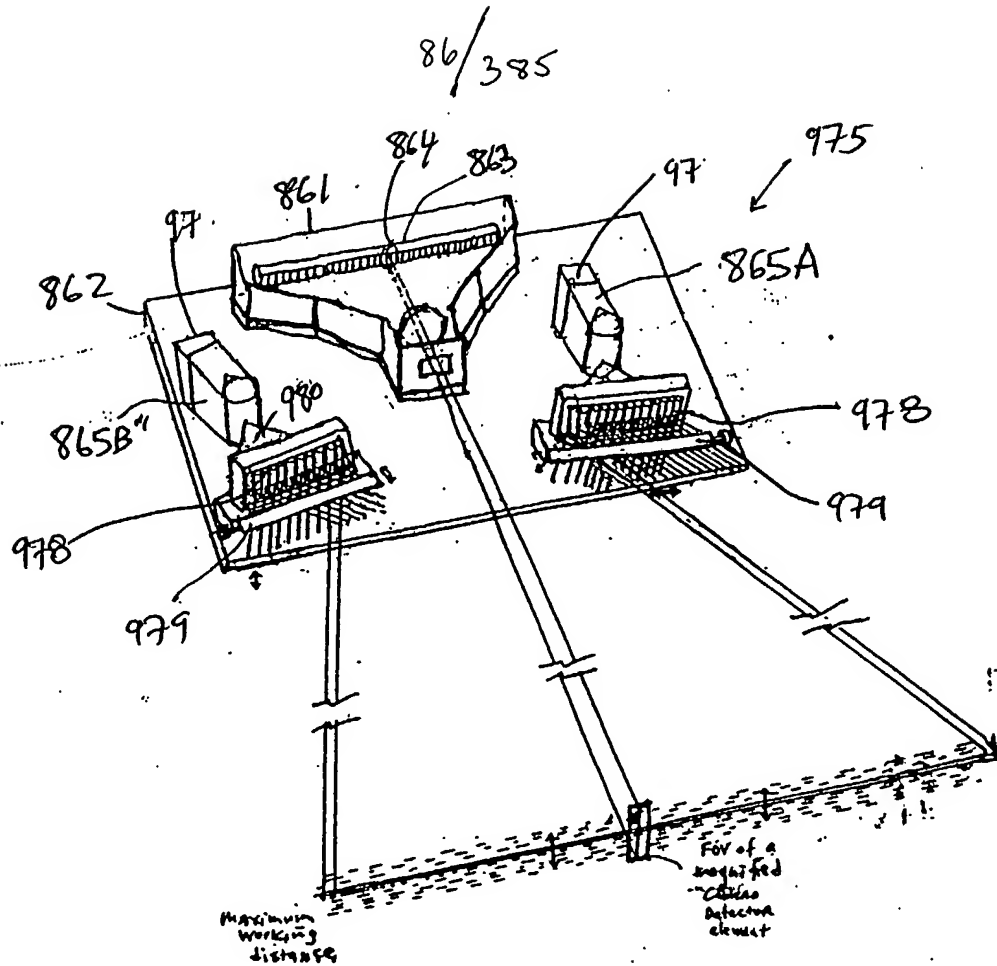


FIG. 1I25K2



- * hybrid =
 - temp freq. mod.
 - spatial phase mod.
- * Transverse Microoscillation of PLIB

FIG. 1I25L1

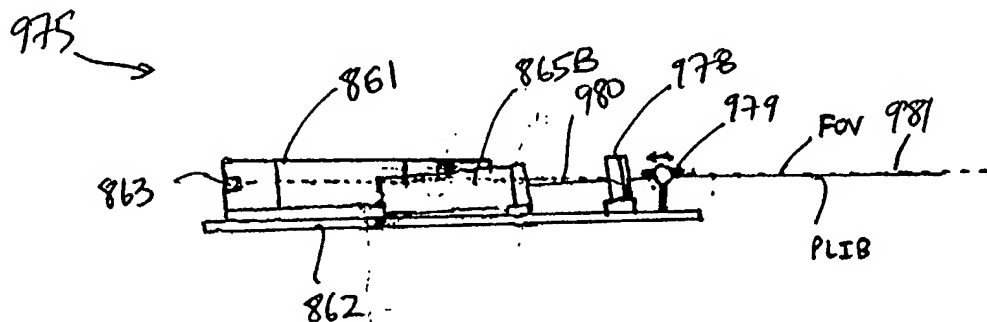
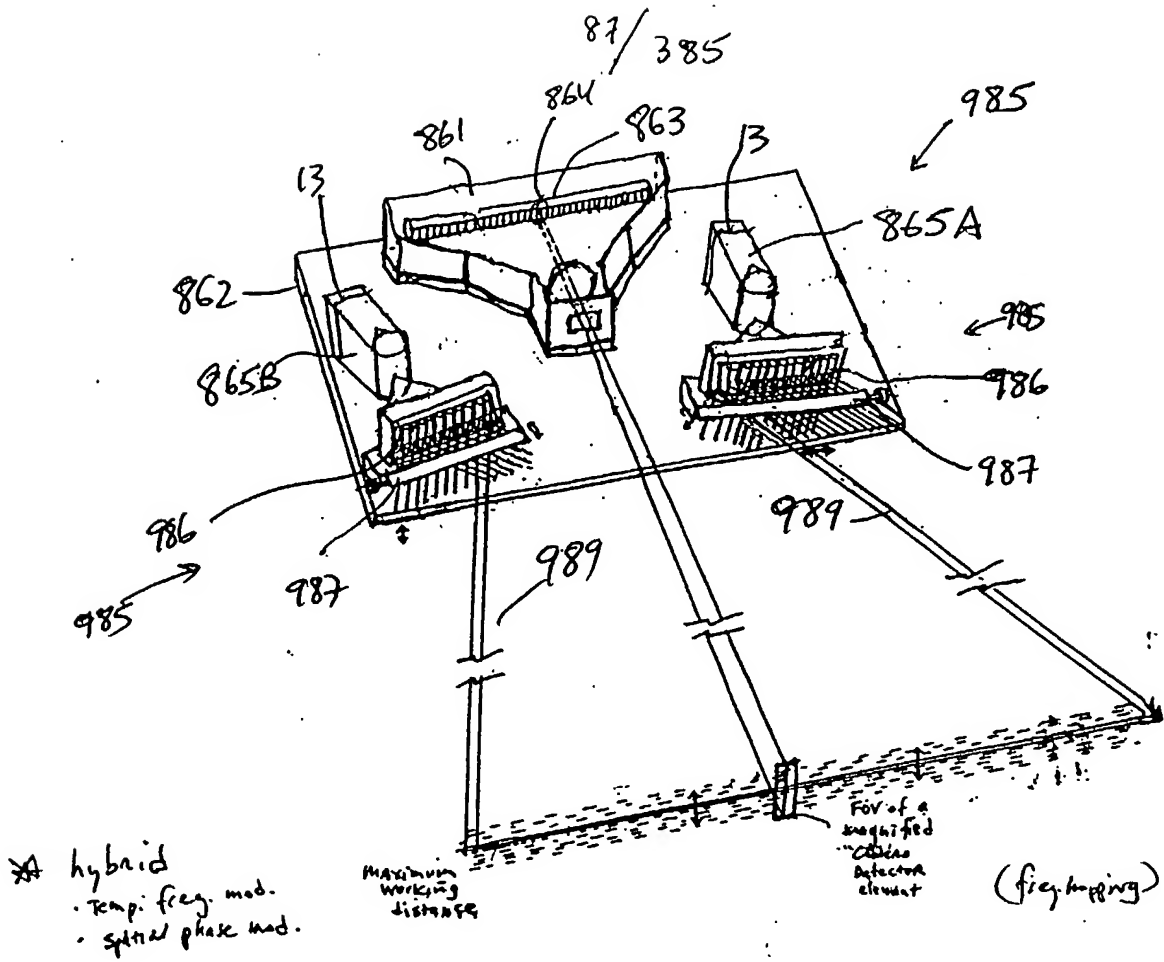


FIG. 1I25L2



* hybrid
 - Temp. freq. mod.
 - Spatial phase mod.

* Transverse
 Modulation of PLIB

FIG. 1I25M1

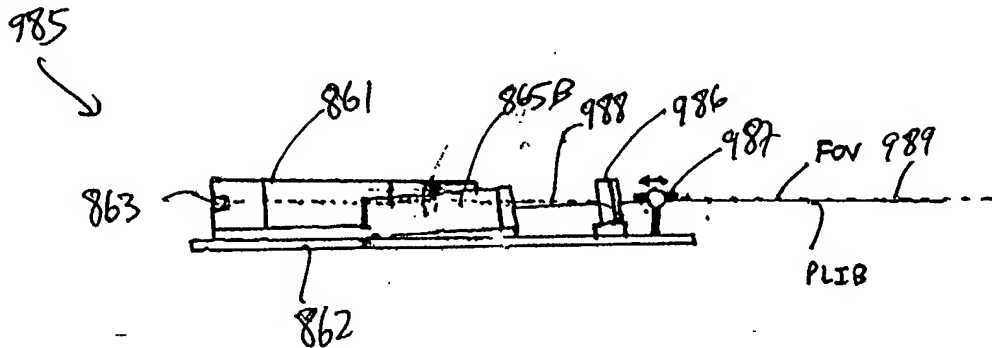
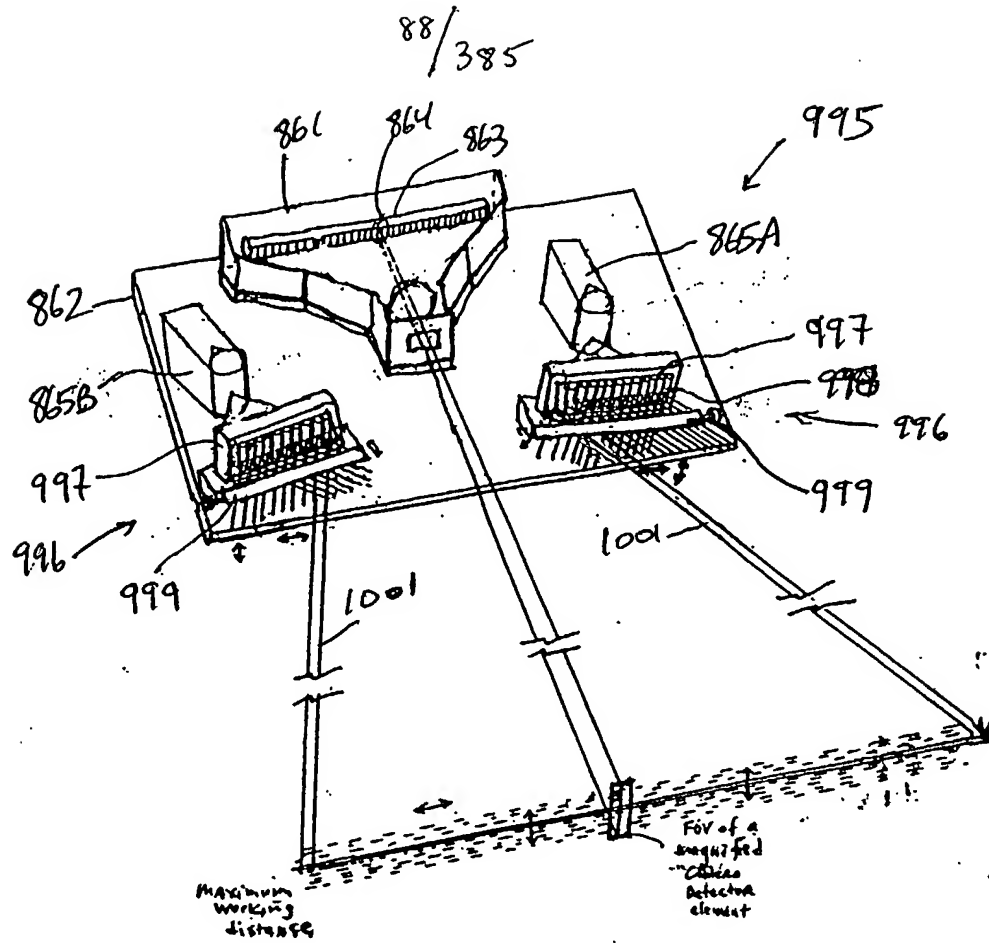


FIG. 1I25M2



- * hybrid:
 - spatial intensity mod.
 - spatial phase
- * lateral and Transverse Modulation of PLIB

FIG. 1I25N1

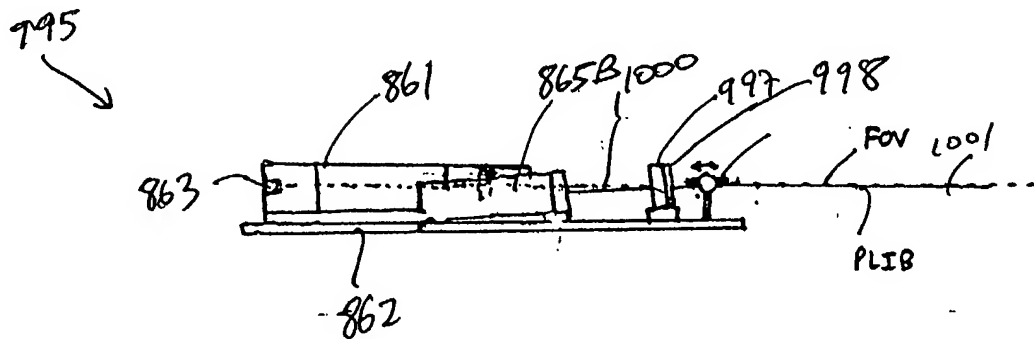


FIG. 1I25NZ

89/385

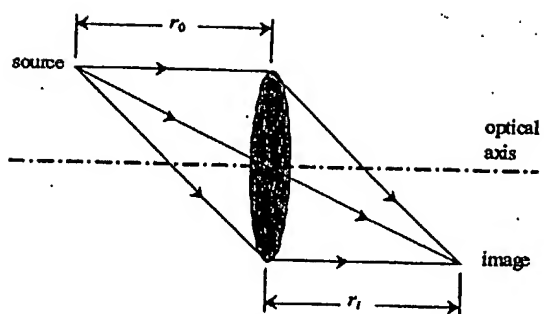


FIG. 1H1

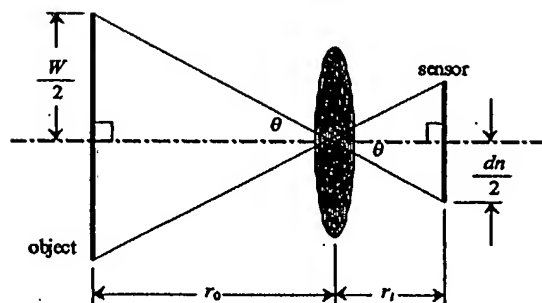


FIG. 1H2

90/385

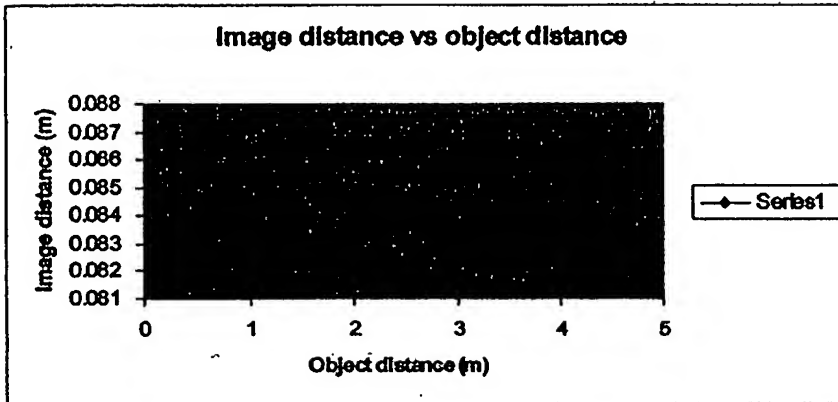


FIG. 1H3

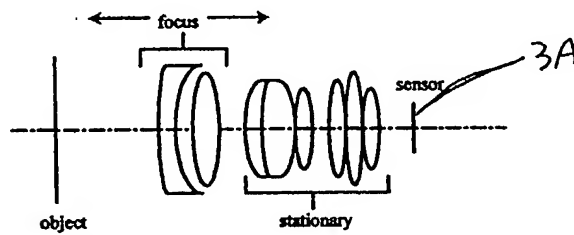


FIG. 1H4

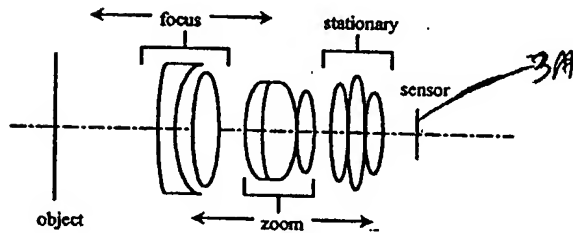
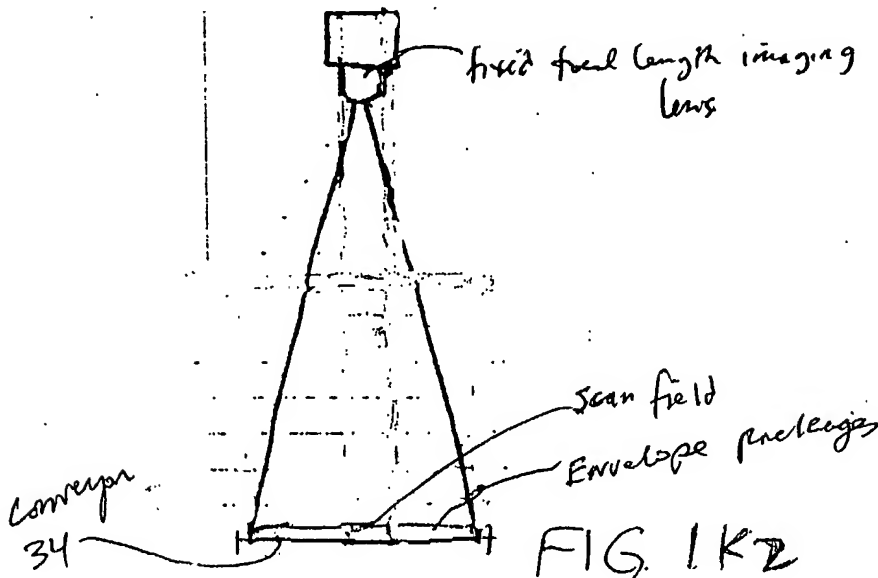
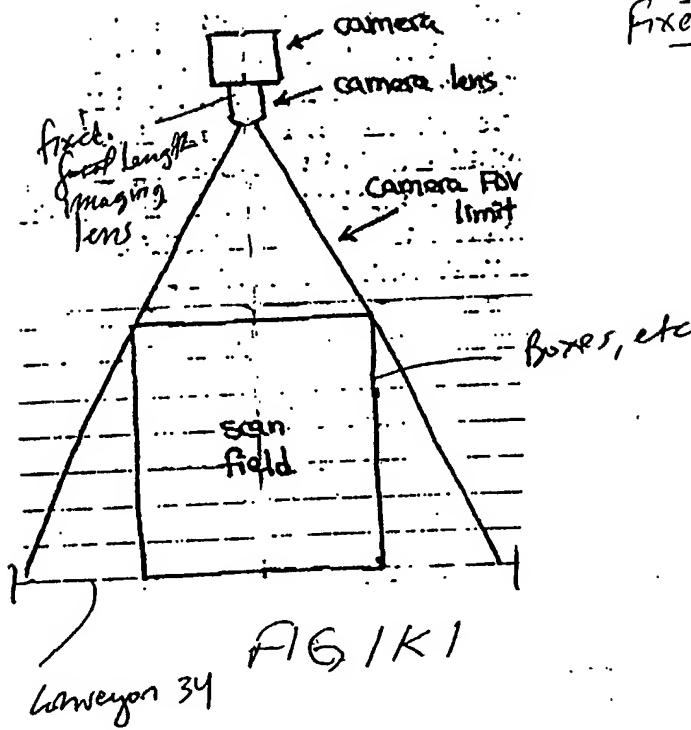


FIG. 1H5

91/385

Fixed focal length lens
cases



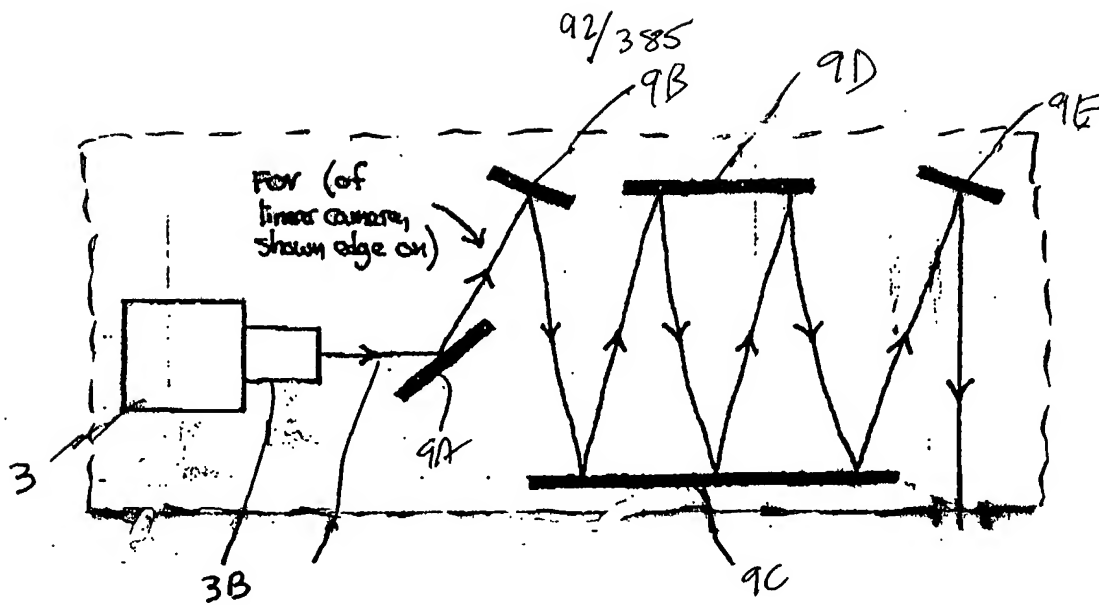


FIG. 1L1

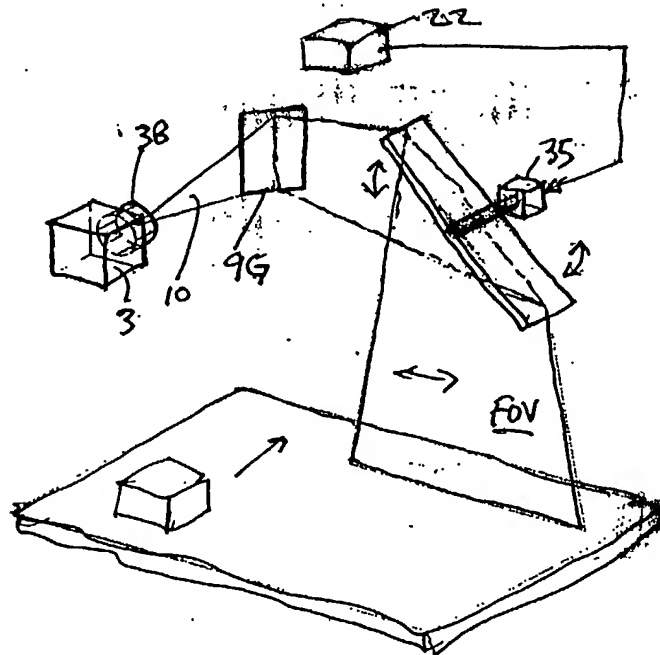


FIG. 1L2

93/385

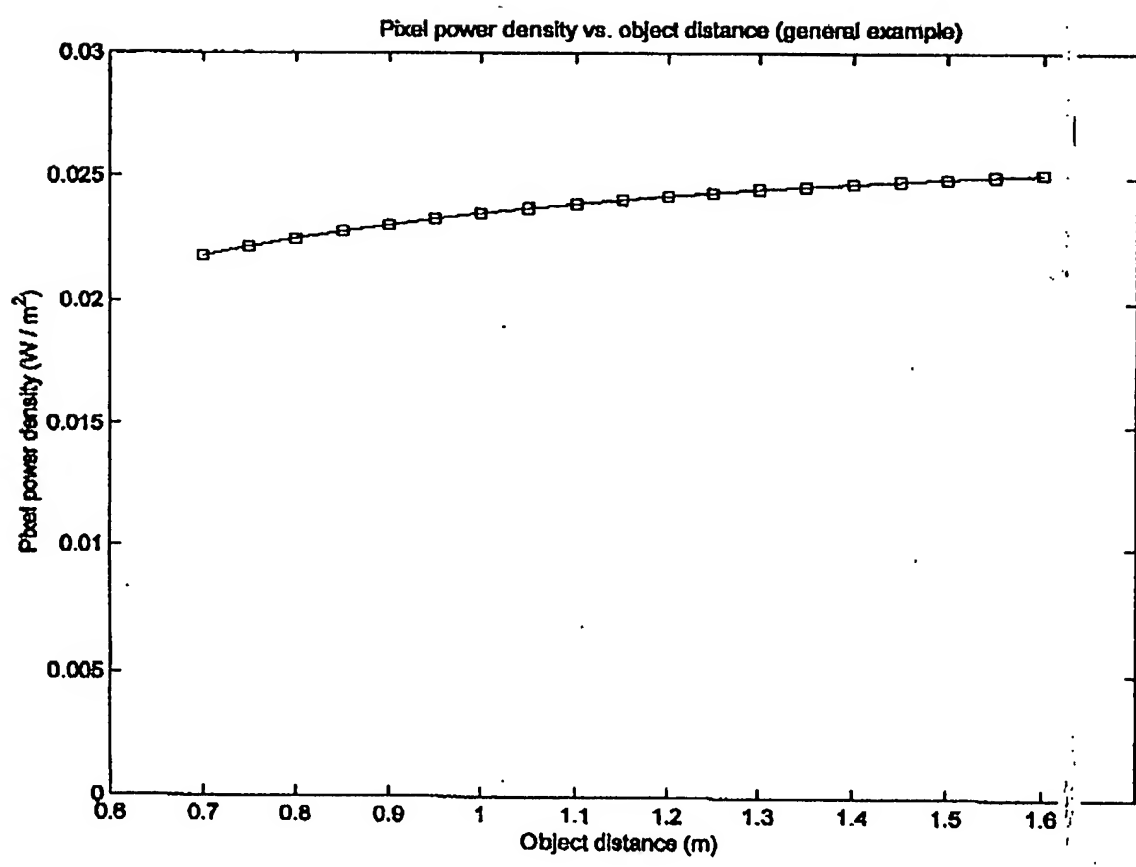


FIG-1M1

94/385

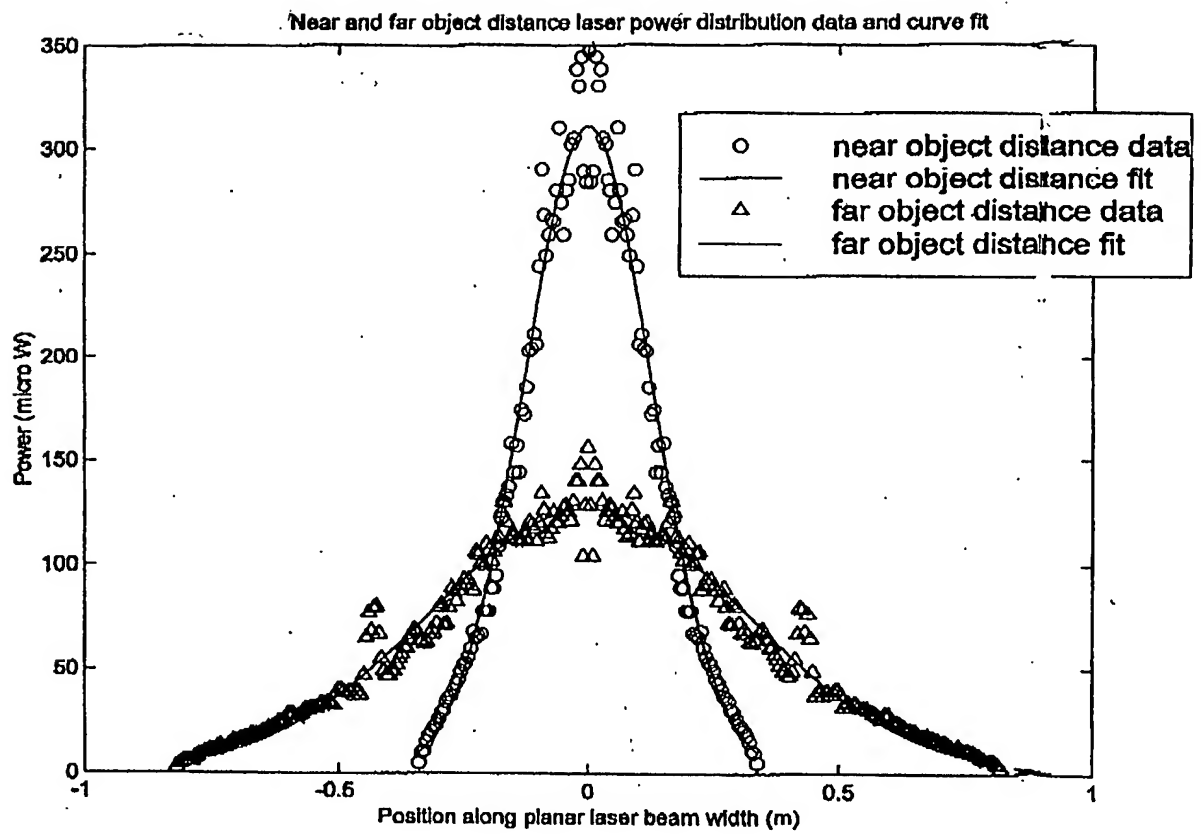


FIG. 1M2

95/385

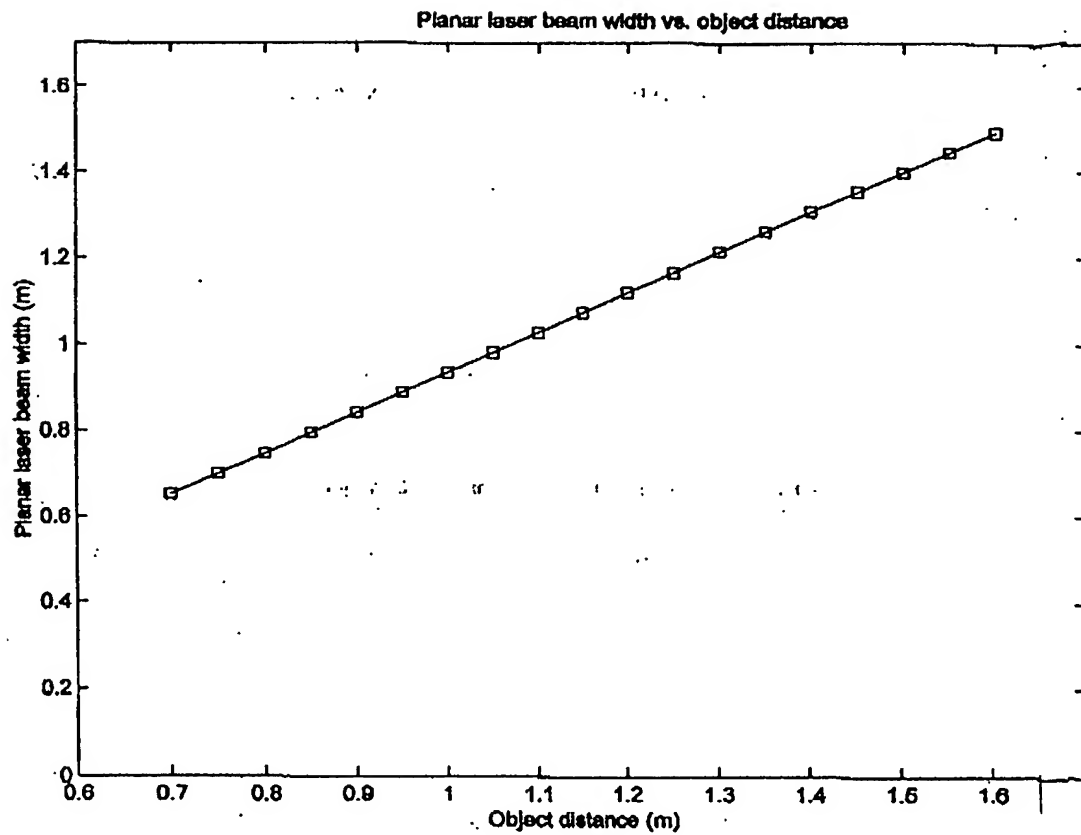
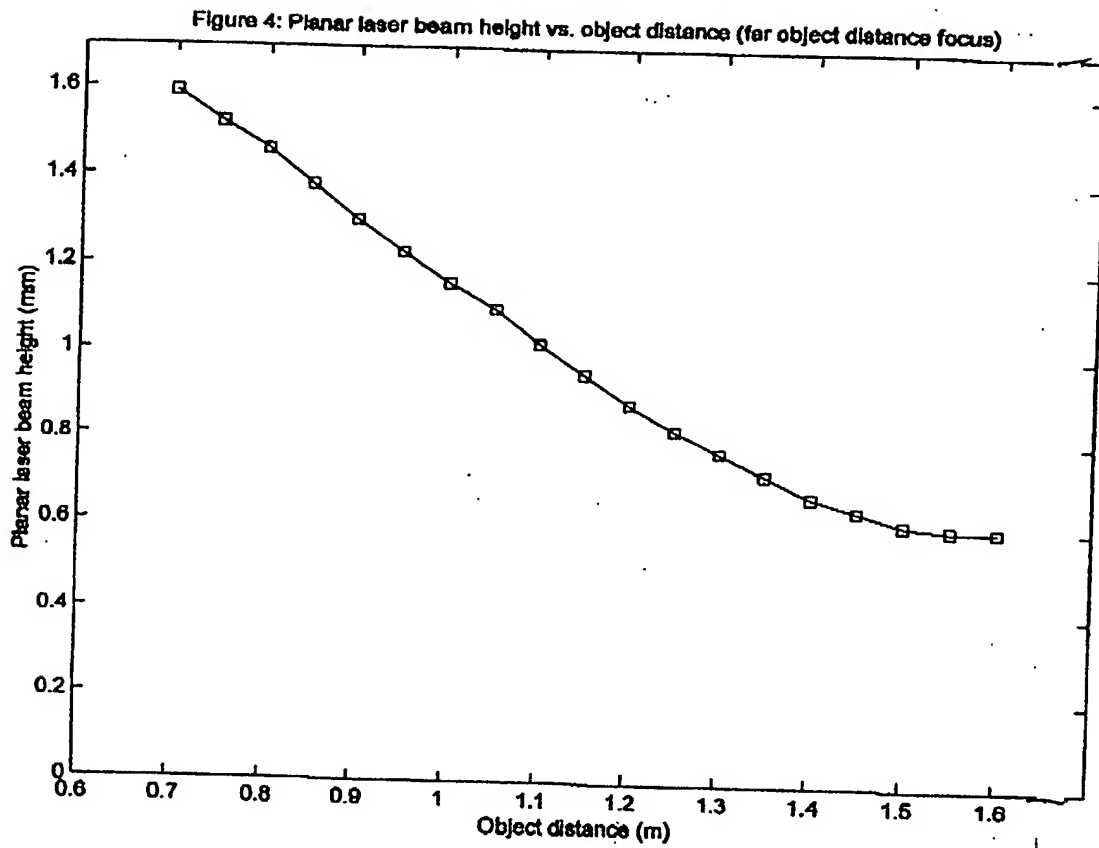


FIG. 1M3

96/385



FIG/M4

97/385

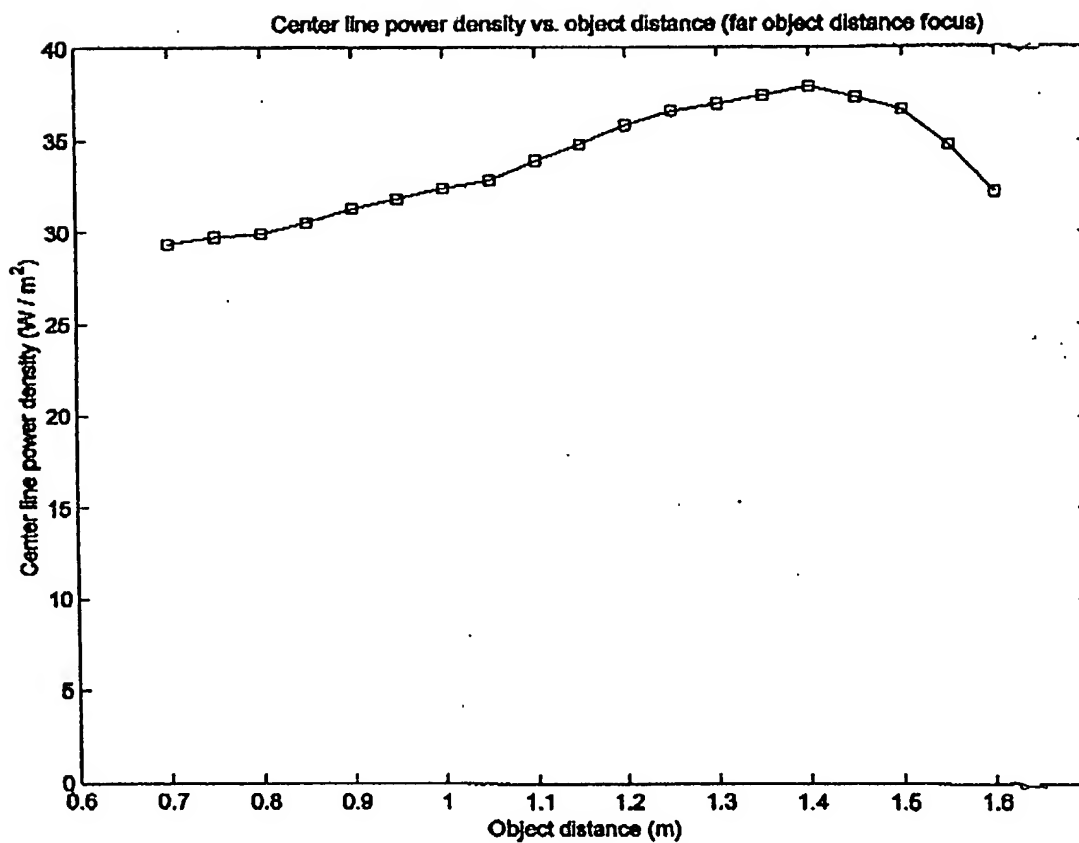


FIG. 1N

98/385

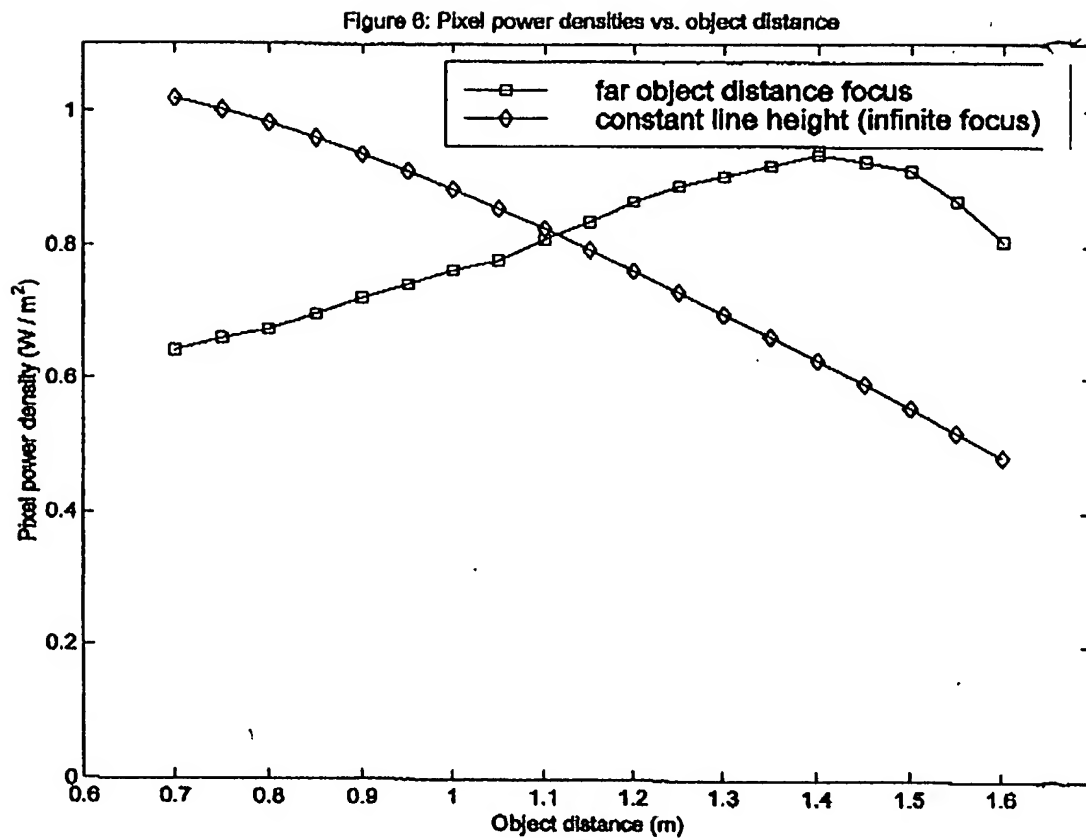


FIG. 10

99/385

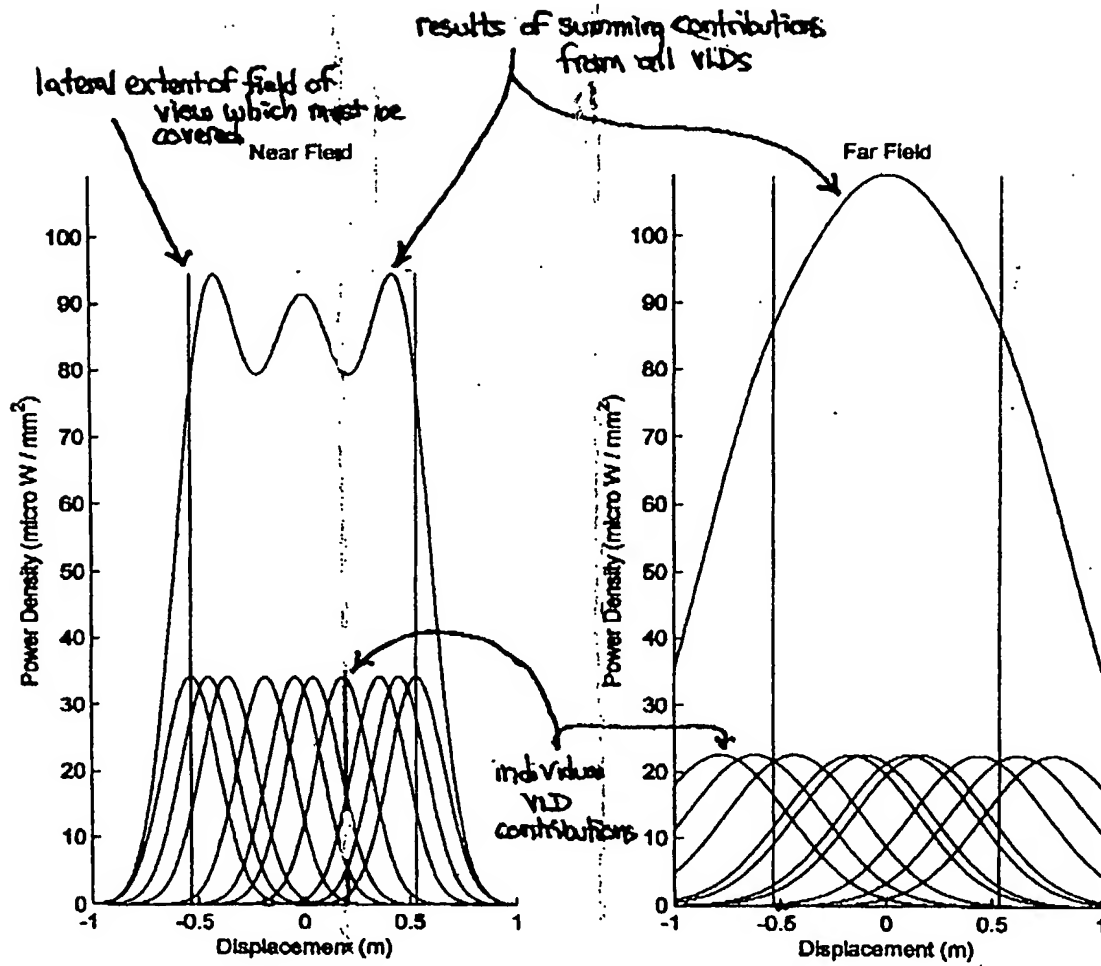


FIG 1P1

FIG 1P2

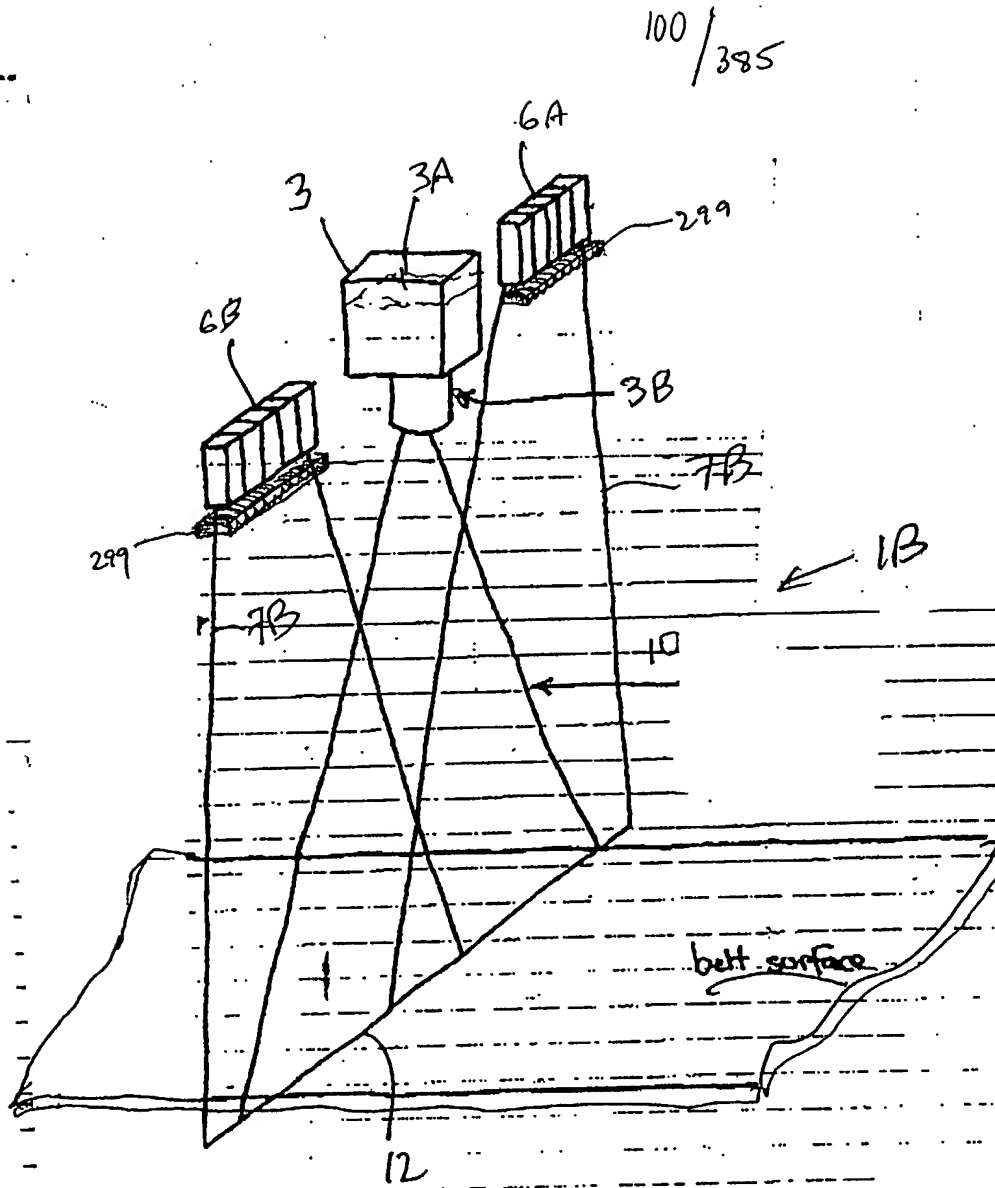


FIG. 1Q1

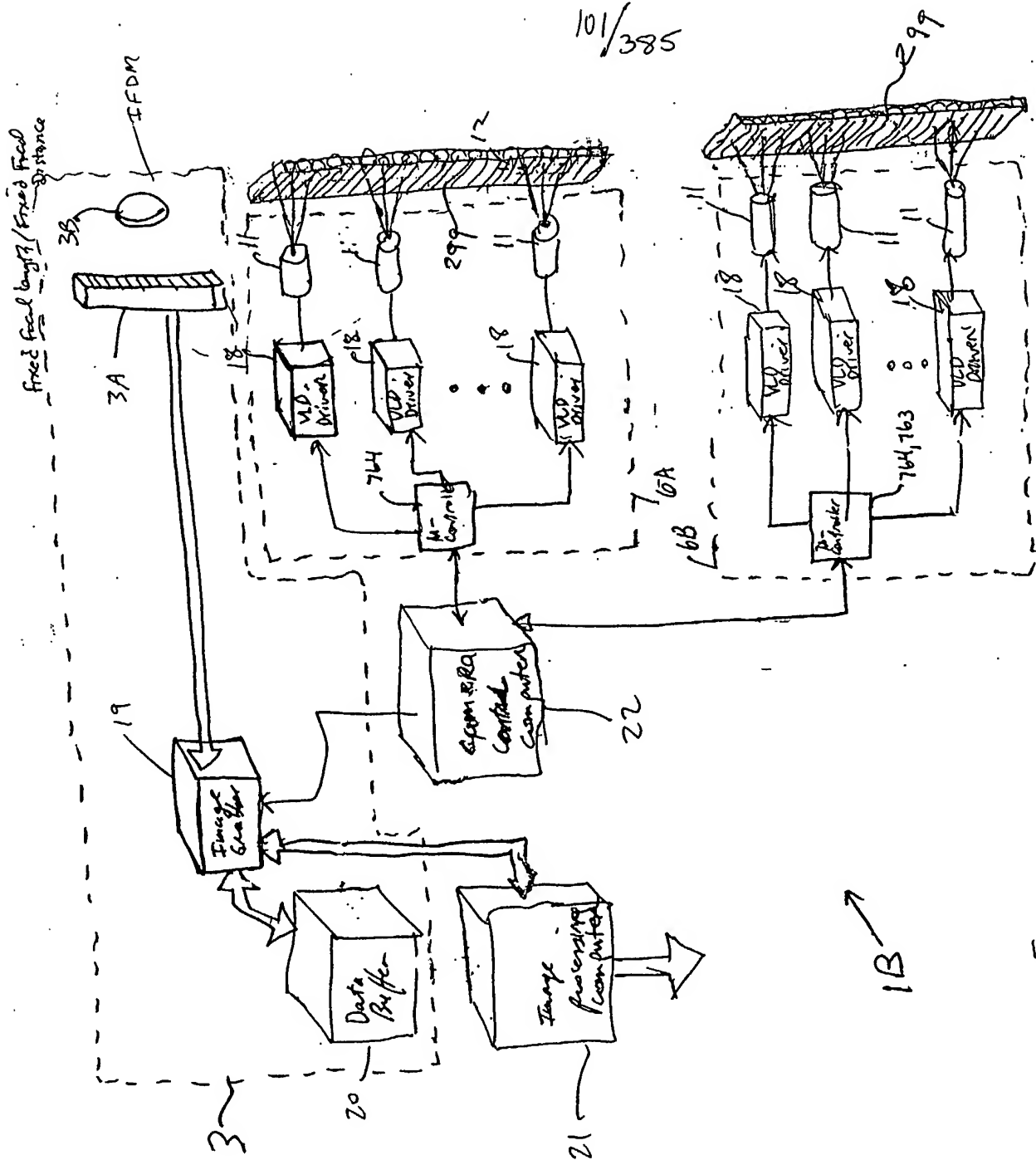
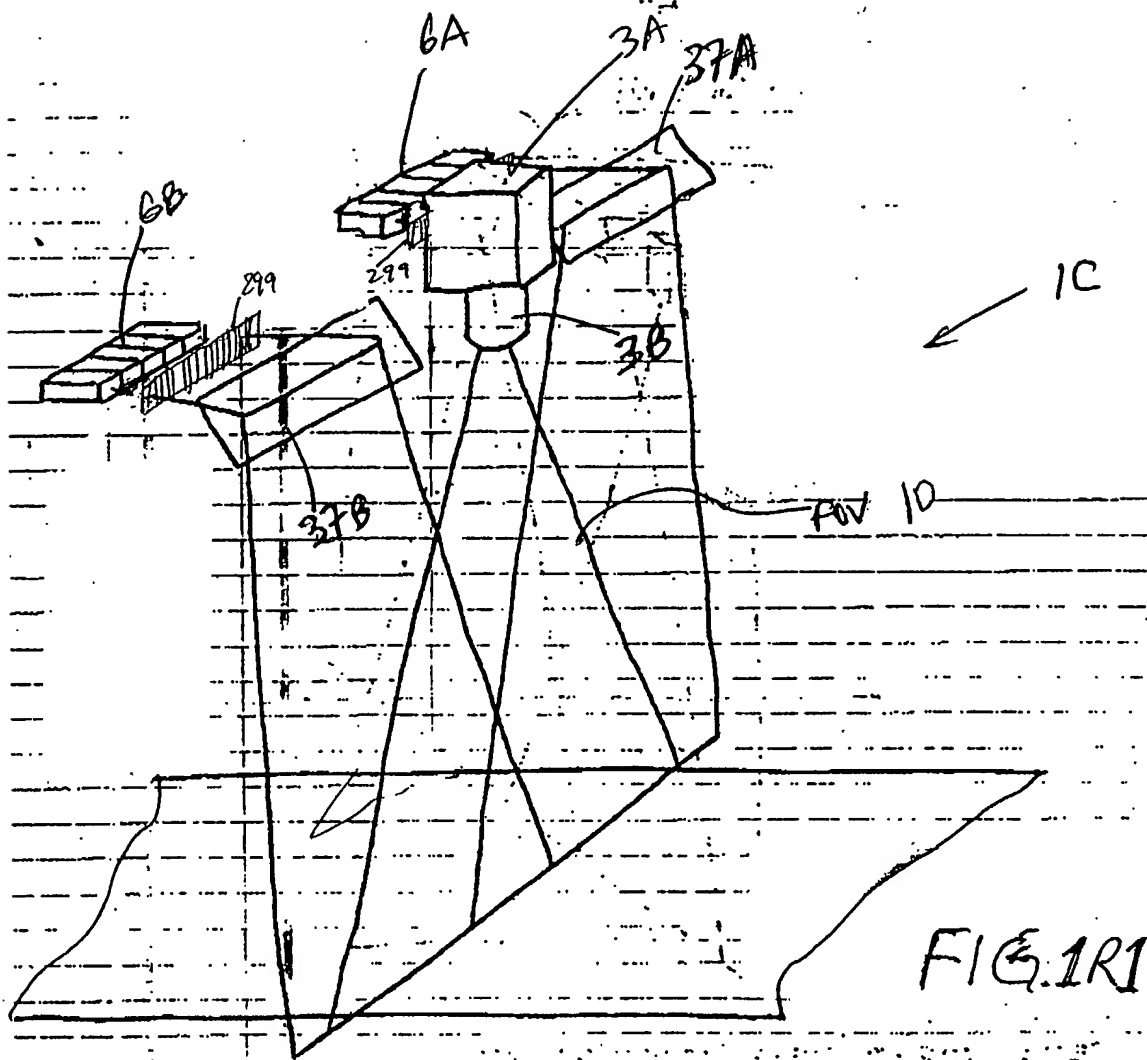
$$101 \overline{) 385}$$


Fig. 102

102/385



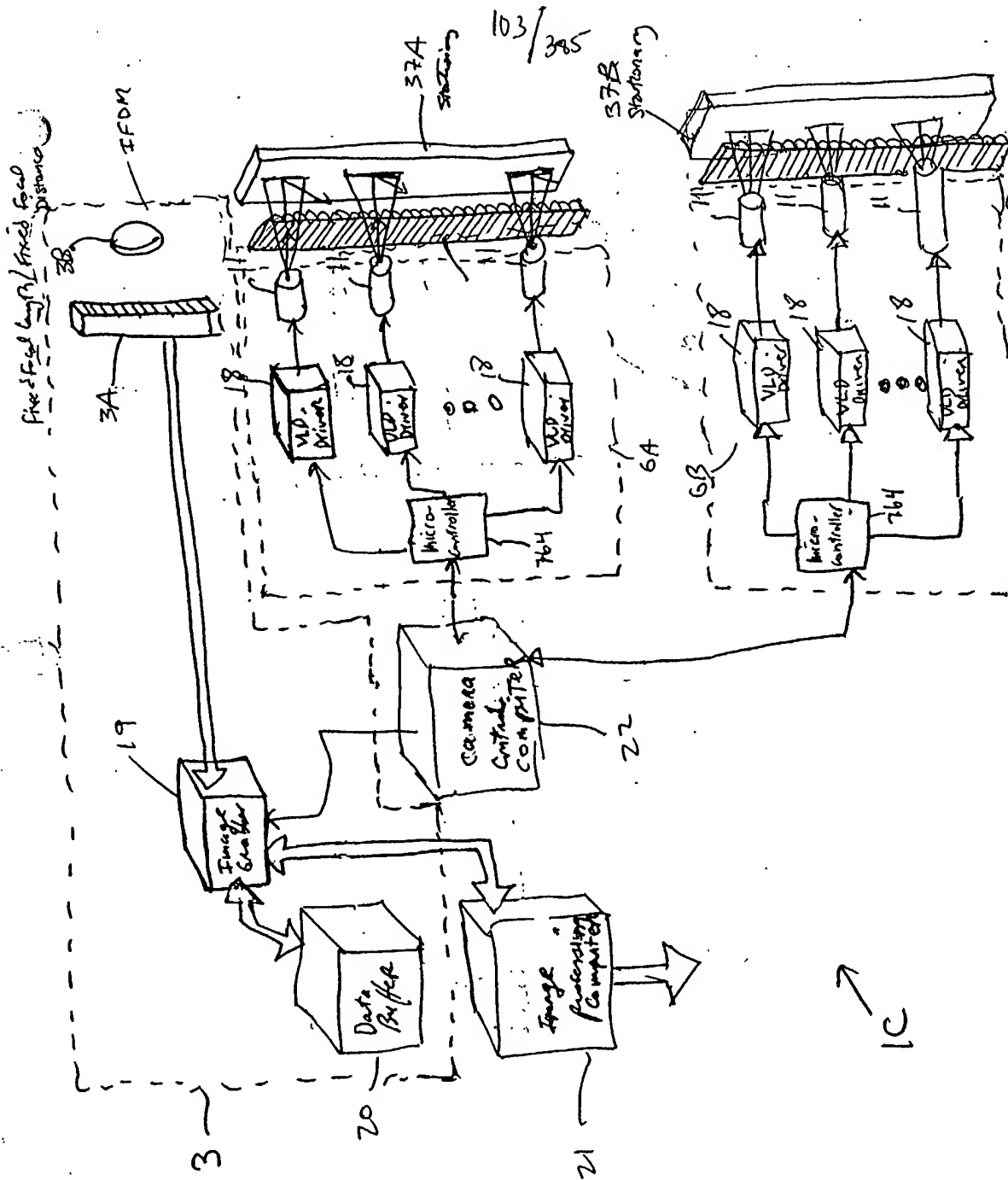


FIG. 1R2

104/385

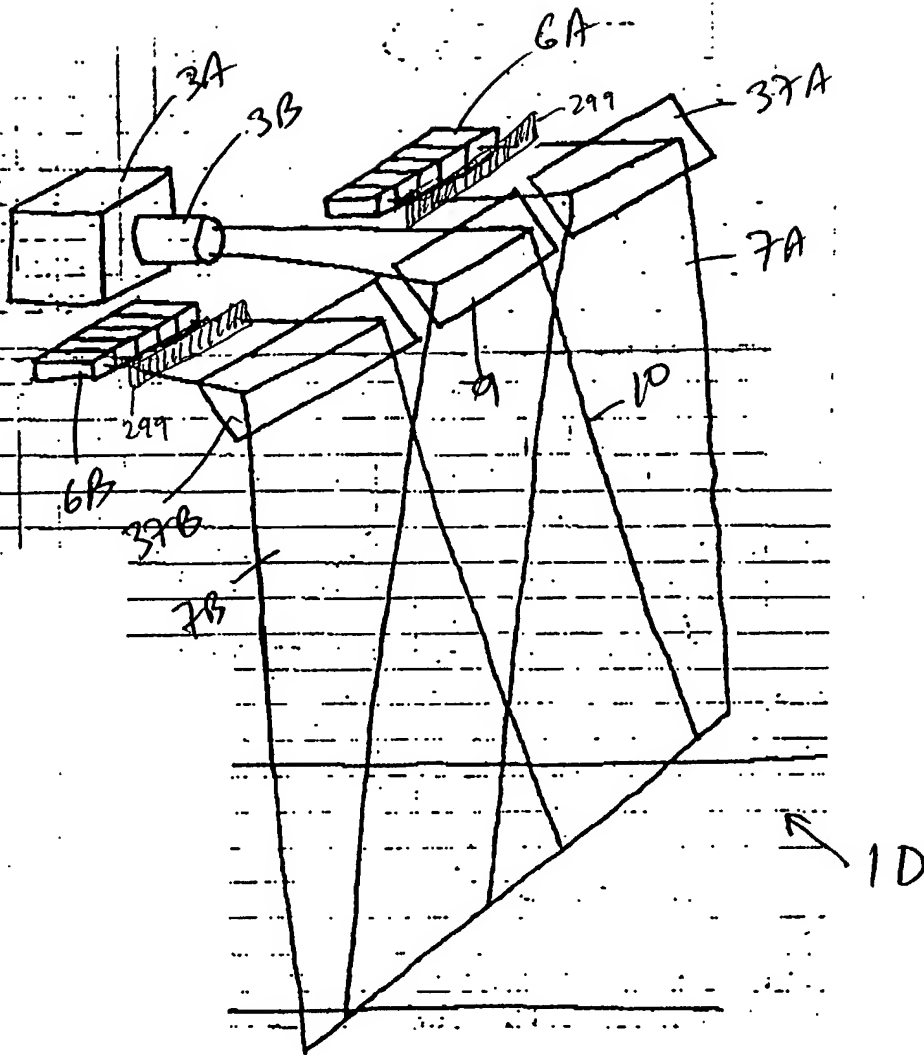


FIG. 1S1

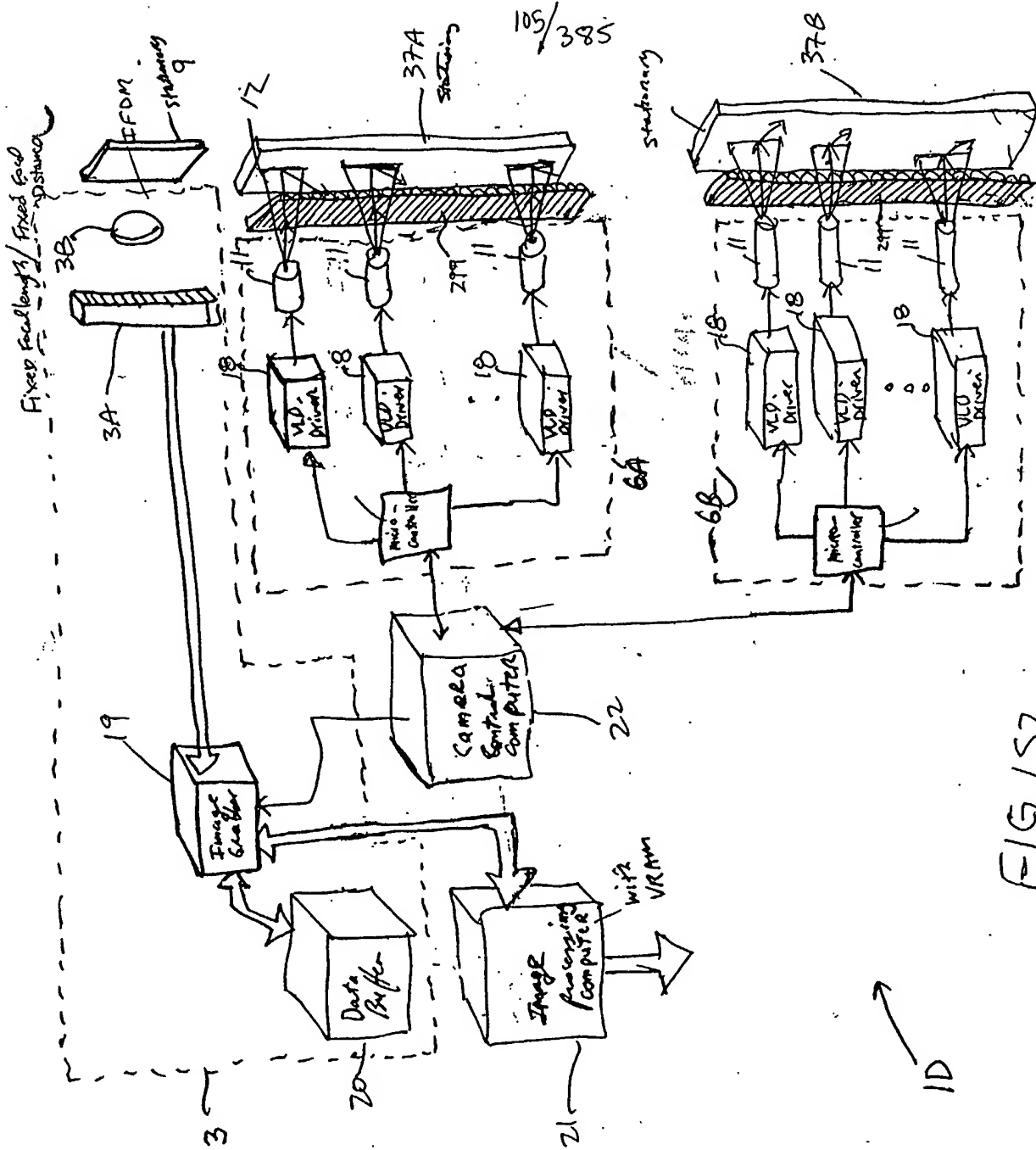


FIG. 1S2

106/385

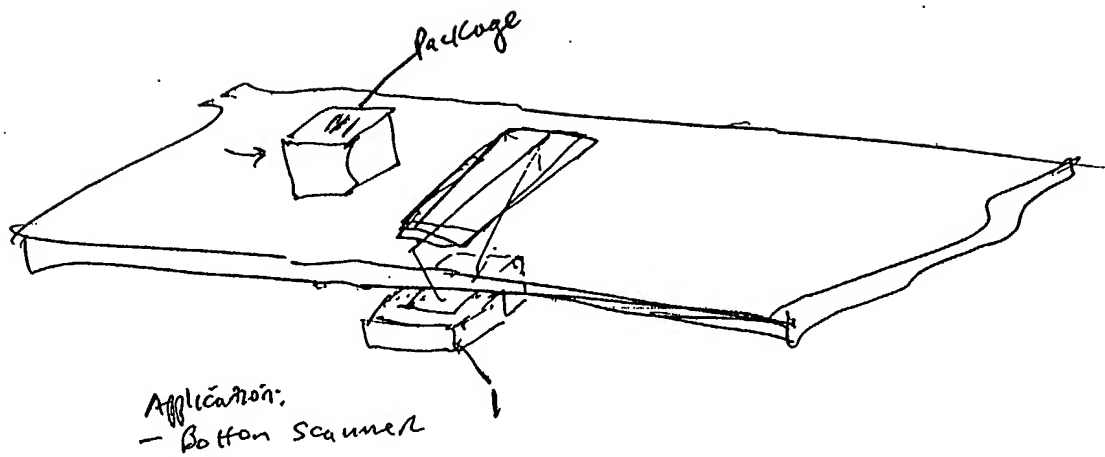
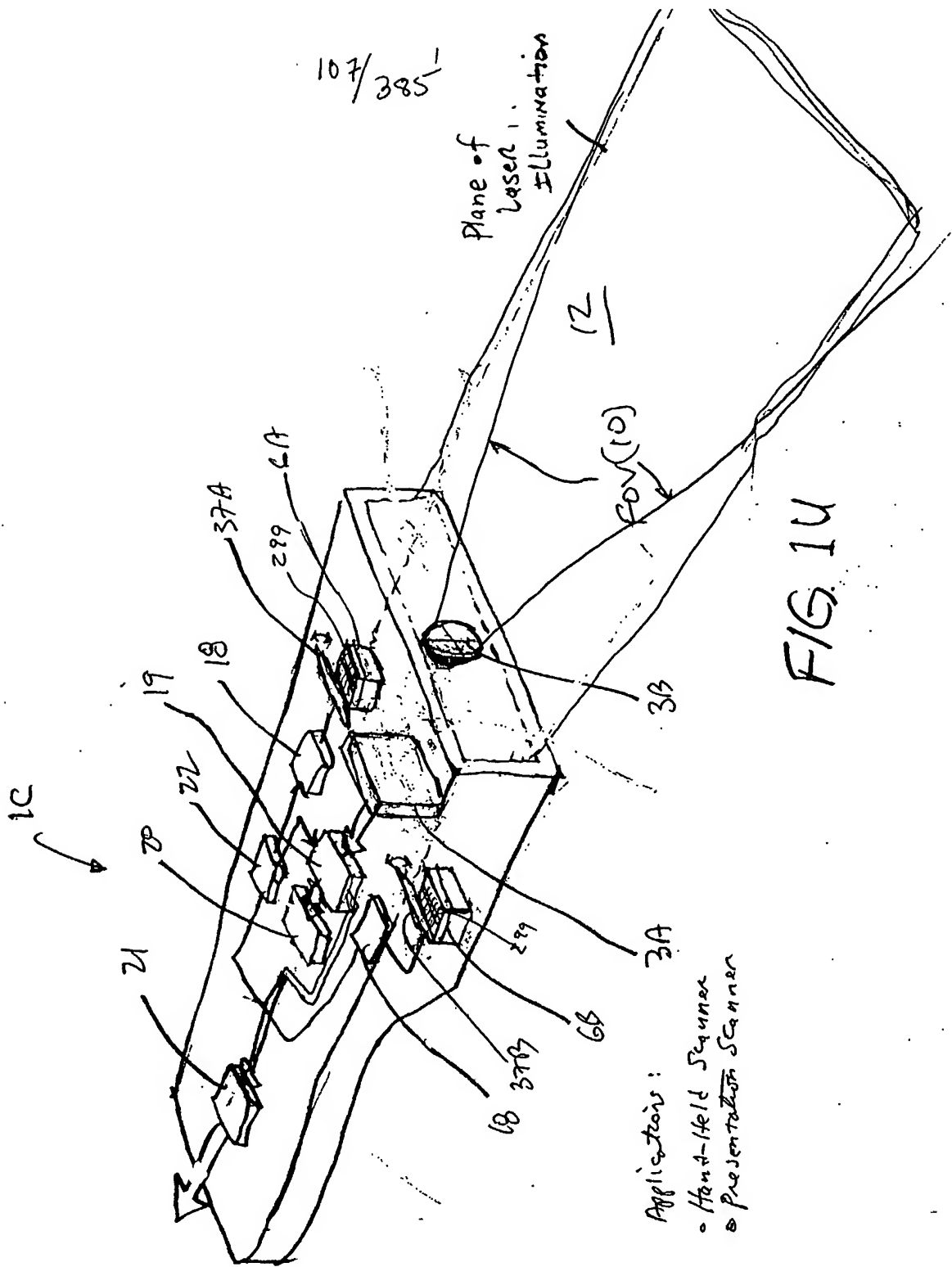


FIG 1T



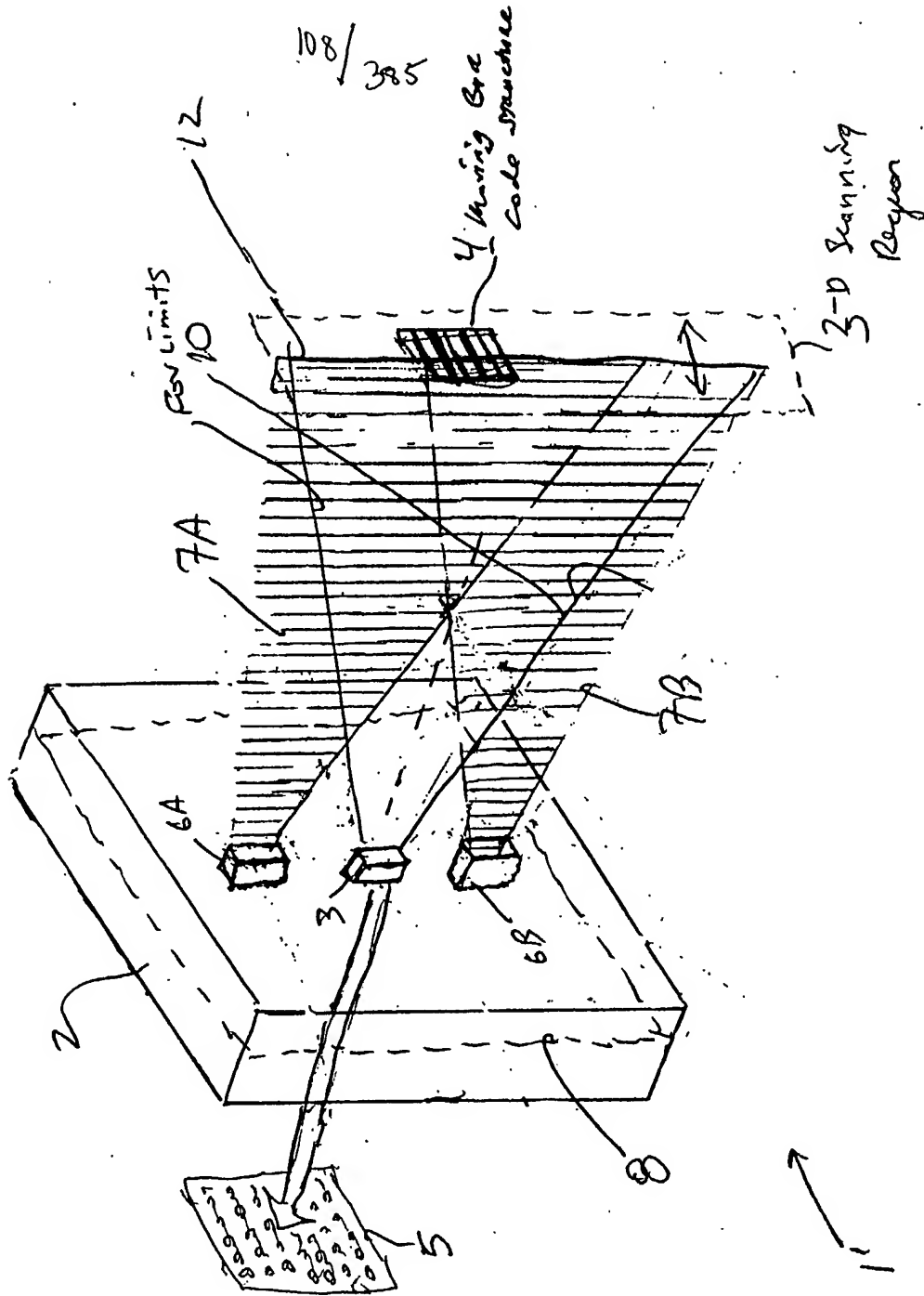


FIG. IVI

109/385

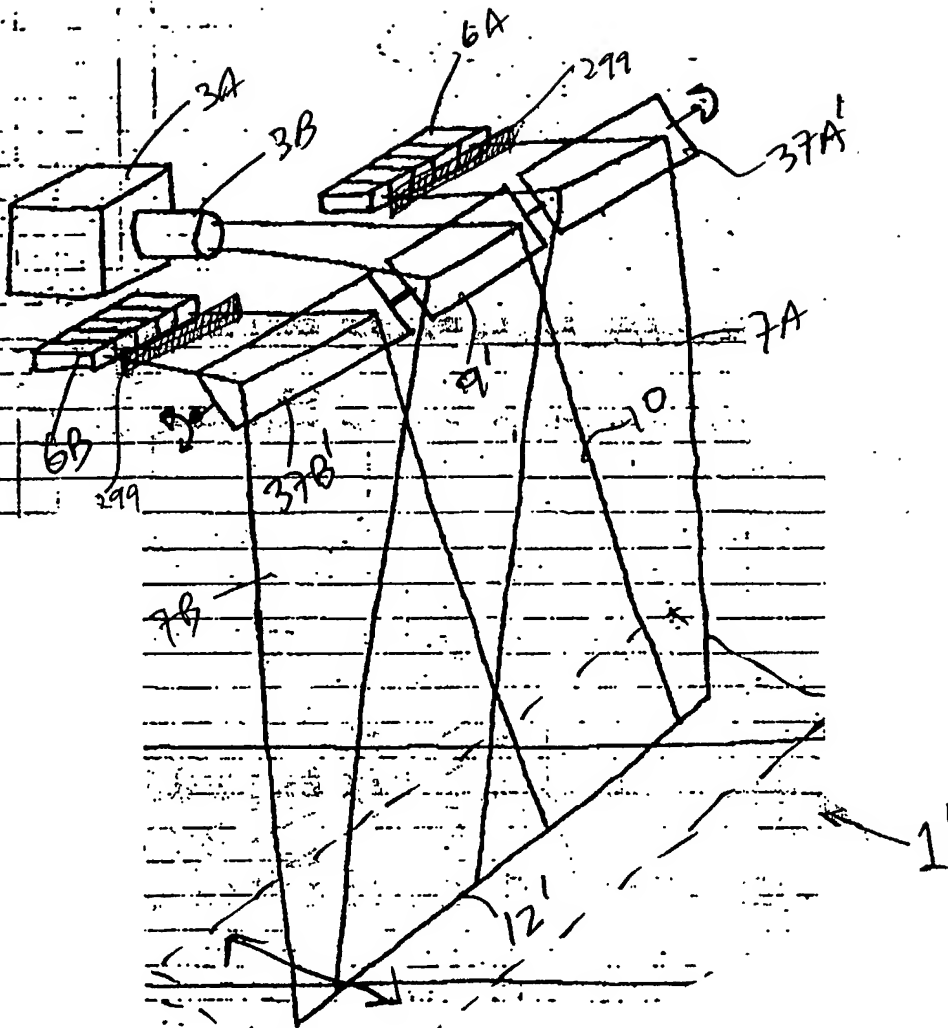
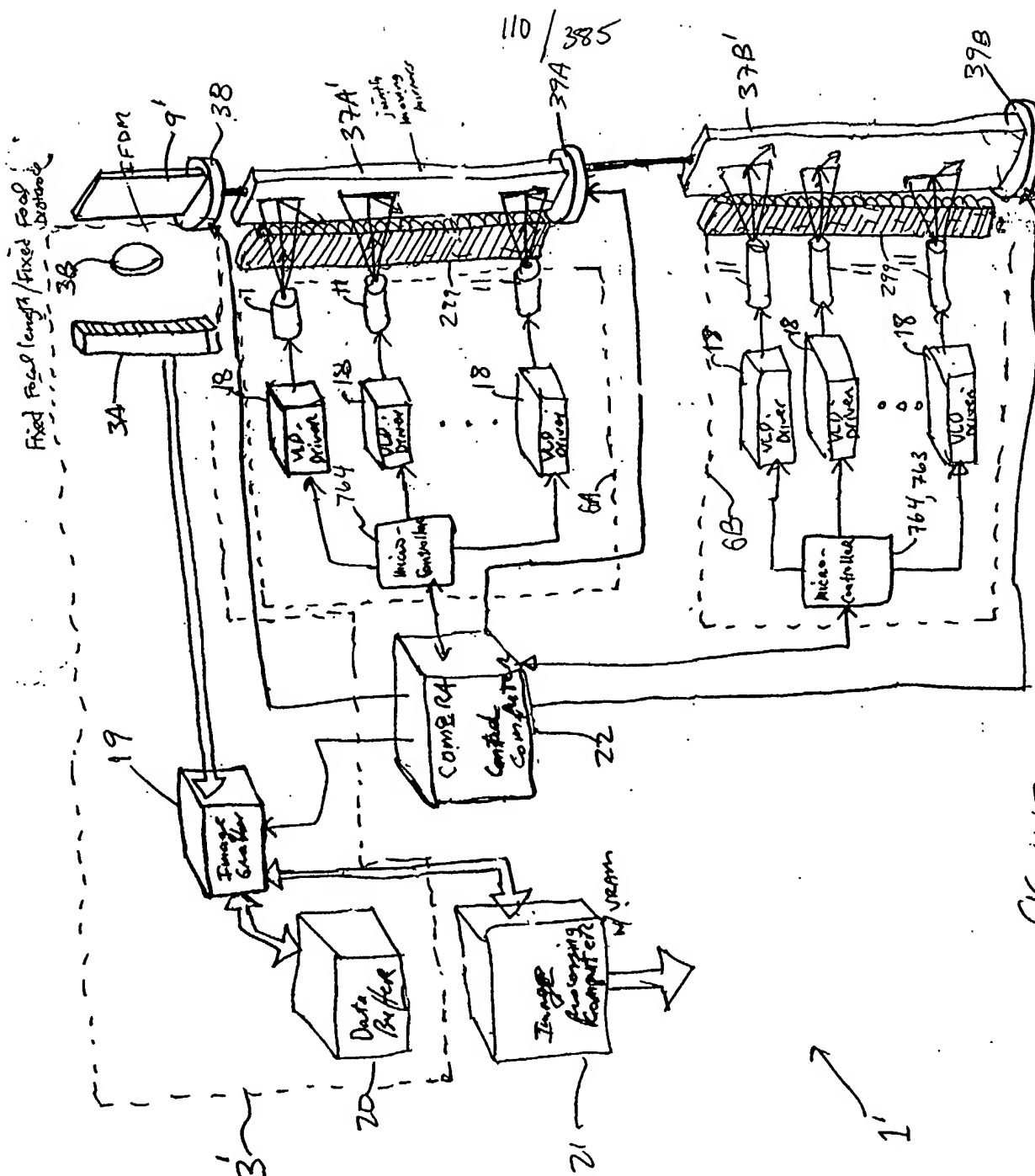
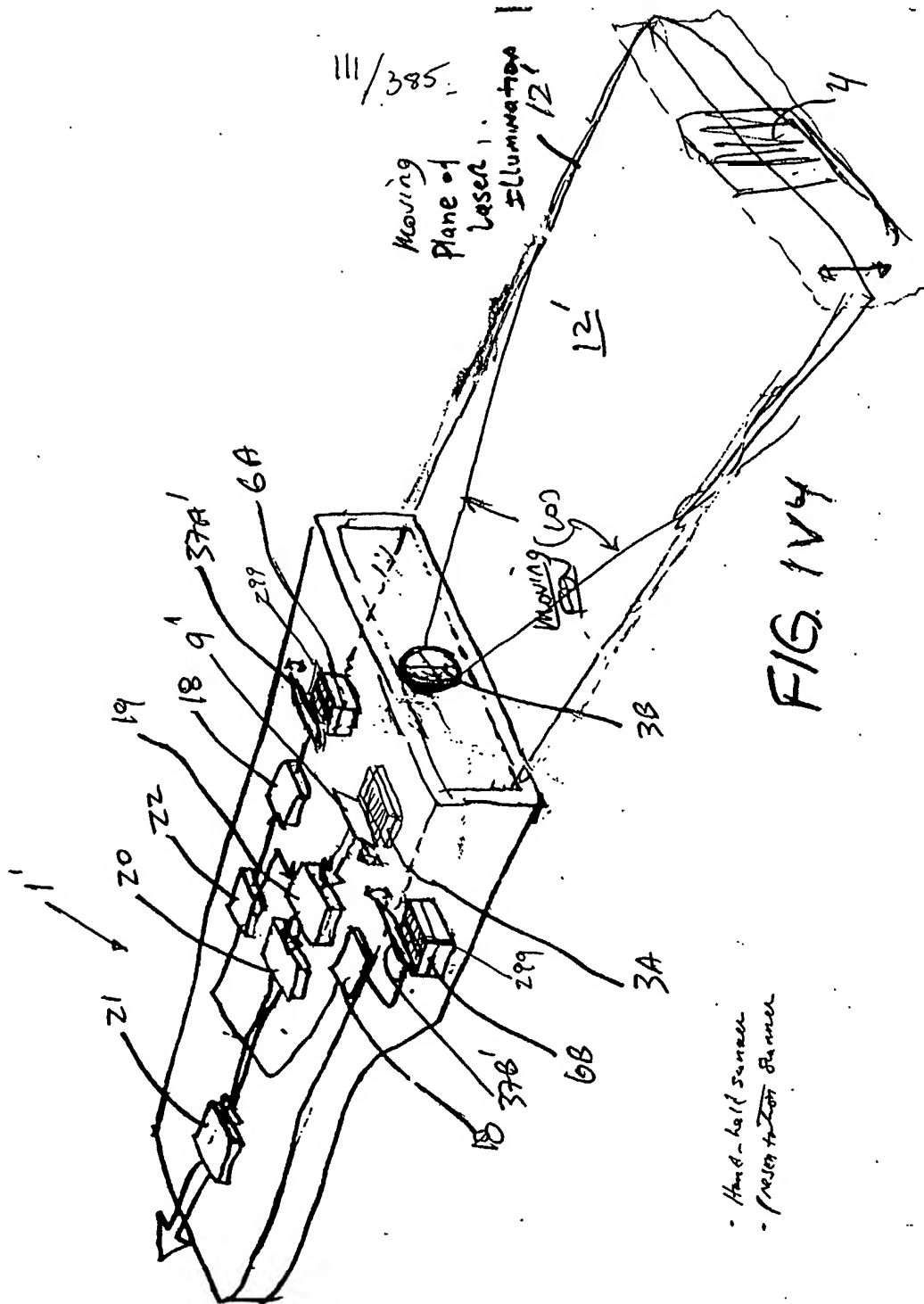


FIG. IV2

2-0
region
of
space



AG.1V3



Hand-held sunshade
Presentation Banner

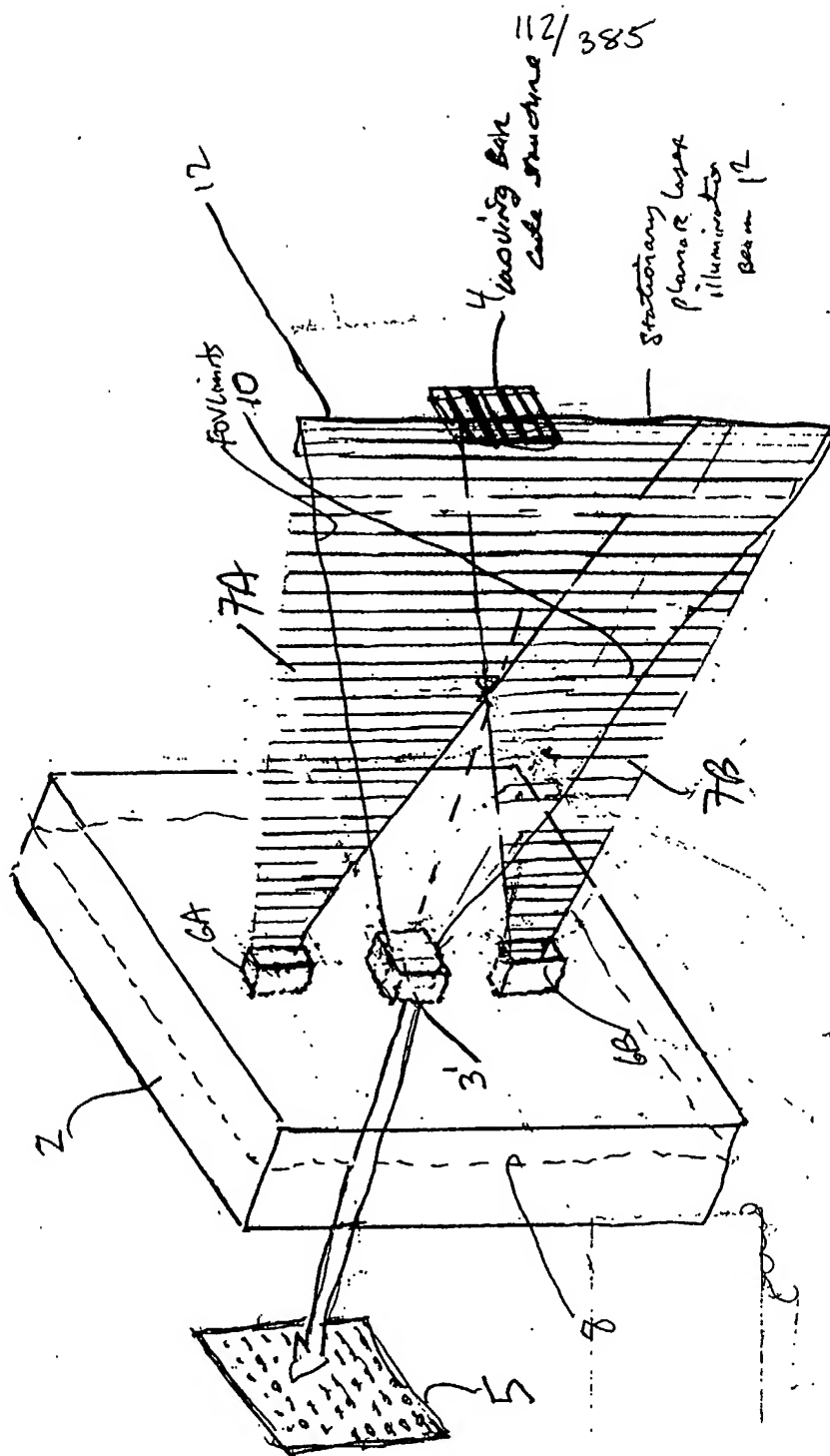


FIG. 2A

40

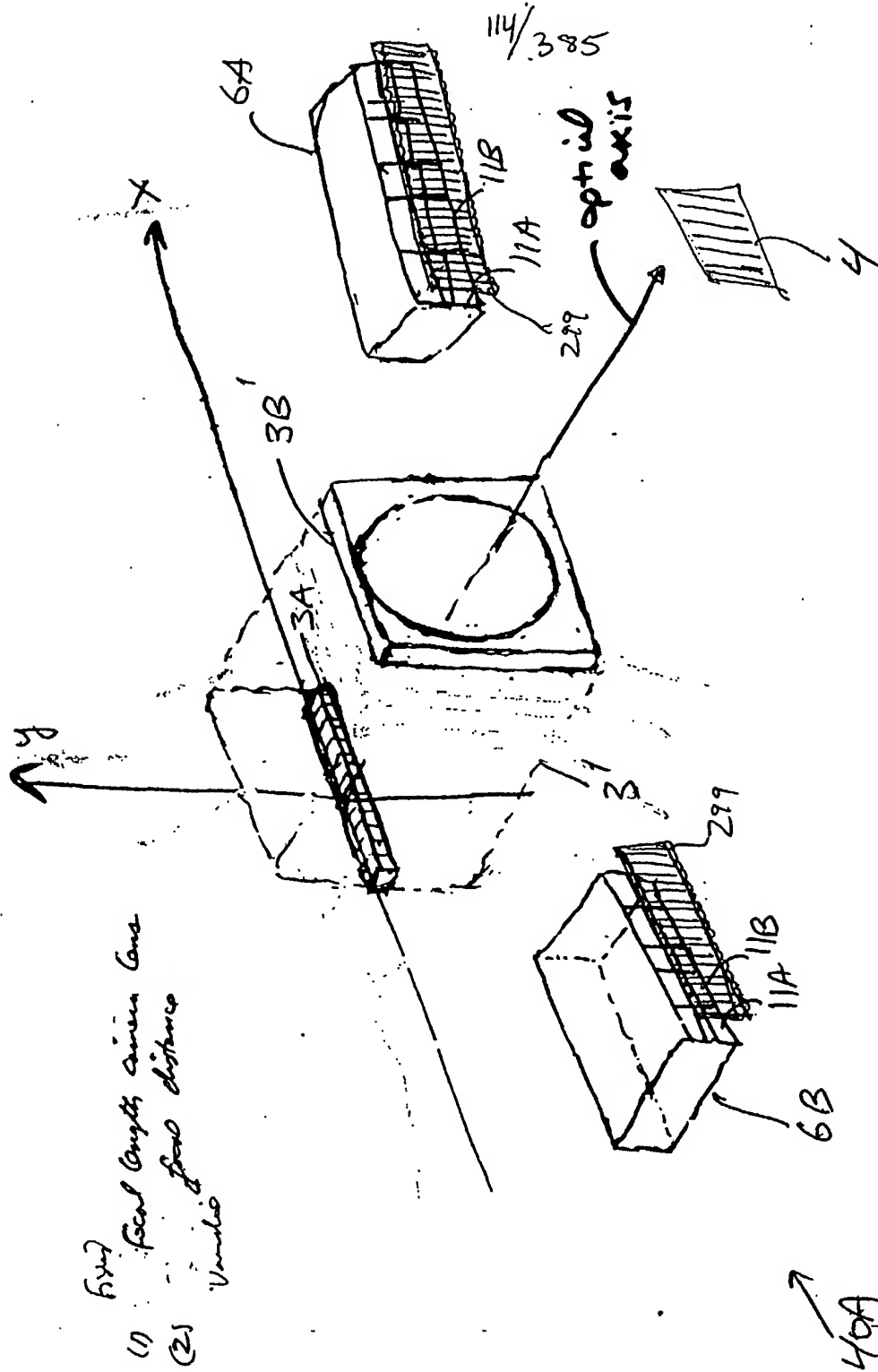


FIG. 2B2

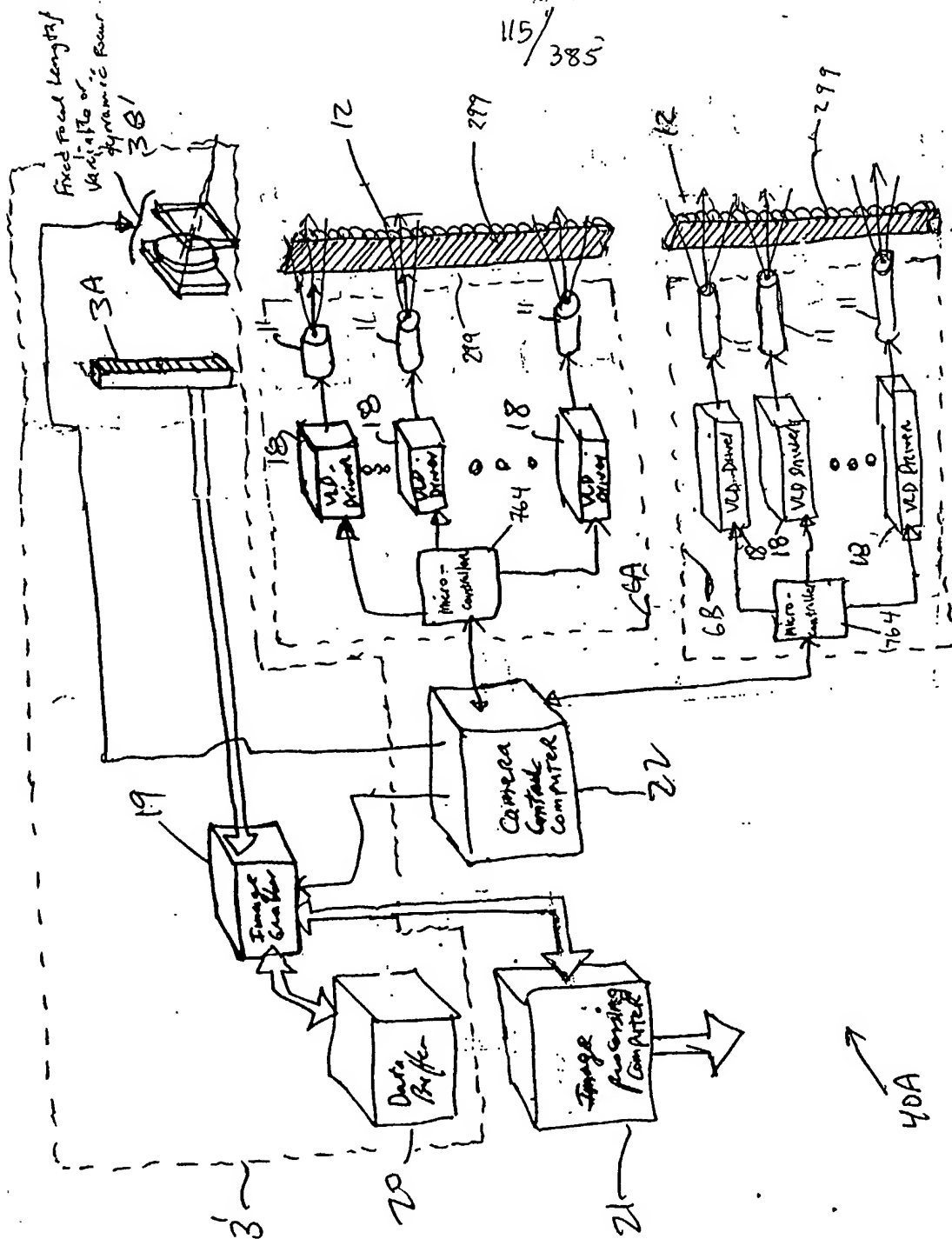


FIG. 2C1

116/385

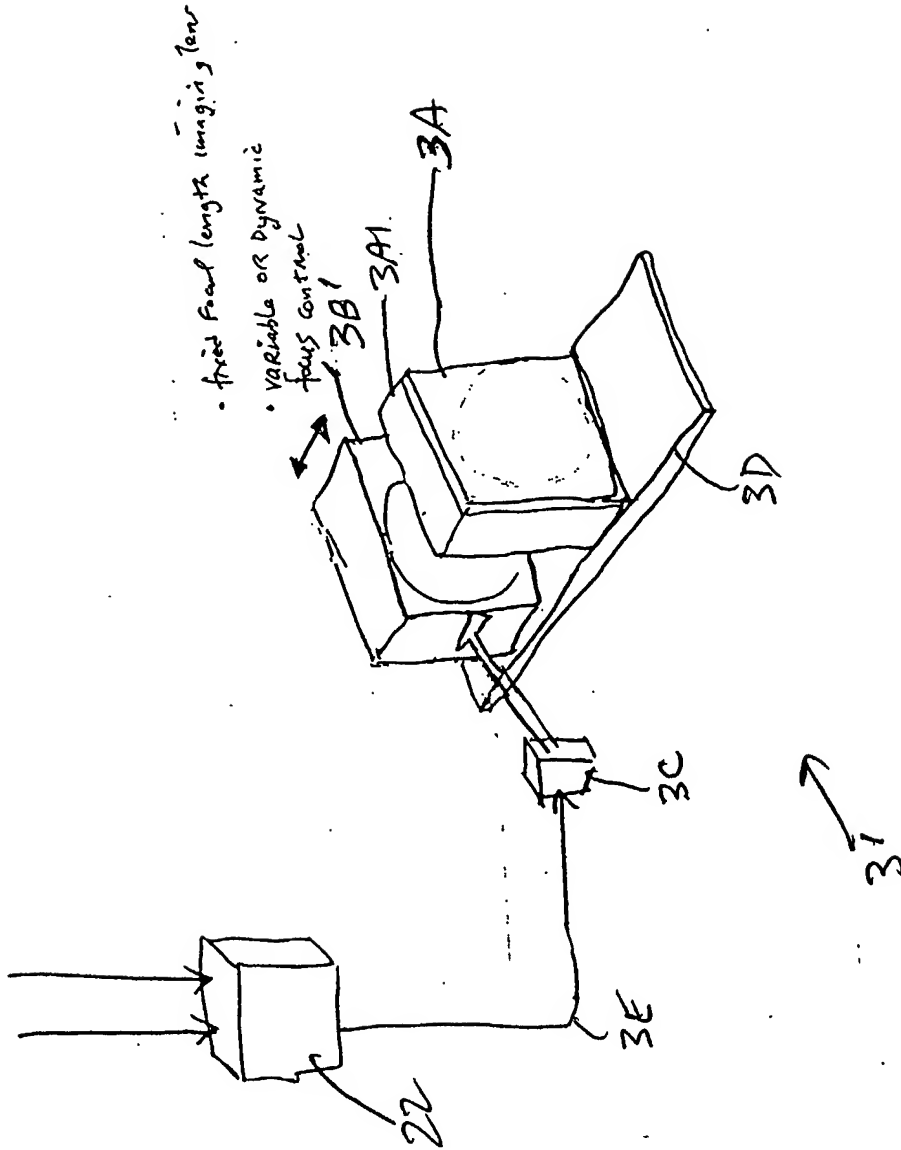
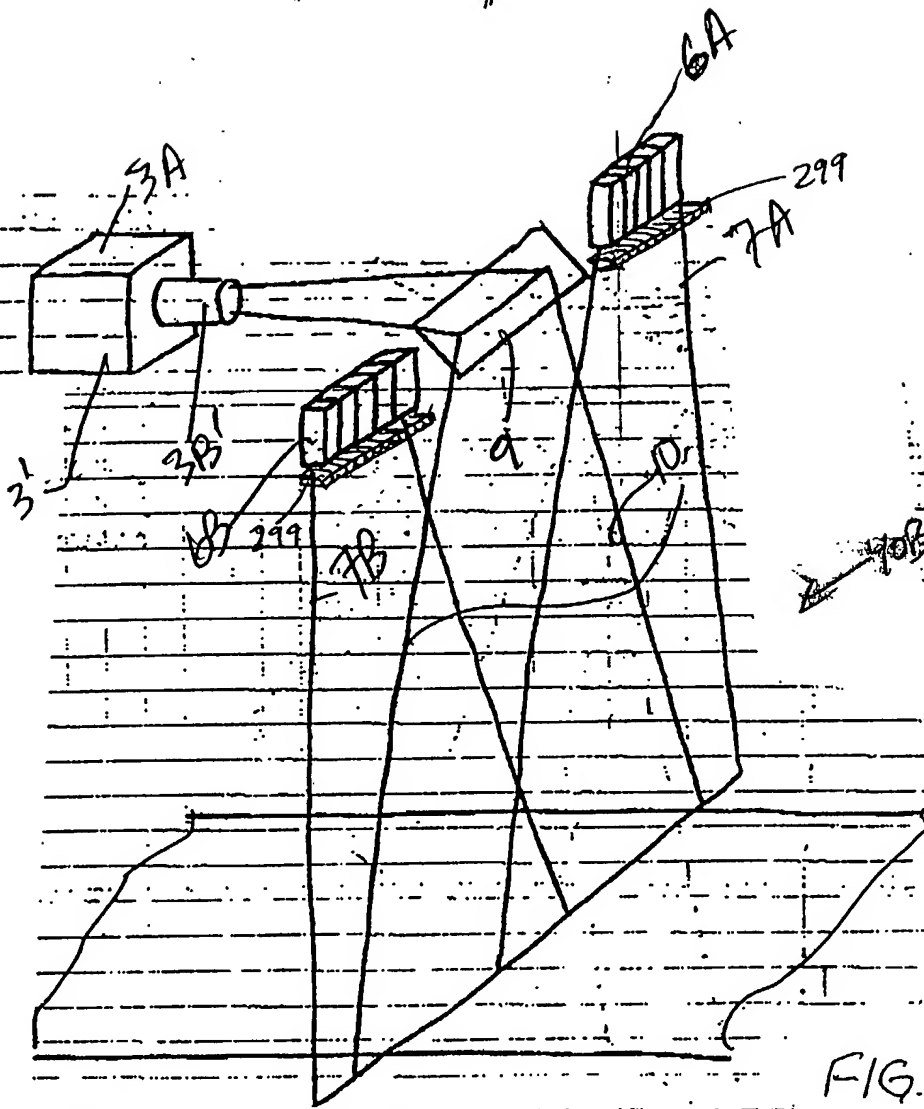


FIG. 2C2

$$117 \overline{) 385}$$


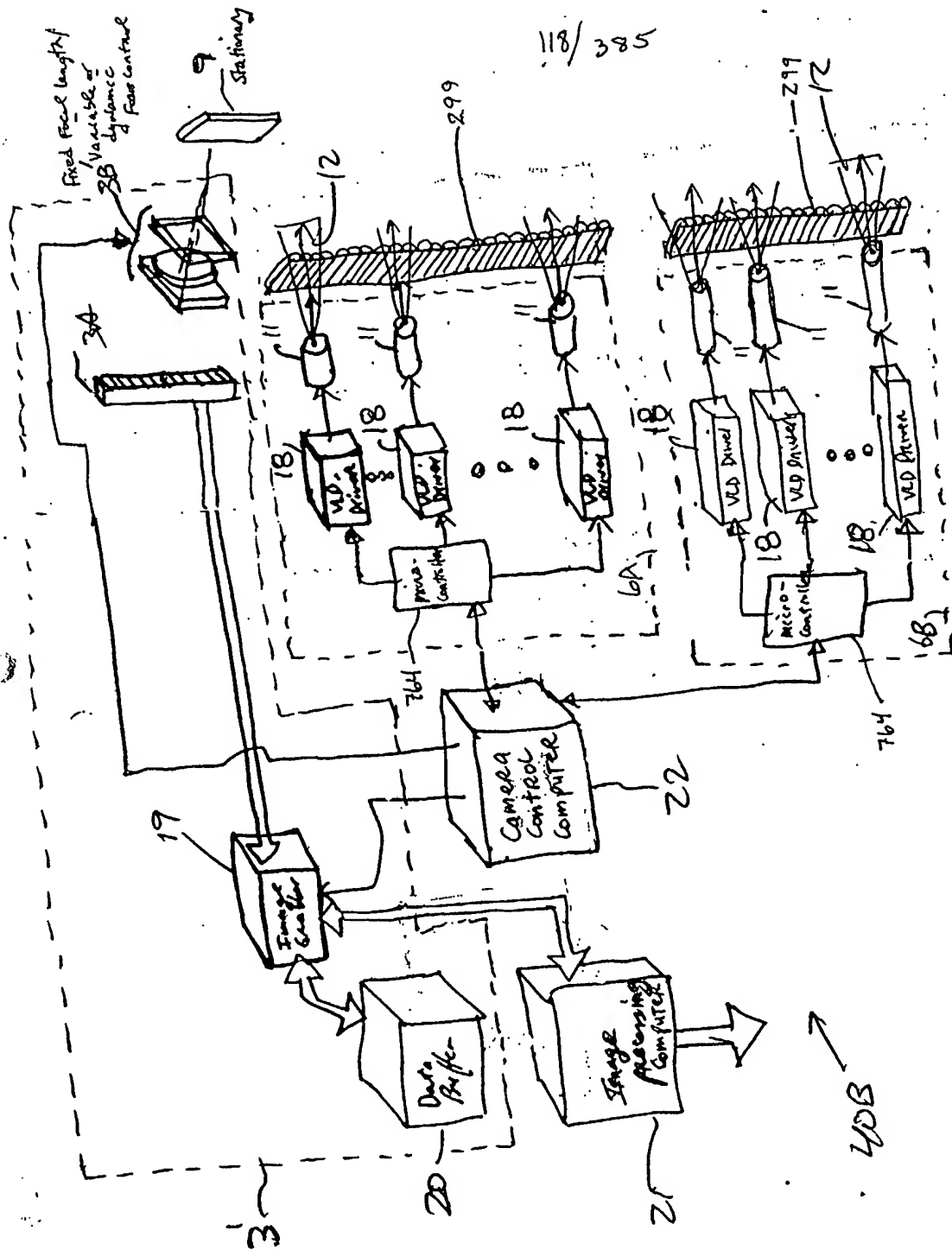


FIG. 2D2

119/385

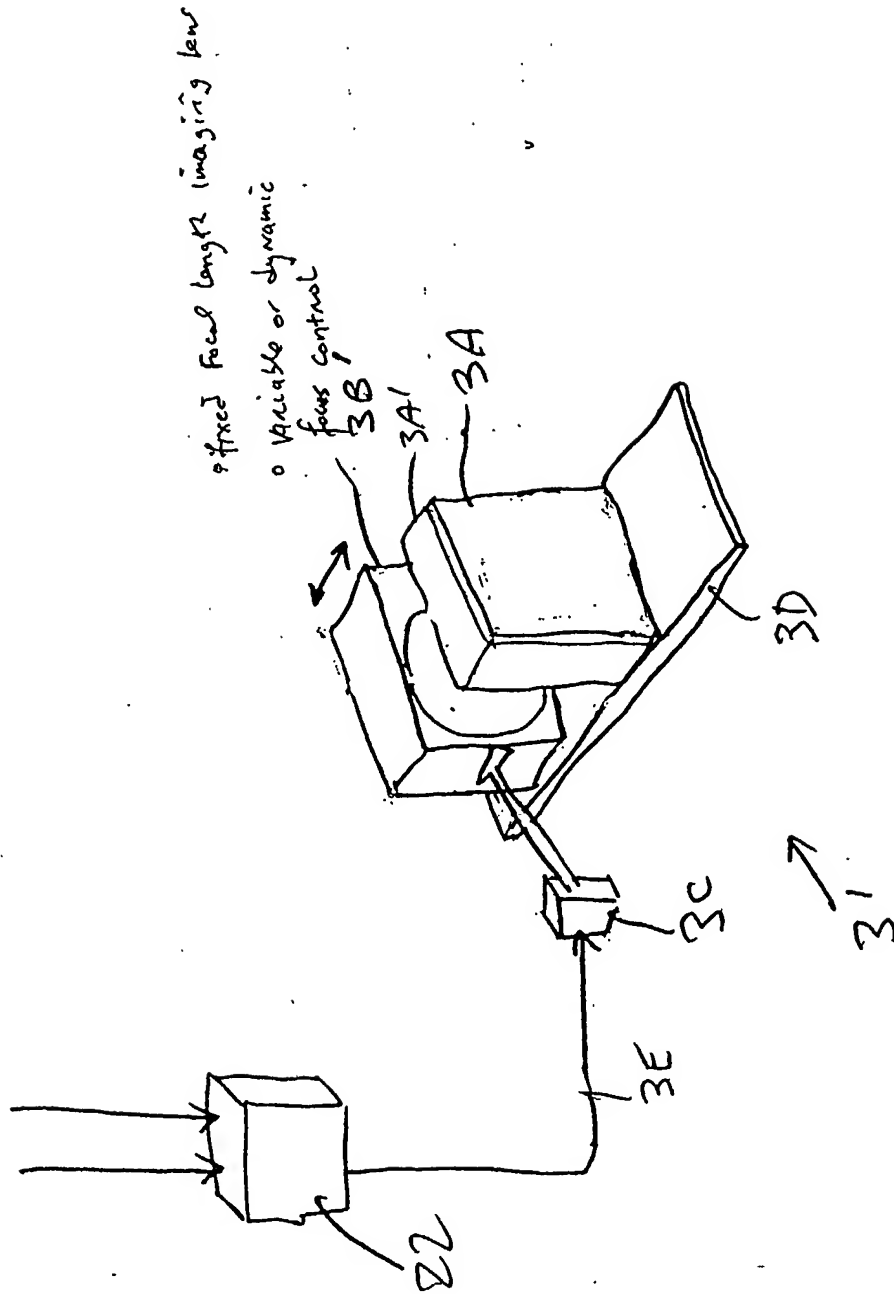
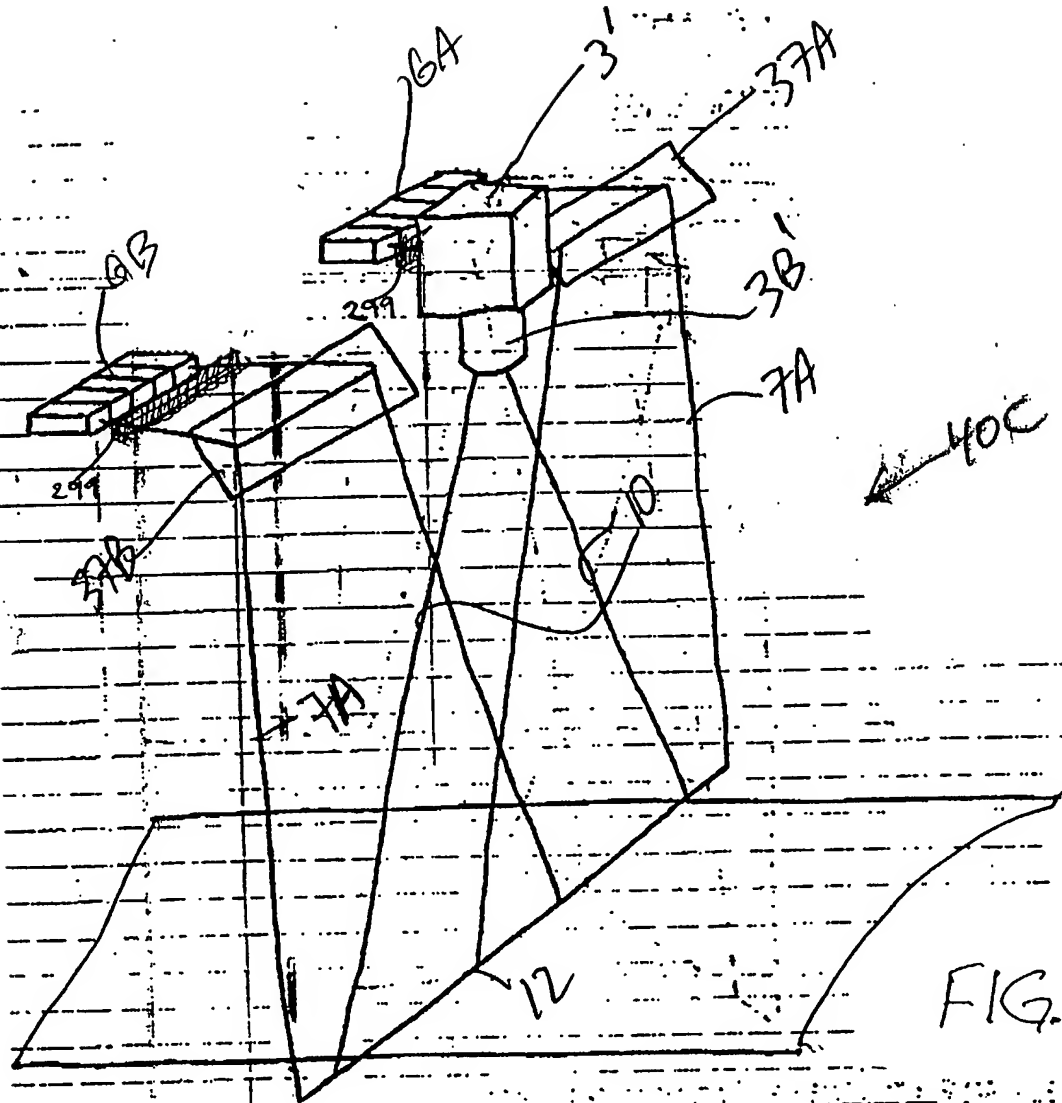


FIG. 2D3

120/385



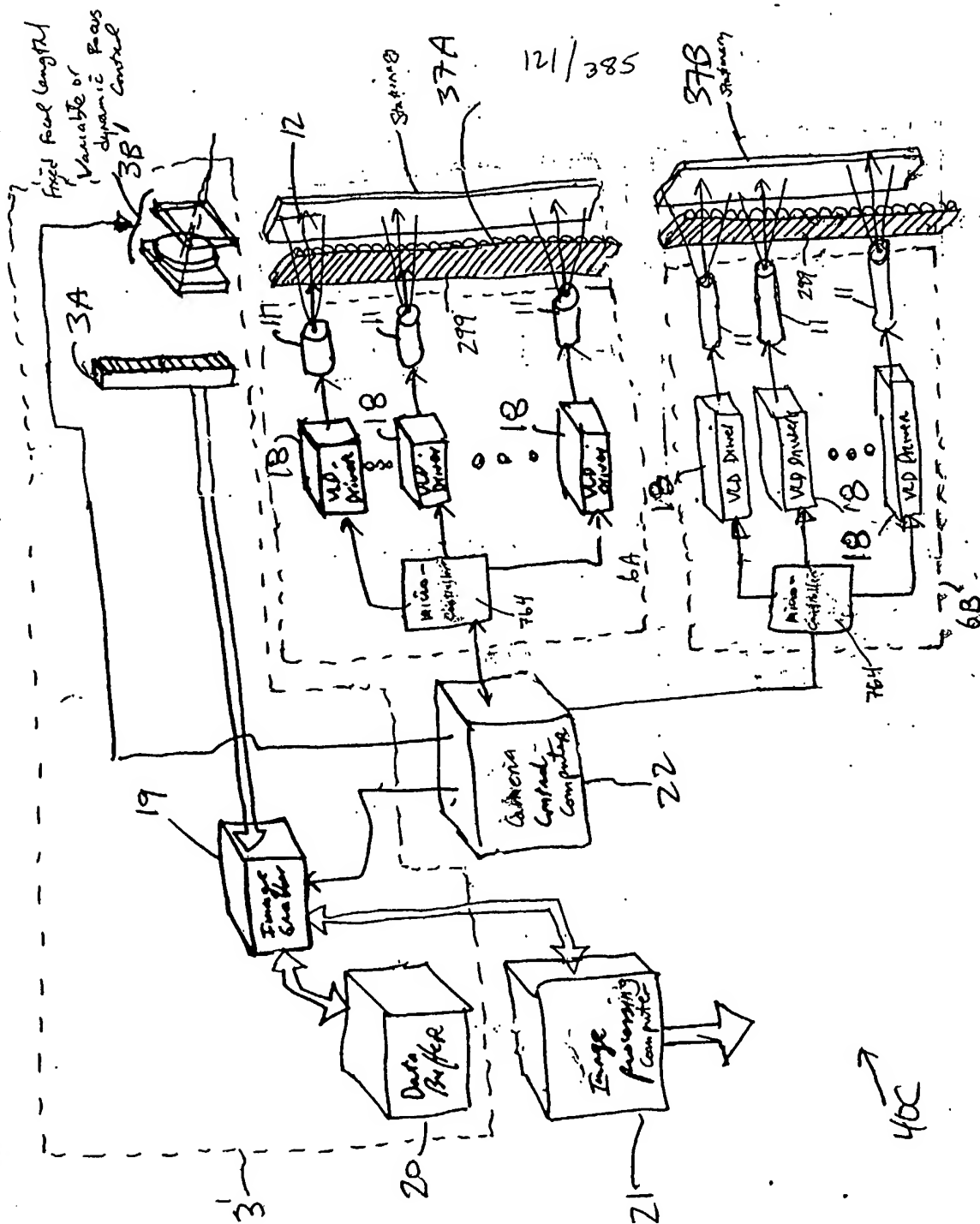


FIG. 2E2

122/385-

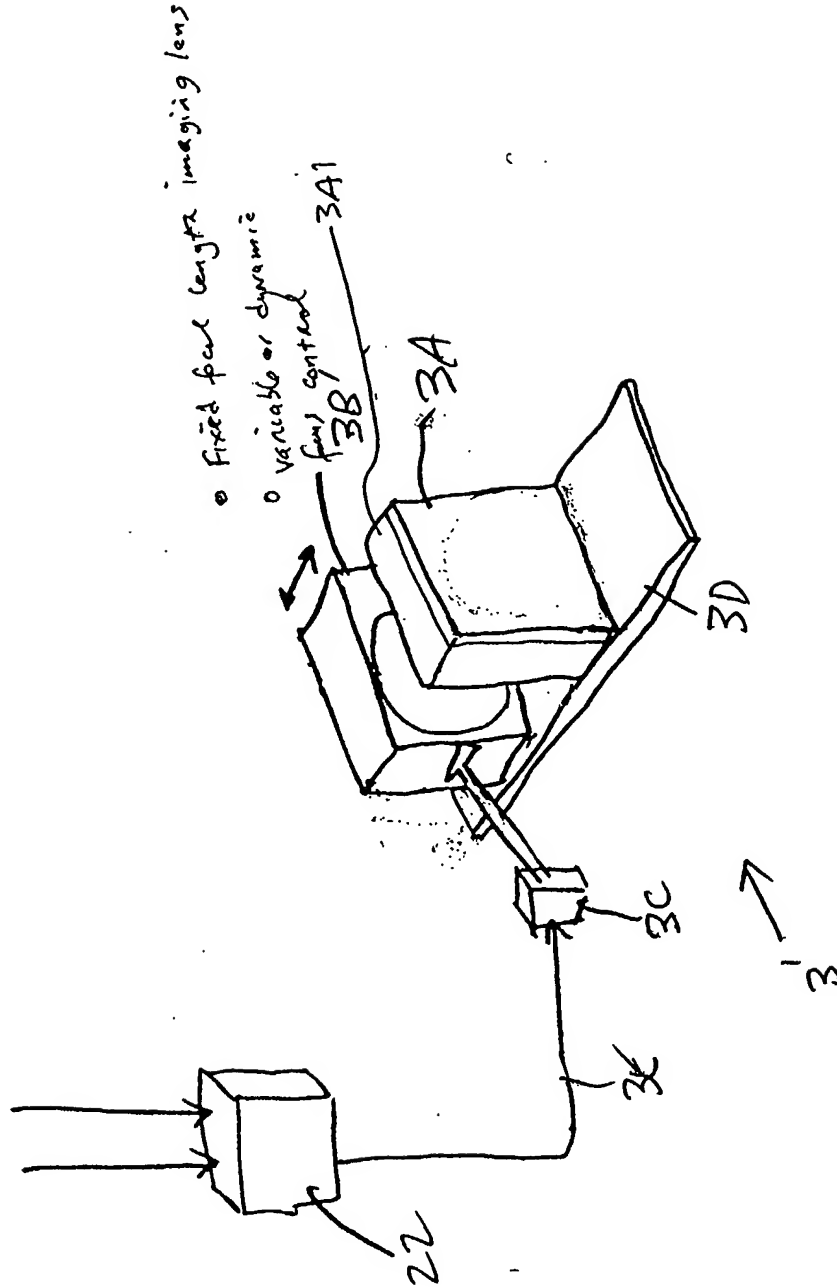


FIG. 2E3

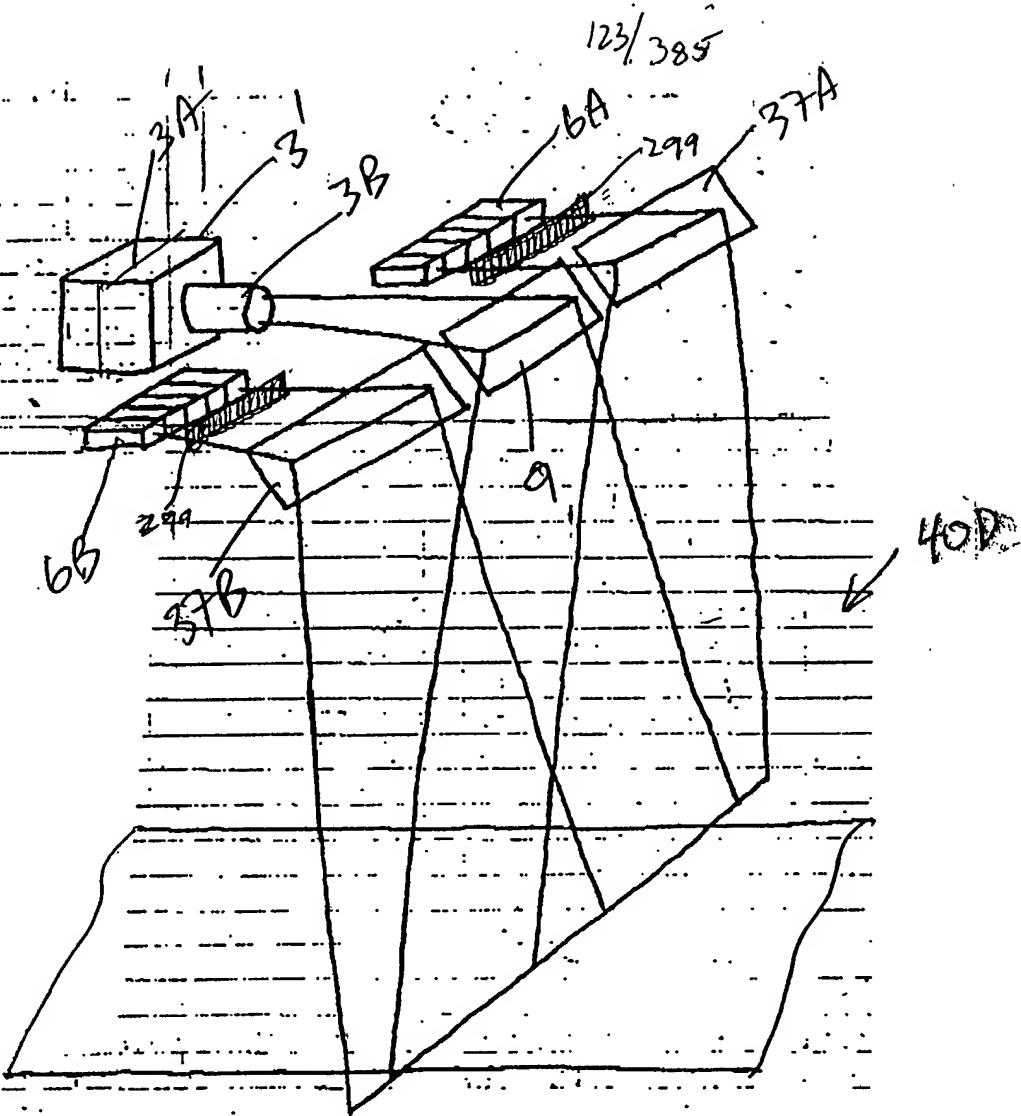


FIG. 2F1

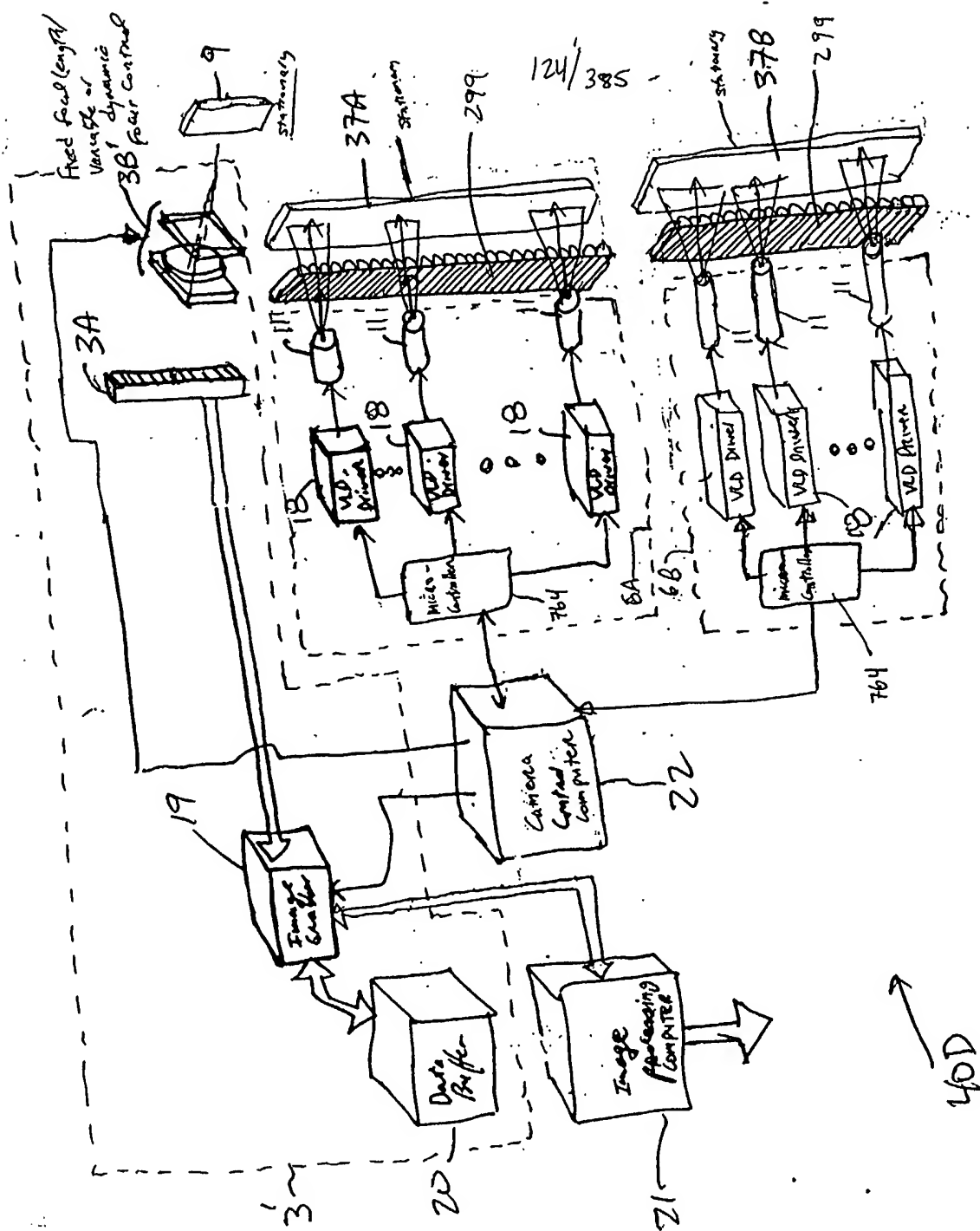


FIG 2F2

40D

125/385

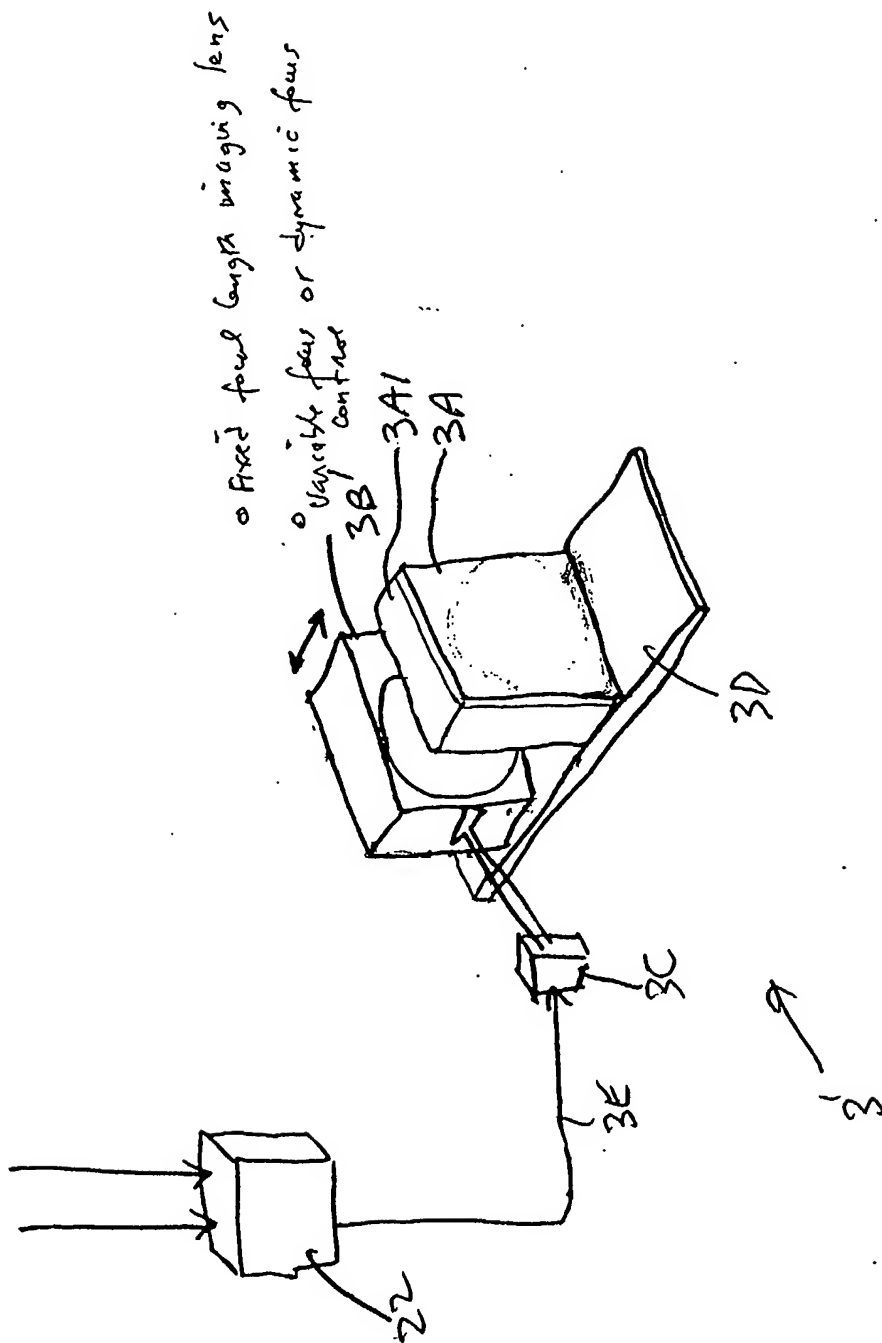


FIG. 2F3

126/385

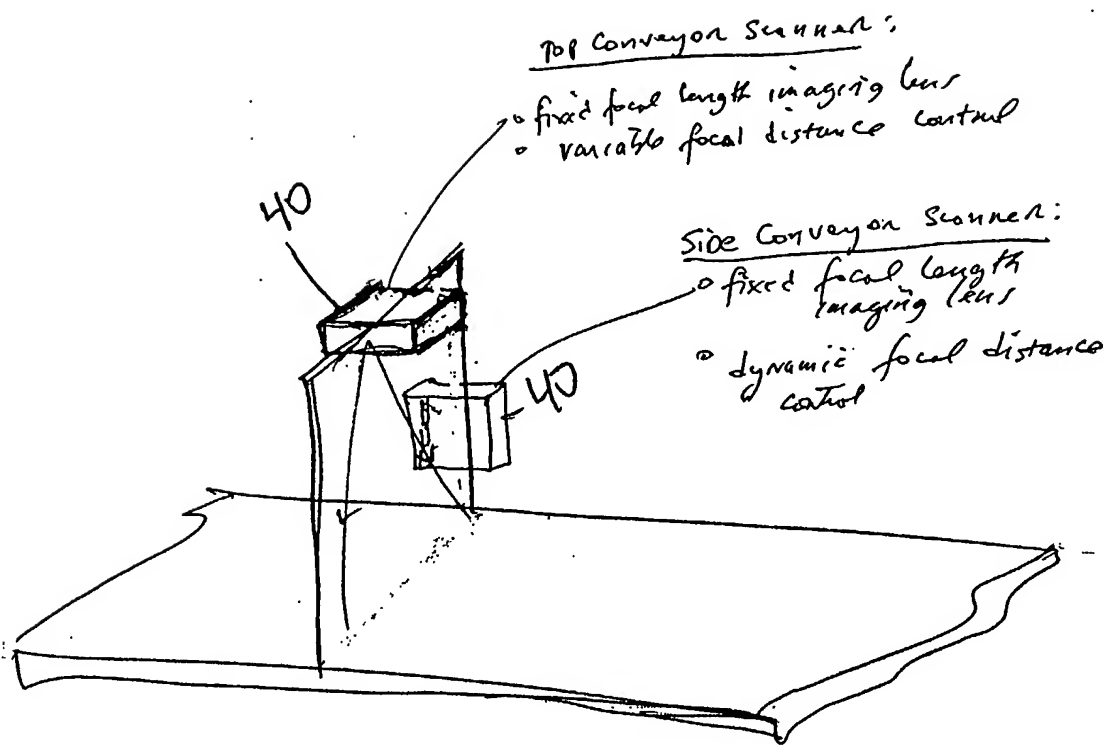
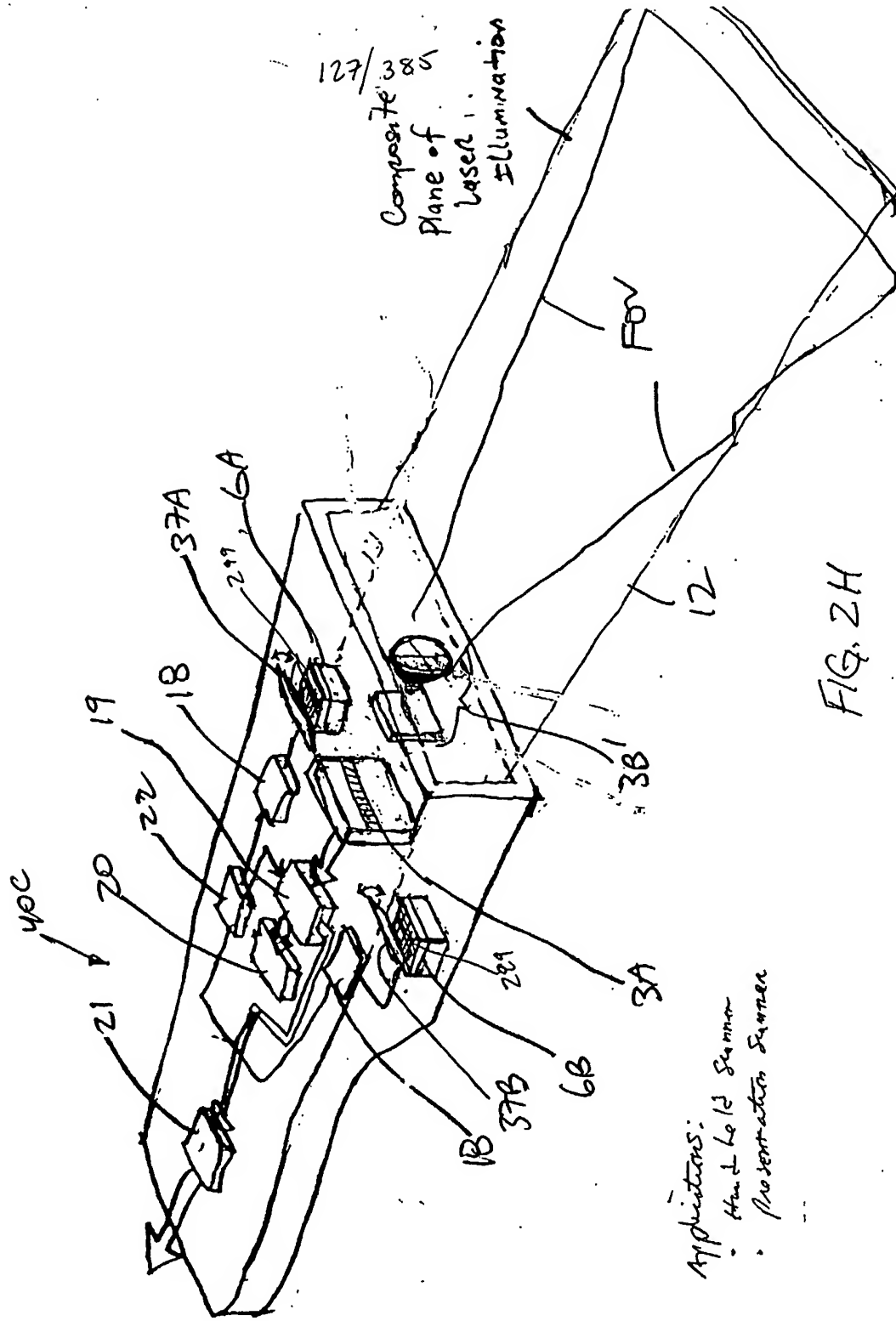


FIG. 2G



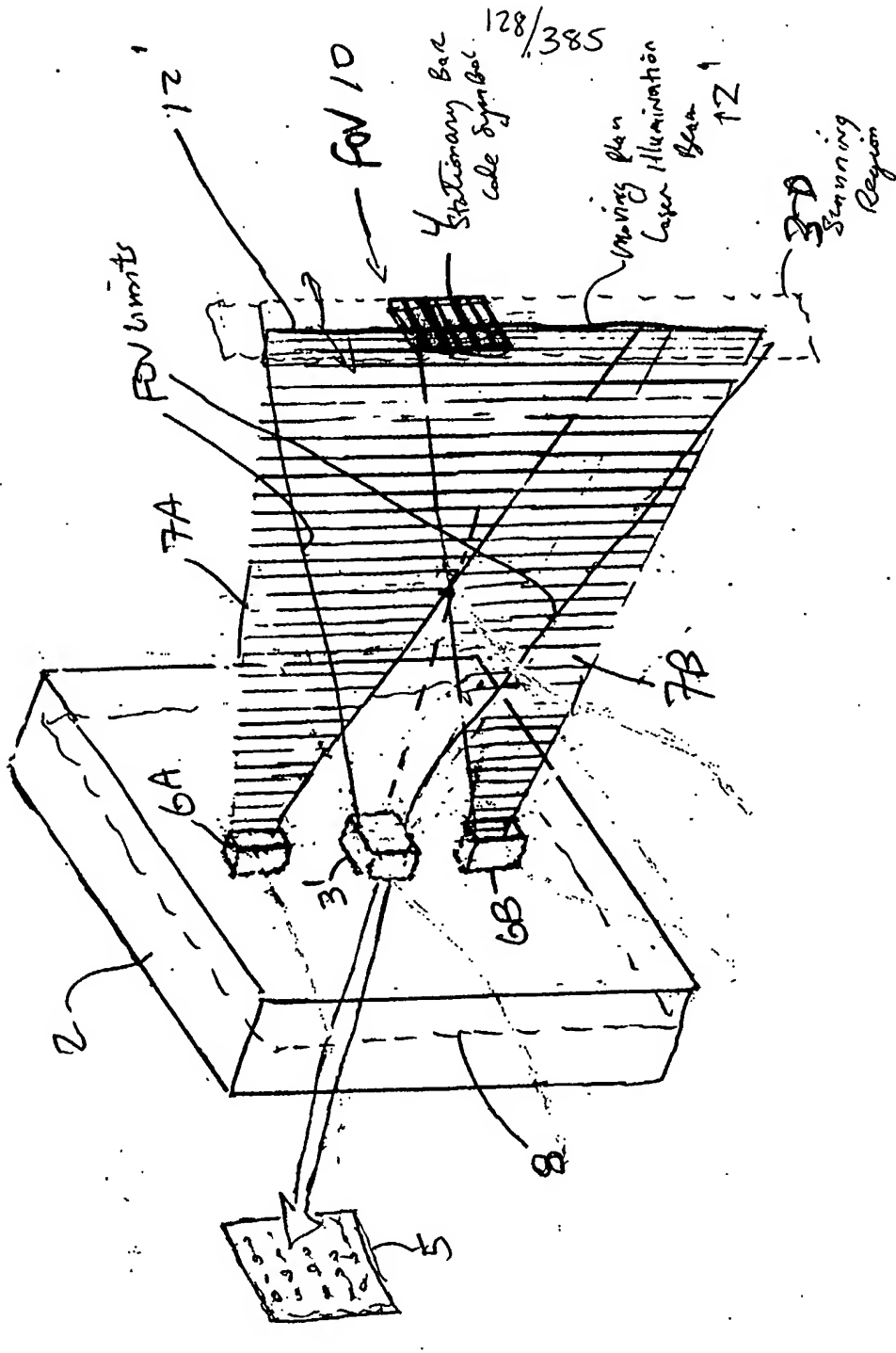
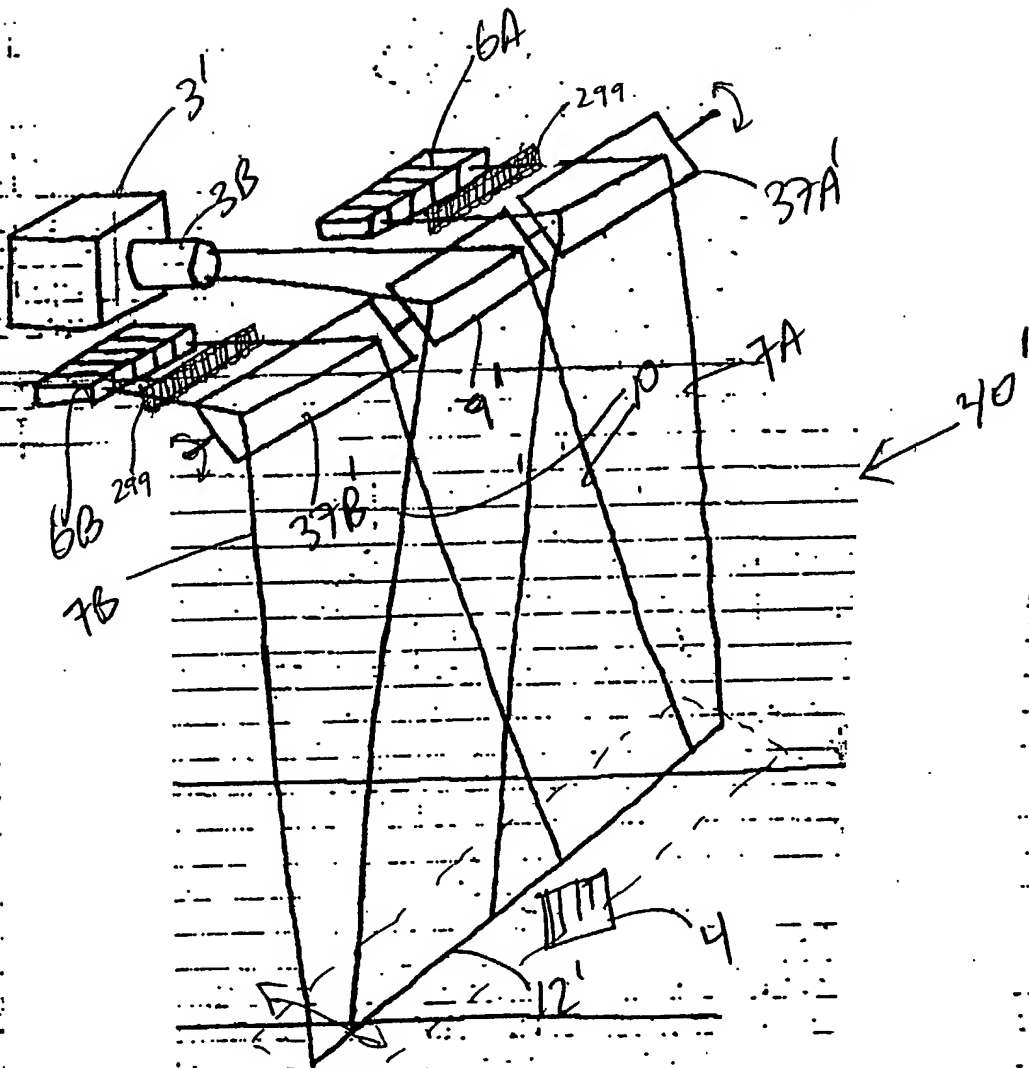


FIG. 2II

129/385



3-D
Examining
Region

FIG 2I2

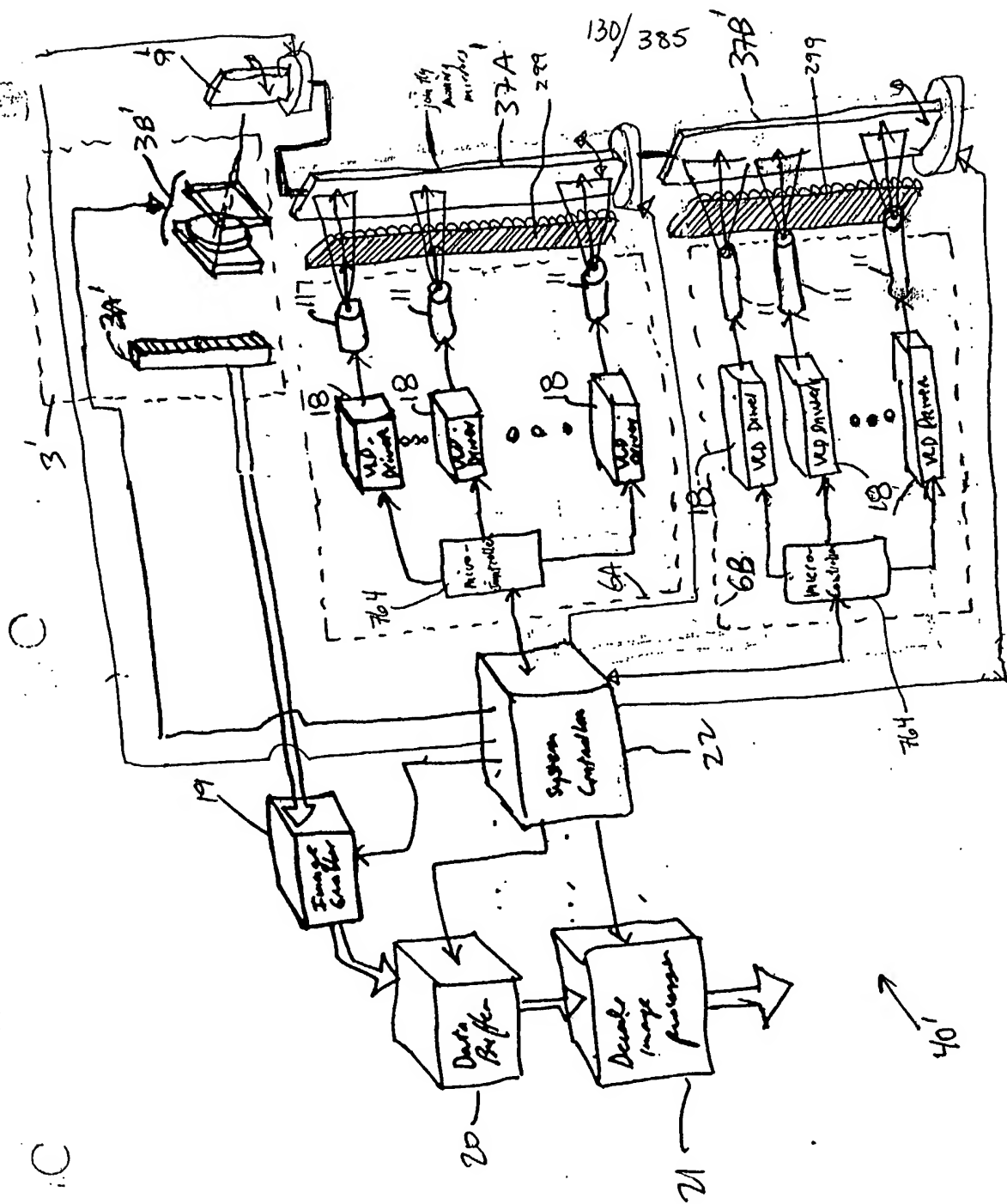


FIG. 2I3

131/385

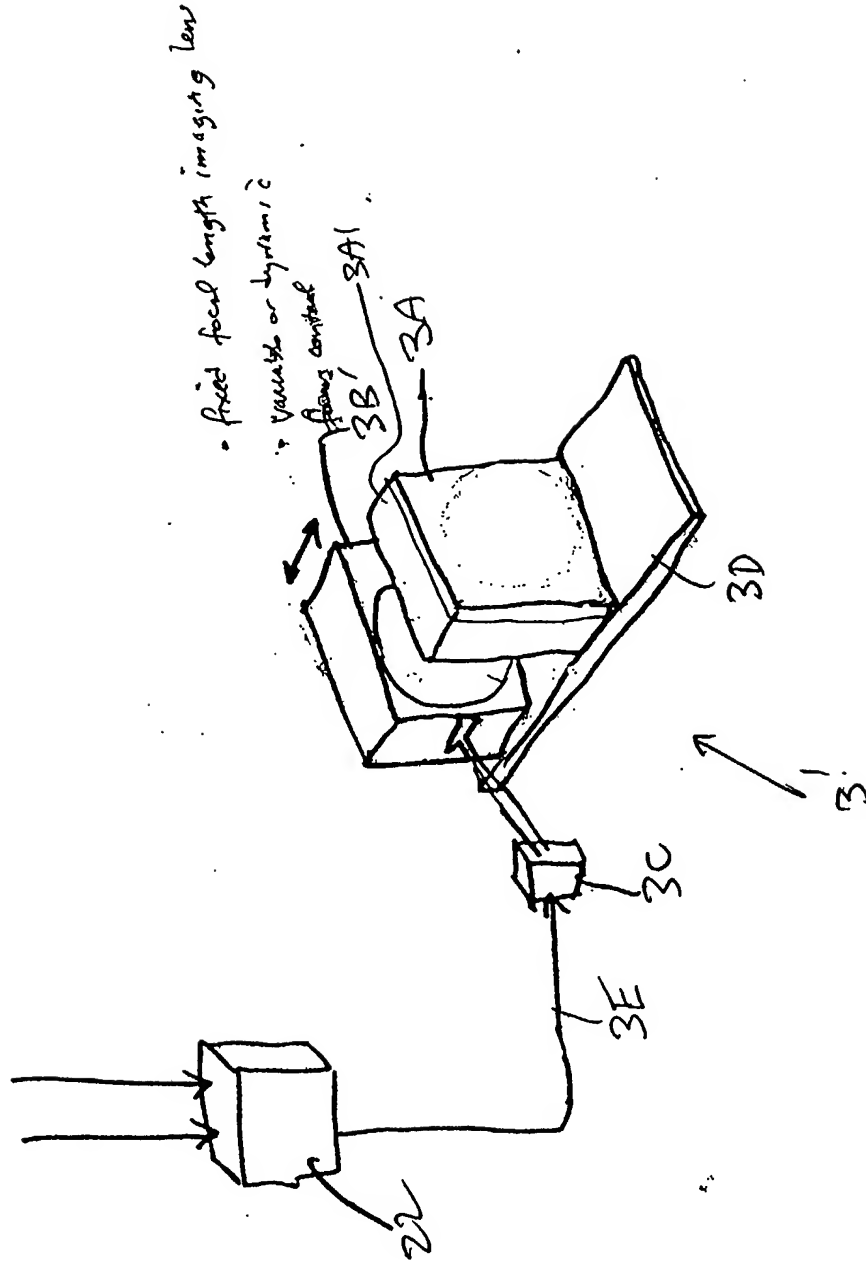
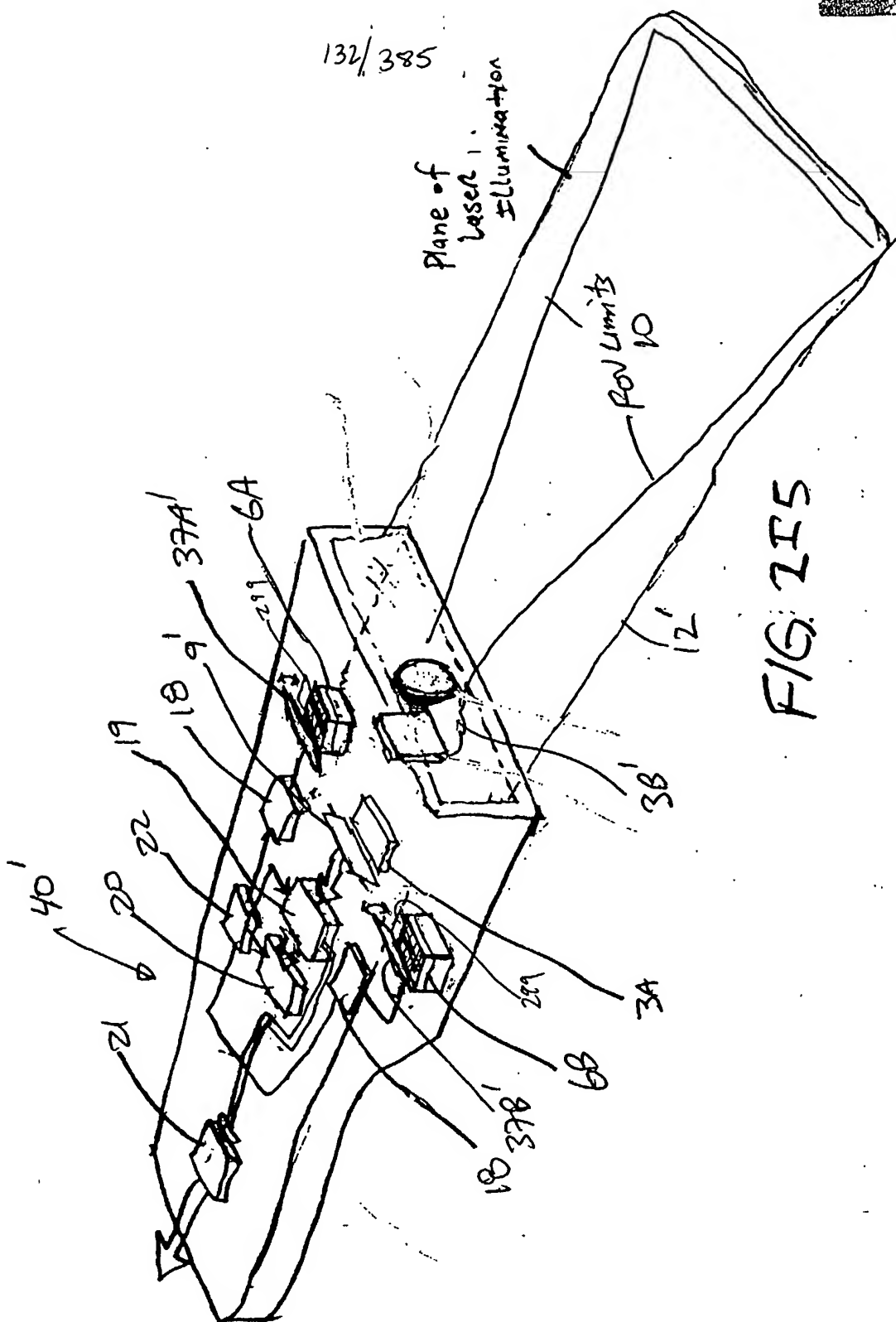


FIG. 2I4



133/385

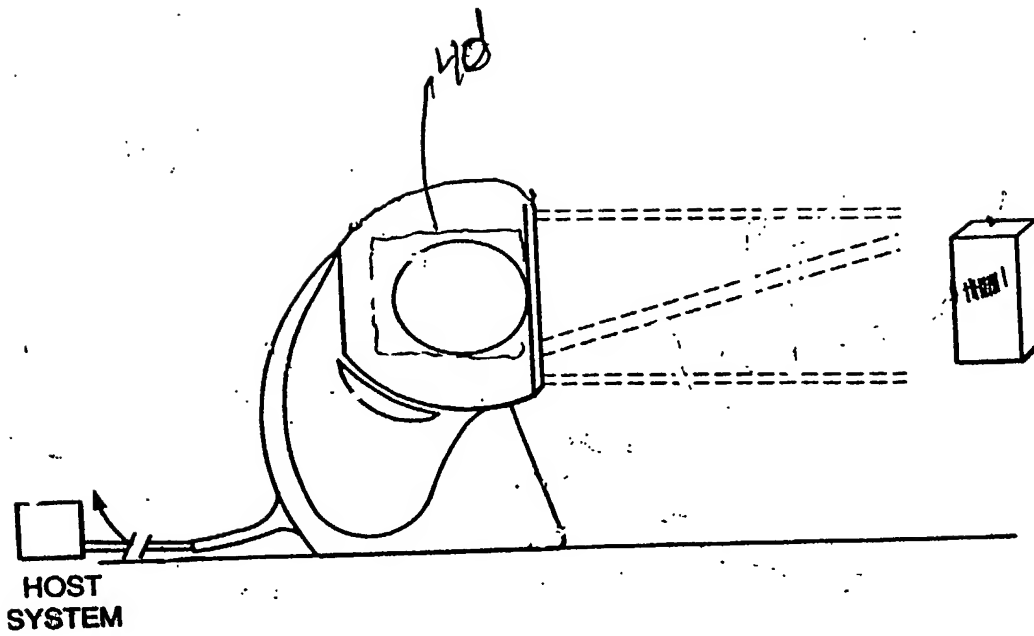
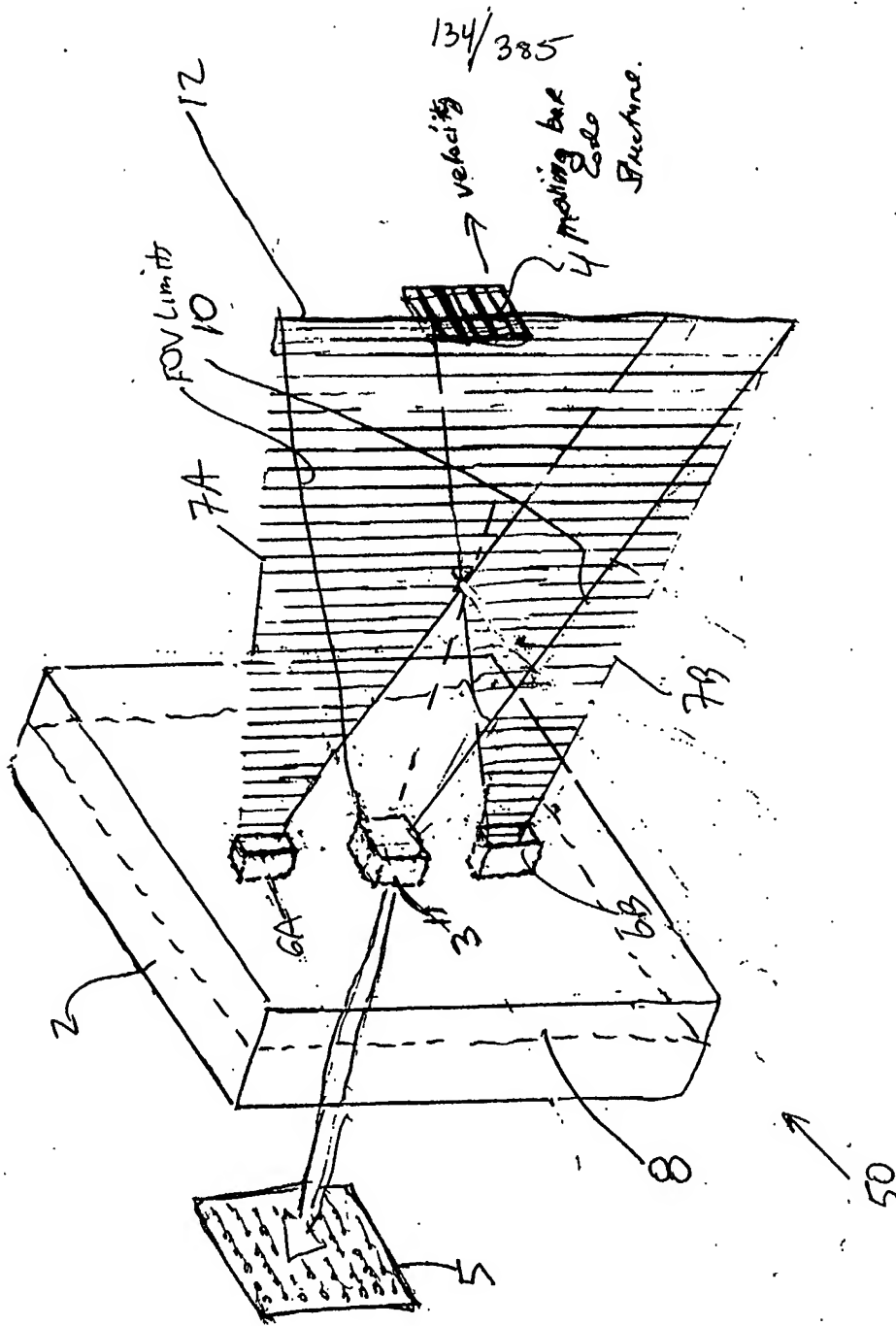


FIG. 2I6



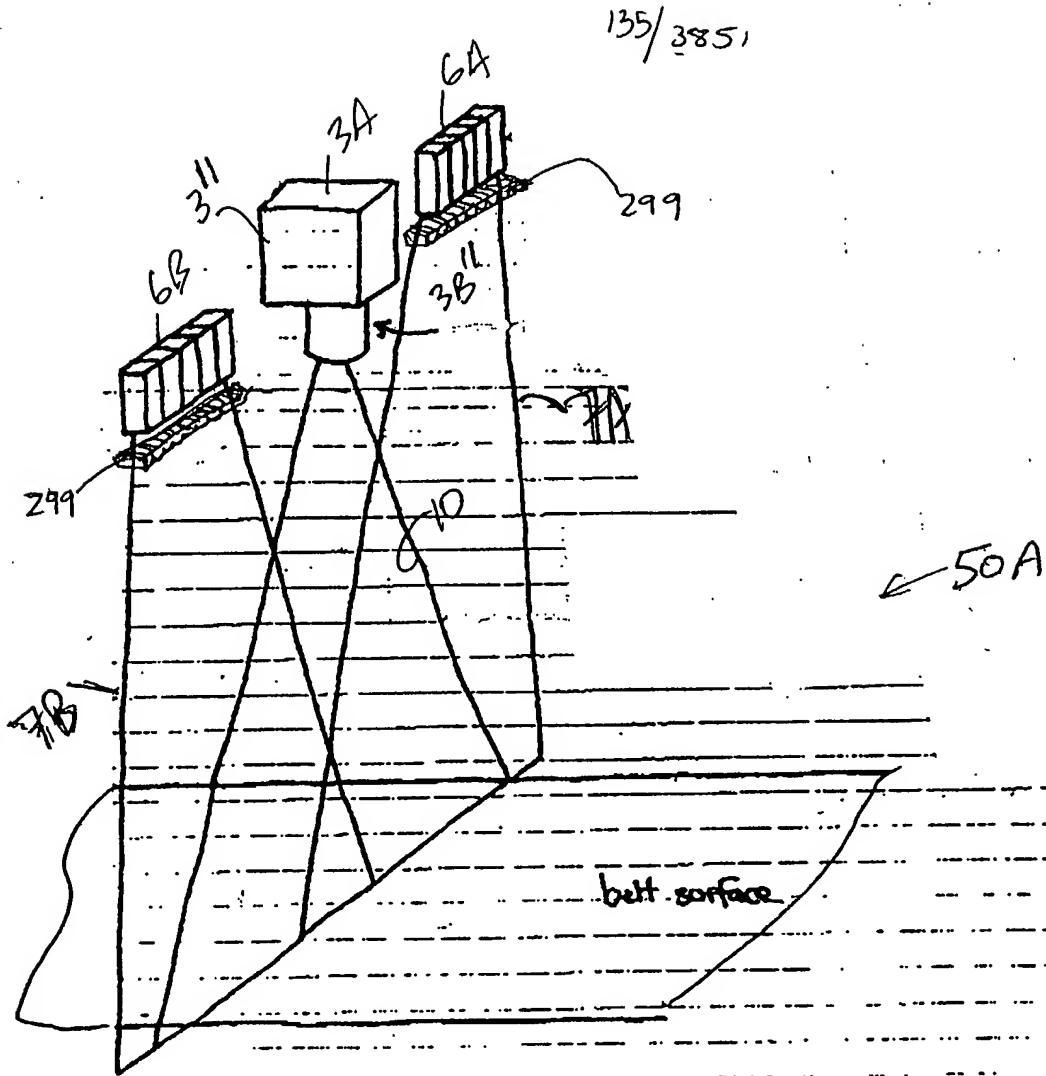
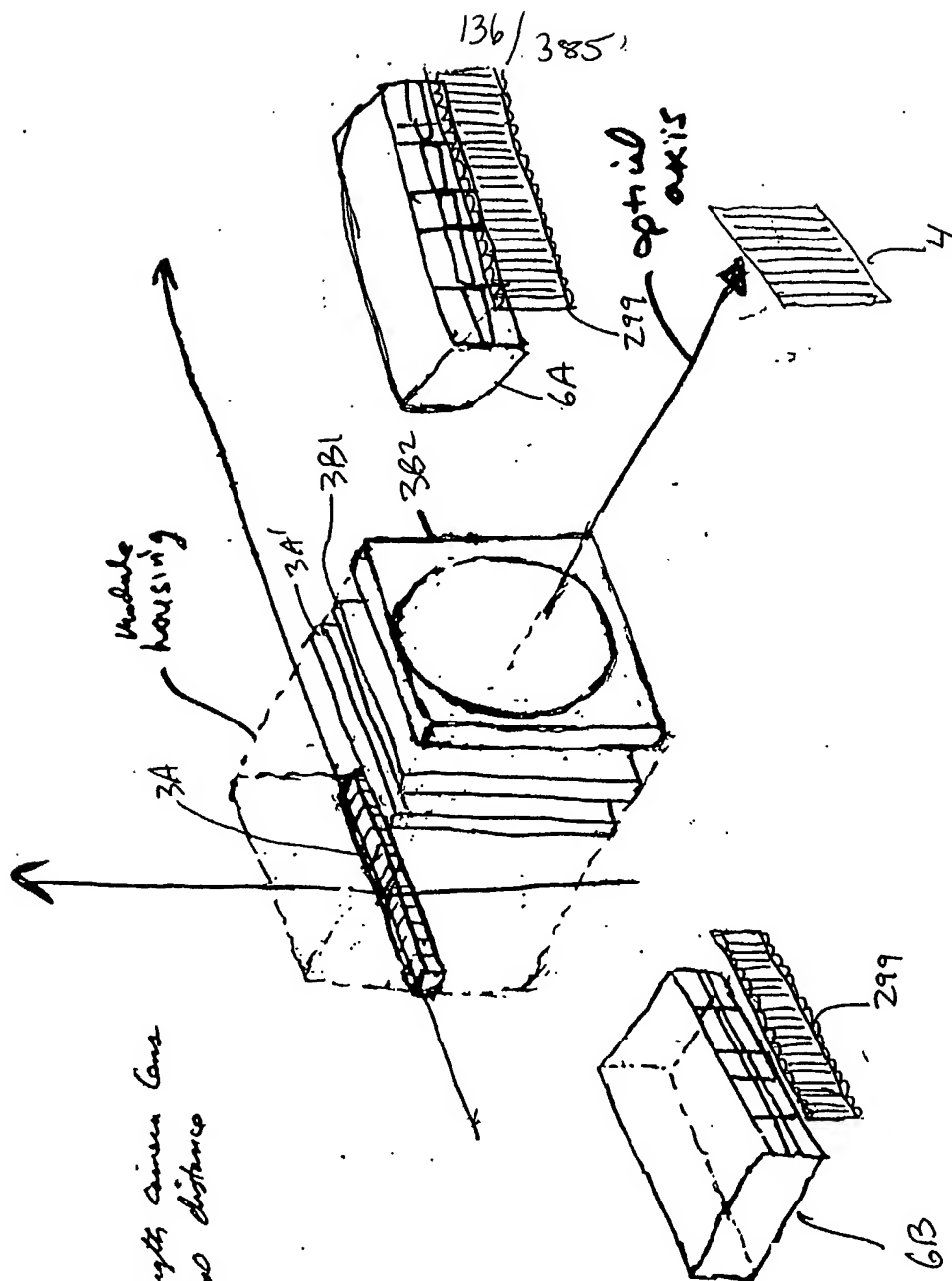
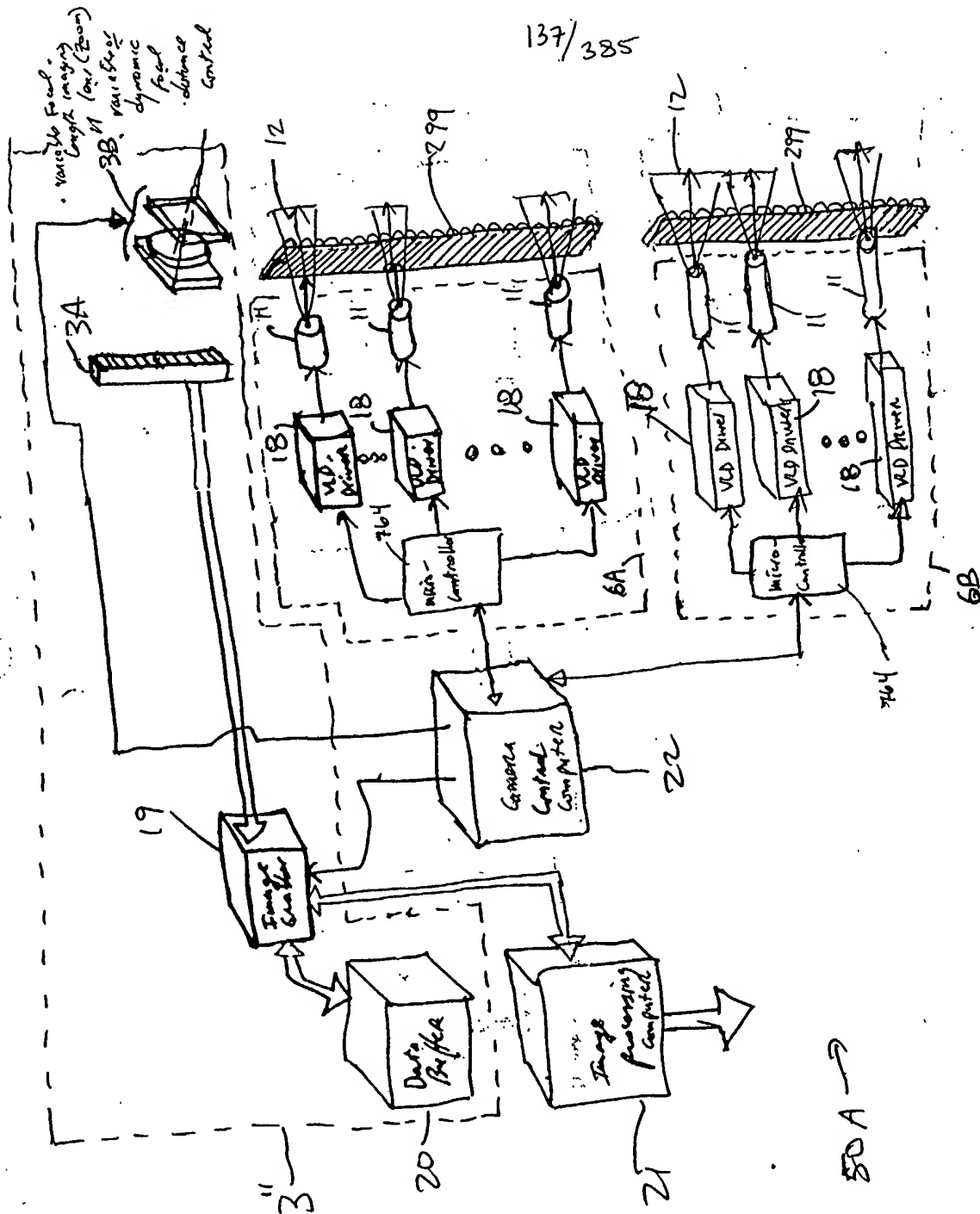


FIG. 3B1



(1) variable focal length camera lens
(2) variable focus distance

FIG. 3B2

$$137 \overline{) 385}$$


↑
A
B

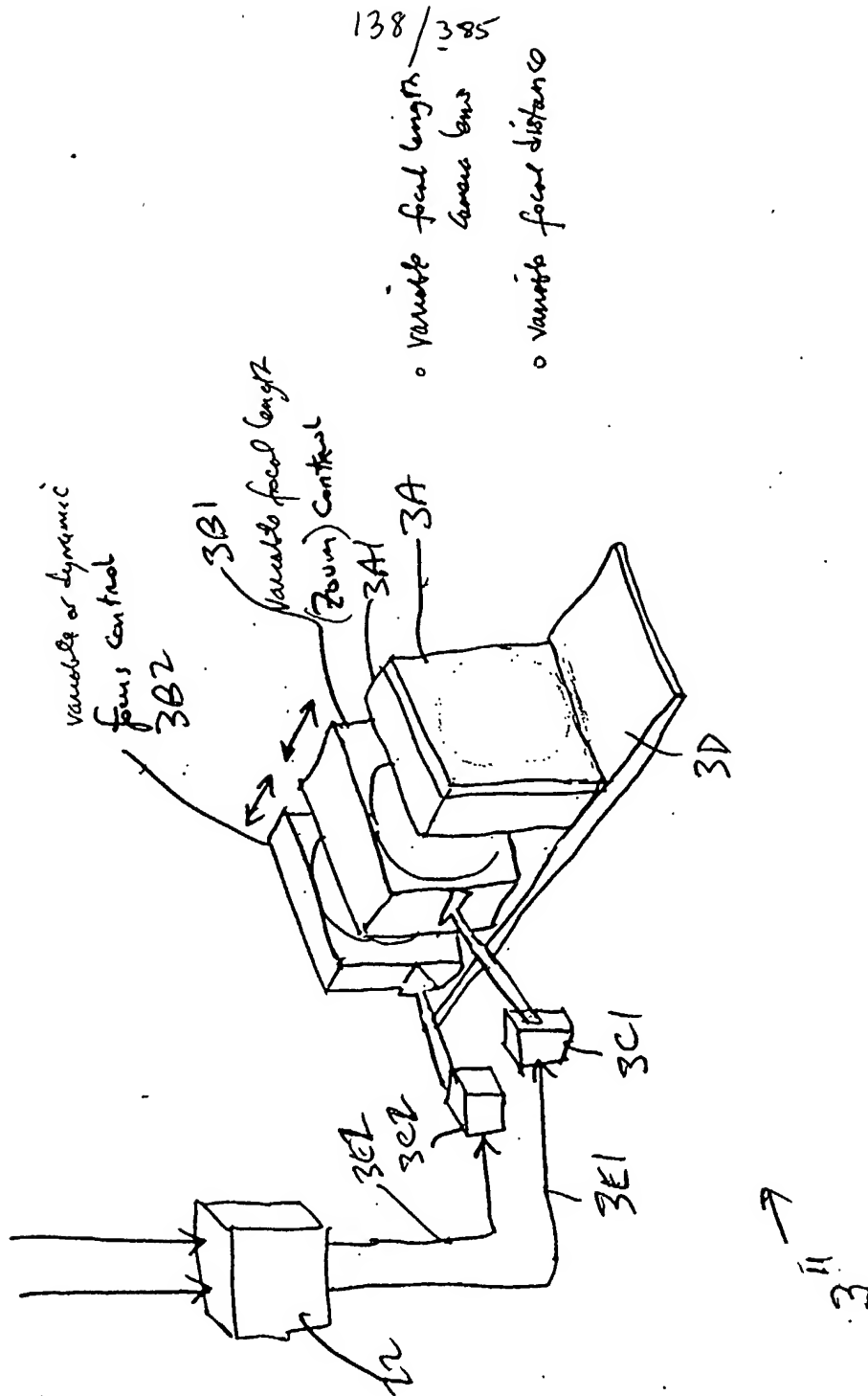
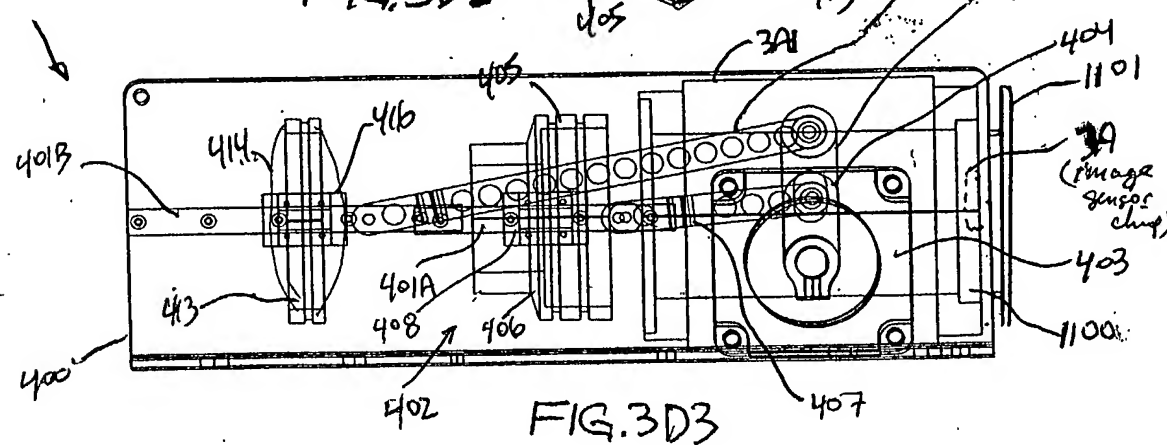
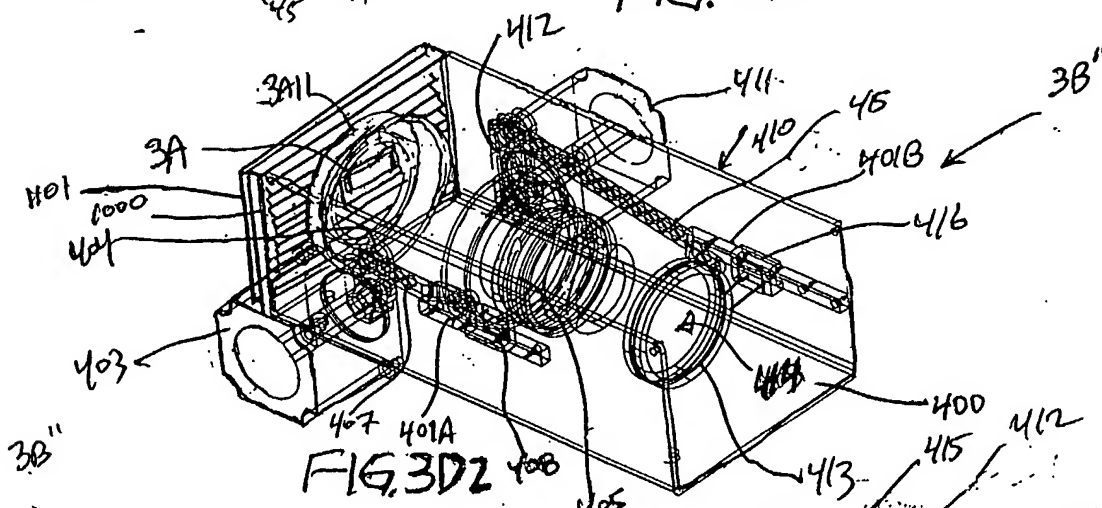
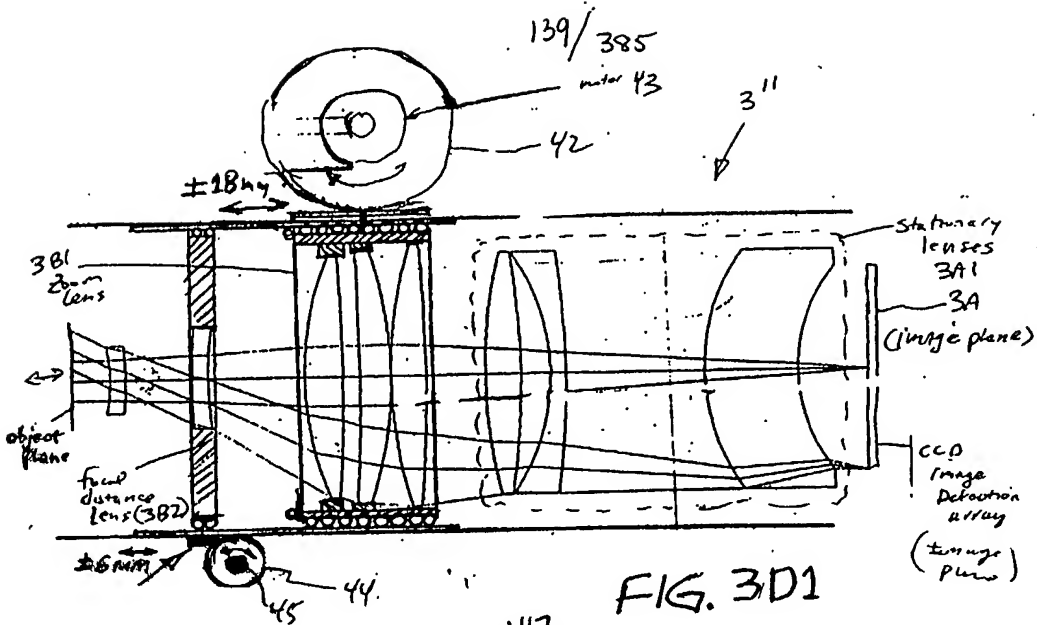
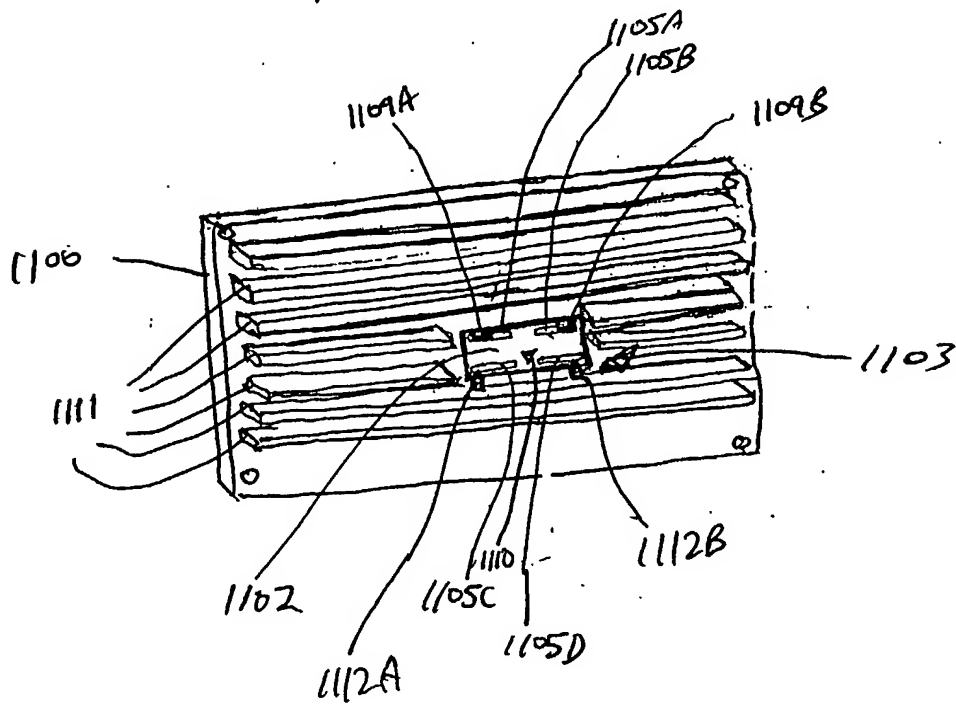
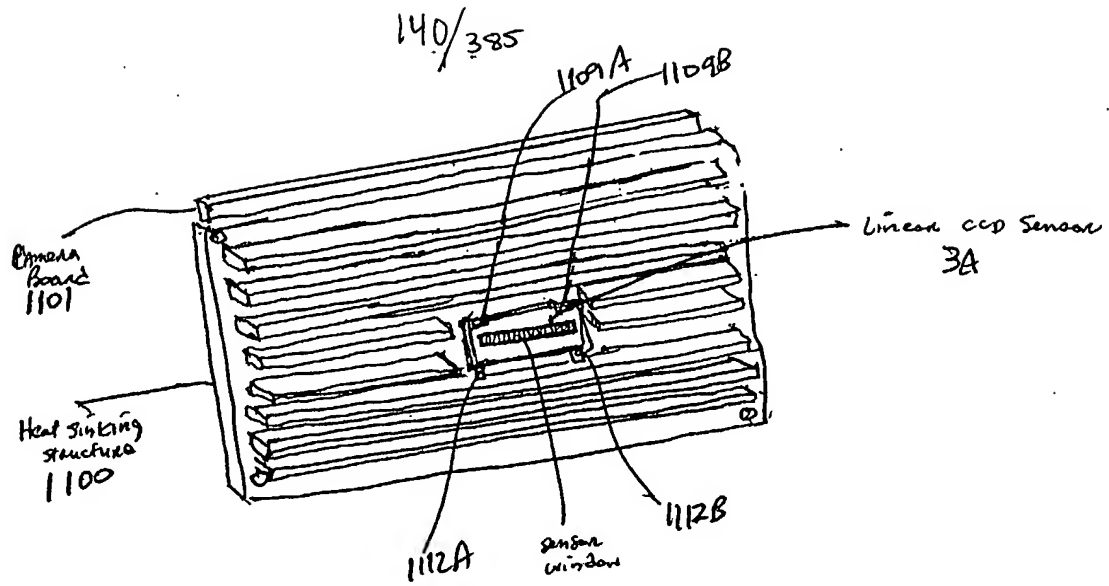


FIG. 3CZ





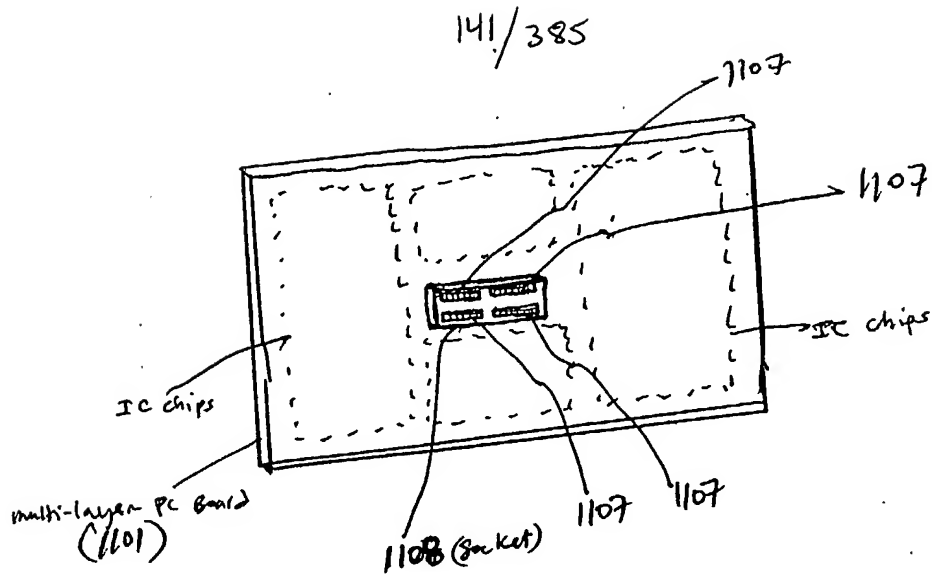


FIG. 3D6

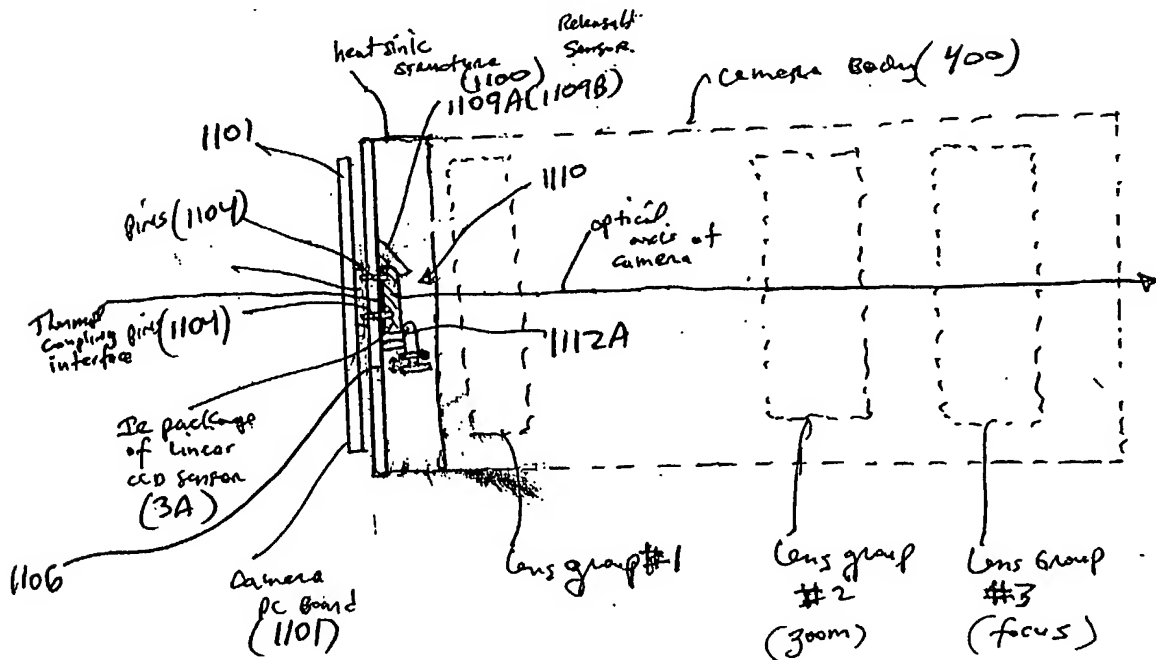
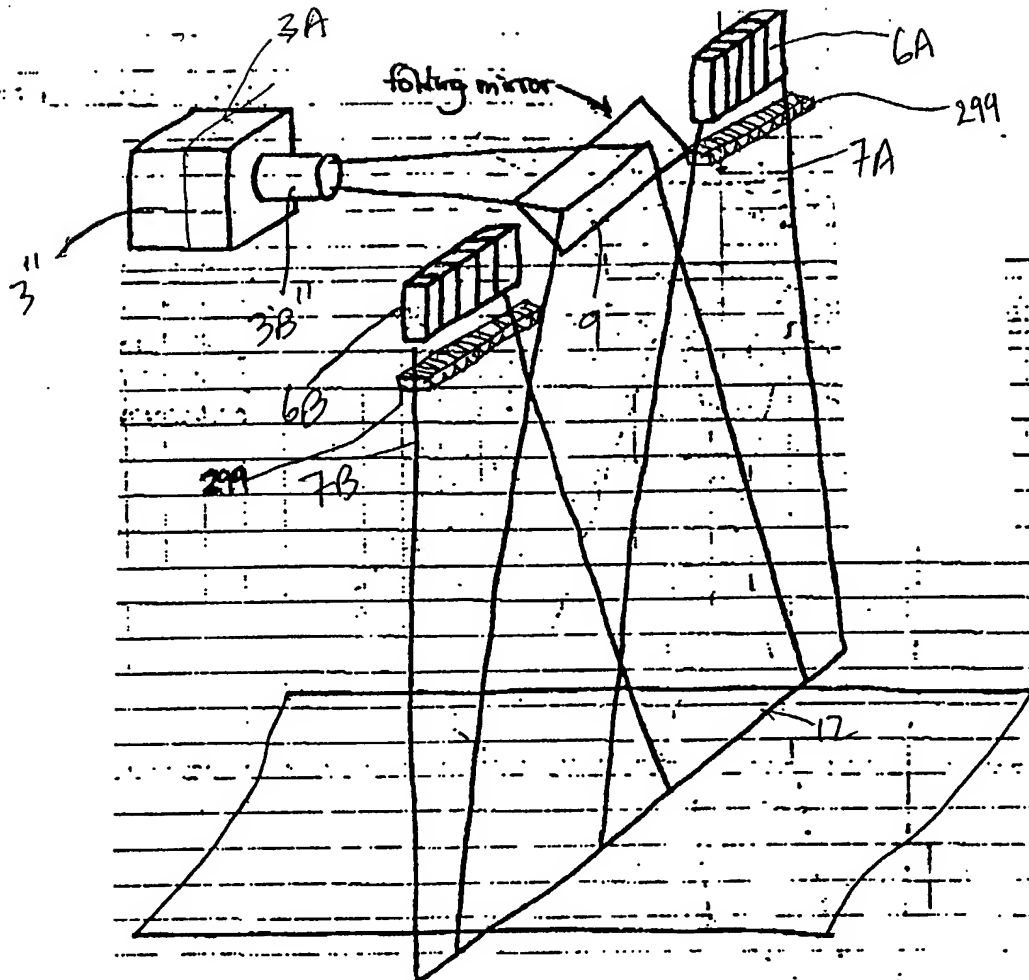


FIG. 3D7

142/385



50B

FIG. 3E1

144/385

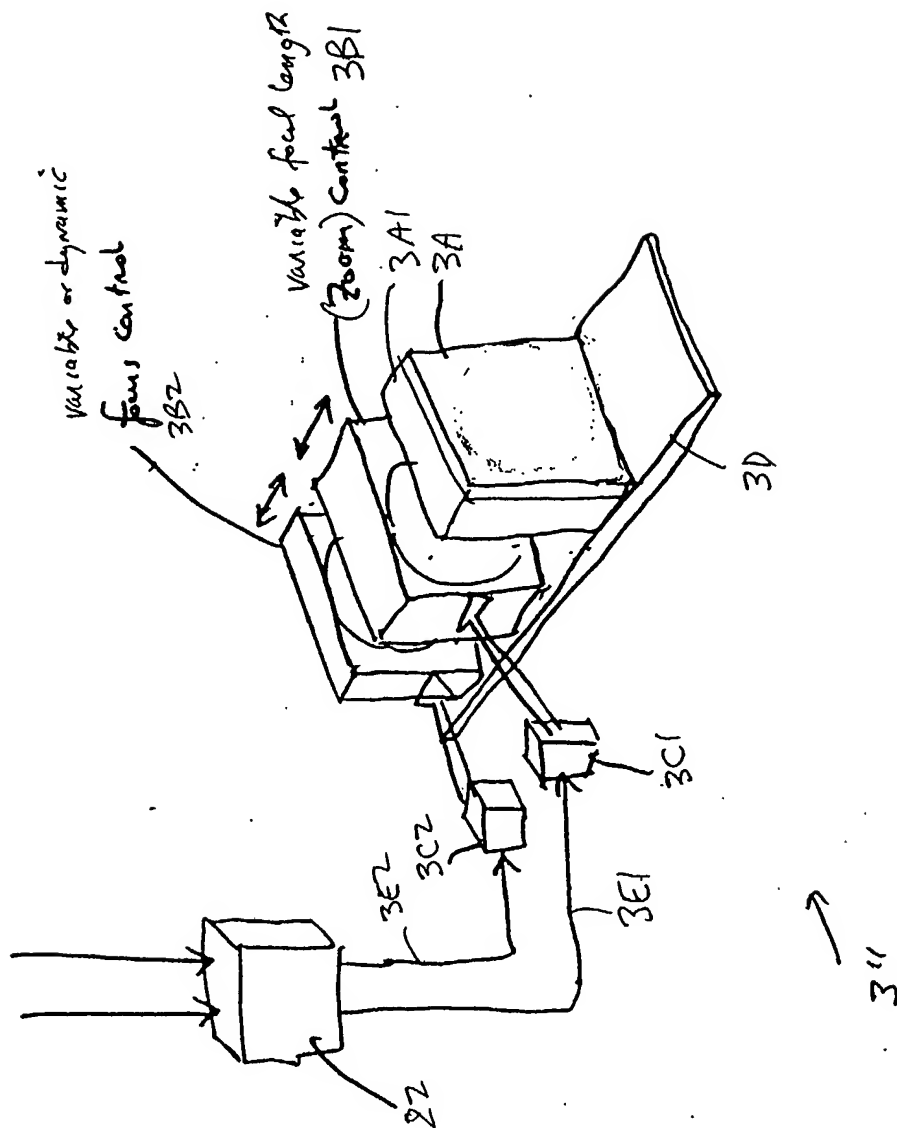
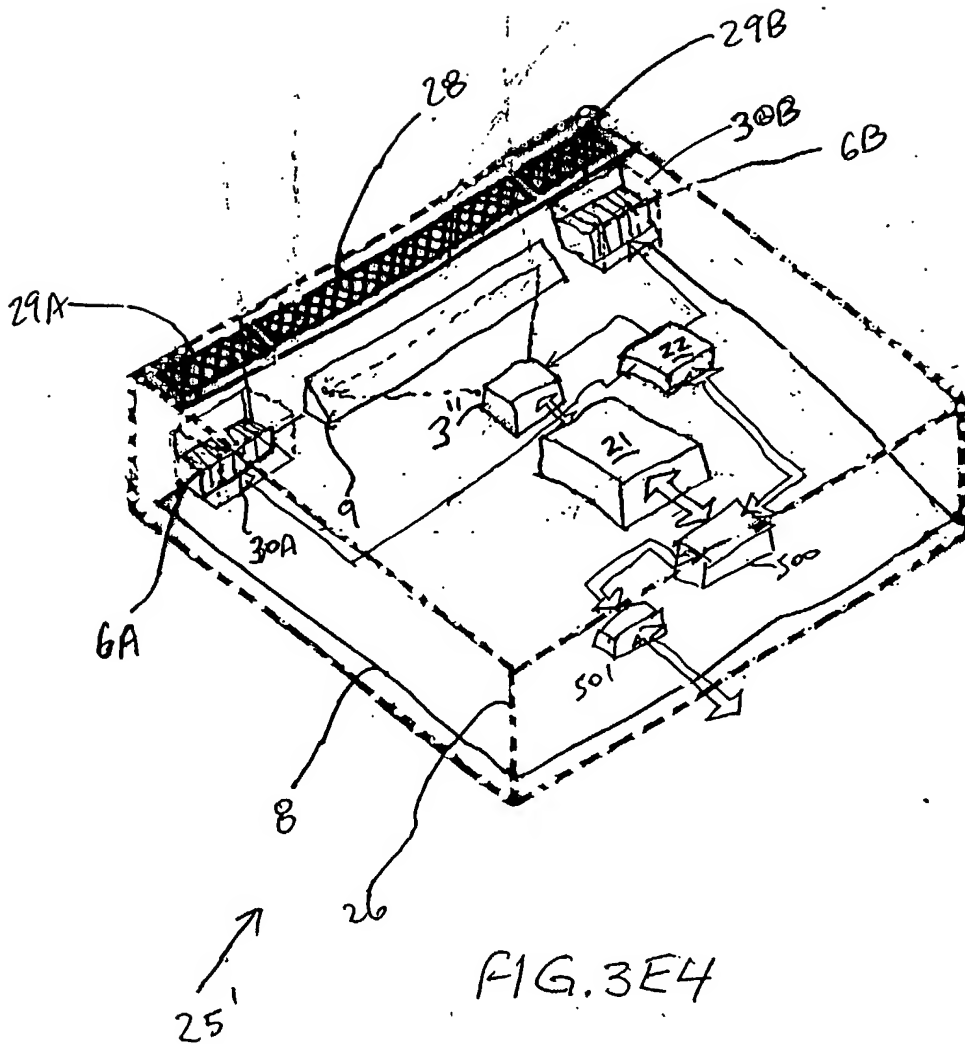


FIG. 3E3

145/385,



146/385

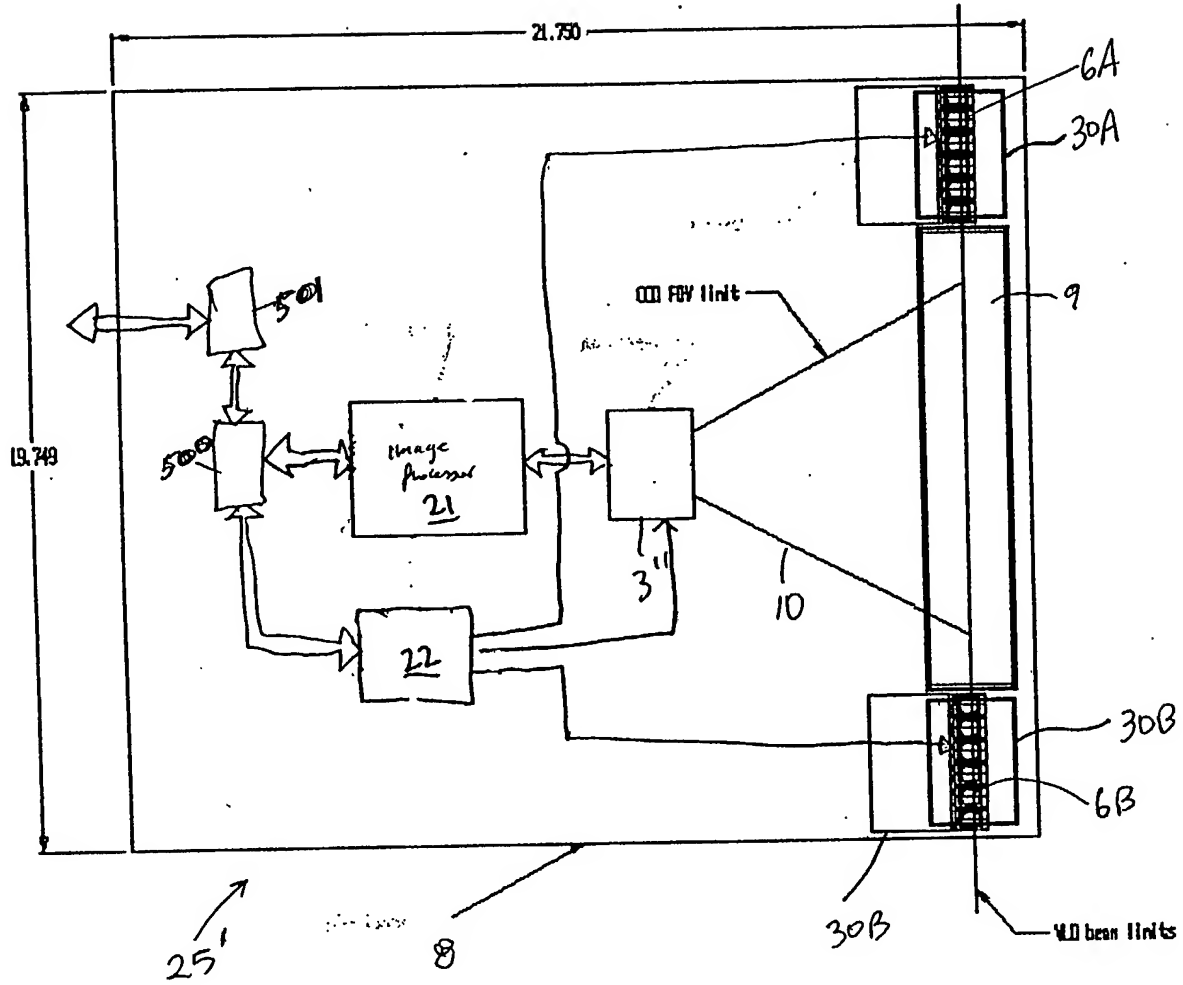


FIG. 3E5

147/385

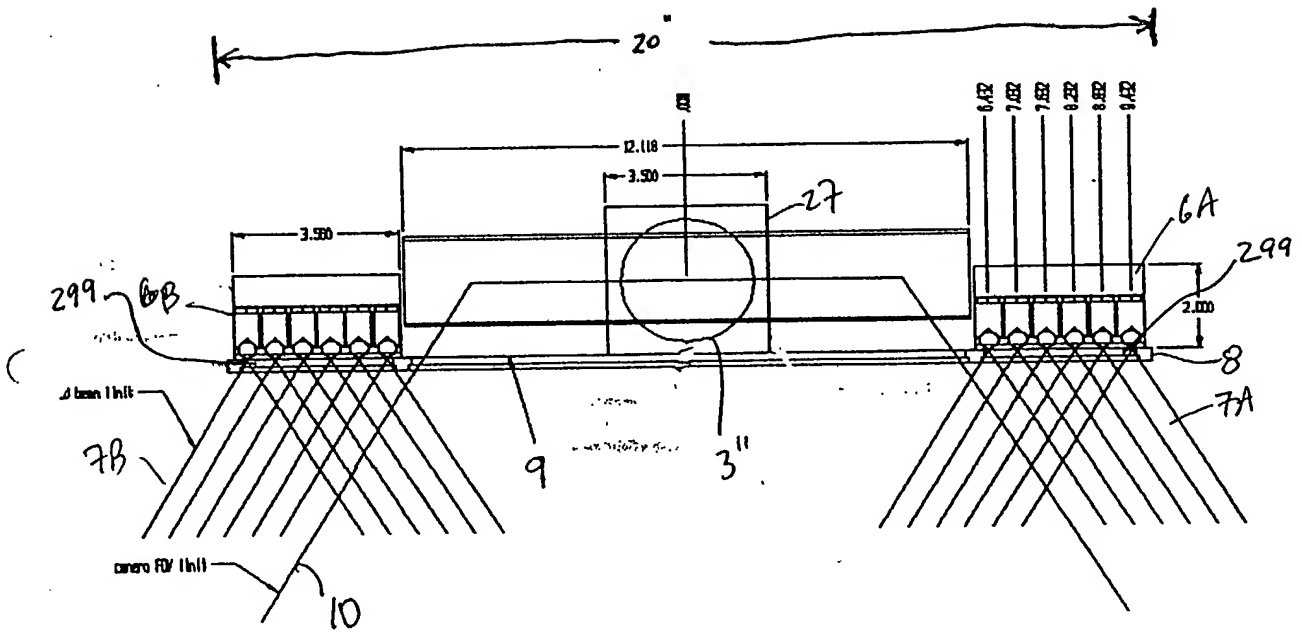


FIG. 3E6

148/385

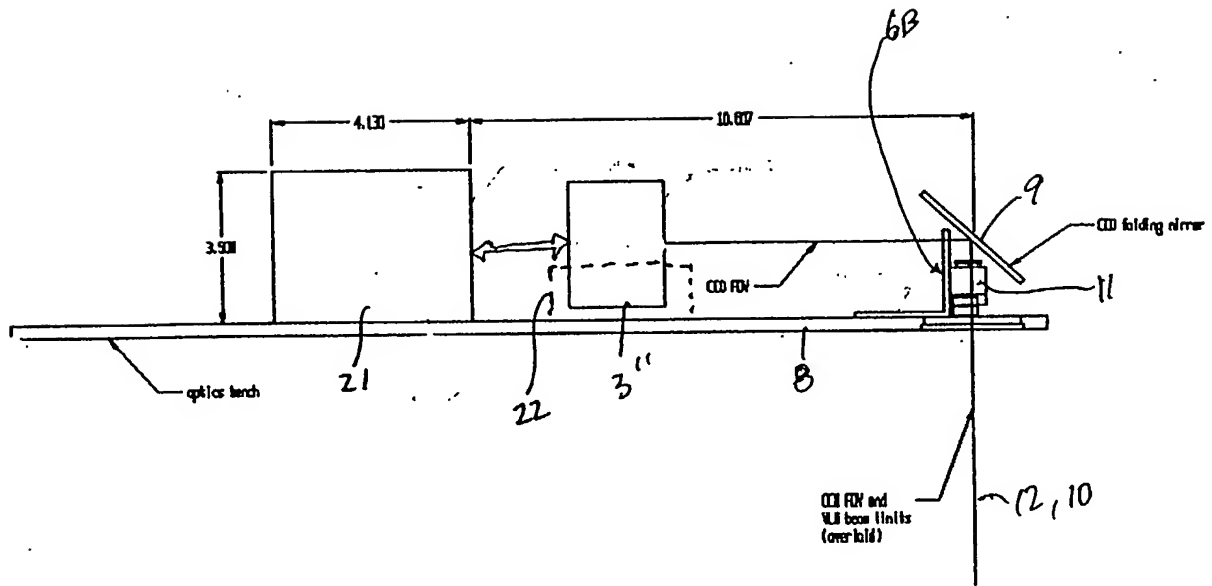


FIG. 3E7

149/385

*variable FOV

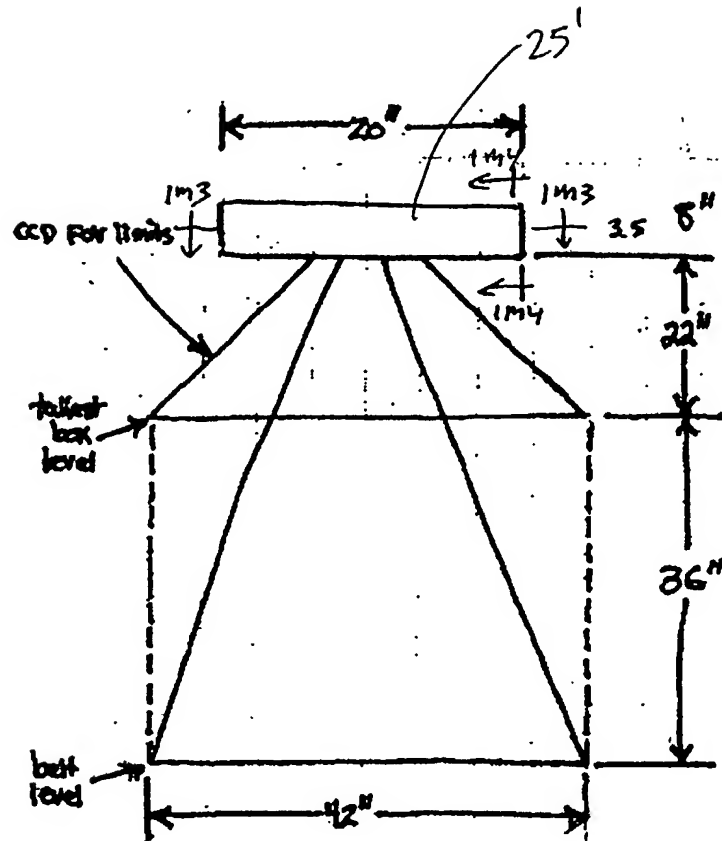


FIG. 3E8

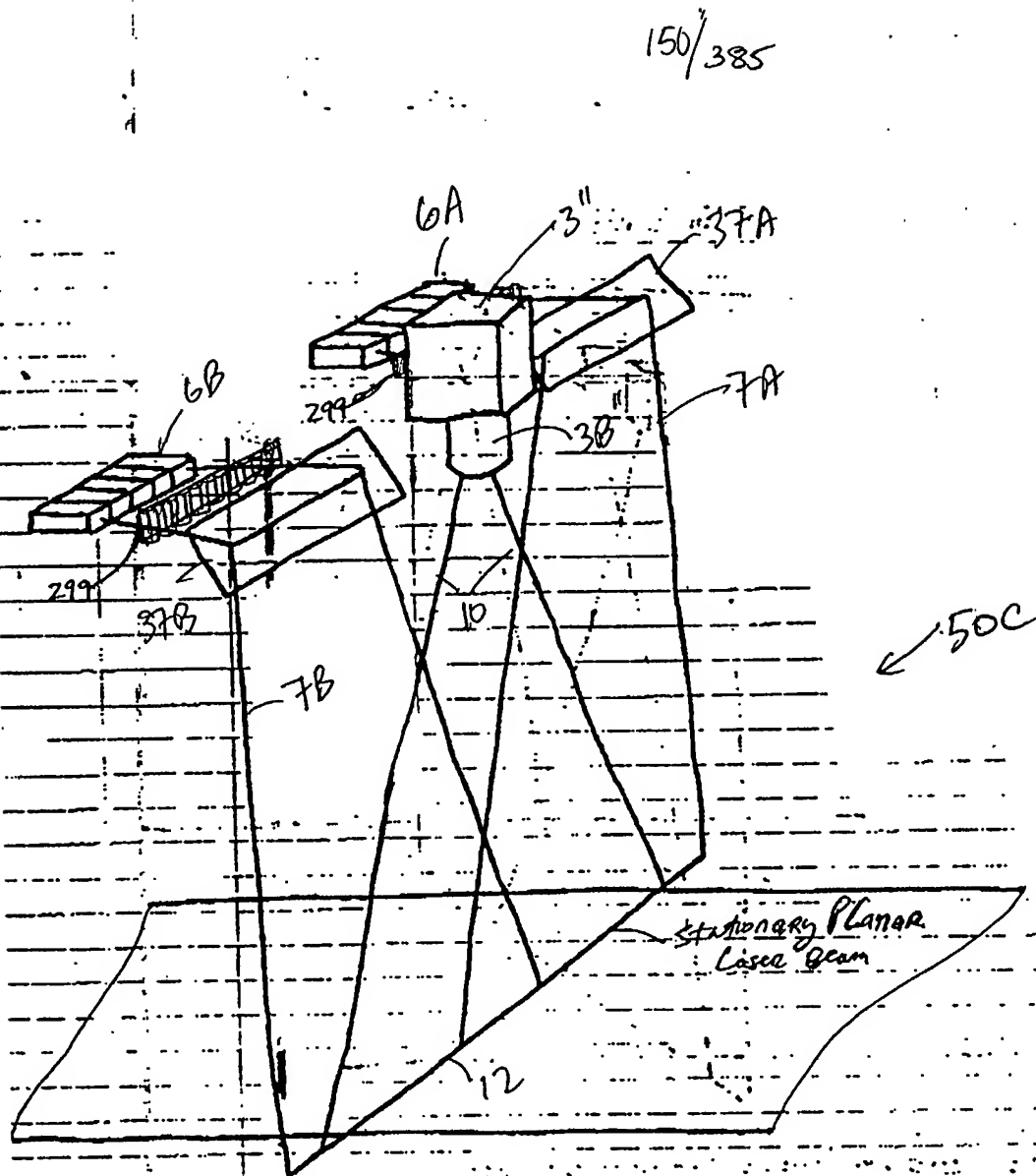
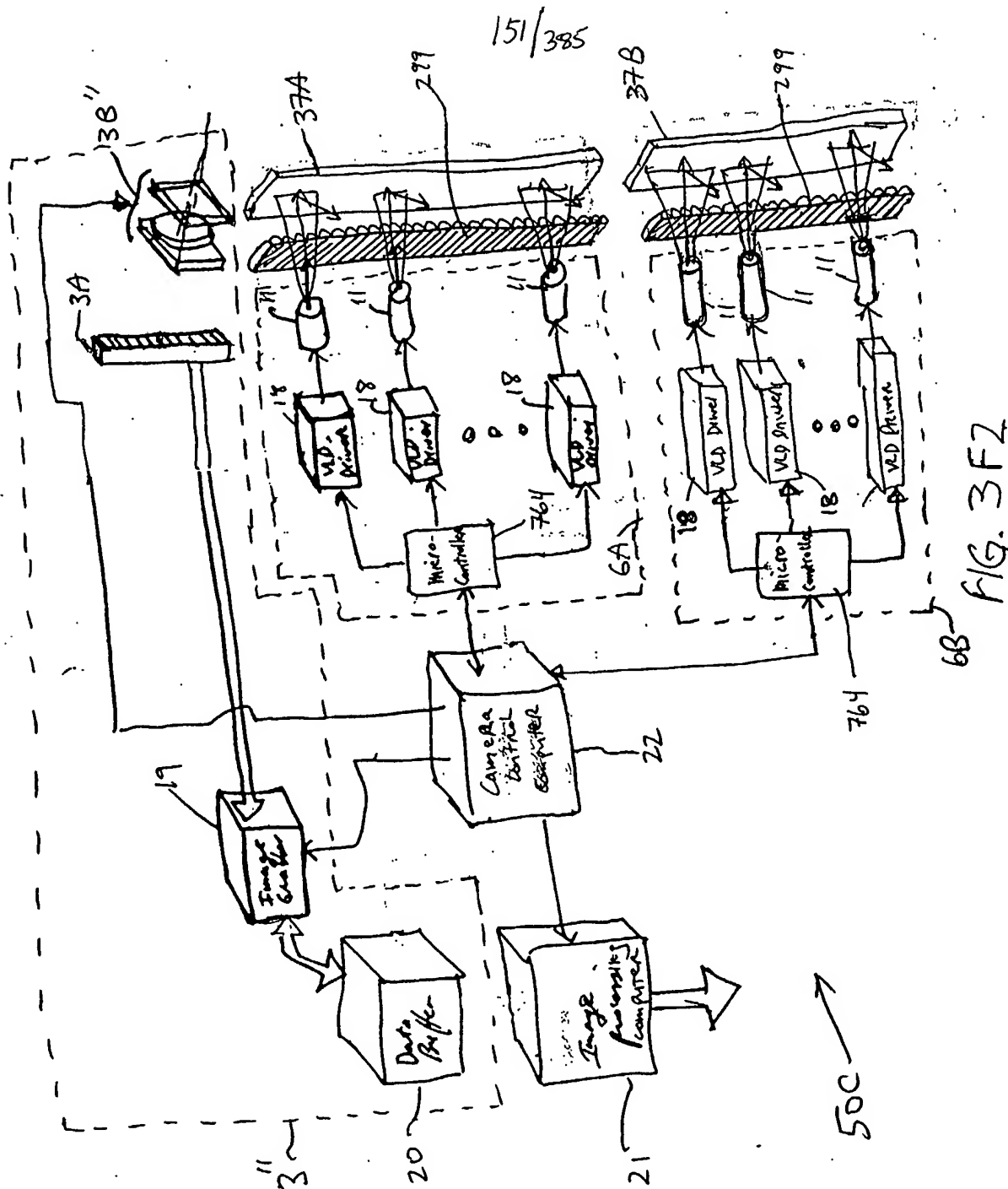


FIG. 3F1



152/385

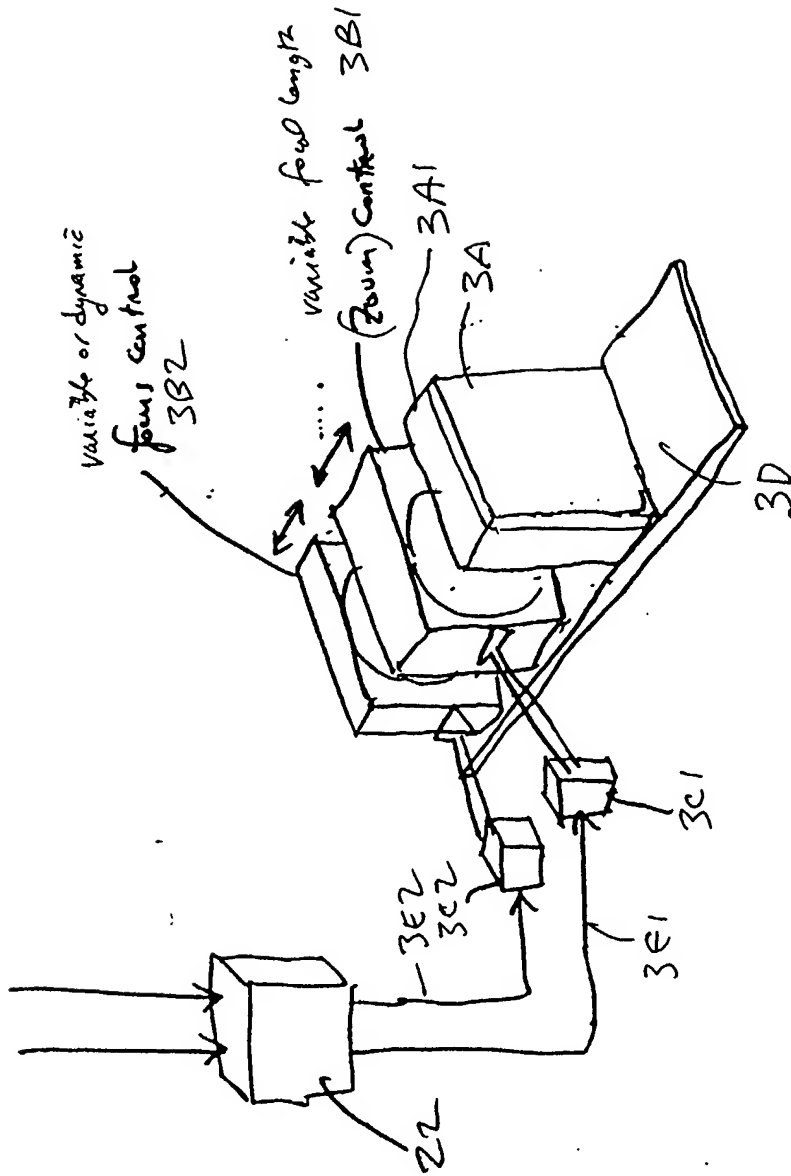


FIG. 3F3

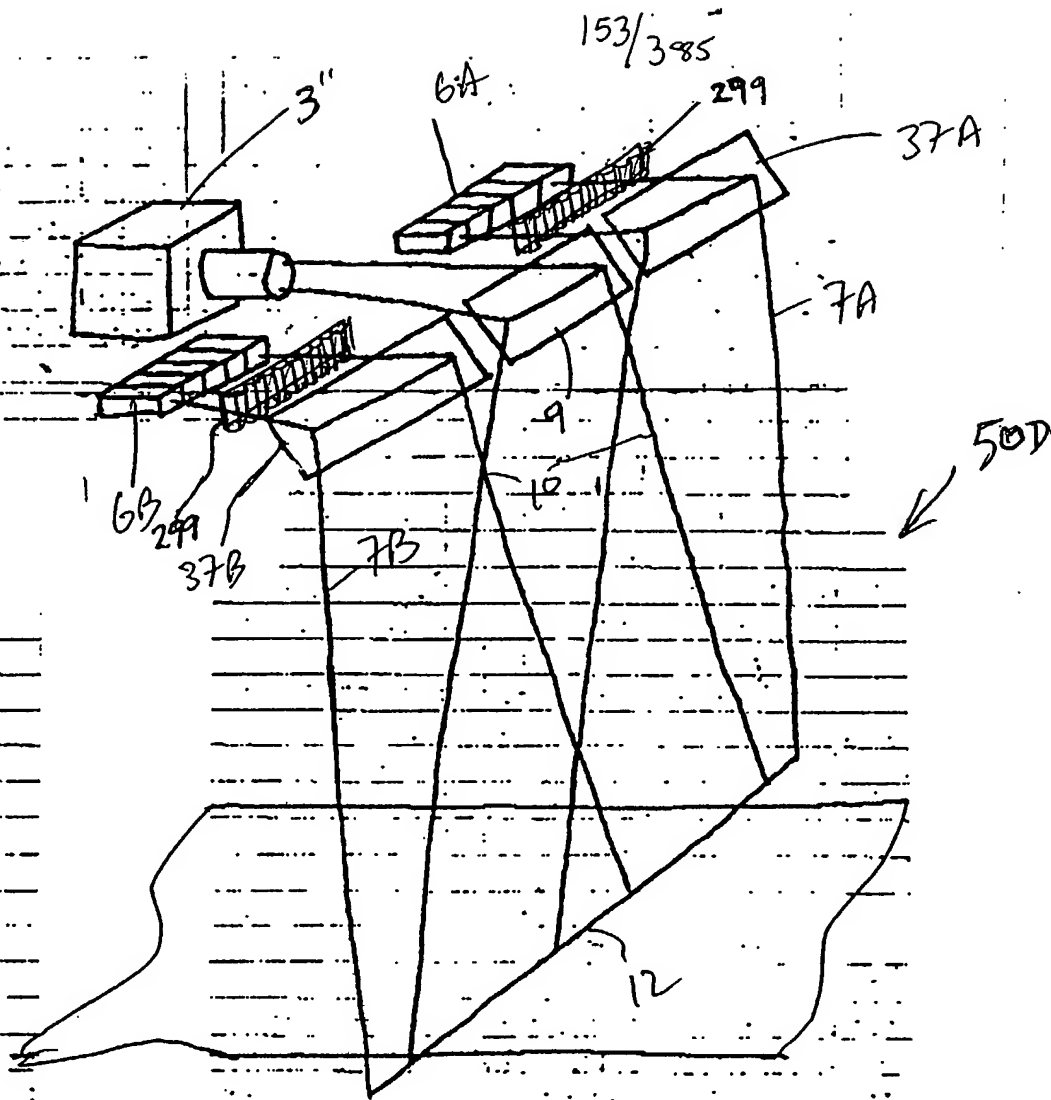


FIG. 351

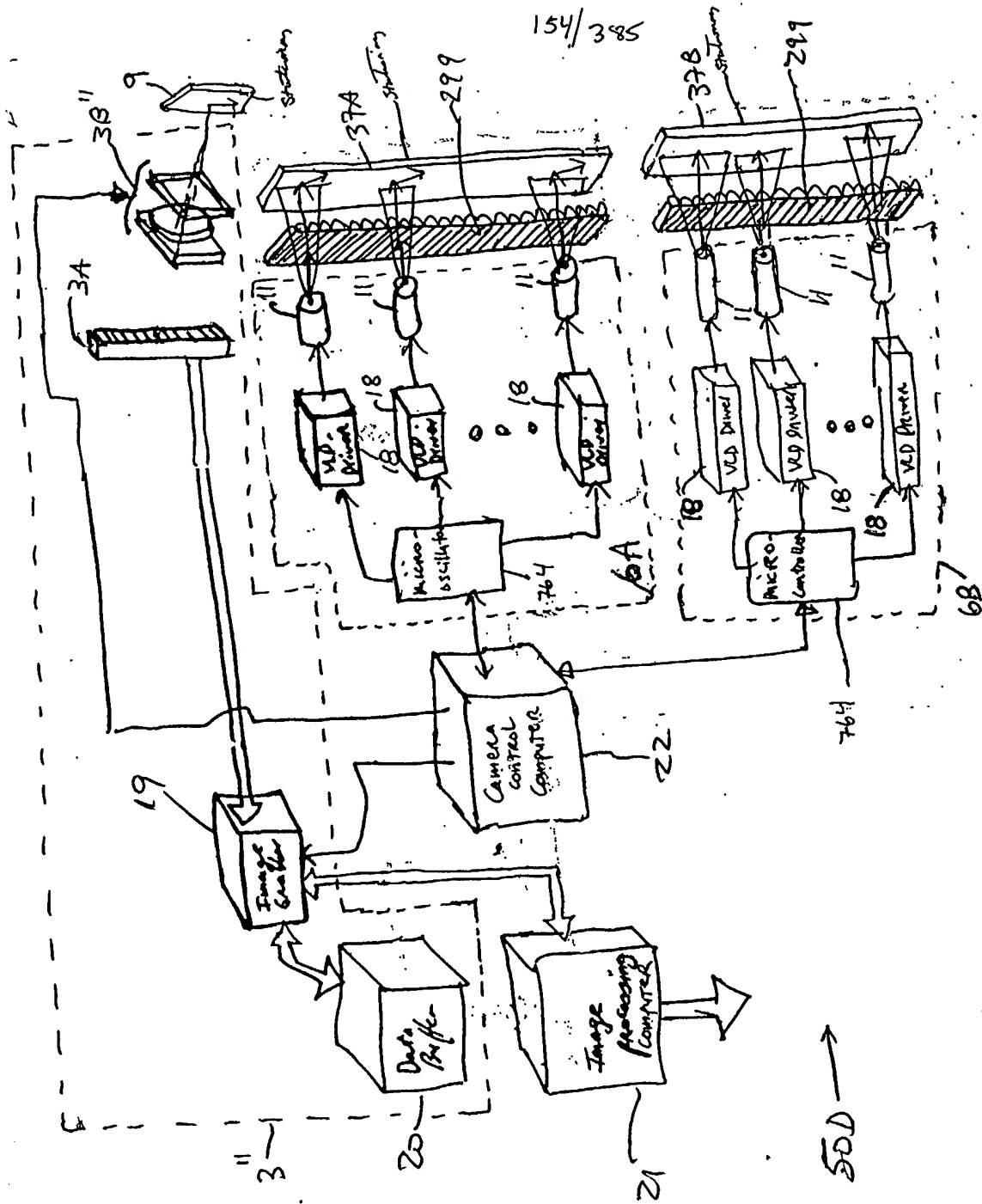


Fig. 362

155/385

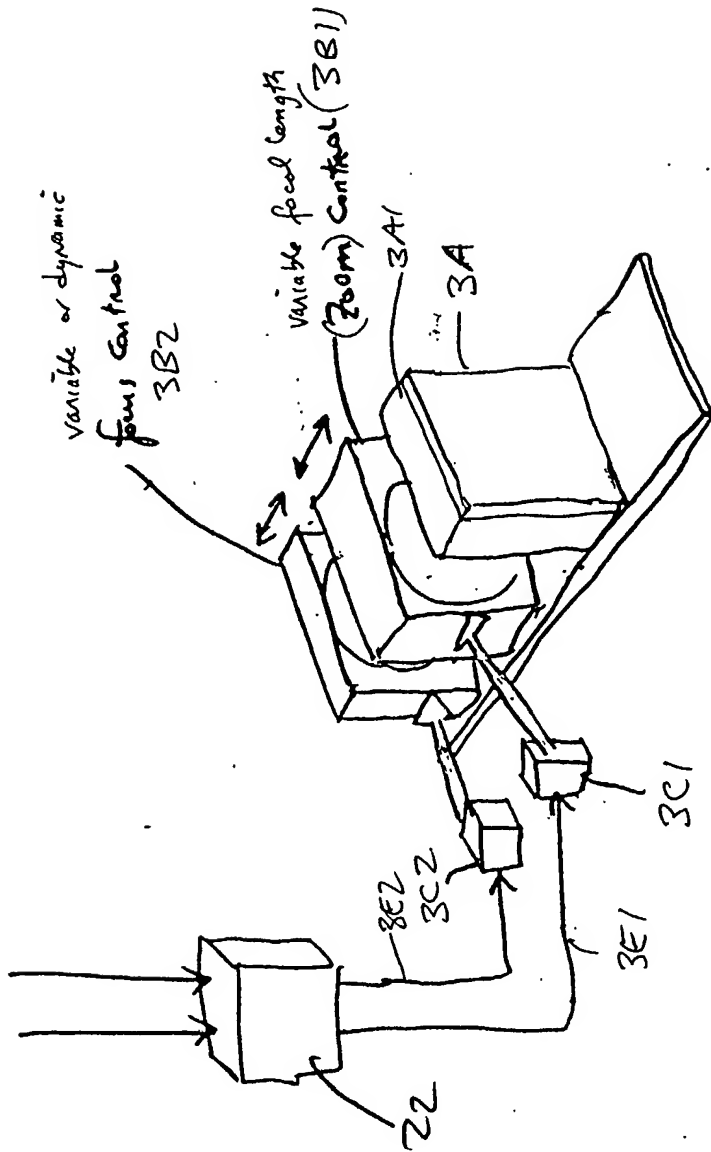


FIG. 393

156/385

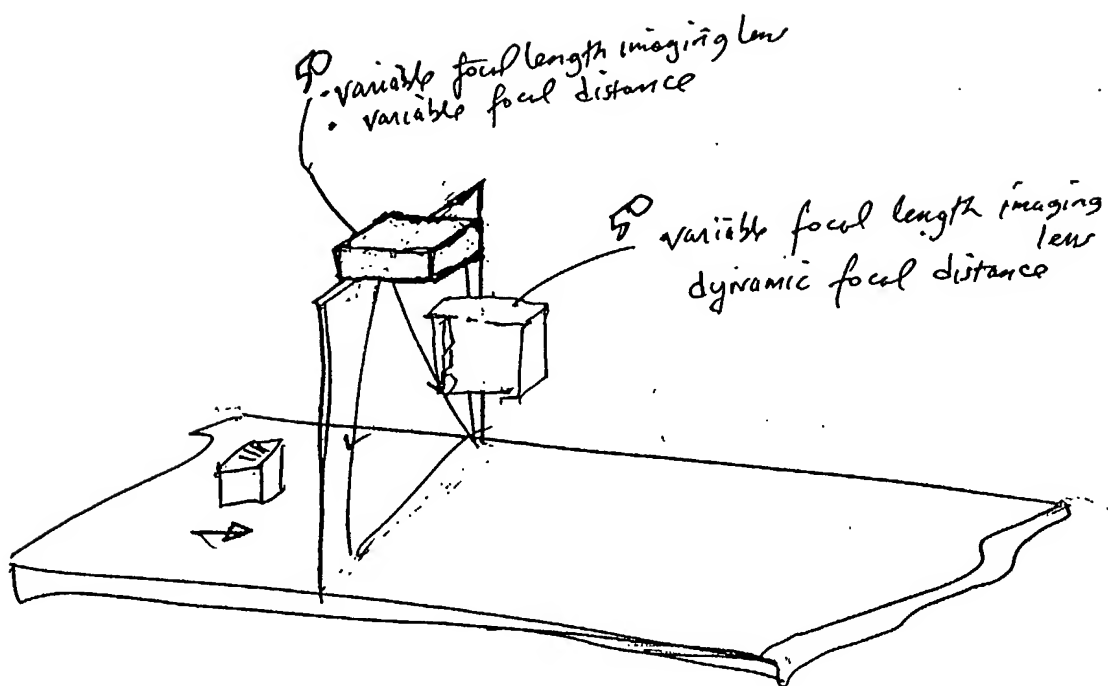


FIG. 3H

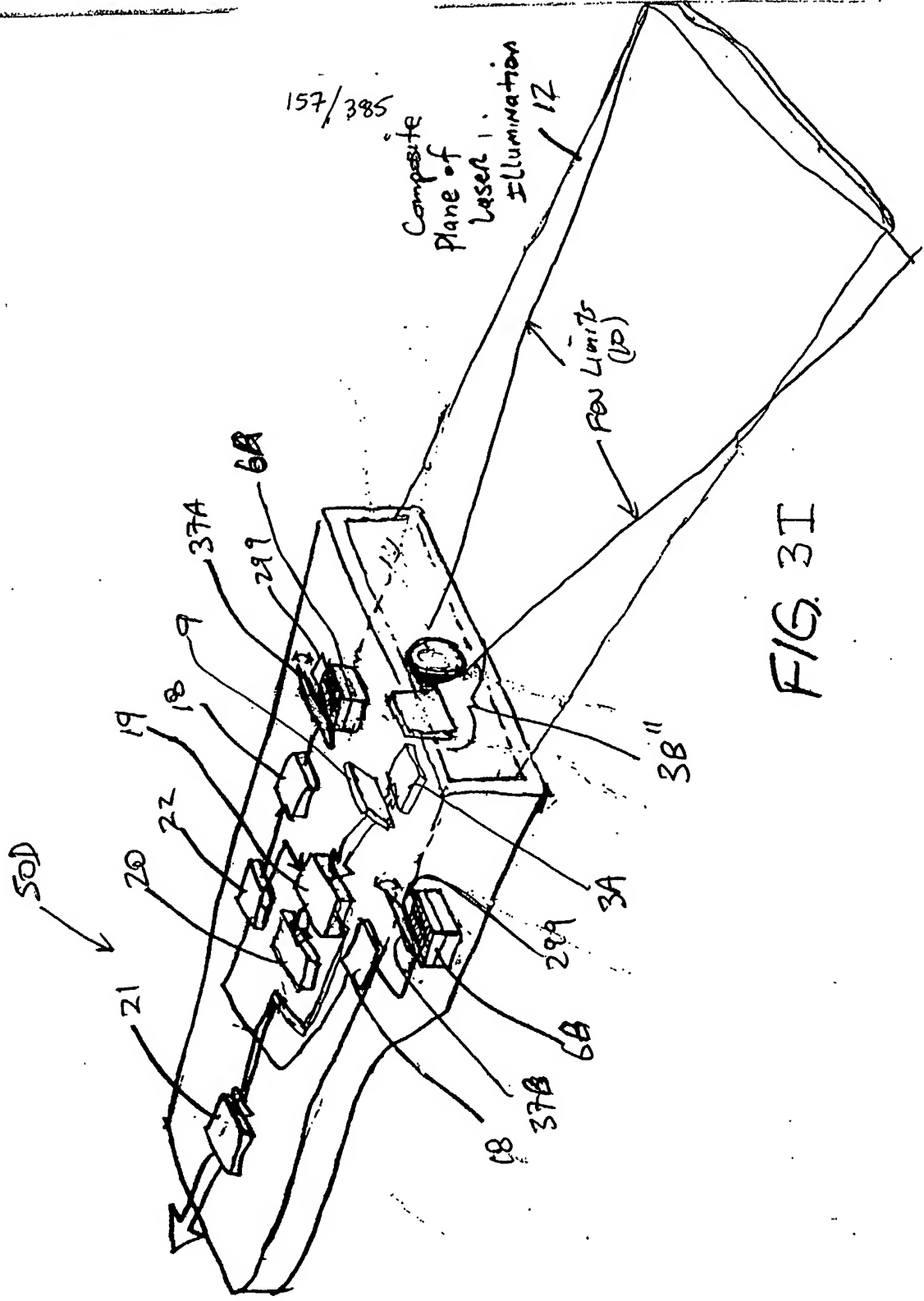


FIG. 3I

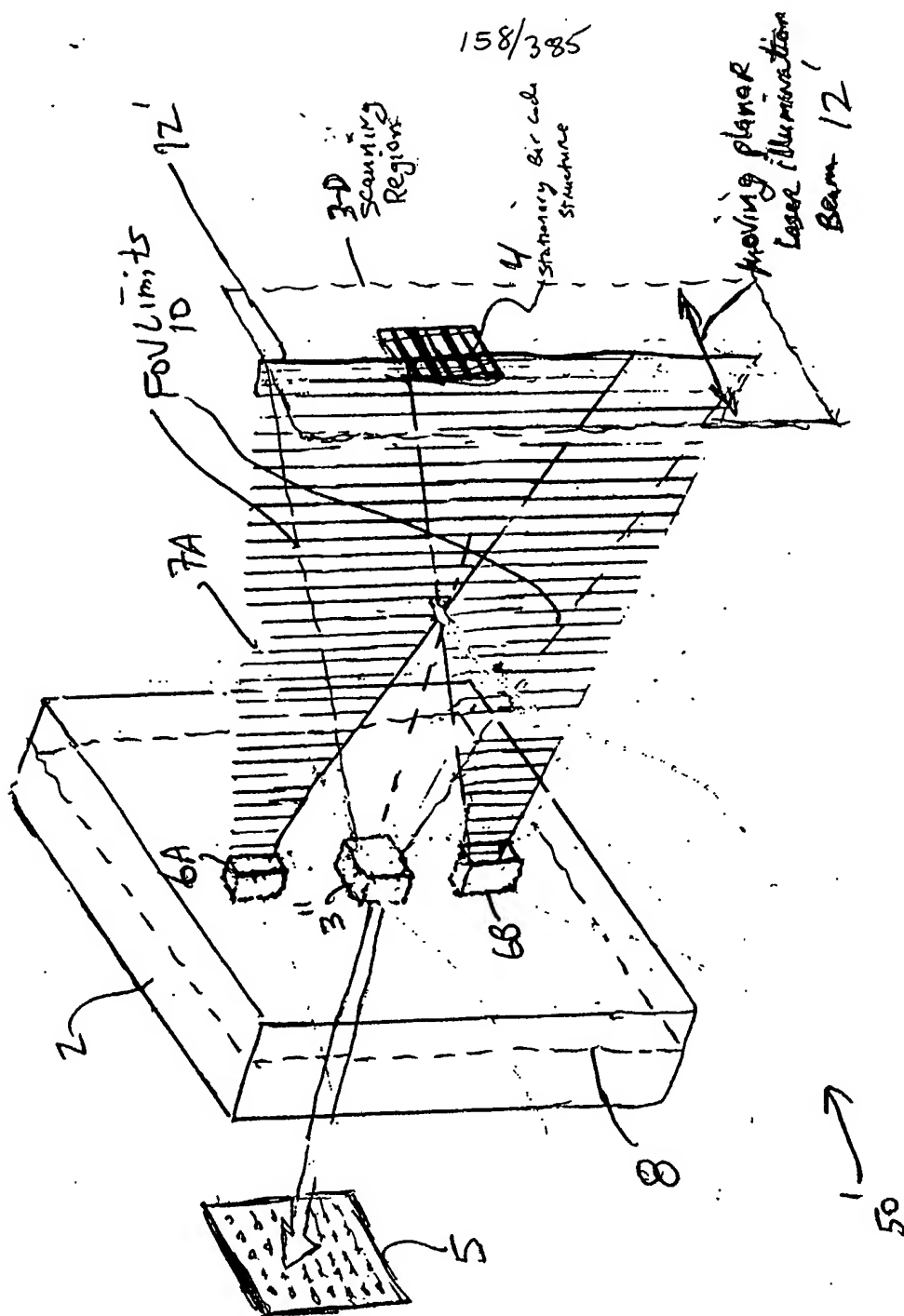


FIG. 3J1

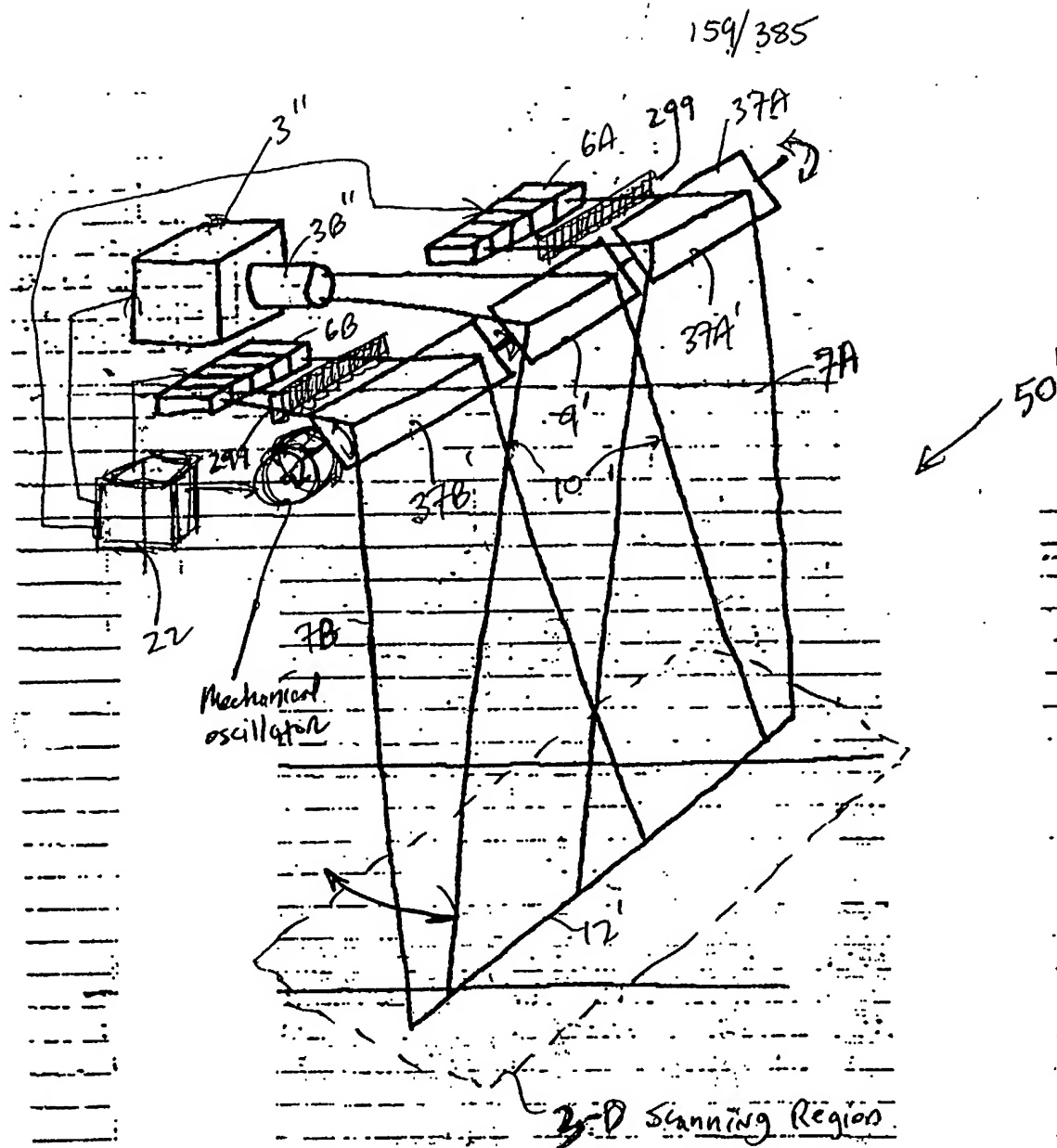


FIG 3J2

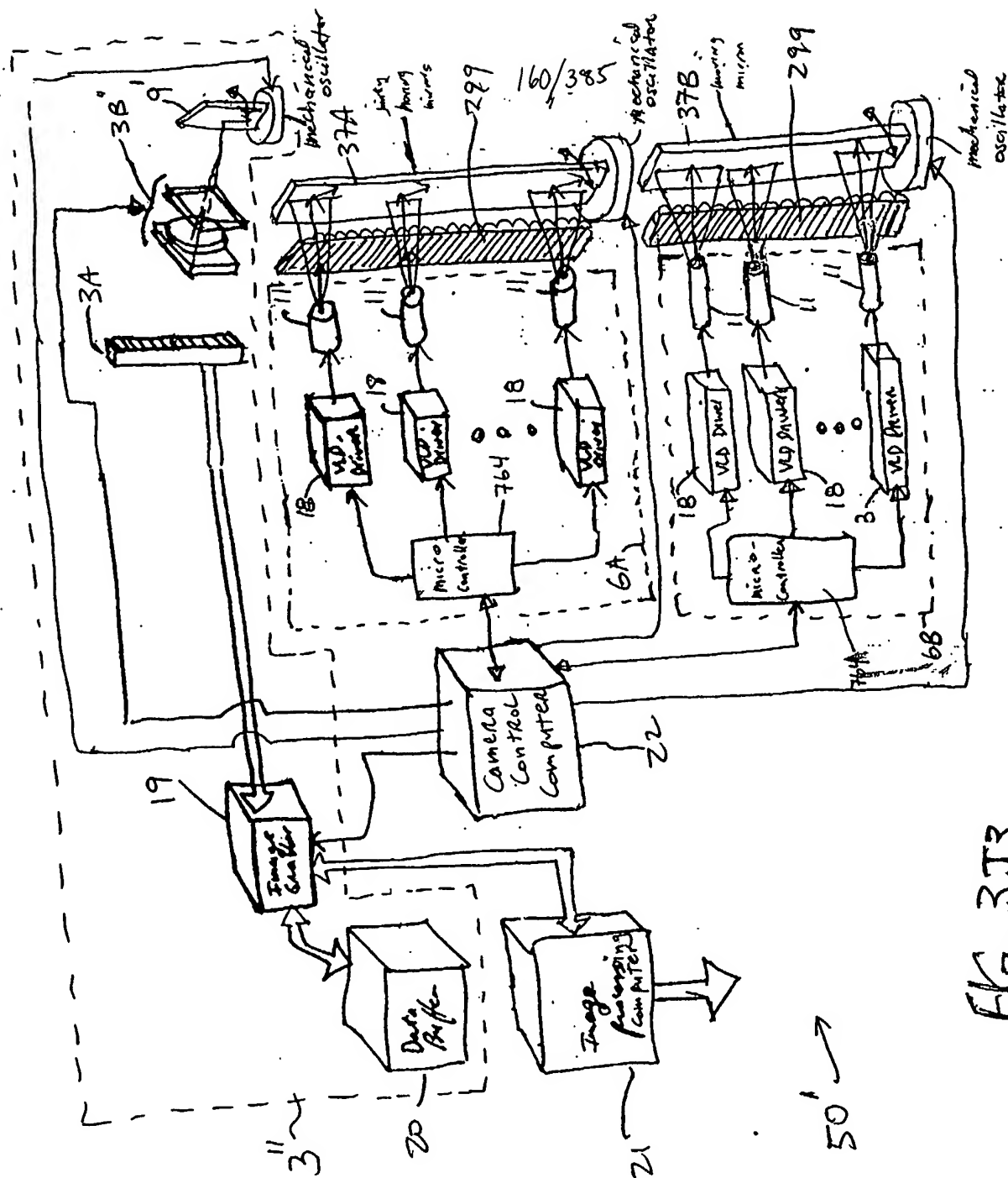


Fig. 3J3

161/385

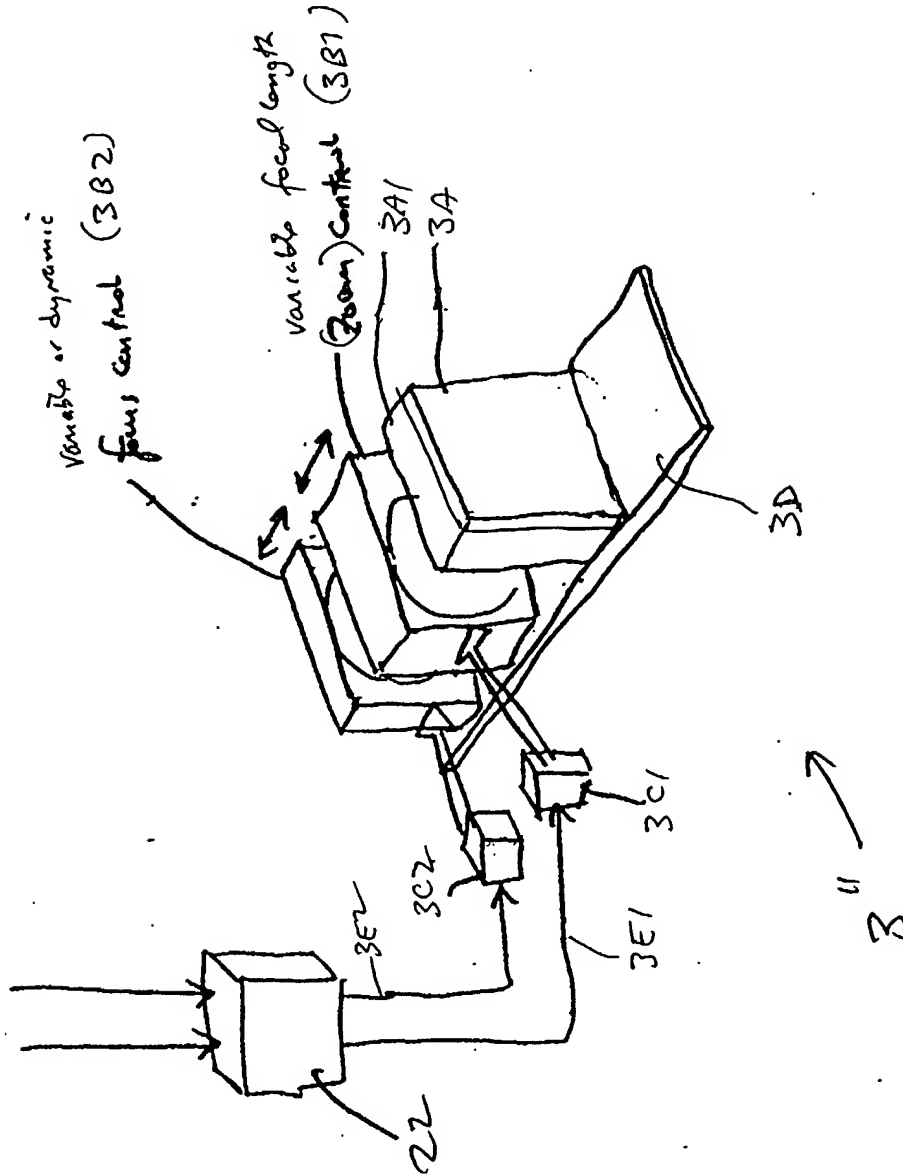
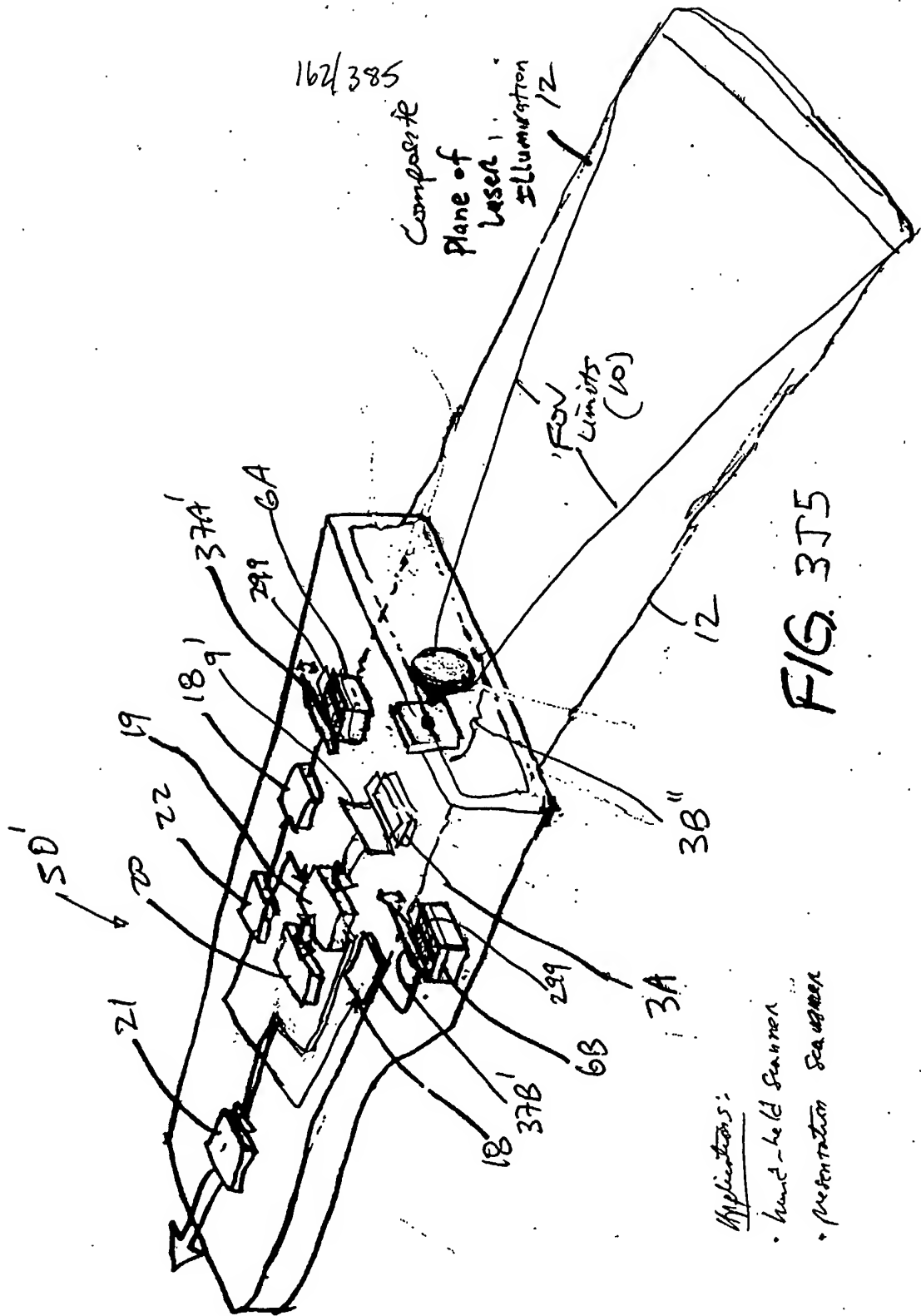


FIG. 3J4



163/385

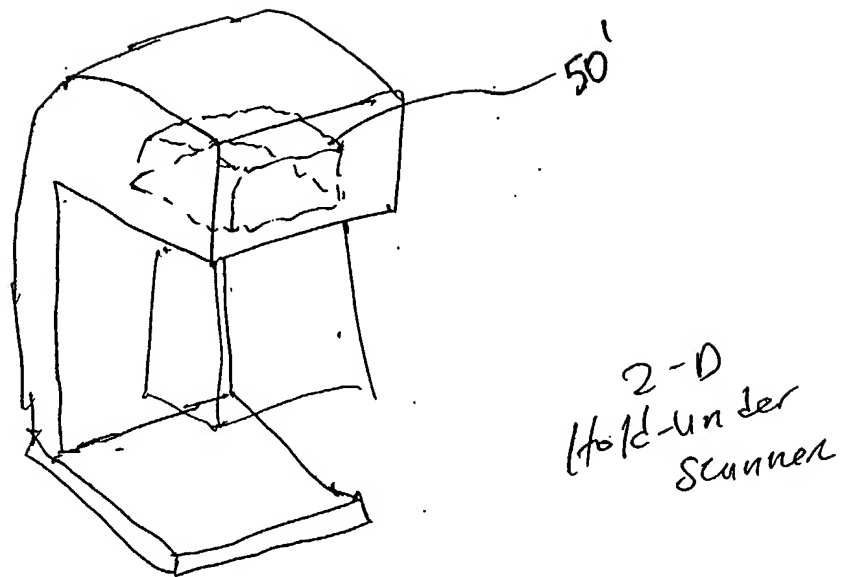


FIG. 316

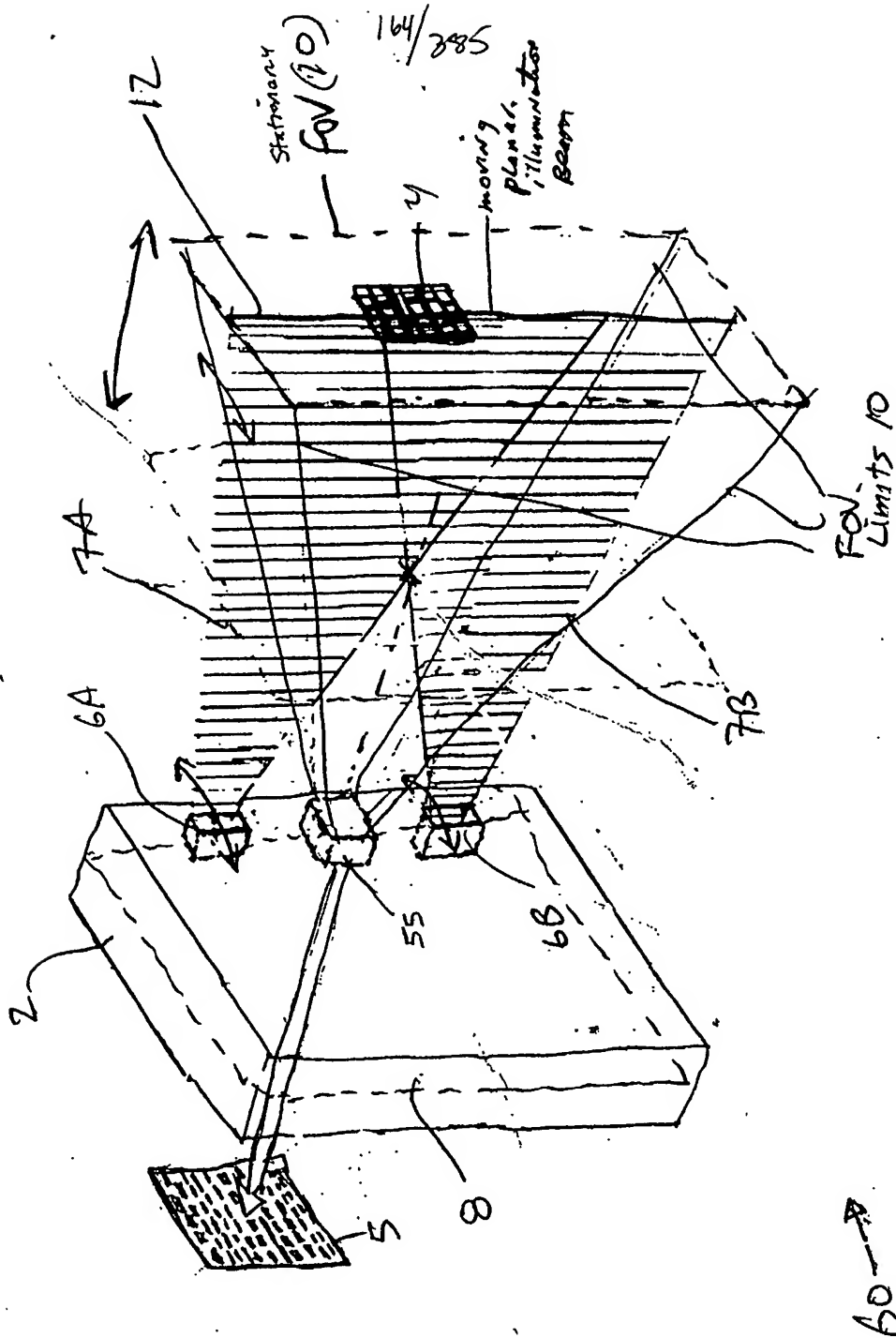


FIG 4A

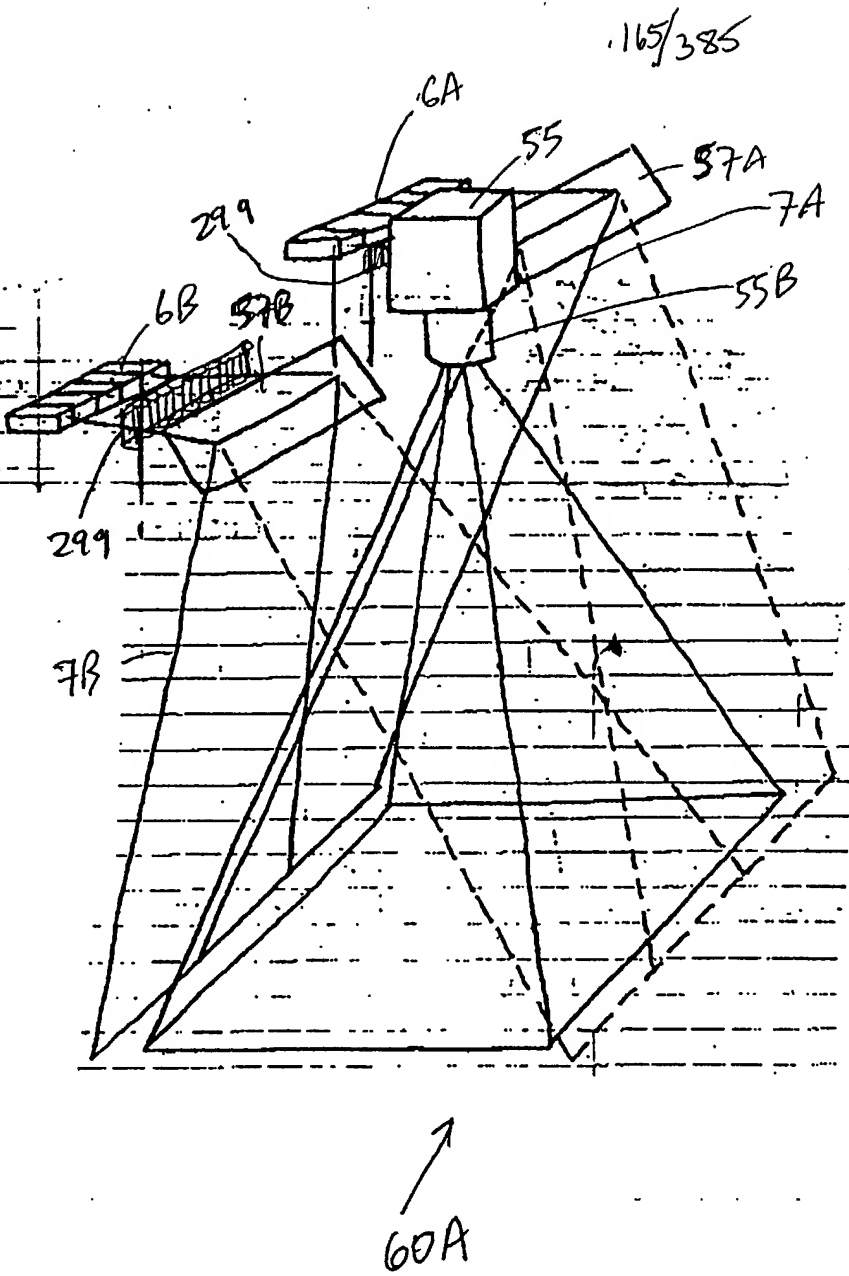


FIG. 4B1

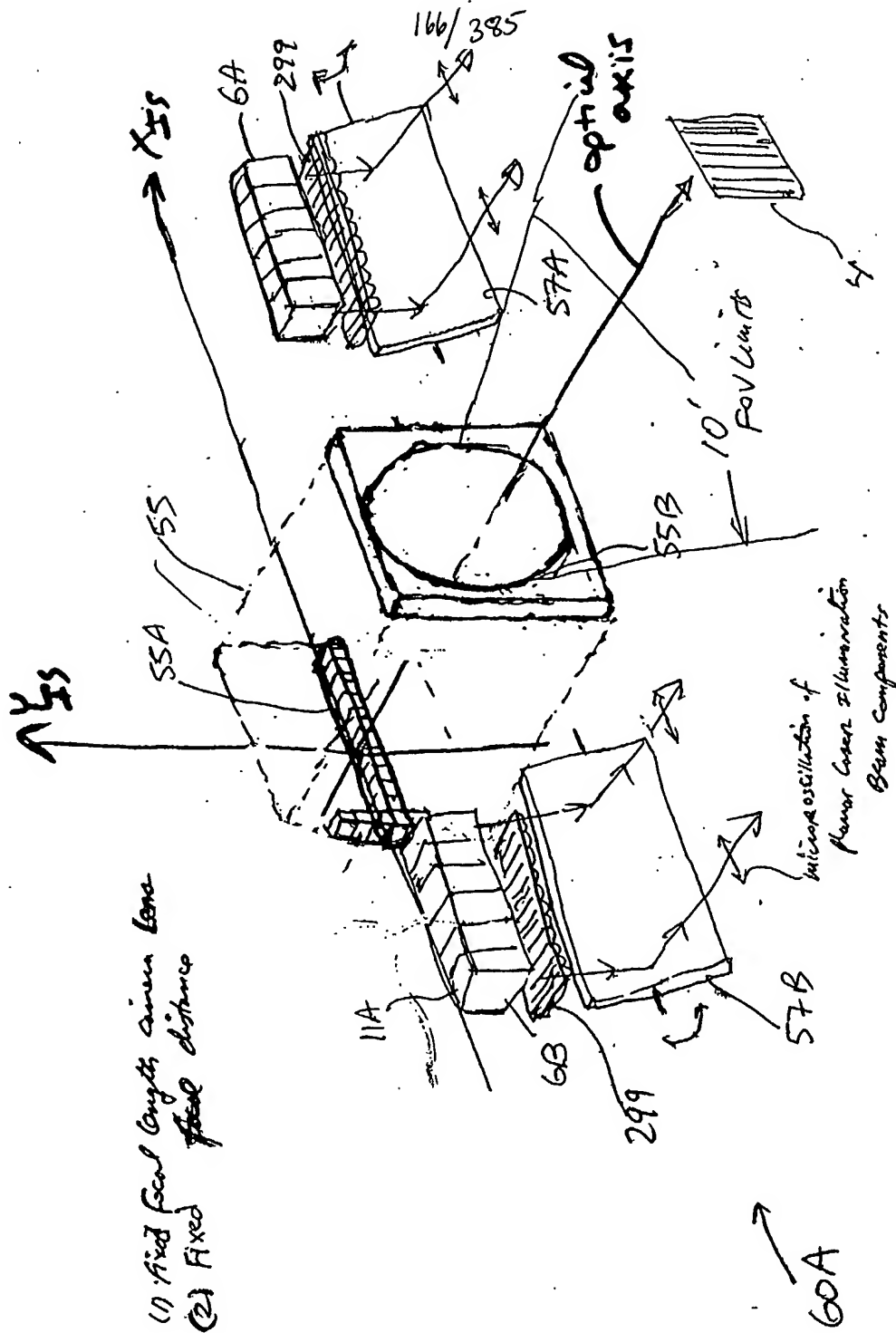
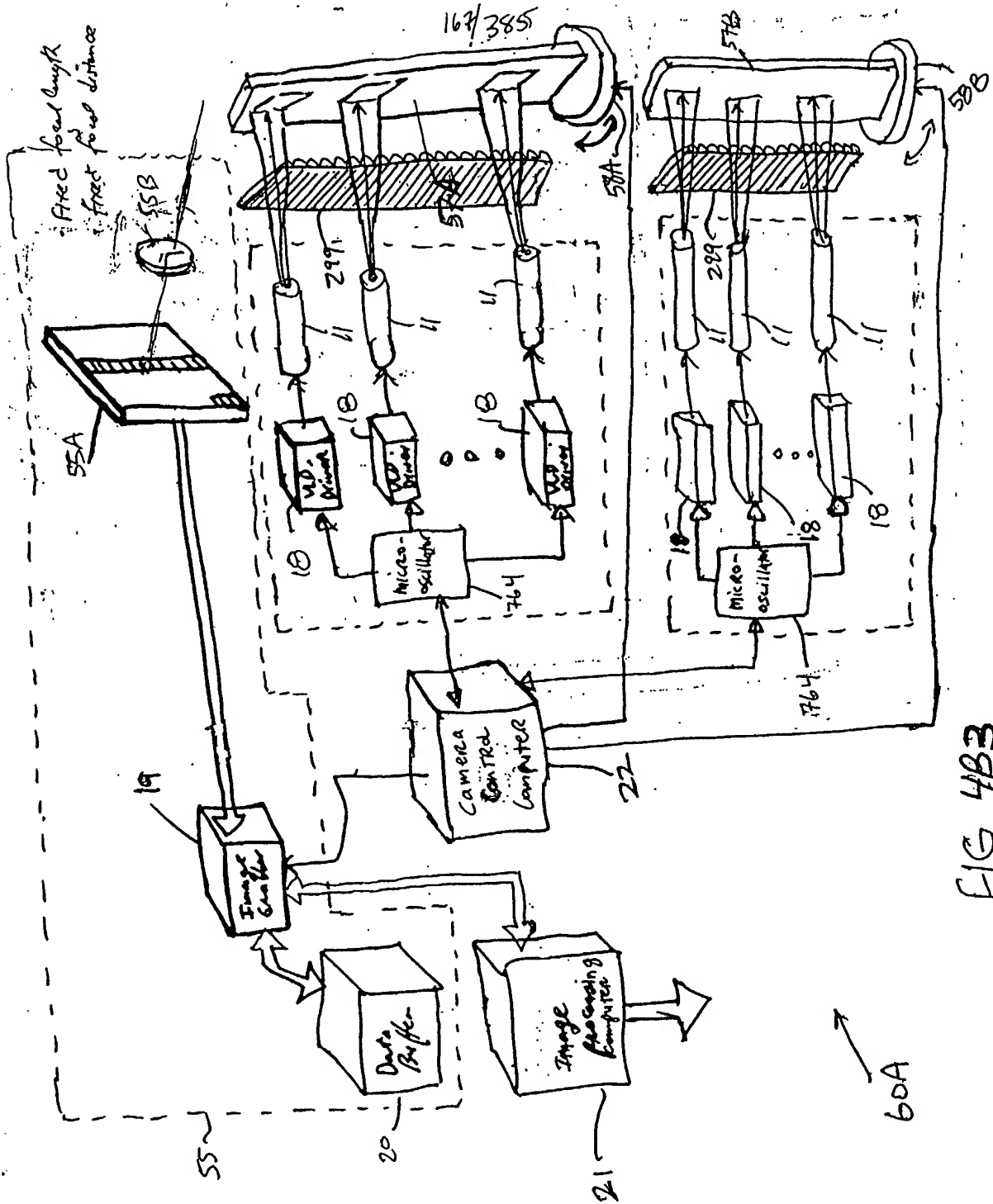


FIG. 4B.Z

- (1) Fixed focal length, same lens
- (2) Fixed focal distance



168/385

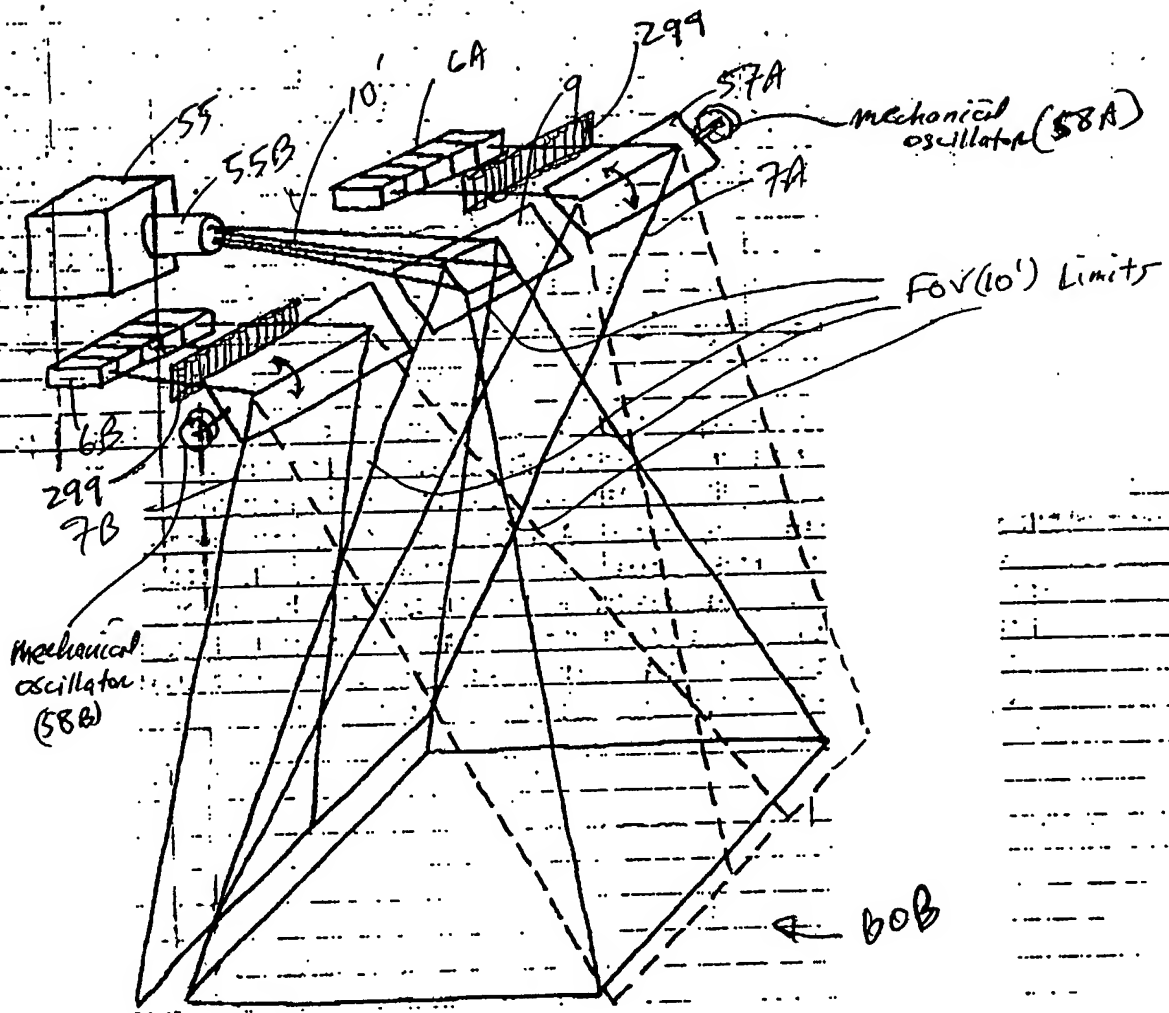


FIG. 4C-1

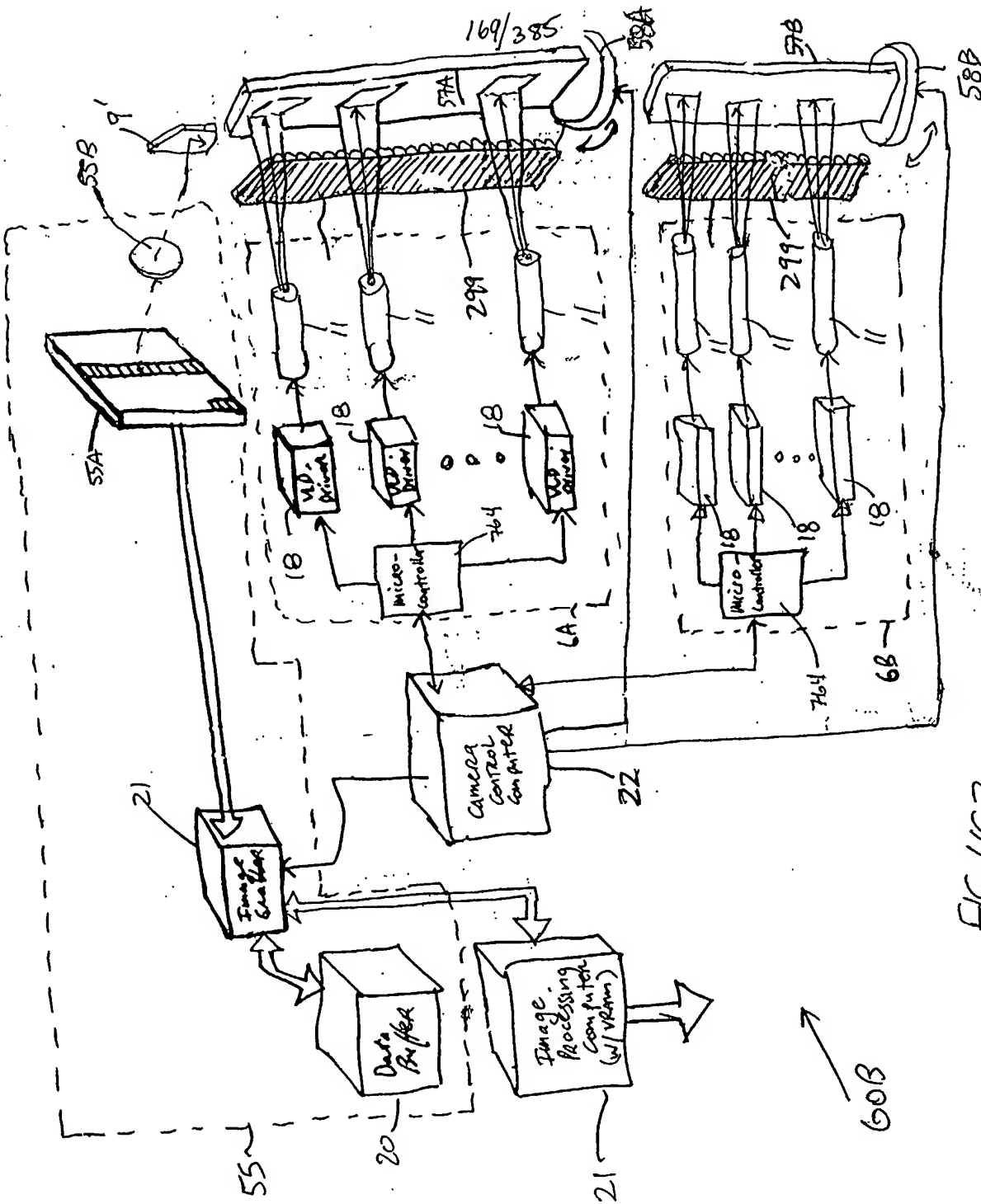


FIG. 4C2

170/385

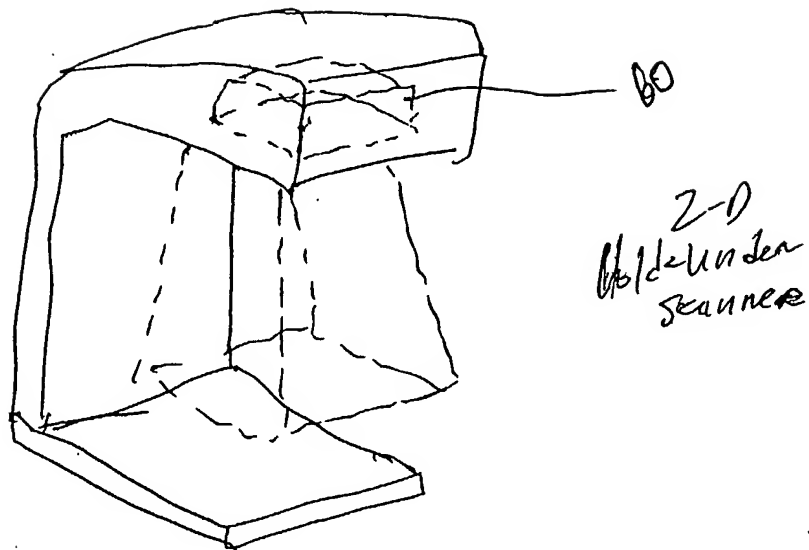


FIG. 4D

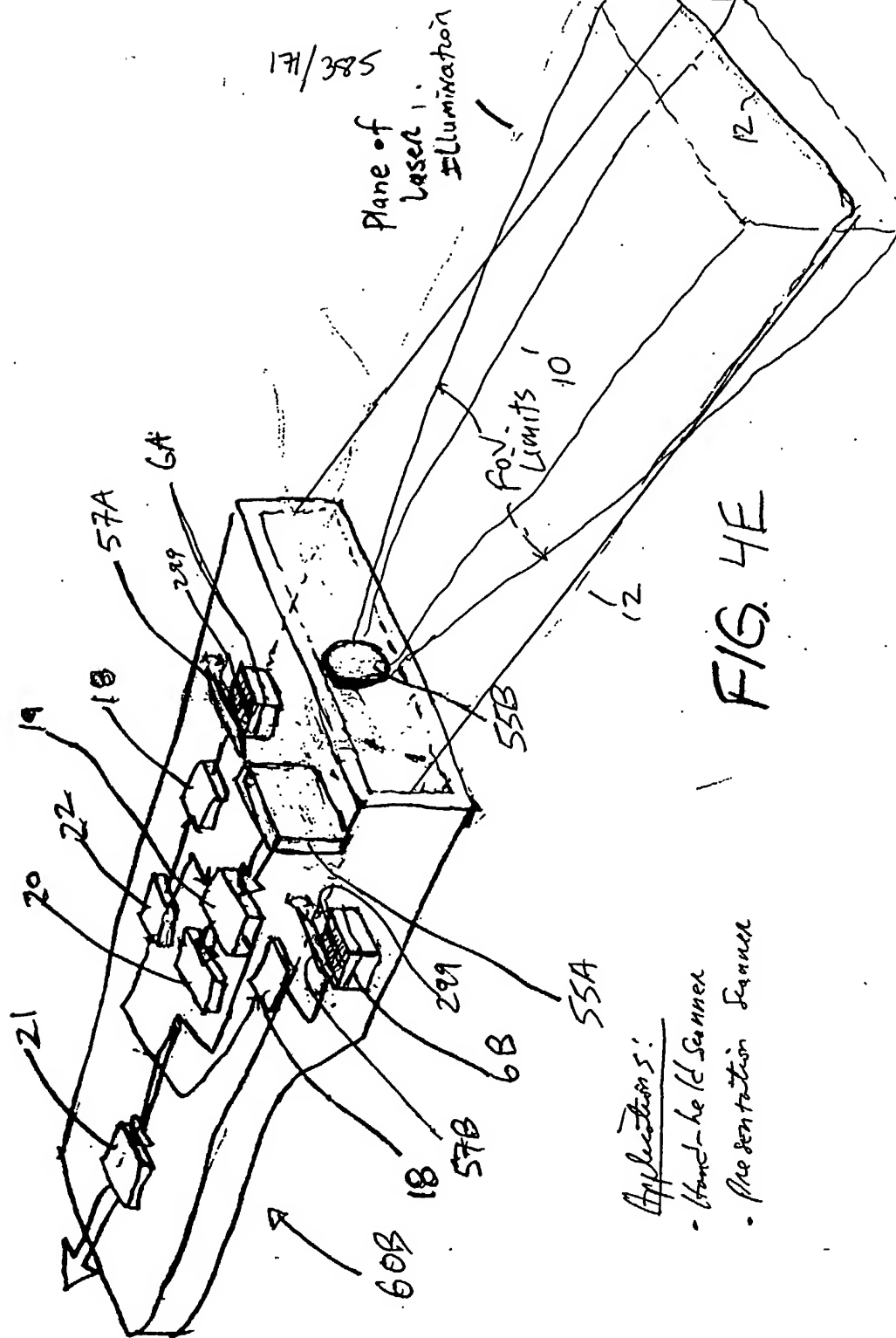


FIG. 4E

Applications:

- Hand-held Scanner
- Presentation Scanner

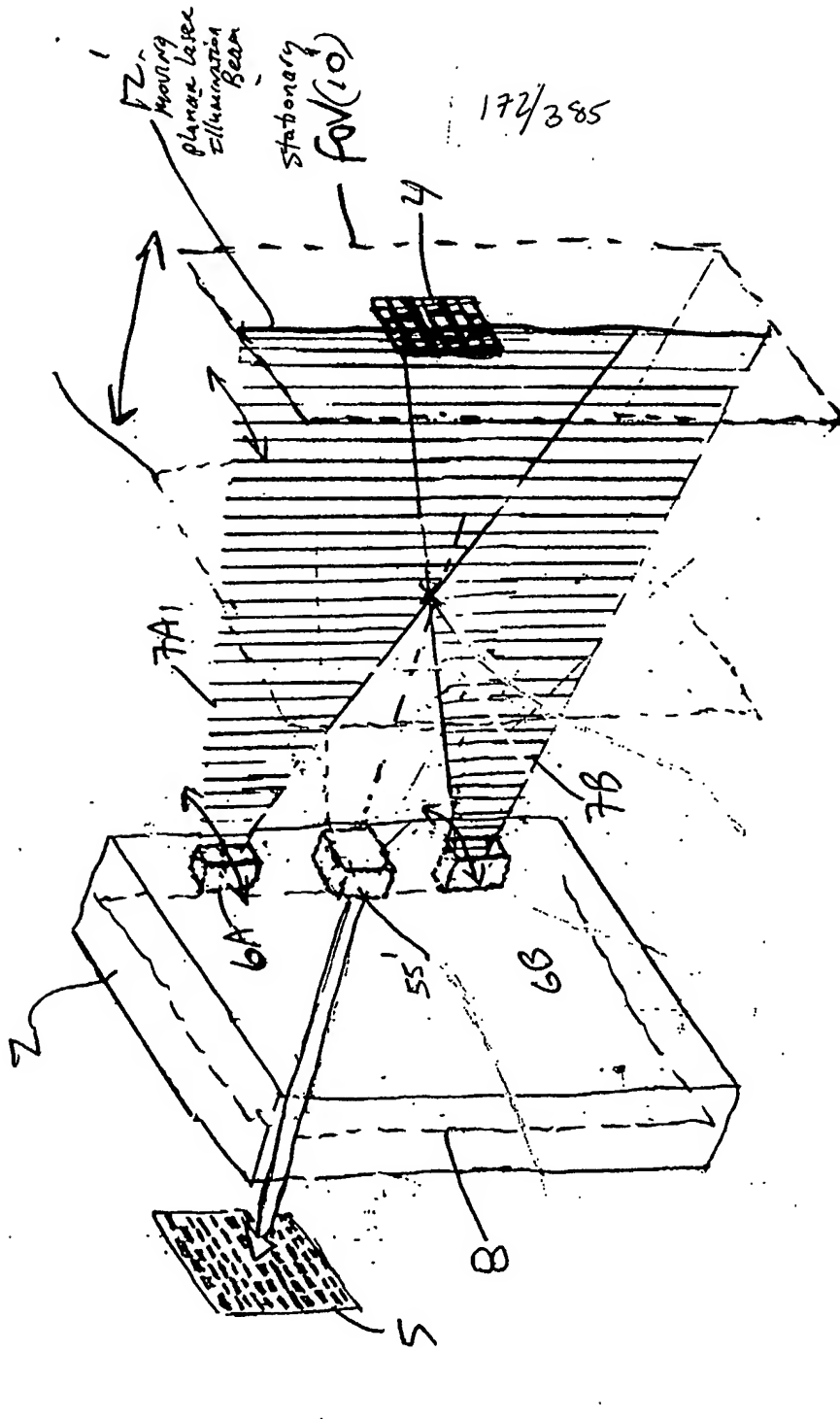


FIG. 5A

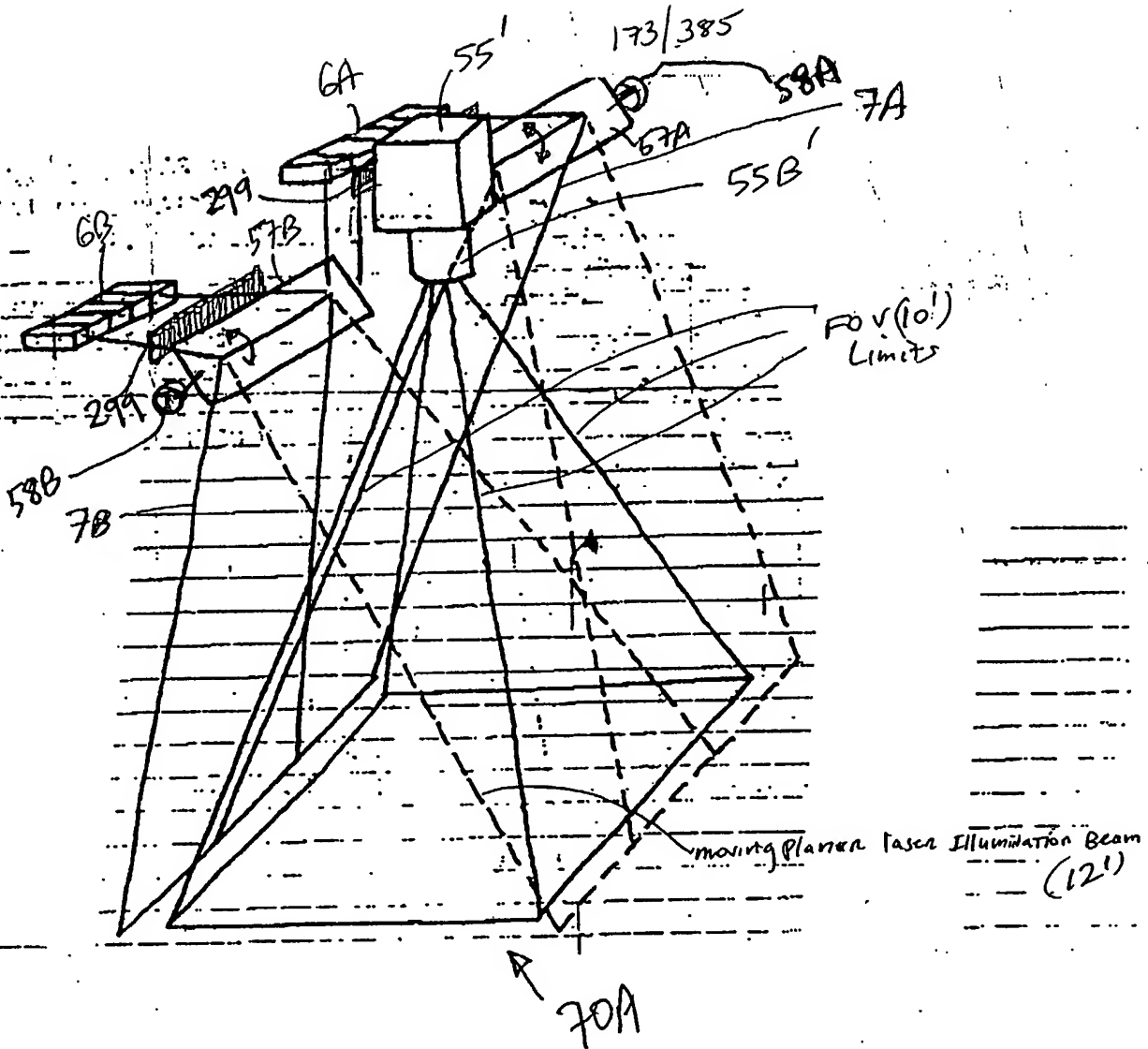


FIG 5B1

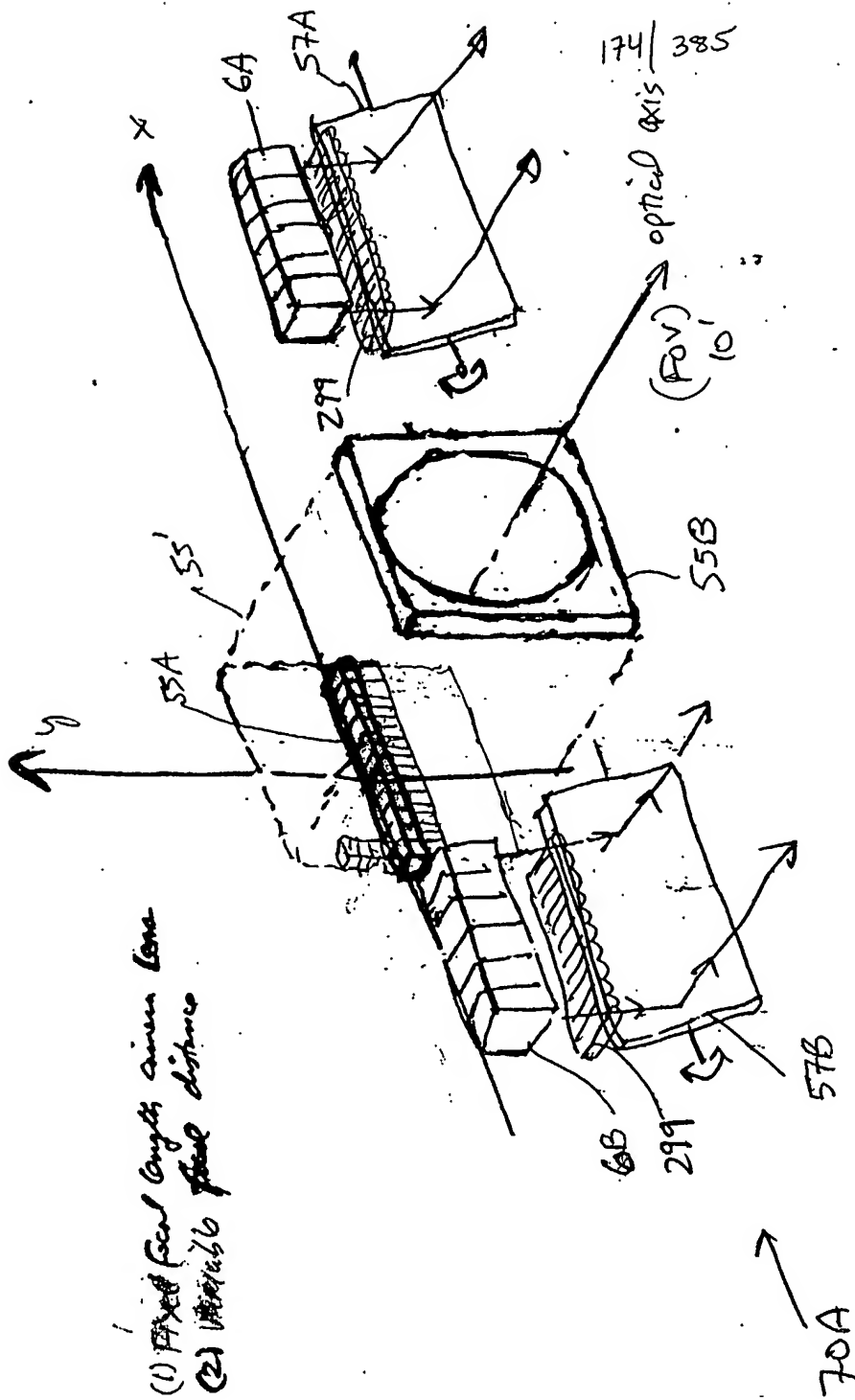


Fig. 5B2

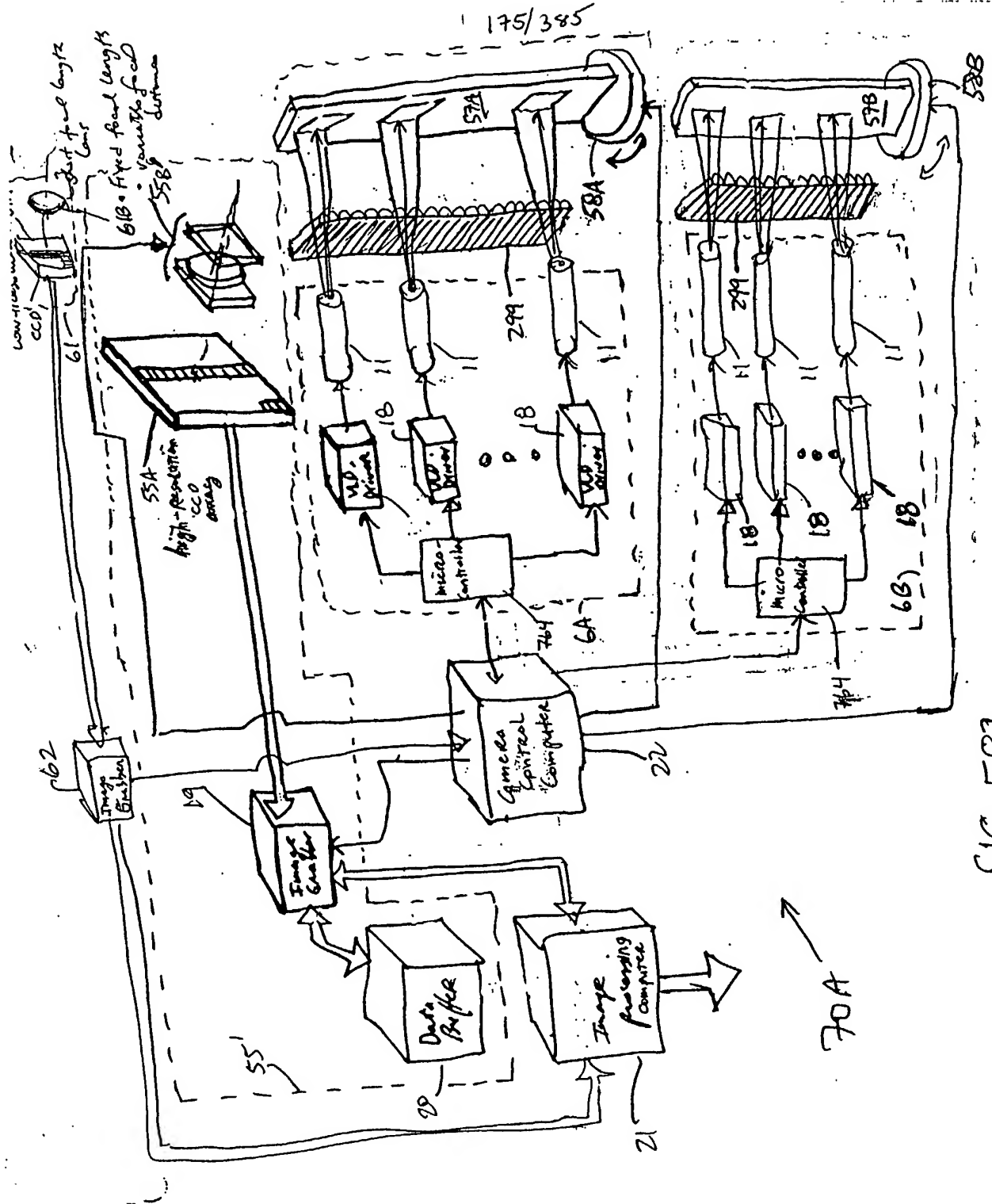


Fig. 533

176/385

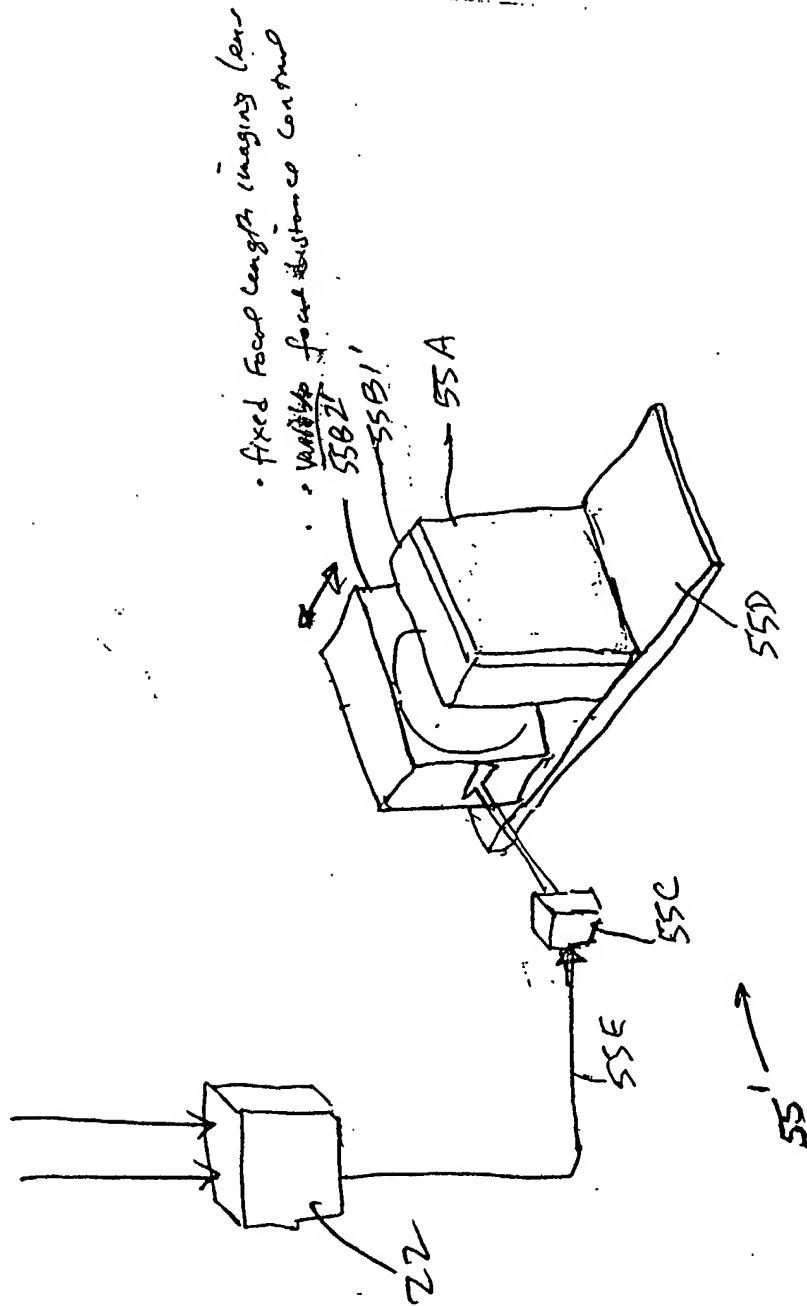


FIG. 5B4

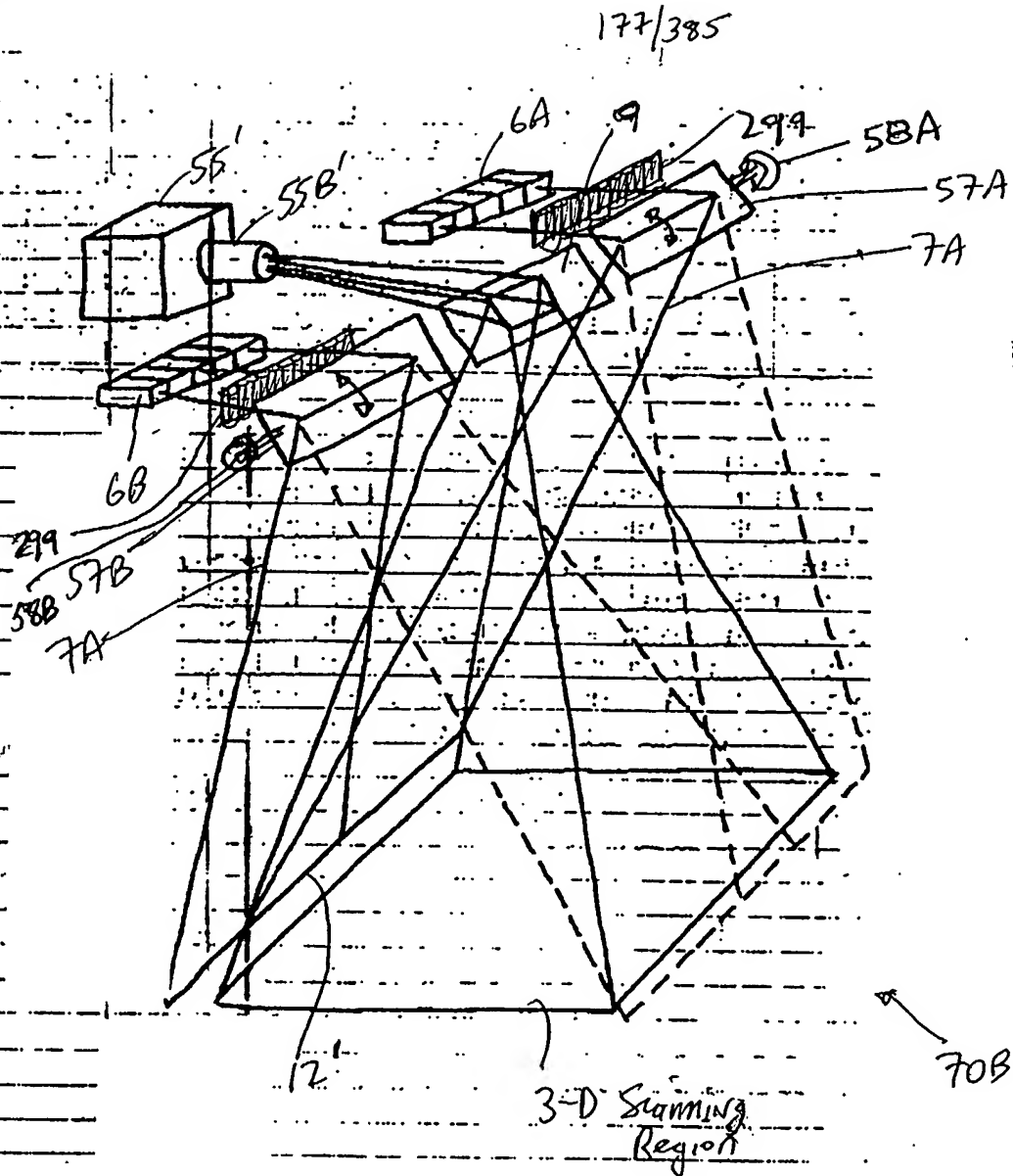
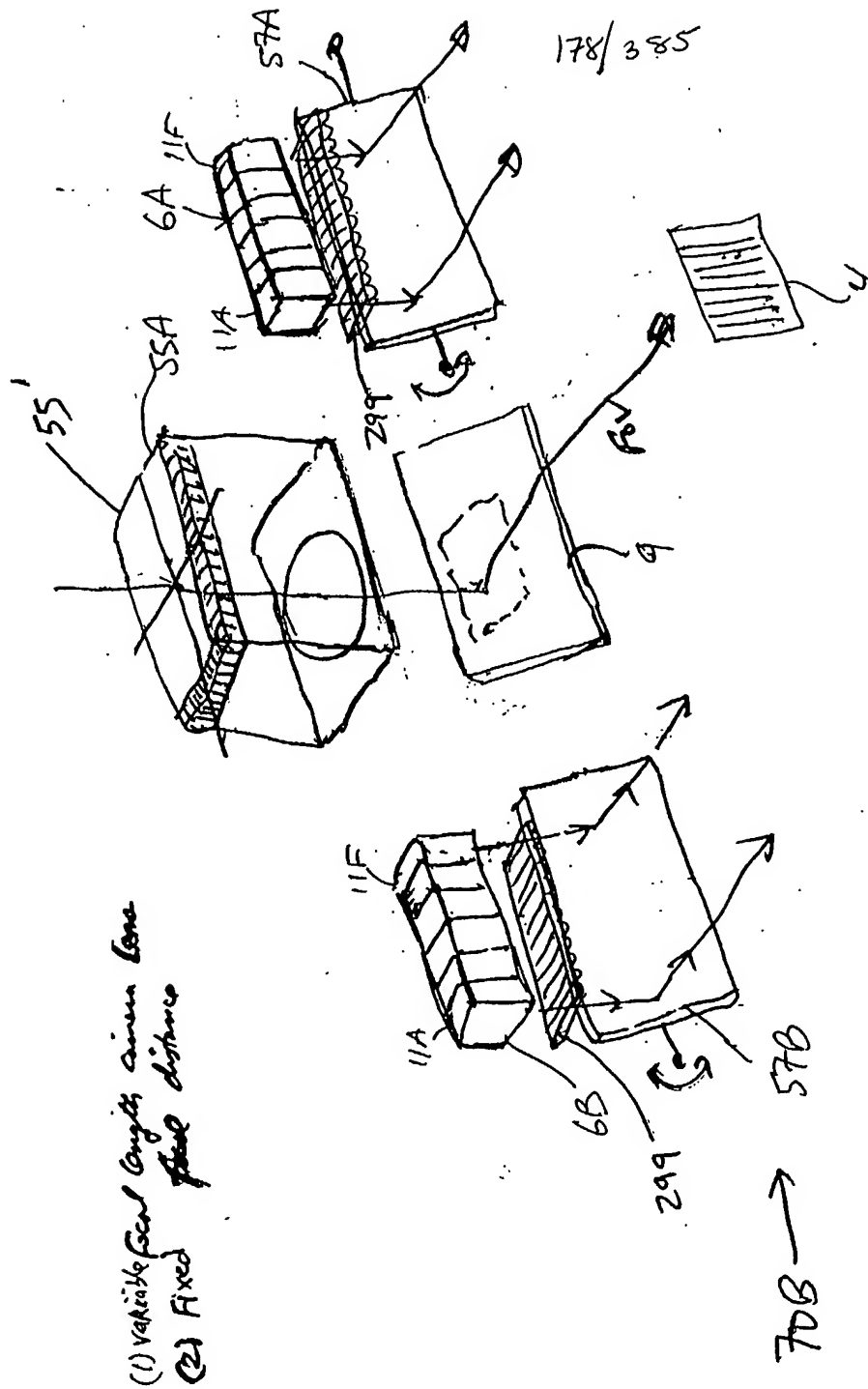


FIG. 5C1



(1) Variable length sinus wave
(2) Fixed peak distance

FIG. 50

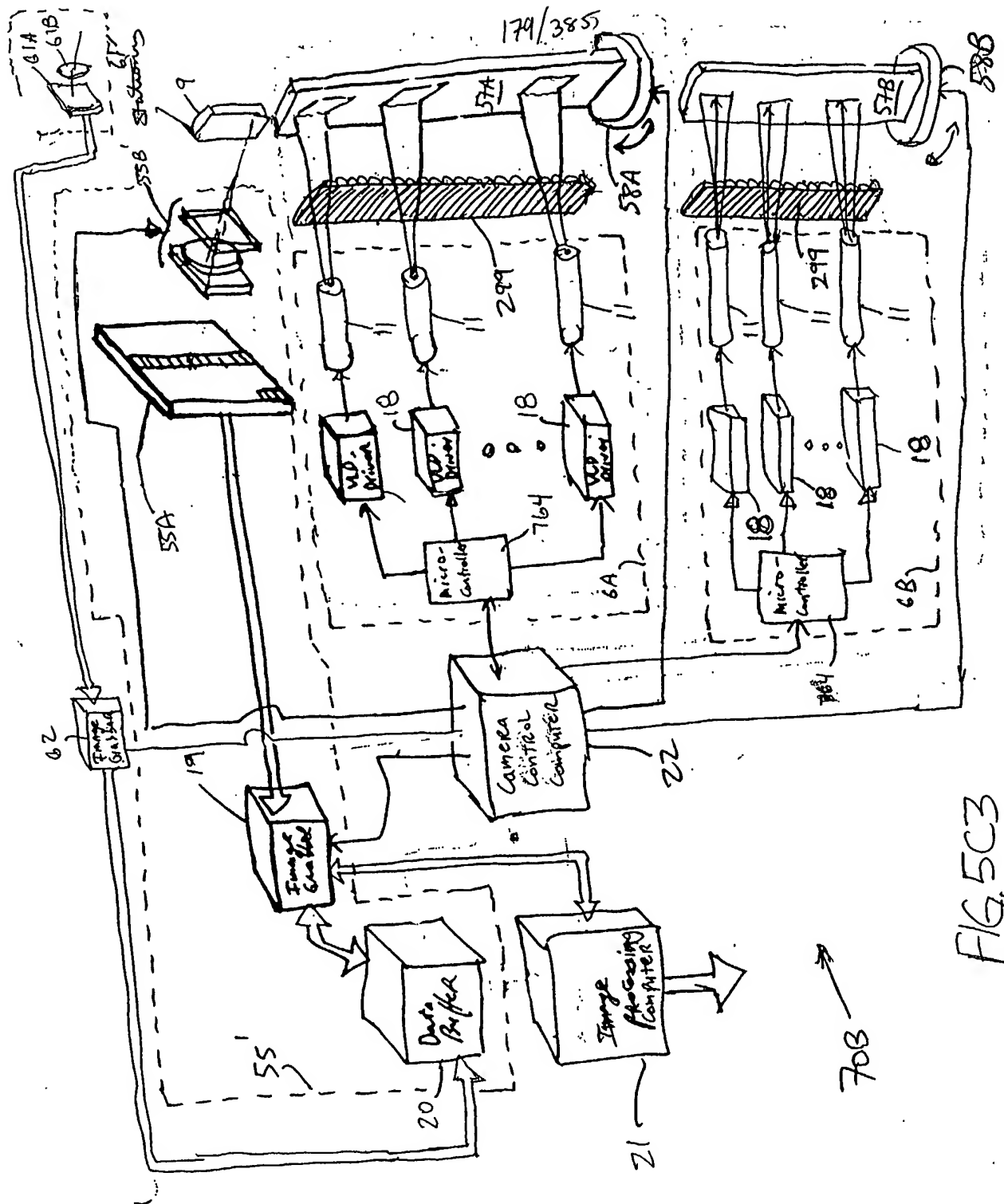


FIG. 5C3

180/385

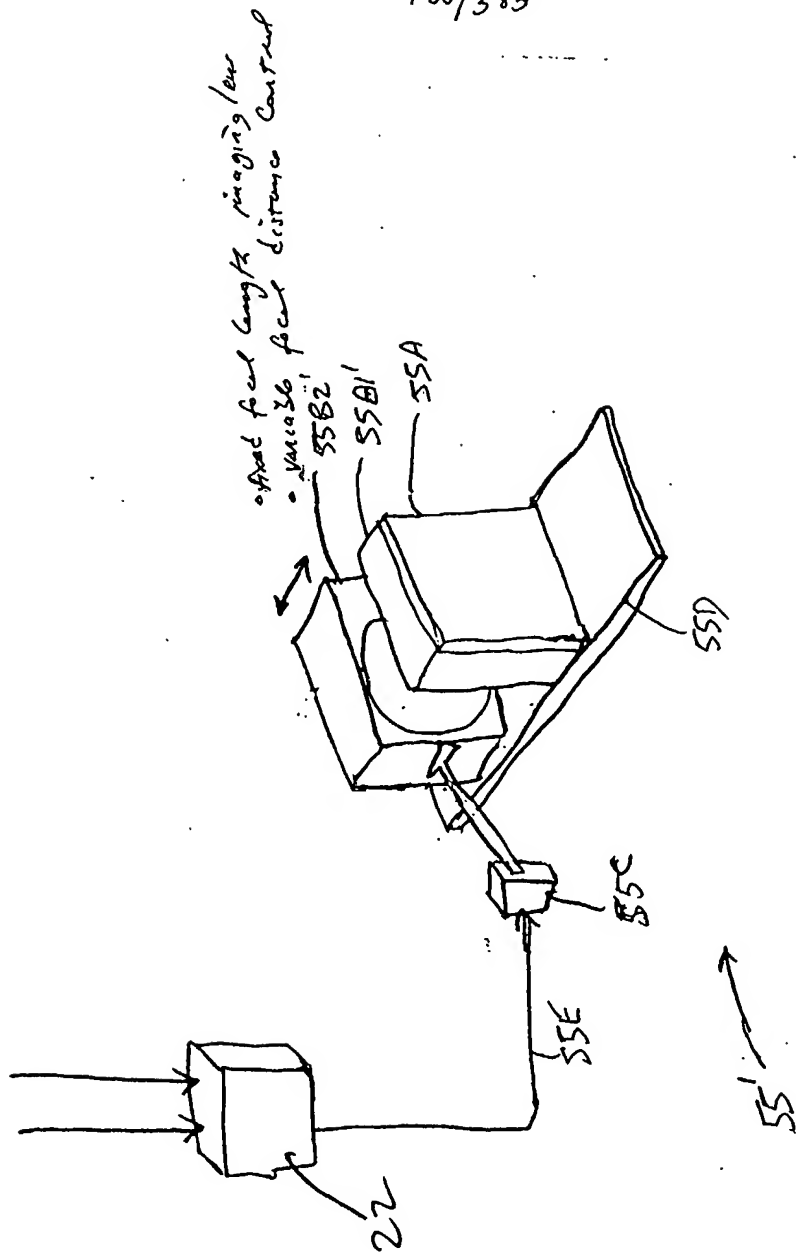


FIG. 5C4

181/385

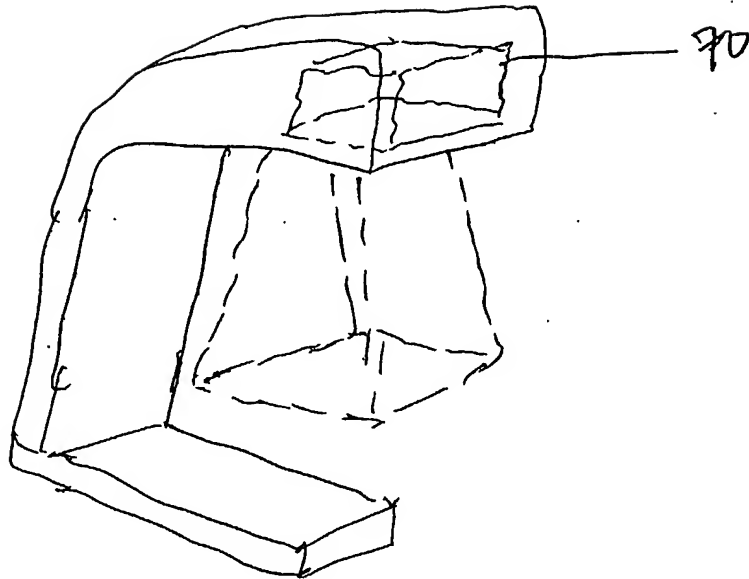


FIG. 5D

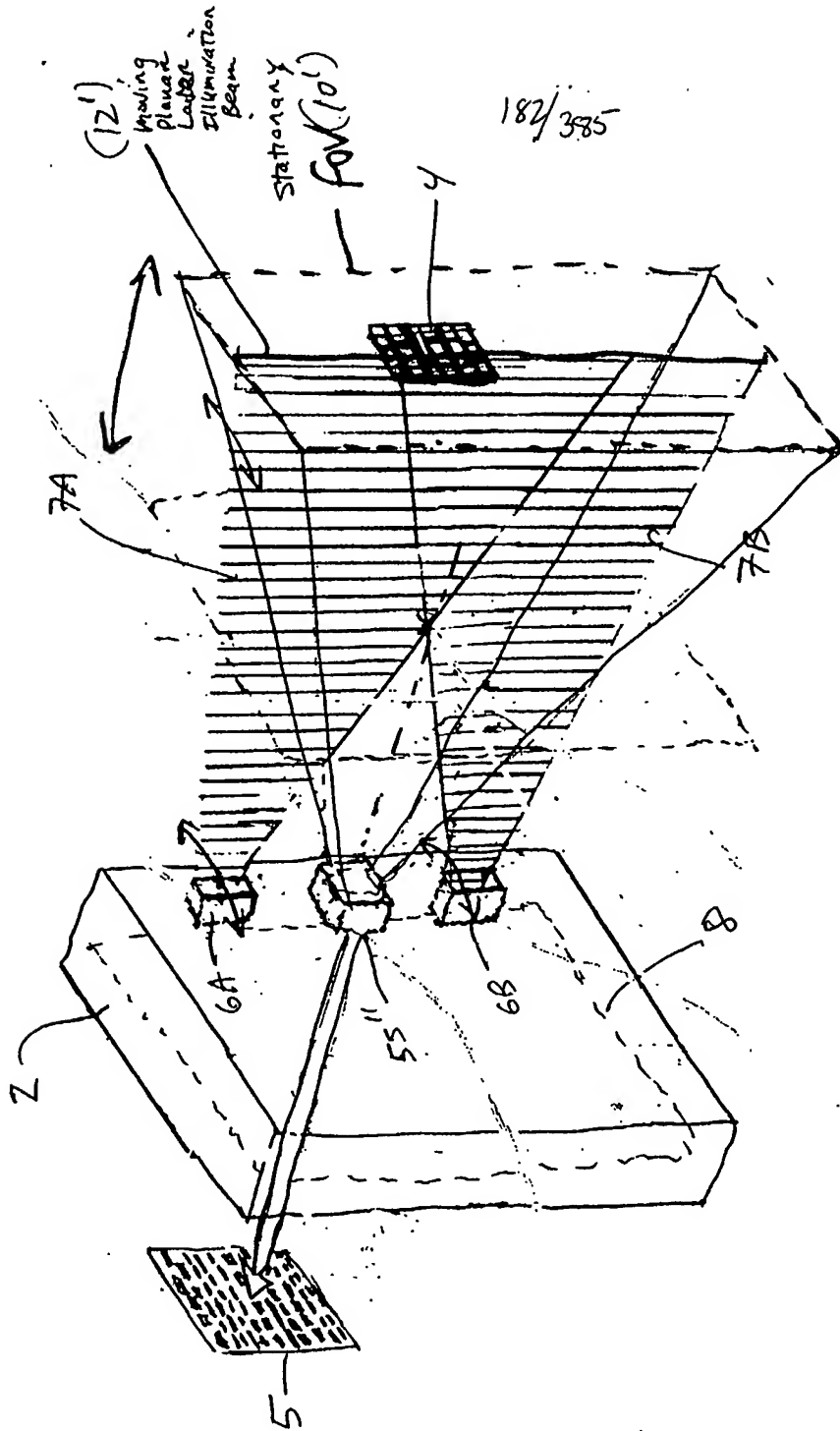


FIG. 6A

86

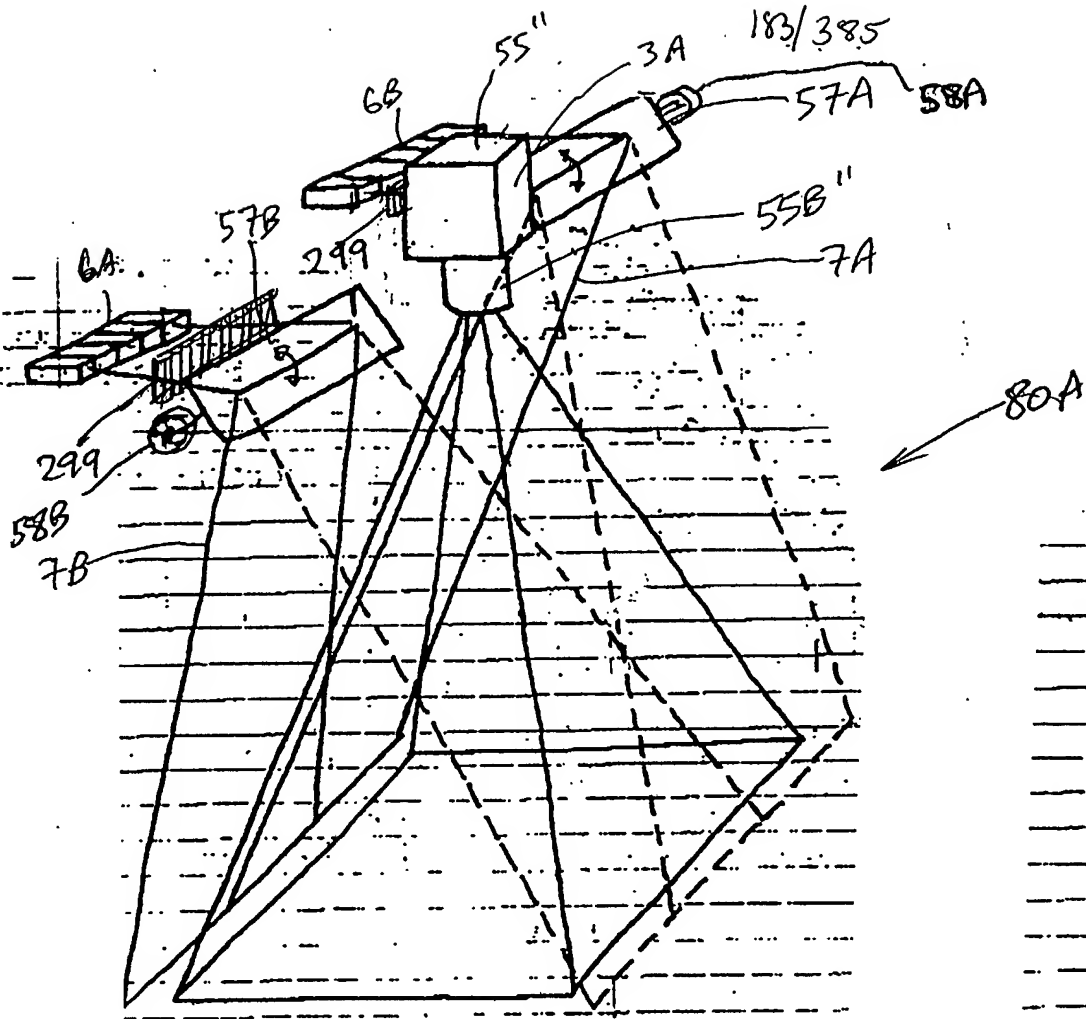
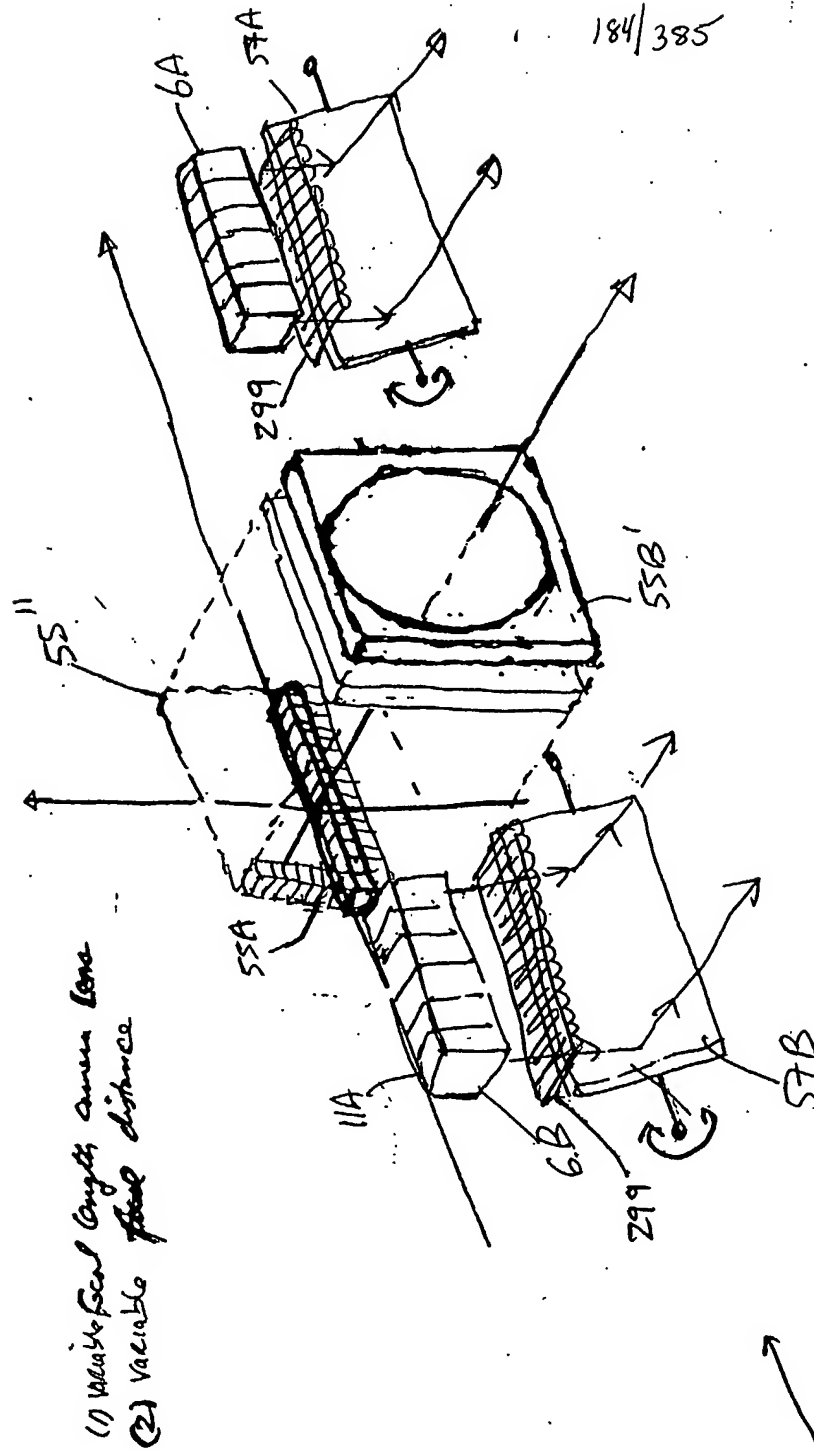


FIG. 6B1



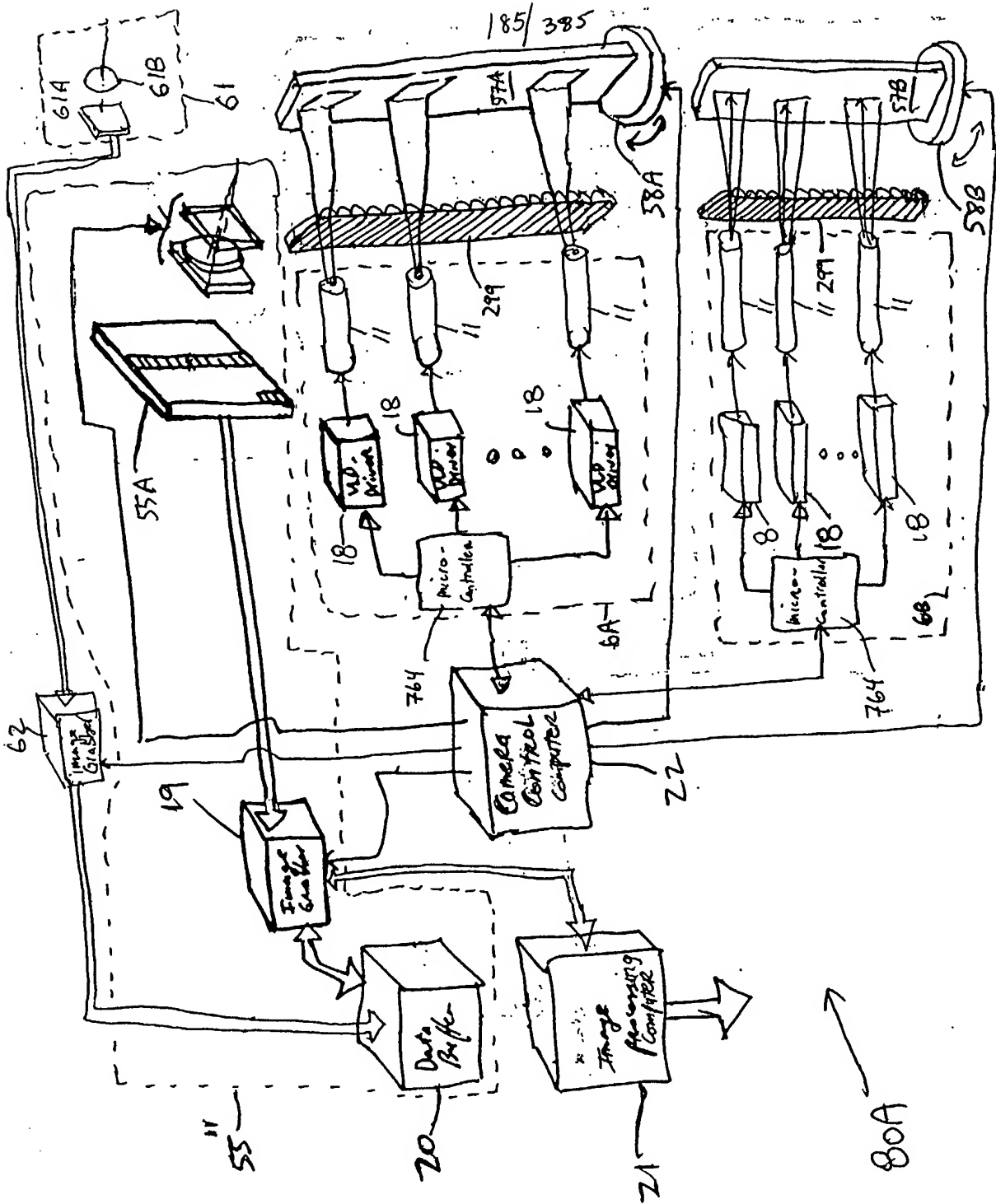


FIG. 6B3

80A

186/385

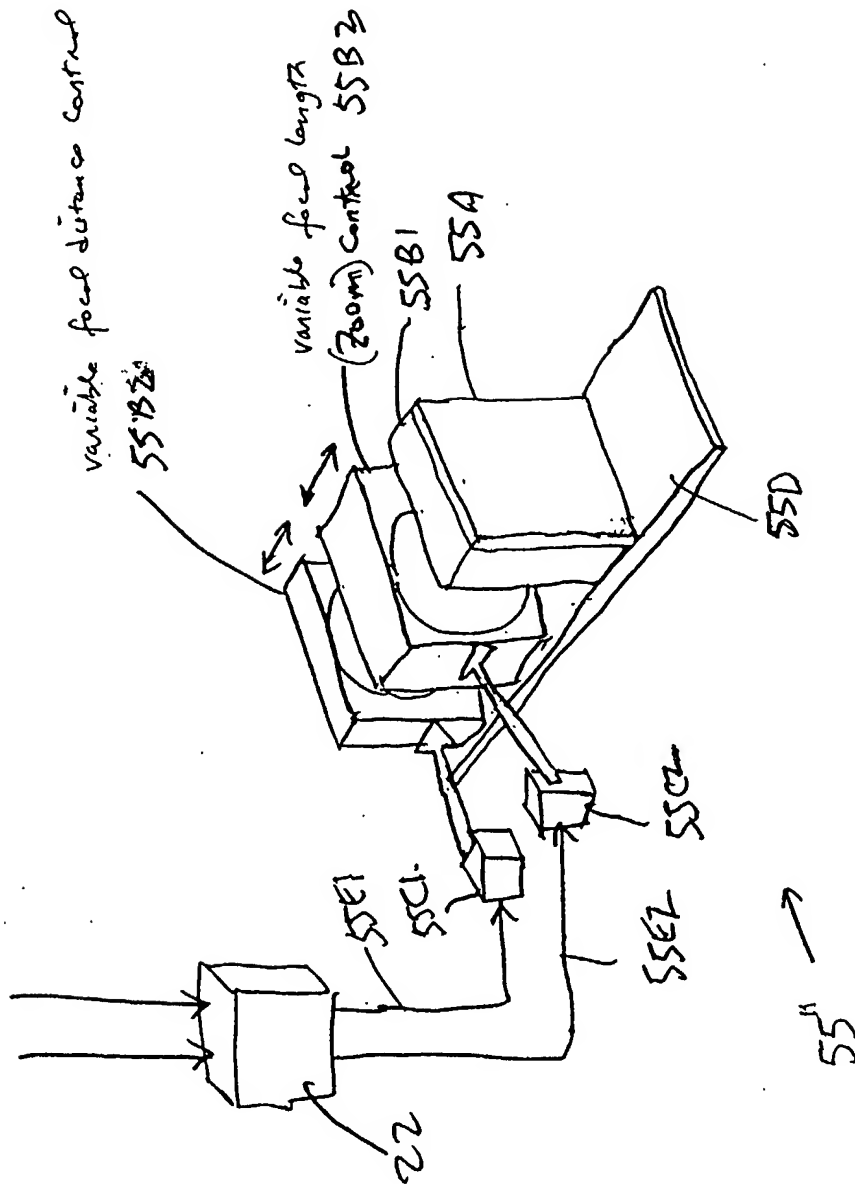


FIG. 6B4

187/385

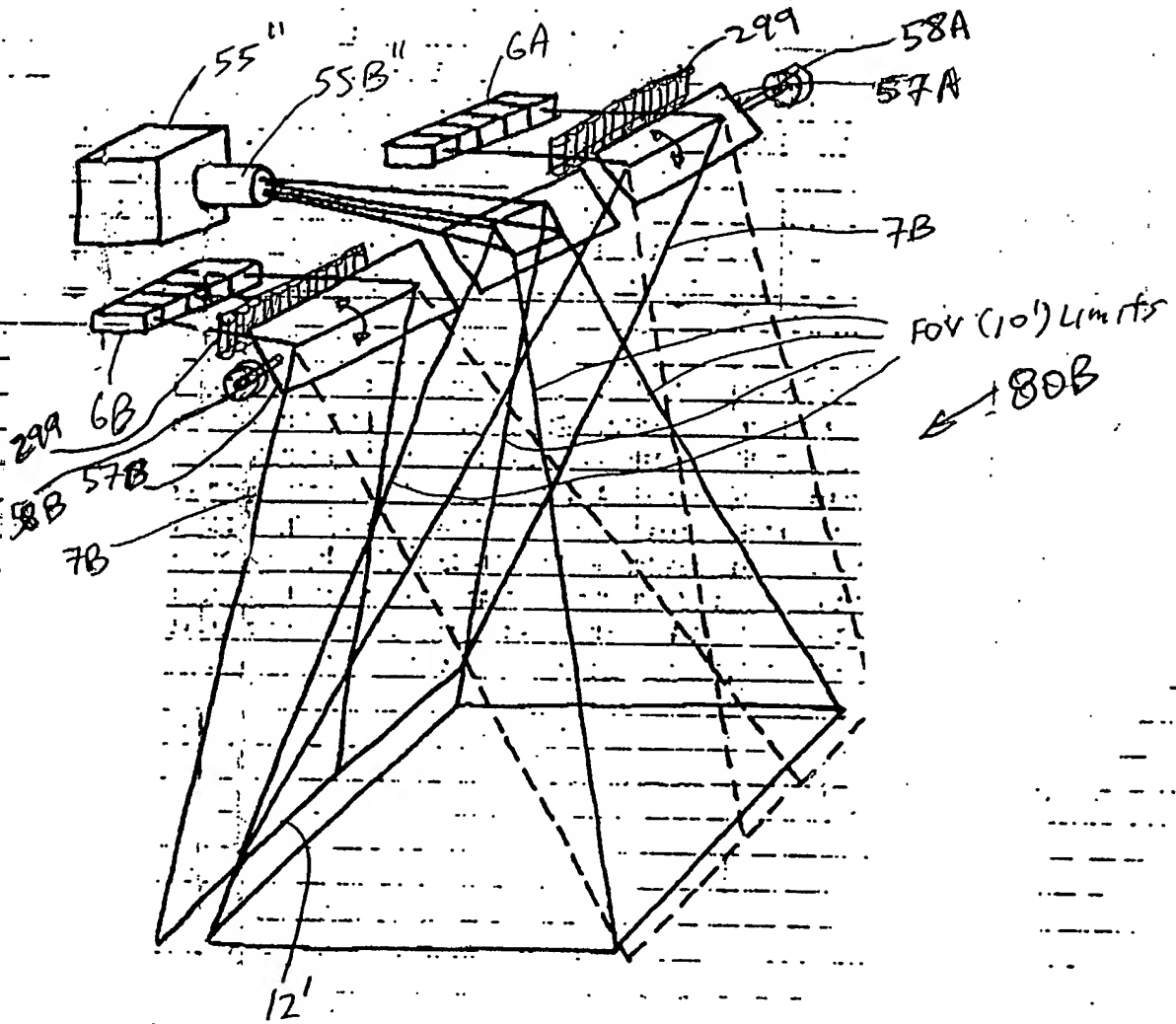


FIG. 6C1

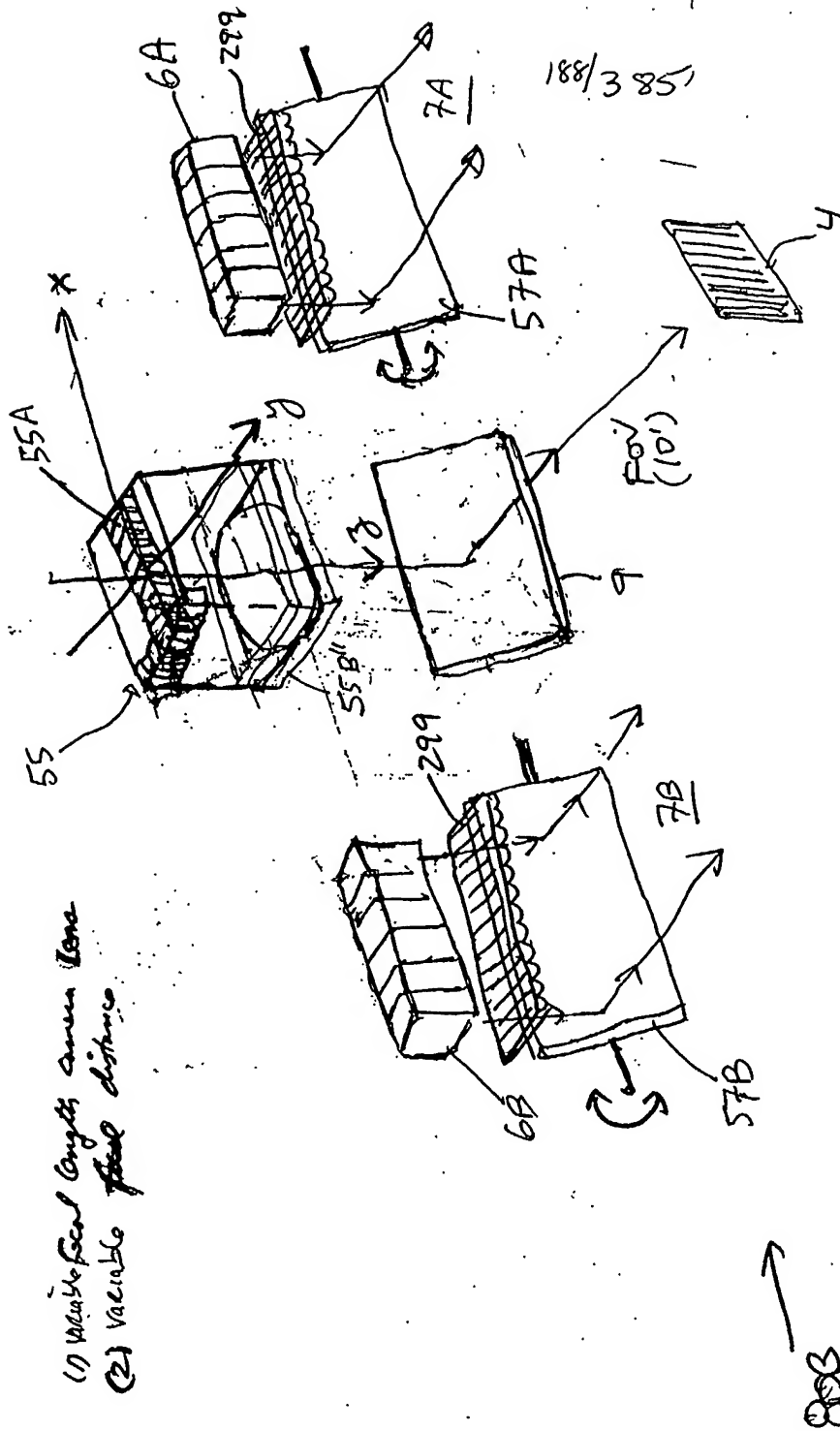
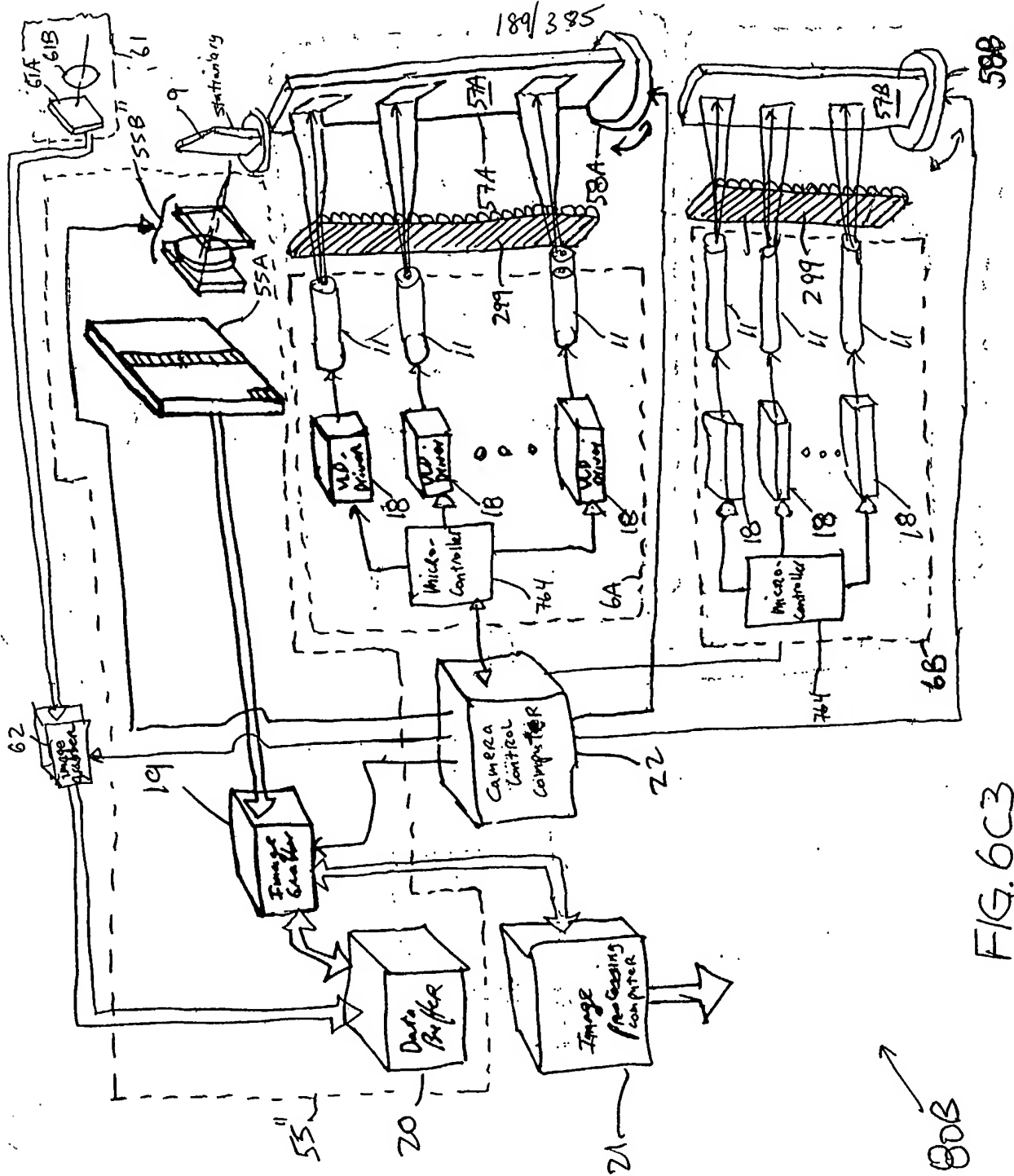


FIG. 6CZ

(1) Variable length inner line
(2) Variable fluid distance





190/385

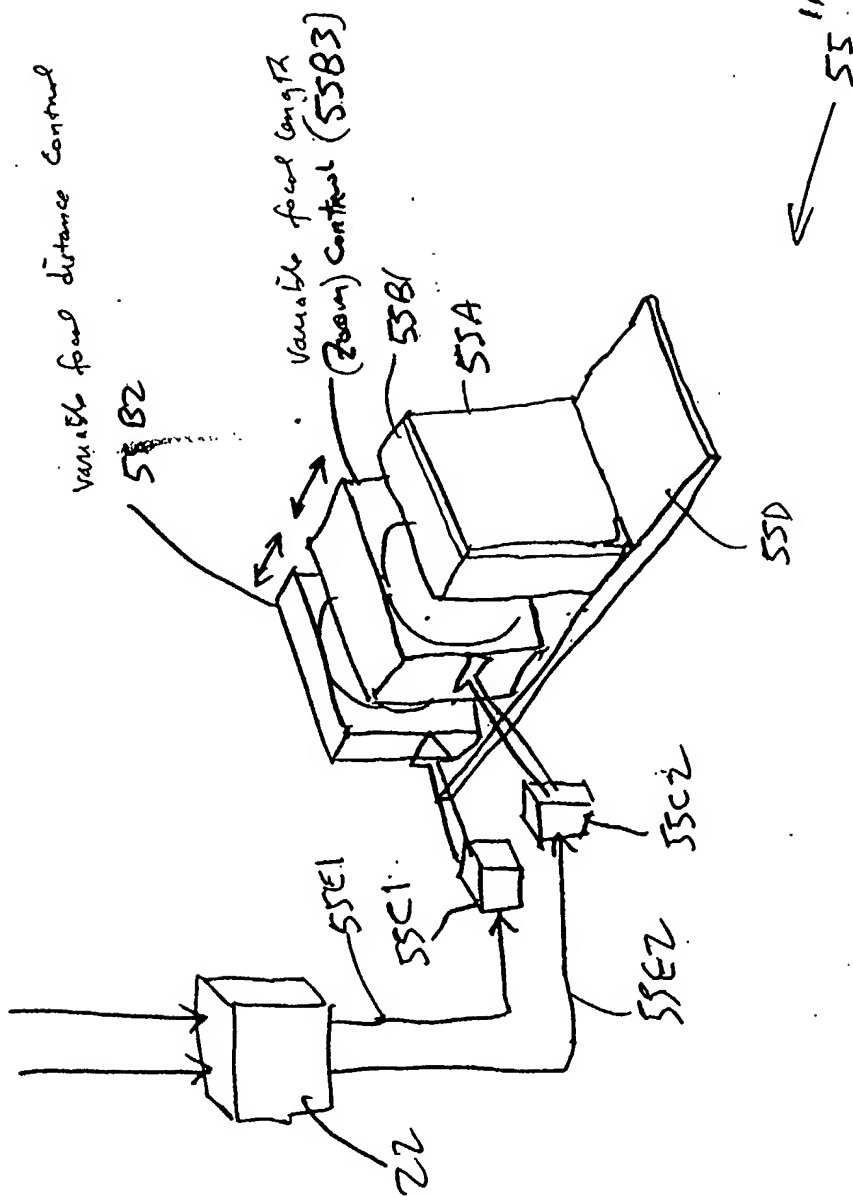


FIG. 6C4

191/385

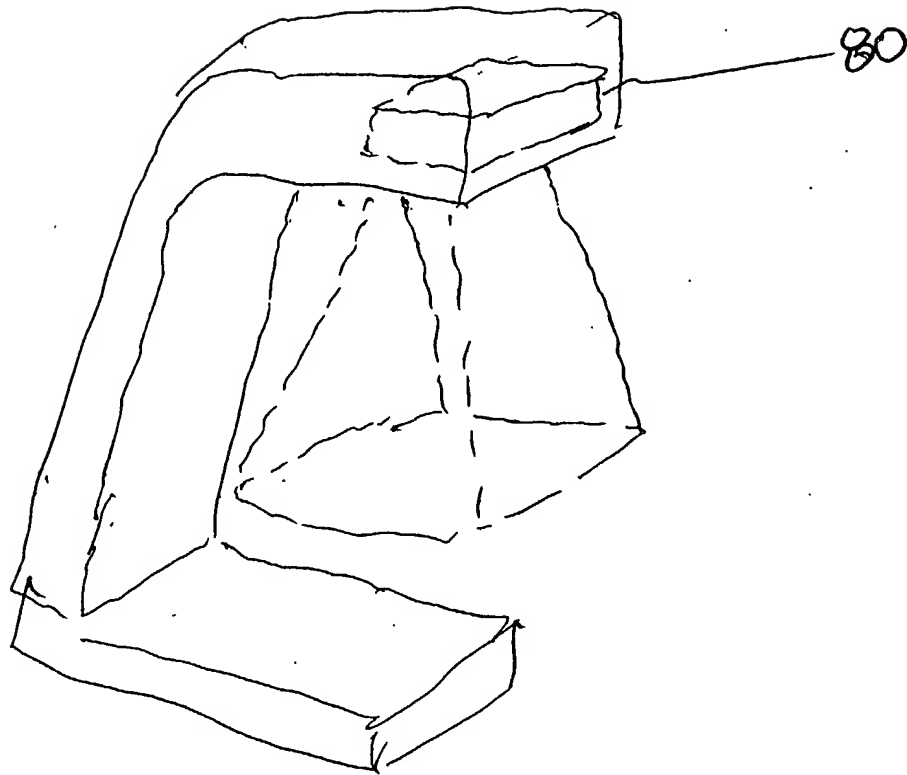


FIG. 6C5

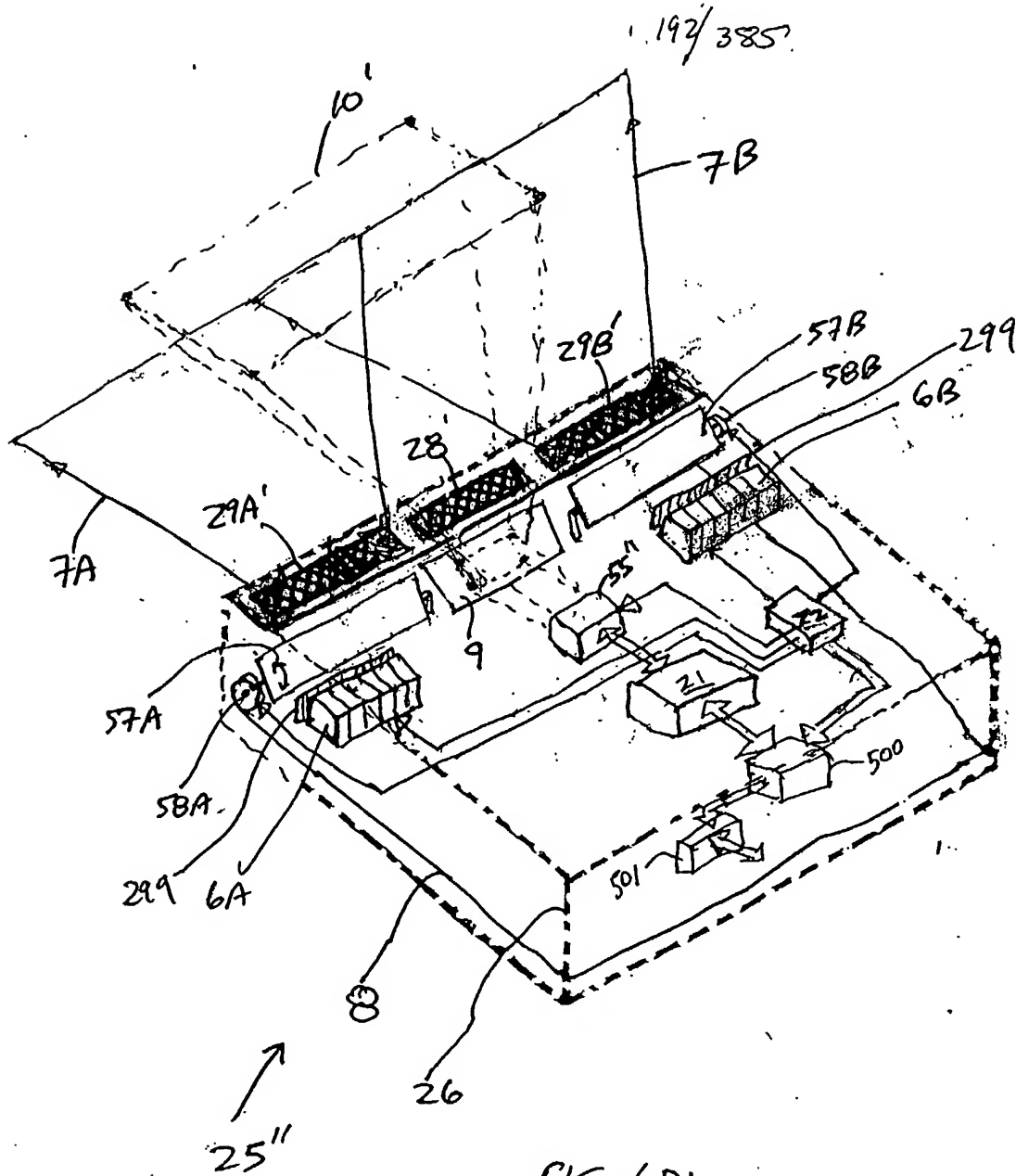
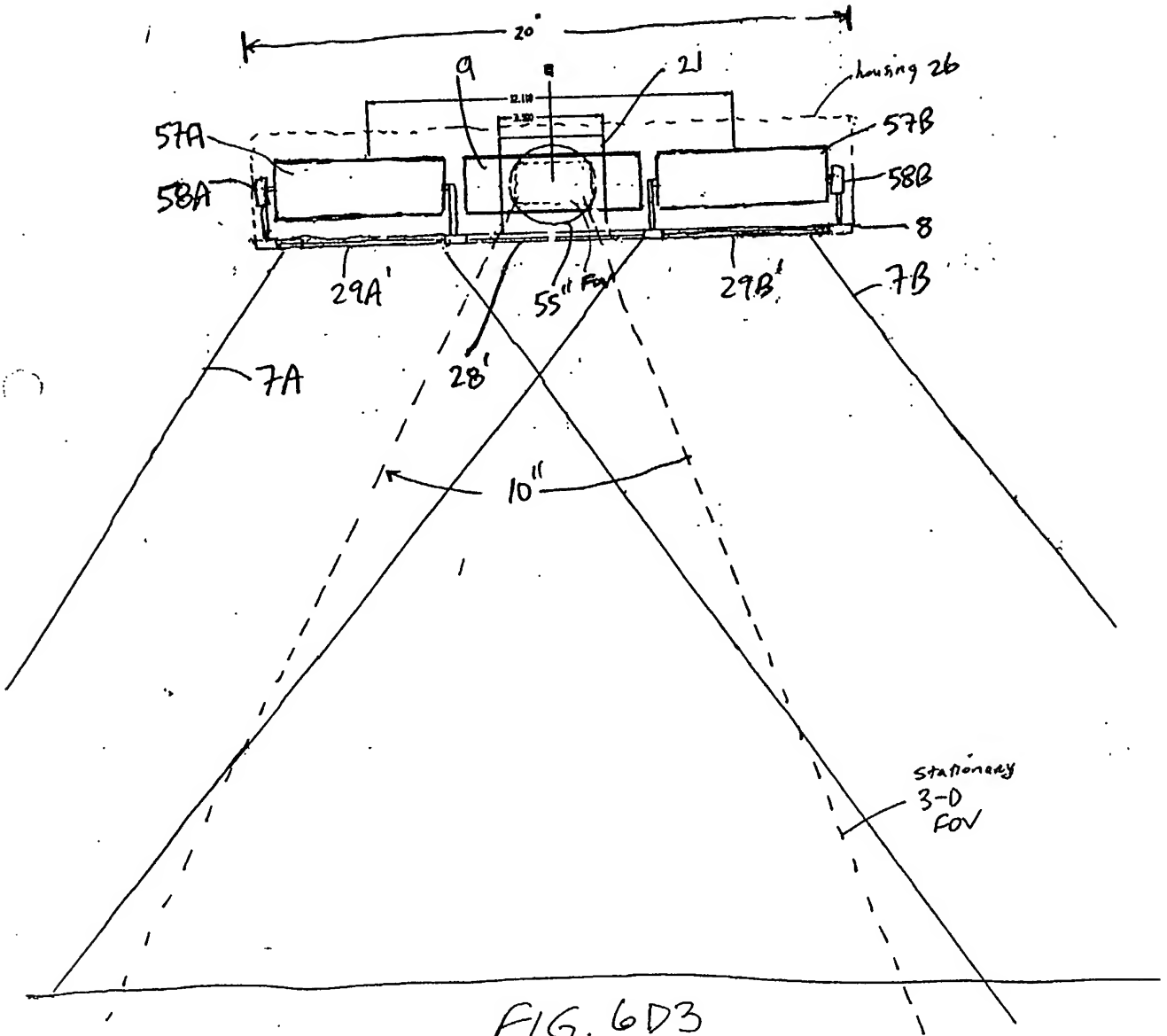


FIG. 6D1

194/385



195/385

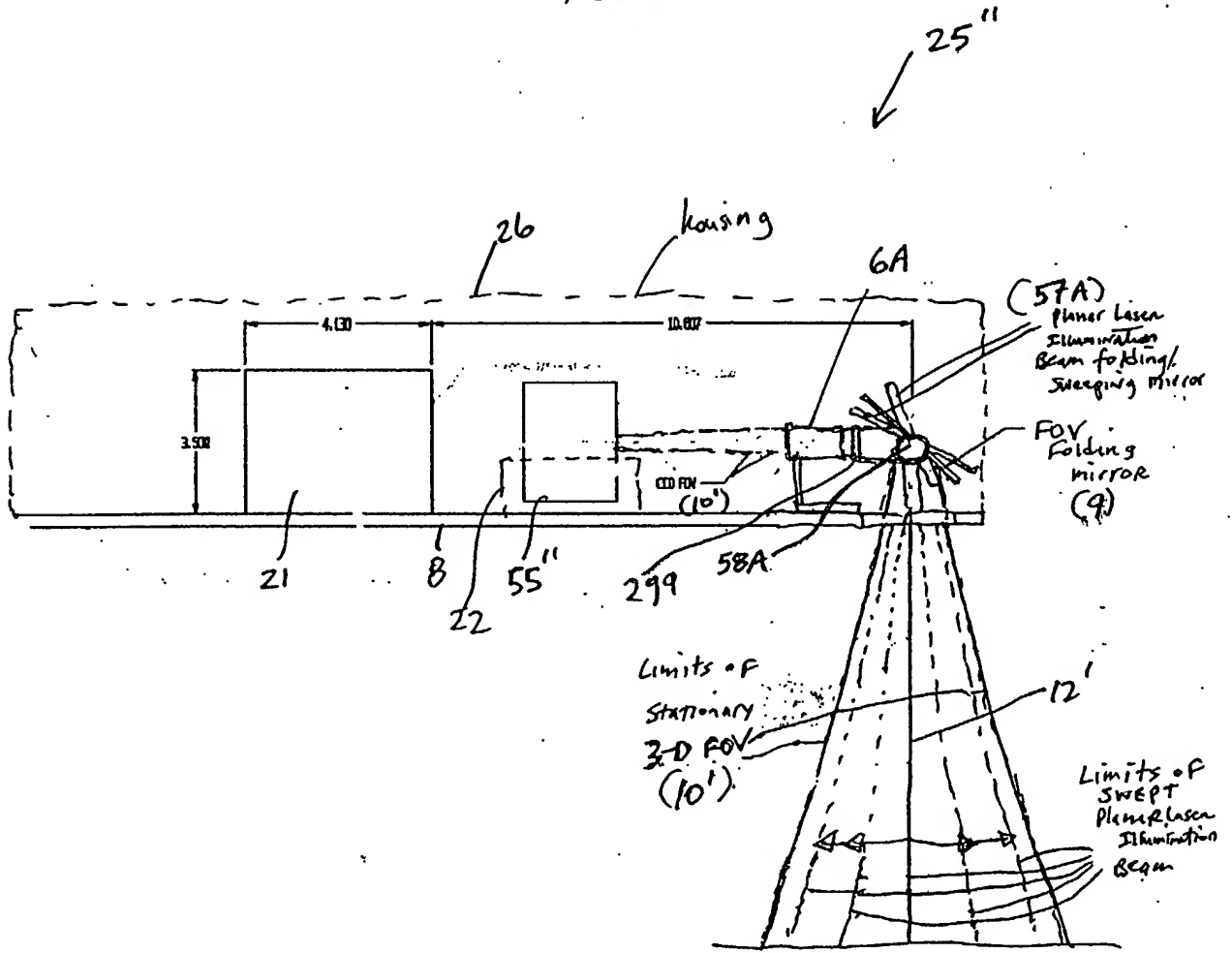


FIG. 6D4

196/385

Variable FOV

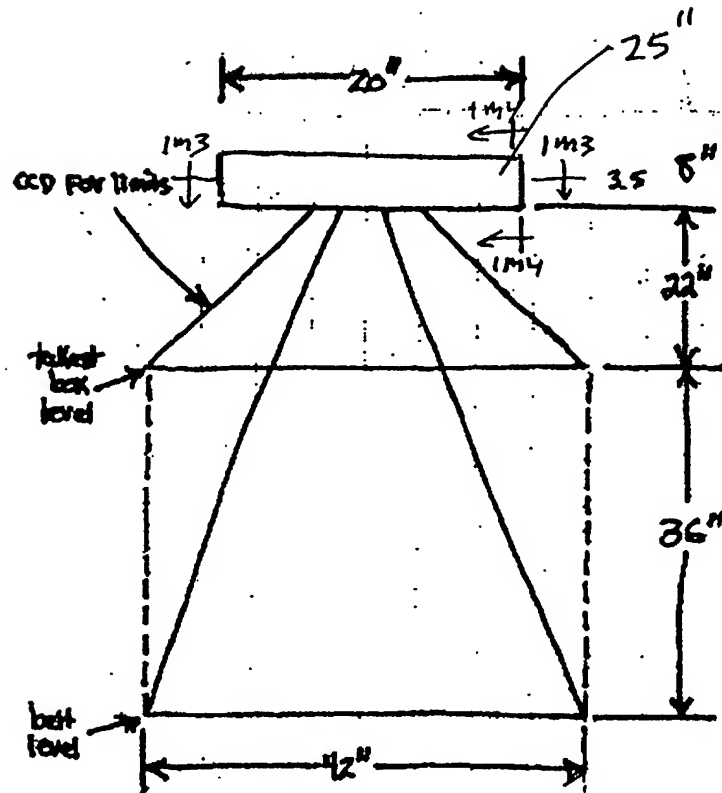


FIG. 6D5

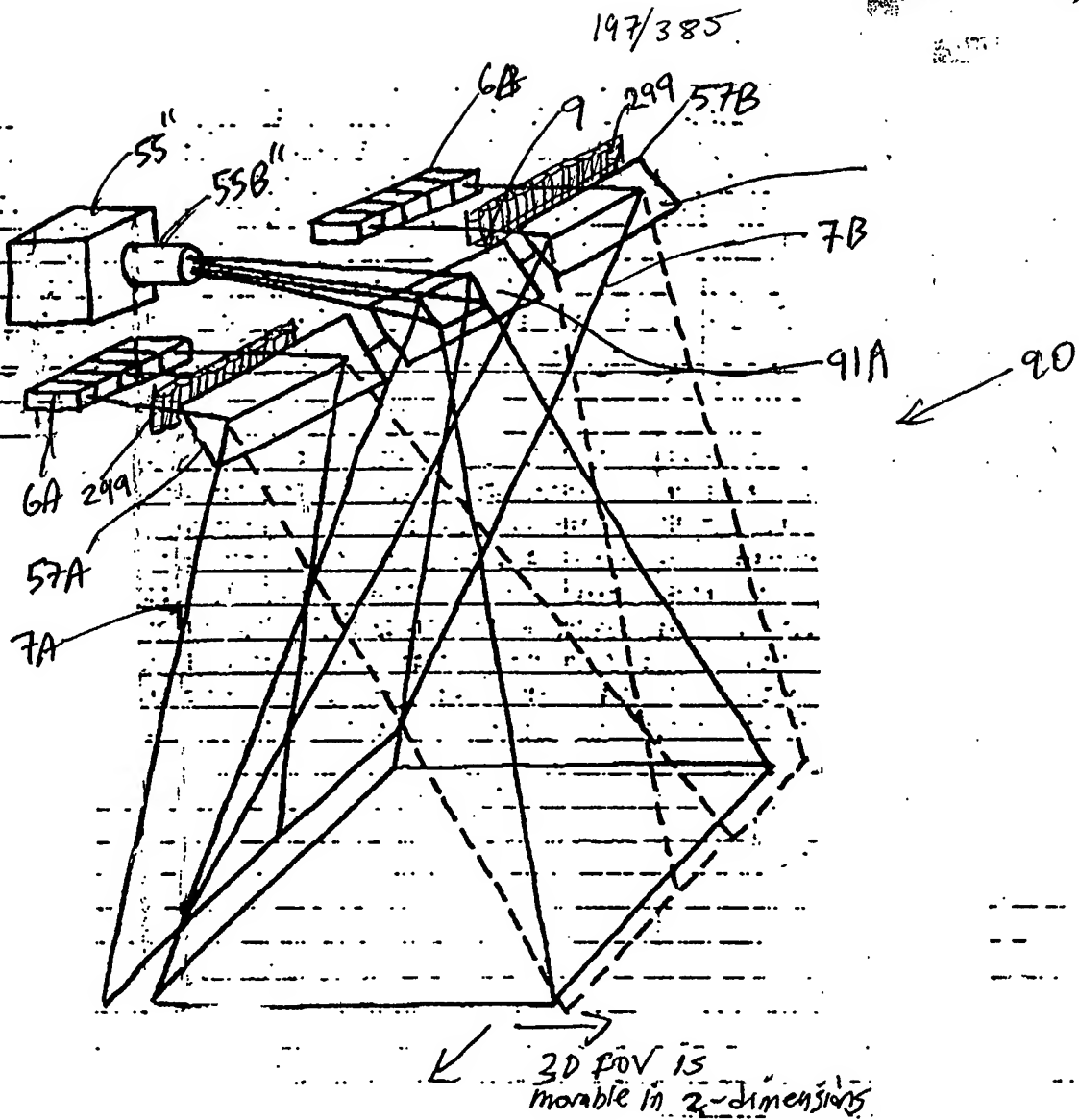


FIG 6E1

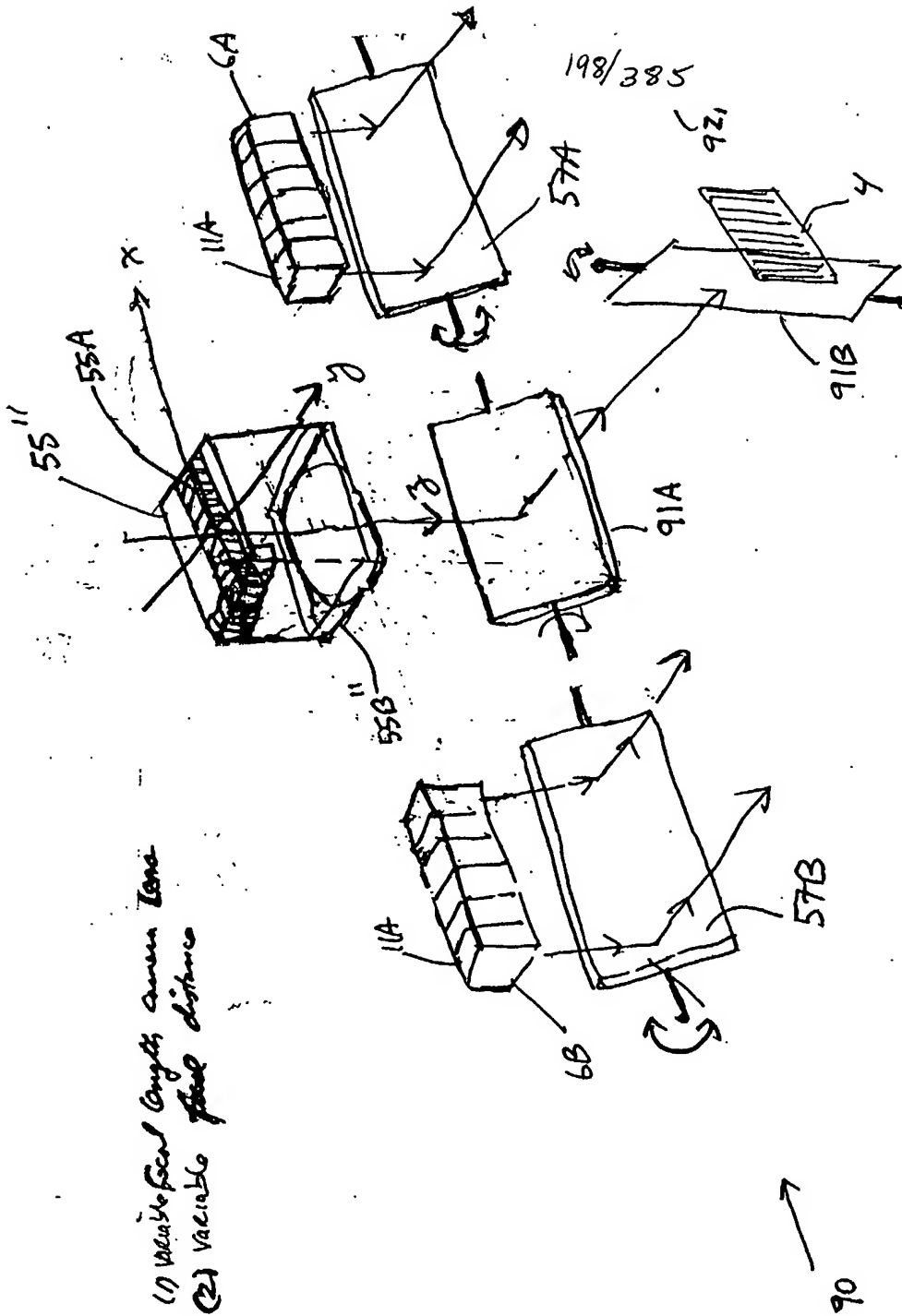


FIG. 6E2

- (1) Variable length array sensor
- (2) Variable fluid distance

90

199/385

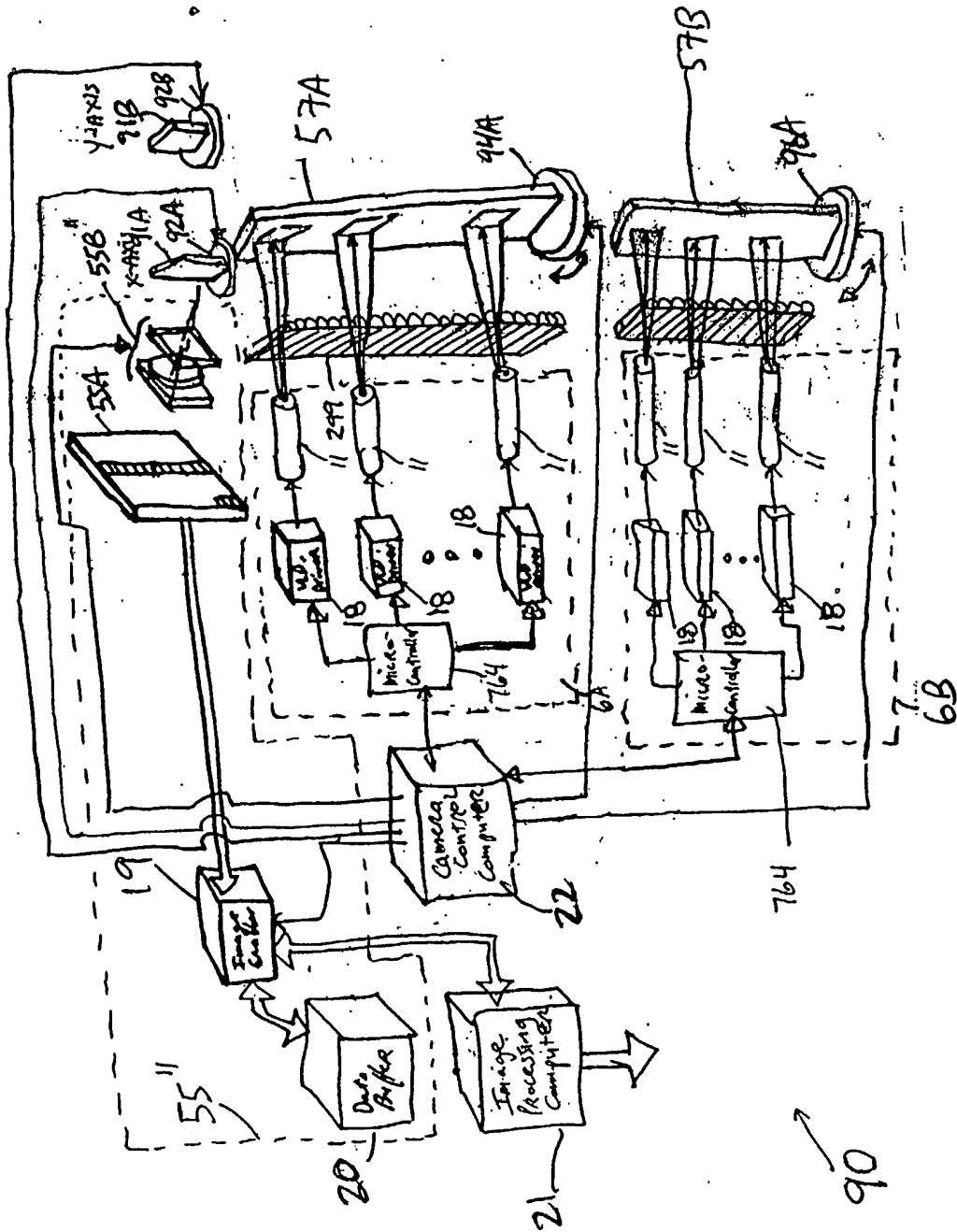
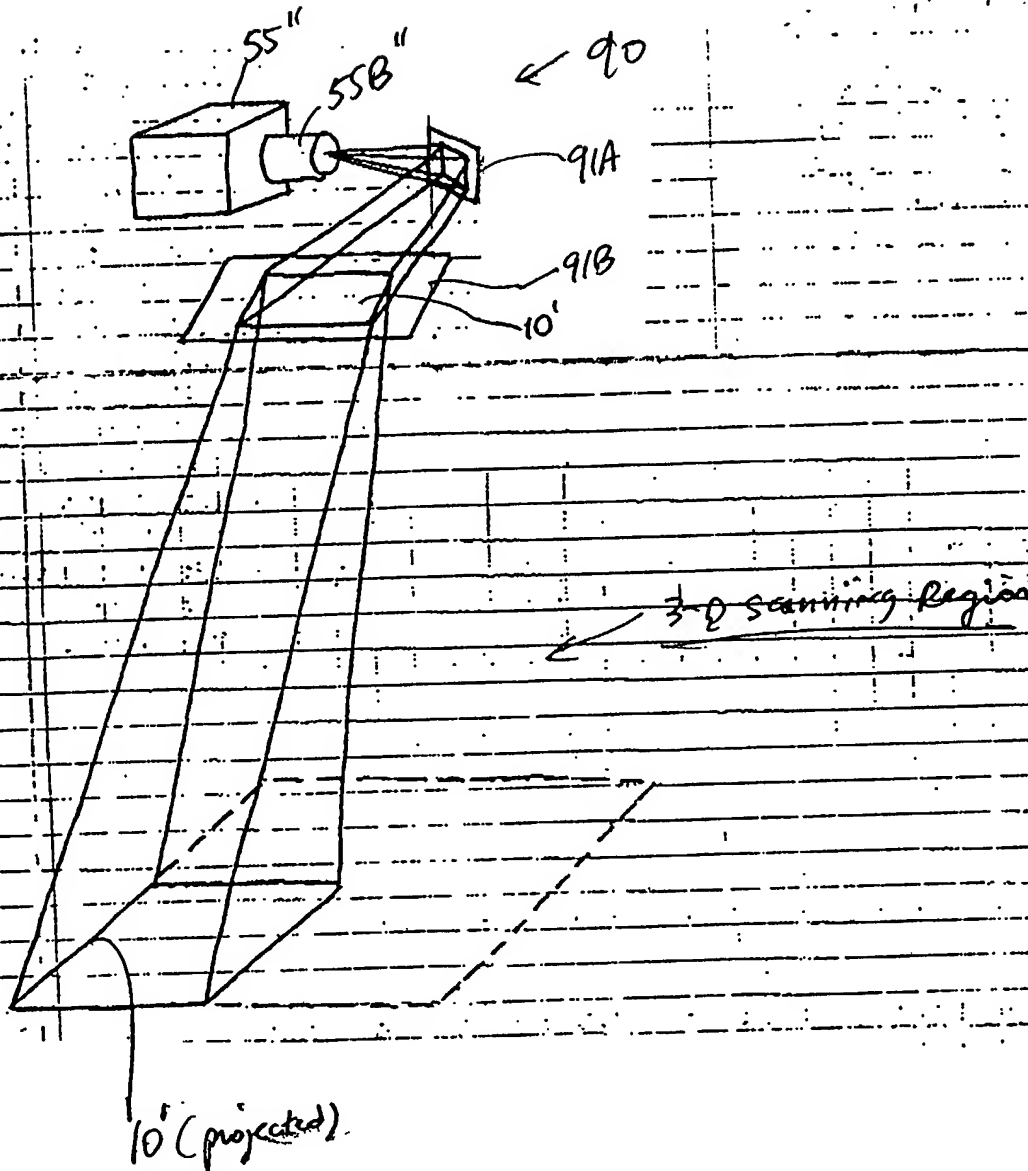


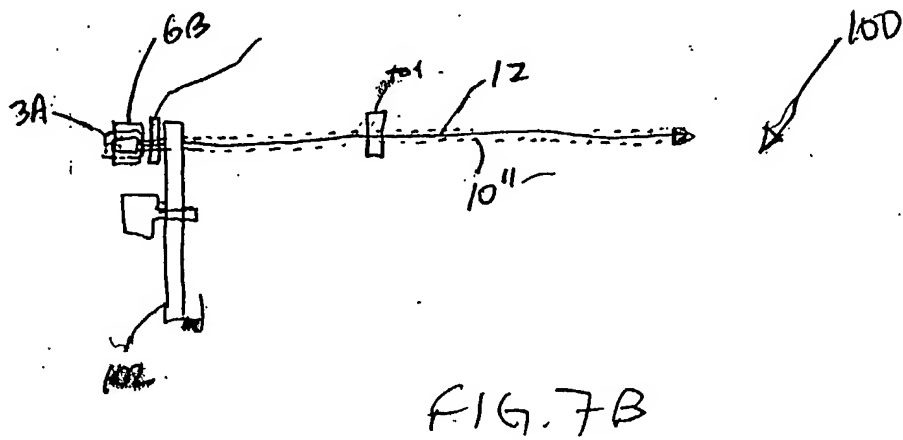
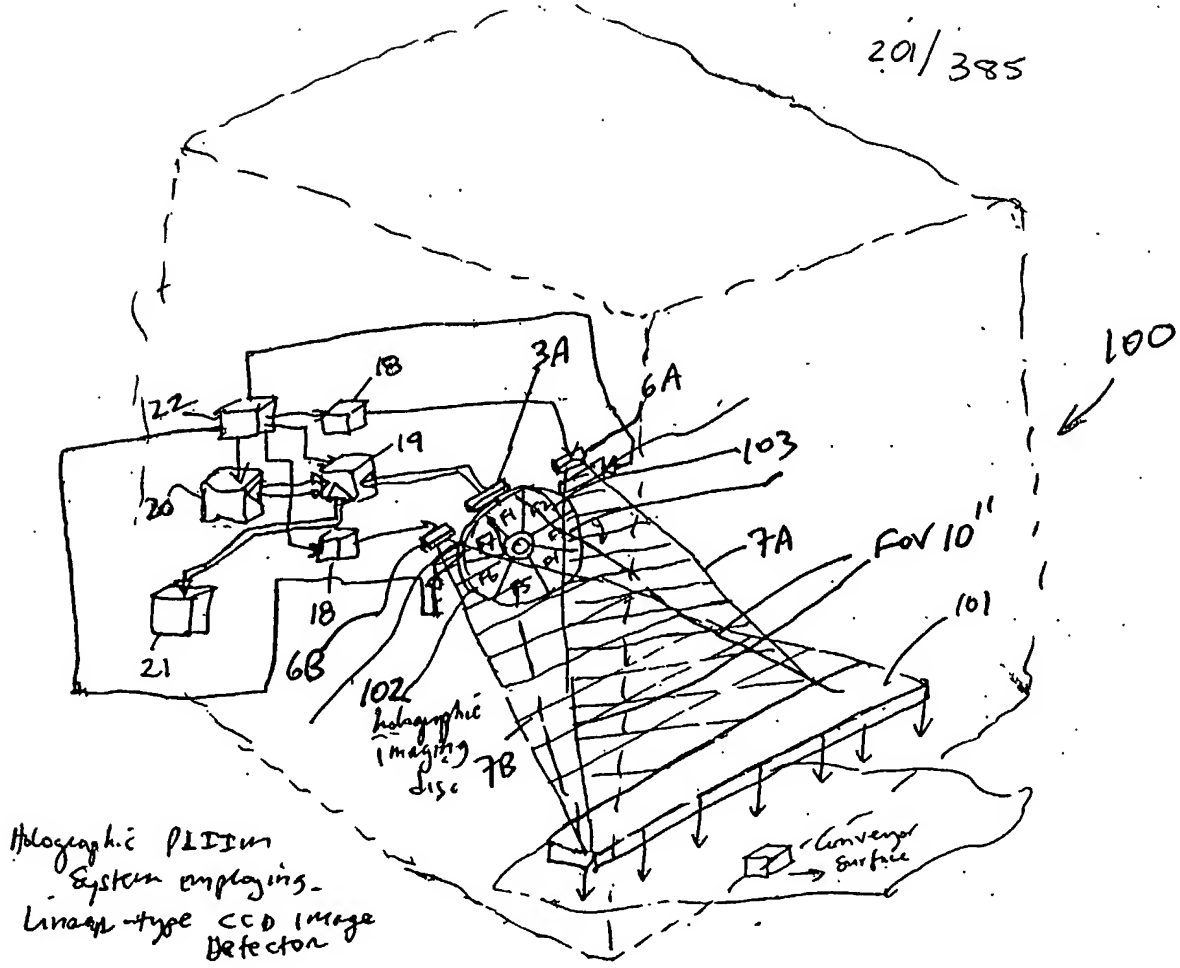
FIG. 6E3

90

200/385



— FIG. 6E4



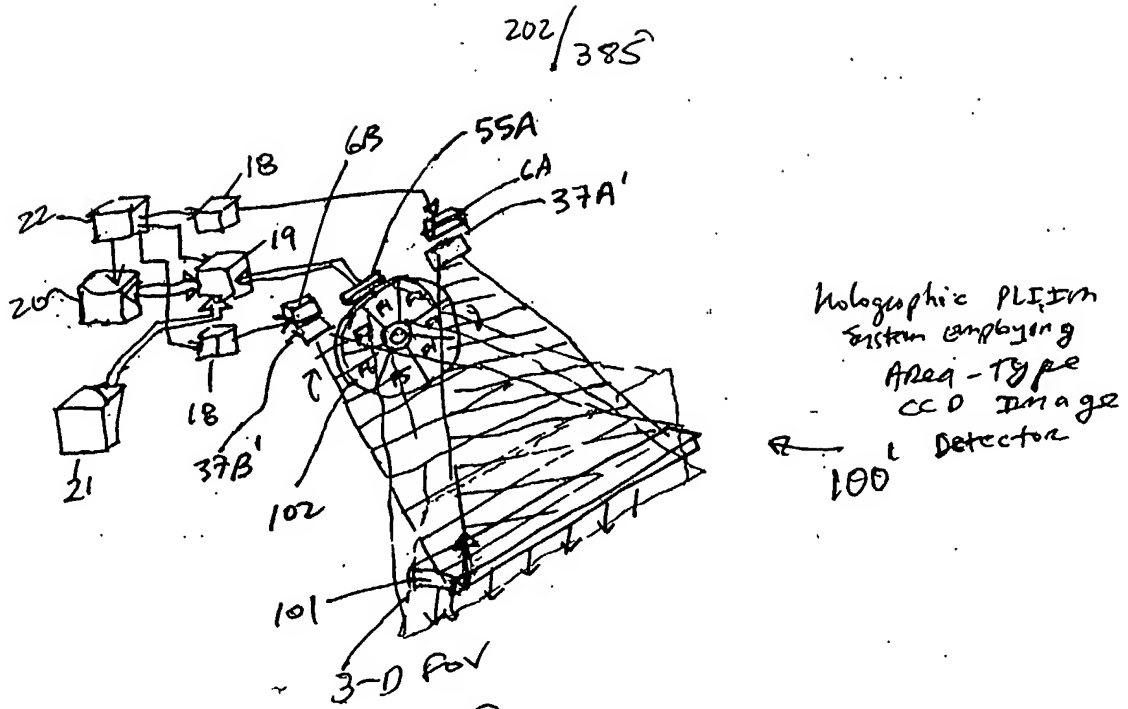


FIG. 8A

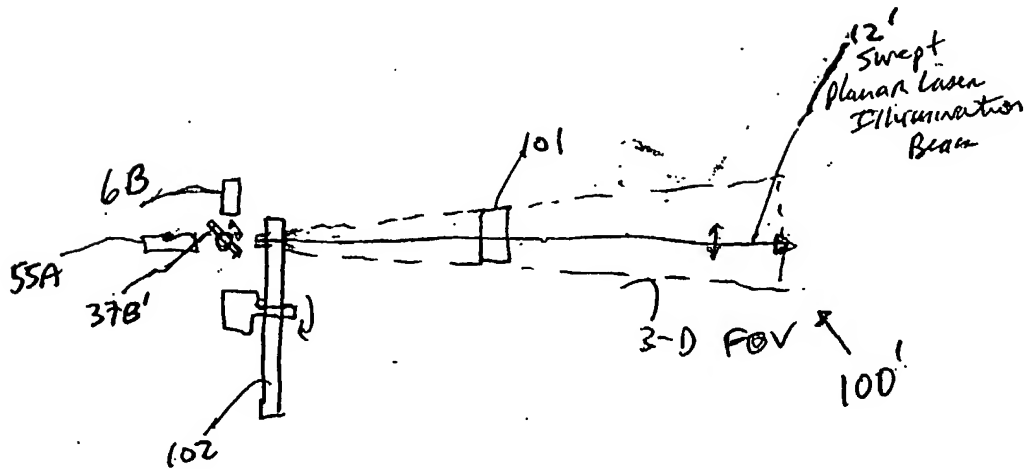


FIG. 8B

203/385

1-D CCD SCANNER EMBODIMENT

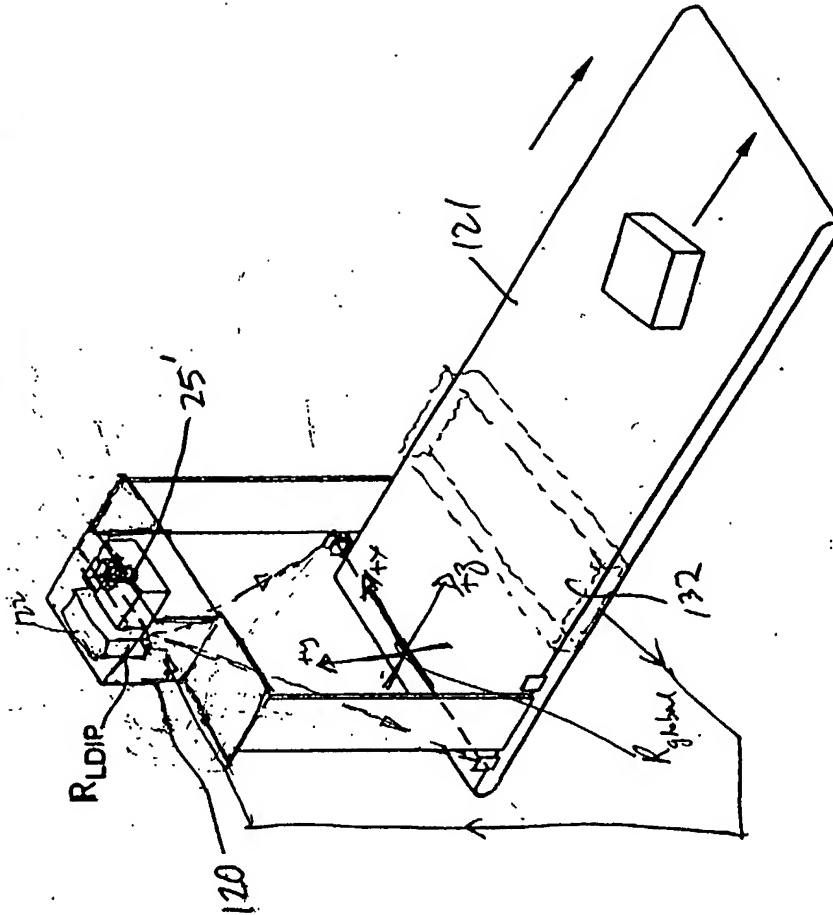
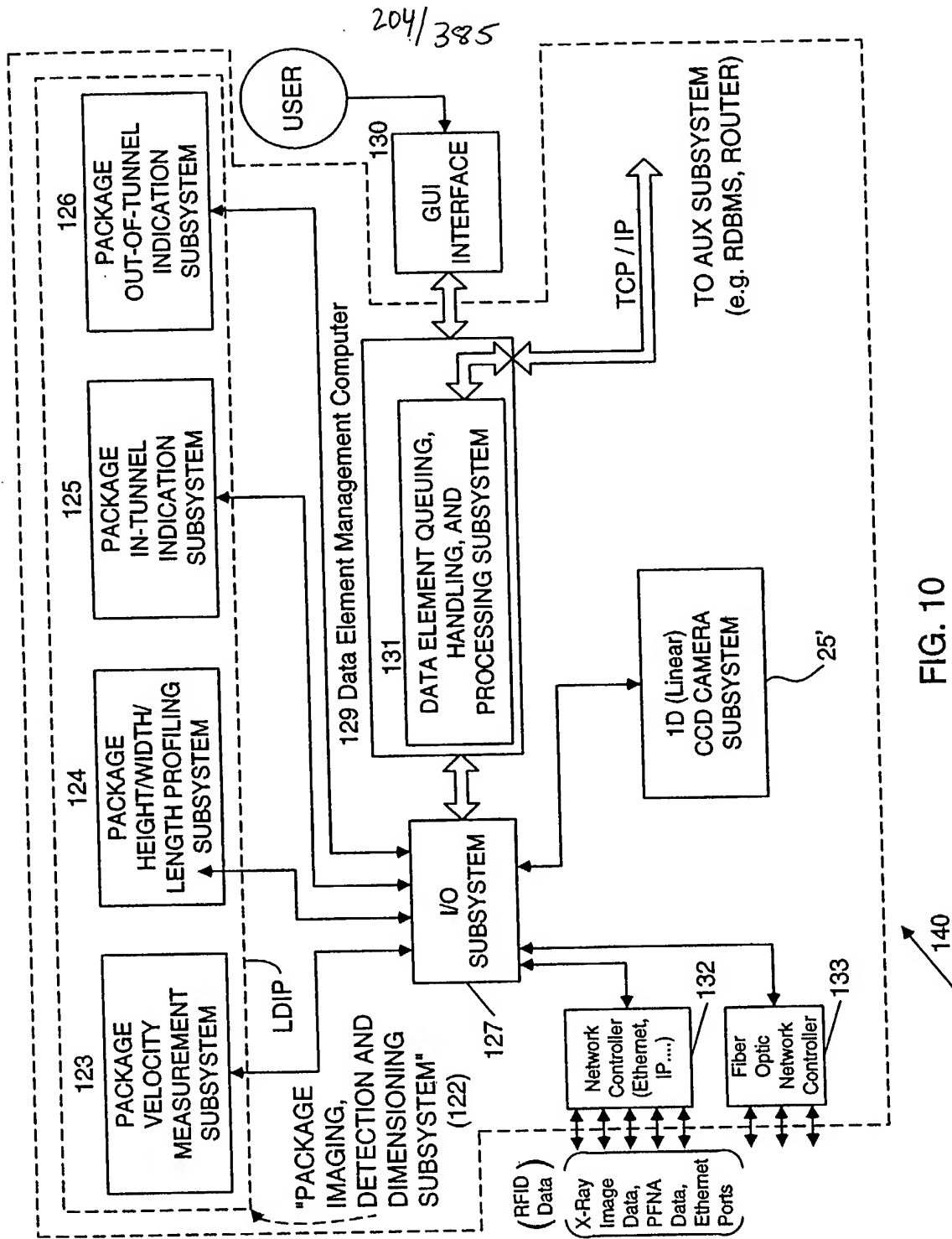


FIG. 9



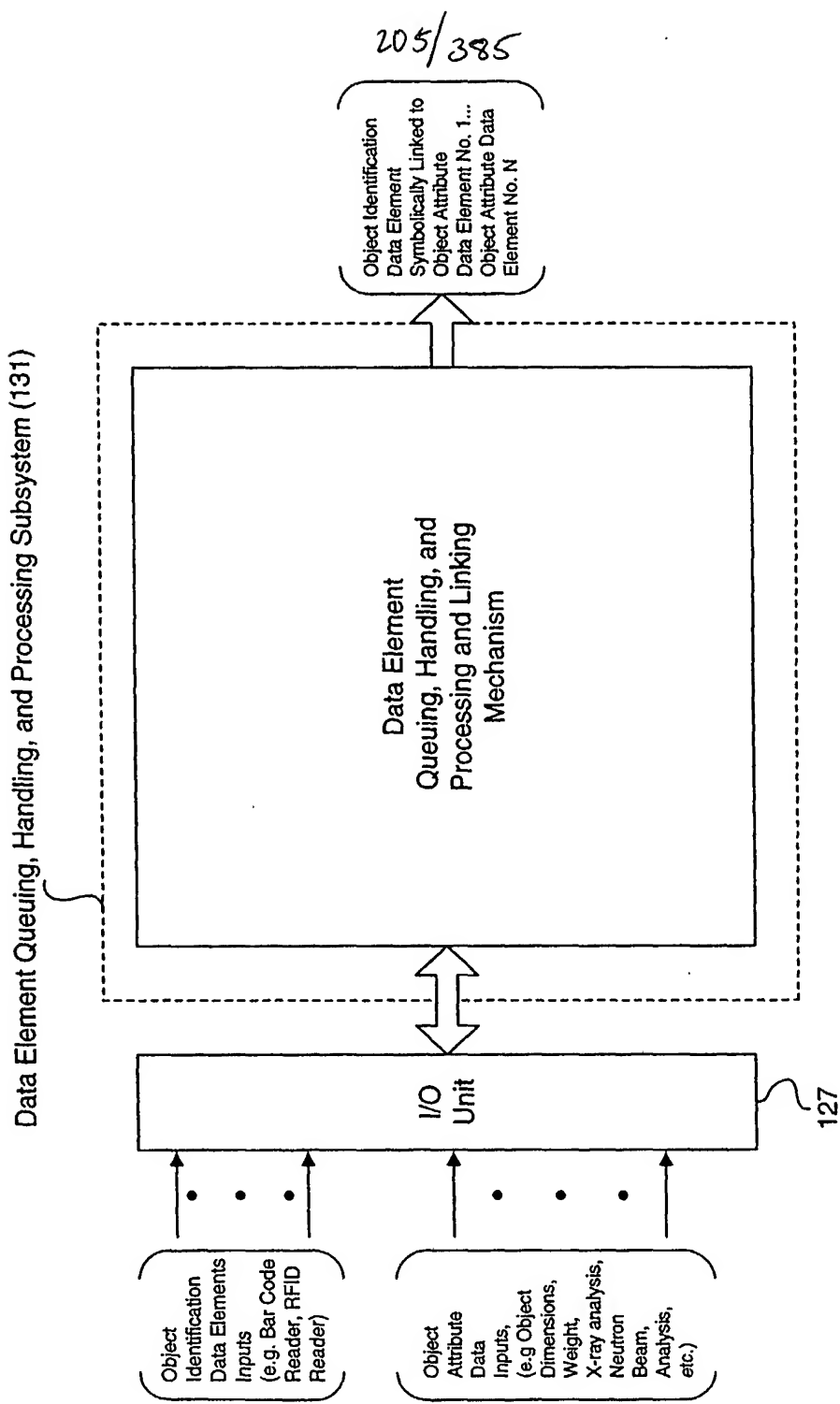


FIG. 10A

Primary Network
and/ or System
Functions:

A. Specification of Object
Detection and
Tracking Capability of
System

B. Specification of Object
Identification
Capability of System

C. Specification of
Object Attribute
Acquisition Capability
of System

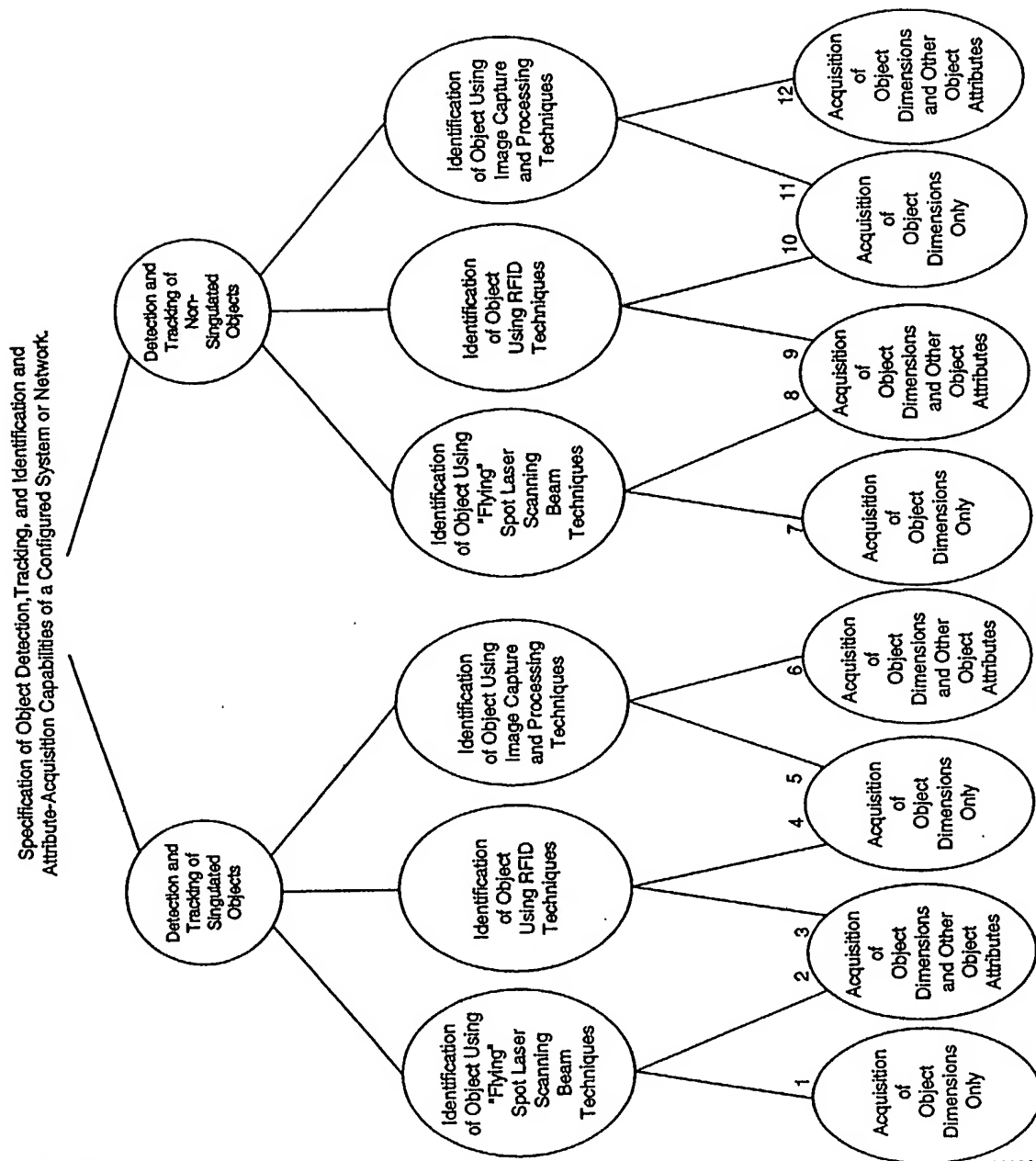


FIG. 10B

206/385

10004077, 002702

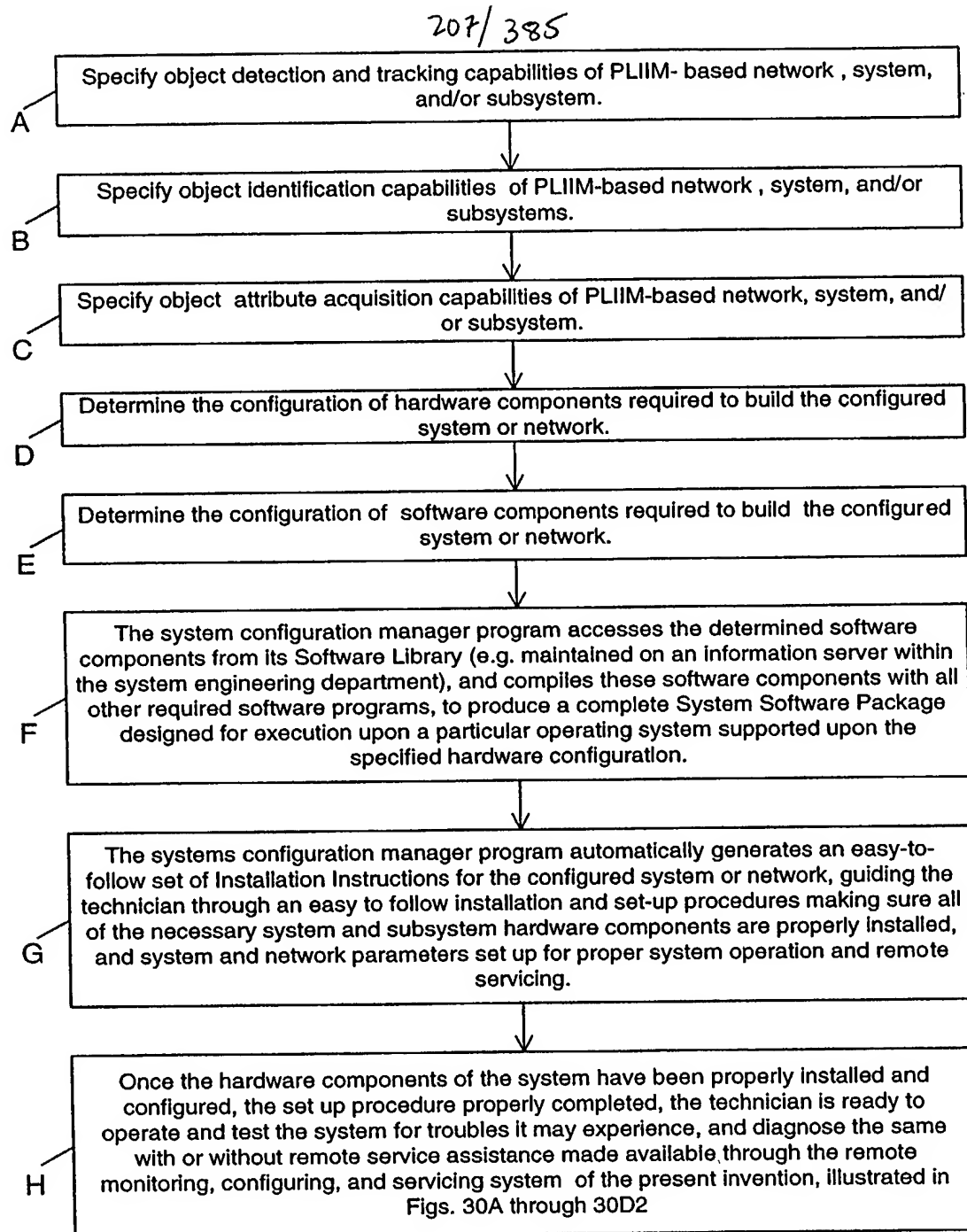


FIG. 10C

208/3857

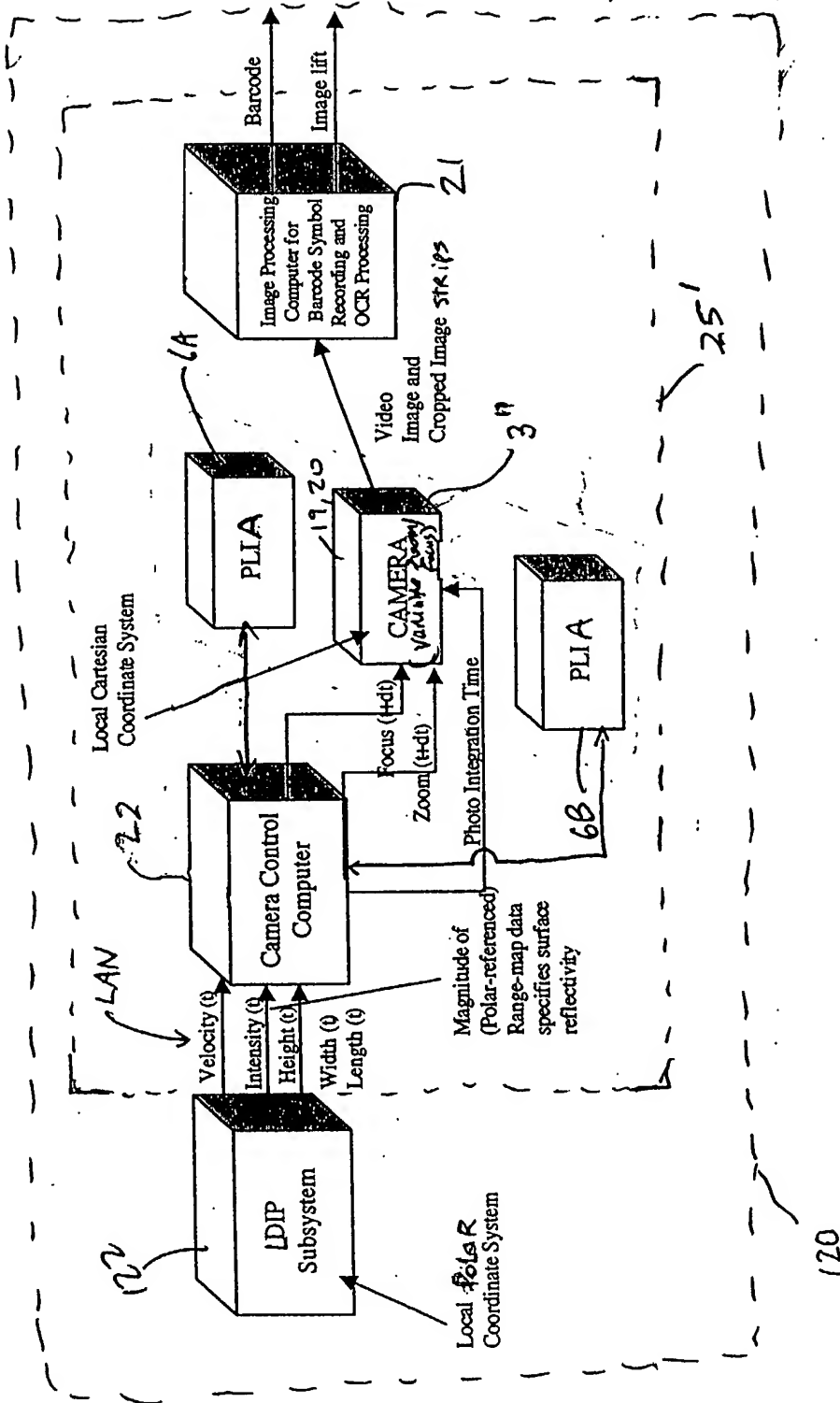


FIG. 11

209/385

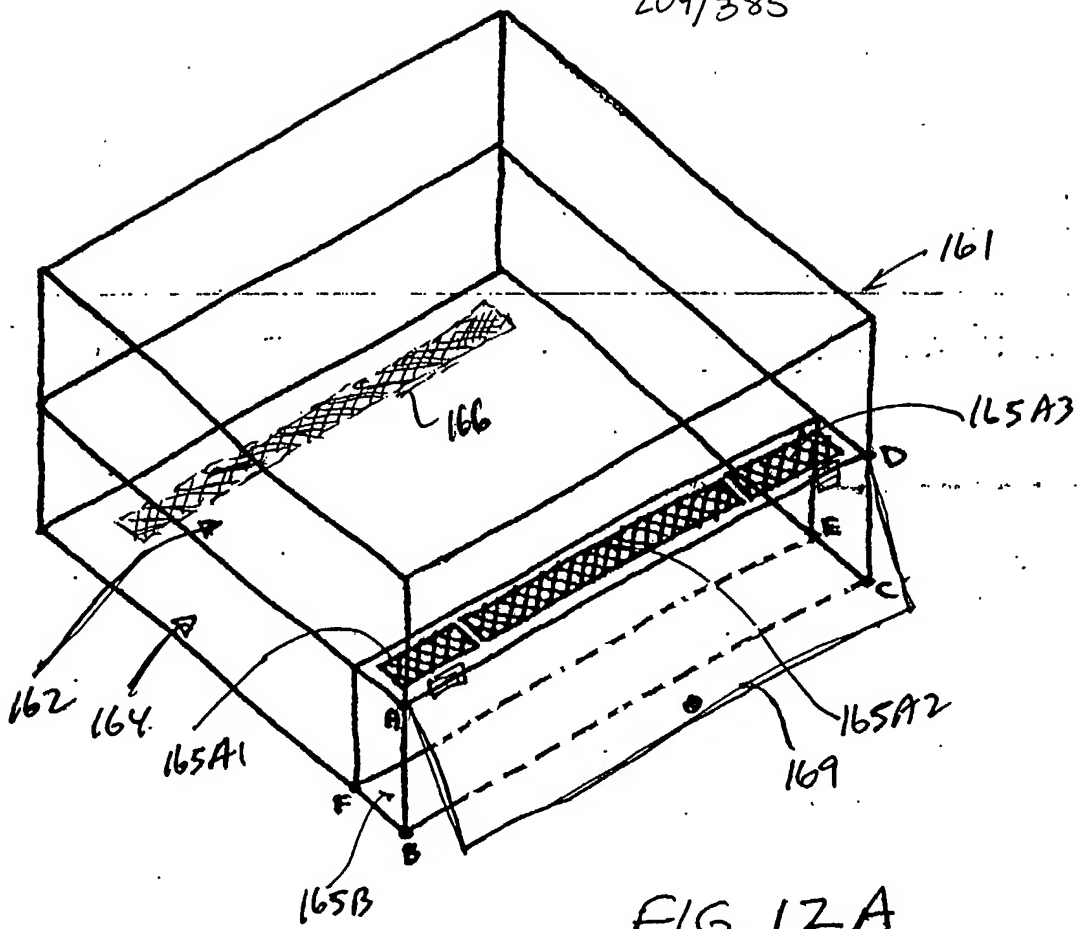


FIG. 12A

210/385

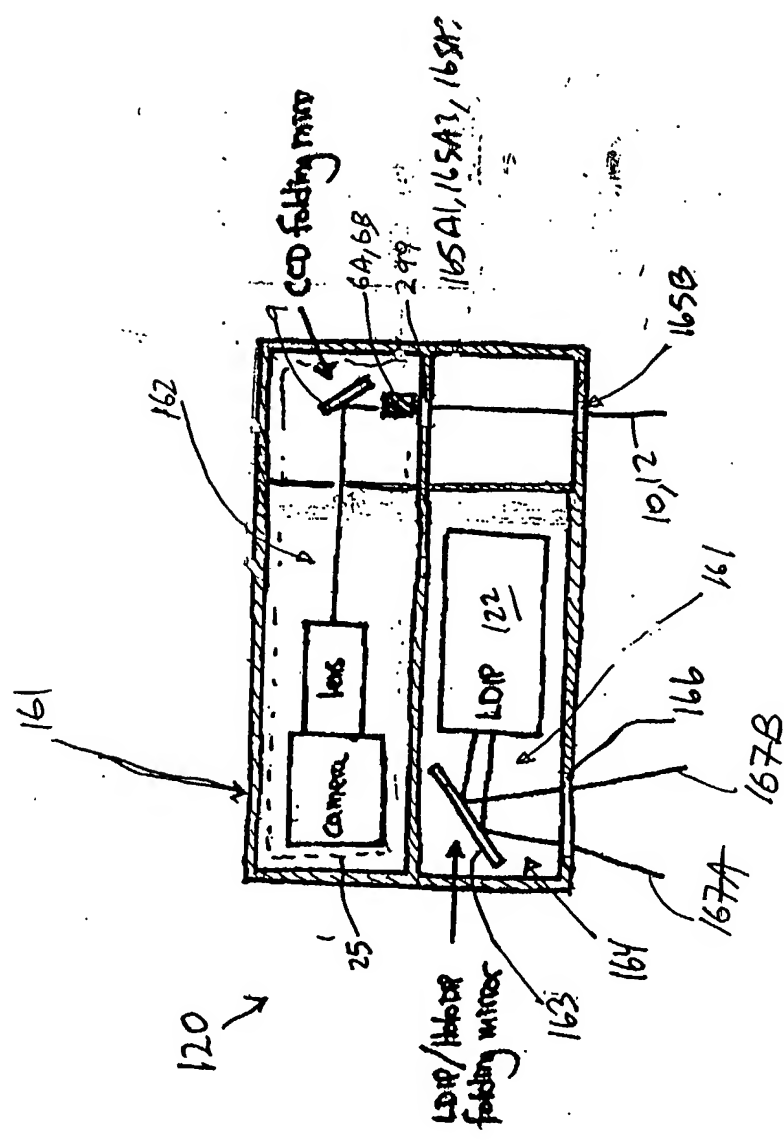


FIG. 12B

211/385

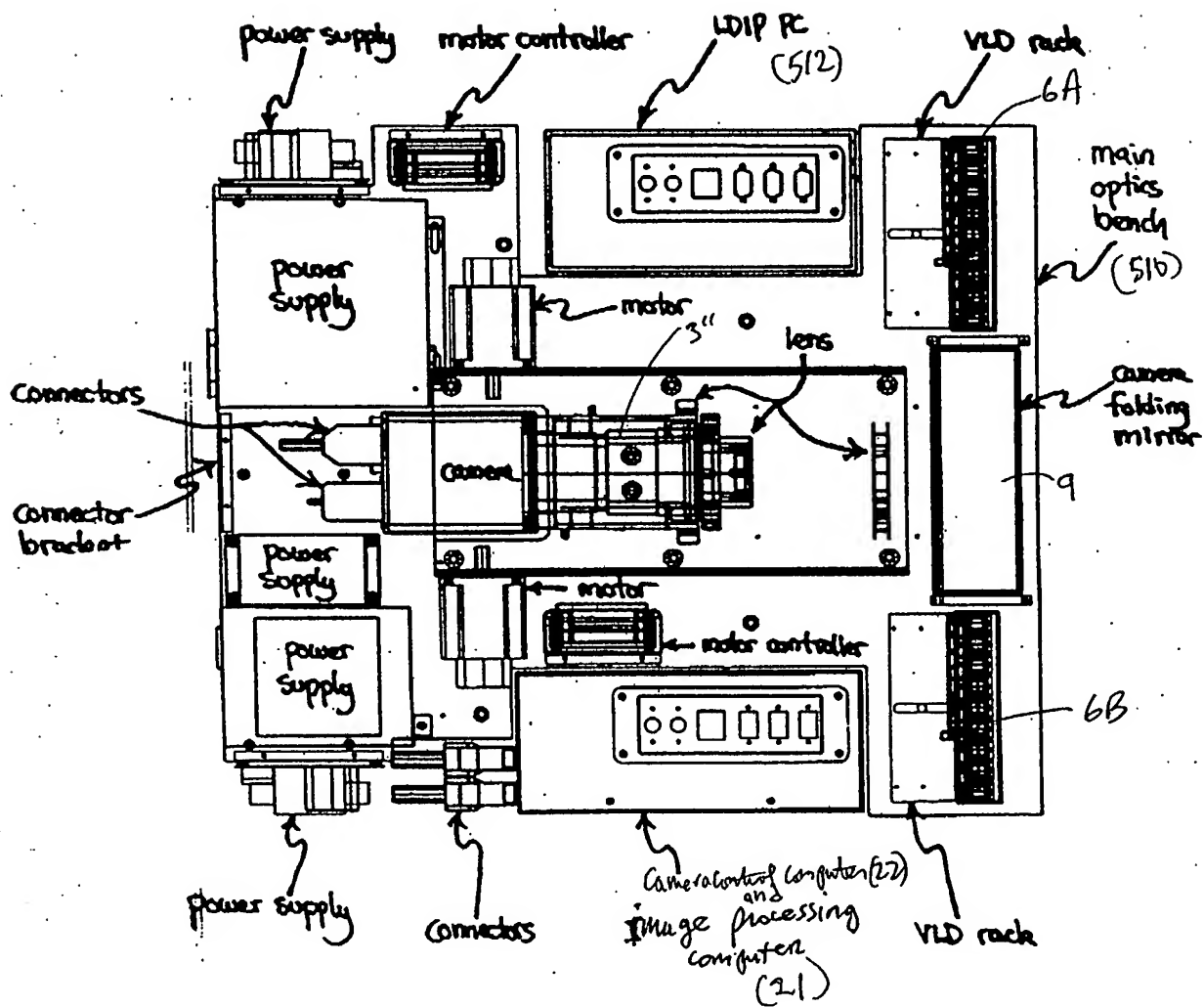


FIG. 12C

212/385

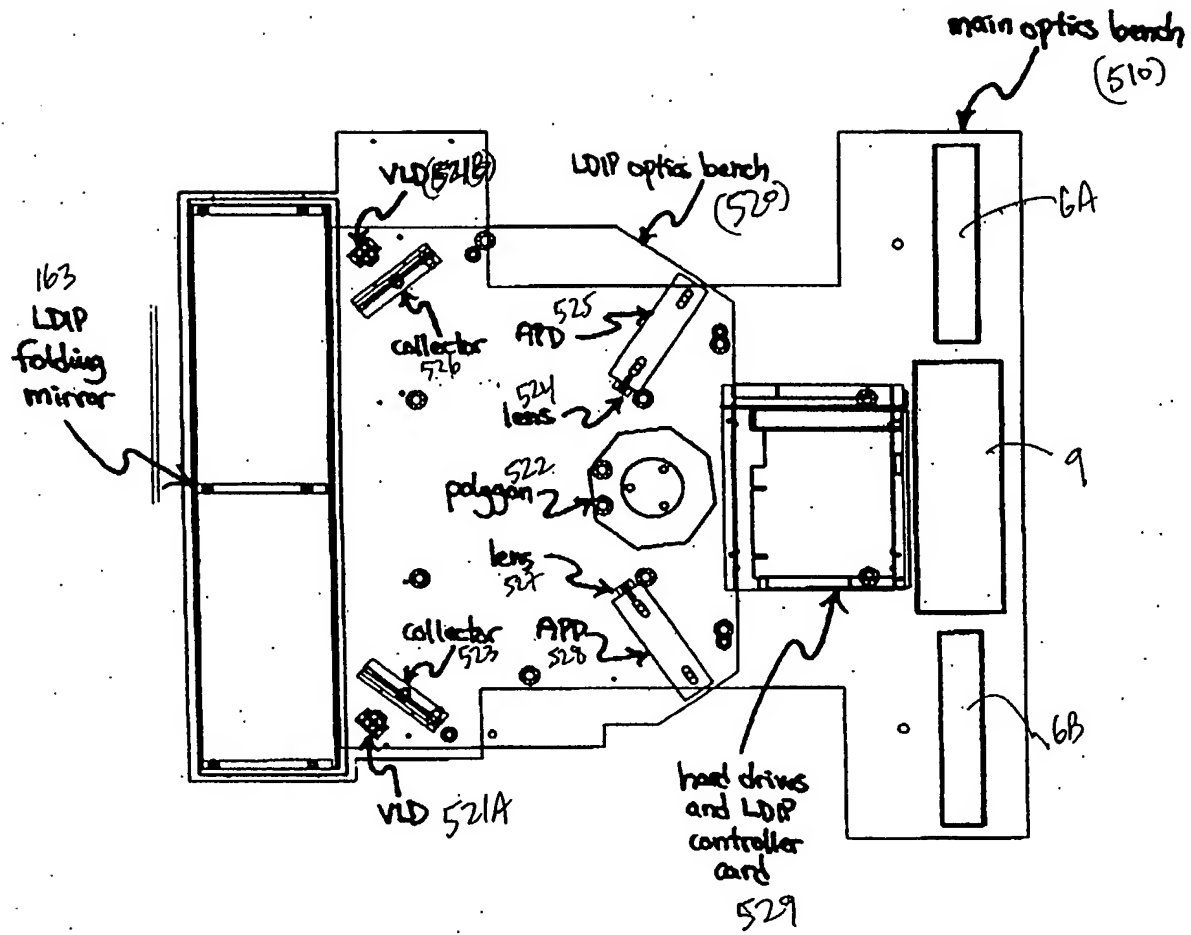
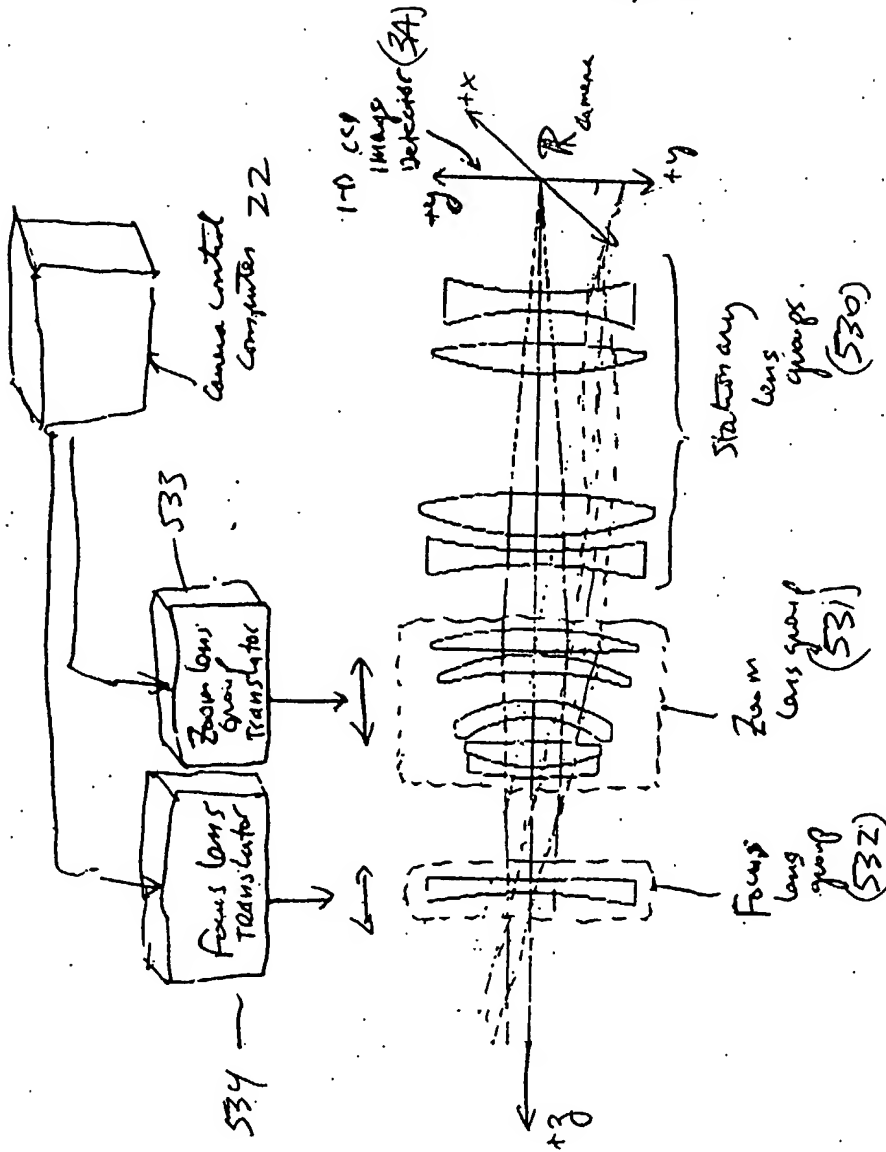


FIG. 12D

213/385



(main optics)
(Lens groups)

FIG. 12E

214/385

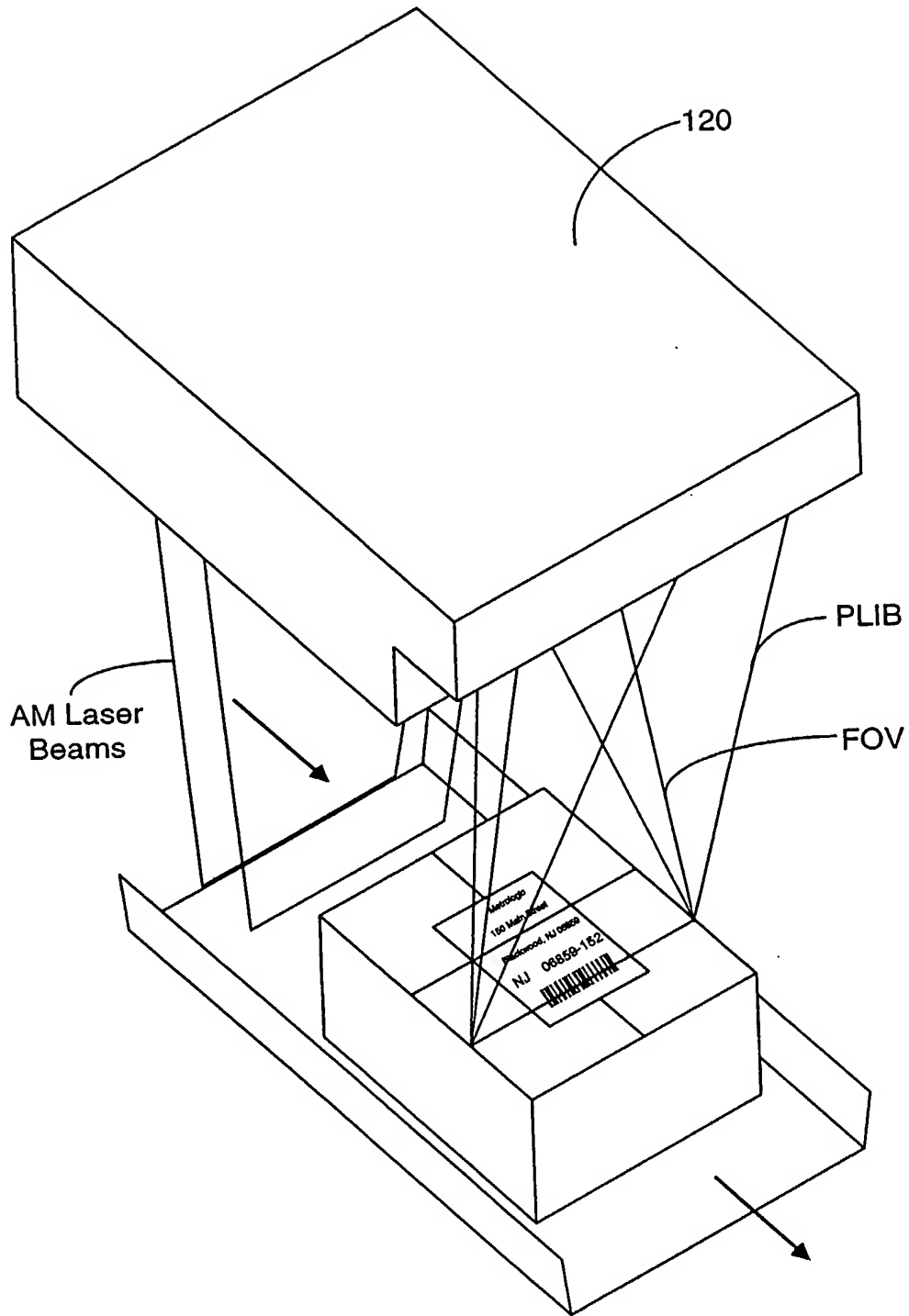


FIG. 13A

216/385

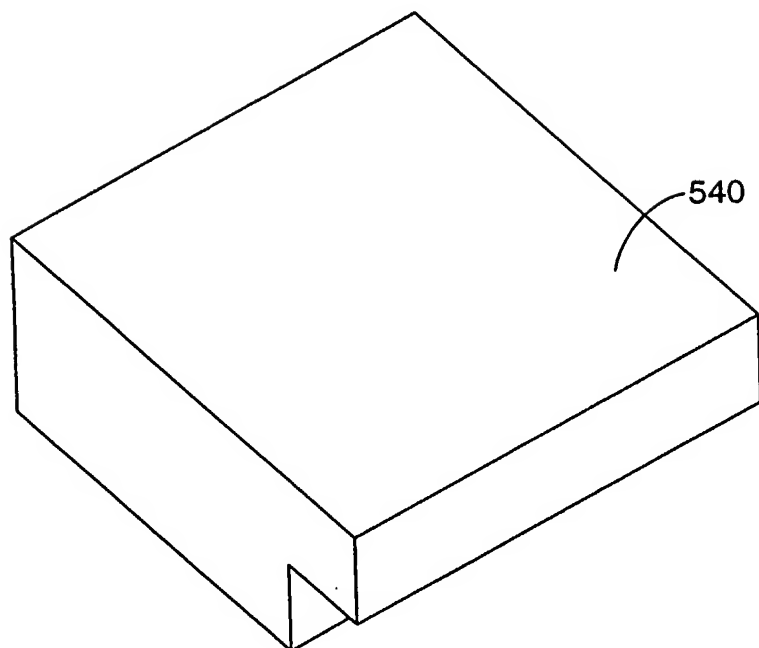


FIG. 13B

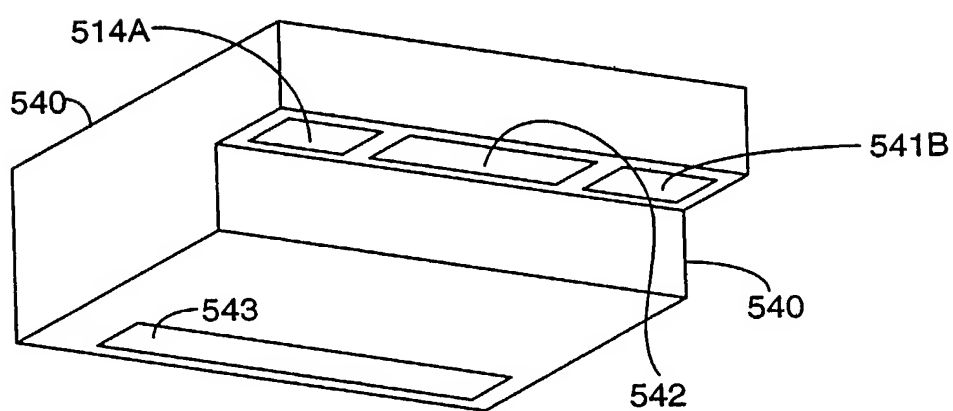


FIG. 13C

27/385

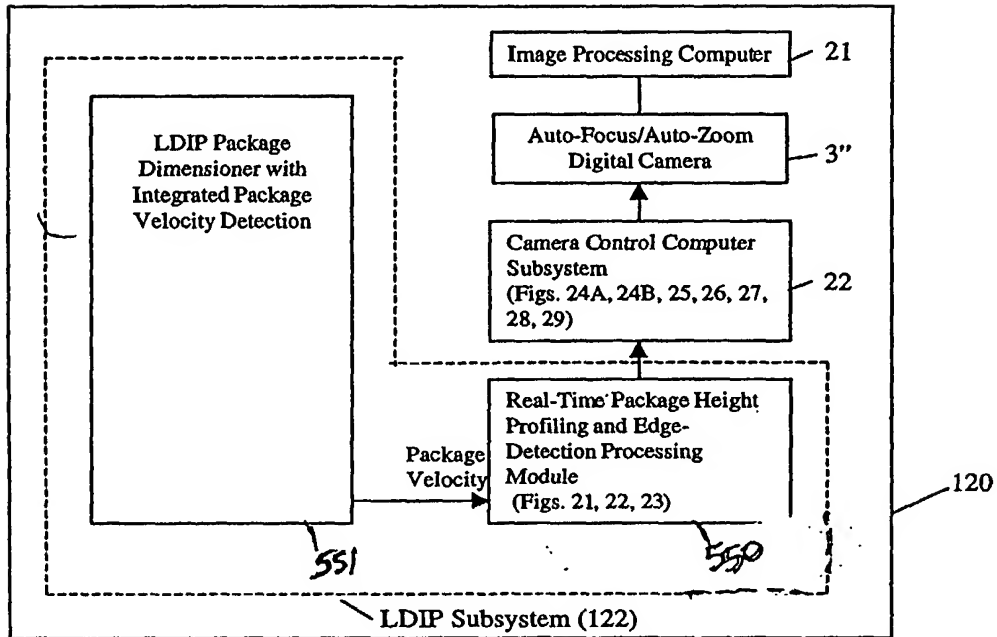
PLLIM-BASED PACKAGE IDENTIFICATION AND
DIMENSIONING (PID) SYSTEM

FIG. 14

218/395

LDIP REAL-TIME PACKAGE HEIGHT PROFILE AND EDGE DETECTION METHOD

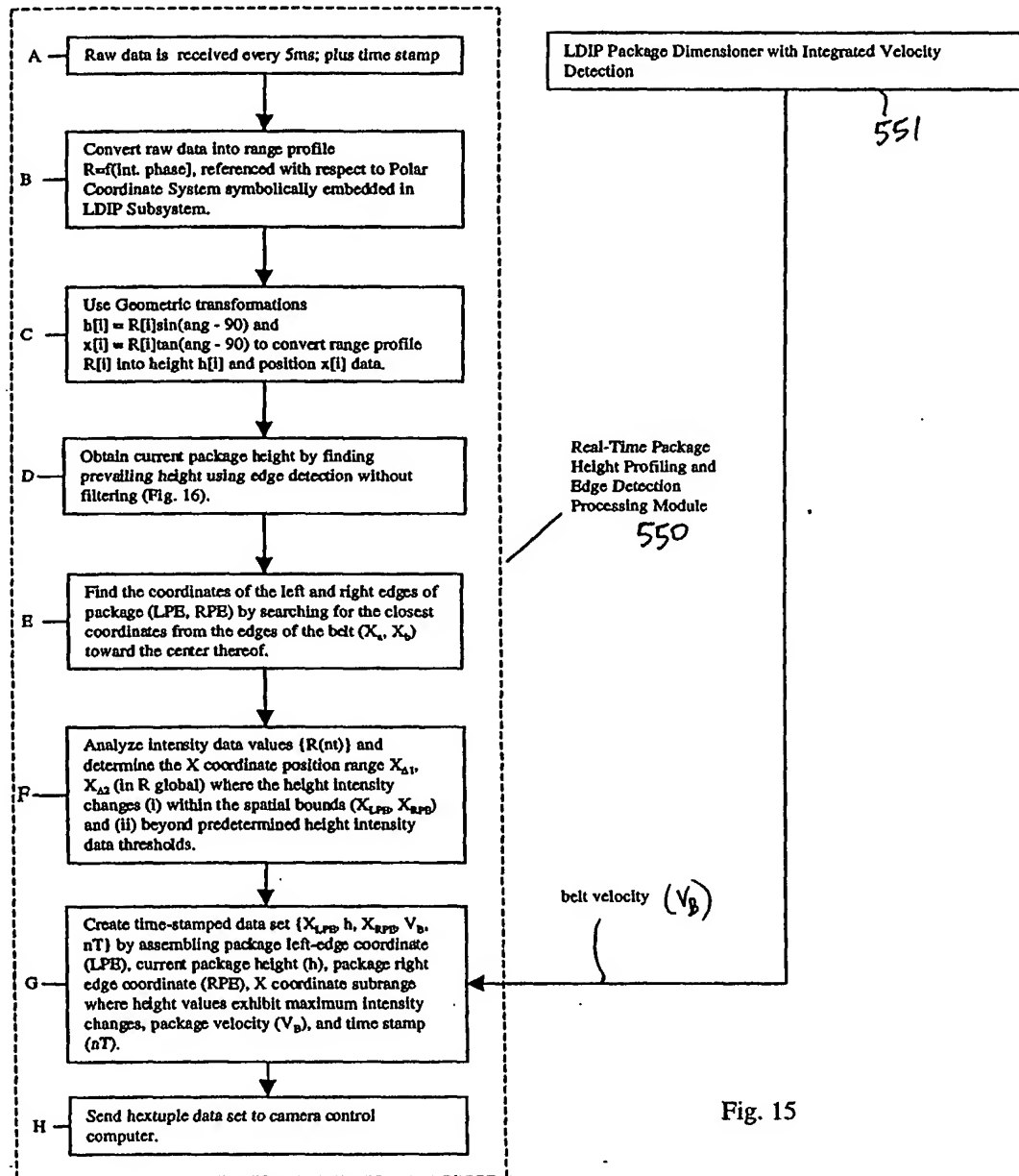


Fig. 15

219/385

LDIP Real Time Package Edge Detection

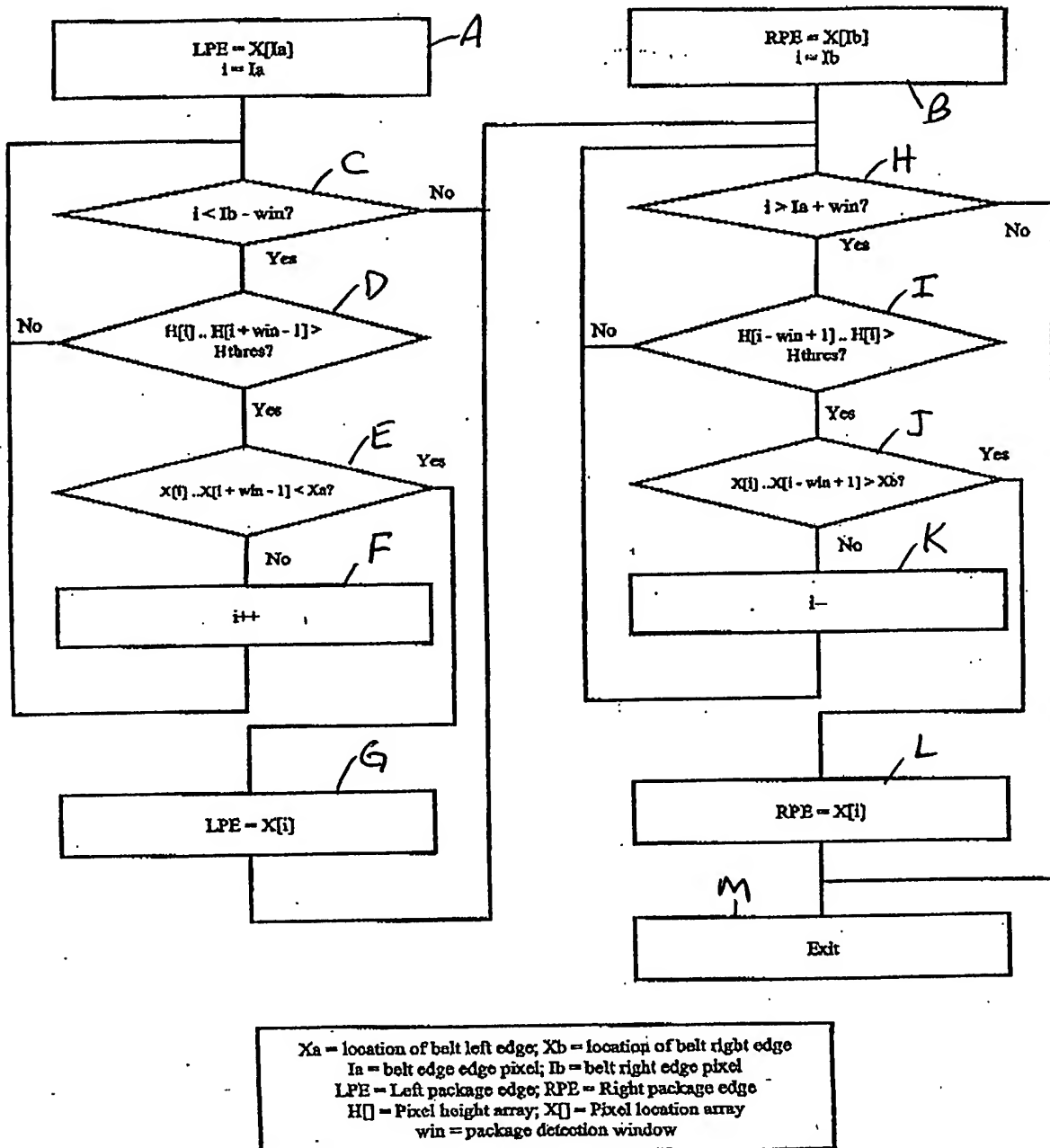


FIG. 16

220/385

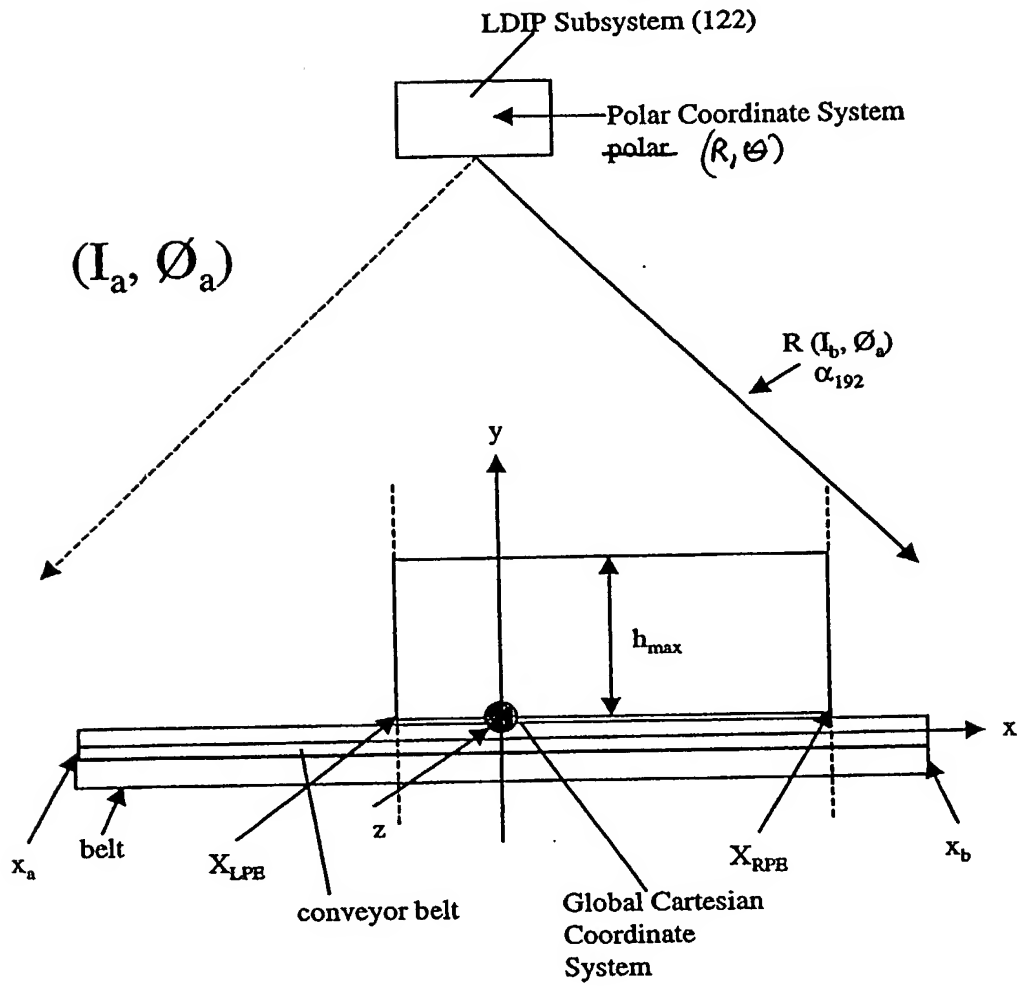


Fig. 17

24/385

INFORMATION MEASURED AT SCAN ANGLES BEFORE COORDINATE TRANSFORMS

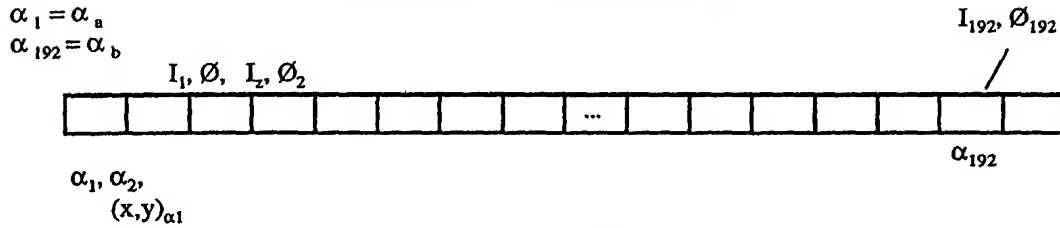


Fig. 17A

RANGE AND POLAR ANGLE MEASURES TAKEN AT SCAN ANGLE α BEFORE COORDINATE TRANSFORMS

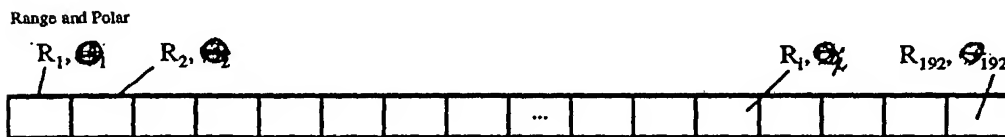


Fig. 17B

MEASURED PACKAGE HEIGHT AND POSITION VALUES AFTER COORDINATE TRANSFORMS

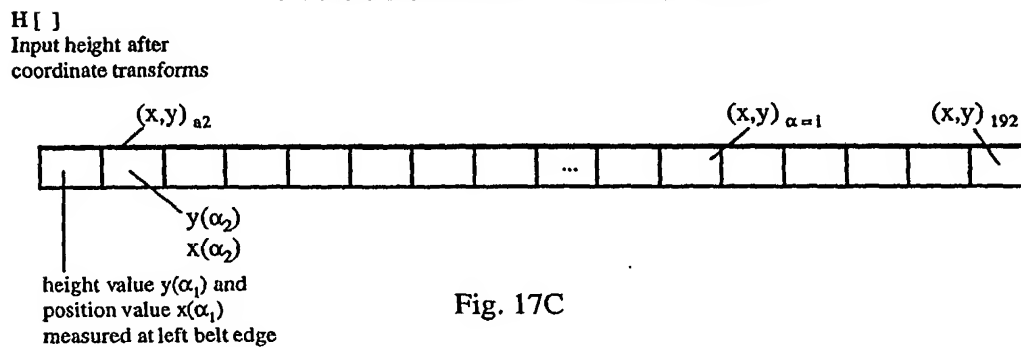
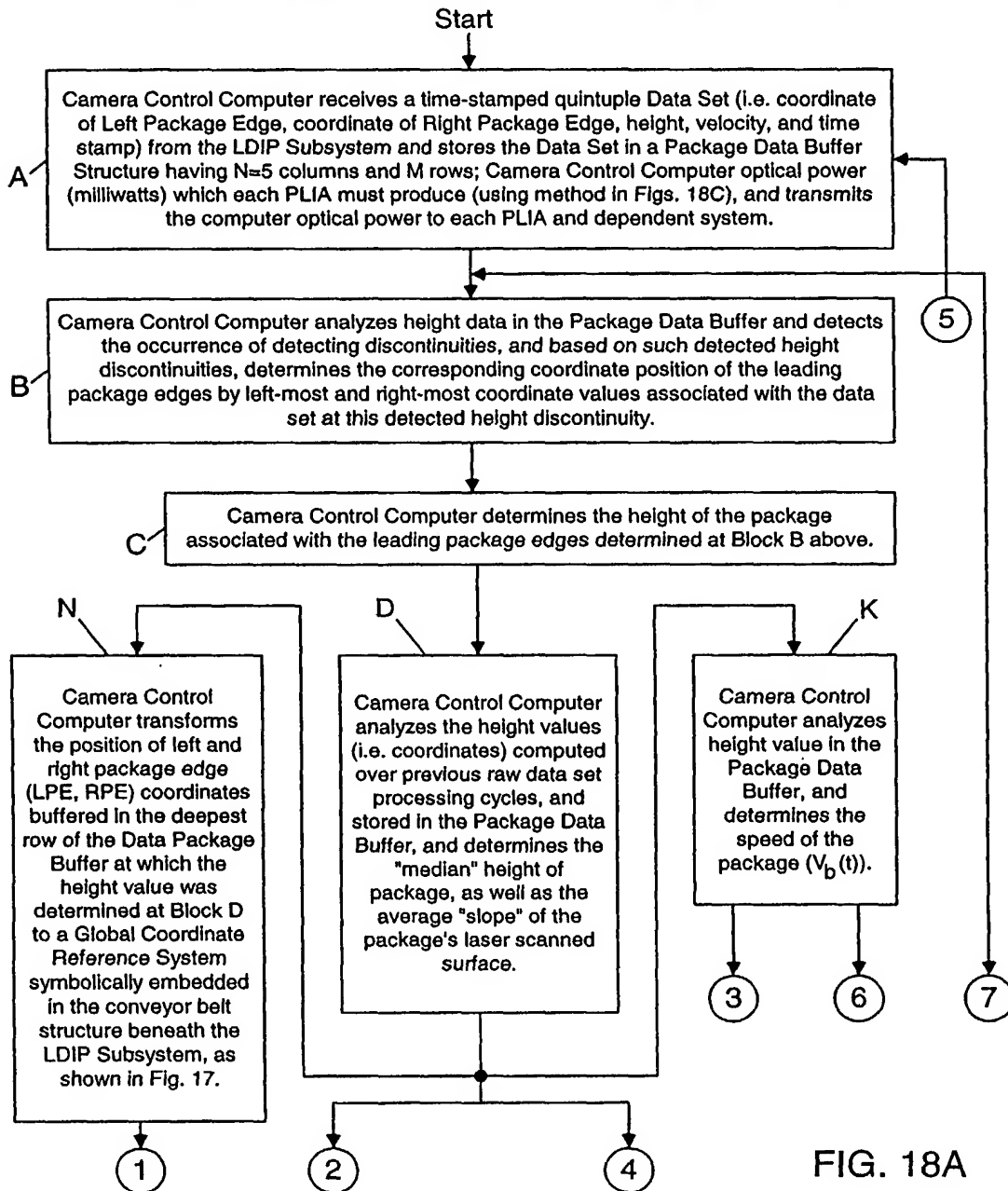


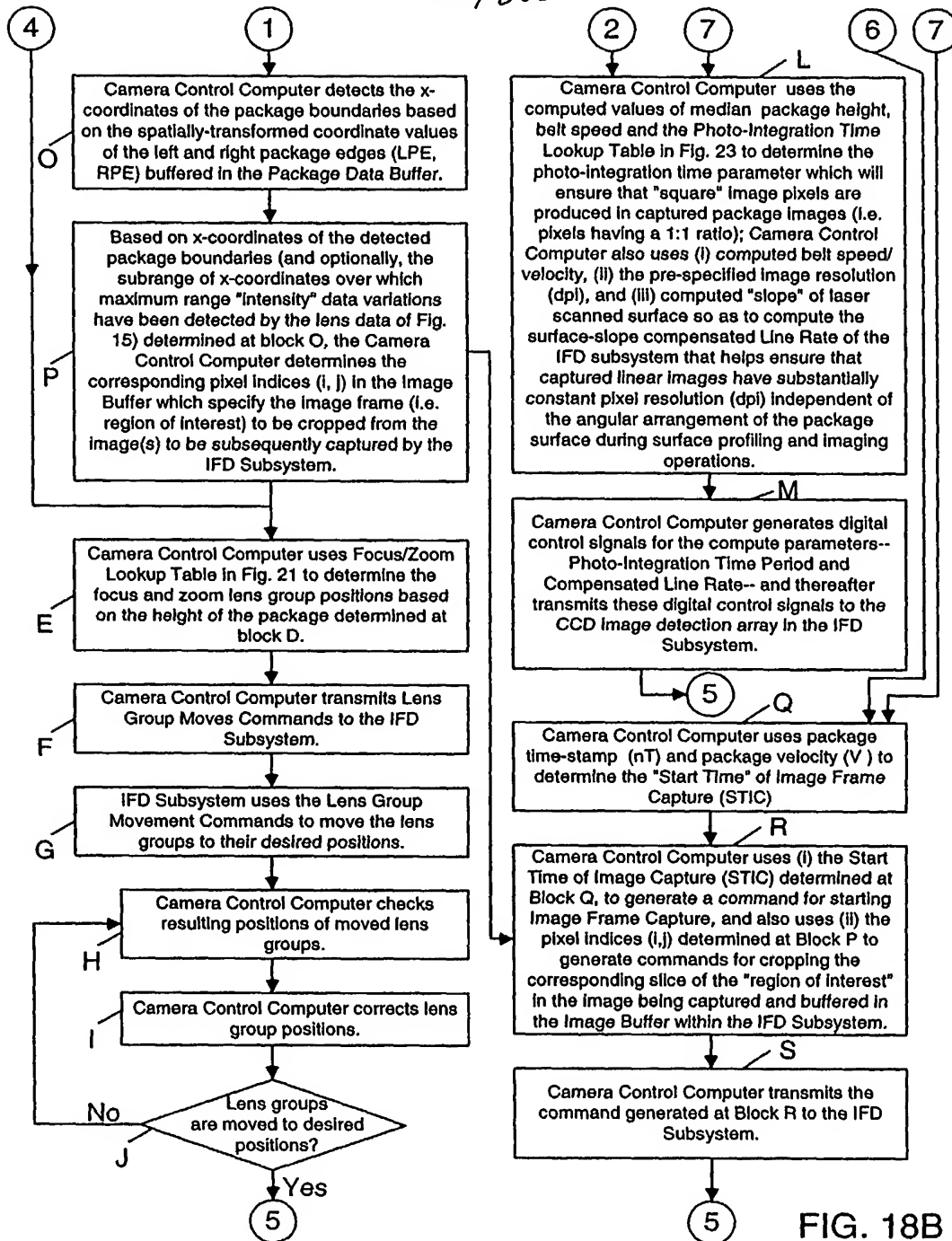
Fig. 17C

222/385

CAMERA CONTROL PROCESS CARRIED OUT WITHIN THE CAMERA
CONTROL SUBSYSTEM OF EACH OBJECT IDENTIFICATION AND
ATTRIBUTE ACQUISITION SYSTEM OF PRESENT INVENTION



223/385



224/385

METHOD OF COMPUTING OPTICAL OUTPUT POWER FROM CASE
DIODES IN PLANAR LASER ILLUMINATION ARRAY (PLIA) FOR
CONTROLLING CONSTANT WHITE LEVEL IN IMAGE PIXELS CAPTURED
BY PLIIM-BASED LINEAR IMAGER

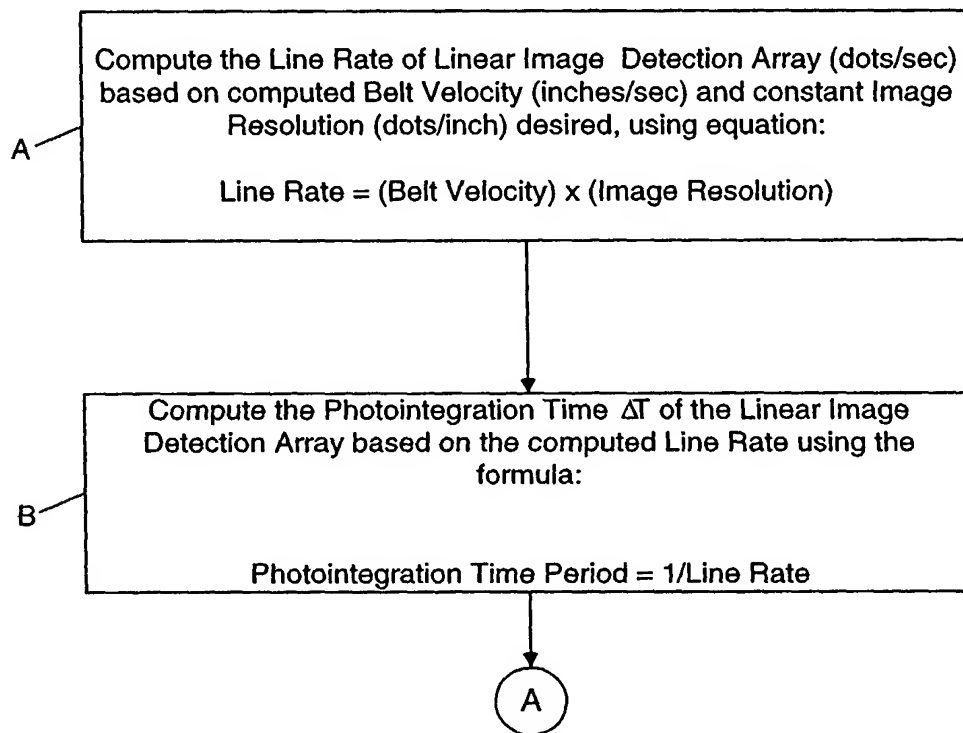


FIG. 18C1

225/385

A



Compute the Optical Power (milliwatts) of each PLIA based on computed Photointegration Time Period (ΔT) using the following formula:

$$\text{Optical Power of VLD (milliwatts)} = \frac{\text{constant}}{\text{Photointegration Time Period } \Delta T}$$

FIG. 18C2

226/ 325

METHOD OF COMPUTING COMPENSATED LINE RATE FOR CORRECTING
VIEWING-ANGLE DISTORTION OCCURING IN IMAGES OF OBJECT
SURFACES CAPTURED AS OBJECT SURFACES MOVE PAST PLIM-
BASED LINEAR IMAGER AT NON-ZERO SKEWED ANGLE

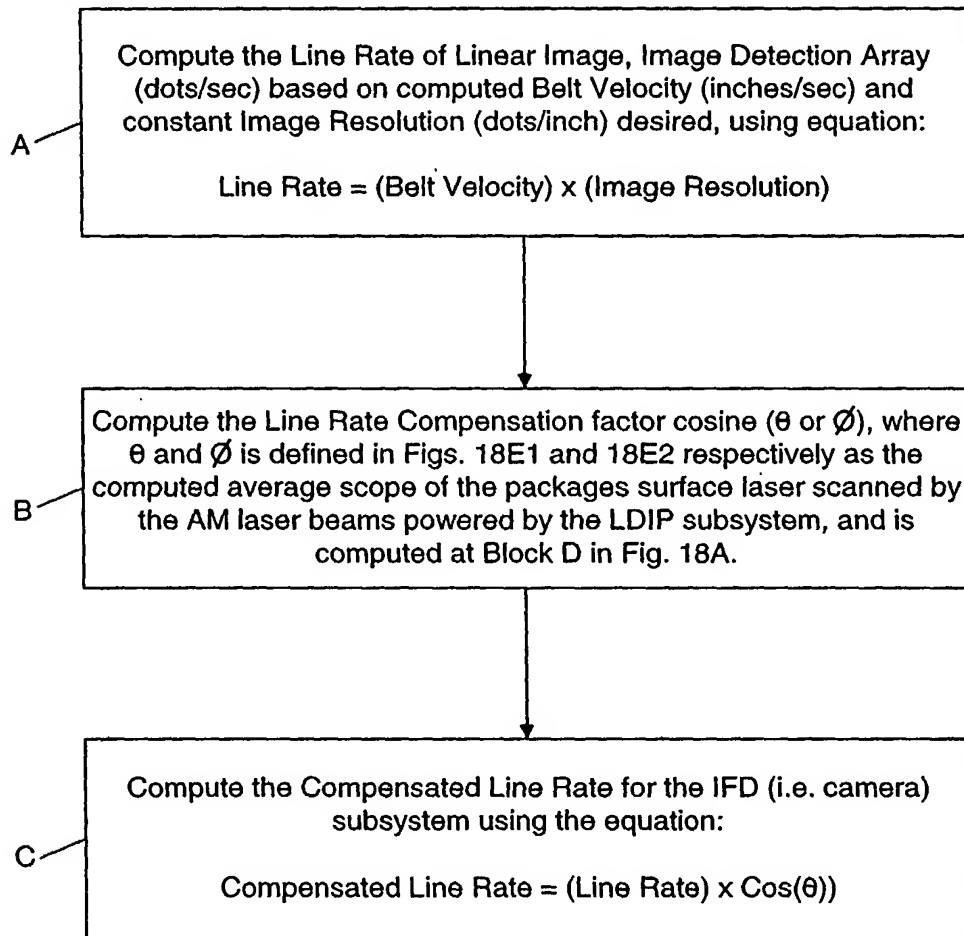


FIG. 18D

CASE 1:
Top Down Imaging

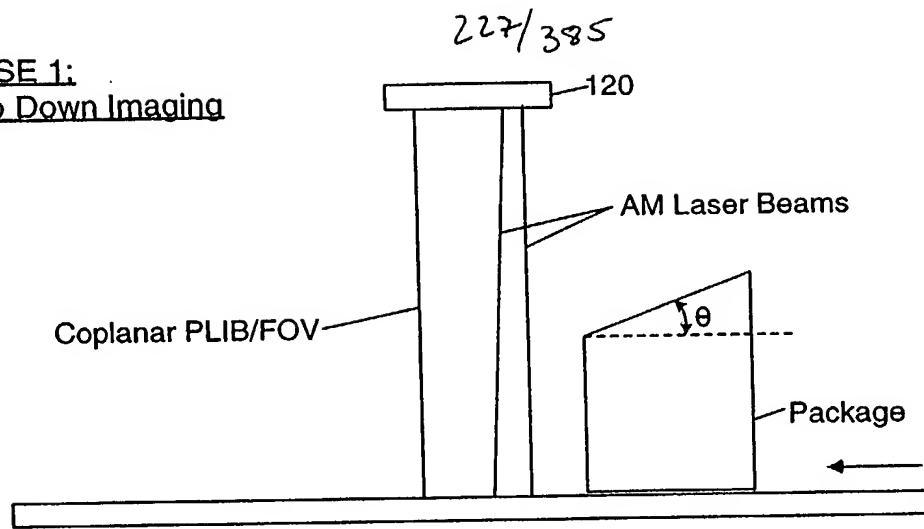


FIG. 18E1

CASE 2:
Side Imaging

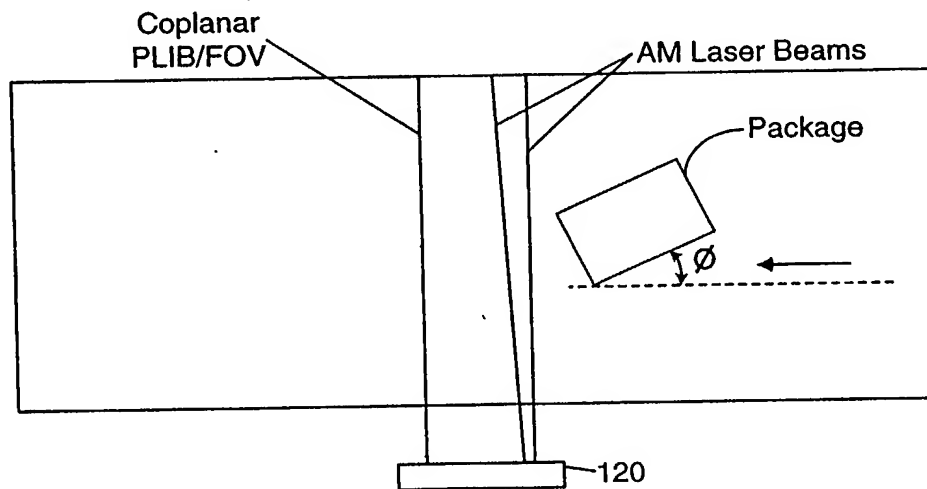


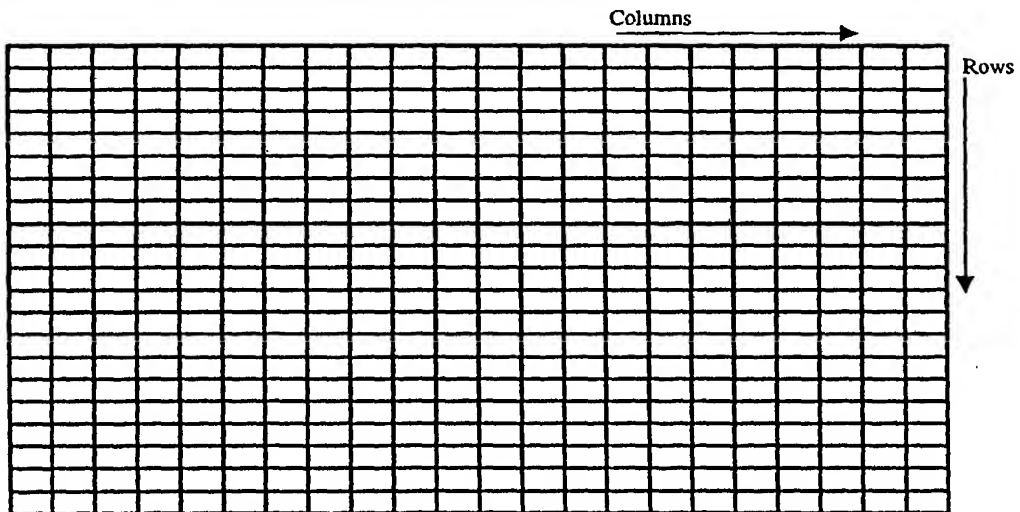
FIG. 18E2

228/385

X coordinate subrange where
maximum range "intensity"
variations have been detected

Left Package Edge (LDE)	Package Height (h)	Right Package Edge (RPE)	Package Velocity	Time-stamp (nT)	
					Row 1
					Row 2
					Row 3
					Row 4
					Row 5
					Row M
Package Data Buffer (FIFO)					

Fig. 19



Camera Pixel Data Buffer
pixel indices (i,j.)

Fig. 20

229/385

Zoom and Focus Lens Group Position
Looking Table

Distance from Camera H (mm)	Zoom group distance (mm) Y (Zoom)	Focus group distance (mm) Y (Focus)
1000	21.57489228	2.47E-05
1100	19.38089696	10.99009783
1200	17.10673434	20.65783177
1300	14.77137314	29.10917002
1400	12.39153565	36.47312595
1500	9.979114358	42.87845436
1600	7.540639114	48.44003358
1700	5.078794775	53.25495831
1800	2.595989366	57.40834303
1900	0.099972739	60.98883615

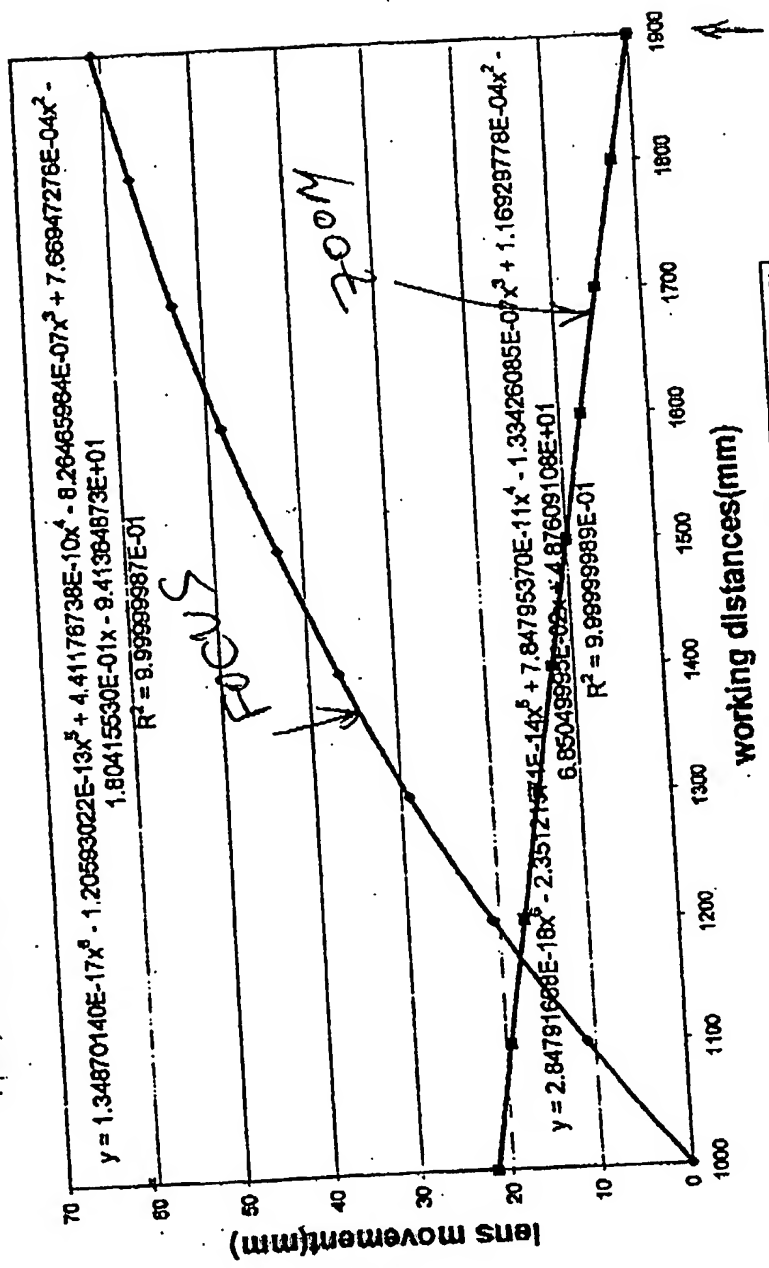
(USE
interpolation
techniques
for walking
distances
between listed
points in
table)

FIG. 21.

230/385

* Note: On feed distance & zoom (left hand graph) in camera lens are coupled (interdependent) in camera has a fixed aperture F5.6 this command on videotape.

Focus and Zoom lens movement vs. working distances



zoom 1 zoom 2 Poly. (zoom 1) Poly. (zoom 2)

conveyor-belt surface

← package height above conveyor

30 above conveyor belt

FIG. 22A

231/385

Photo-Integration Time Look-Up Table

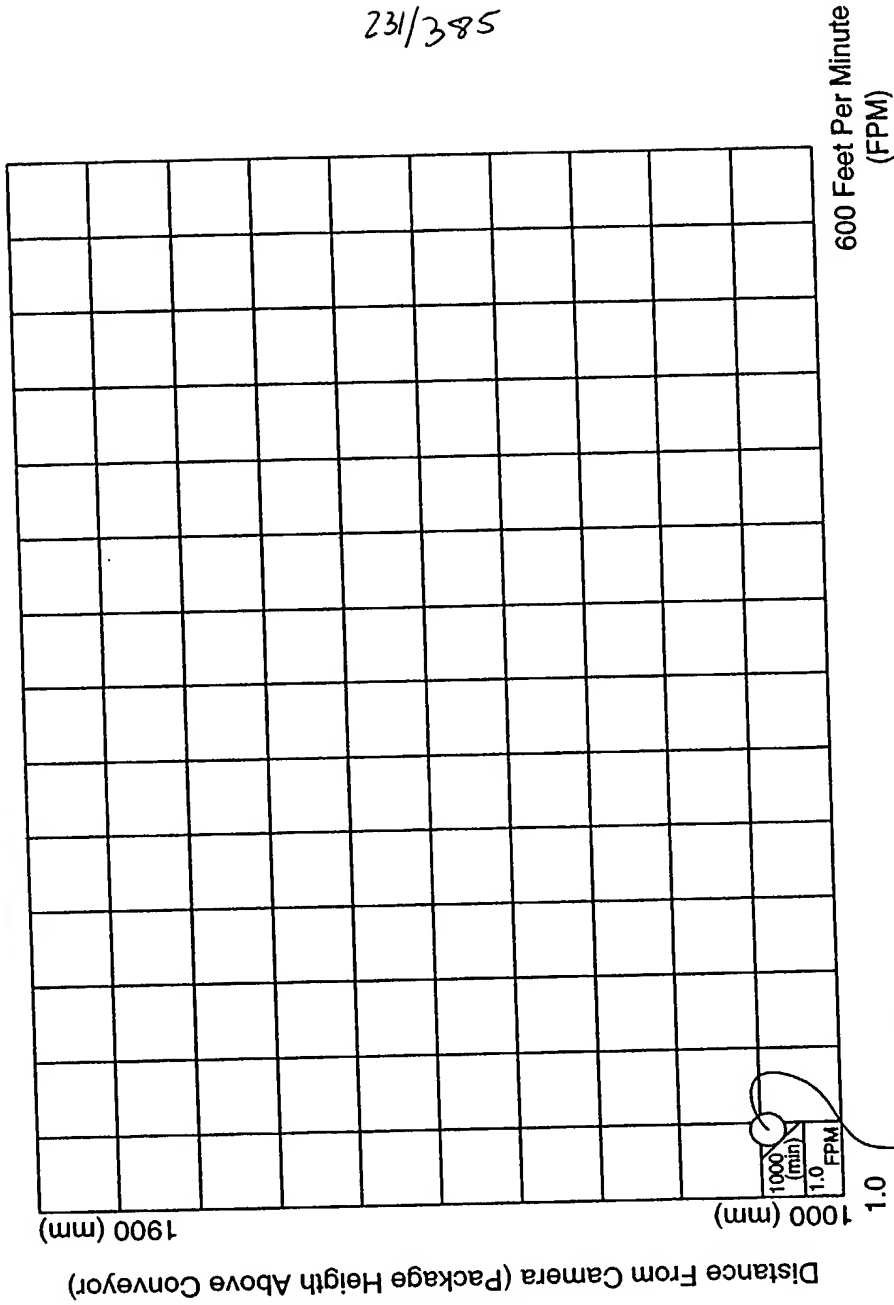


FIG. 22B

232/385

3D Surface Profile And High Resolution
Linear Image Data Capture
At PLIIM-Based Profiling
And Imaging System

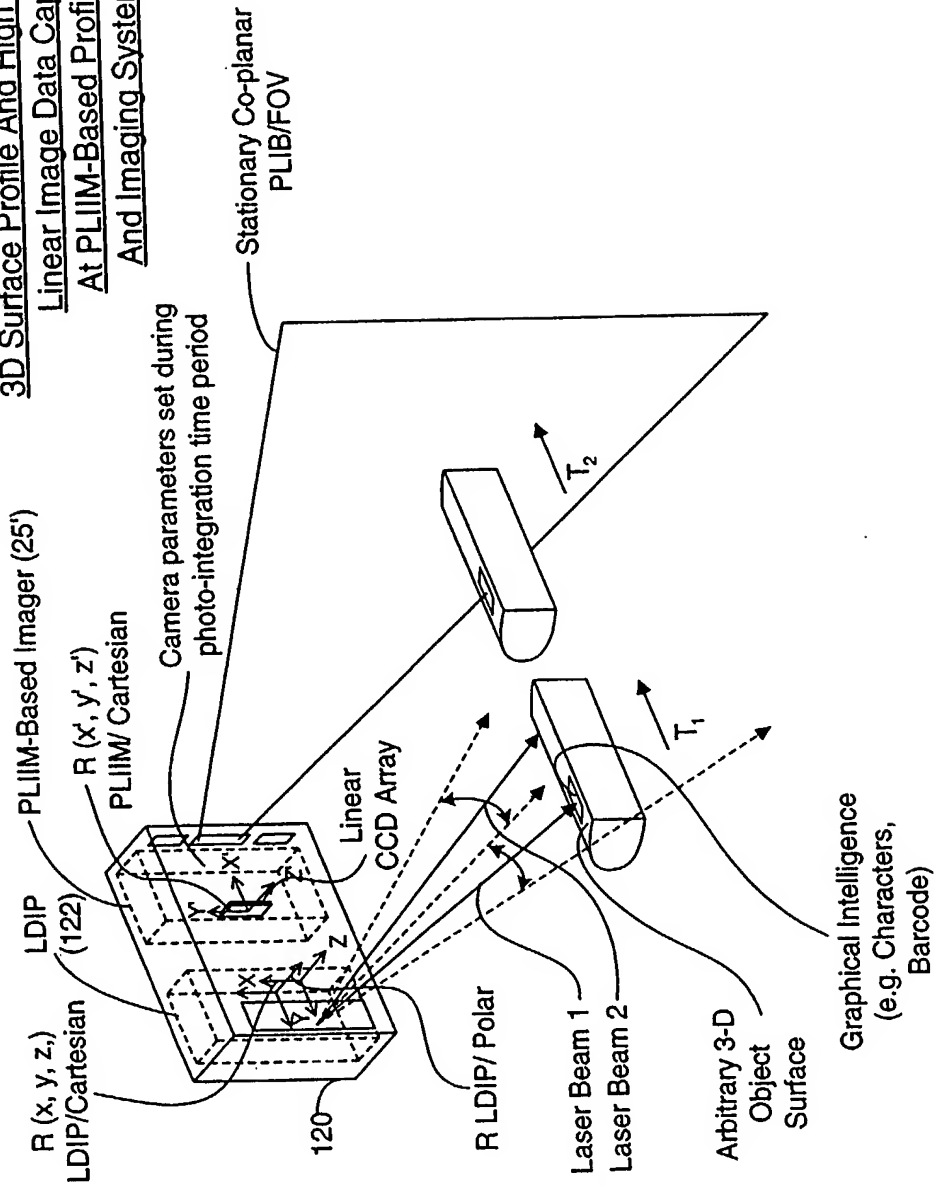


FIG. 23A

233/385

Geometrical Modelling Of Arbitrary 3-D Object Surface
At Image Processing Computer

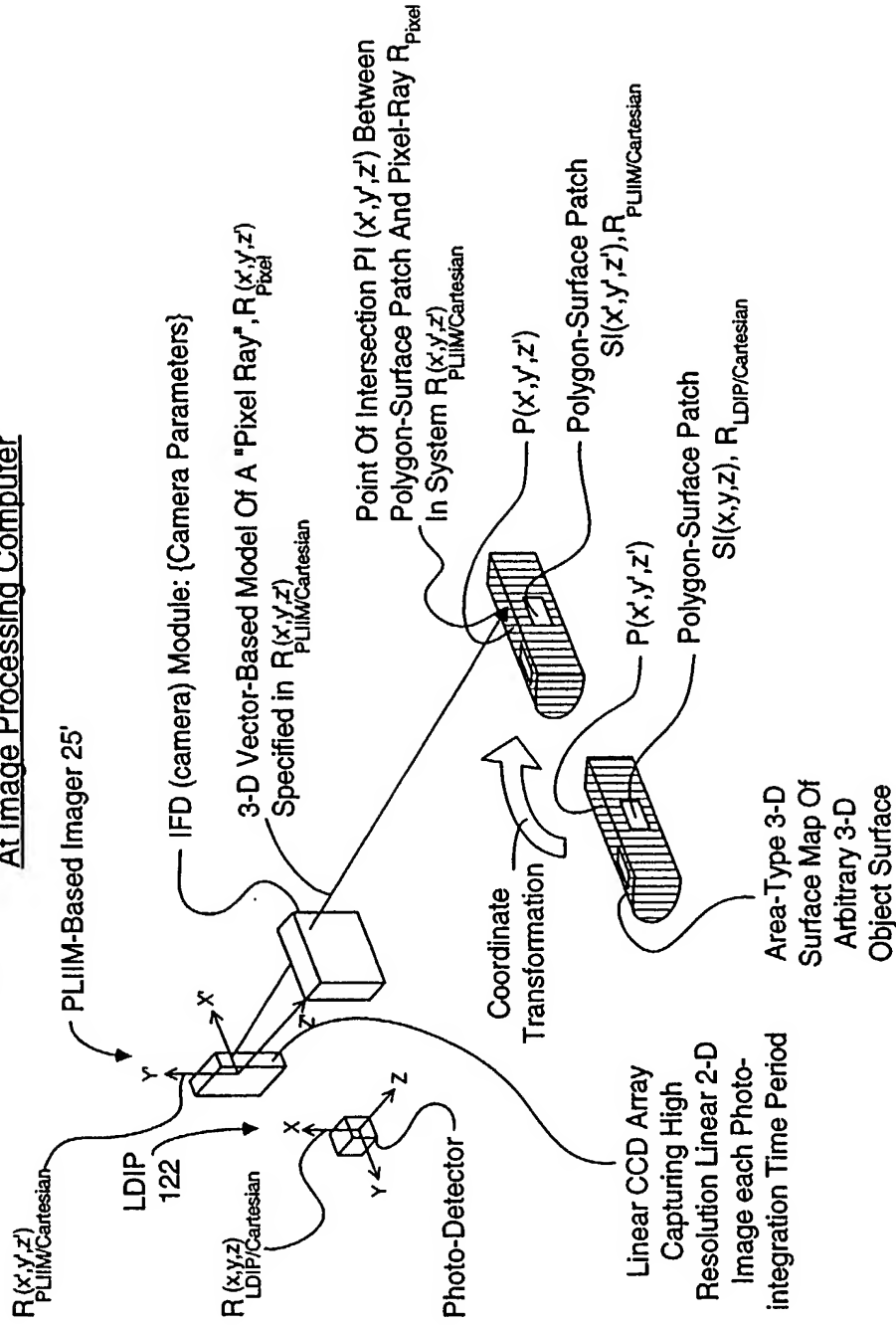


FIG. 23B

234/ 385

METHOD OF AND APPARATUS FOR PERFORMING AUTOMATIC
RECOGNITION OF GRAPHICAL INTELLIGENCE CONTAINED IN 2-D
IMAGES CAPTURED FROM ARBITRARY 3-D OBJECT SURFACES

STEP 1: At the unitary PLIIM-based object imaging and profiling system, use the laser doppler imaging and profiling (LDIP) subsystem employed therein to (i) consecutively capture a series of linear 3-D surface profile maps on a targeted arbitrary (e.g. non-planar or planar) 3-D object surface bearing forms of graphical intelligence and (ii) measure the velocity of the arbitrary 3-D object surface, wherein the polar coordinates of each point in the captured linear 3-D surface profile map are specified in a local polar coordinate system $R_{LDIP/polar}$, symbolically embedded within the LDIP subsystem.

A

STEP 2: At the unitary PLIIM-based object imaging and profiling system, use coordinate transforms to automatically convert the polar coordinates of each point $p(\alpha, R)$ in the captured linear 3-D surface profile map into x,y, z Cartesian coordinates specified as $p(x,y,z)$ in a local Cartesian coordinate system $R_{LDIP/Cartesian}$, symbolically embedded within the LDIP subsystem.

B

STEP 3: At the unitary PLIIM-based object imaging and profiling system, use the PLIIM-based imager employed therein to consecutively capture high-resolution linear 2-D images of the arbitrary 3-D object surface bearing forms of graphical intelligence (e.g. symbol character strings), wherein (i) the x', y' coordinates of each pixel in each said captured high-resolution linear 2-D image is specified in local Cartesian coordinate system $R_{PLIIM/Cartesian}$ symbolically embedded within the PLIIM-based imager, and (ii) the intensity value of the pixel $I(x',y')$ is associated with the x', y' Cartesian coordinates of the image detection element in the linear image detection array at which the pixel is detected, and (iii) wherein also the planar laser illumination beam (PLIB) of the PLIIM-based imager is spaced from the amplitude modulated (AM) laser scanning beam of the LDIP subsystem is about D centimeters.

C

A

FIG. 23C1

235/385
A

STEP 4: At the unitary PLIIM-based object imaging and profiling system, capture and buffer the camera (IFD) parameters used to form and detect each linear high-resolution 2-D image captured during the corresponding photo-integration time period ΔT_K , by the PLIIM-based imager.

D

STEP 5: At the end of each photo-integration time period ΔT_K , use the unitary PLIIM-based object imaging and profiling system to transmit the following information elements to the Image Processing Computer for data storage and subsequent information processing:

(1) the converted coordinates x, y, z , of each point in the linear 3-D surface profile map of the arbitrary 3-D object surface captured during photo-integration time period ΔT_K ;

(2) the measured velocity(ies) of the arbitrary 3-D object surface during photo-integration time period ΔT_K ;

(3) the x', y' coordinates and intensity value $I(x', y')$ of each pixel in each high-resolution linear 2-D image captured during photo-integration time period ΔT_K and specified in the local Cartesian coordinate system $R_{PLIIM/Carthesian}$; and

(4) the captured camera (IFD) parameters used to form and detect each linear high-resolution 2-D image captured during the photo-integration time period ΔT_K

E

STEP 6: At the Image Processing Computer, receive the data elements transmitted from the PLIIM-based profiling and imaging system during Step 5, buffer data elements (1) and (2) in a first FIFO buffer memory structure, and data elements (3) and (4) in a second FIFO buffer memory structure.

F

B

FIG. 23C2

236/385

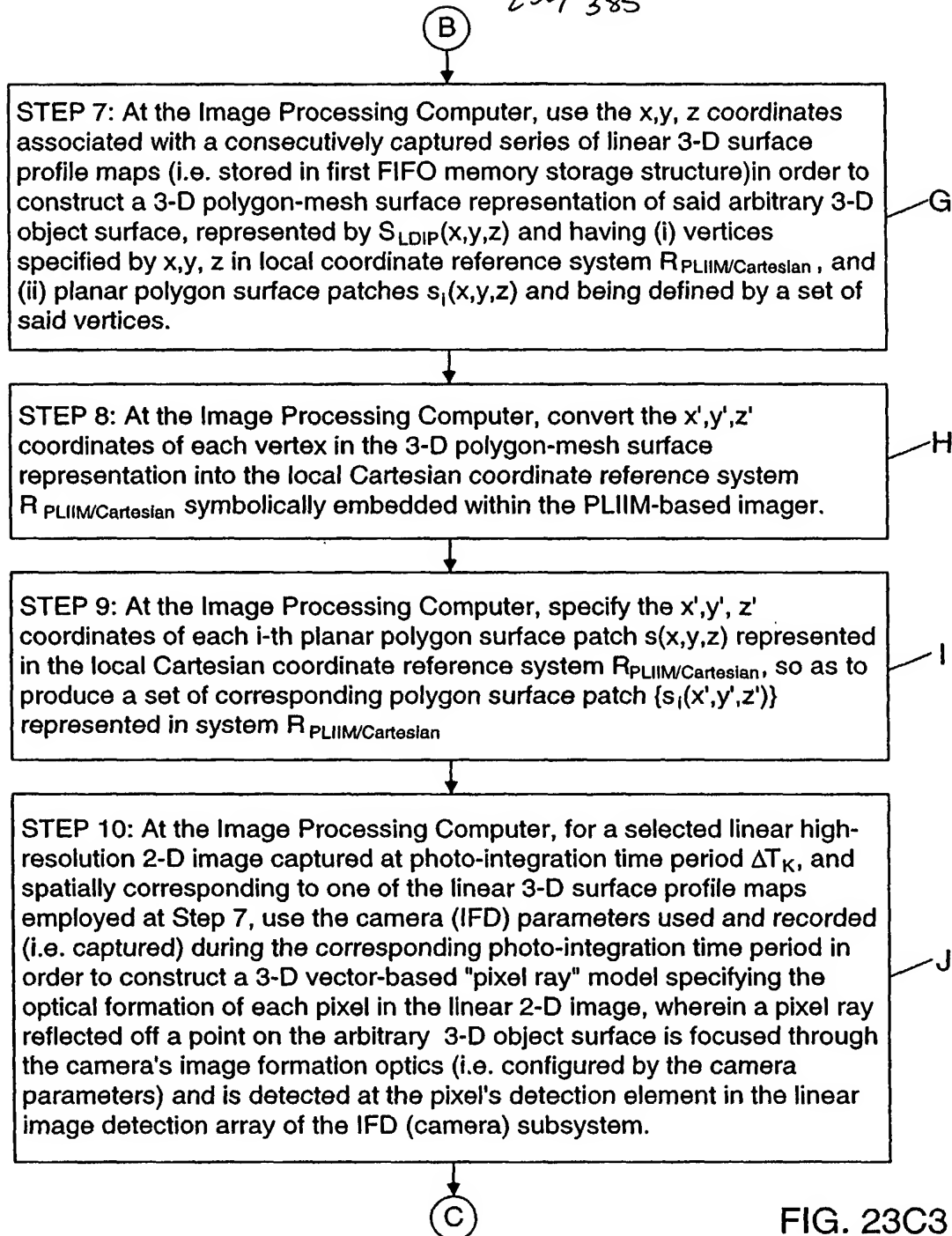


FIG. 23C3

C

237/385

STEP 11: At the Image Processing Computer, for each laser beam ray (producing one of the pixels in said selected linear 2-D image), (i) determine which polygon surface patch $s_i(x, y, z)$ the pixel ray intersects, (ii) compute the x, y, z coordinates of the point of intersection (POI) between the pixel ray and the polygon surface patch represented in Cartesian coordinate reference system $R_{PLIIM/Cartesian}$, and (iii) designate the computed set of points of intersection as $\{p_i(x, y, z)\}$.

K

STEP 12: At the Image Processing Computer, for each laser beam ray passing through a determined polygon surface patch $s(x', y', z')$ at a computed point of intersection $p_i(x, y, z)$, assign the intensity value $I(x', y')$ of the pixel ray to the x', y', z' coordinates of the point of intersection, thereby producing a linear high-resolution 3-D image comprising a 2-D array of pixels, each said pixel pixel having as its attributes (i) an Intensity value $I(x', y', z')$ and (ii) coordinates x', y', z' specified in the local Cartesian coordinate reference system $R_{PLIIM/Cartesian}$.

L

STEP 13: Put the computed linear high-resolution 3-D image in a third FIFO memory storage structure in the image processing computer.

M

STEP 14: Repeat Steps 1-6 to update the first and second FIFO data queues maintained in the image processing computer, and Steps 7-13 to update the consecutively computed linear high-resolution 3-D image stored in the third FIFO memory storage structure.

N

STEP 15: Assemble in an image buffer in the image processing computer, a set of consecutively computed linear high-resolution 3-D images retrieved from the third FIFO data storage device so as to construct an "area-type" high-resolution 3-D image of said arbitrary 3-D object surface.

O

D

FIG. 23C4

D

238/385

STEP 16: At the Image Processing Computer, map the intensity value $I(x', y', z')$ of each pixel in the computed area-type 3-D image onto the x', y', z' coordinates of the points on a uniformly-spaced apart "grid" positioned perpendicular to the optical axis of the camera subsystem (i.e. to model the 2-D planar substrate on which the forms of graphical intelligence was originally rendered), wherein said mapping process involves using an intensity weighing function based on the x', y', z' coordinate values of each pixel in the area-type high-resolution 3-D image, thereby producing an area-type high-resolution 2-D image of the 2-D planar substrate surface bearing said forms of graphical intelligence (e.g. symbol character strings).

P

STEP 17: At the Image Processing Computer, use said OCR algorithm to perform automated recognition of graphical intelligence contained in said area-type high-resolution 2-D image of said 2-D planar substrate surface so as to recognize said graphical intelligence and generate symbolic knowledge structures representative thereof.

Q

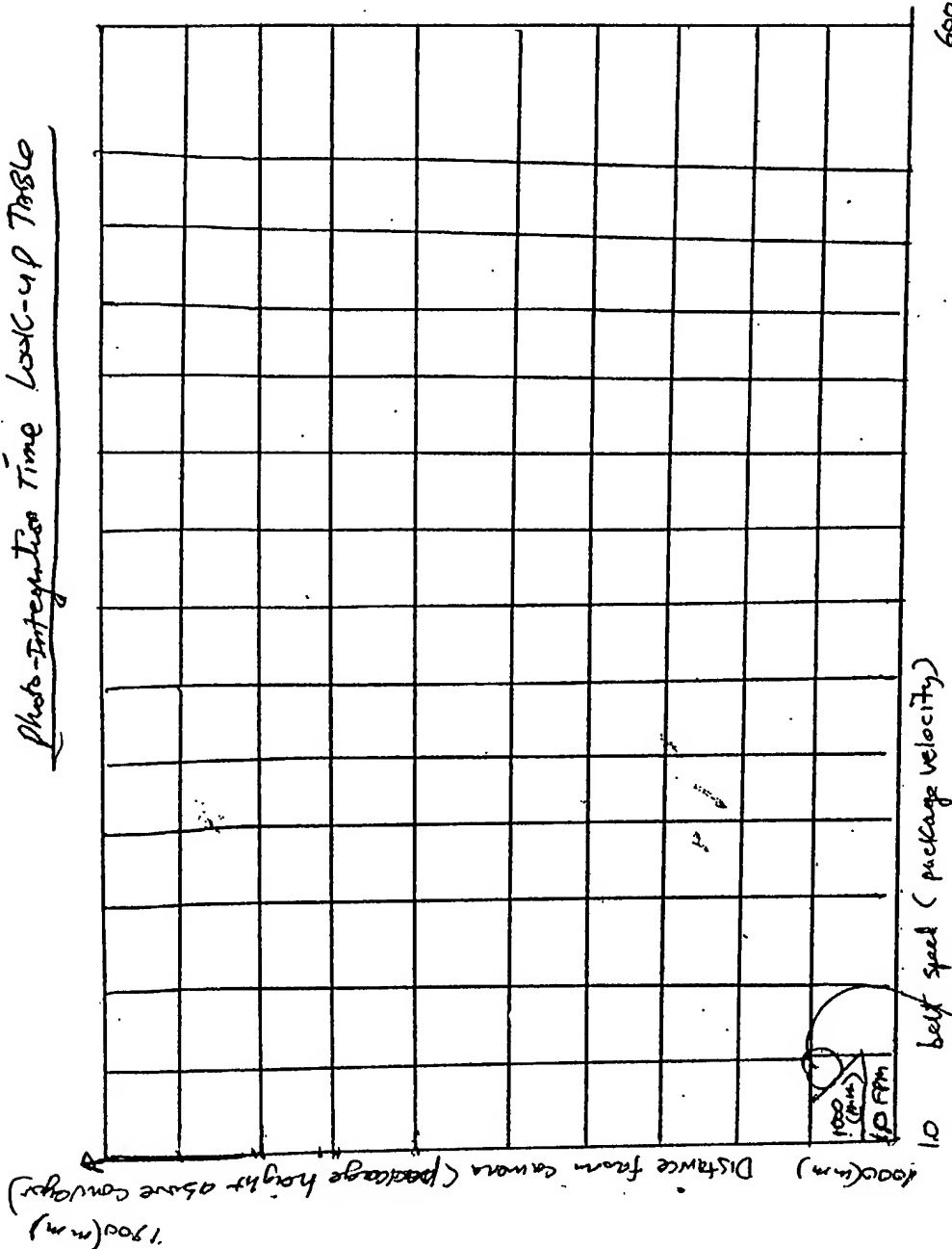
STEP 18: Repeat Steps 1-17 as often as required to recognize changes in graphical intelligence on the arbitrary moving 3-D object surface.

R

FIG. 23C5

239/385

Photo-Integration Time Look-up Table



600 feet per minute
(FPM)

FIG. 22B

240/395

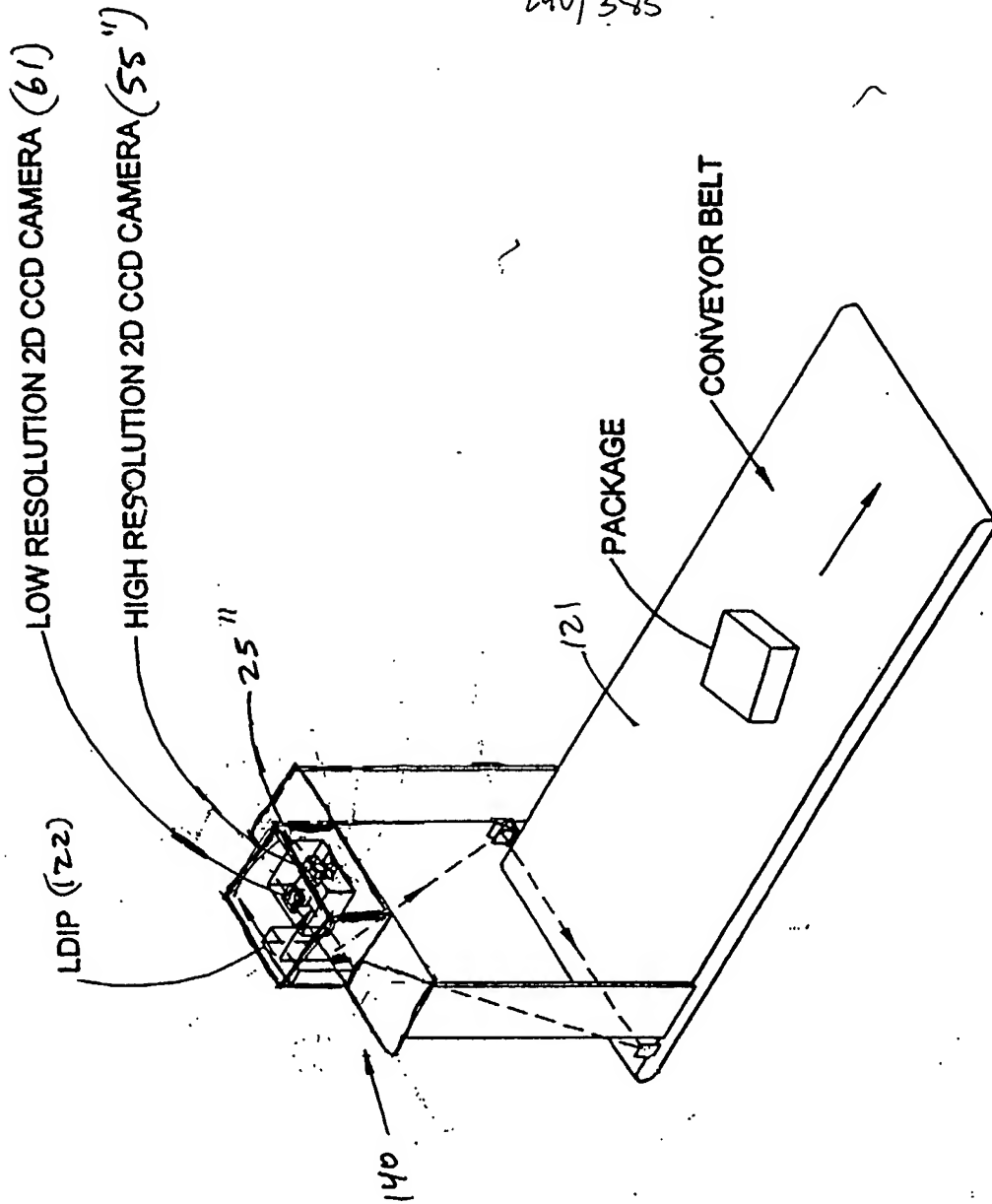
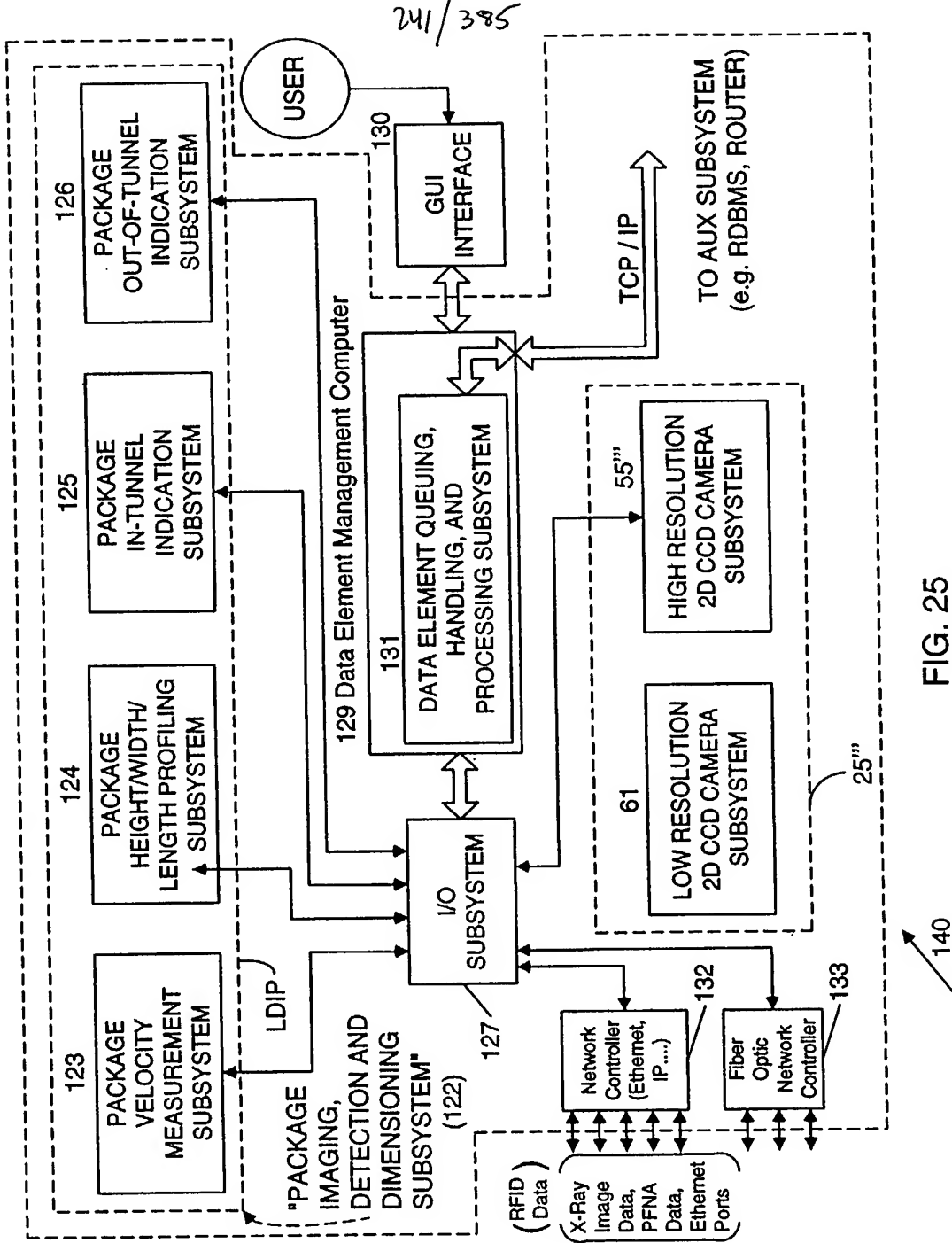


FIG 24



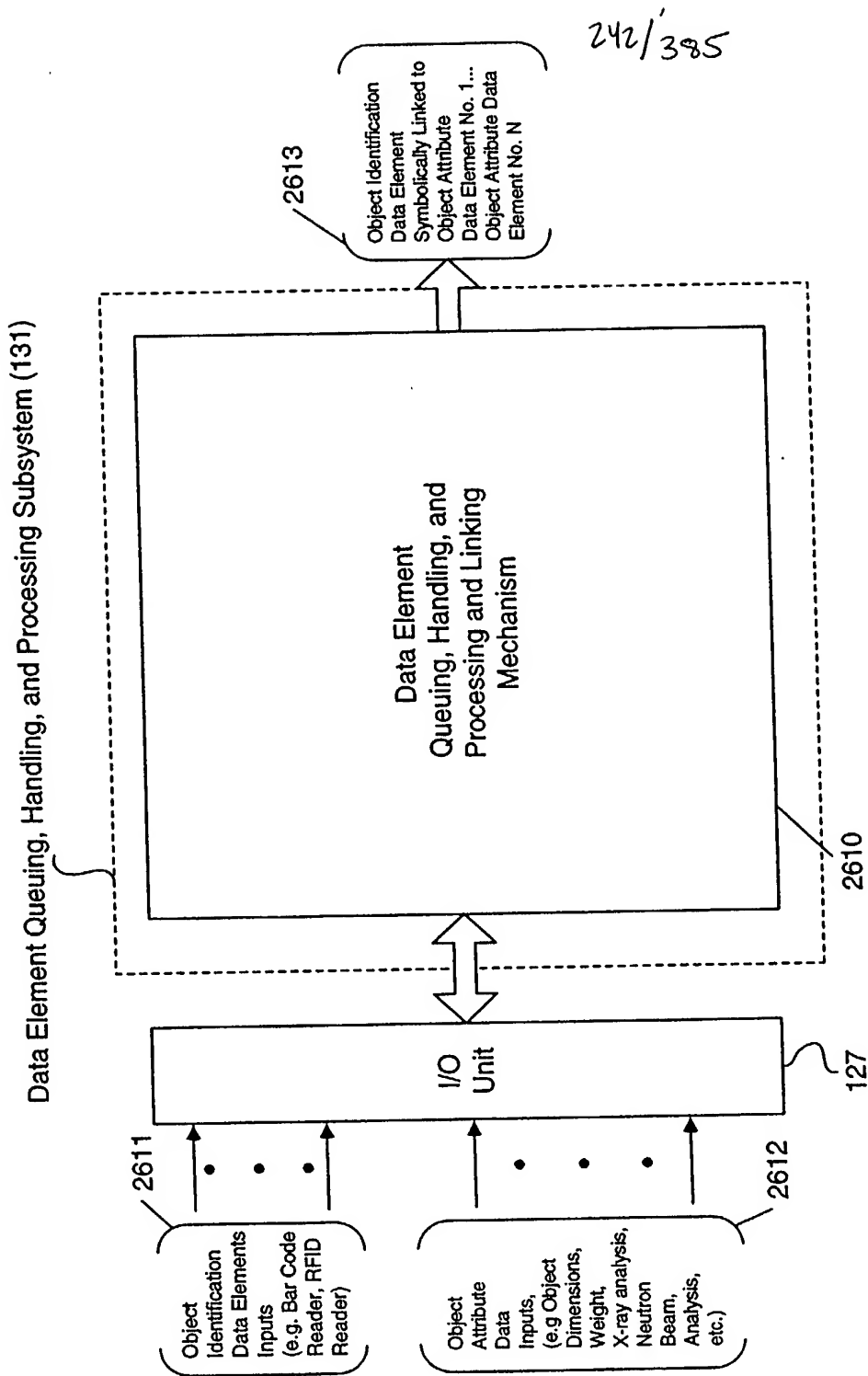


FIG. 25A

Primary Network:
and/or System
Functions:

A. Specification of Object
Detection and
Tracking Capability of
System

B. Specification of Object
Identification
Capability of System

C. Specification of
Object Attribute
Acquisition Capability
of System

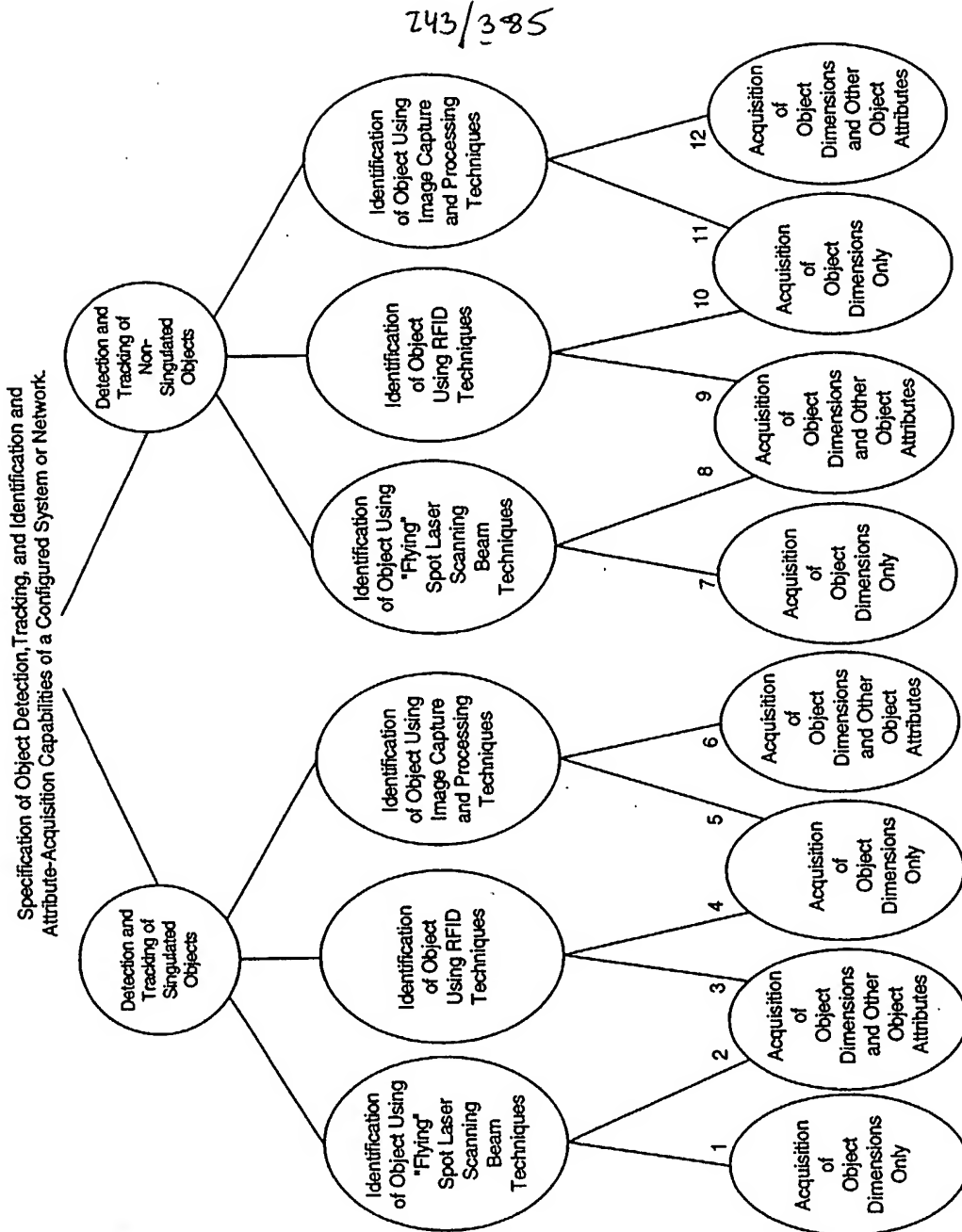


FIG. 25B

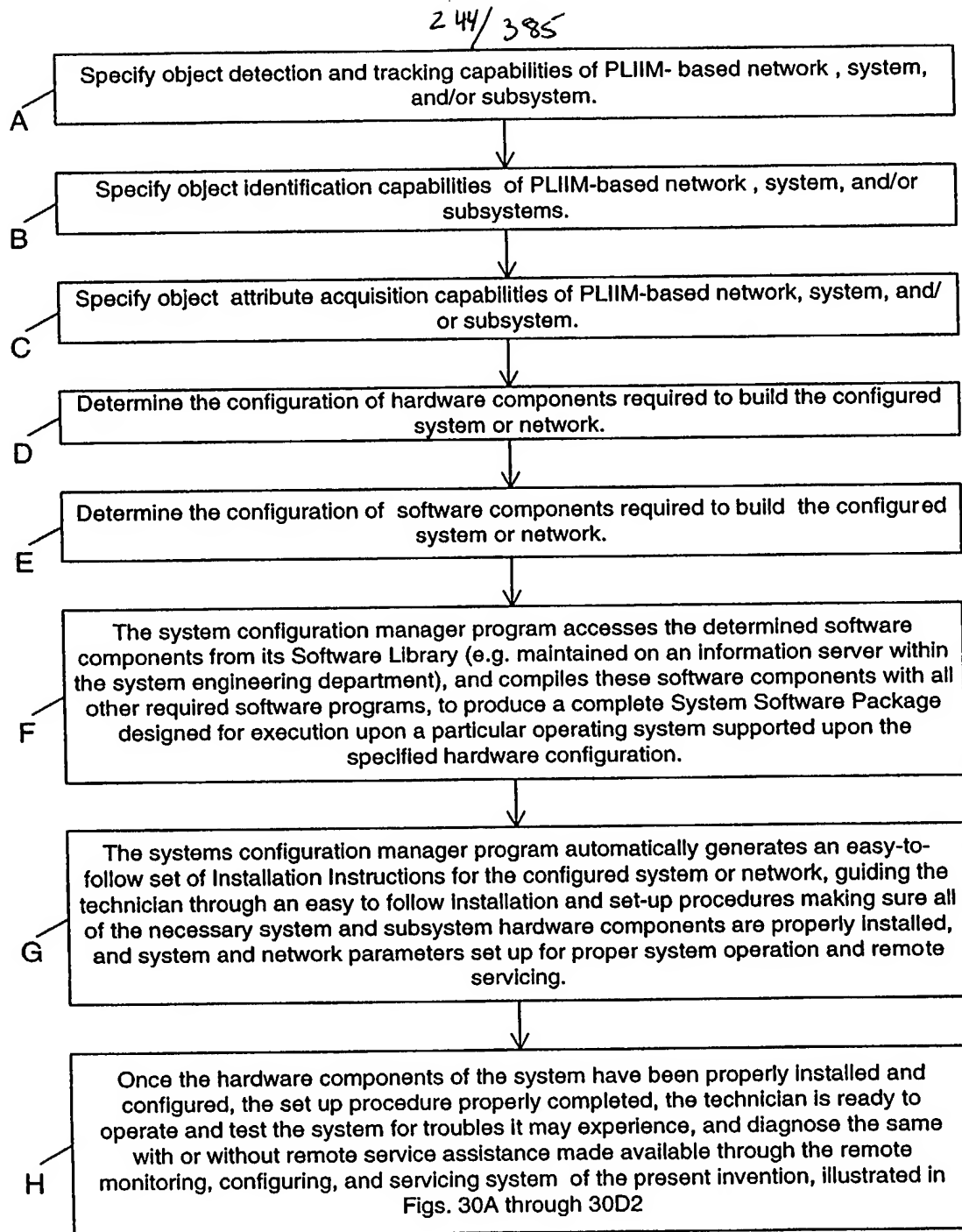


FIG. 25C

245/385

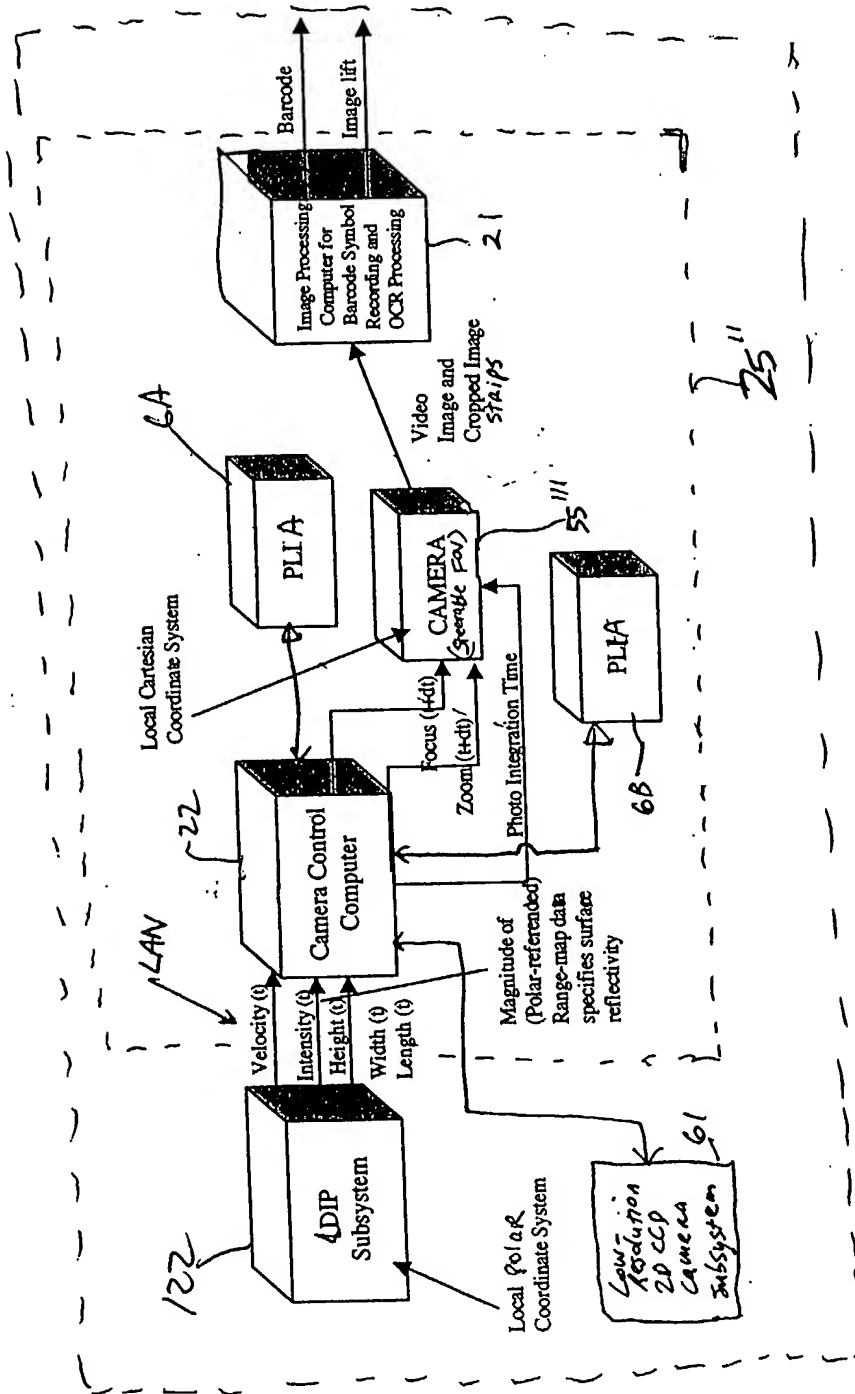
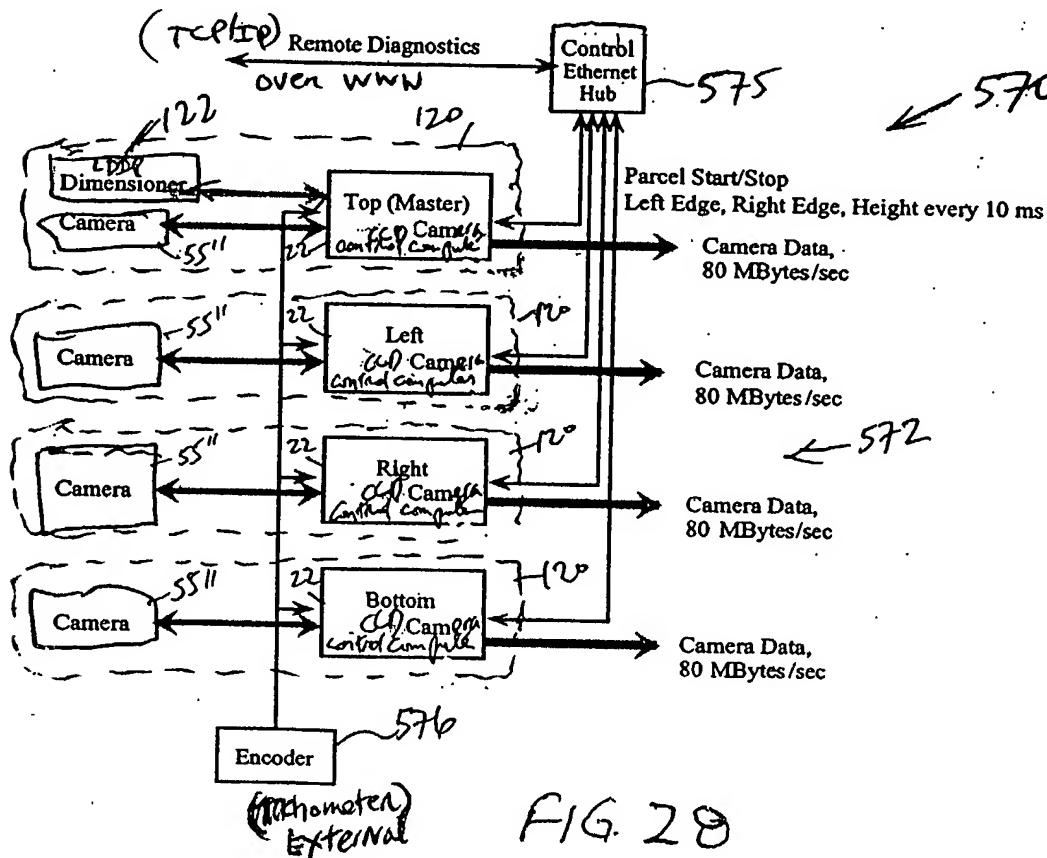
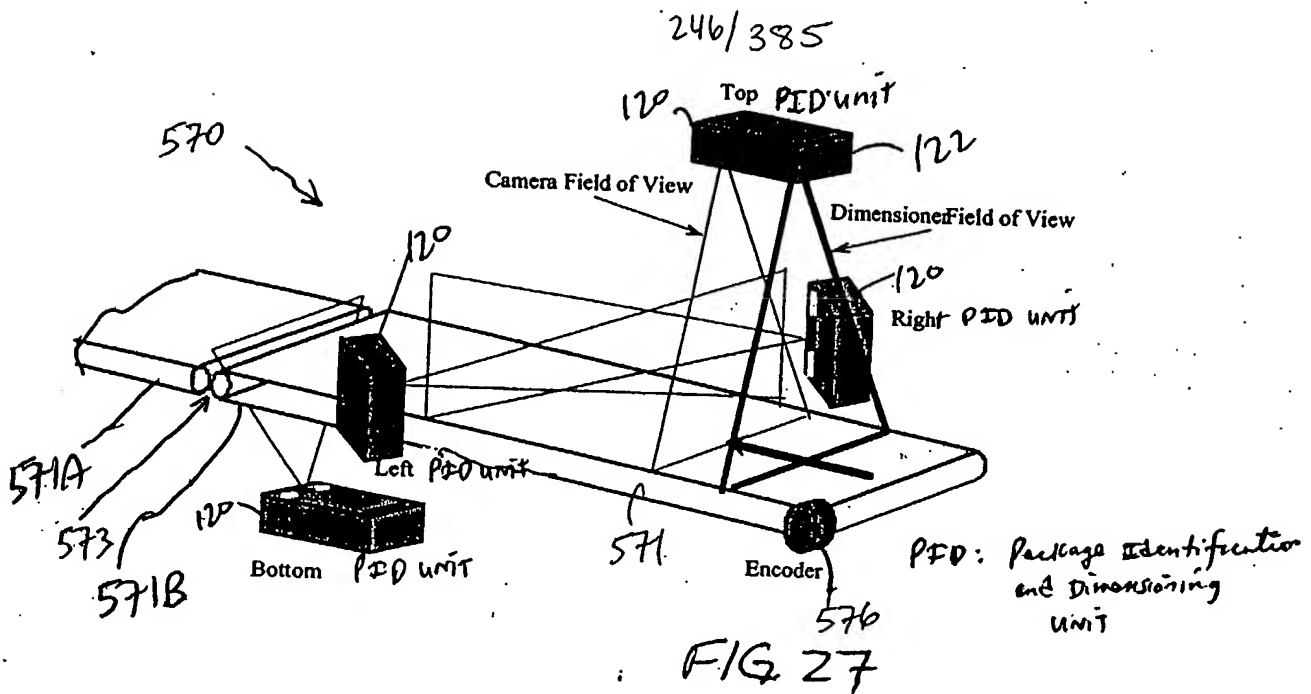


FIG. 26



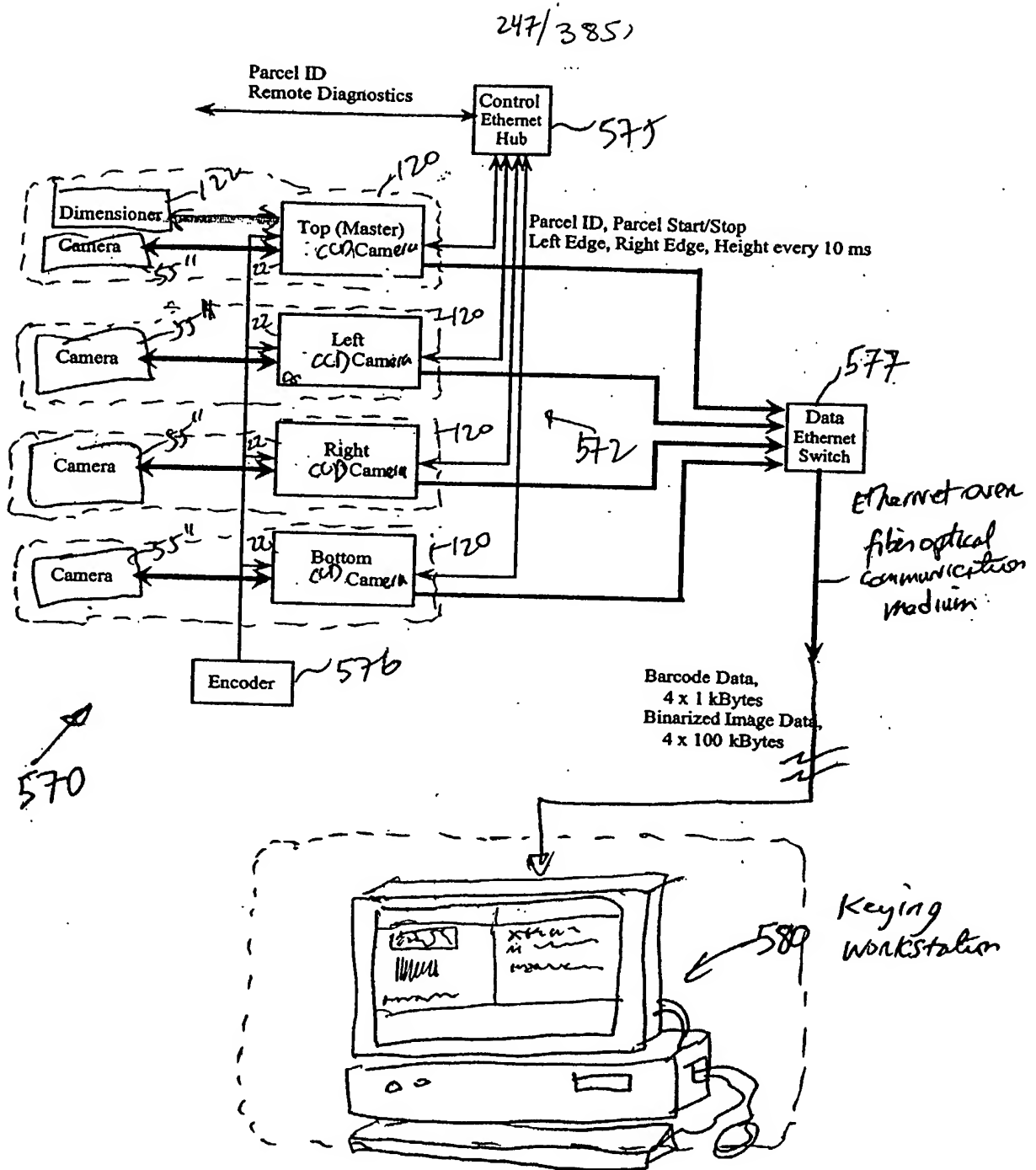
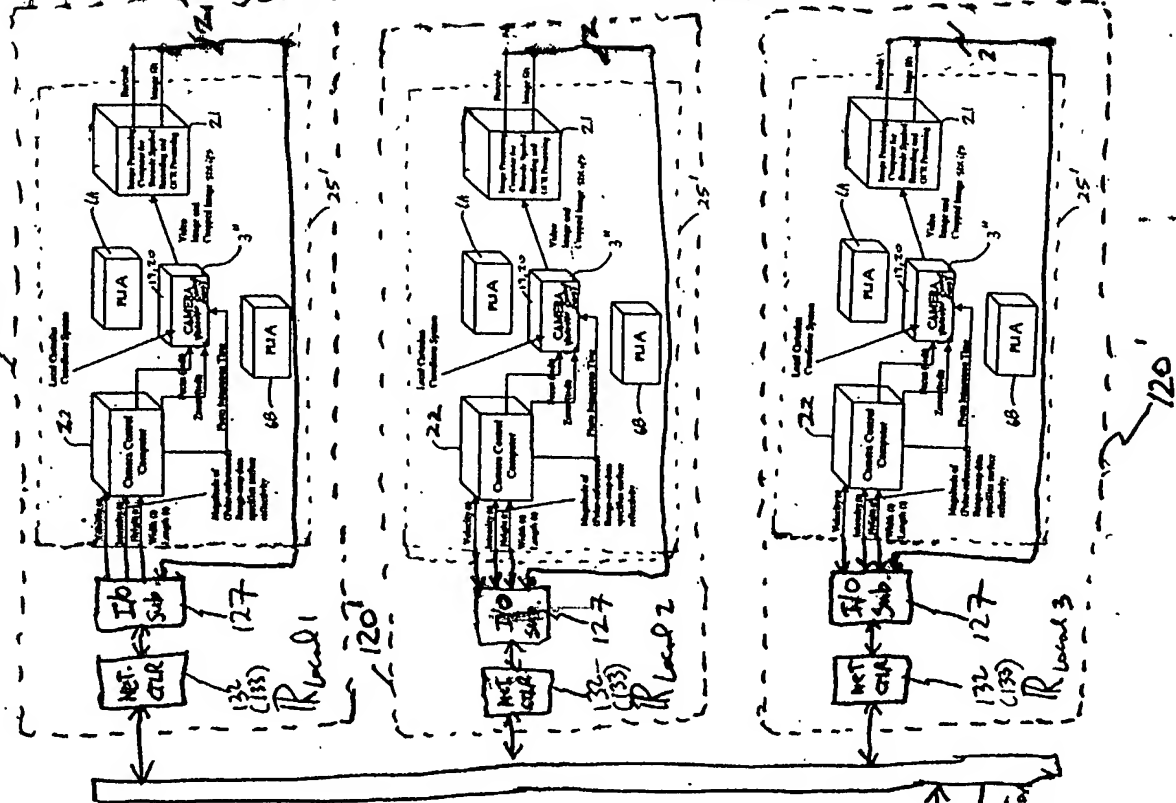


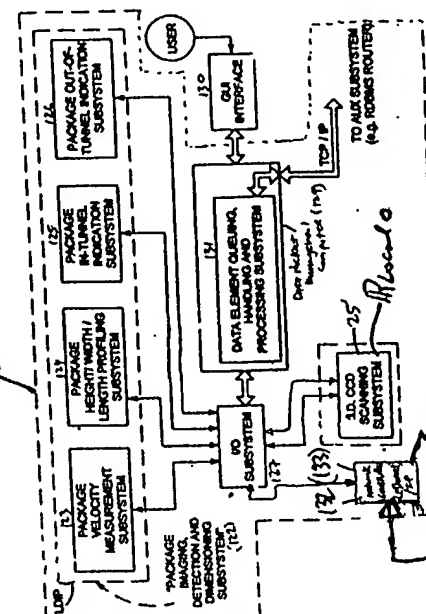
FIG. 29

249/385



570

120



Coordinate Data
Reference
with respect to
Global

$\left\{ \begin{array}{l} \text{Velocity}(t) \\ \text{Intensity}(t) \\ \text{Height}(t) \\ \text{Width}(t) \\ \text{Length}(t) \end{array} \right\}$

Network
Communication
Medium

FIG 30

249/385

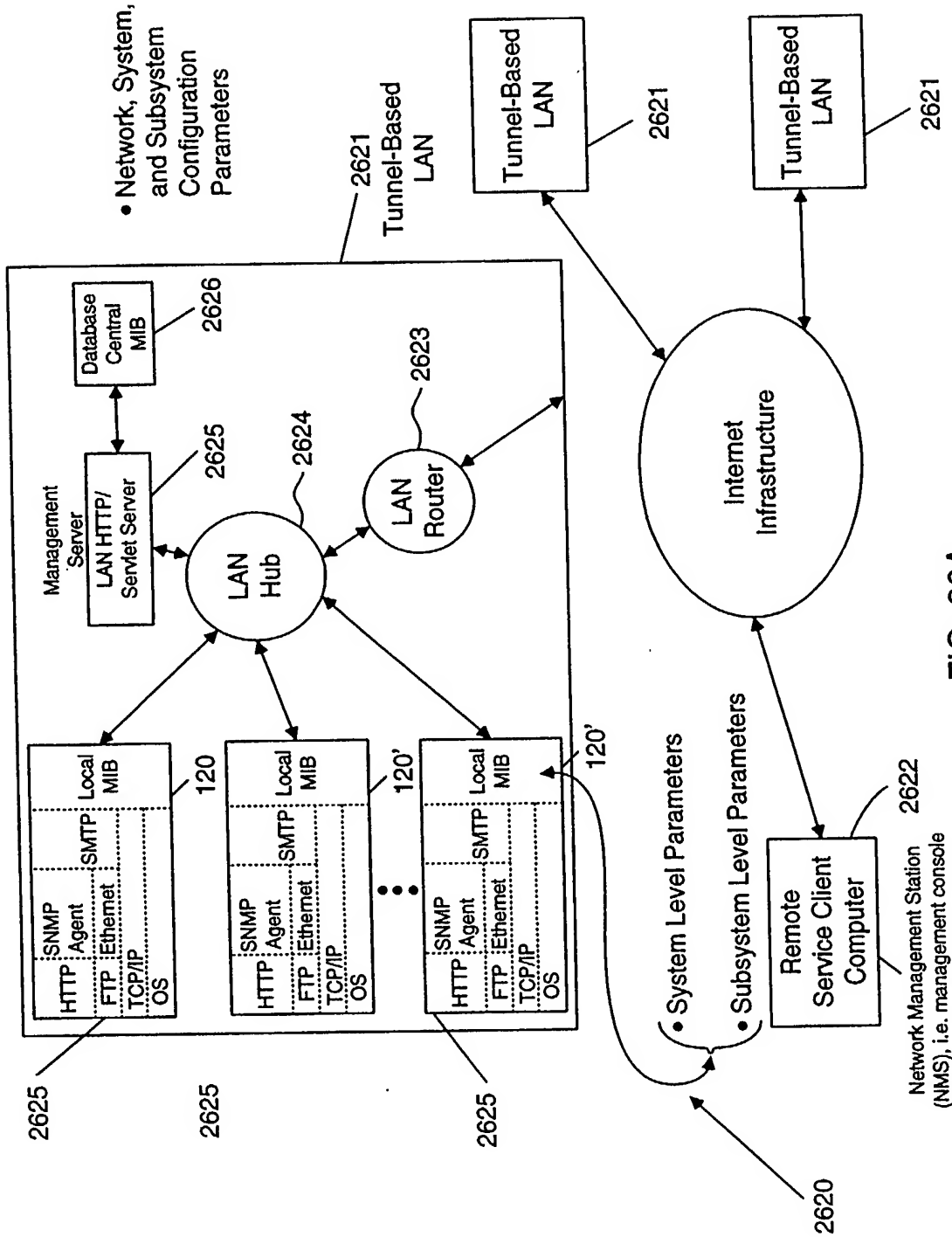


FIG. 30A

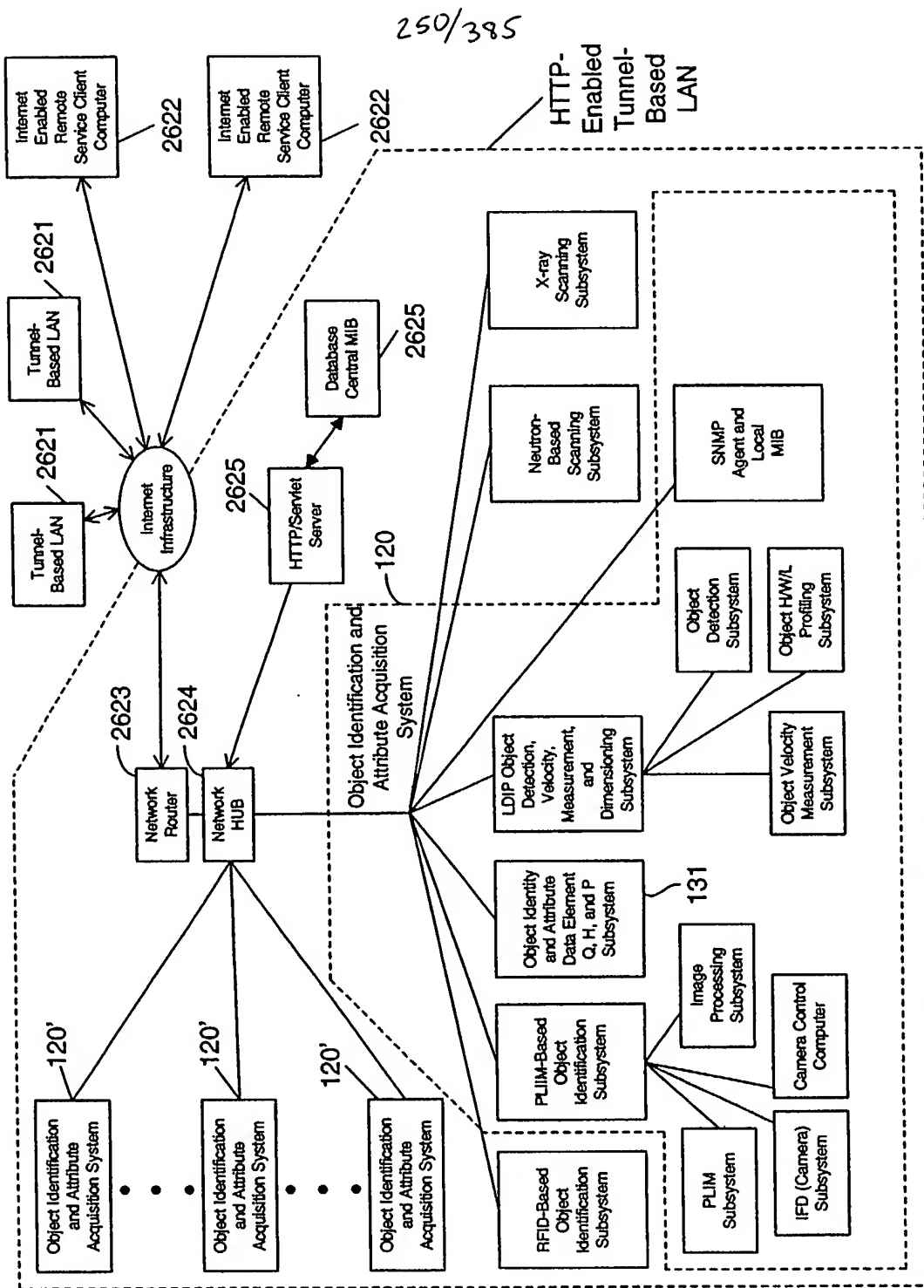


FIG. 30B

251/385

Network Configuration Parameters:

[Router IP address; no. of nodes (i.e. systems) in LAN; passwords, LAN location; name of customer facility; technical contact; phone no.; domain name; object identity codes; object attribute acquisition codes;.....]

System Configuration Parameters:

[System IP Address; passwords; object identity codes; object attribute acquisition codes;.....]

Monitorable and/or Configurable Parameters for Subsystems Within Each System:

- | | |
|--|--|
| <p>These subsystems generate object identity parameters</p> | <p><input type="checkbox"/> PLIIM-based object identification subsystem: [object identity code; object attribute acquisition codes;.....]</p> <p><input type="checkbox"/> PLIM Subsystem: [VLD status; power VLD; TIM function; temp;.....]</p> <p><input type="checkbox"/> IFD (Camera) Subsystem: [sensor temp;]</p> <p><input type="checkbox"/> Image Processing Subsystem (Computer): [processor load history; system up time; # of frames (pgs); barcode read rate; current line rate;.....]</p> <p><input type="checkbox"/> Camera Contact Subsystem (Computer): [number of frames dropped; number of focused zoom commands; number and kinds of motor control errors;.....]</p> |
| <p>This system links object attribute data element parameters (i.e. object identity data element) to corresponding object identity parameters (i.e. object attribute data element)</p> | <p><input type="checkbox"/> RFID-based object identification subsystem: [....]</p> <p><input type="checkbox"/> Object identity and attribute data element queuing, handling and processing subsystem: [....]</p> |
| <p>These subsystems generate object attribute parameters</p> | <p><input type="checkbox"/> LDIP object identification, velocity-measurement, and dimensioning subsystem: [....]</p> <p><input type="checkbox"/> Object velocity measurement subsystem: [polygon RPM; polygon laser output X; channel X drift; channel X noise; trigger error events; instant lock reference drift; temperature]</p> <p><input type="checkbox"/> Object HWW/L profiling subsystem</p> <p><input type="checkbox"/> Object detection subsystem: [non- singulation/ singulation code;.....]</p> <p><input type="checkbox"/> X-ray scanning subsystem: [....]</p> <p><input type="checkbox"/> Neutron-beam scanning subsystem: [....]</p> |

FIG. 30C

252/385

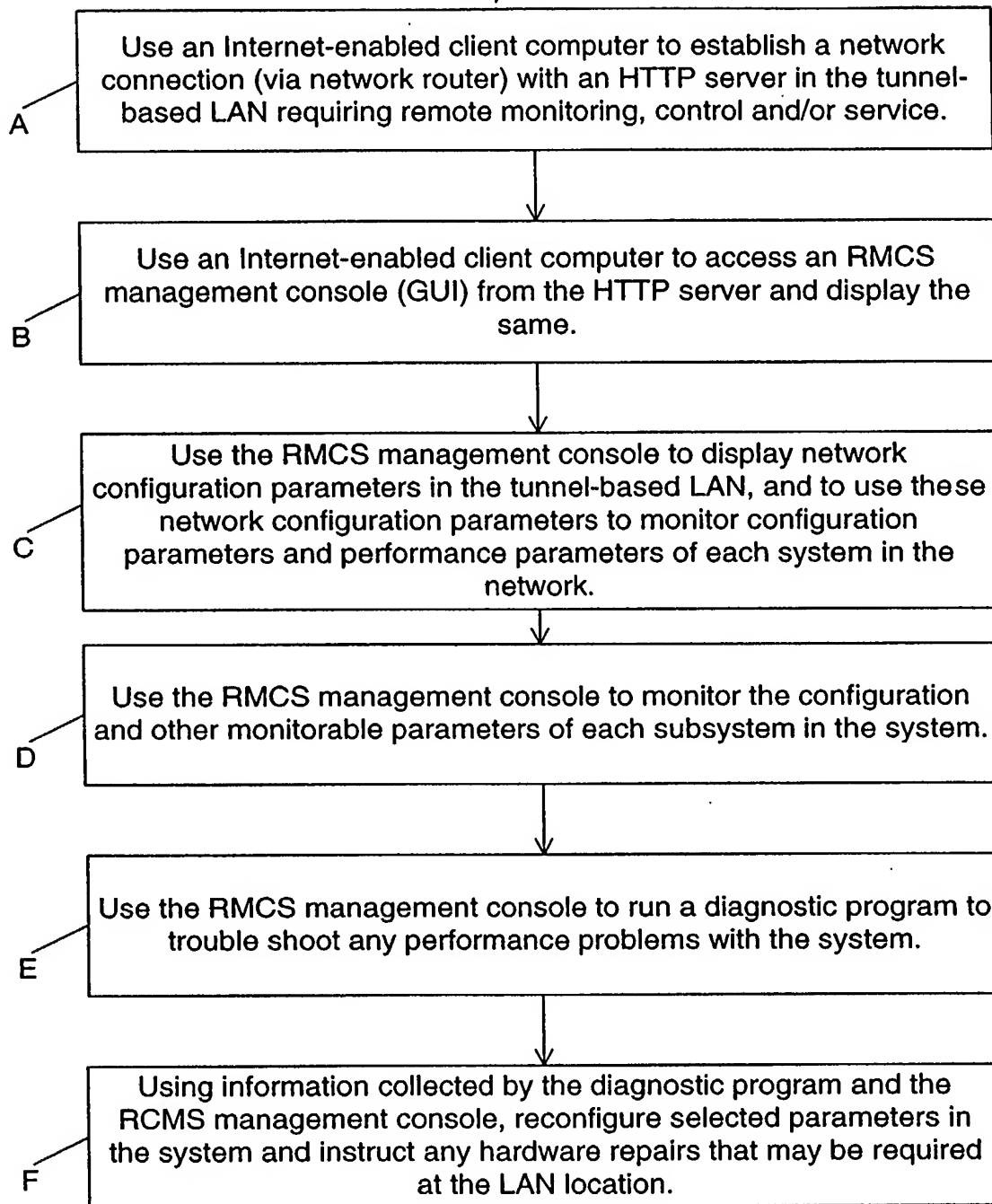


FIG. 30D1

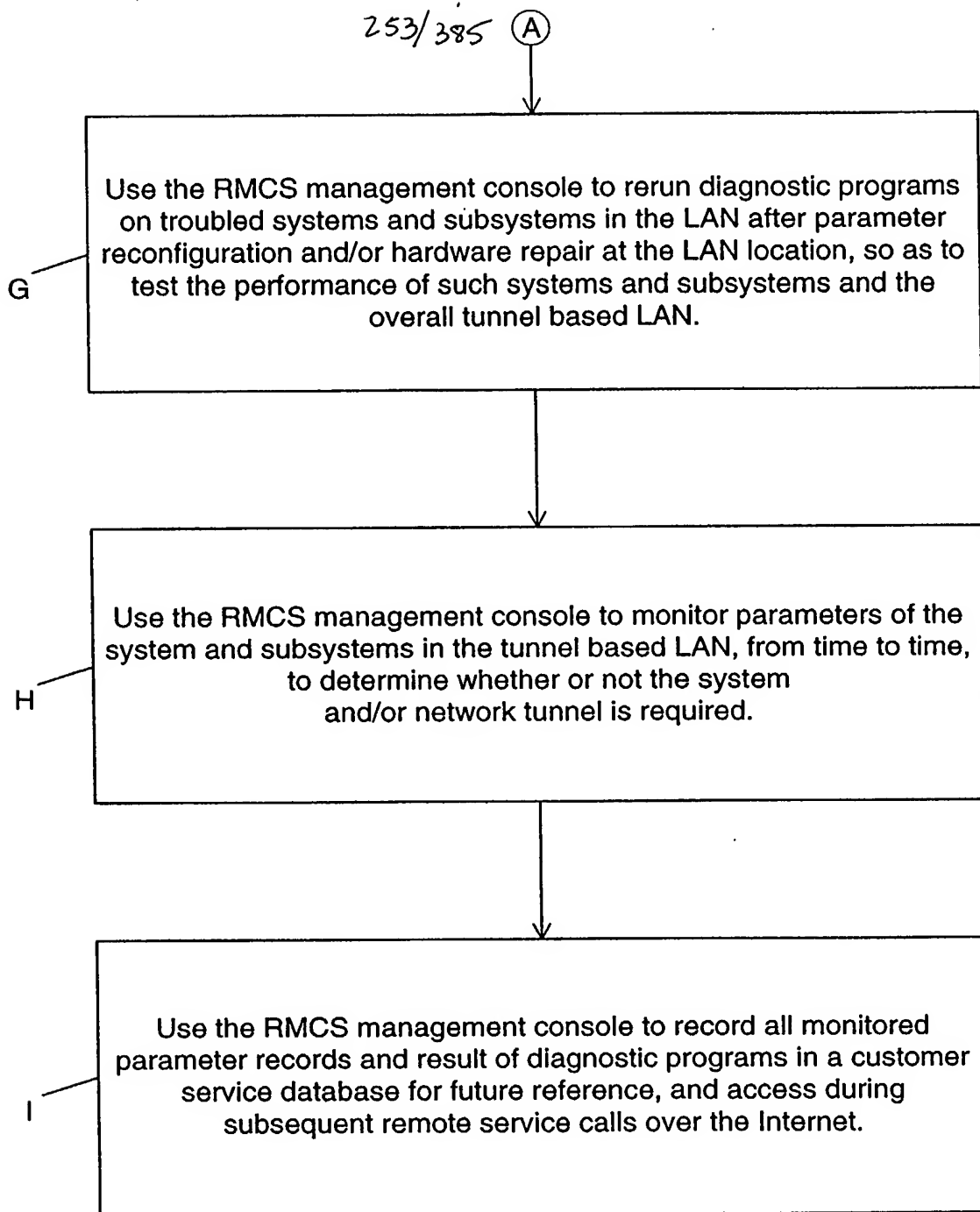
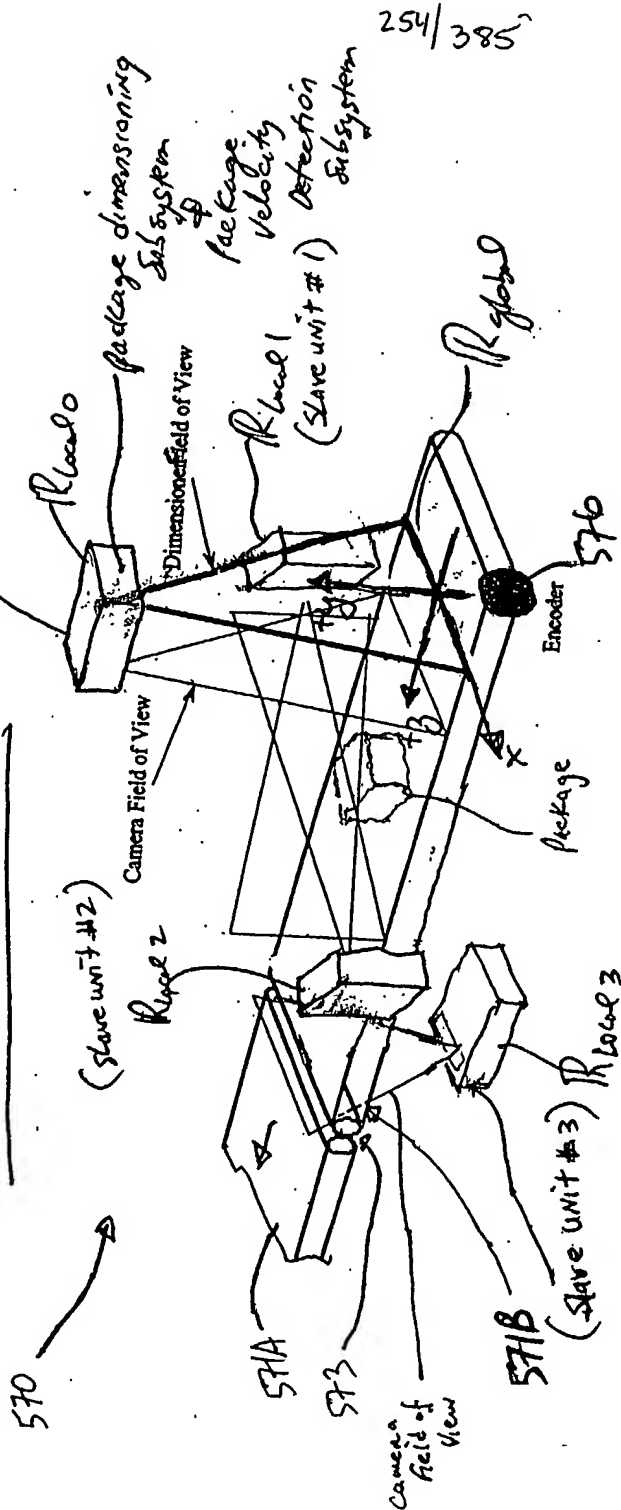


FIG. 30D2

CCD Camera-Based Tunnel System
Employing Package Coordinate Data
Driven Method of Automatic Camera
Zoom and Focus Control



Package coordinate data \parallel \Rightarrow Package coordinate data \parallel \Rightarrow Package coordinate data

FIG. 31

255/385

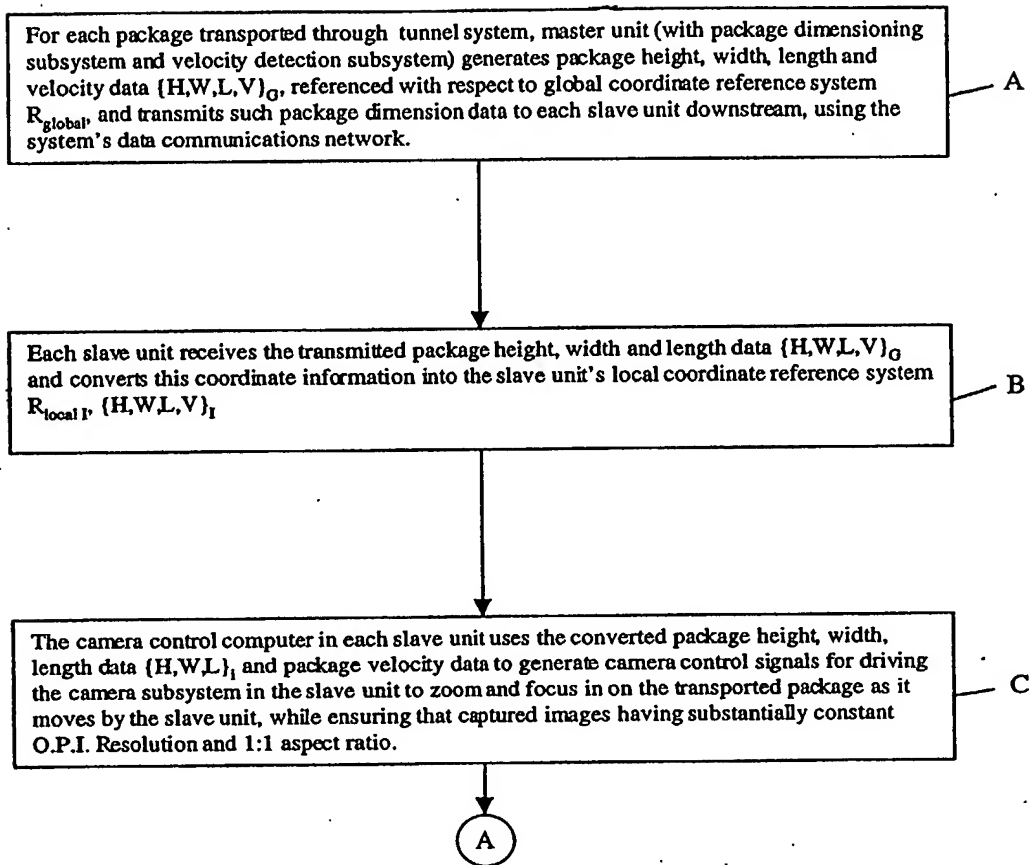


FIG. 32A

(A)

256/385

Each slave unit captures images acquired by its intelligently controlled camera subsystem, buffers the same, and processes the images to decode bar code symbol identifiers represented in said images, and/or to perform optical character recognition (OCR) thereupon.

D

The slave unit which decodes a bar code symbol in a processed image automatically transmits a package identification data element (containing symbol character data representative of the decoded bar code symbol) to the master unit (or other designated system control unit employing data element management functionalities) for package data element processing.

E

Master unit time-stamps received package identification data element, places said data element in a data queue, and processes package identification data elements and time-stamped package dimension data elements in said queue to link each package identification data element with one said corresponding package dimension data element.

F

FIG. 32B

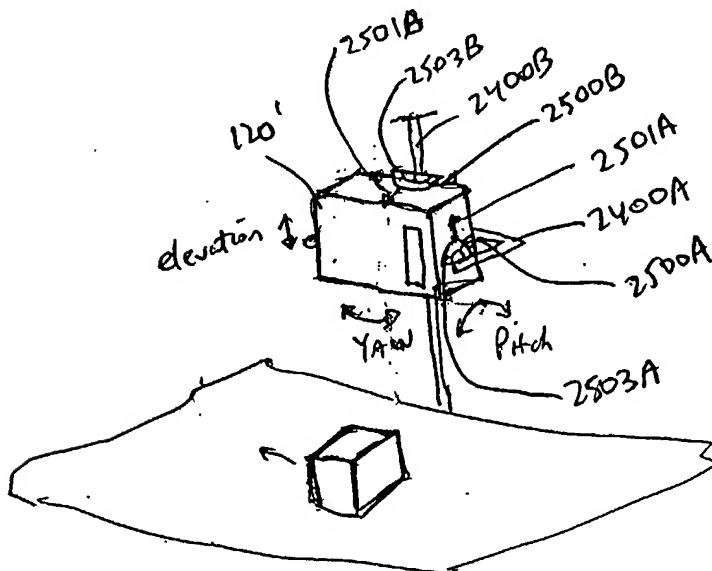
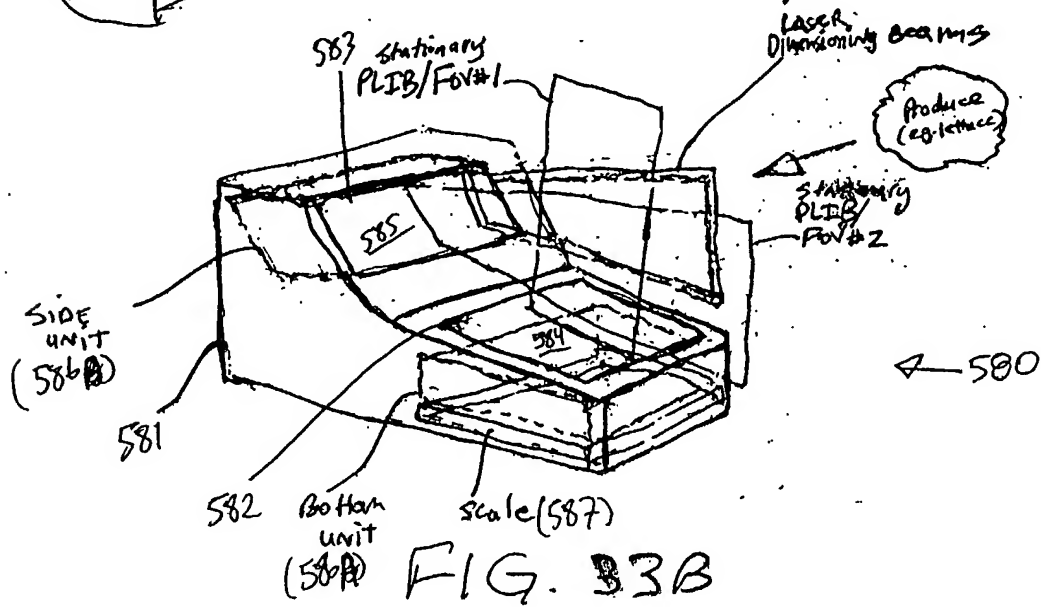
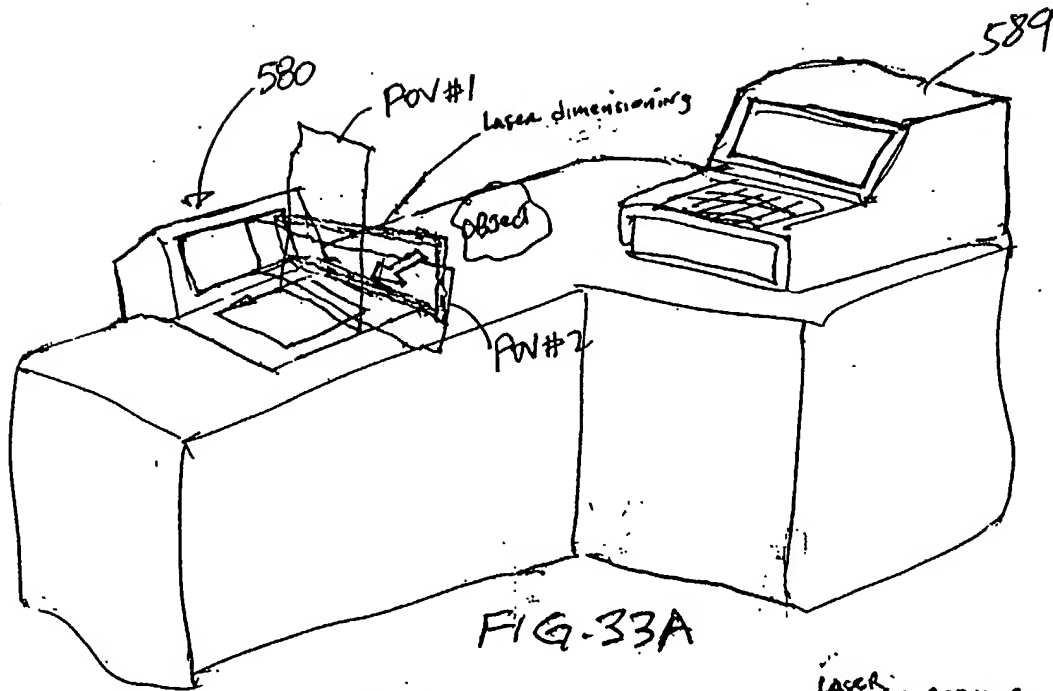
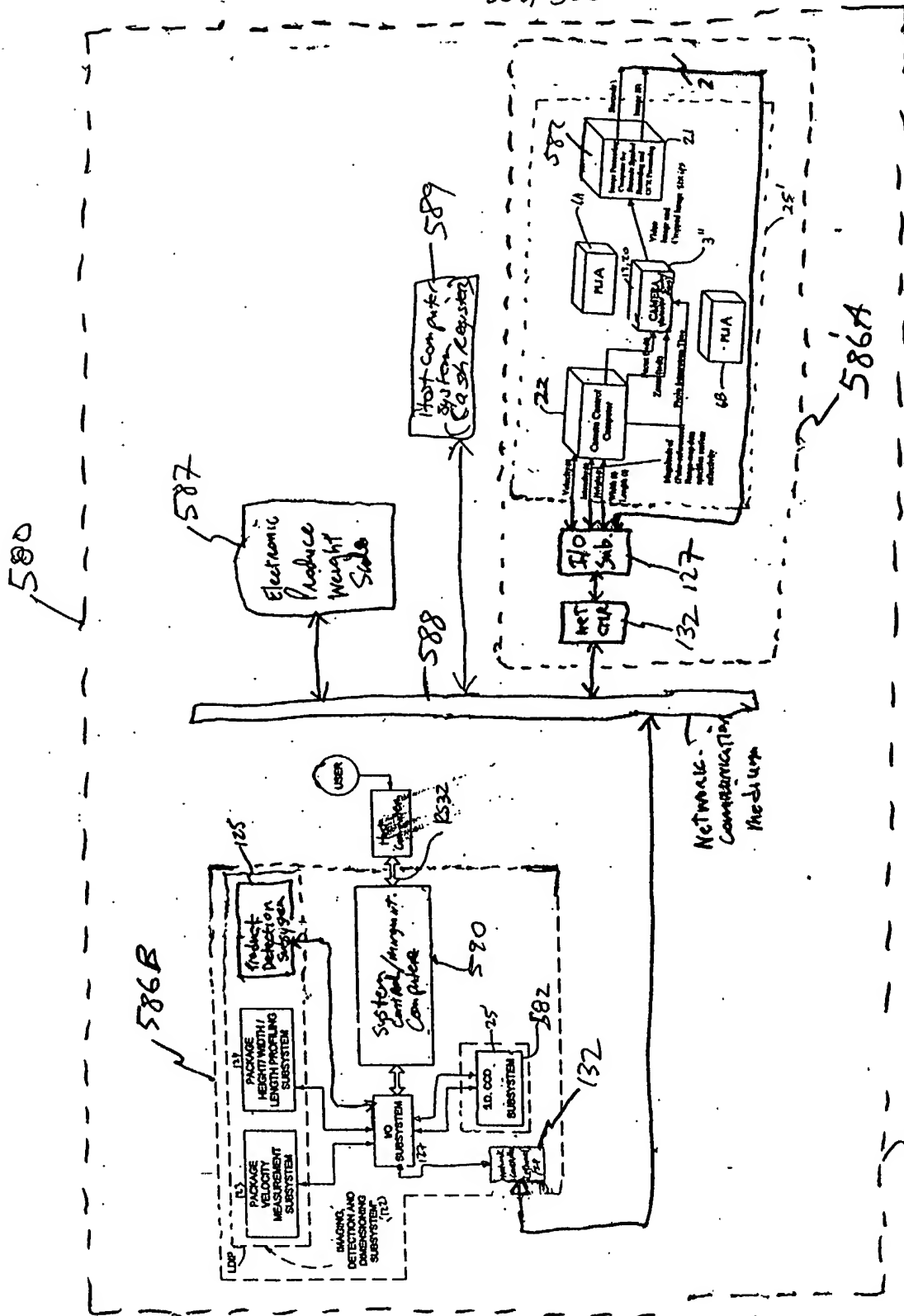


FIG. 31A

257/385



258/385'



259/385

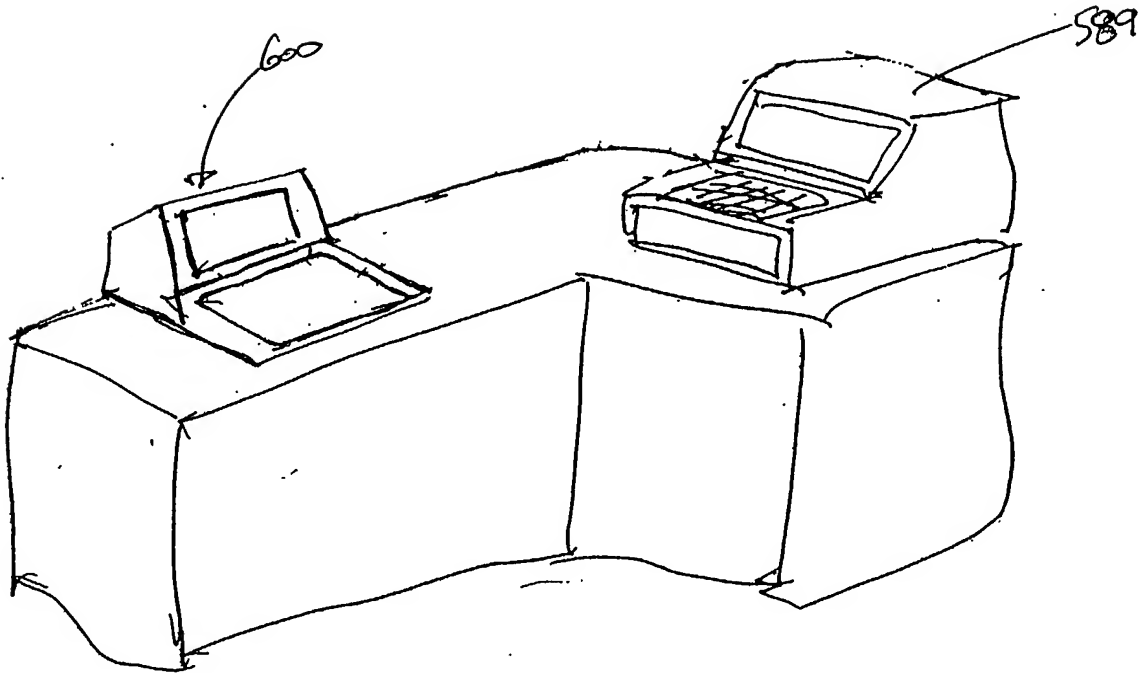


FIG. 34A

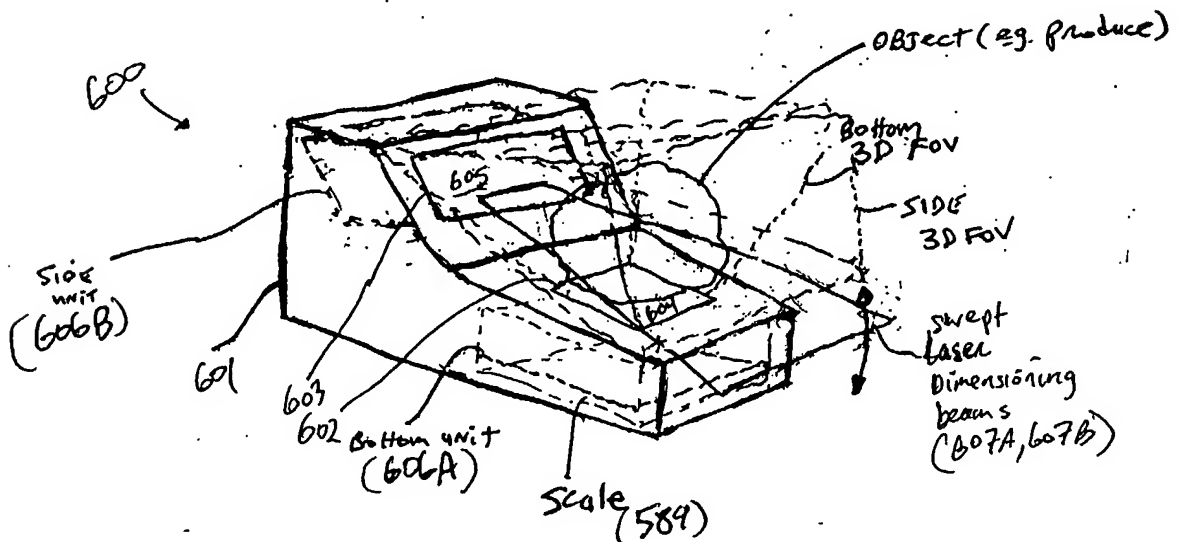


FIG. 34B

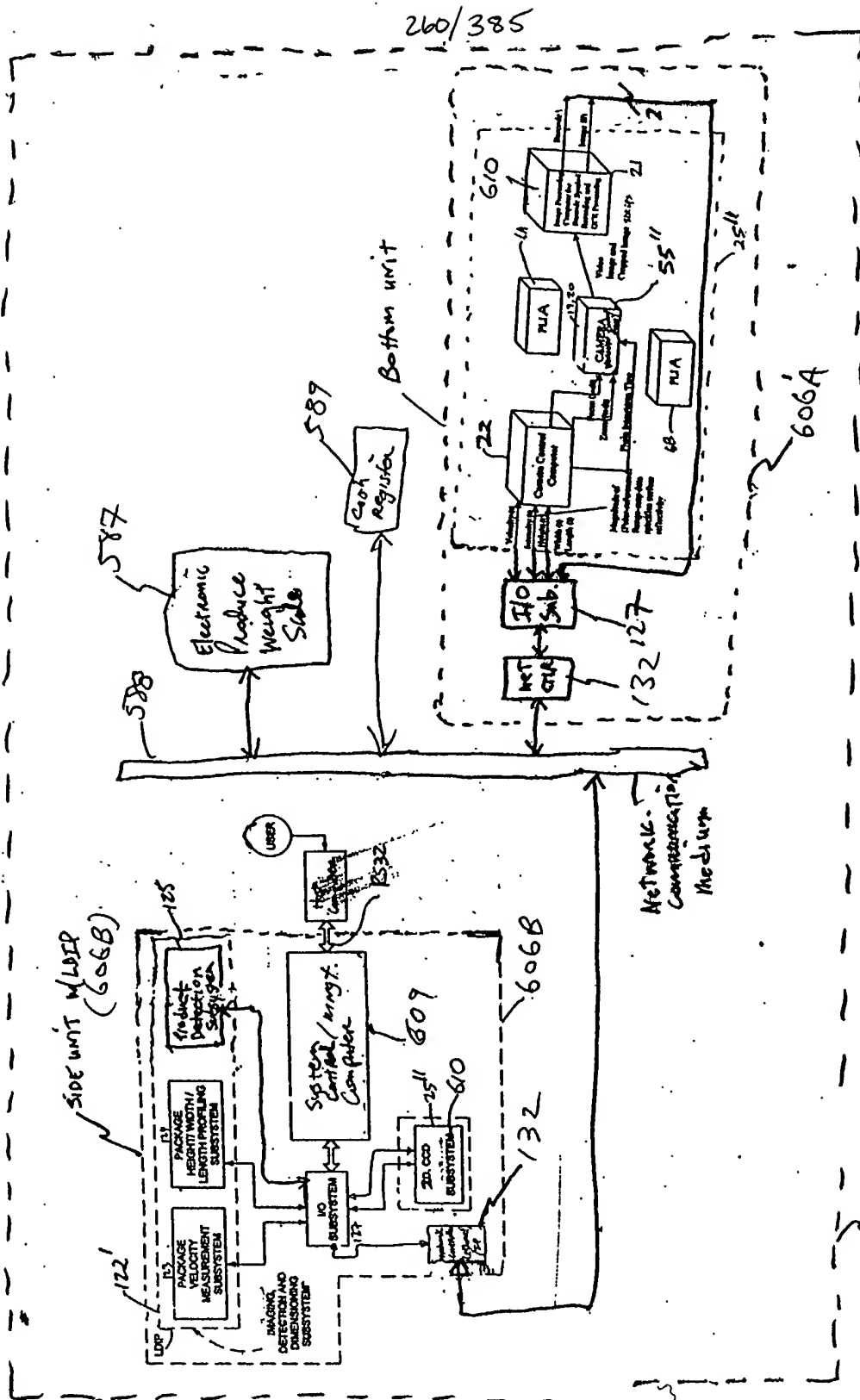
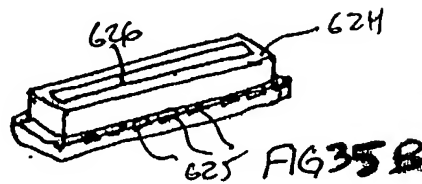
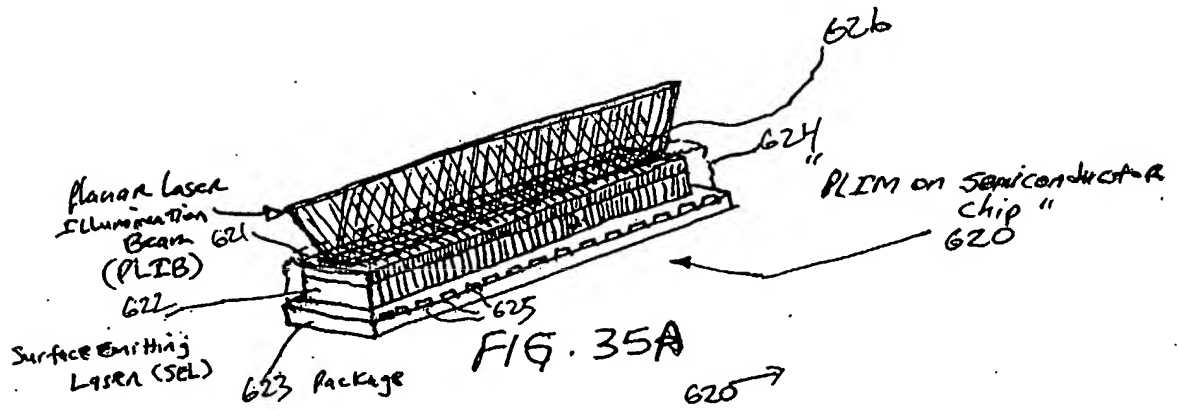
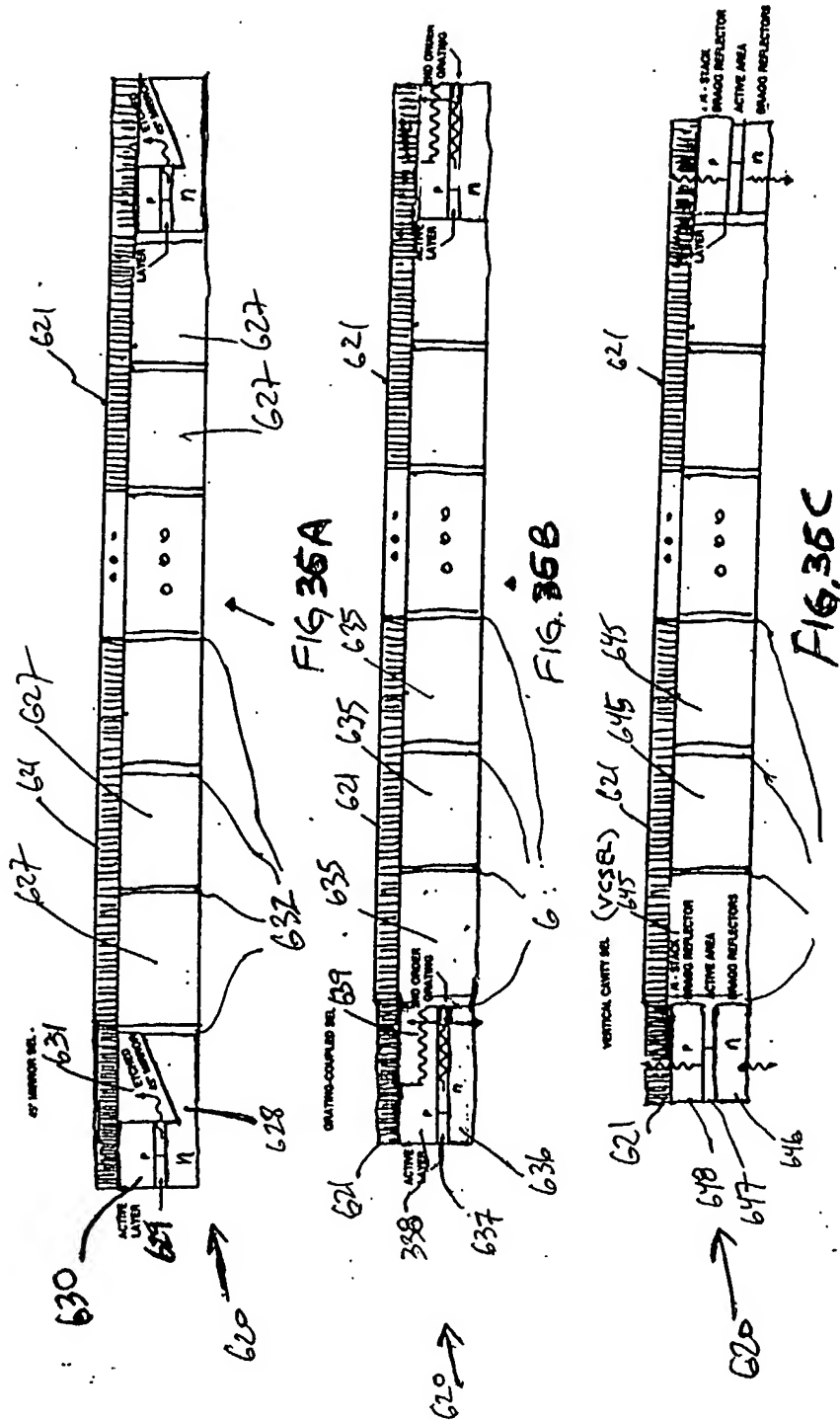


FIG. 34C

261/385



262/385



2 63/3857

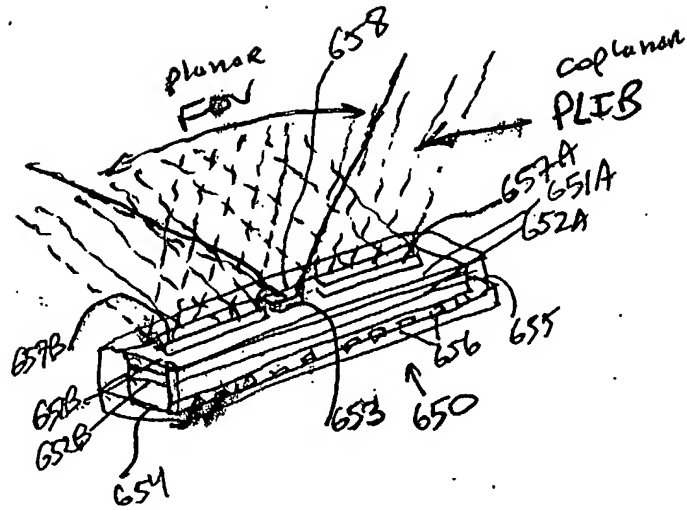


FIG. 37

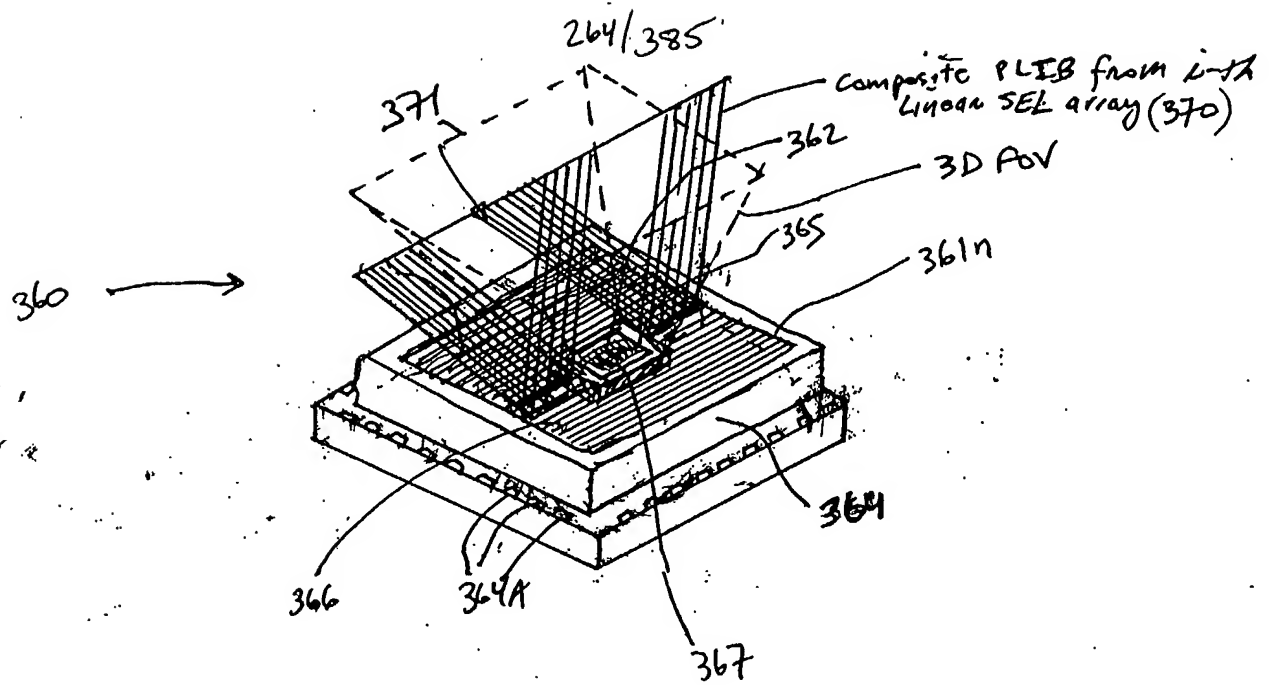


FIG. 38A

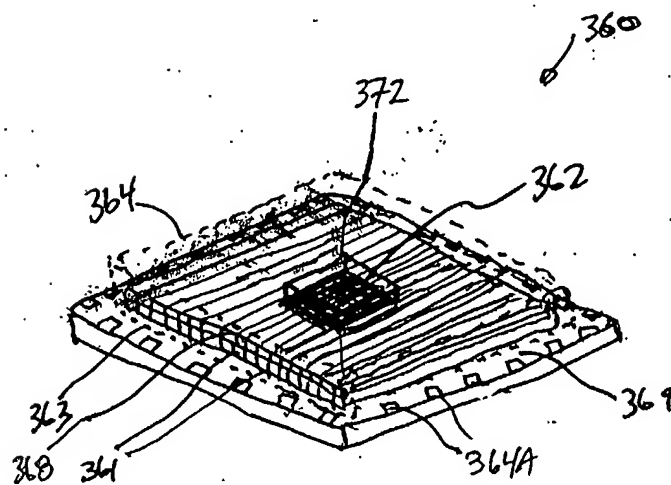
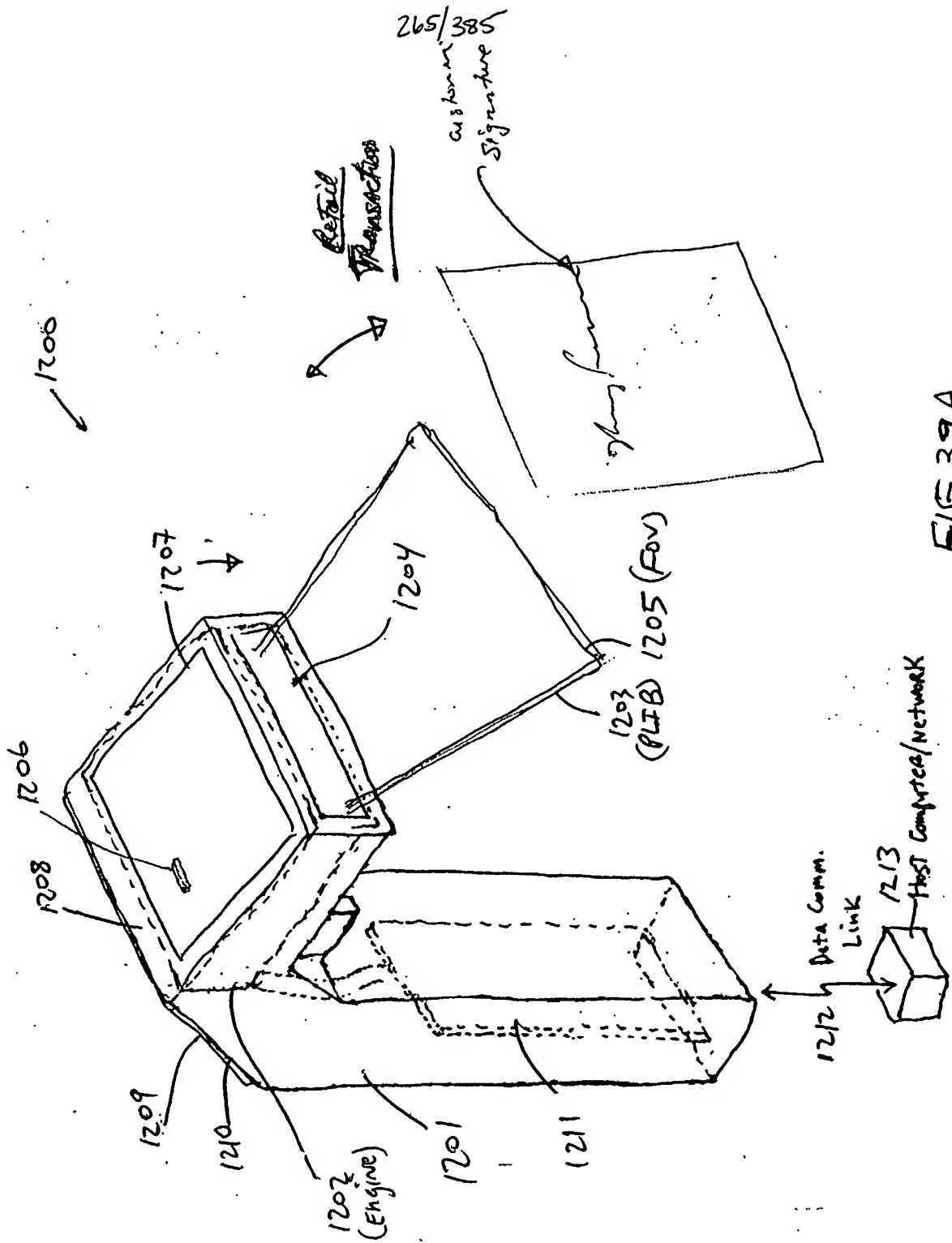


FIG. 38B



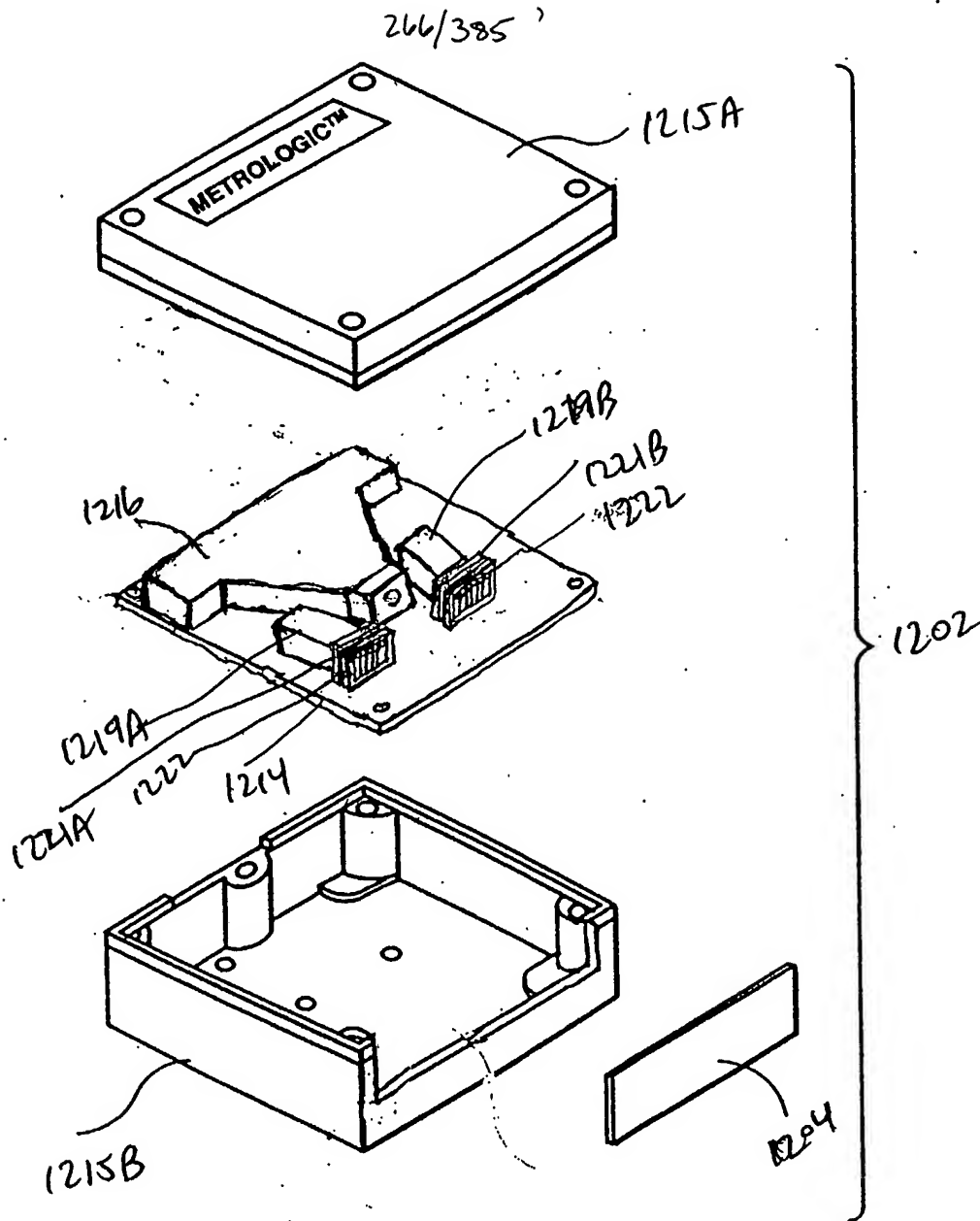


FIG. 39B

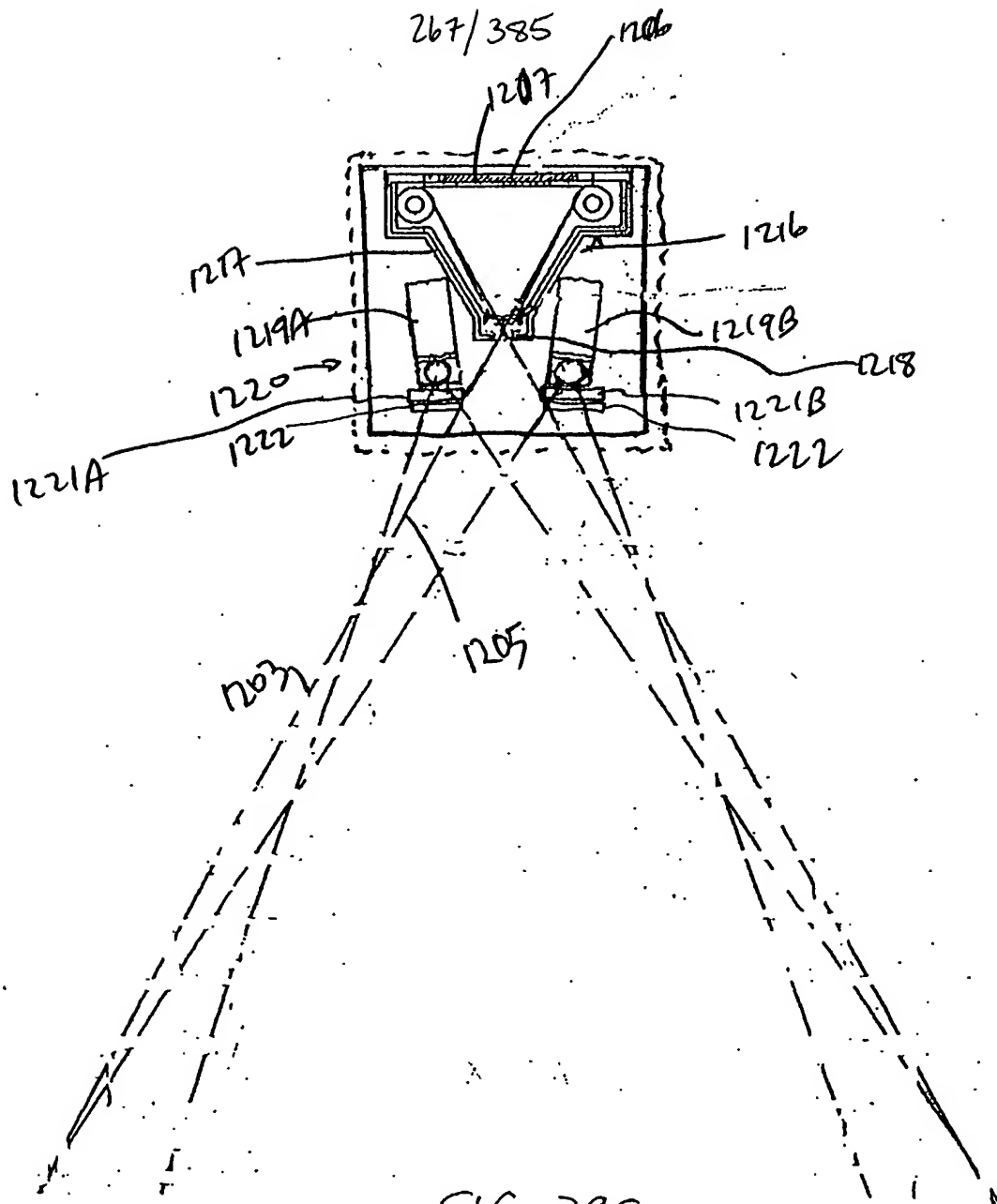


FIG. 39C

268/385

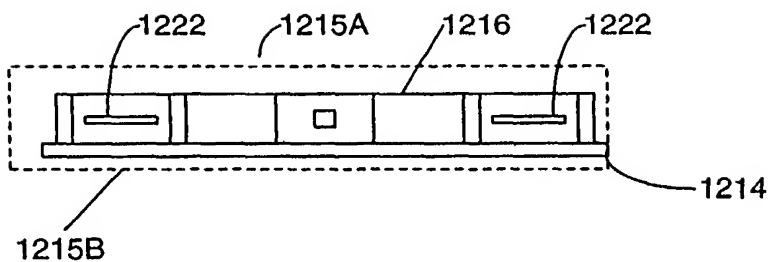


FIG. 39D

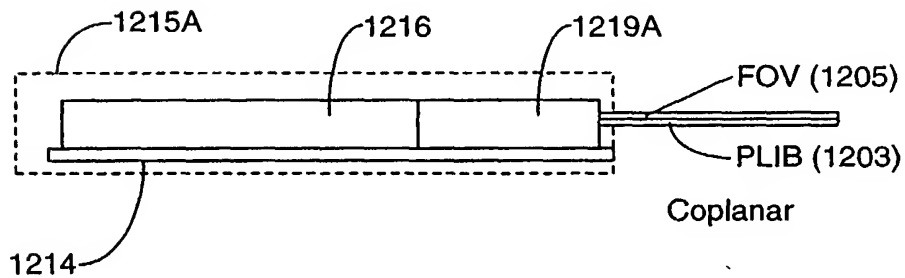


FIG. 39E

269/385

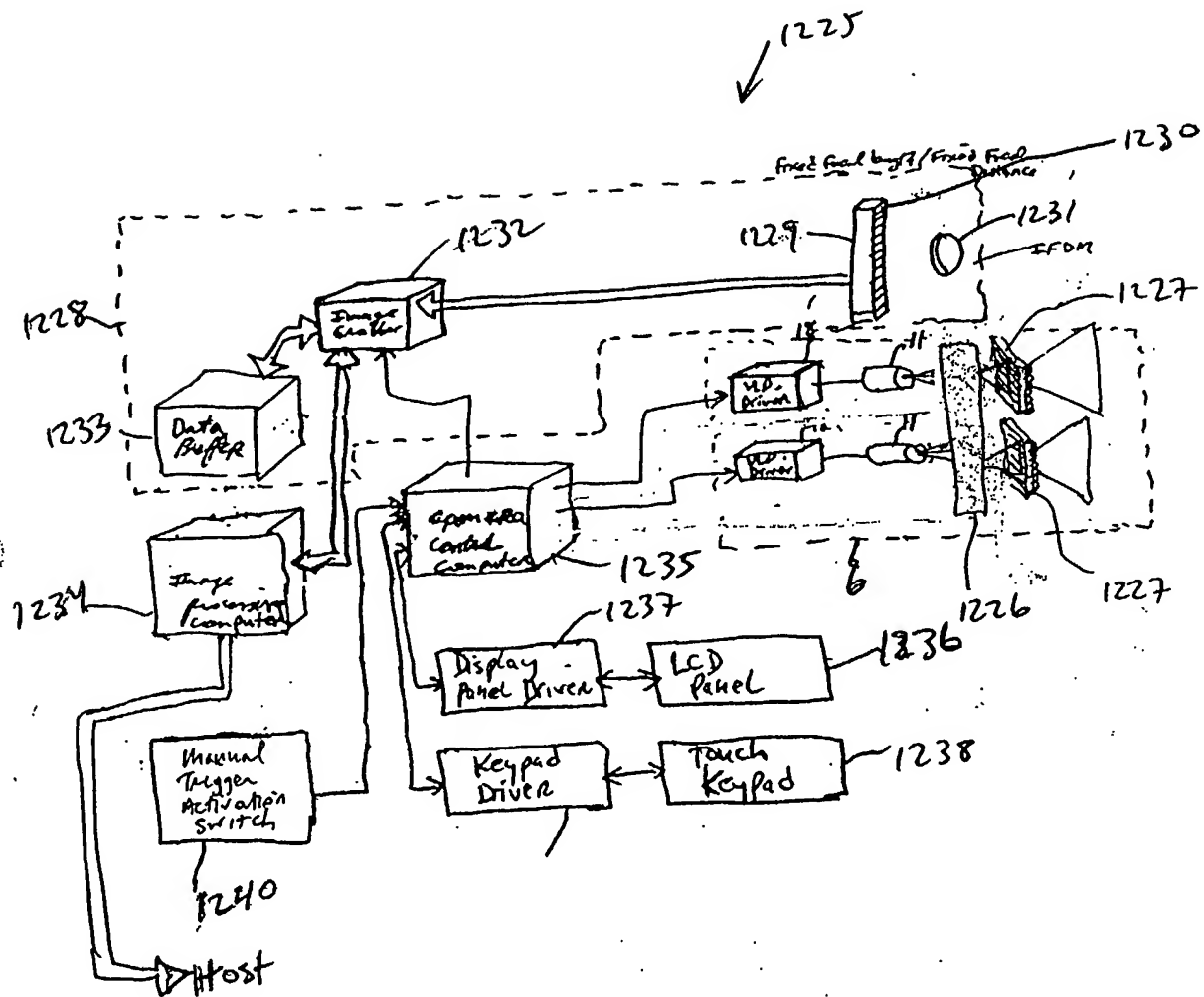
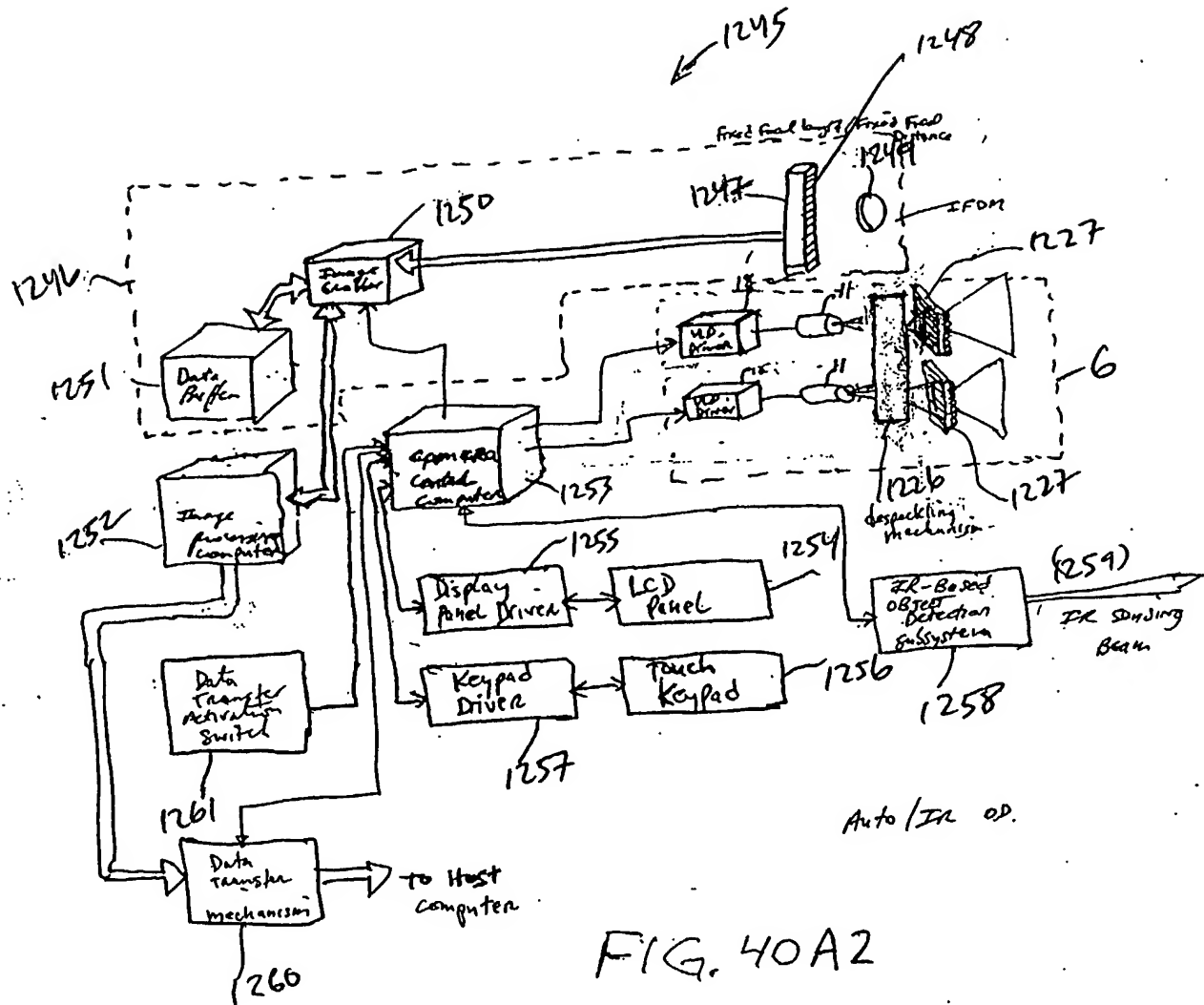
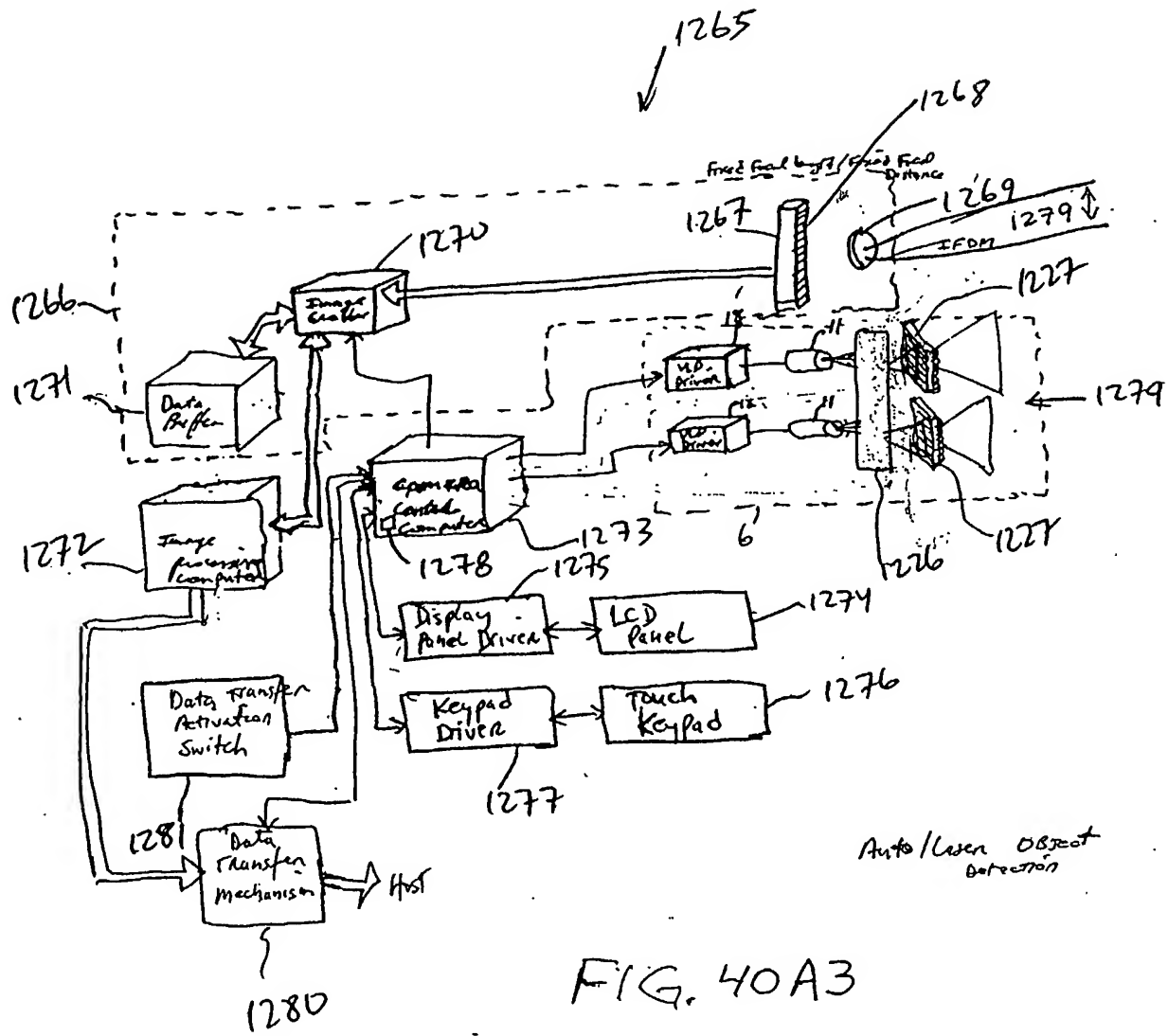


FIG. 40A1

$$270/385$$


271/385



272/385

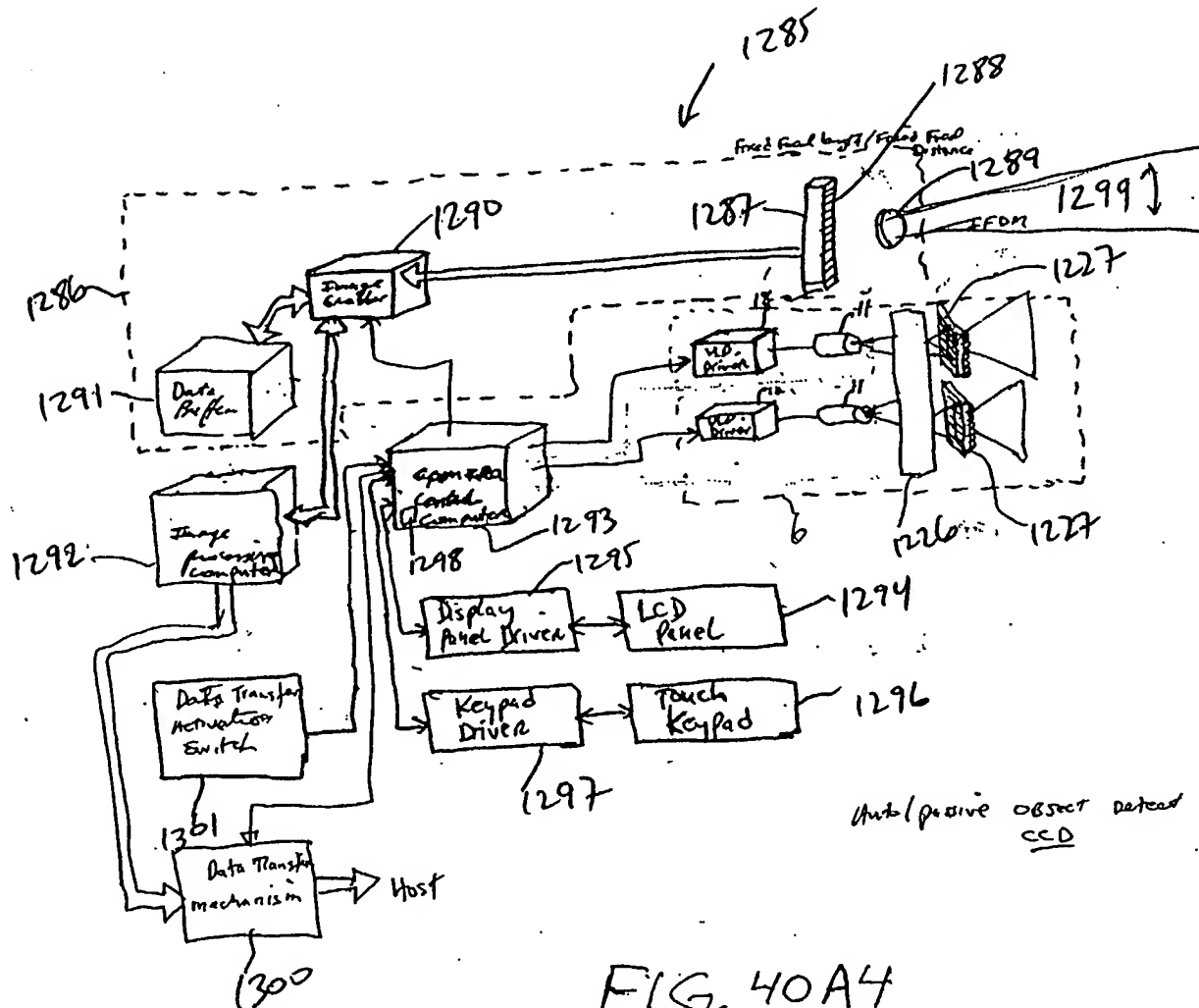
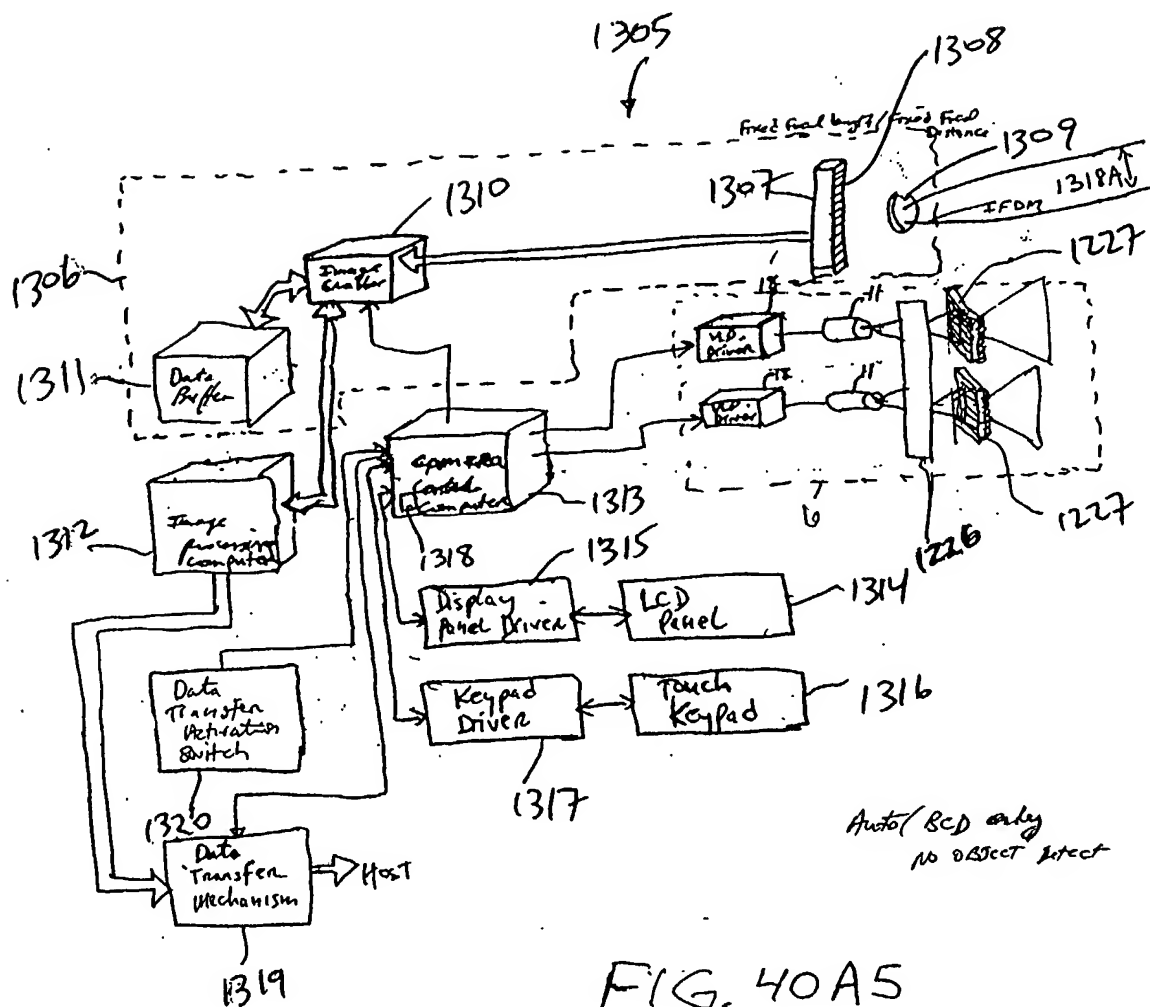


FIG. 40A4

273/385



27/385

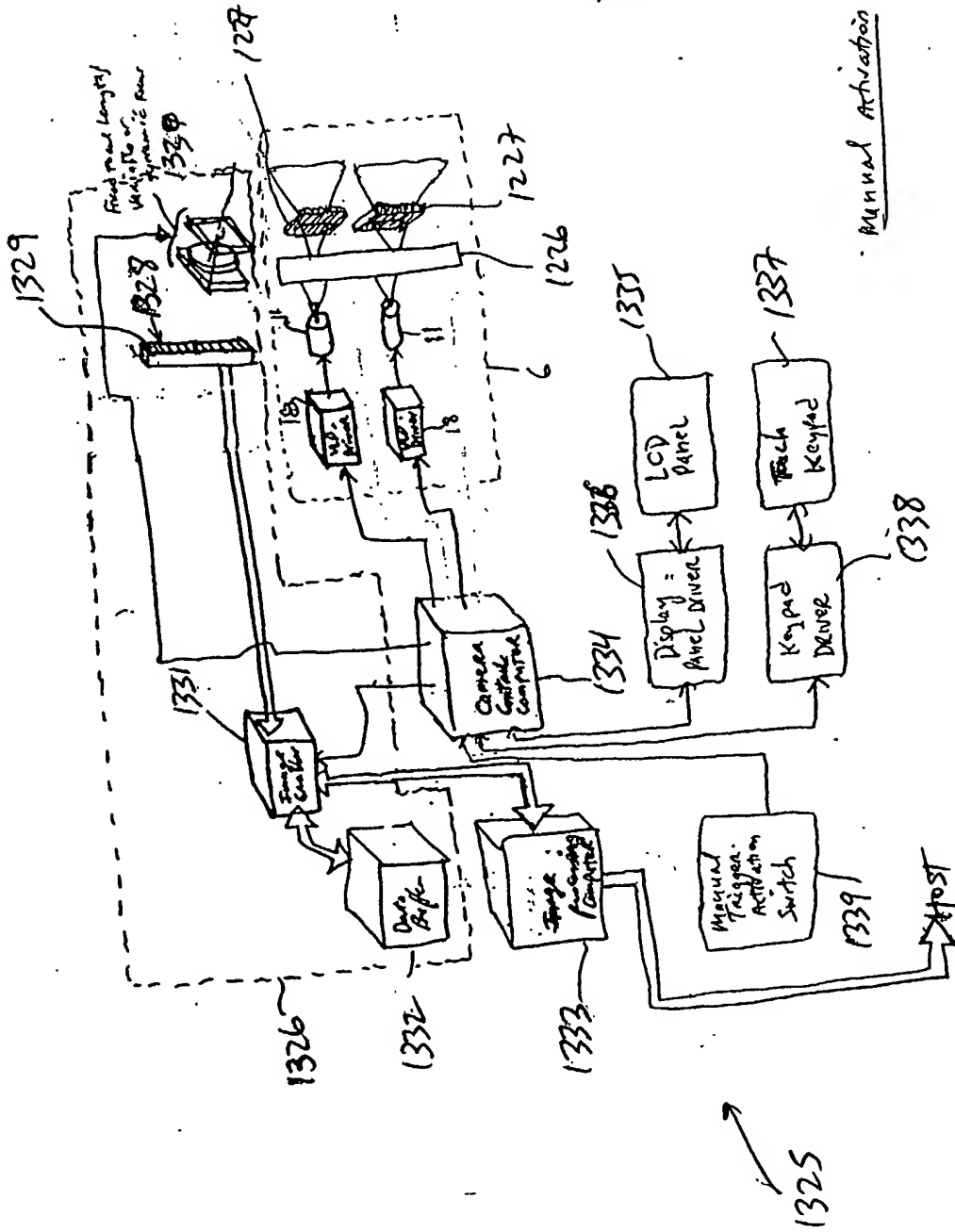
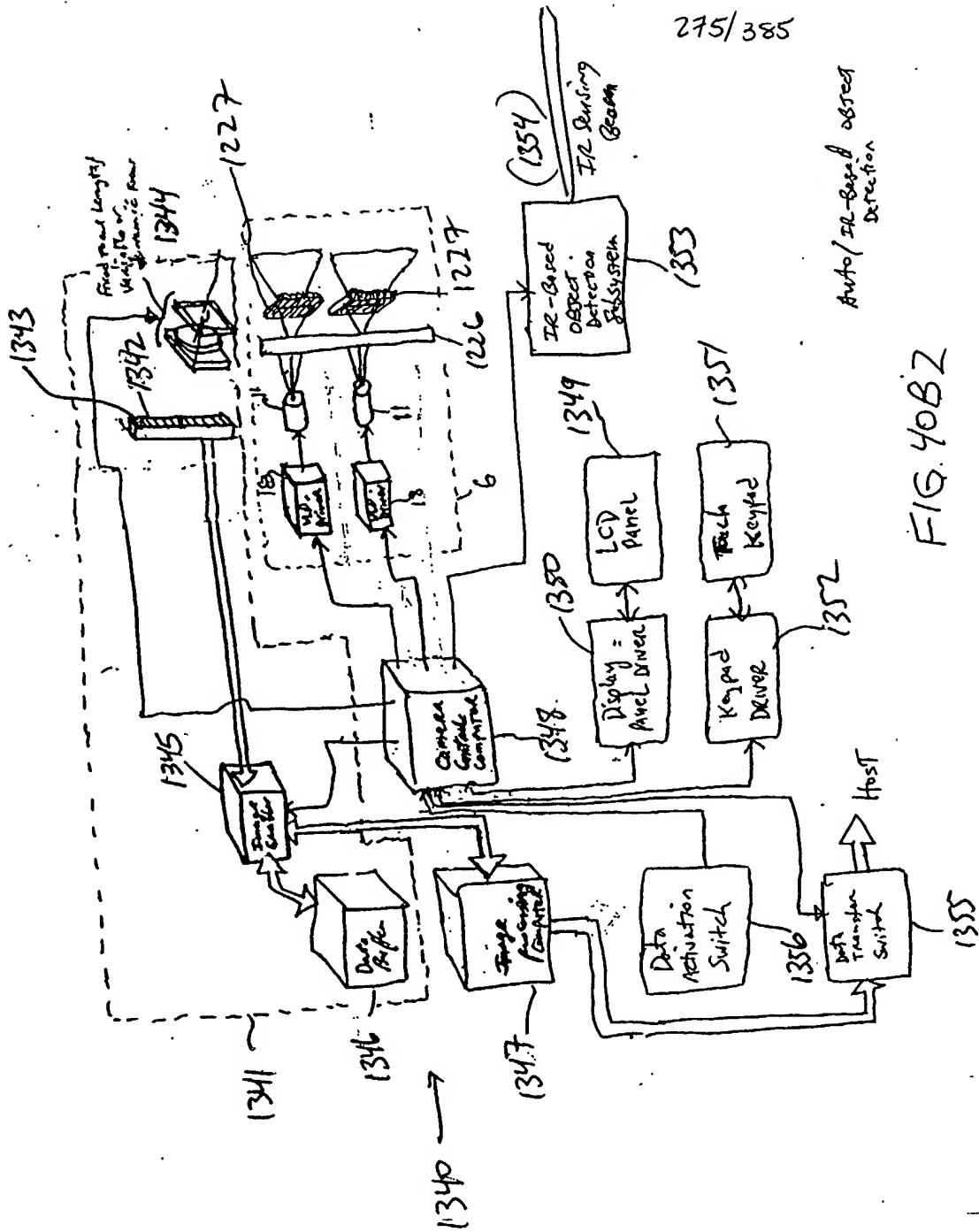


FIG. 40B1



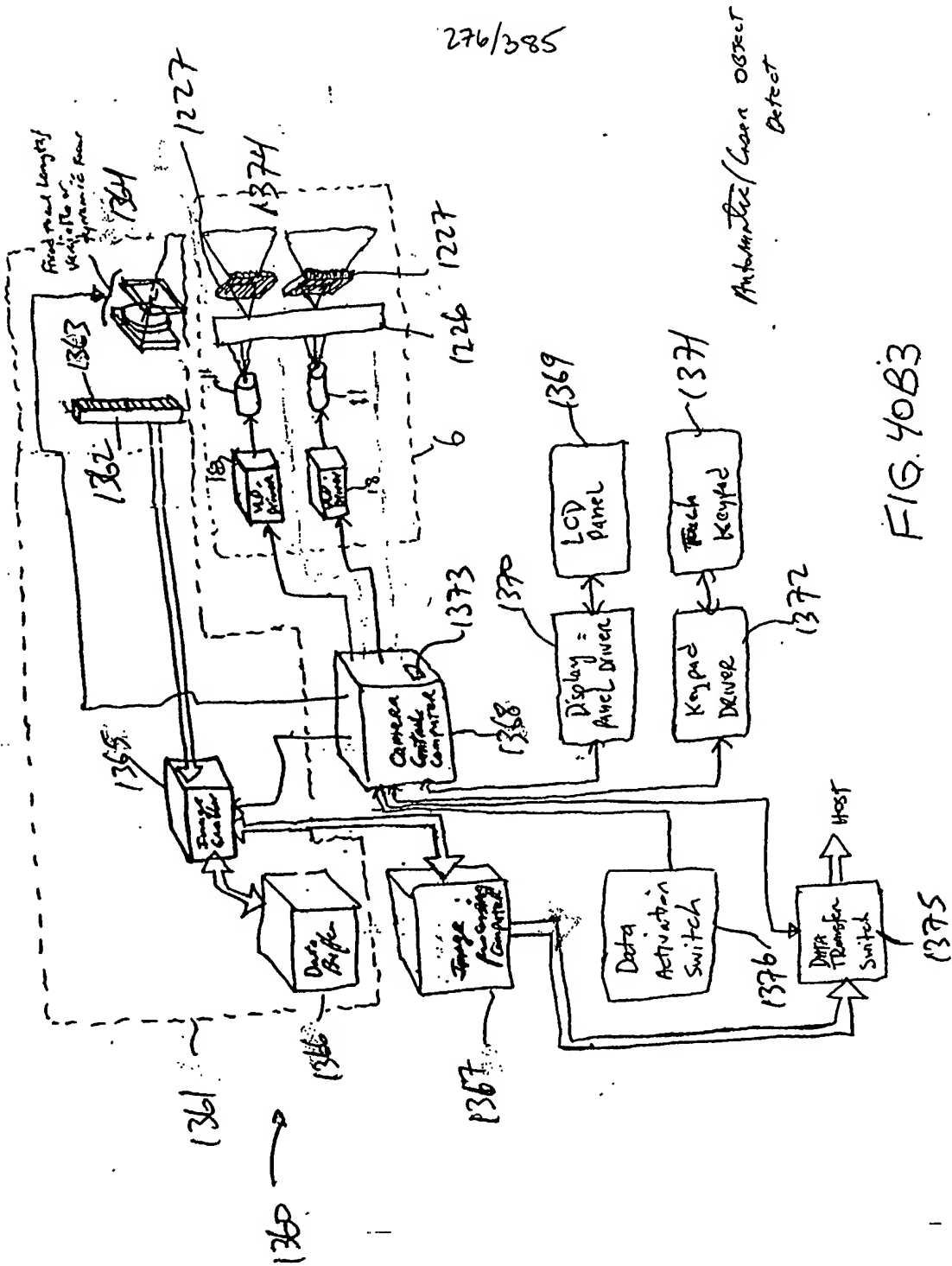
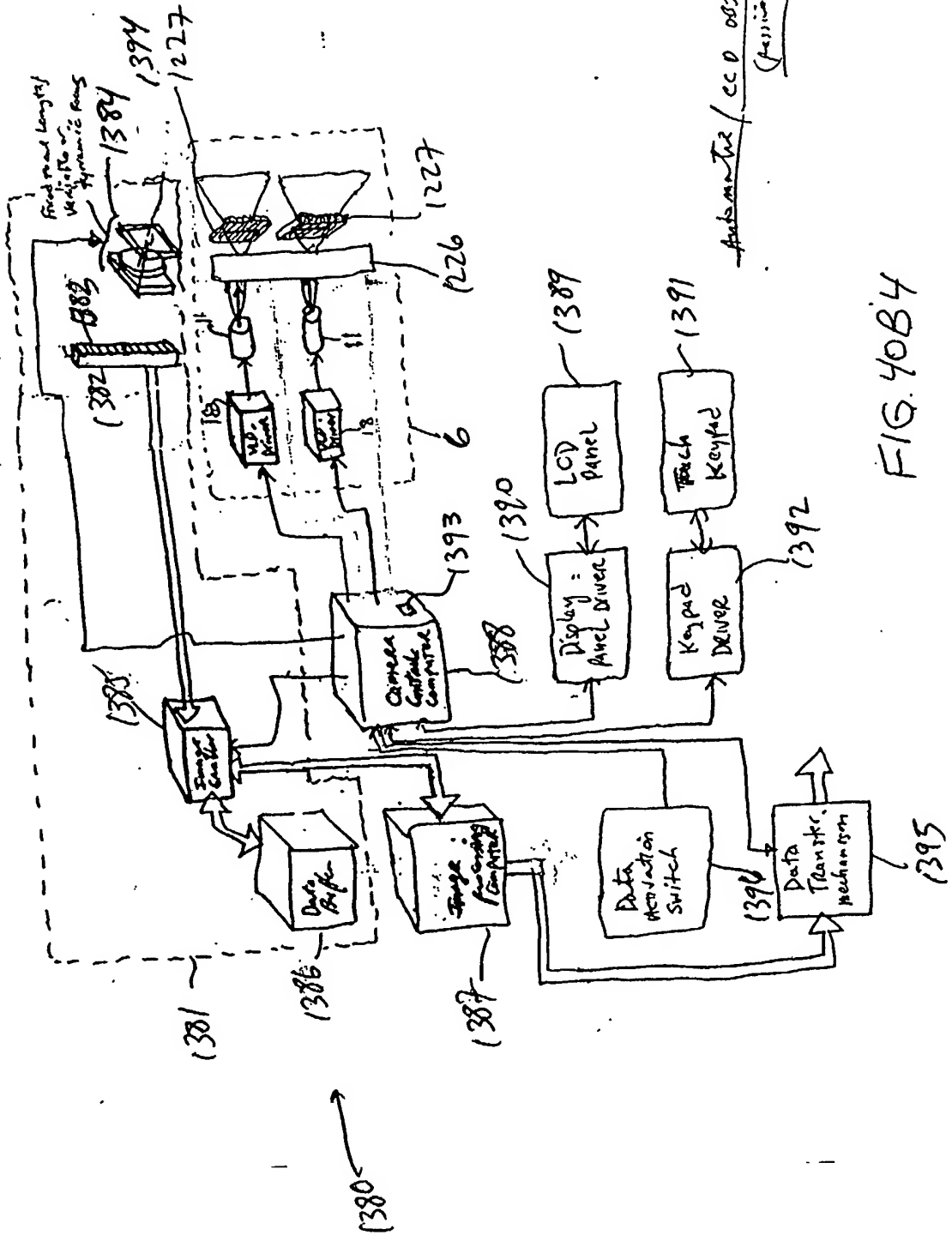
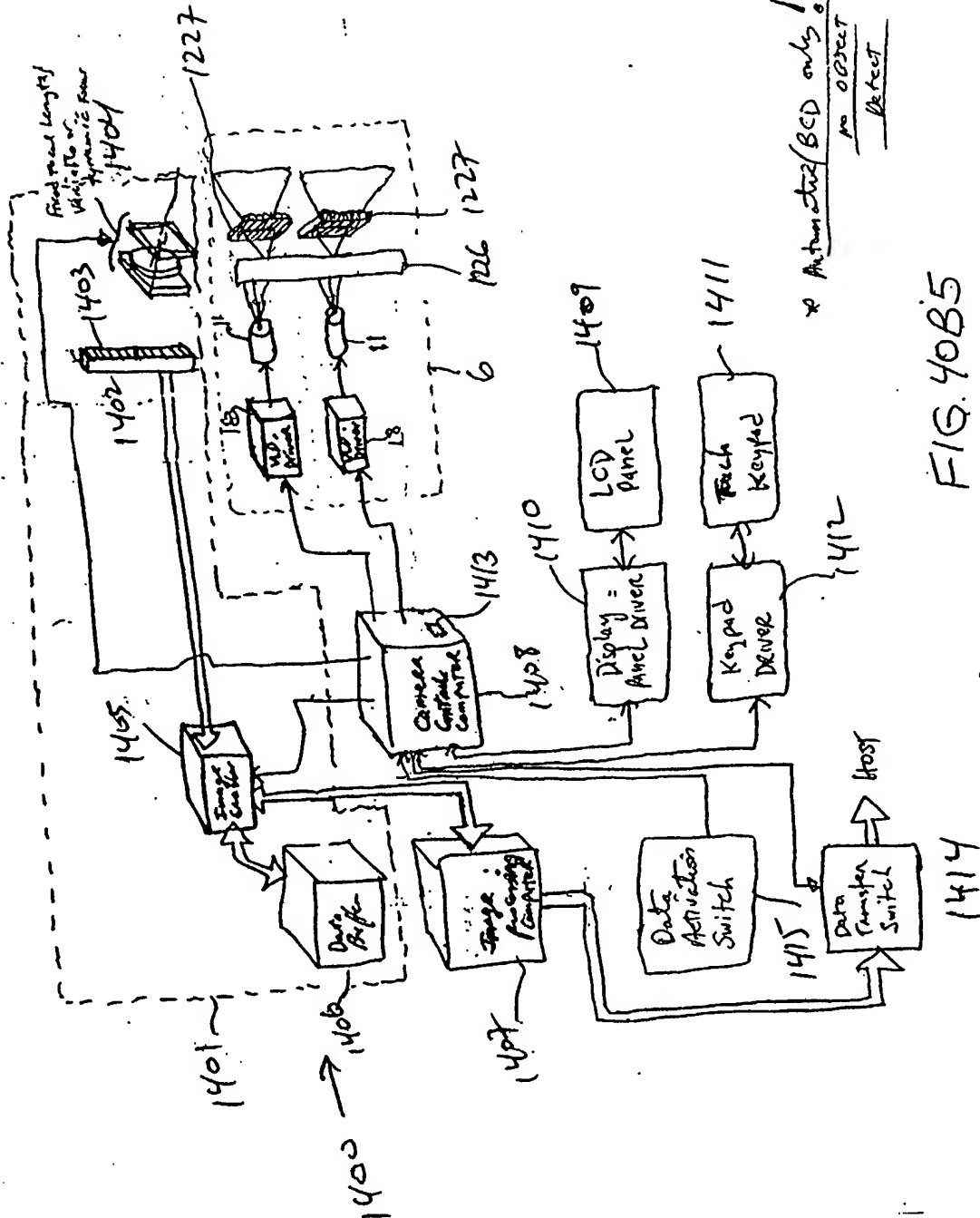


FIG. 40B3



278/385



279/385

Manual Activation

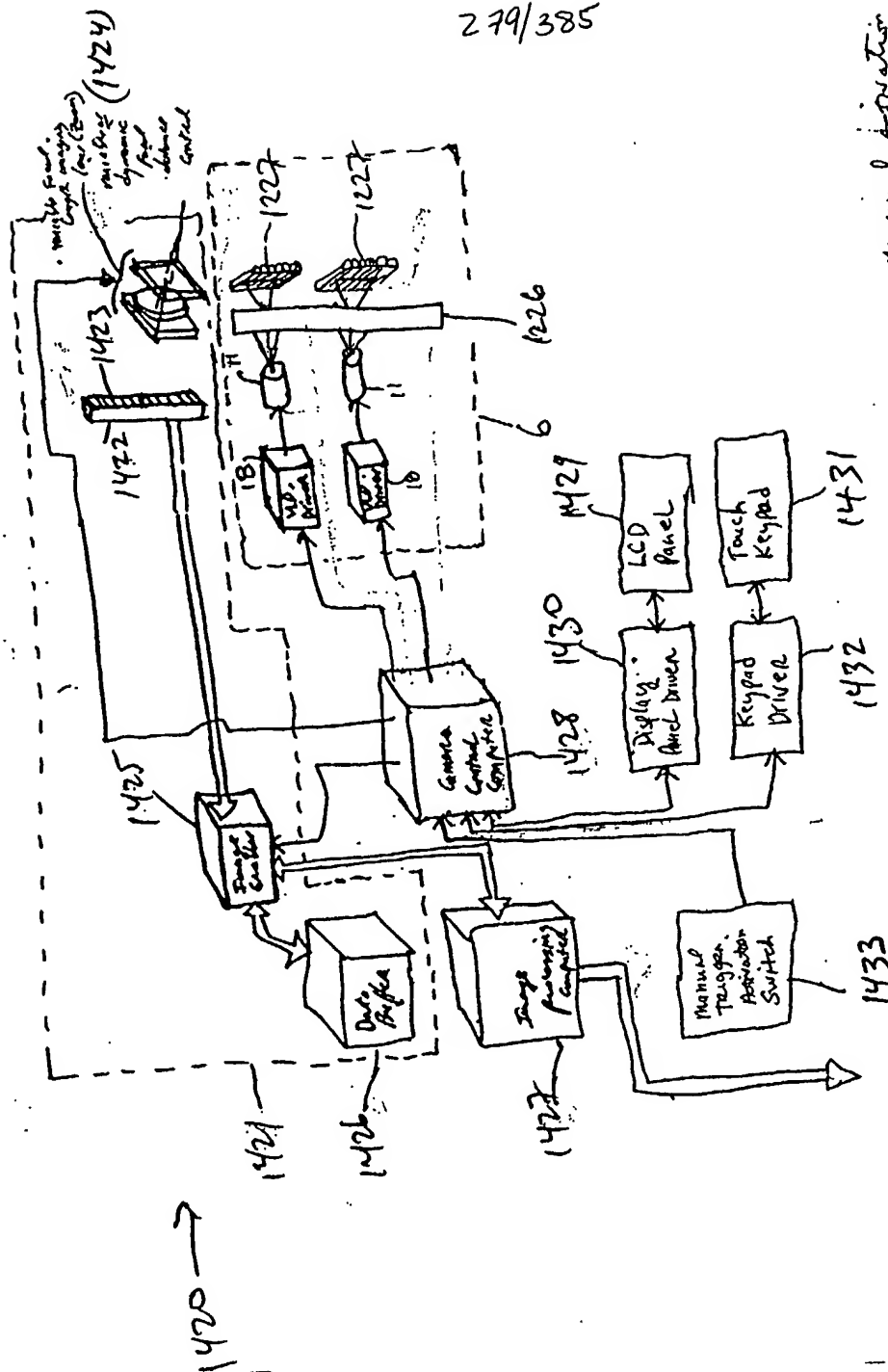


FIG. 40C1

280/385,

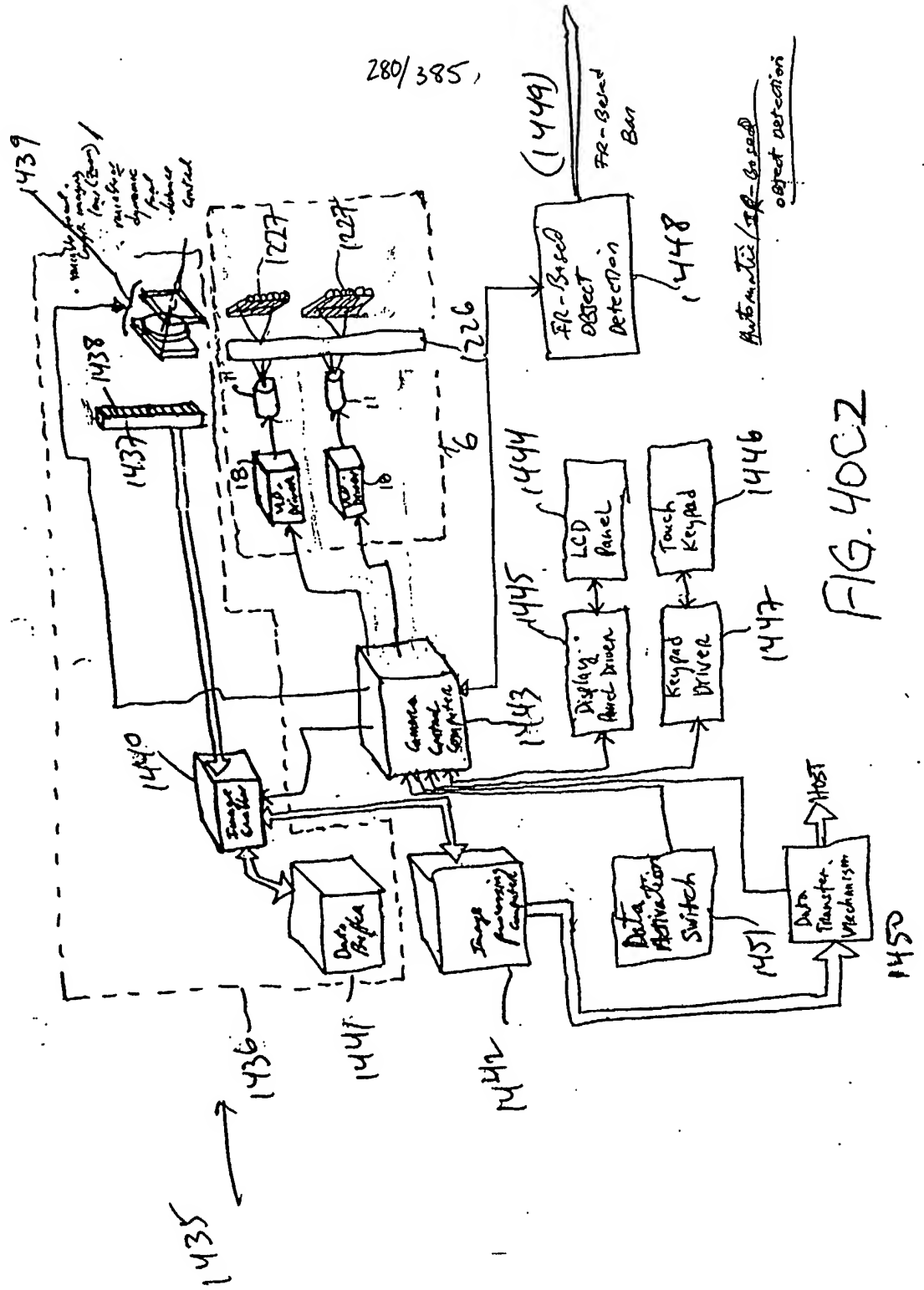
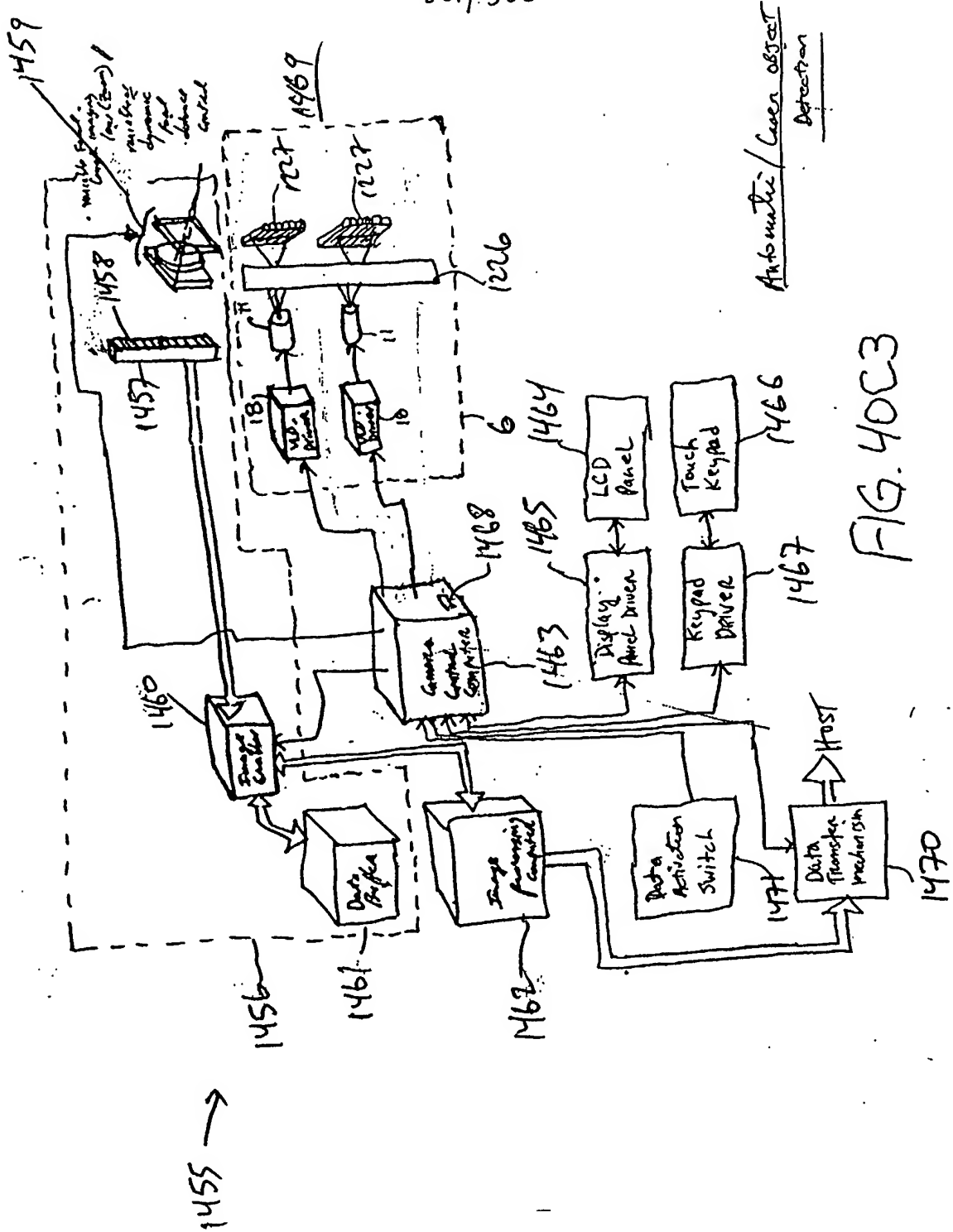
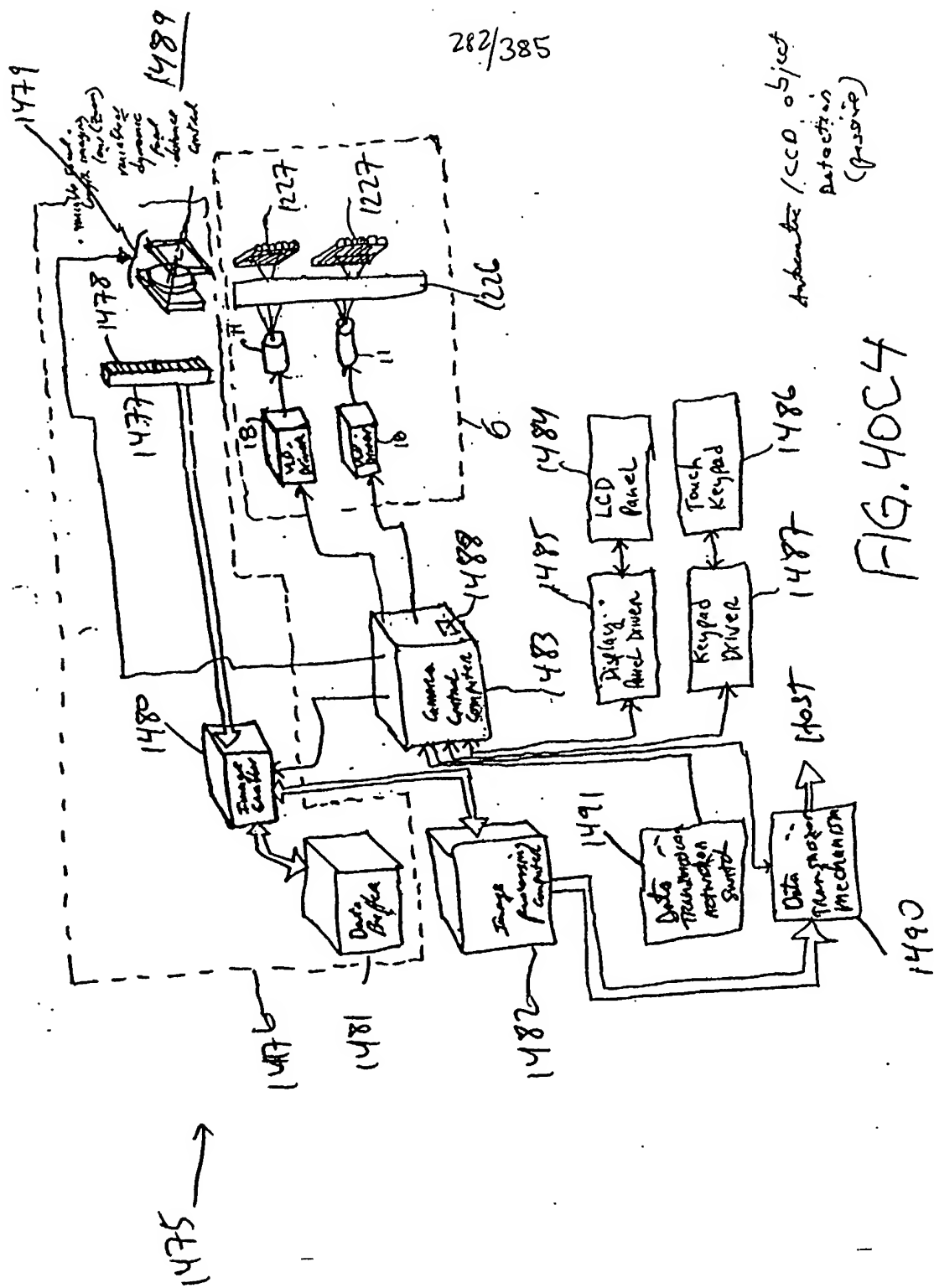


FIG. 40C2

281/385

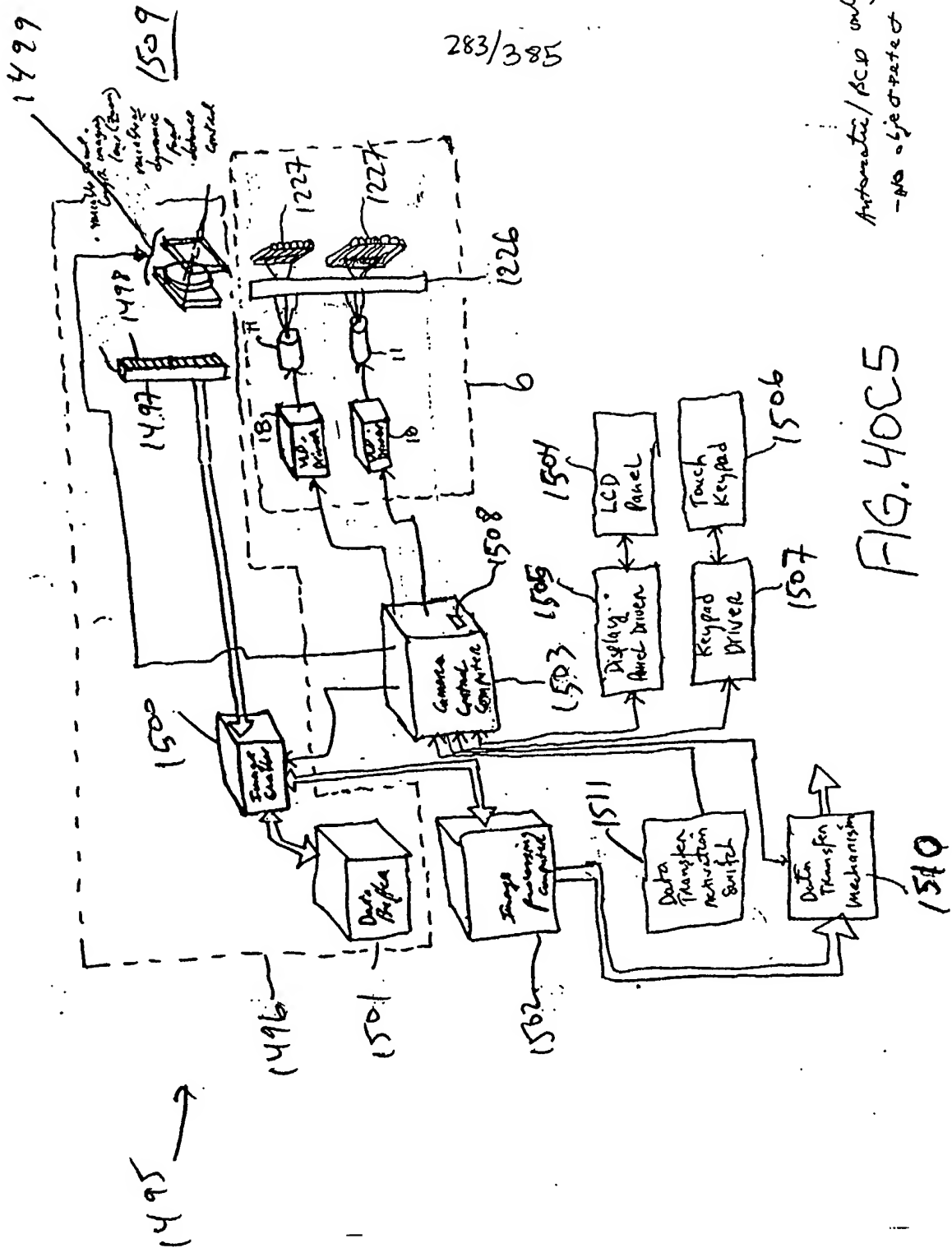


282/385



$$283/385$$

Automatic/BCD only
-No object detect



284/385

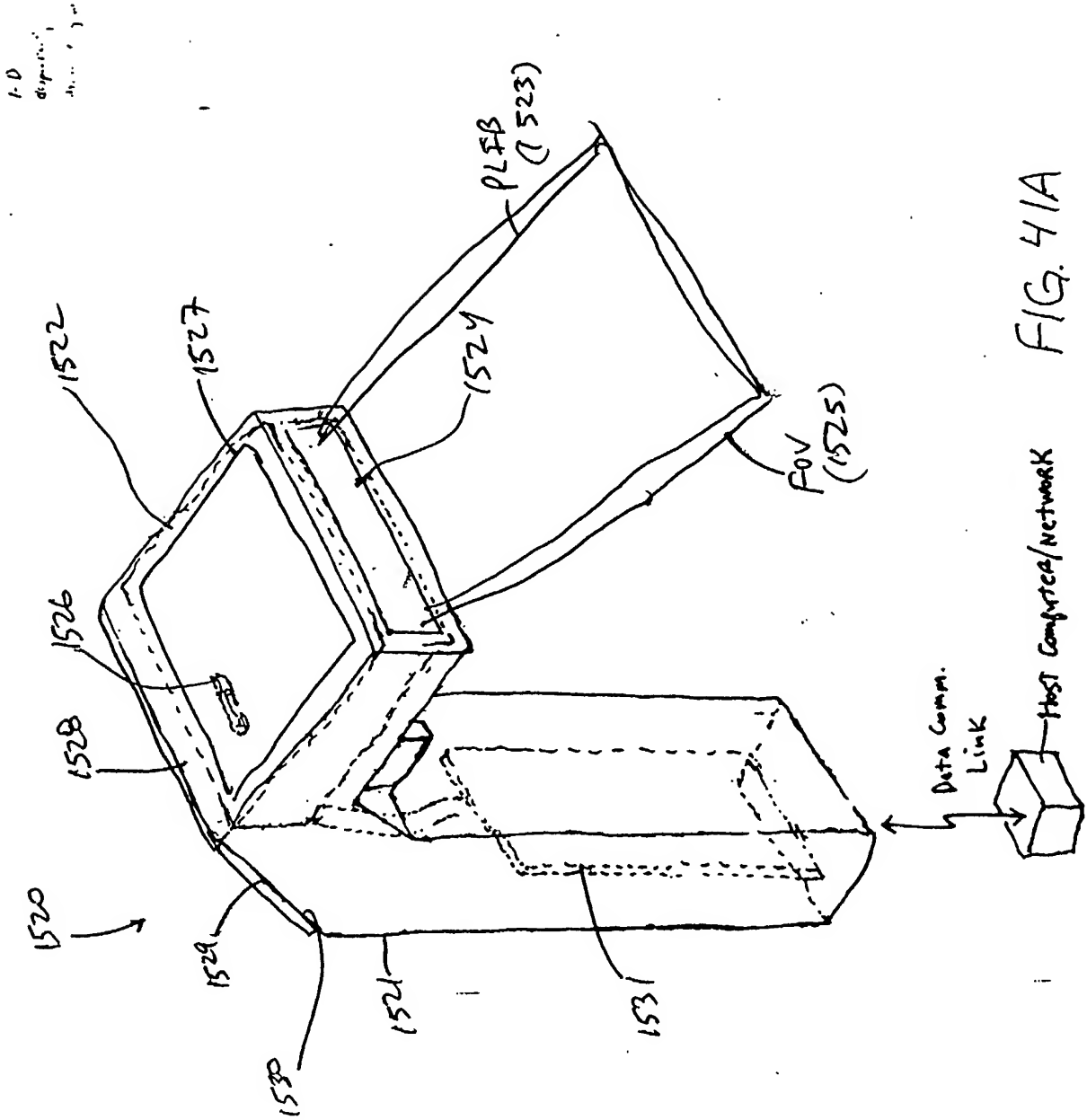


FIG. 41A

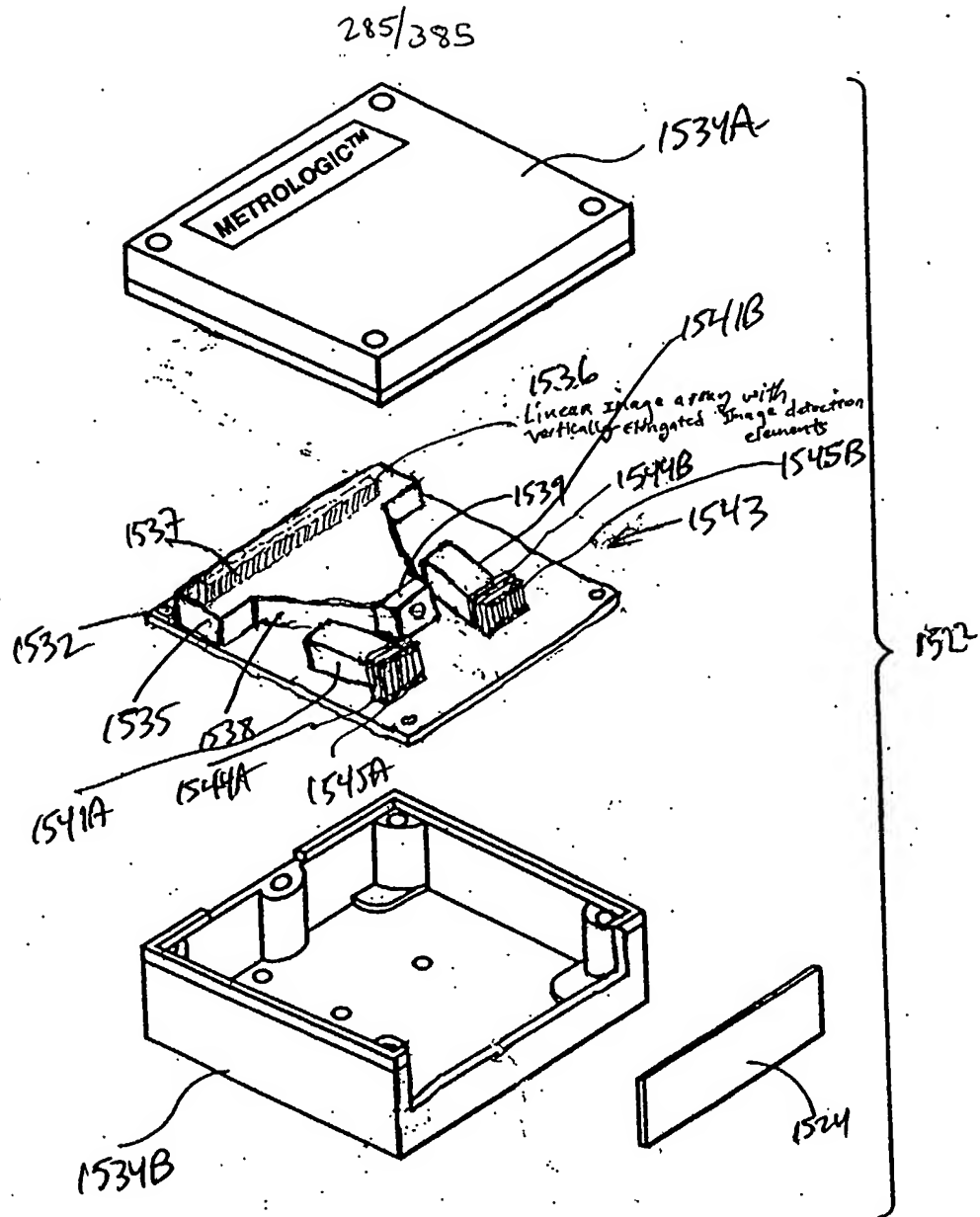


FIG. 41B

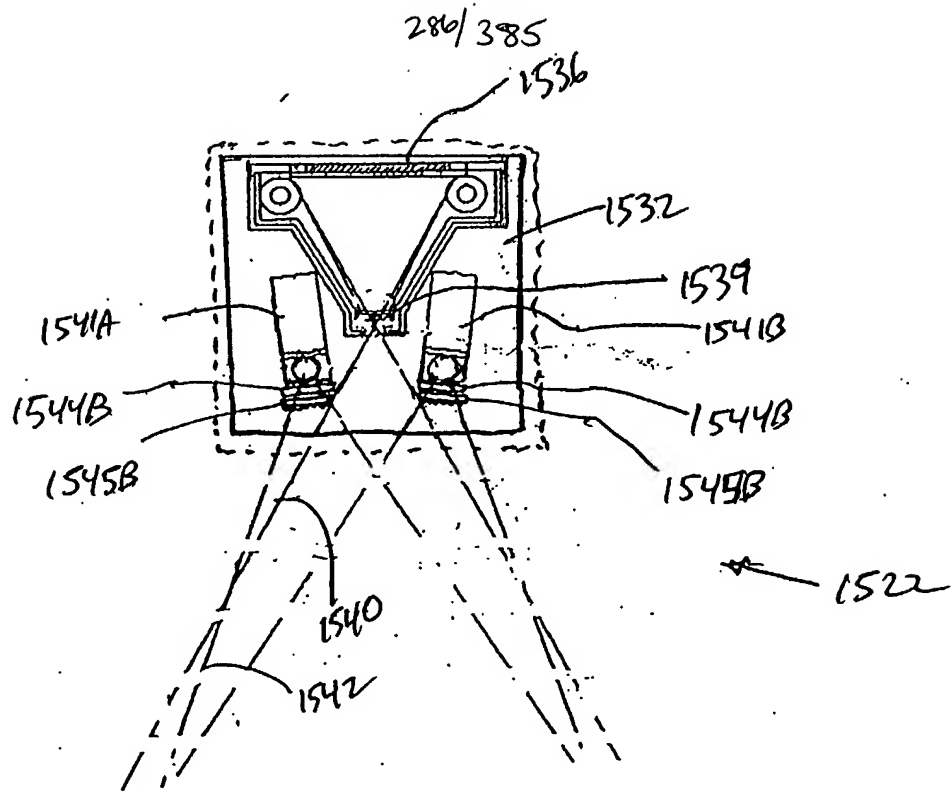


FIG. 41C

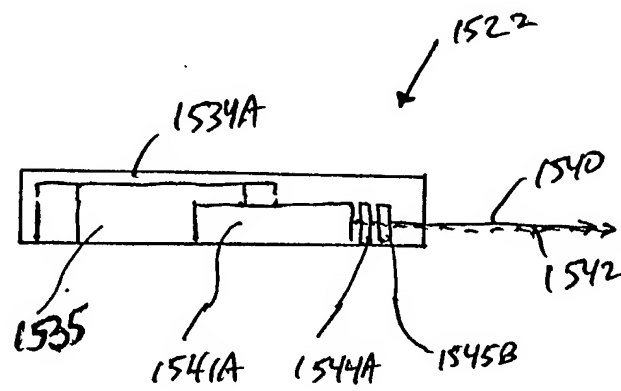


FIG. 41D

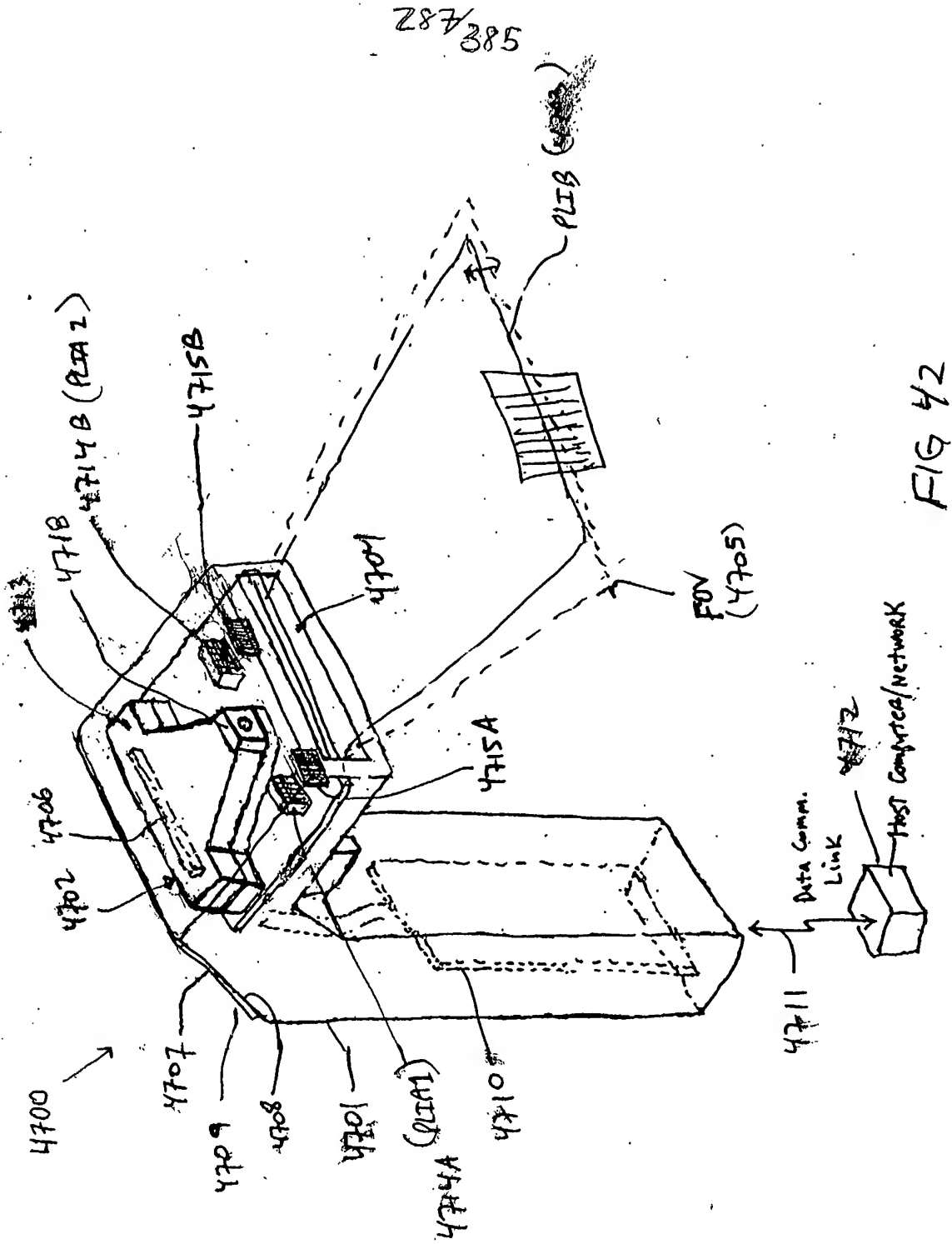


FIG 42

1-D
display
unit

288/385

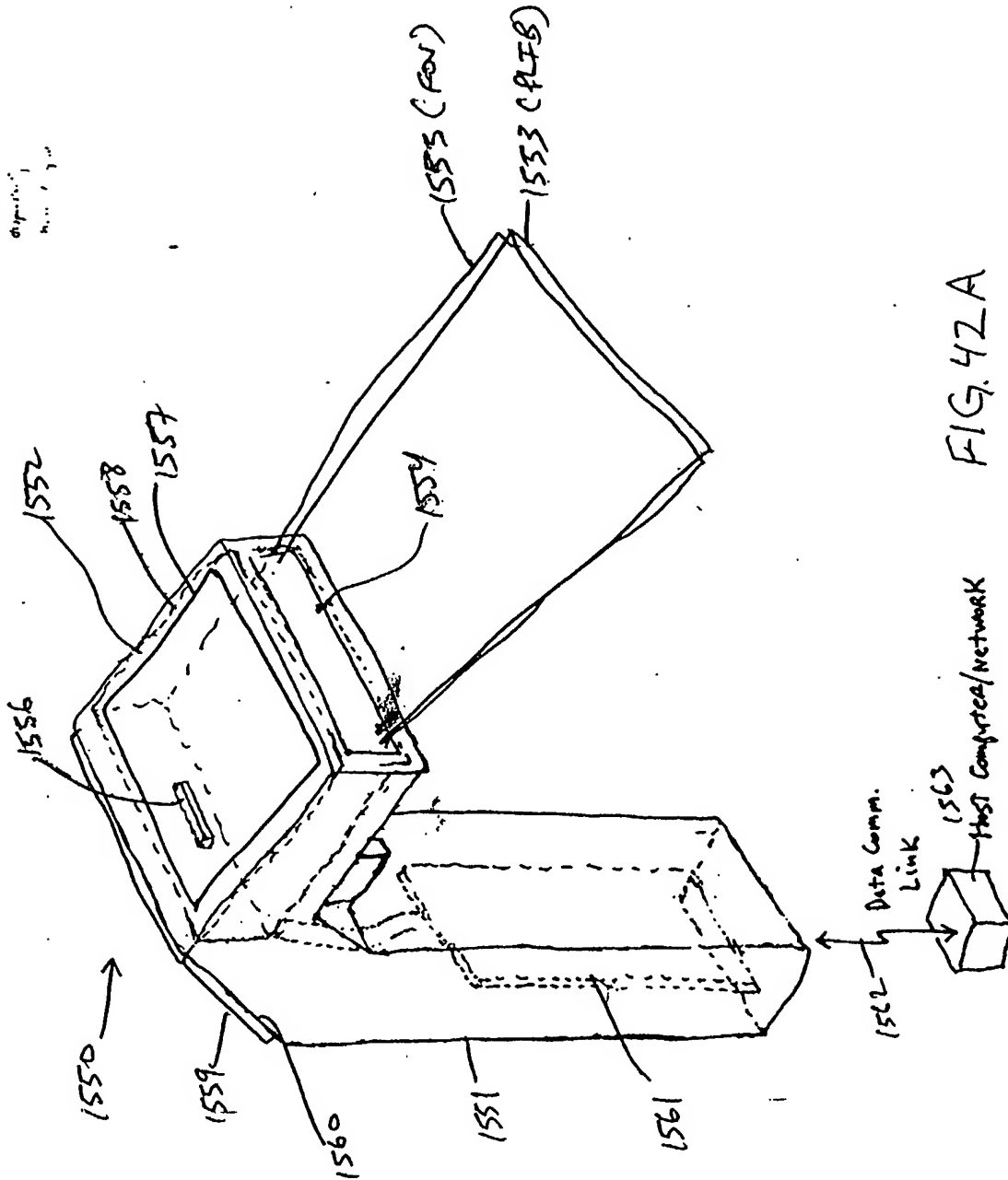


FIG. 42A

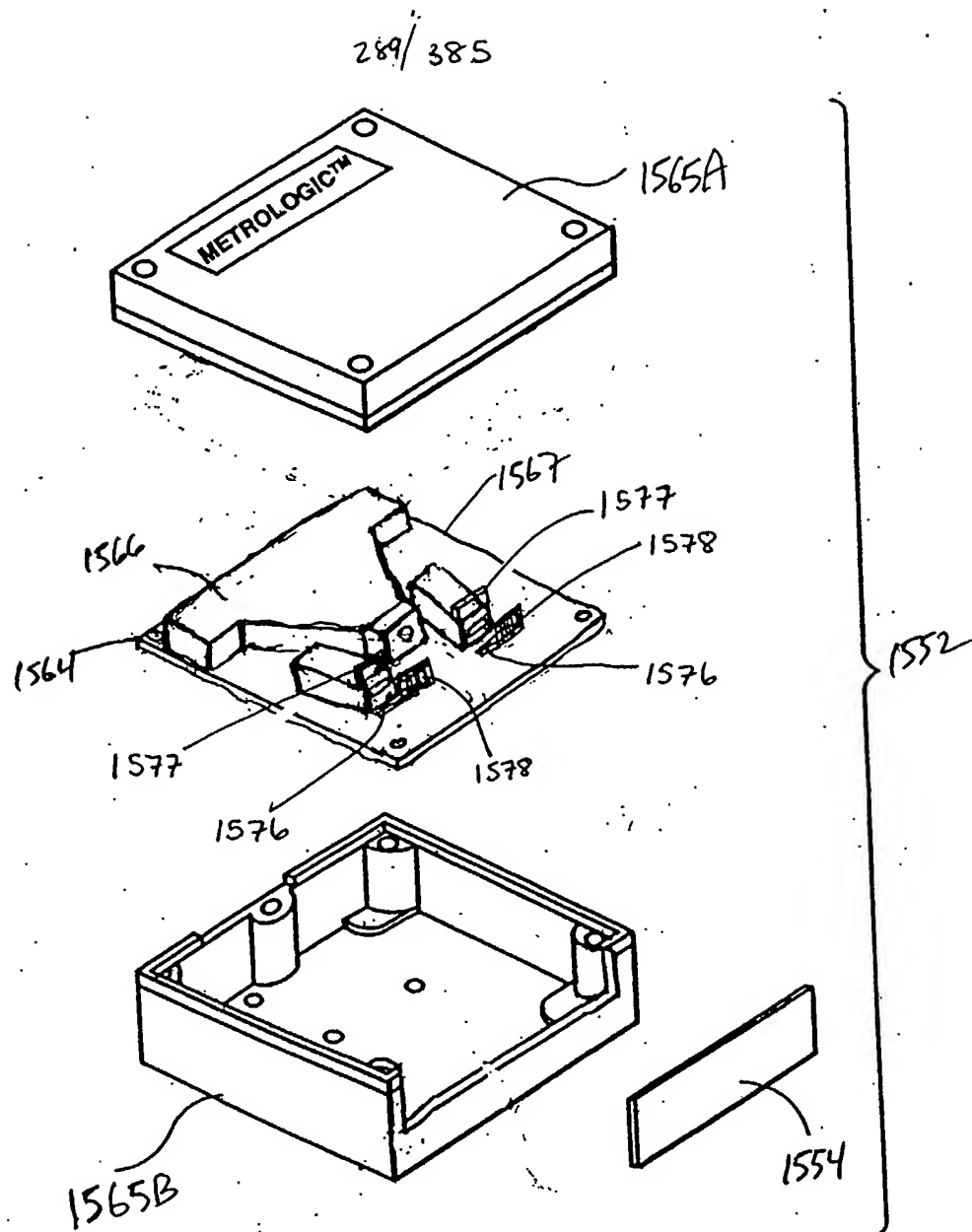


FIG. 42B

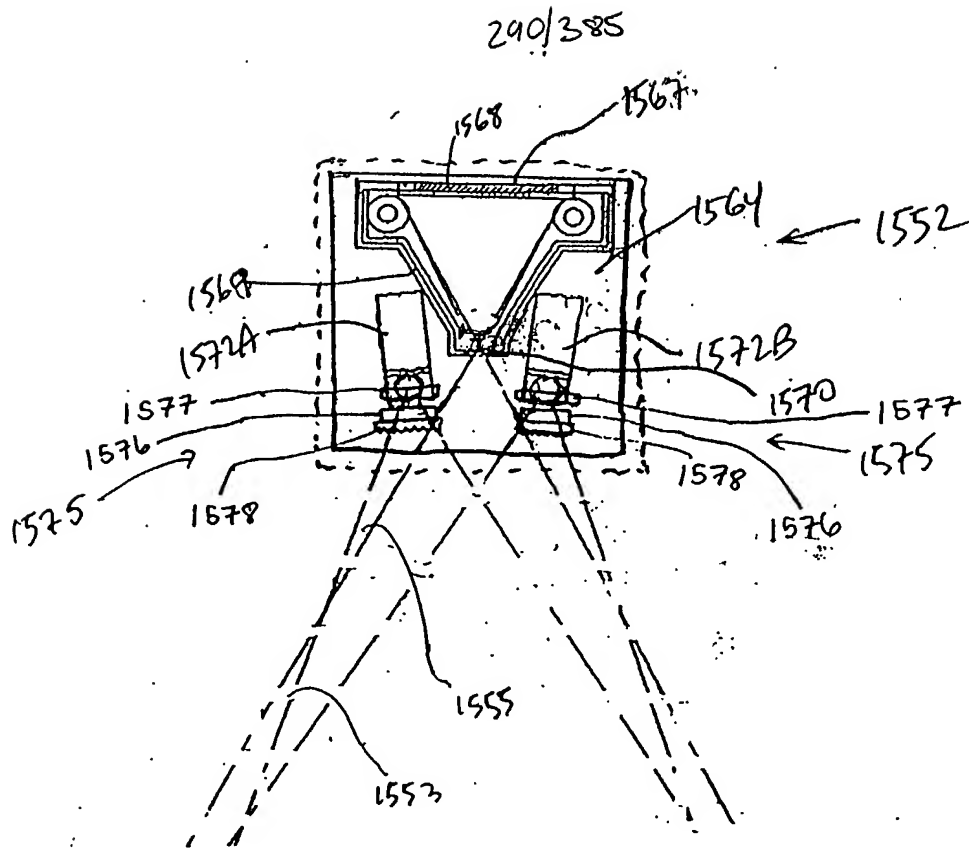


FIG. 42C

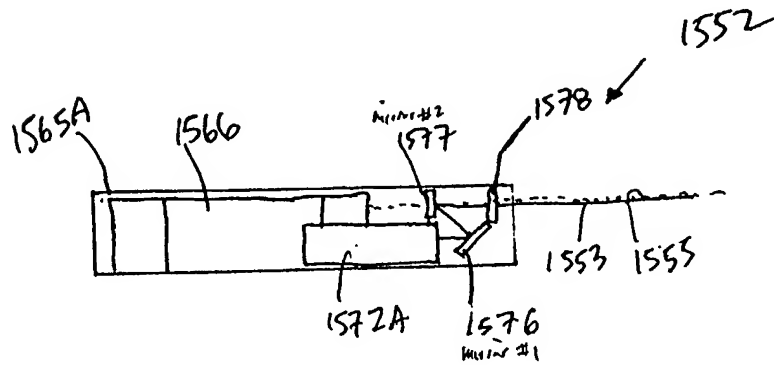


FIG. 42D

291/385

1-D
display
Area

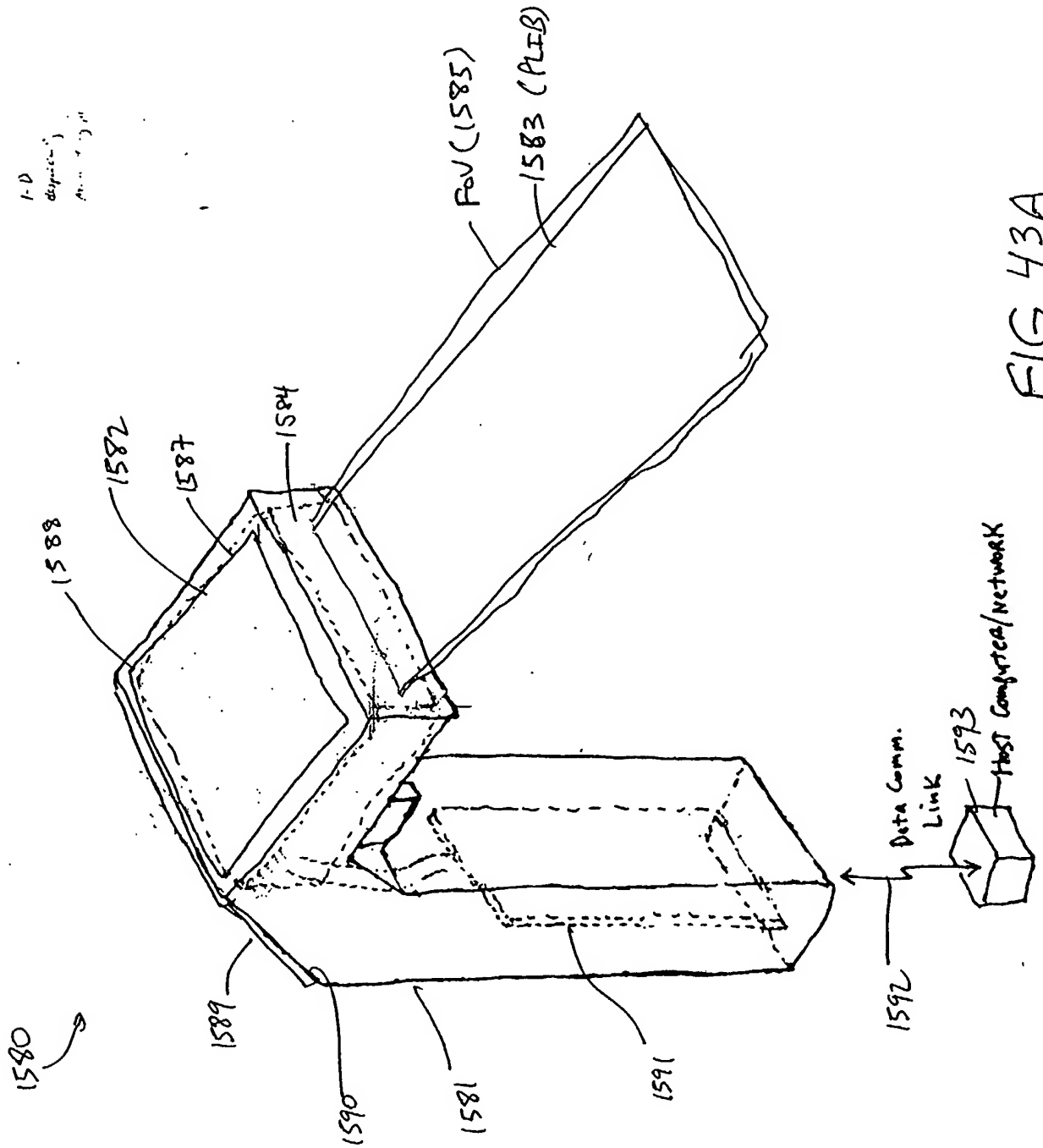


FIG. 43A

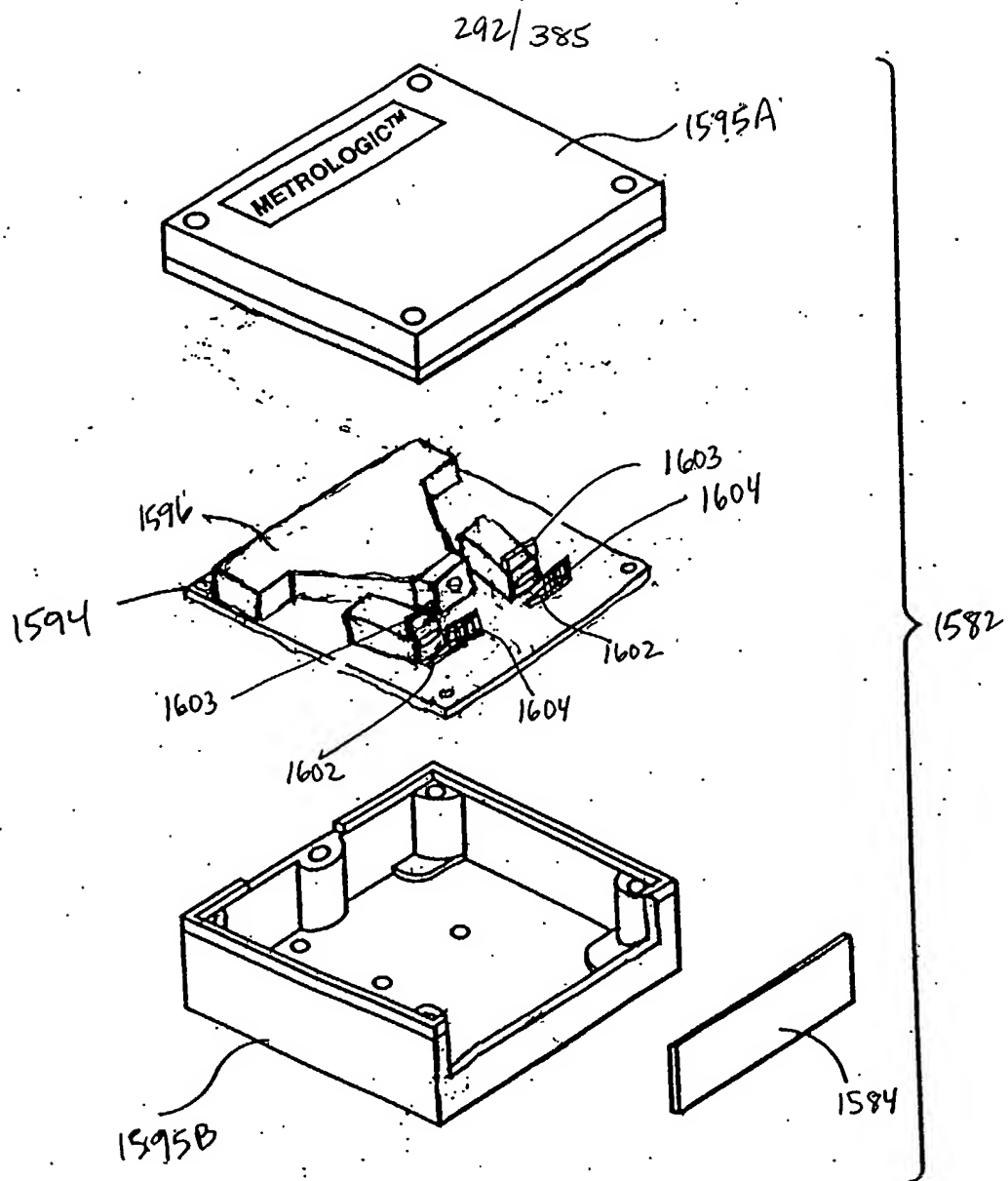


FIG. 43B

293/385

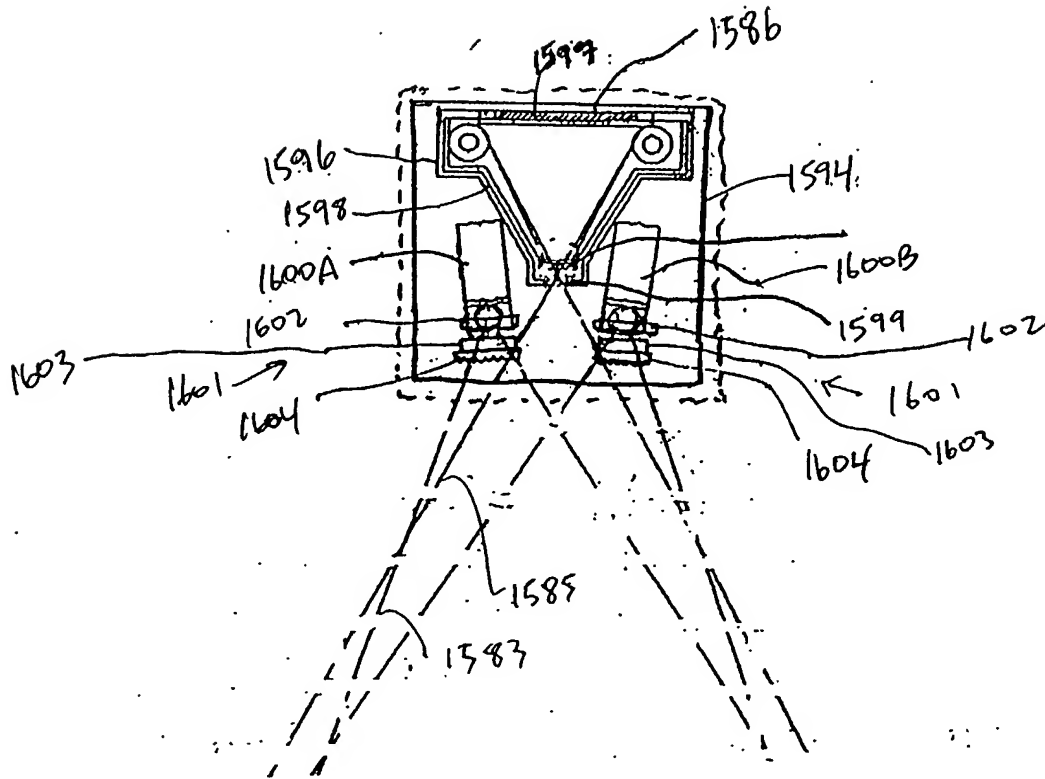


FIG. 43C

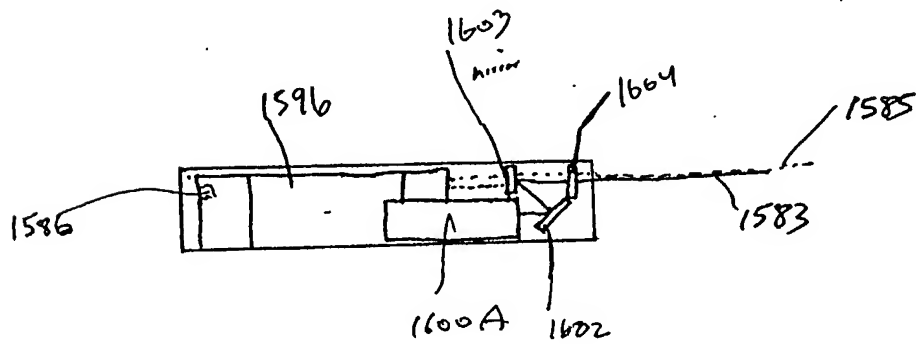


FIG. 43D

294/285

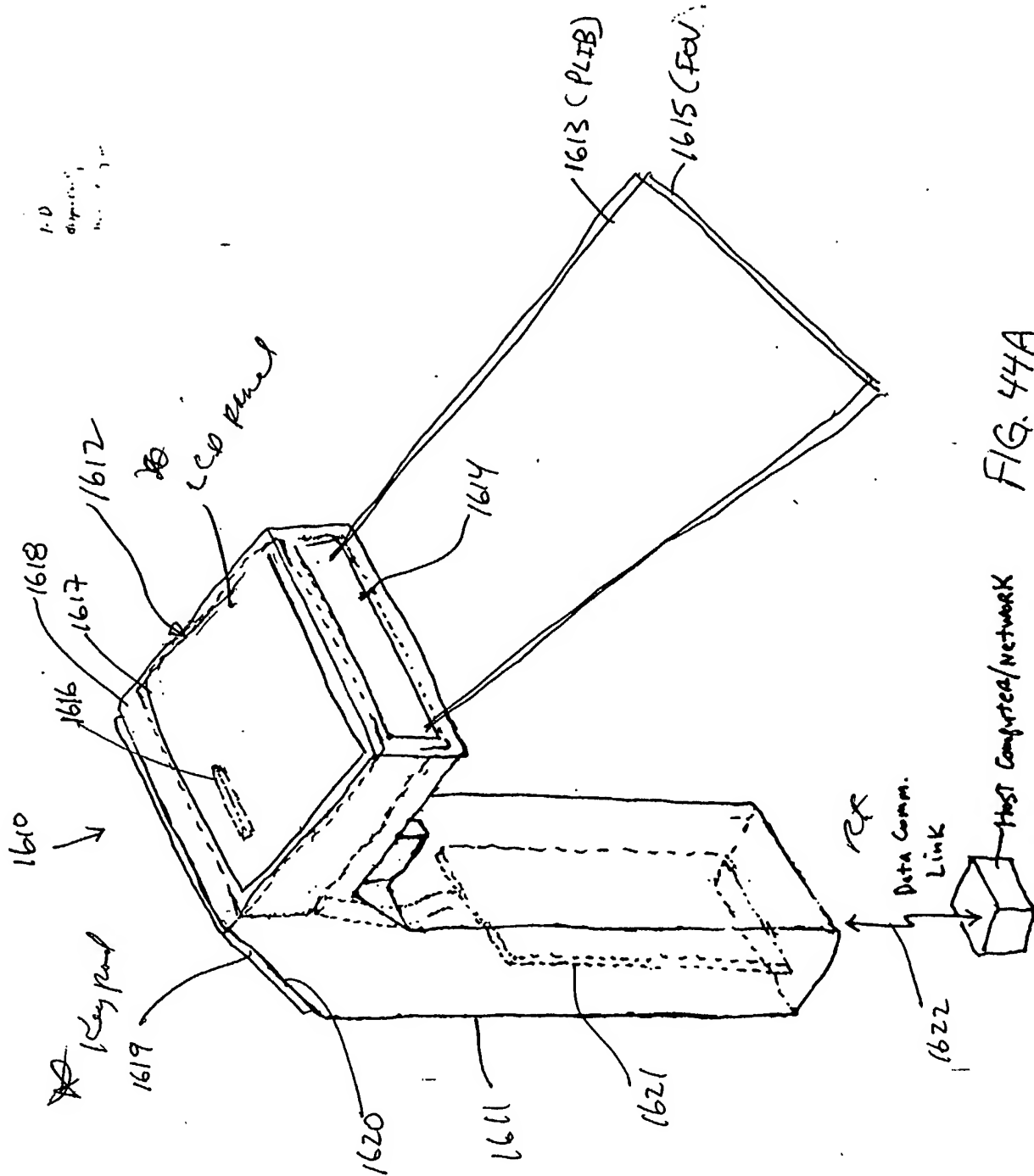


FIG. 44A

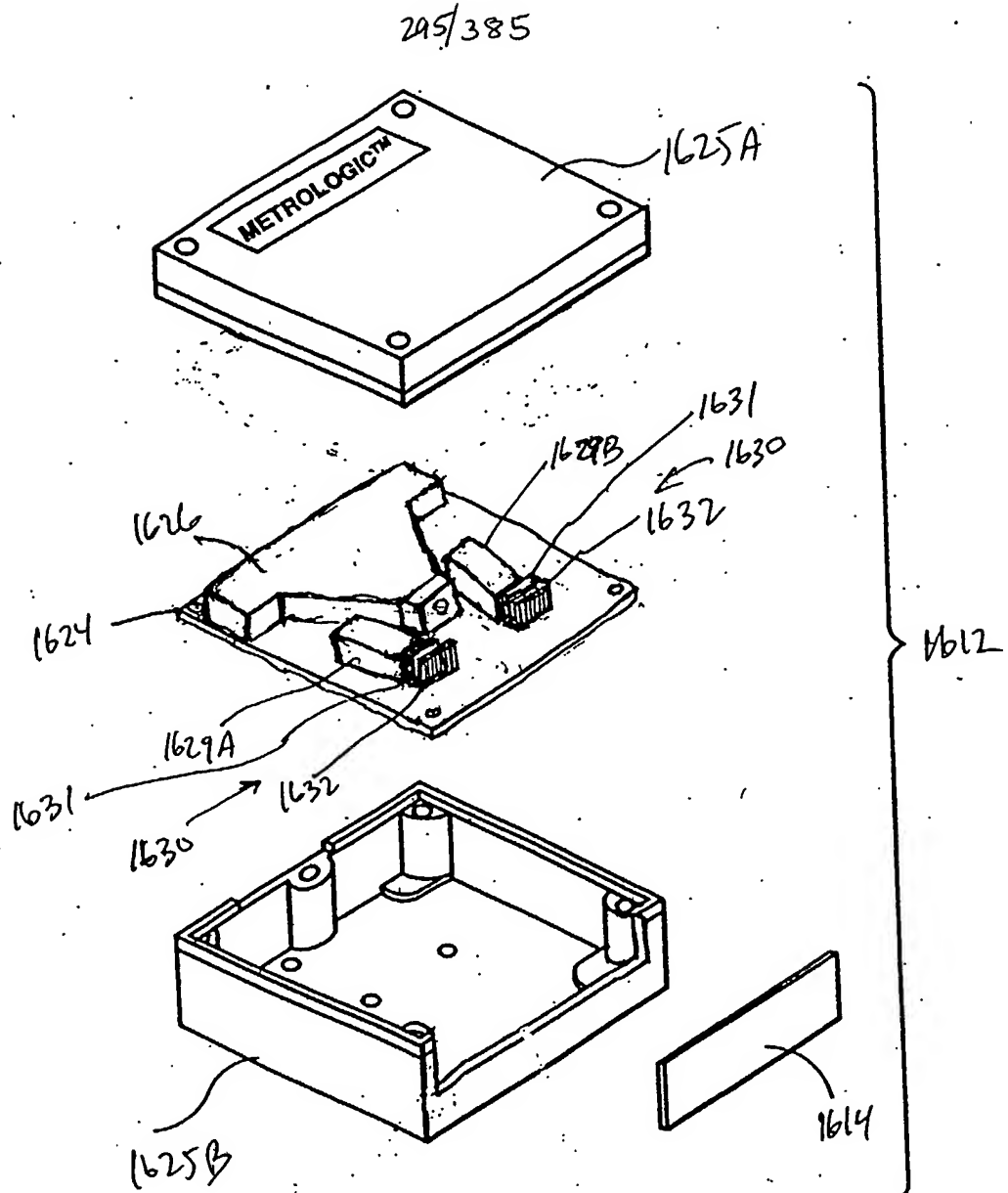


FIG. 44B

296/3857

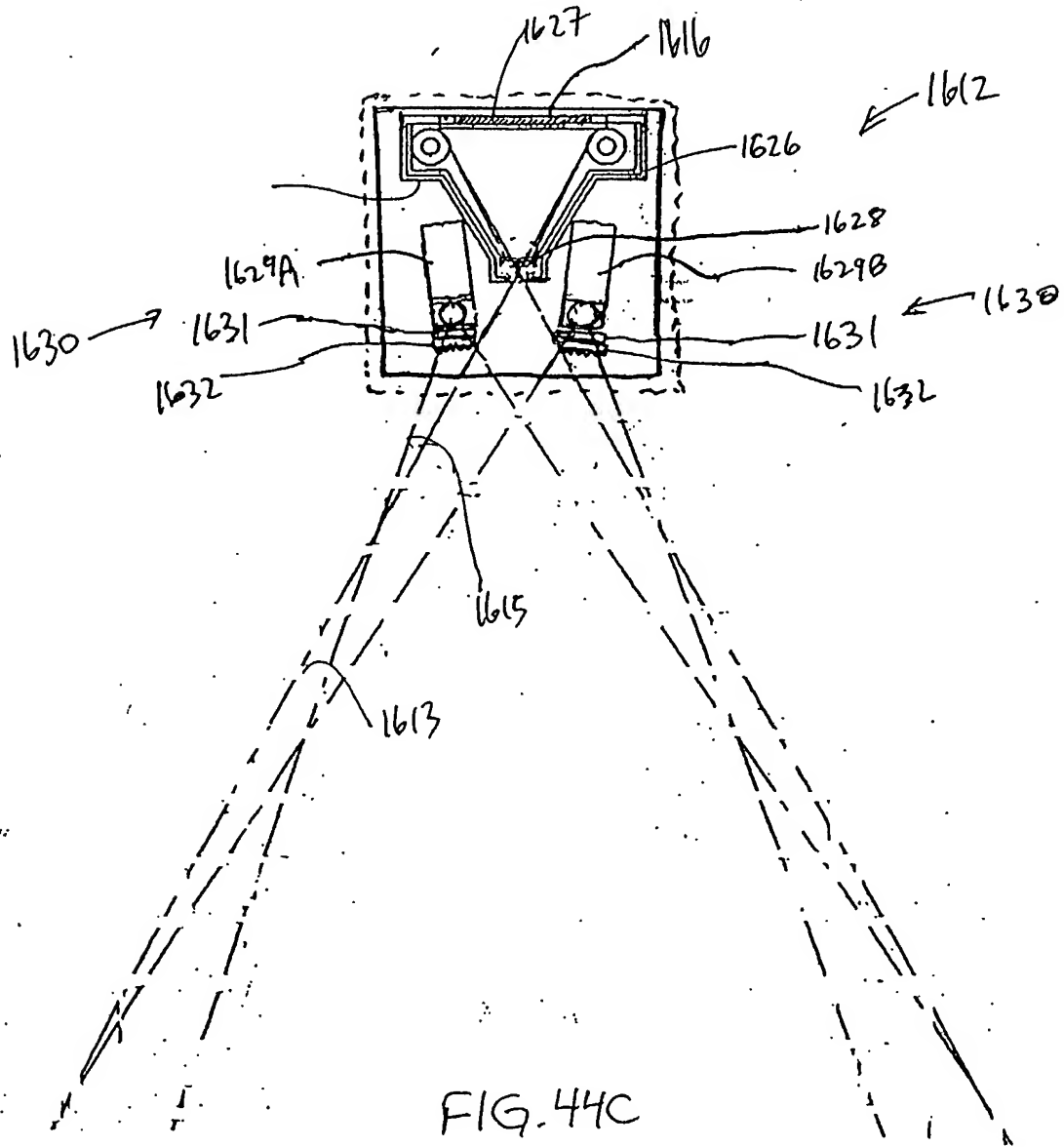


FIG. 44C

297/385

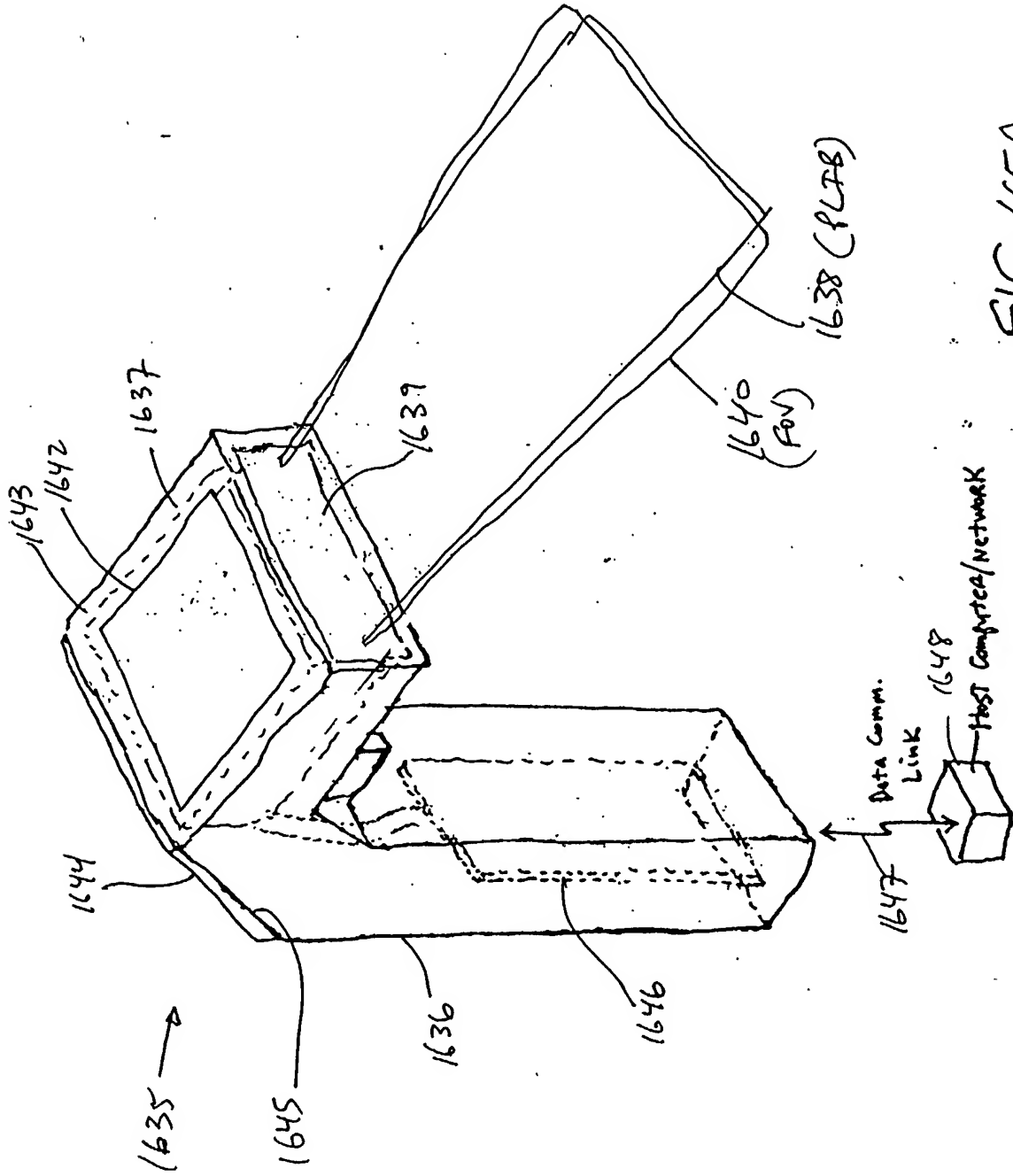


FIG. 45A

298/385

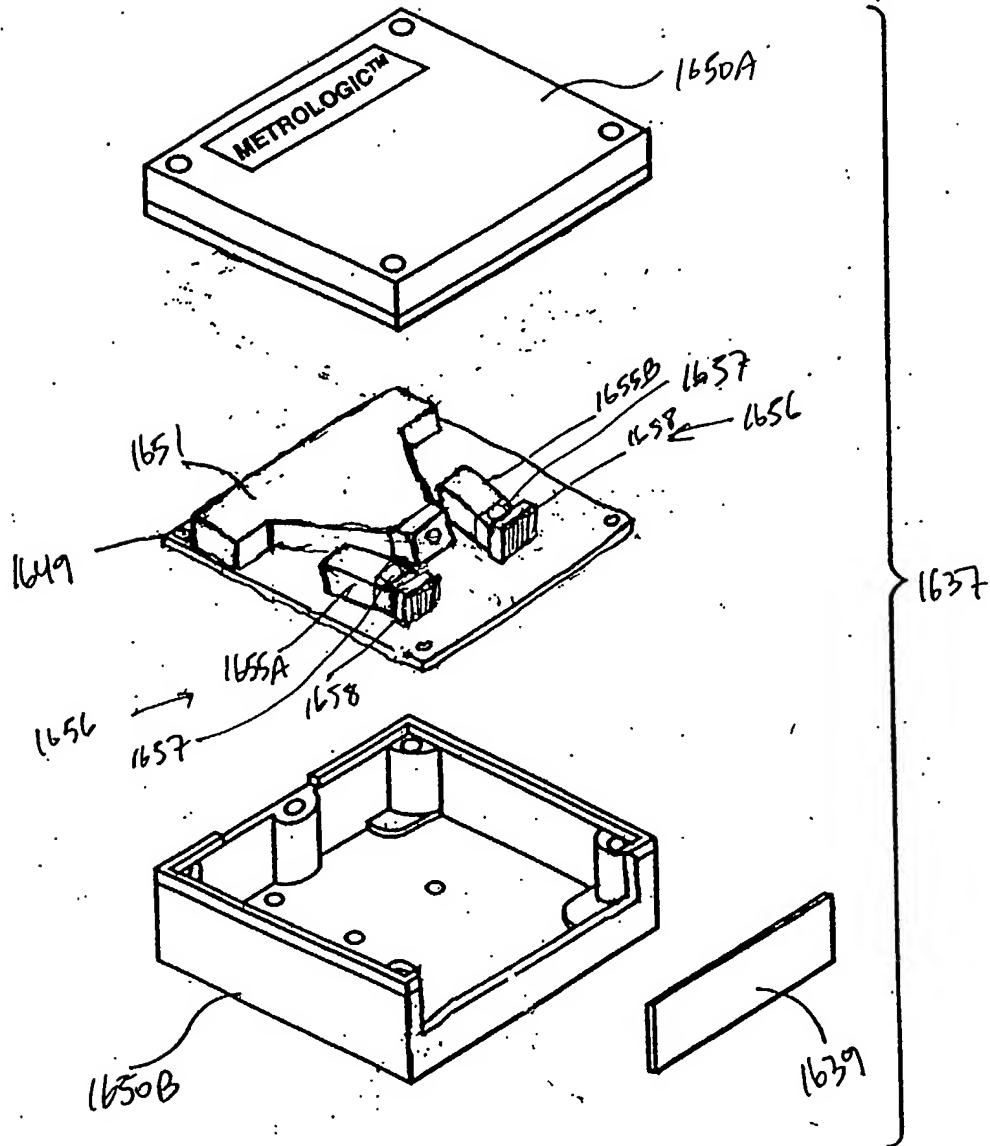
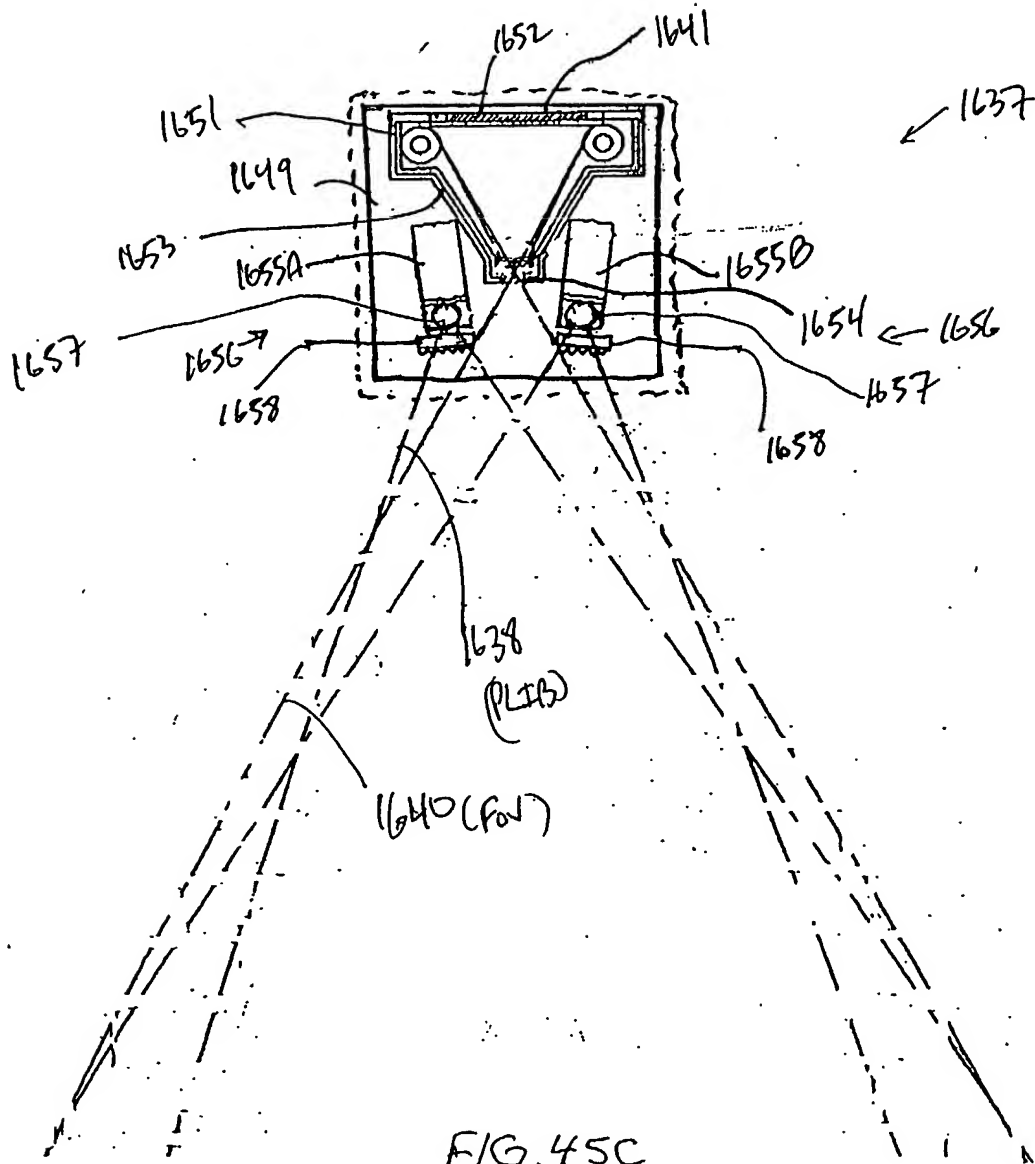
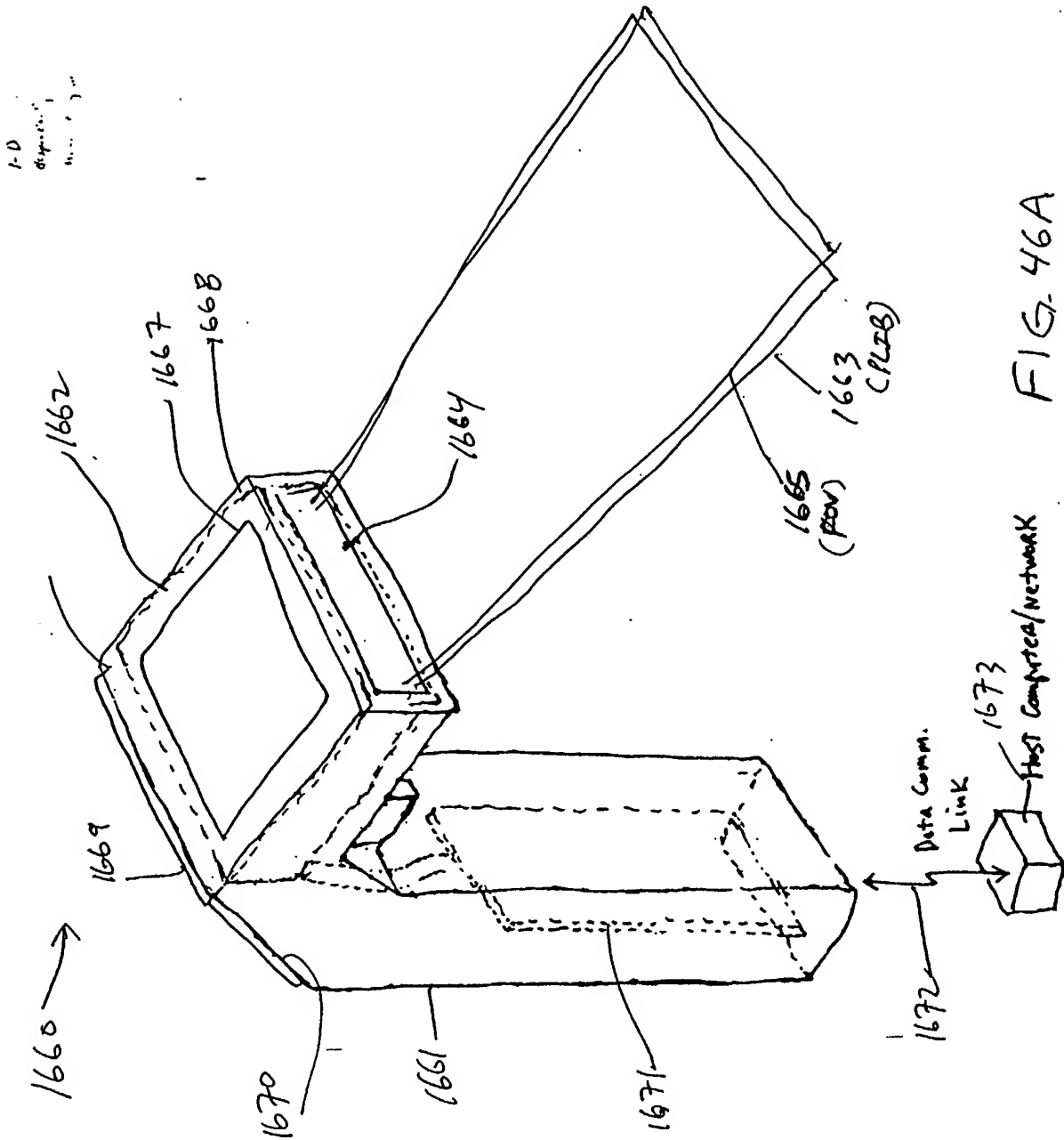


FIG. 45B

299/385



300/385



301/385

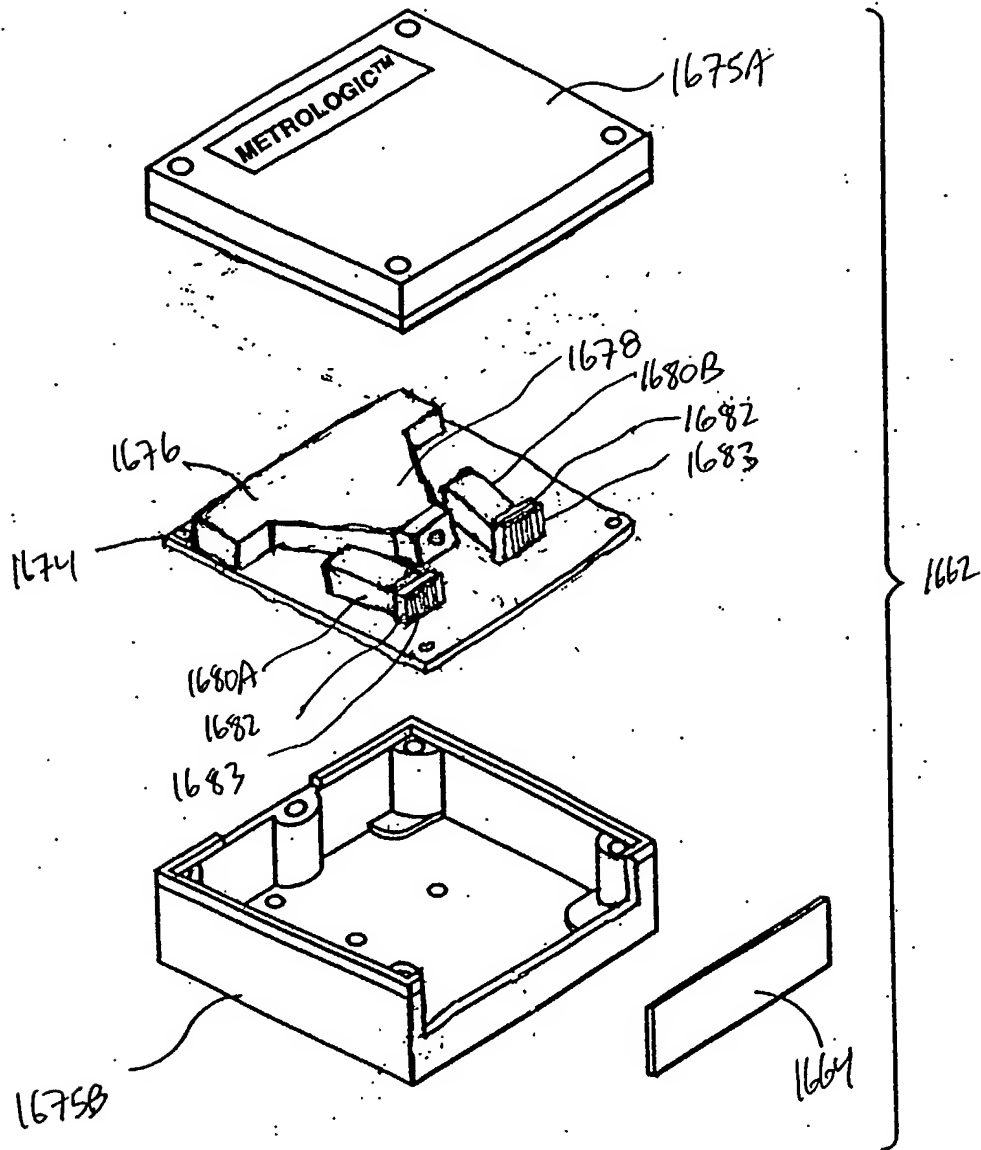
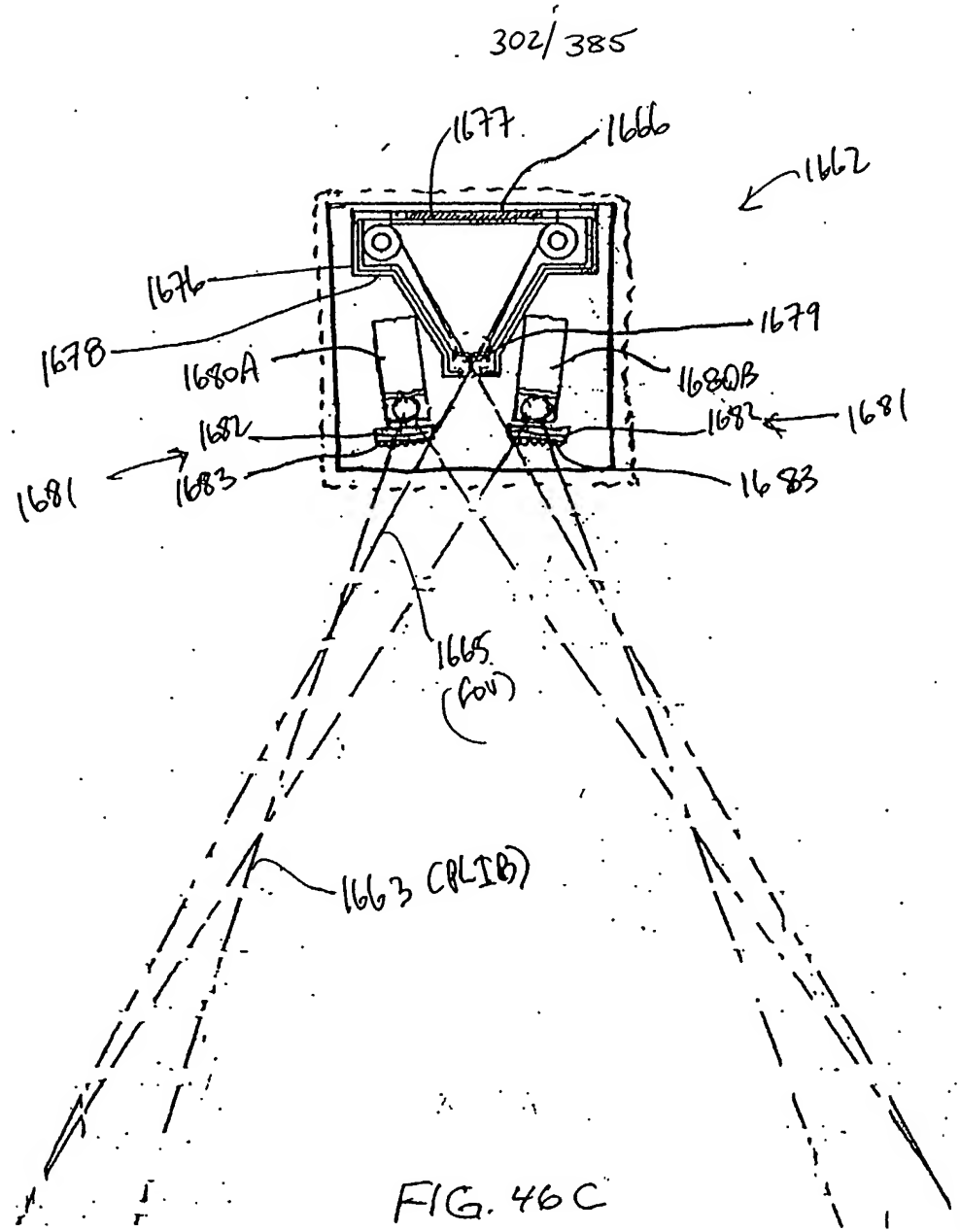
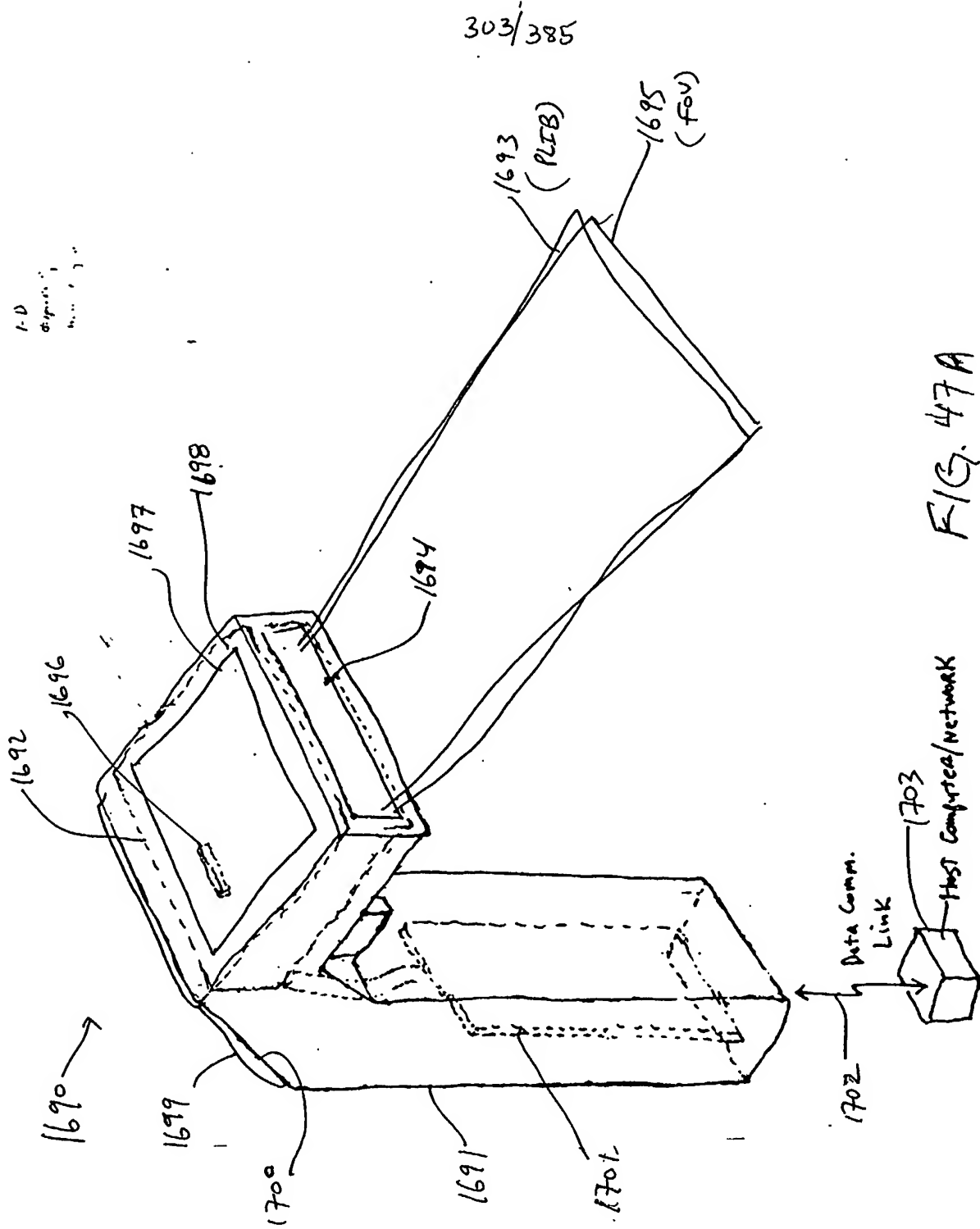


FIG. 46B





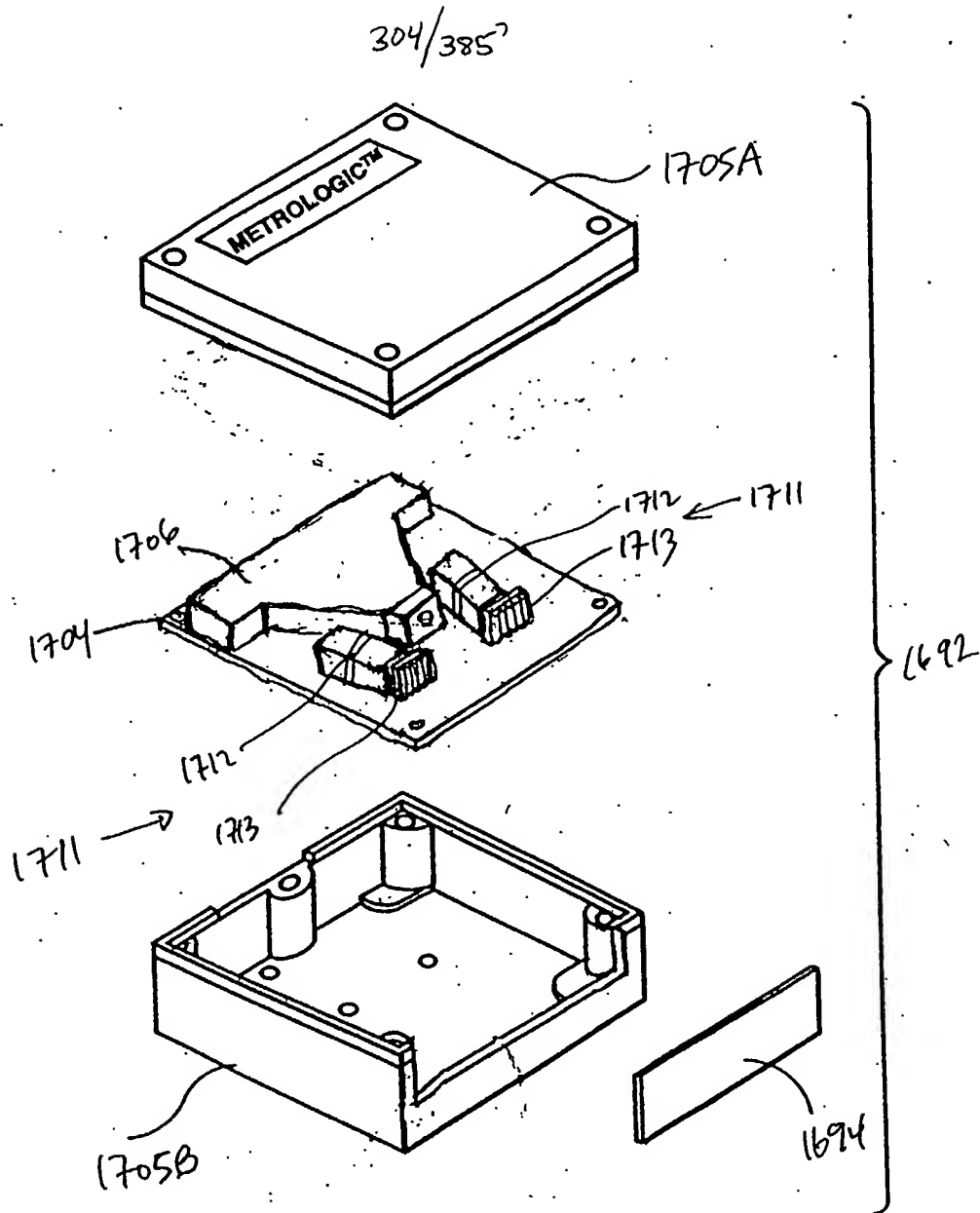


FIG. 47B

305/385

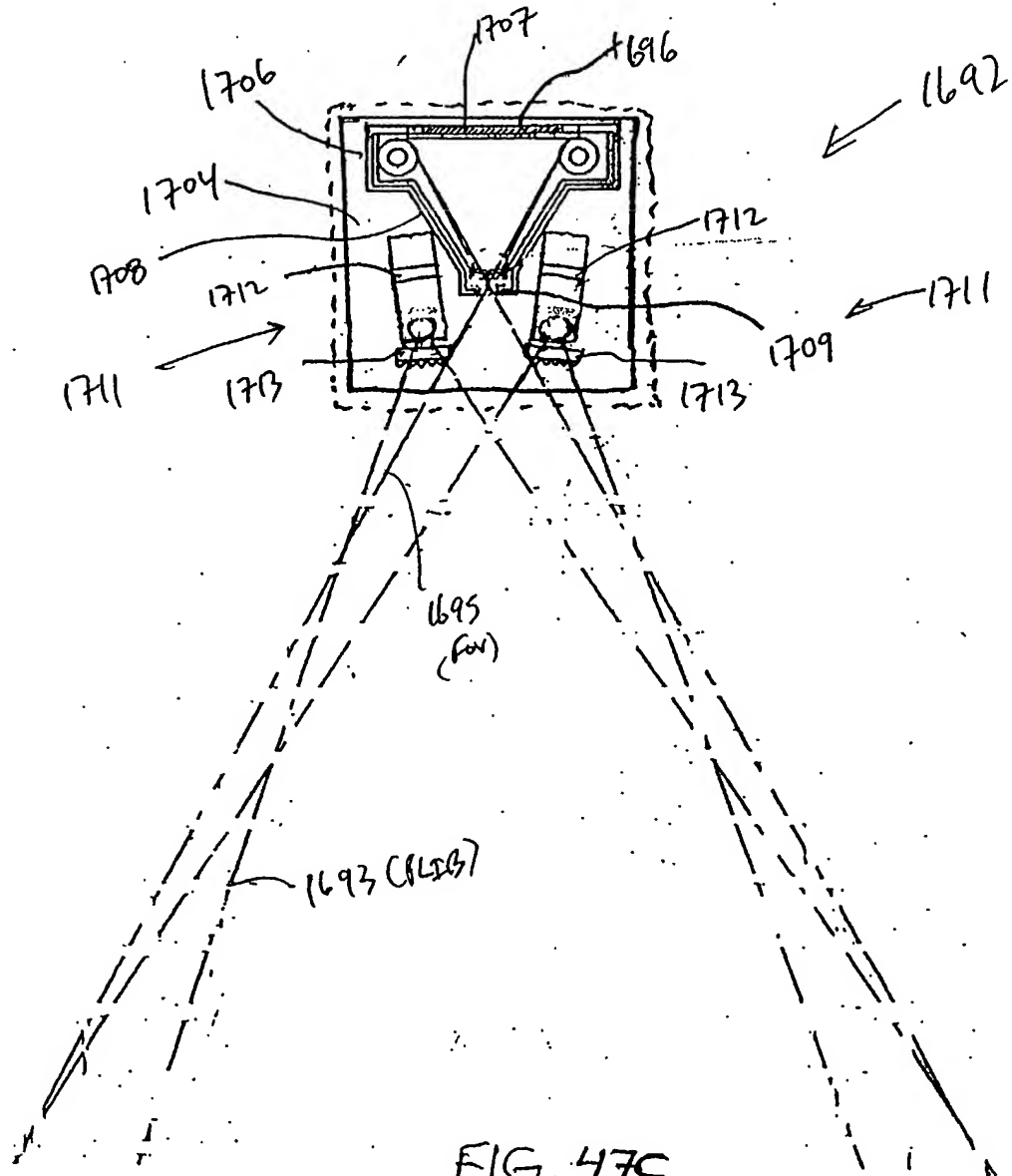


FIG. 47C

306/385

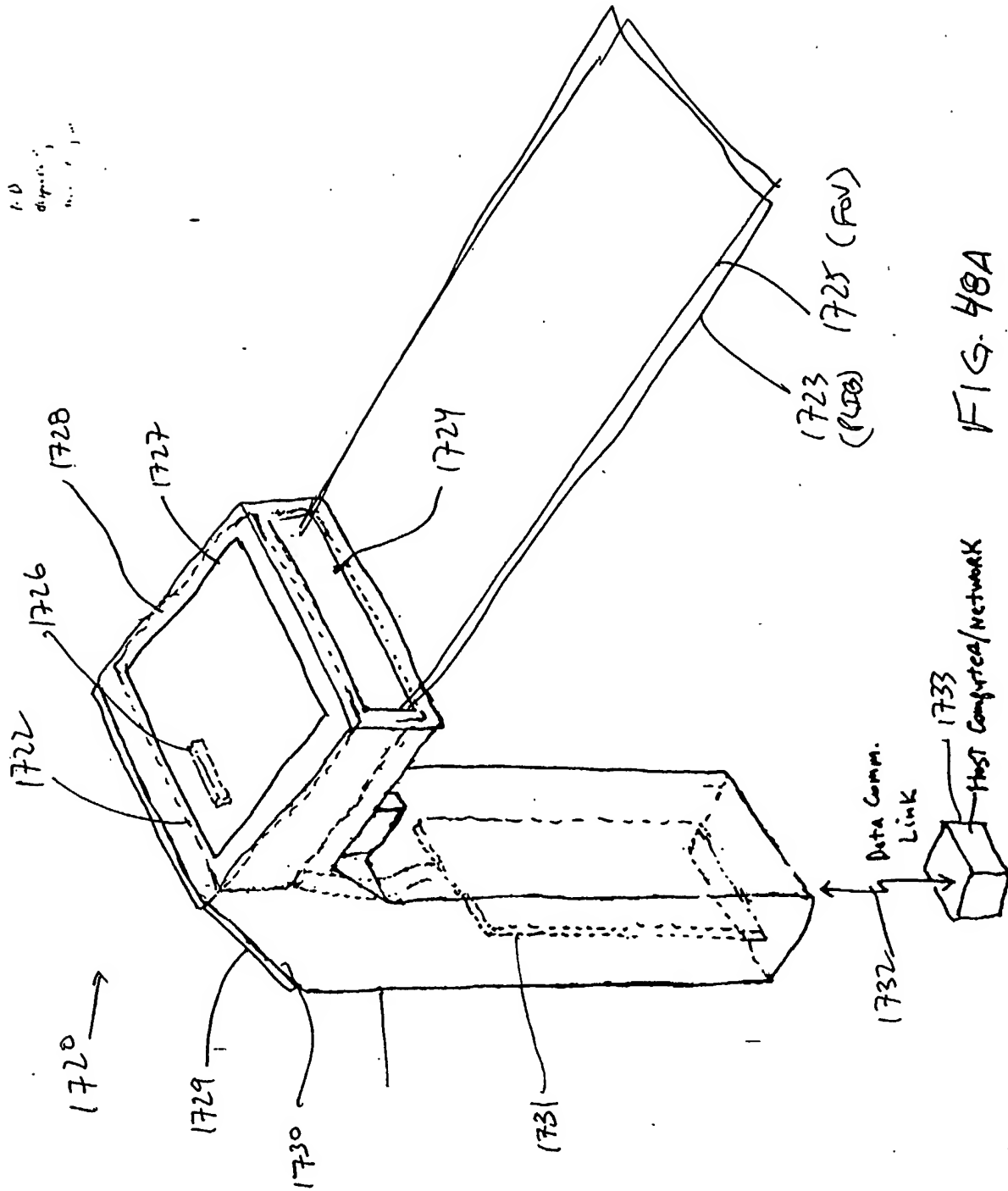


FIG. 48A

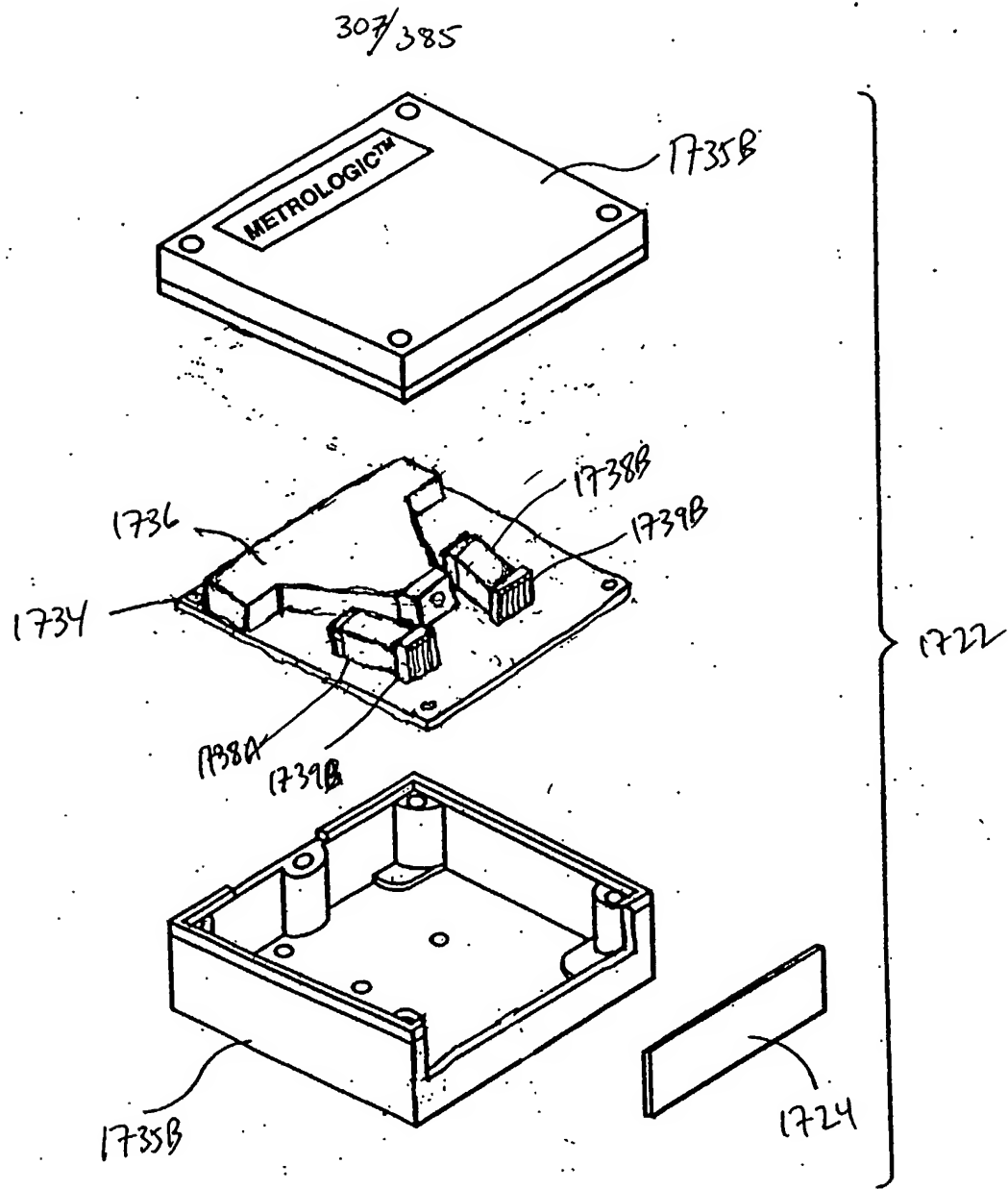
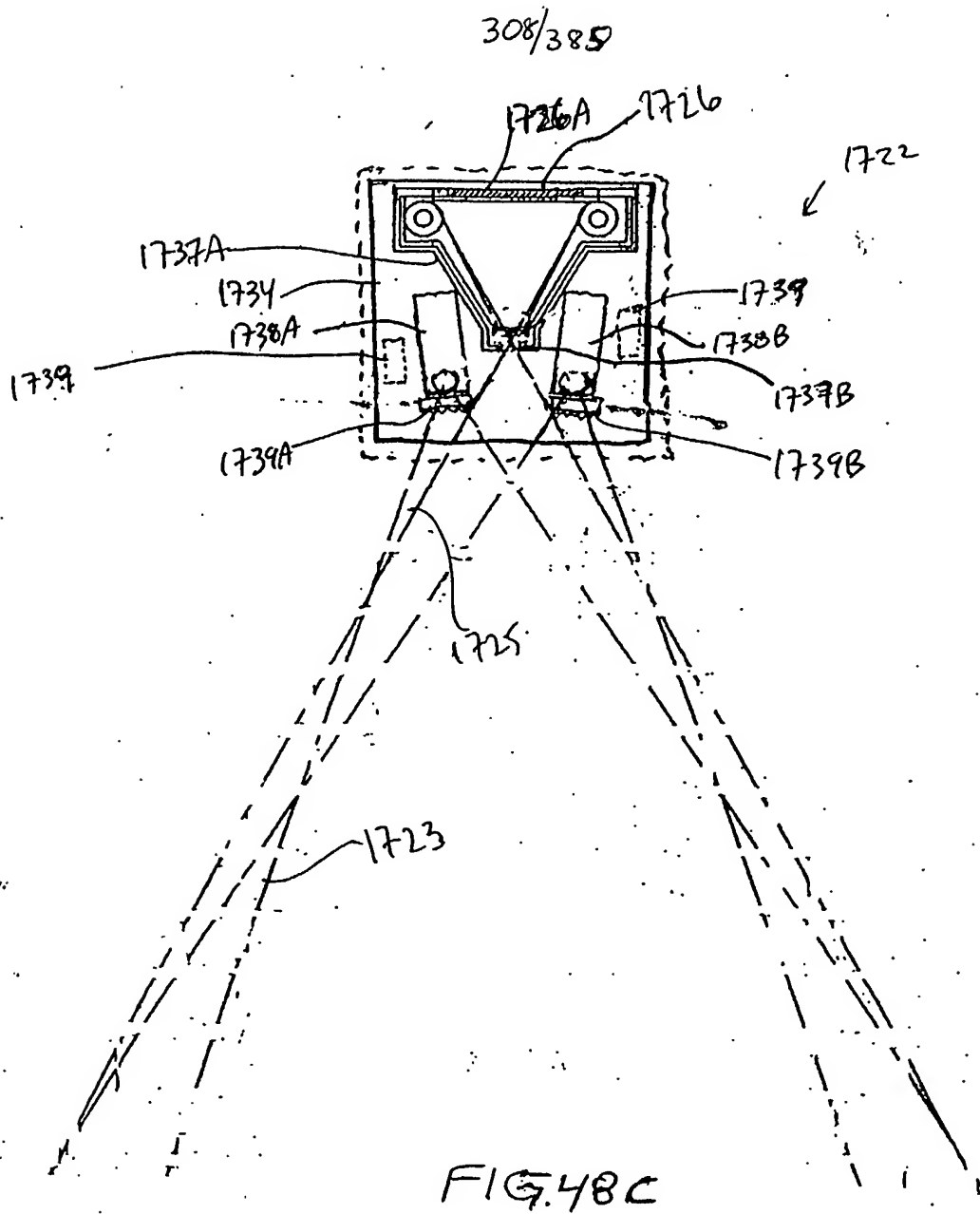


FIG. 48B



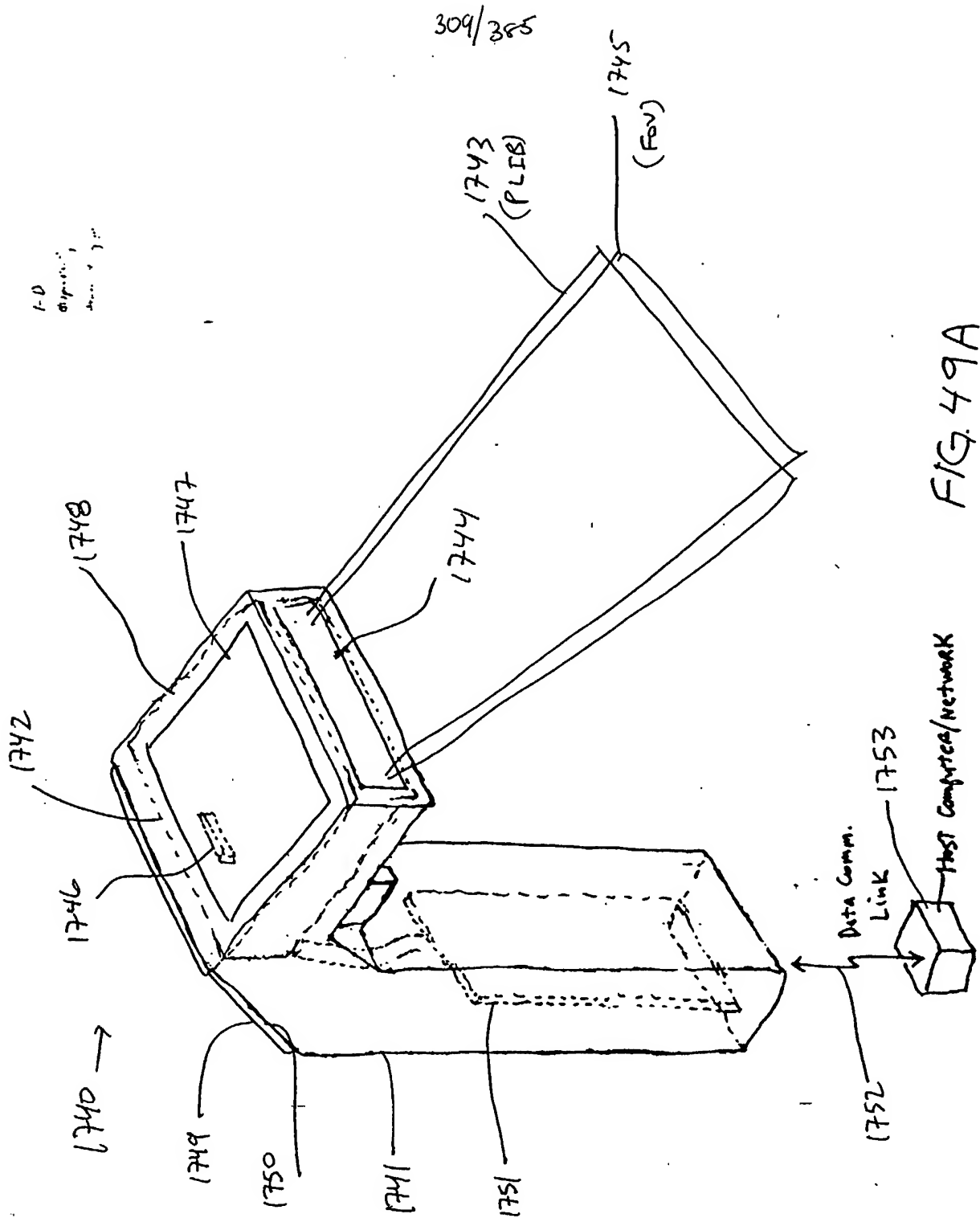


FIG. 49A

310/385

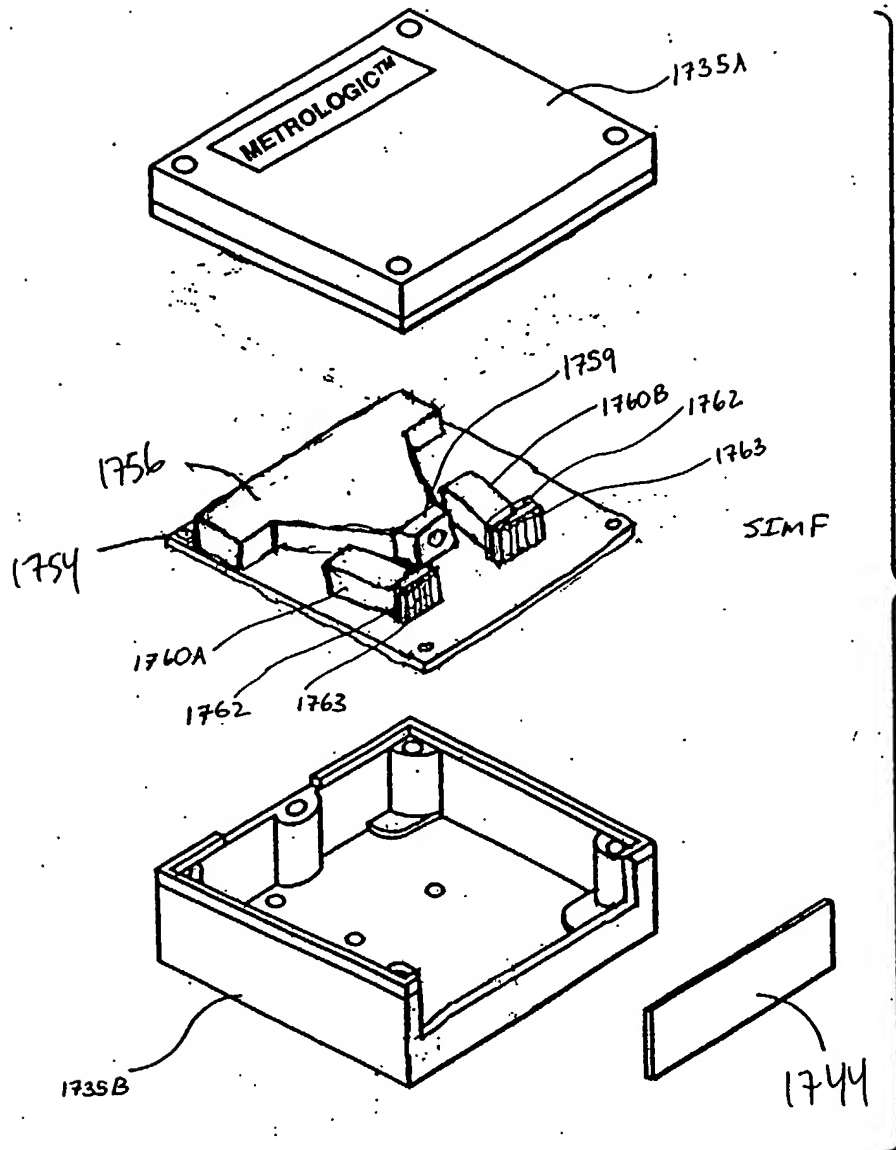
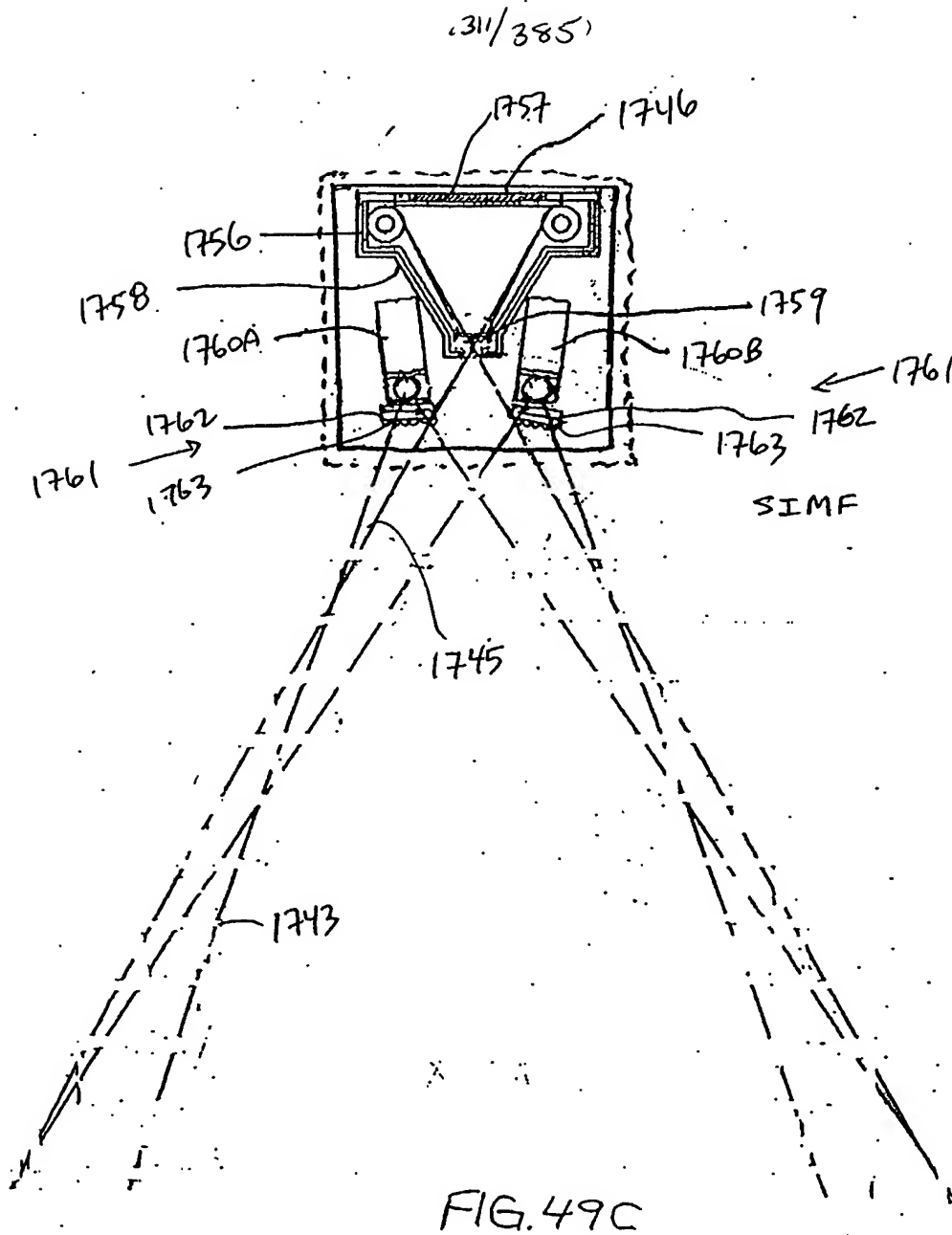


FIG. 49B



312/385

1-D
display
showing 3D

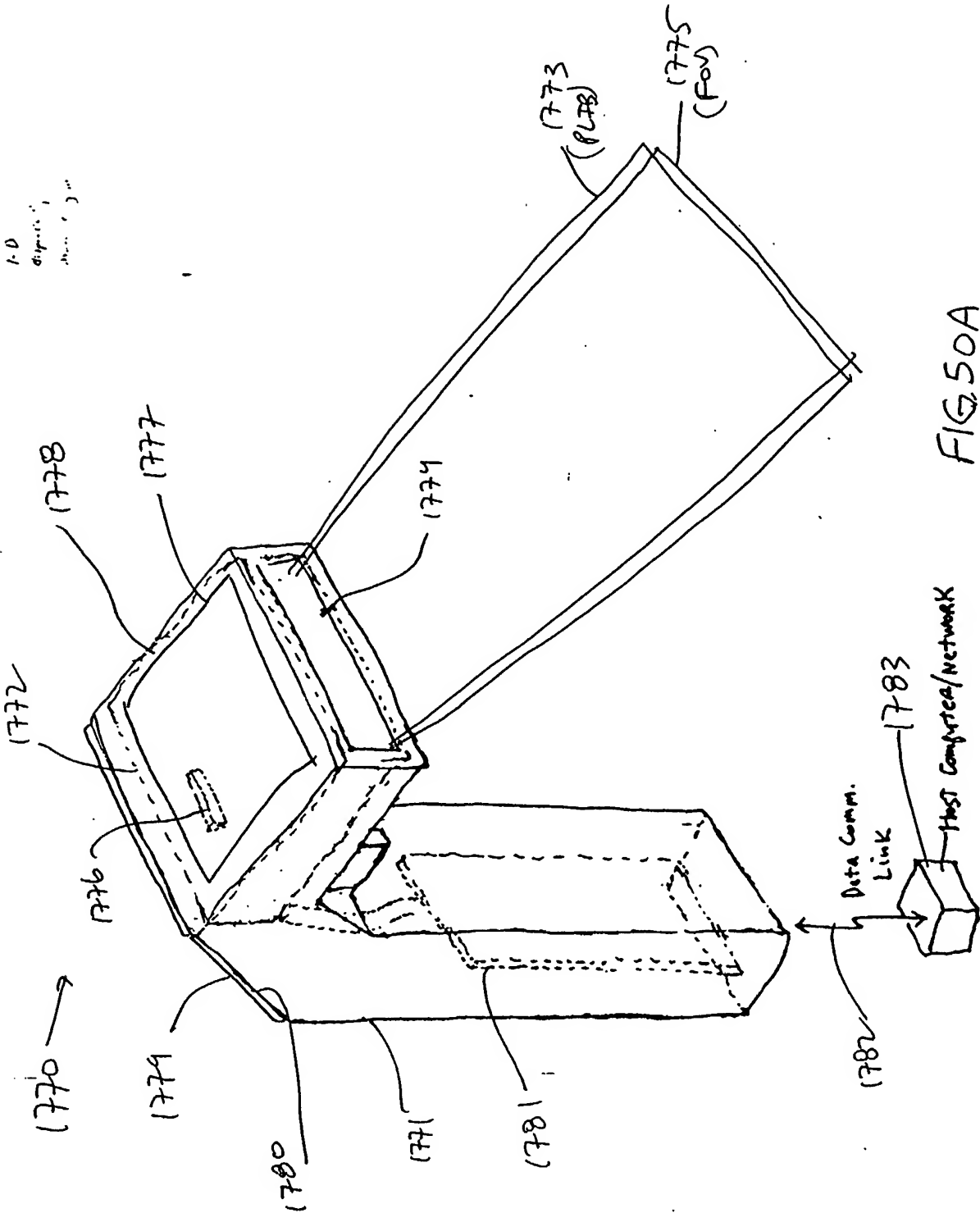


FIG. 50A

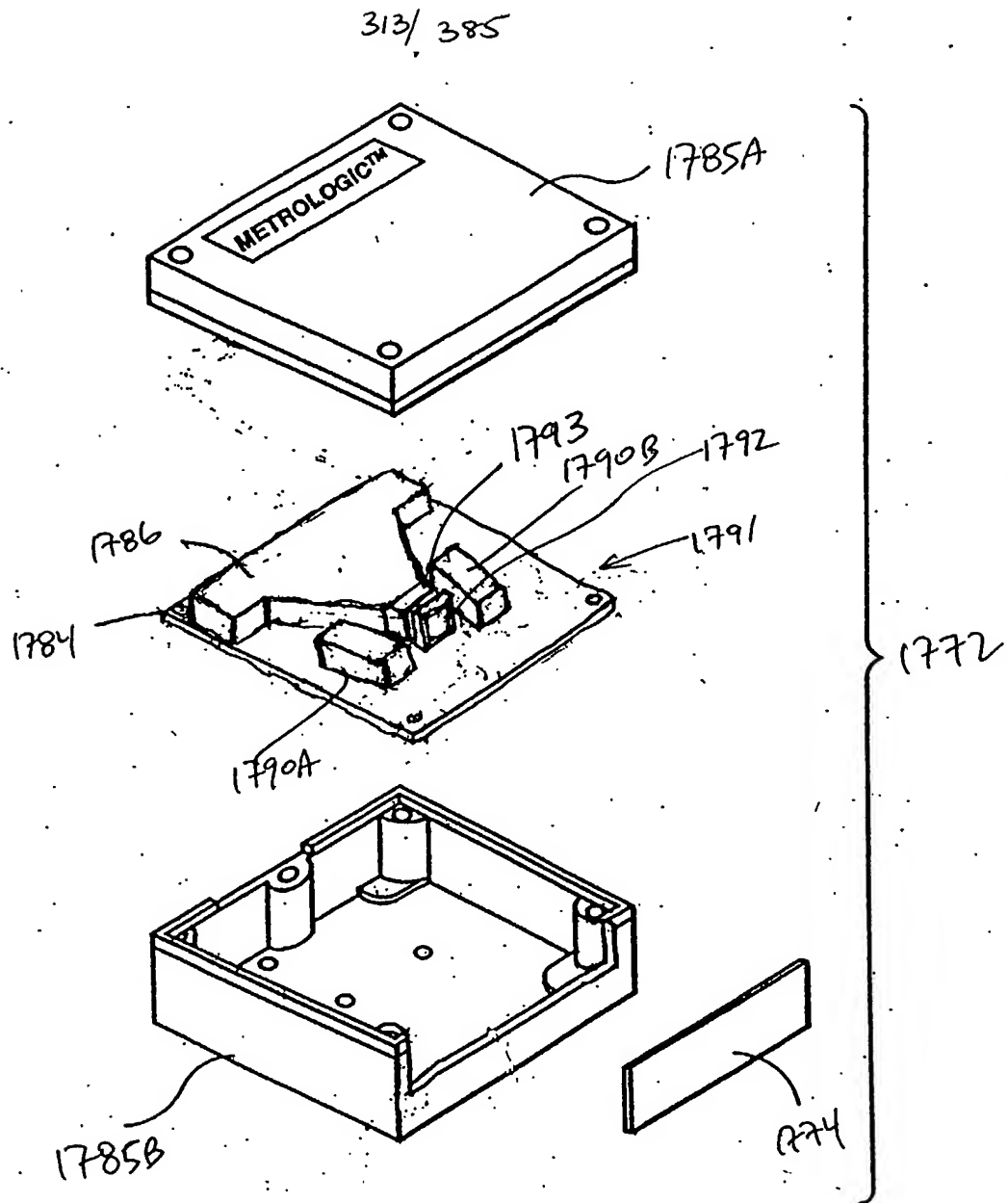


FIG. 50B

314/385

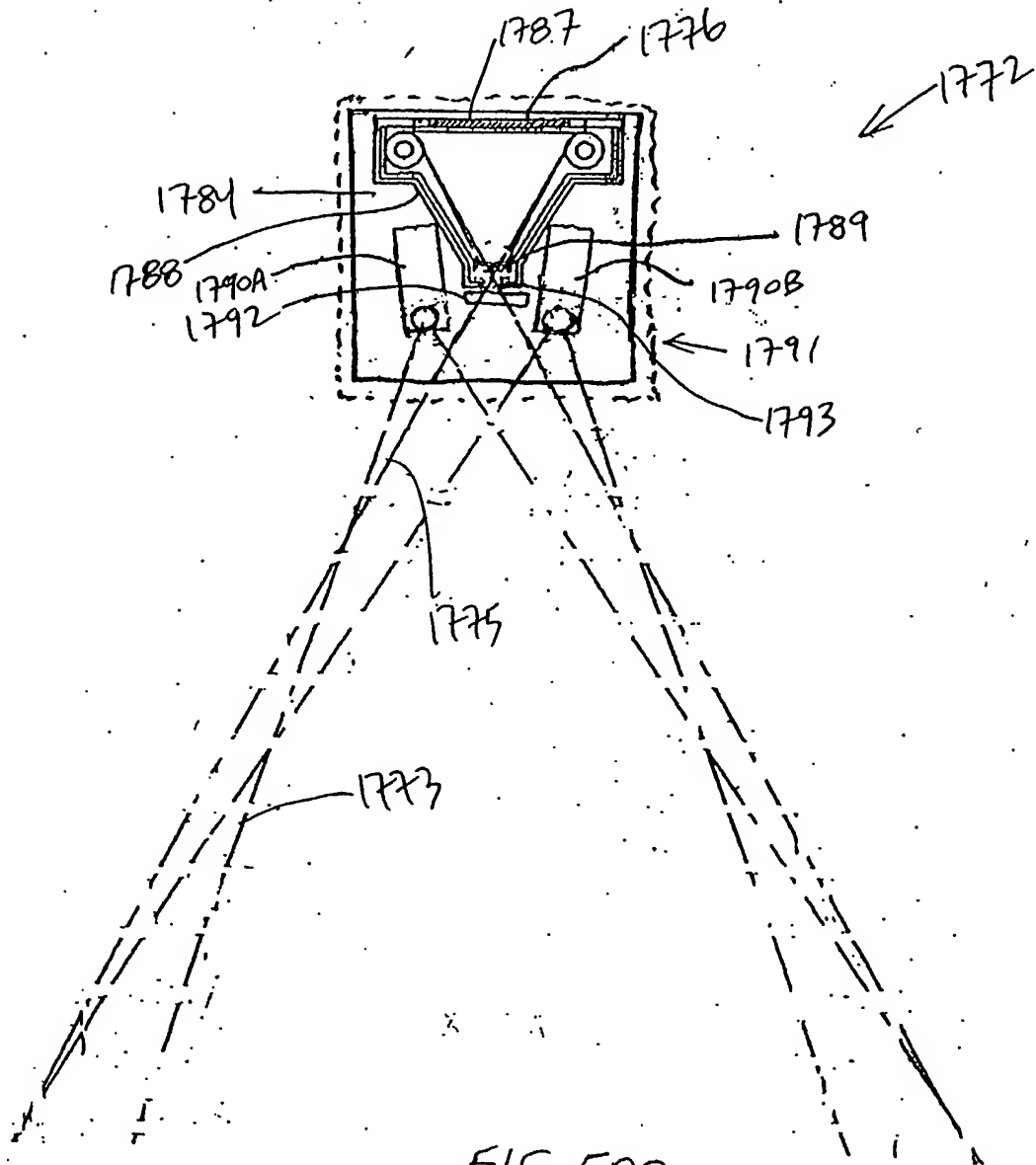
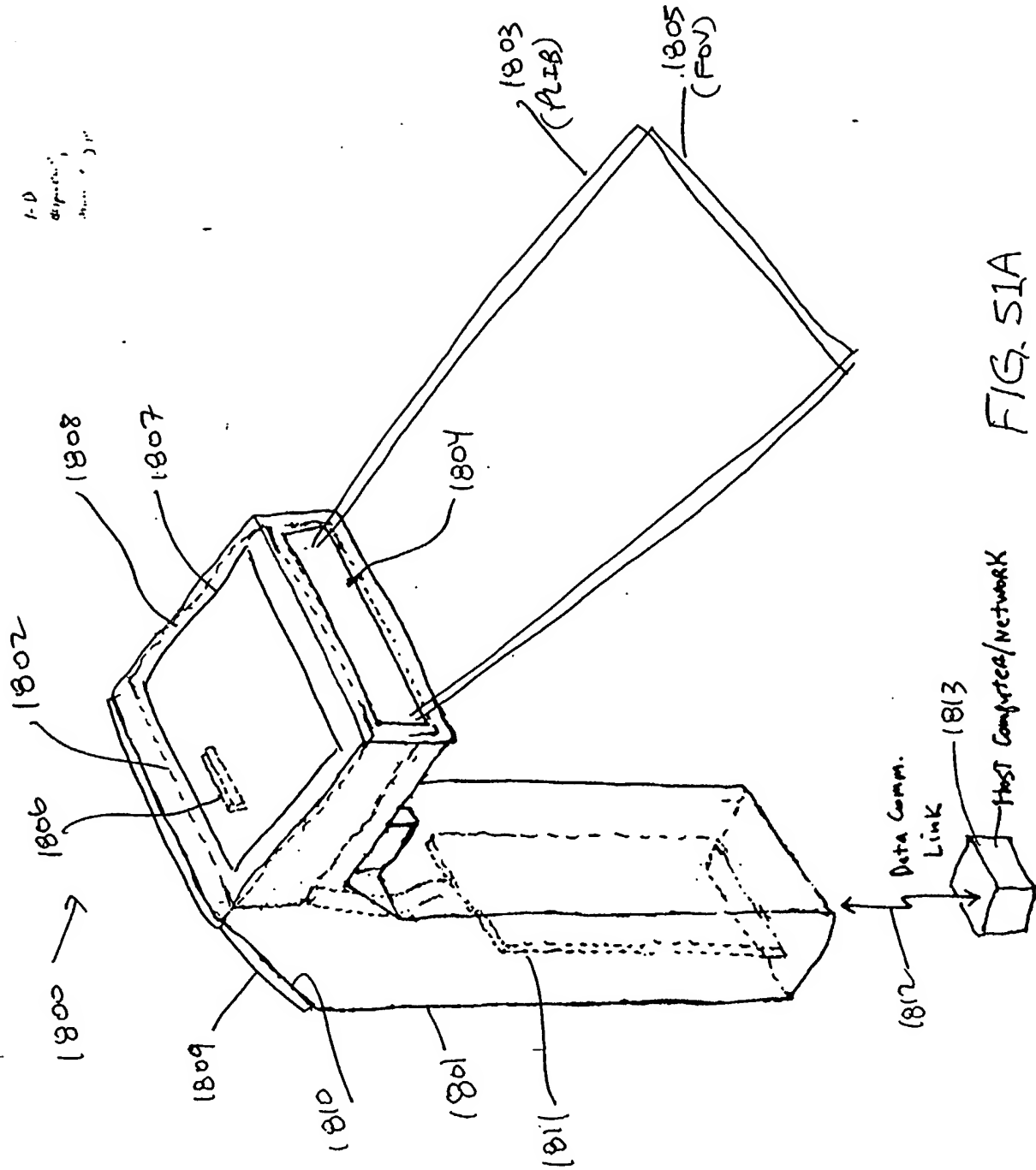


FIG. 50C

3/5/385

1-D
display
area



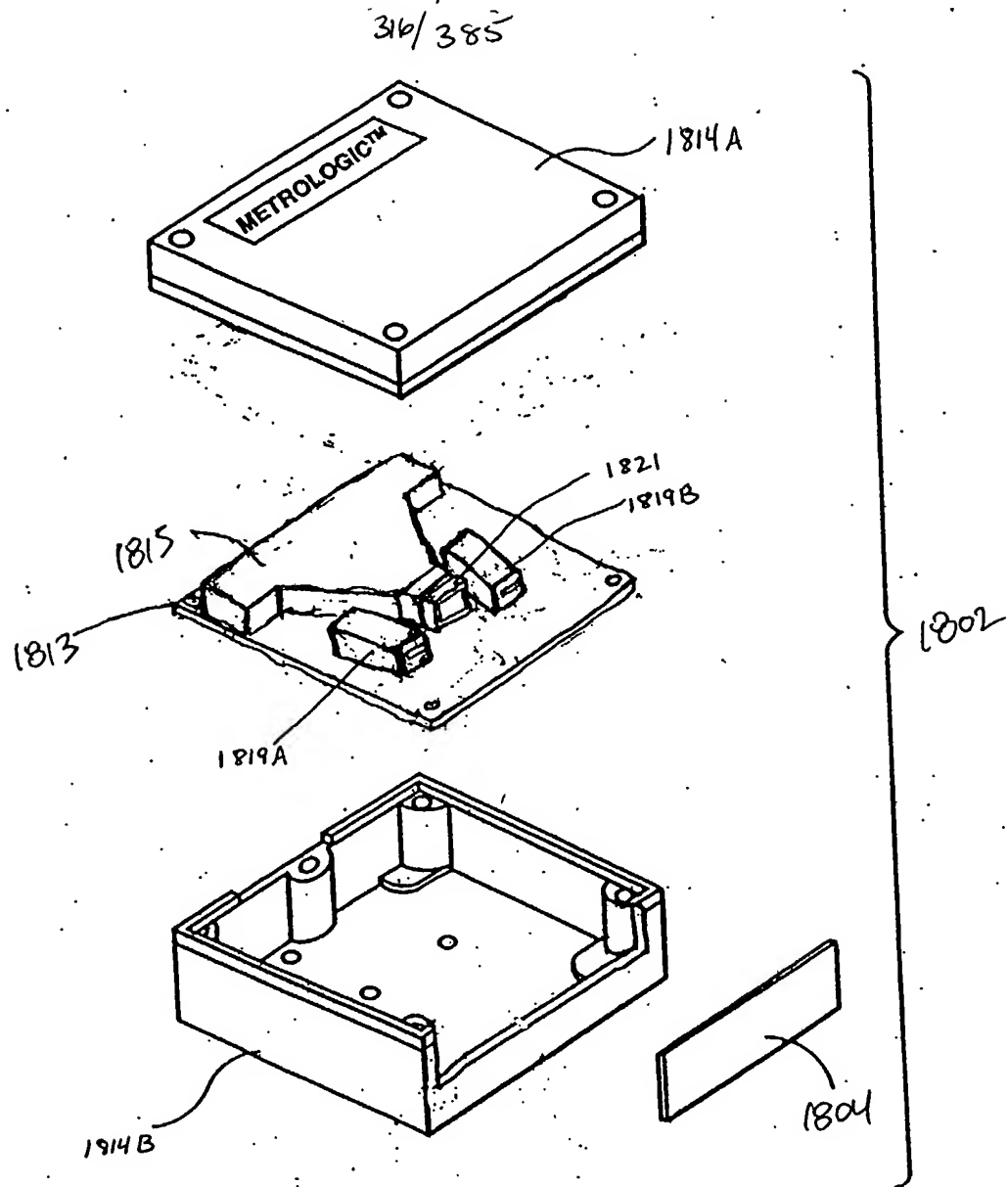
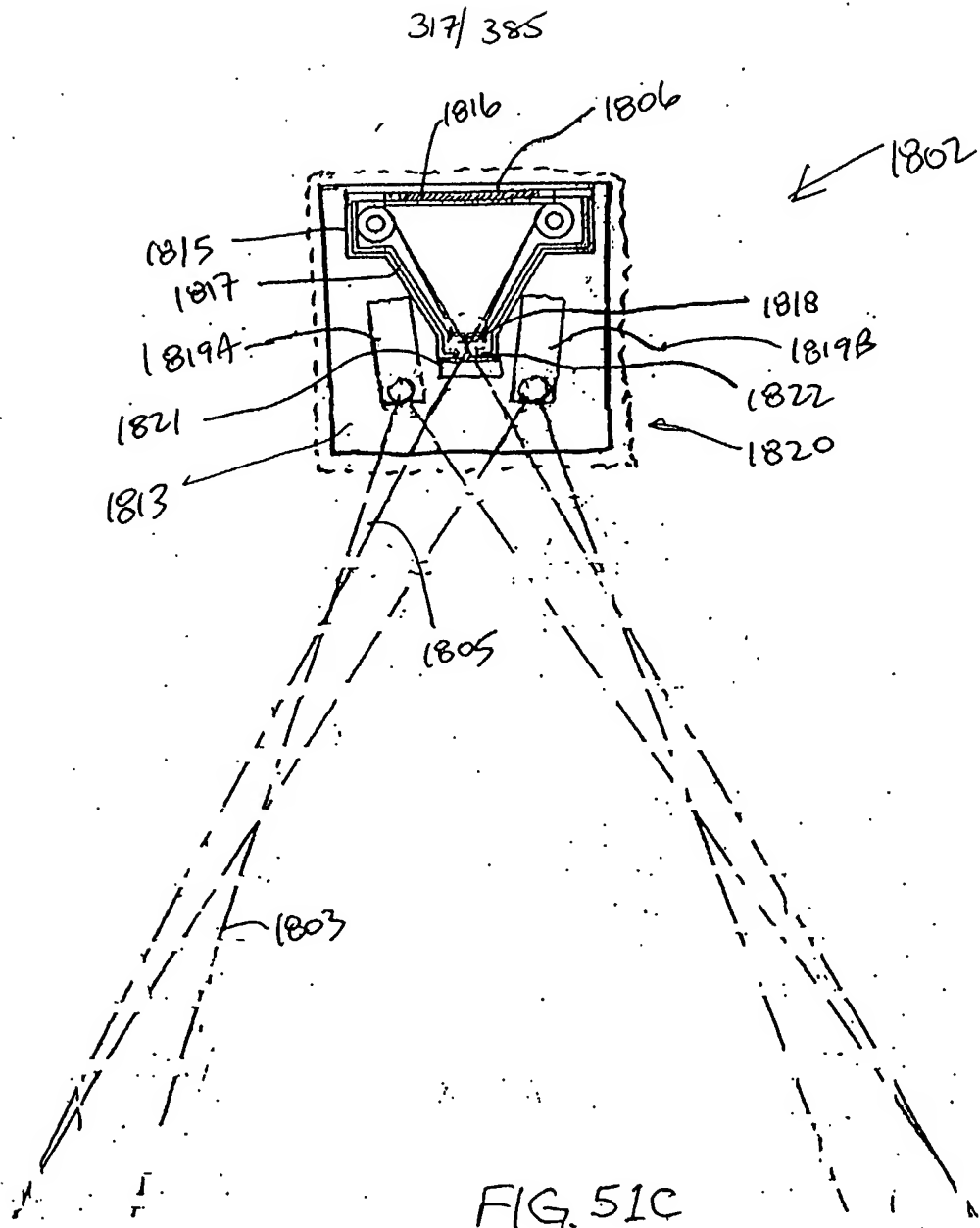


FIG. 51B



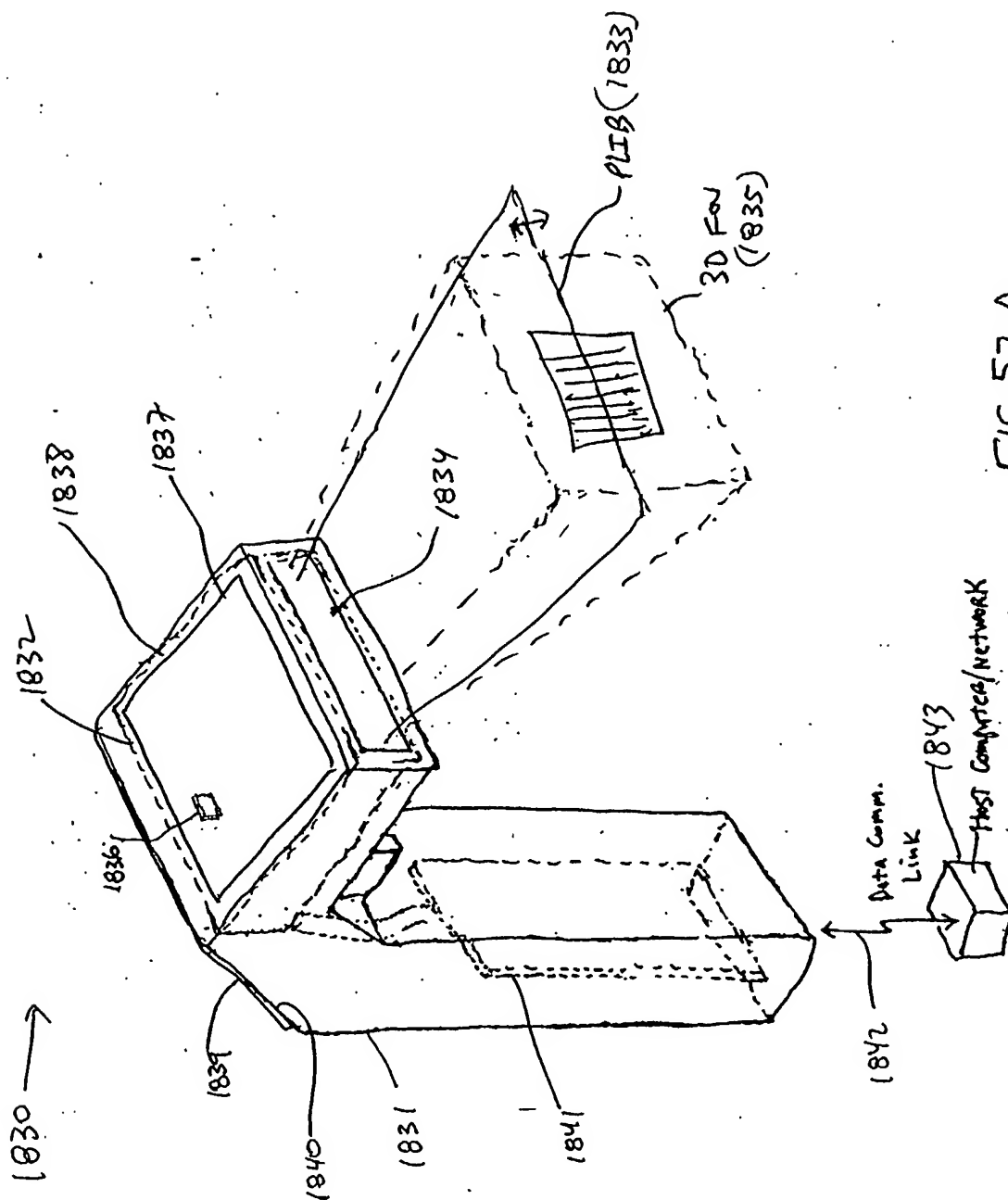


FIG. 52A

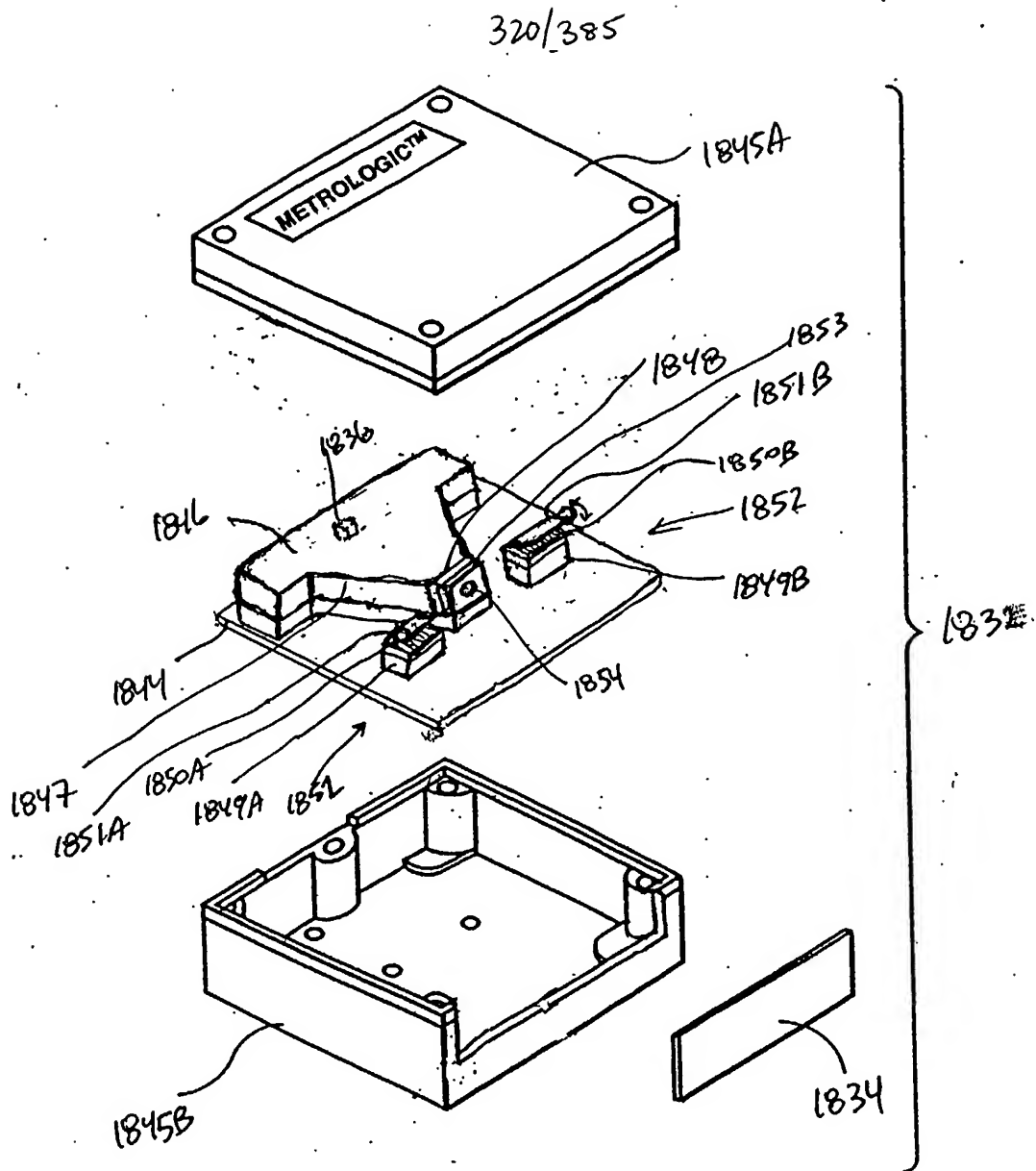
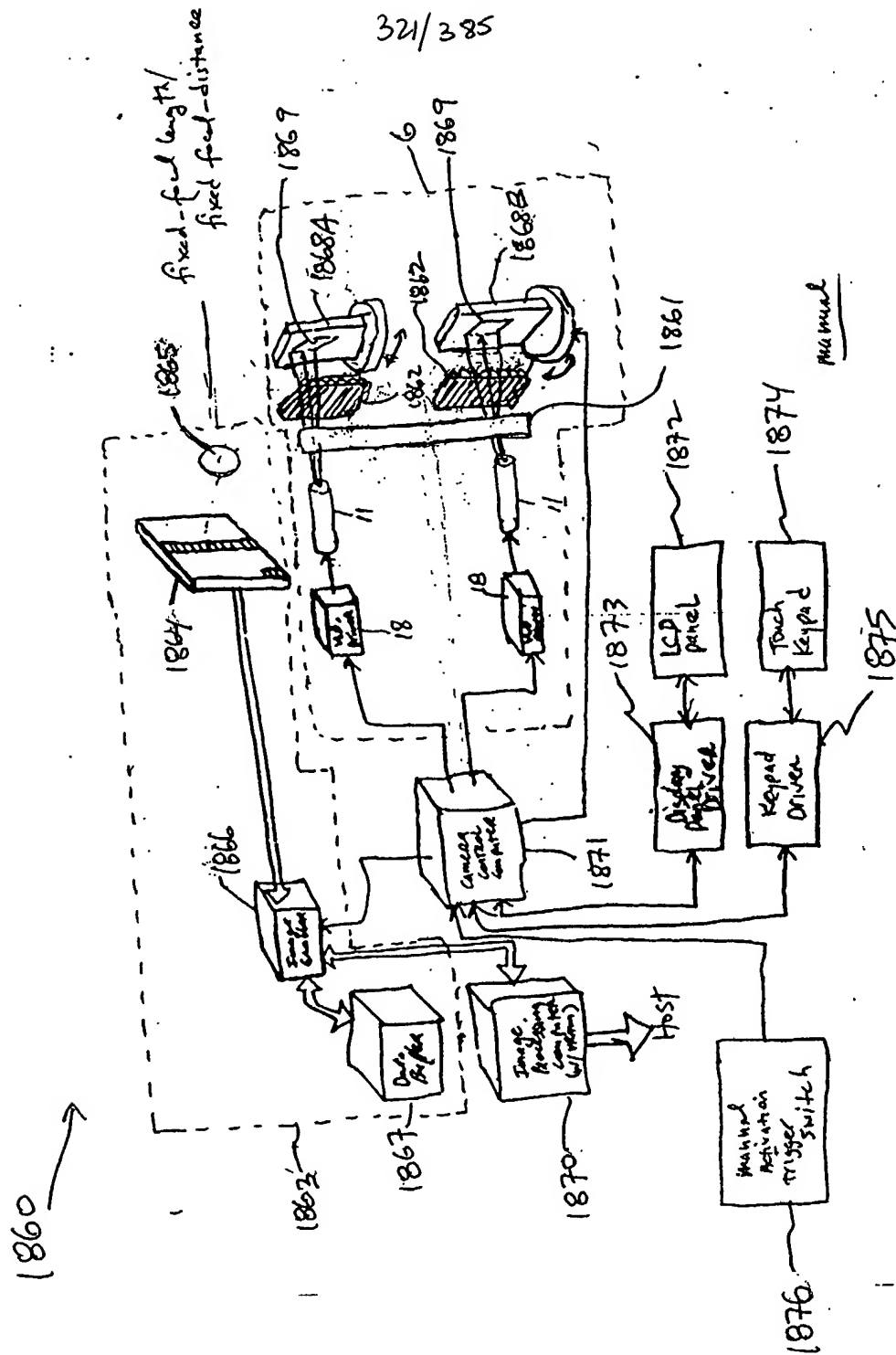


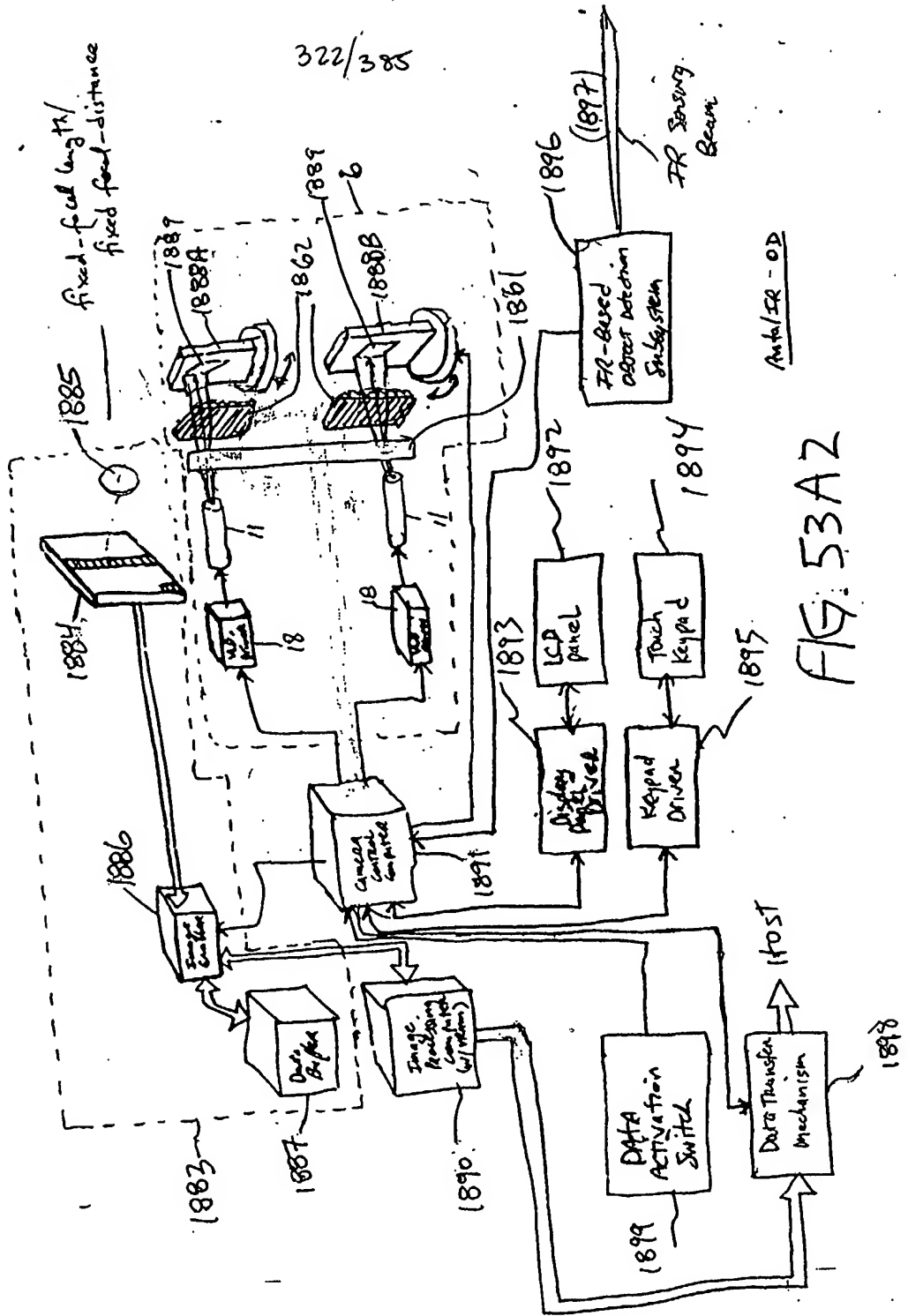
FIG. 52B

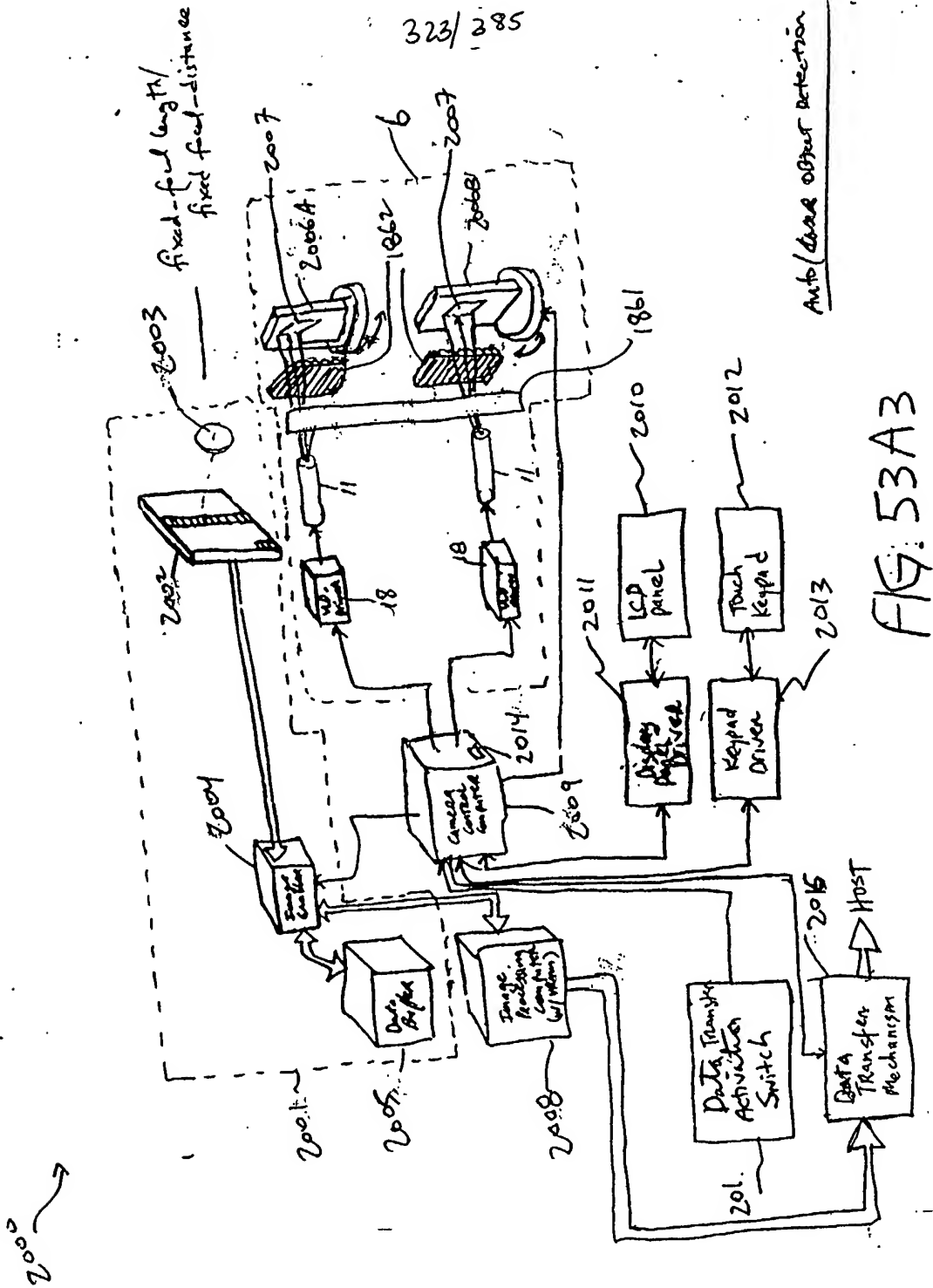
Fig. 1I3A-3B

321/385



1880





2020 →

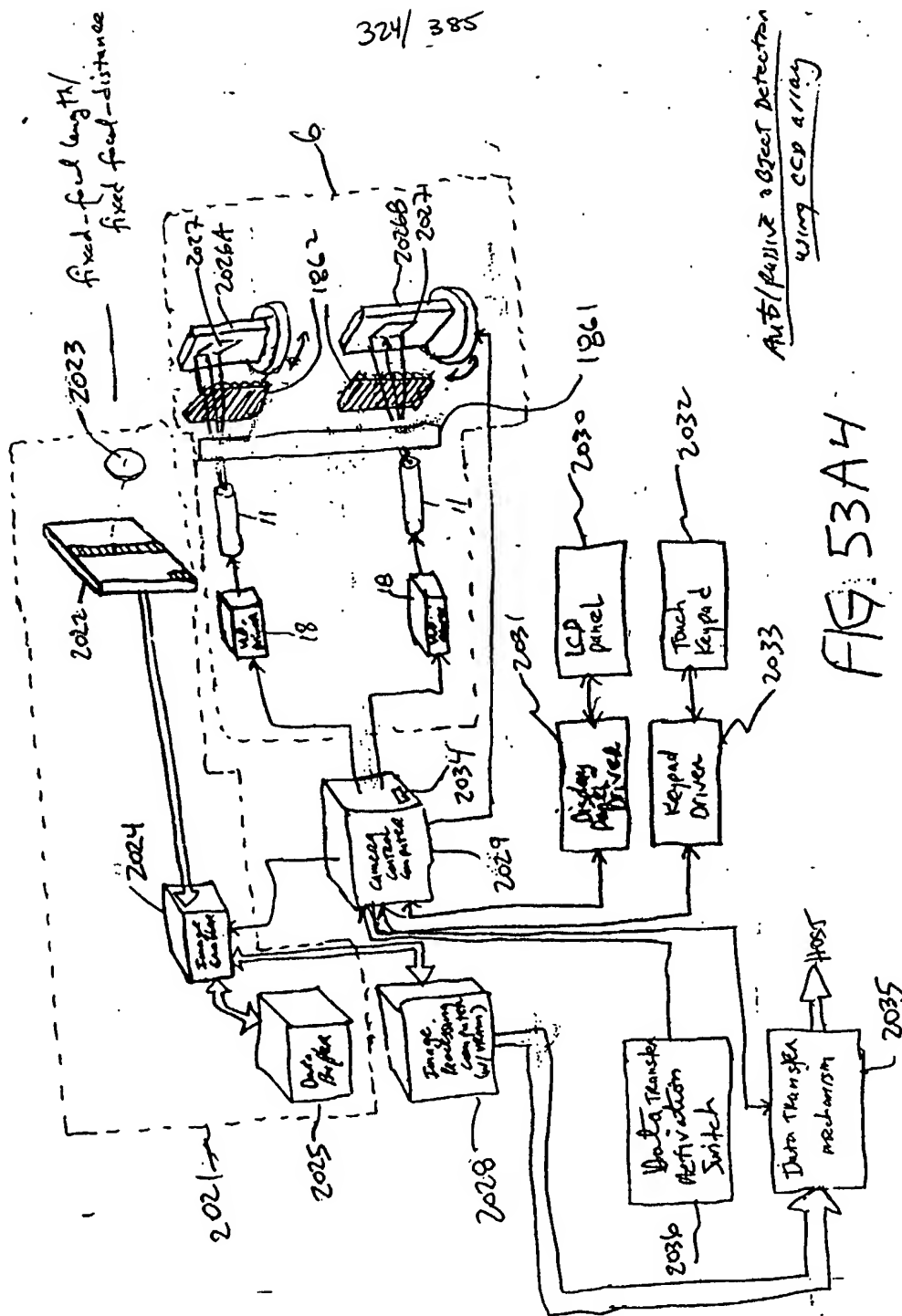


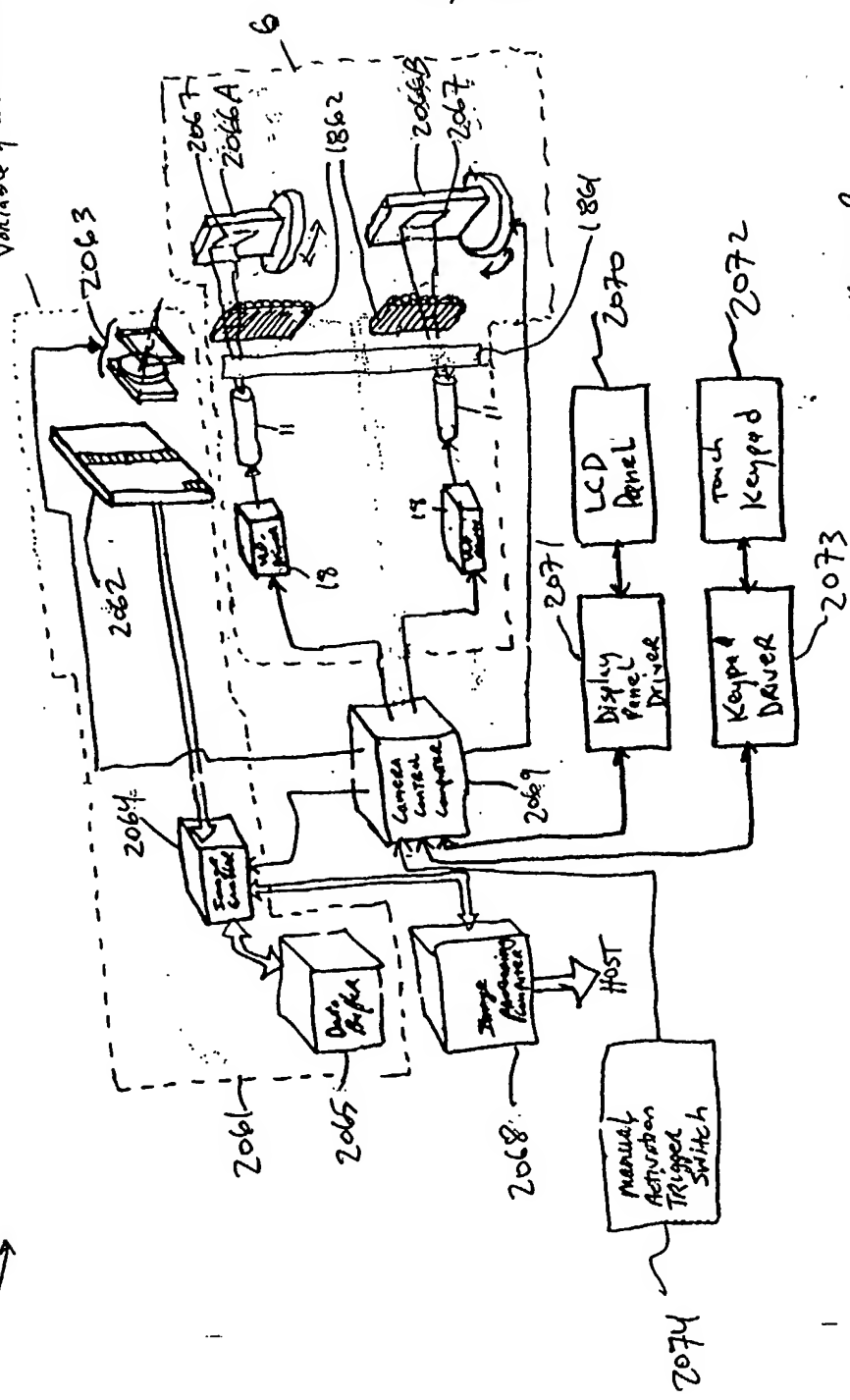
FIG. 53A4

Anti/Passive Object Detection
using CCD array

fixed focal length/
variable focal distance

326/385

2060 →



Manual

FIG. 53B1

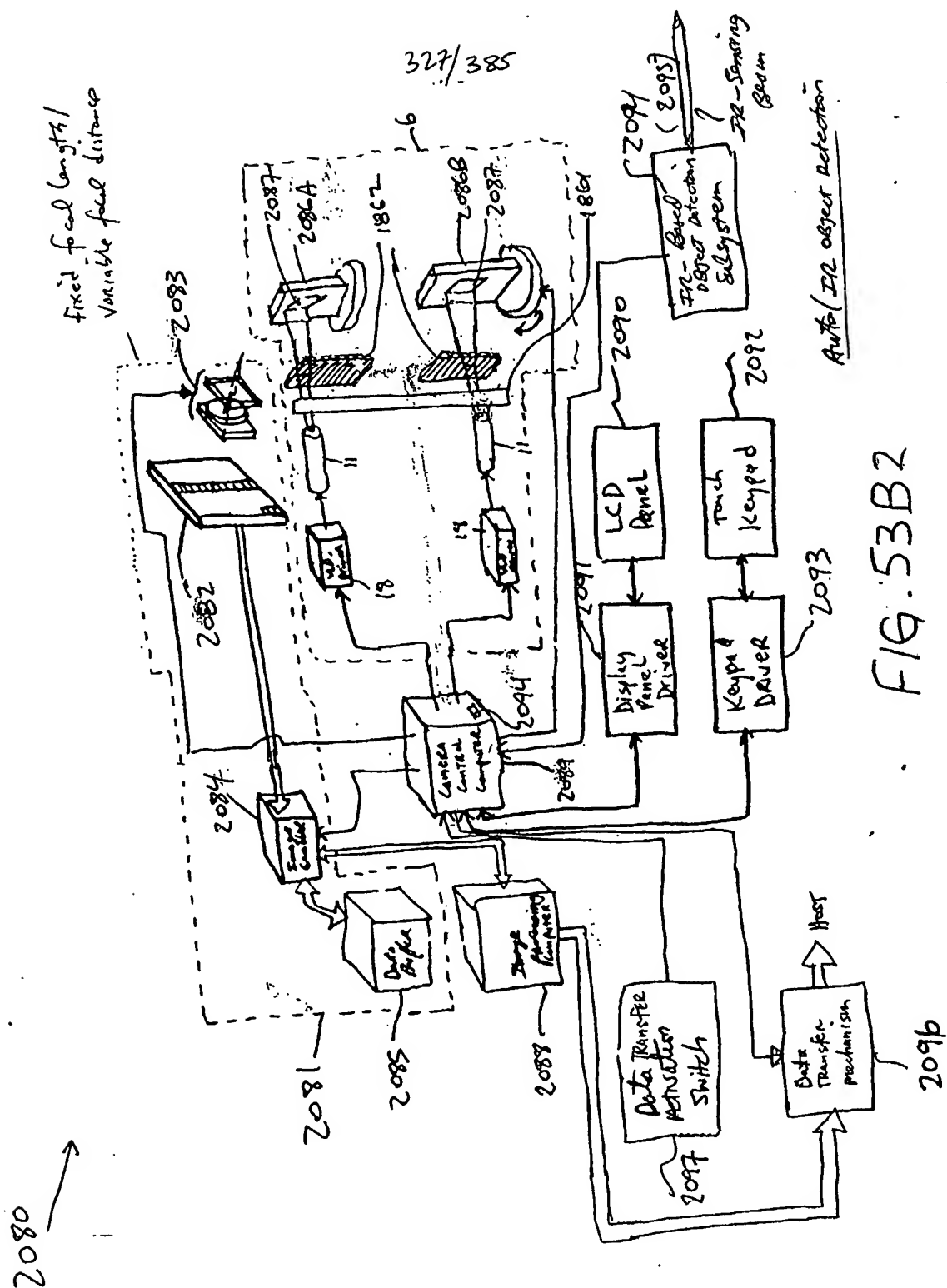


FIG. 53B2

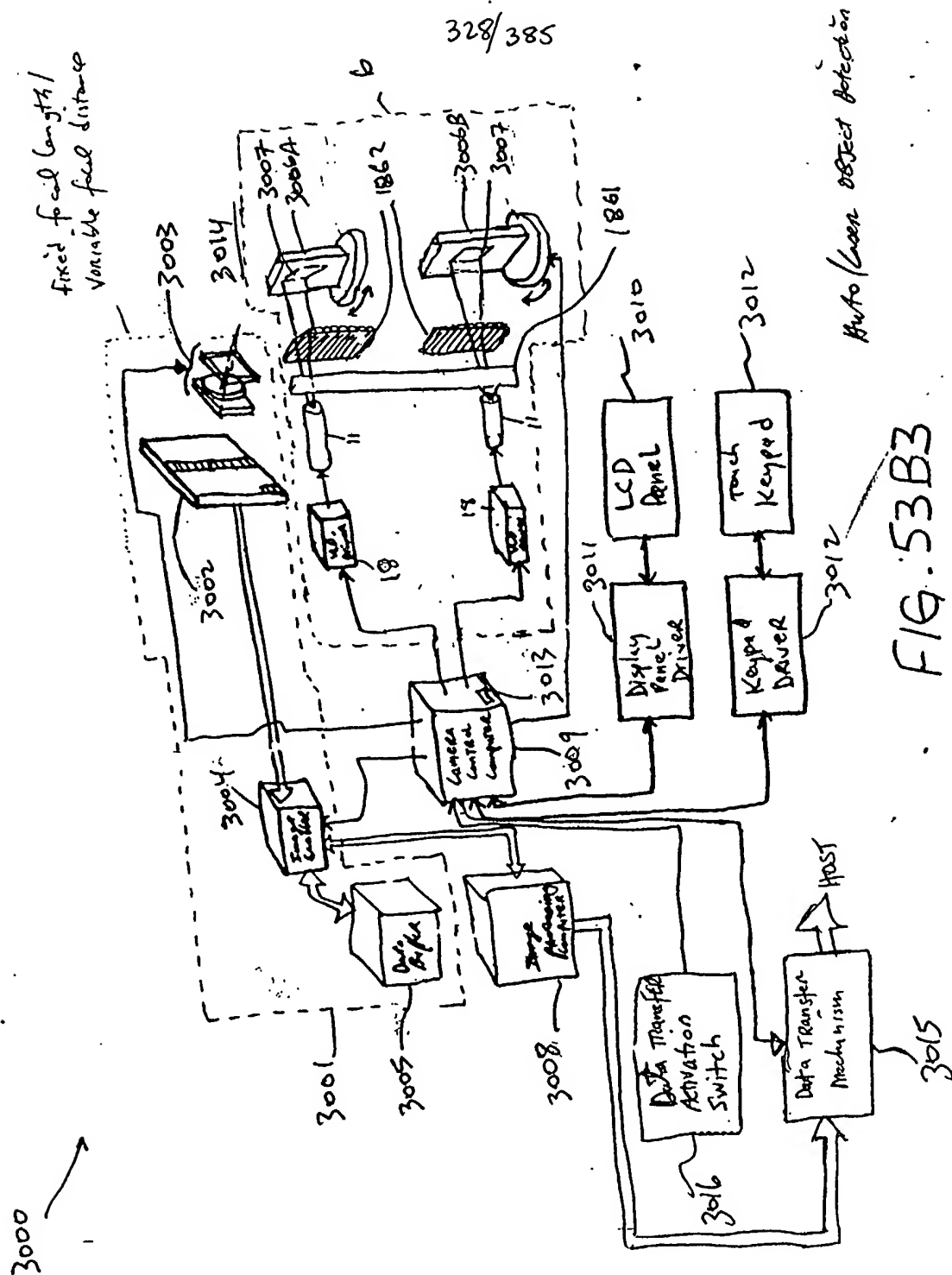
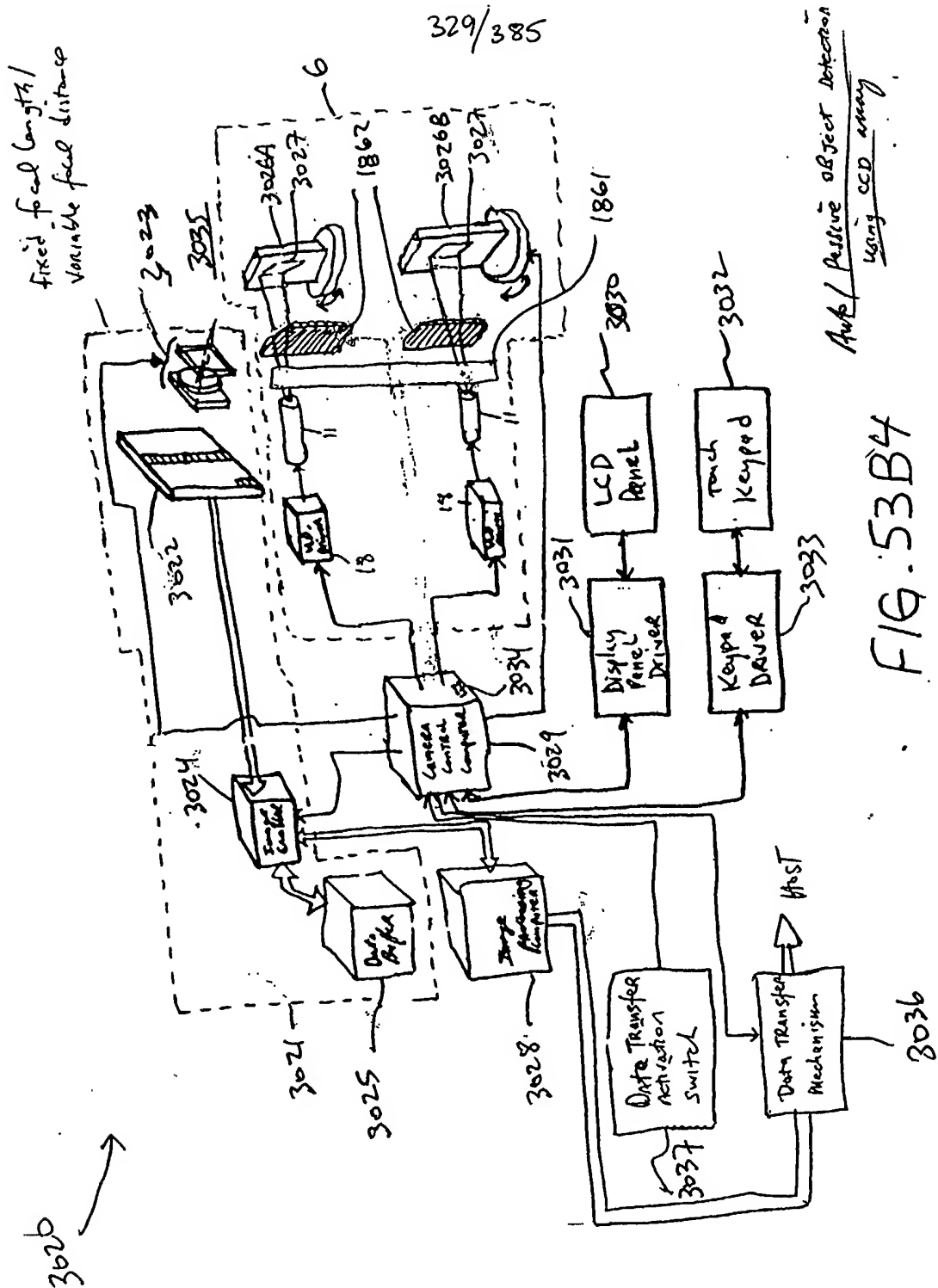
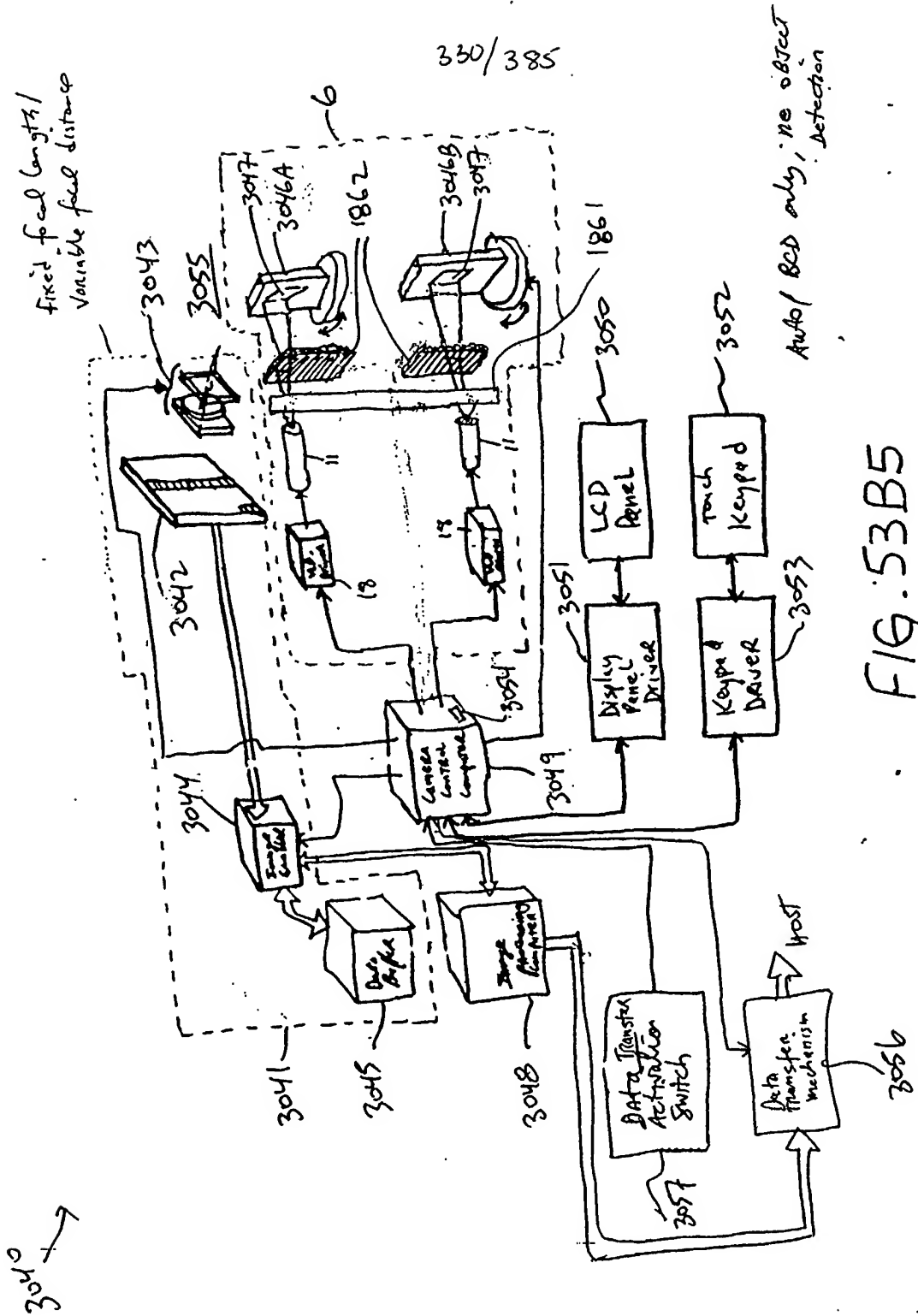


FIG. 53B3





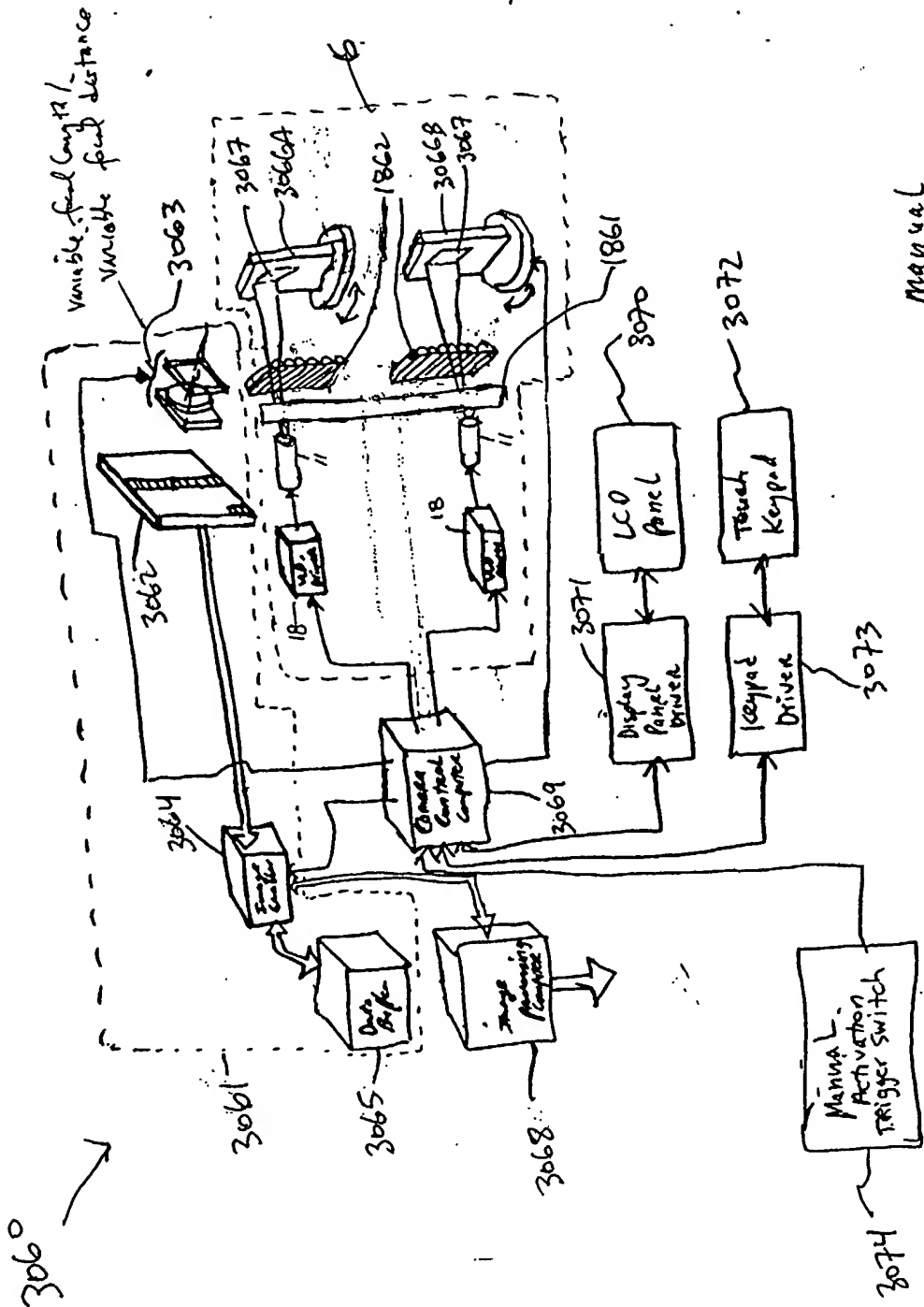
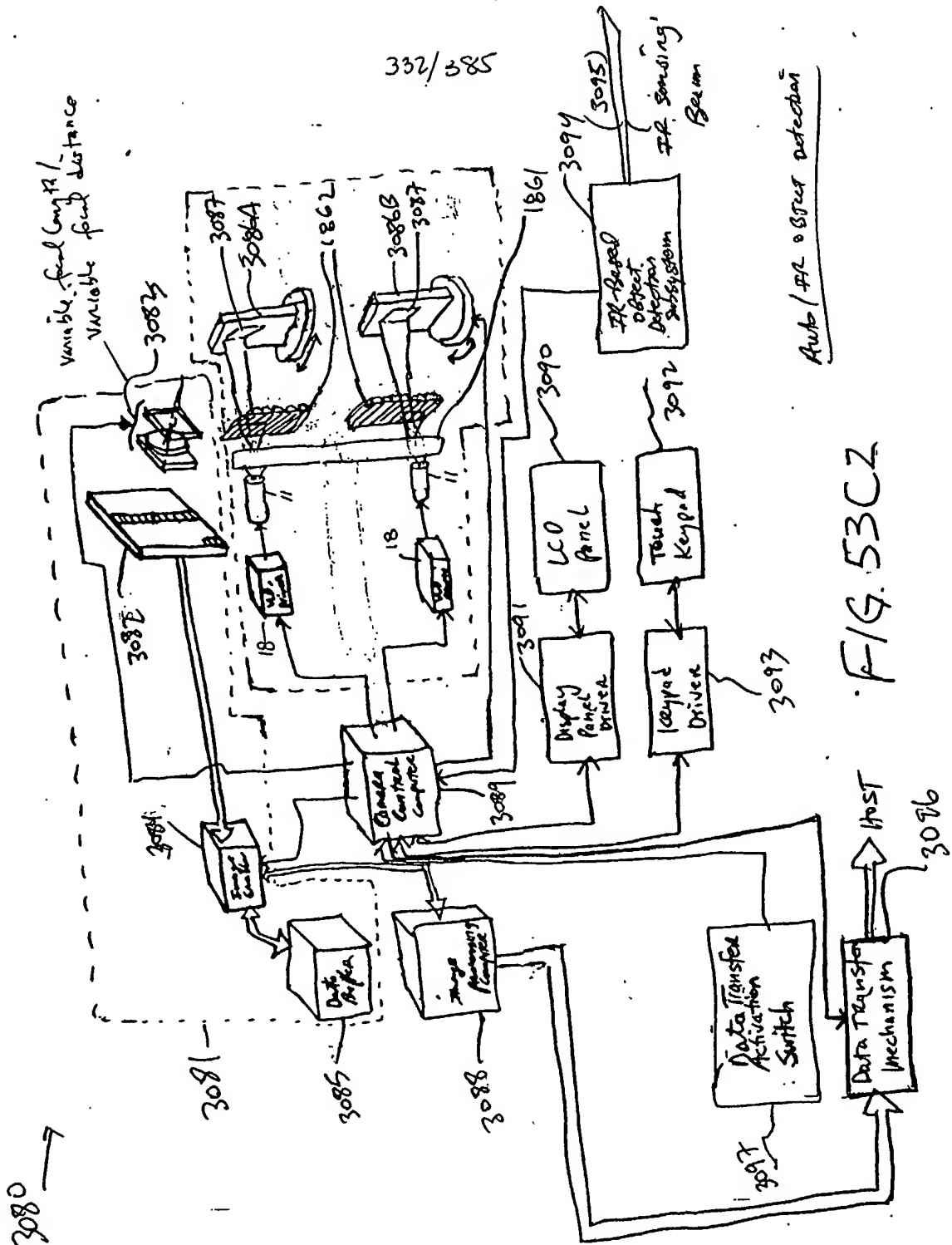


FIG. 53C1

Manual



333/385

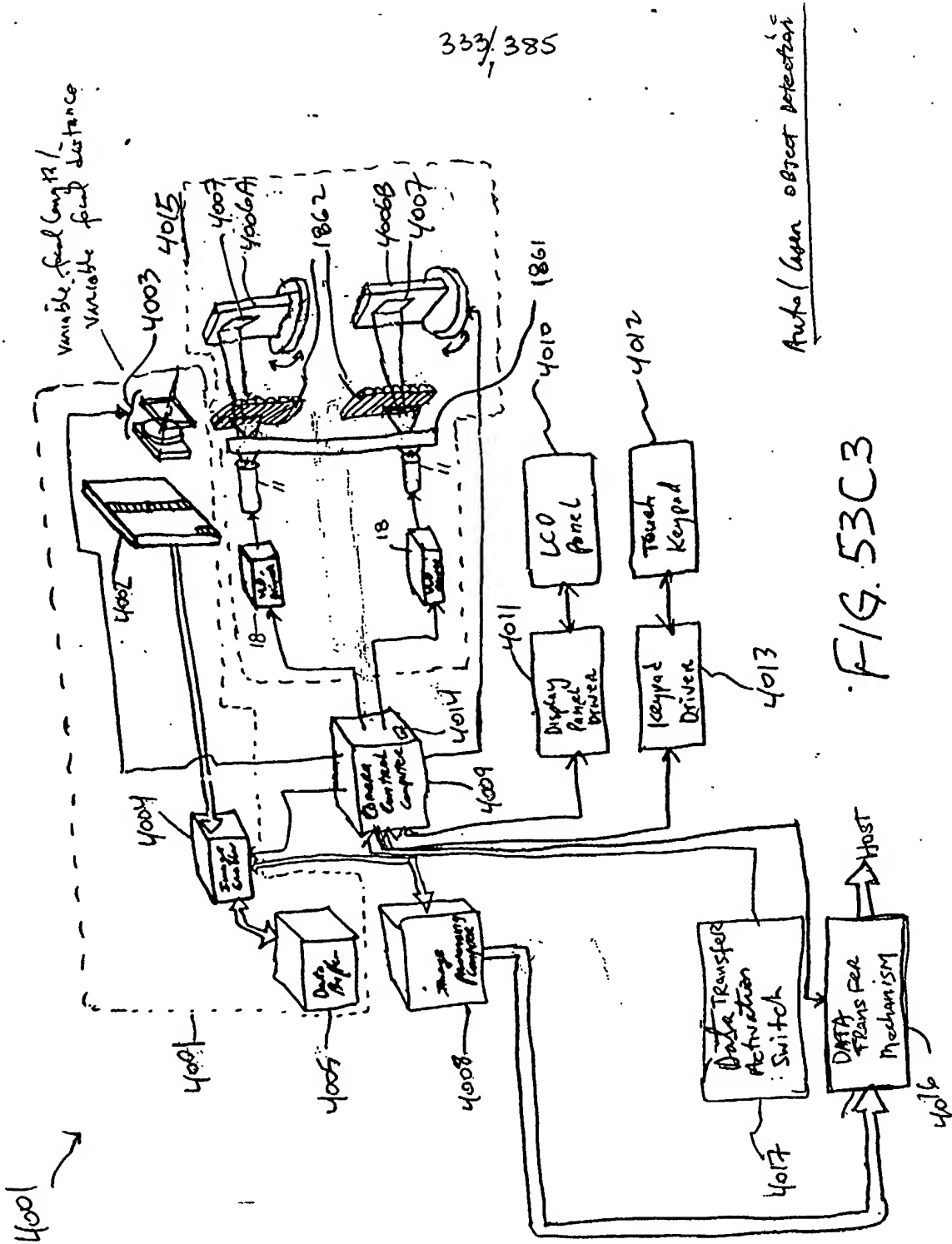
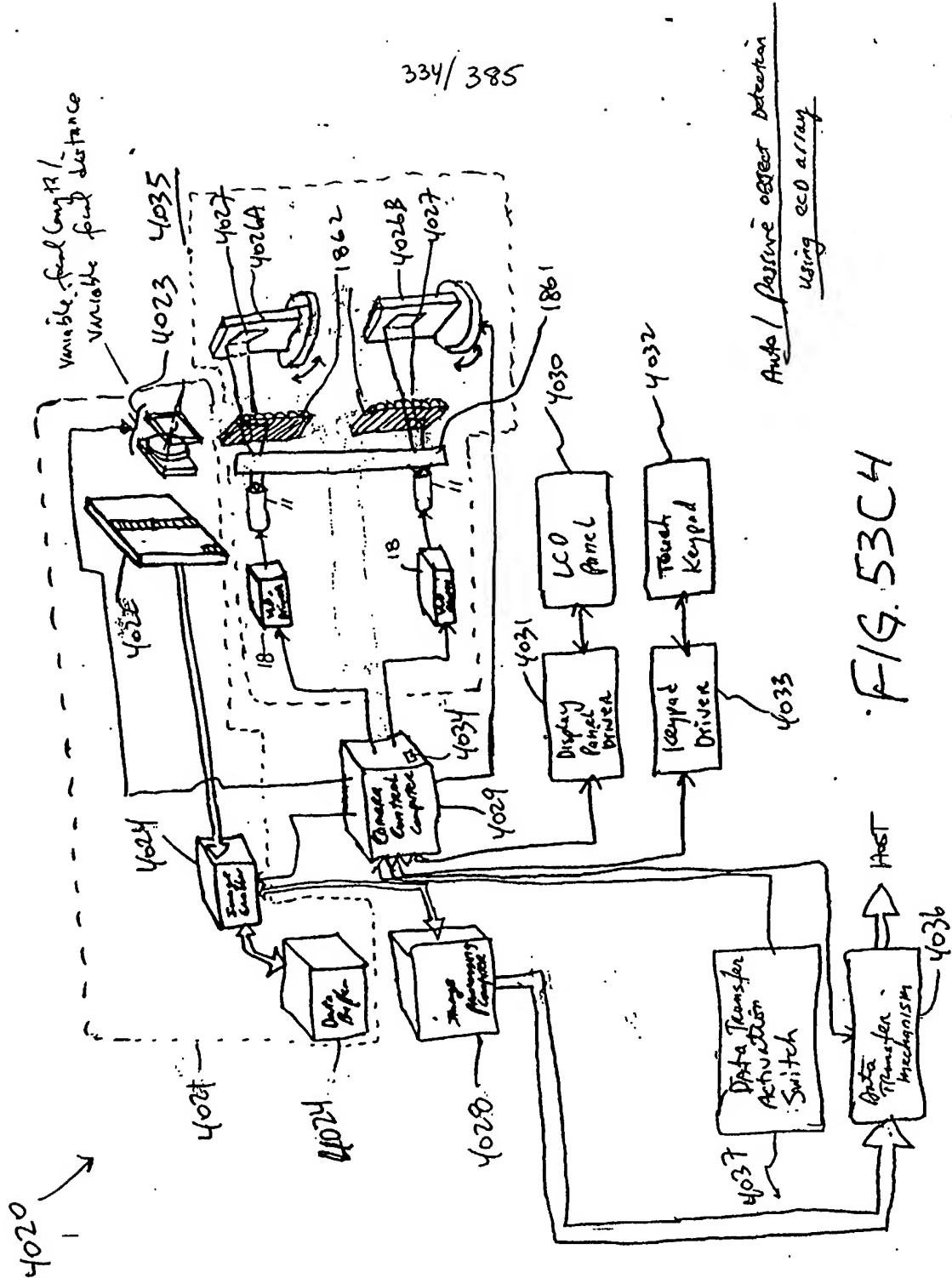


FIG. 53C3

Auto/Camera Object Detection

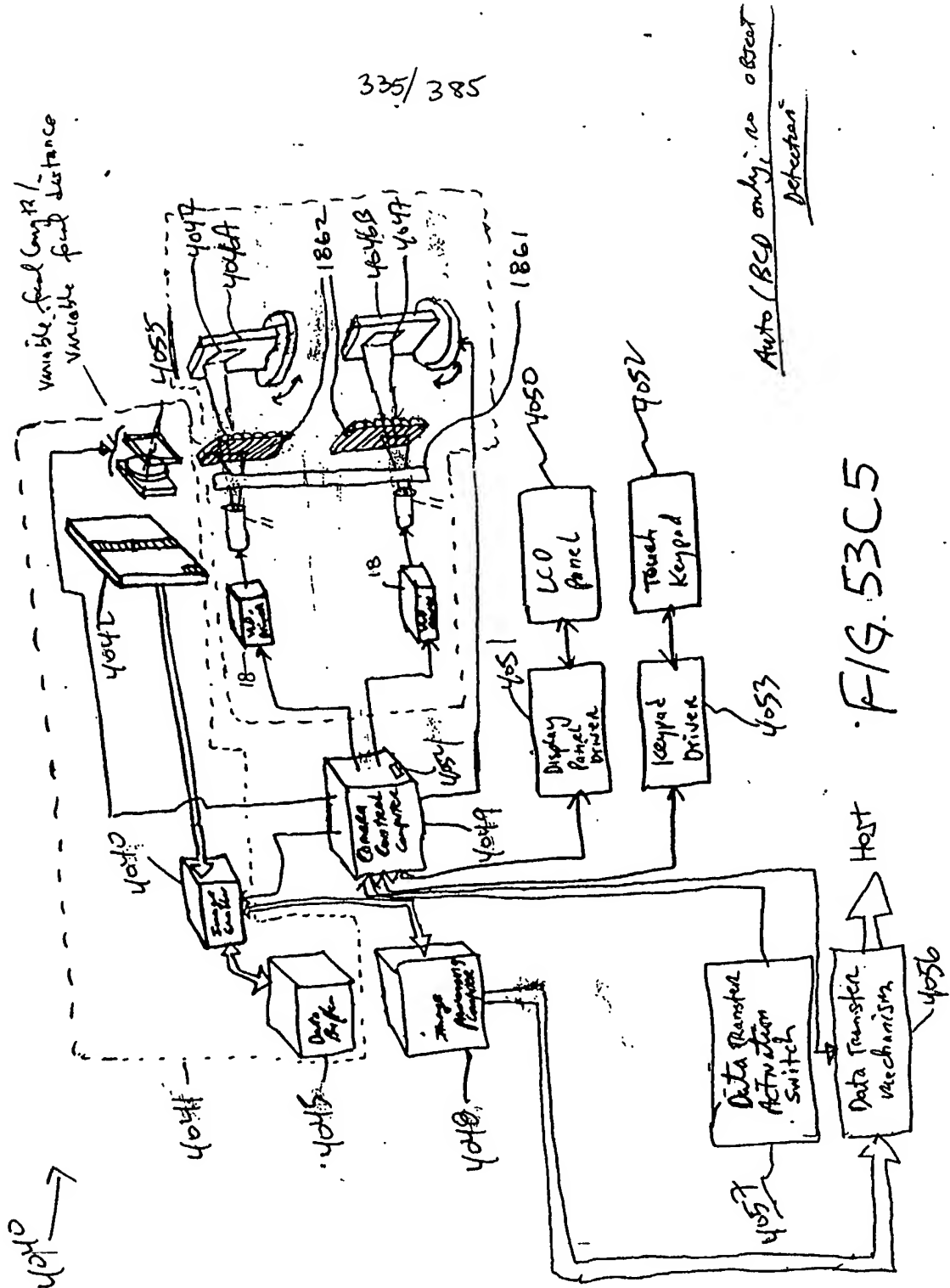
334/385



Auto / Passive object detection
using CCD array

FIG. 53C4

335/385



336/385

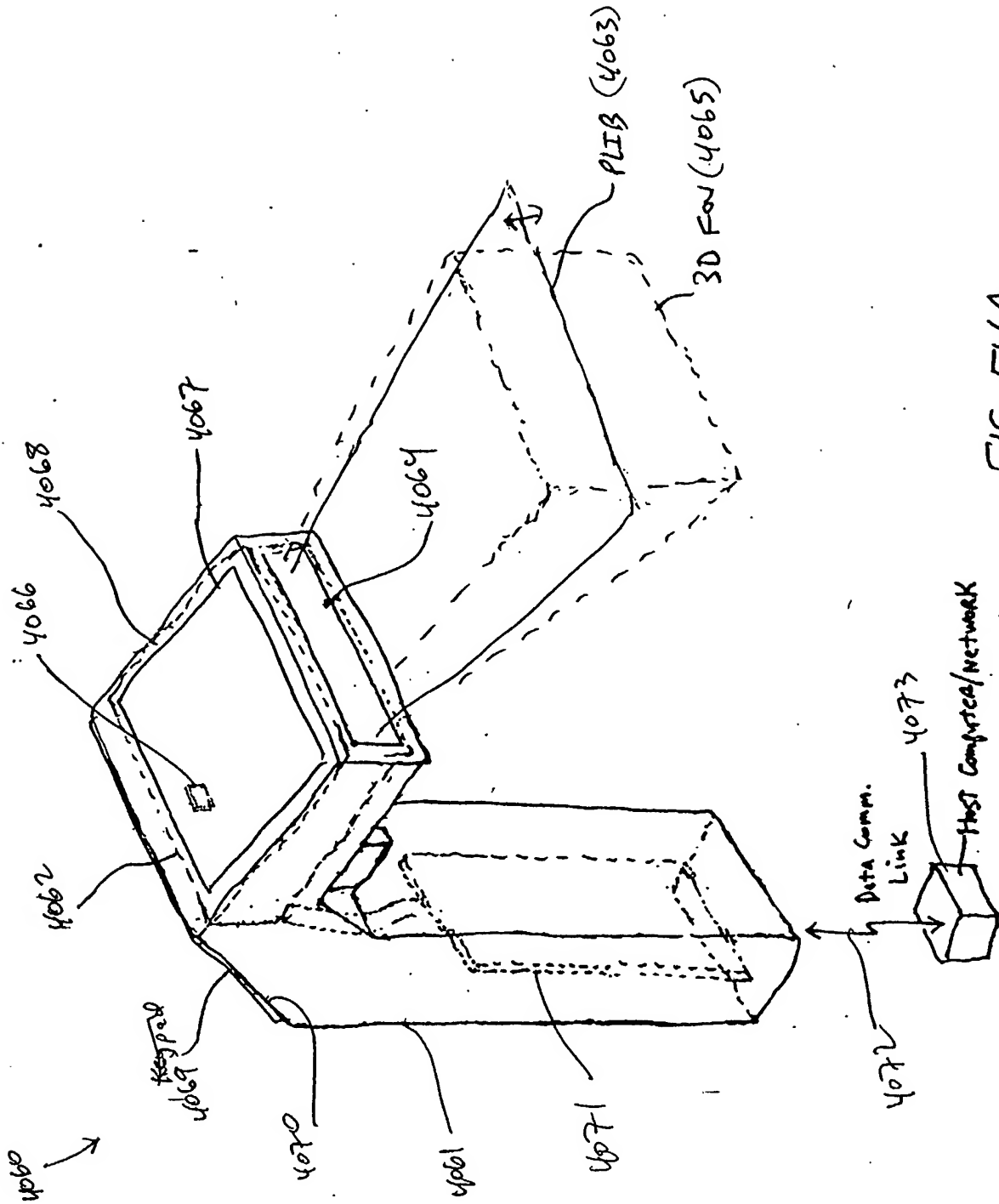


FIG. 54A

337/385

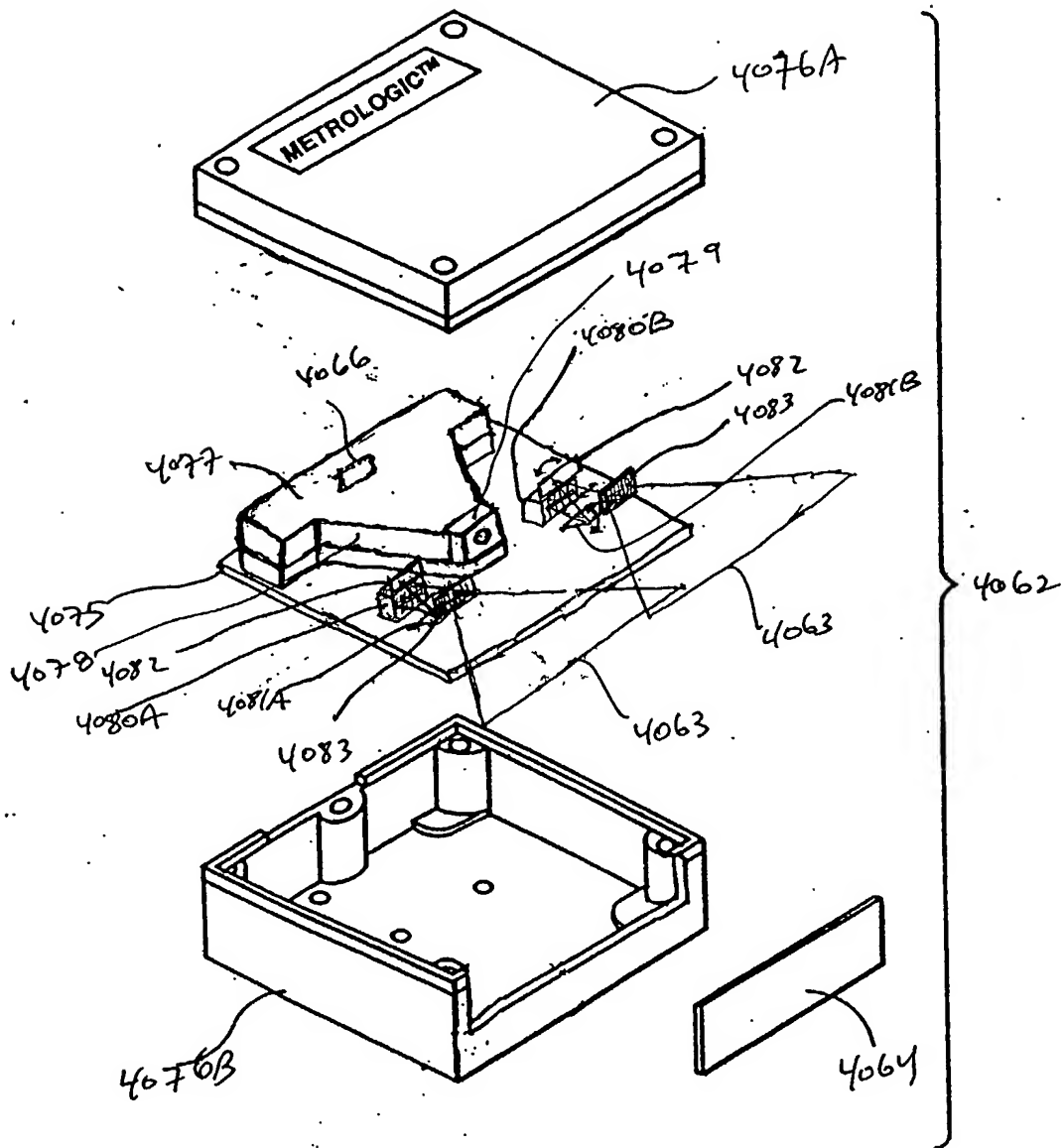


FIG. 54B

(Dual mirrors)

Fig. 175A-SP1

338/385

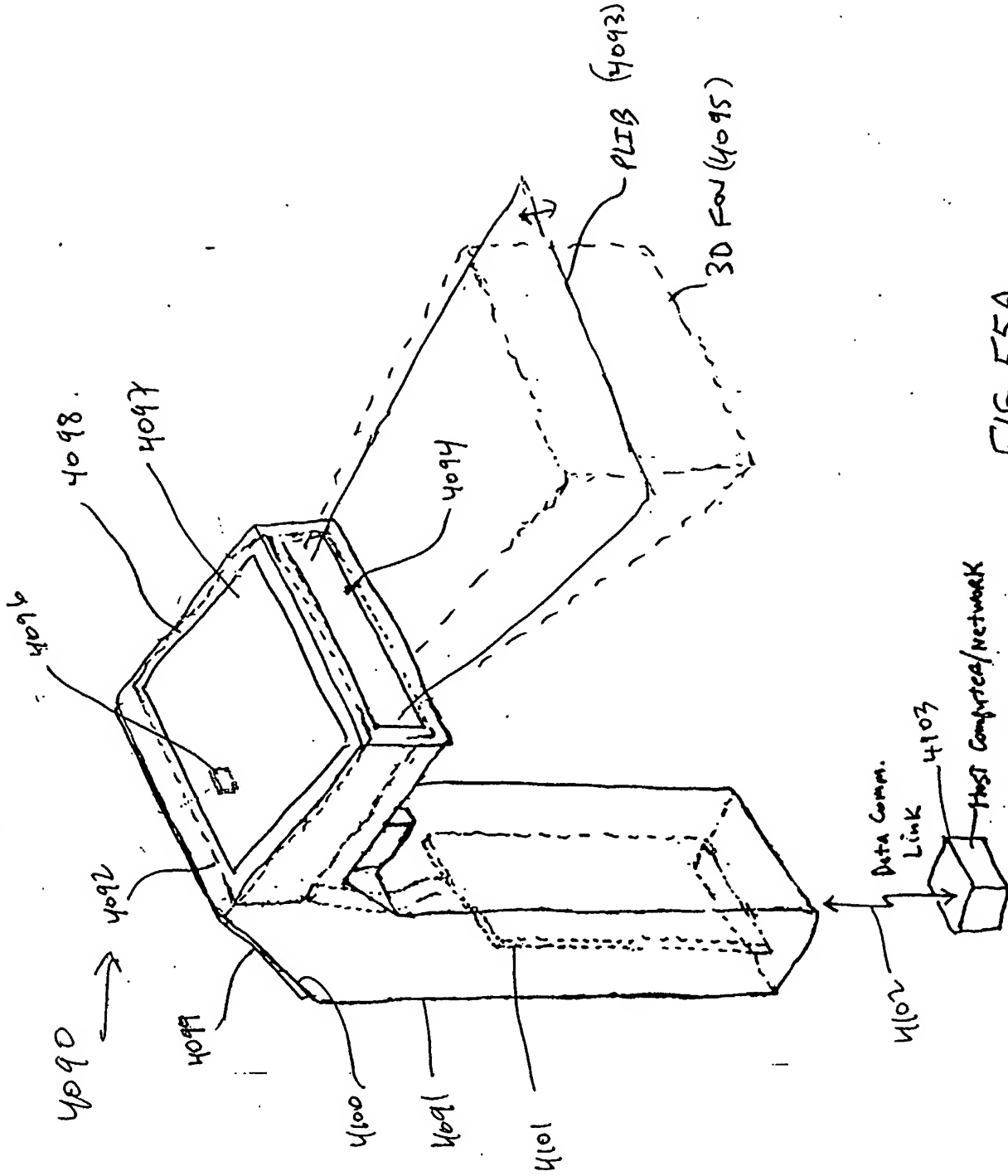


FIG. 55A

339/385

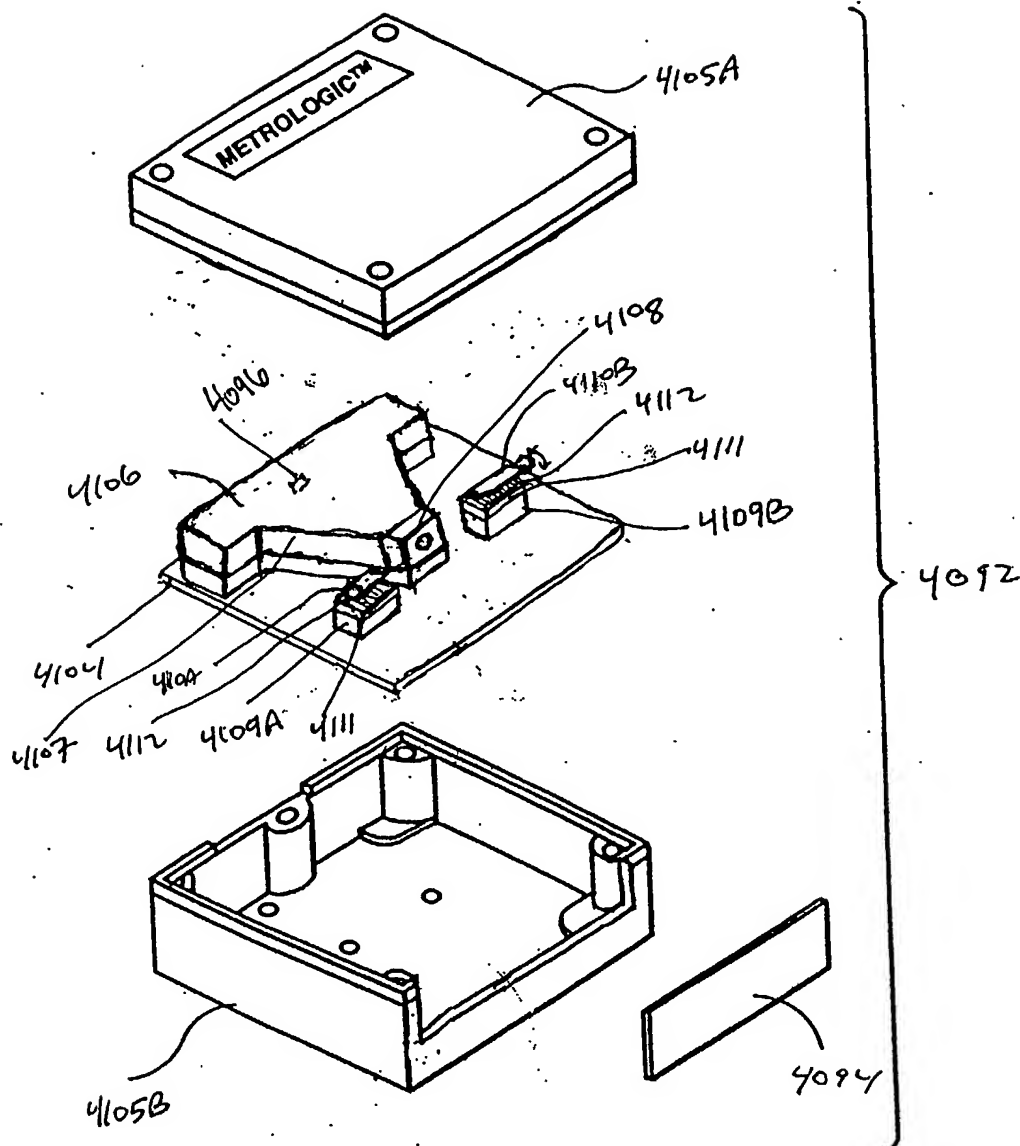


FIG. 55B

Brogg cell
Fig. 116A-6B

340/385

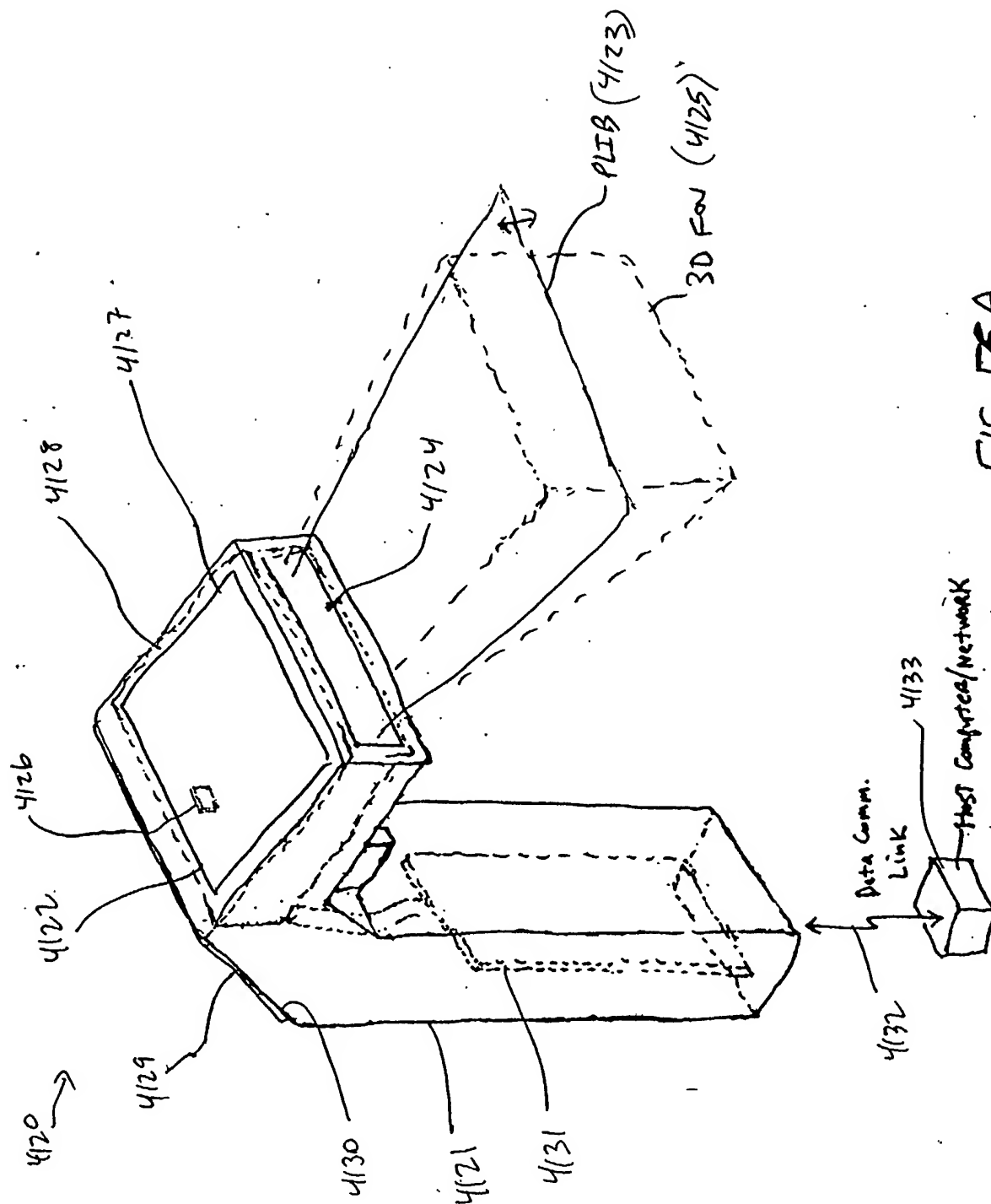


FIG. 56A

341/385

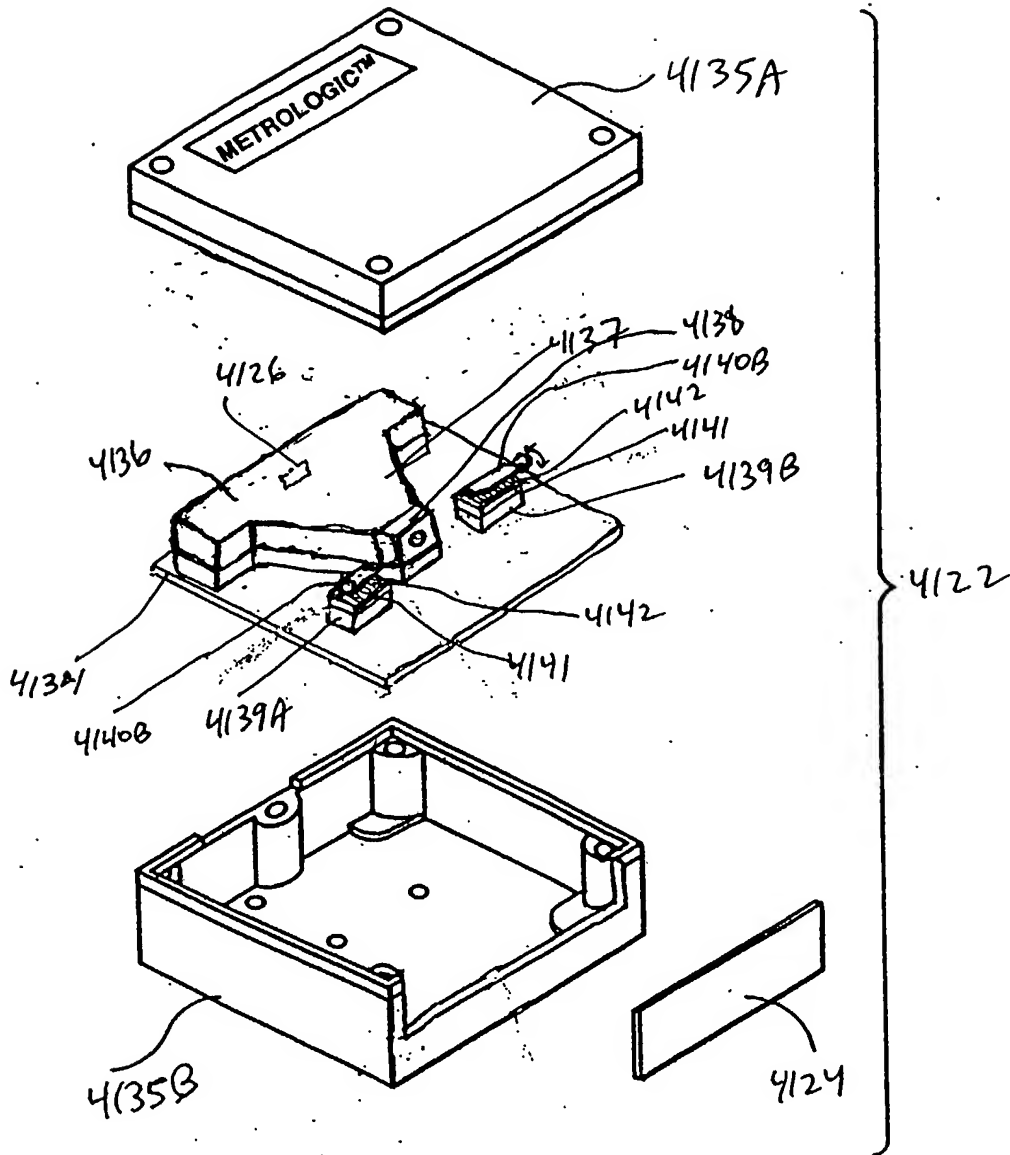


FIG. 56B

DM

Fig. 1I 7A-7C

342/385

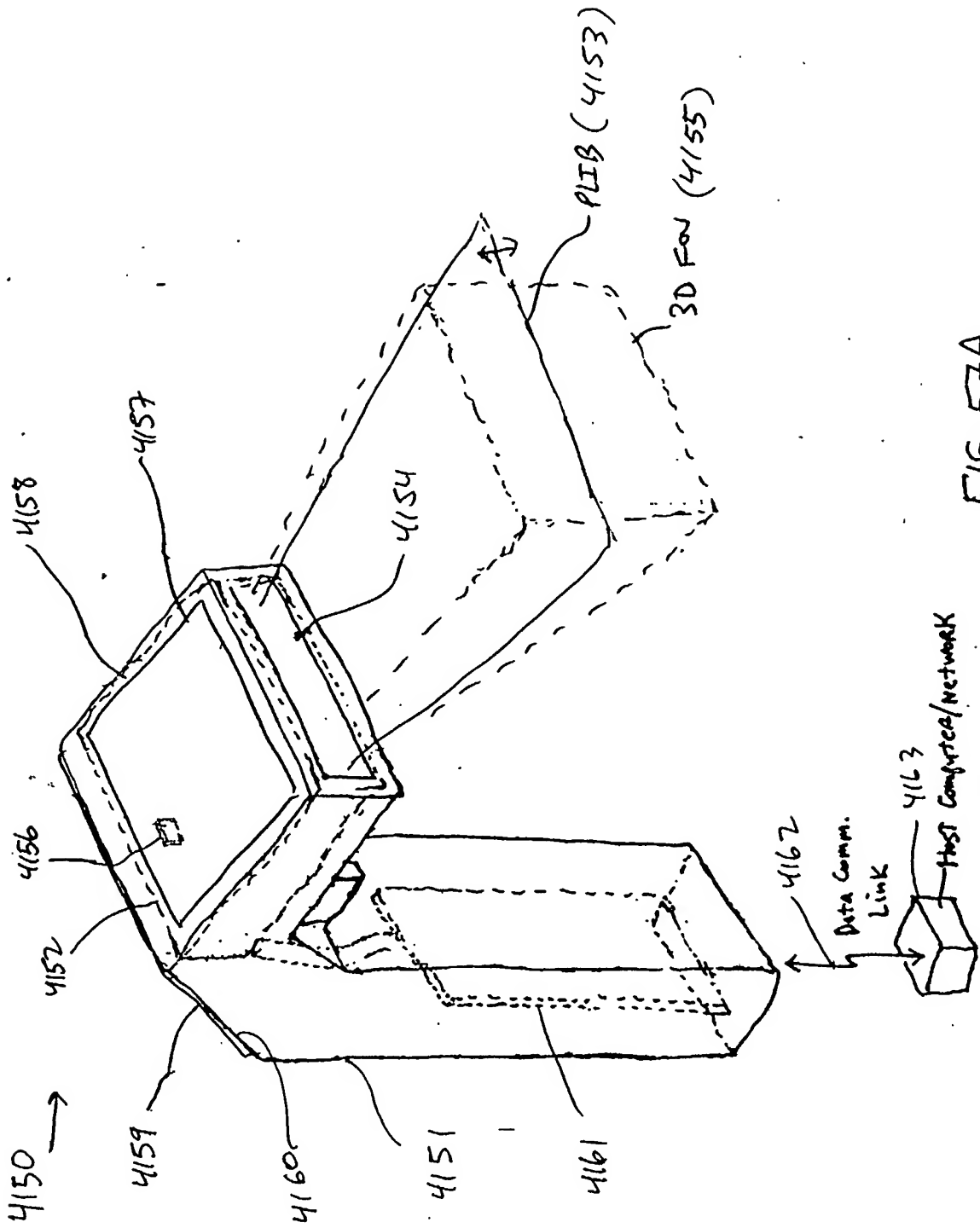


FIG. 57A

343/385

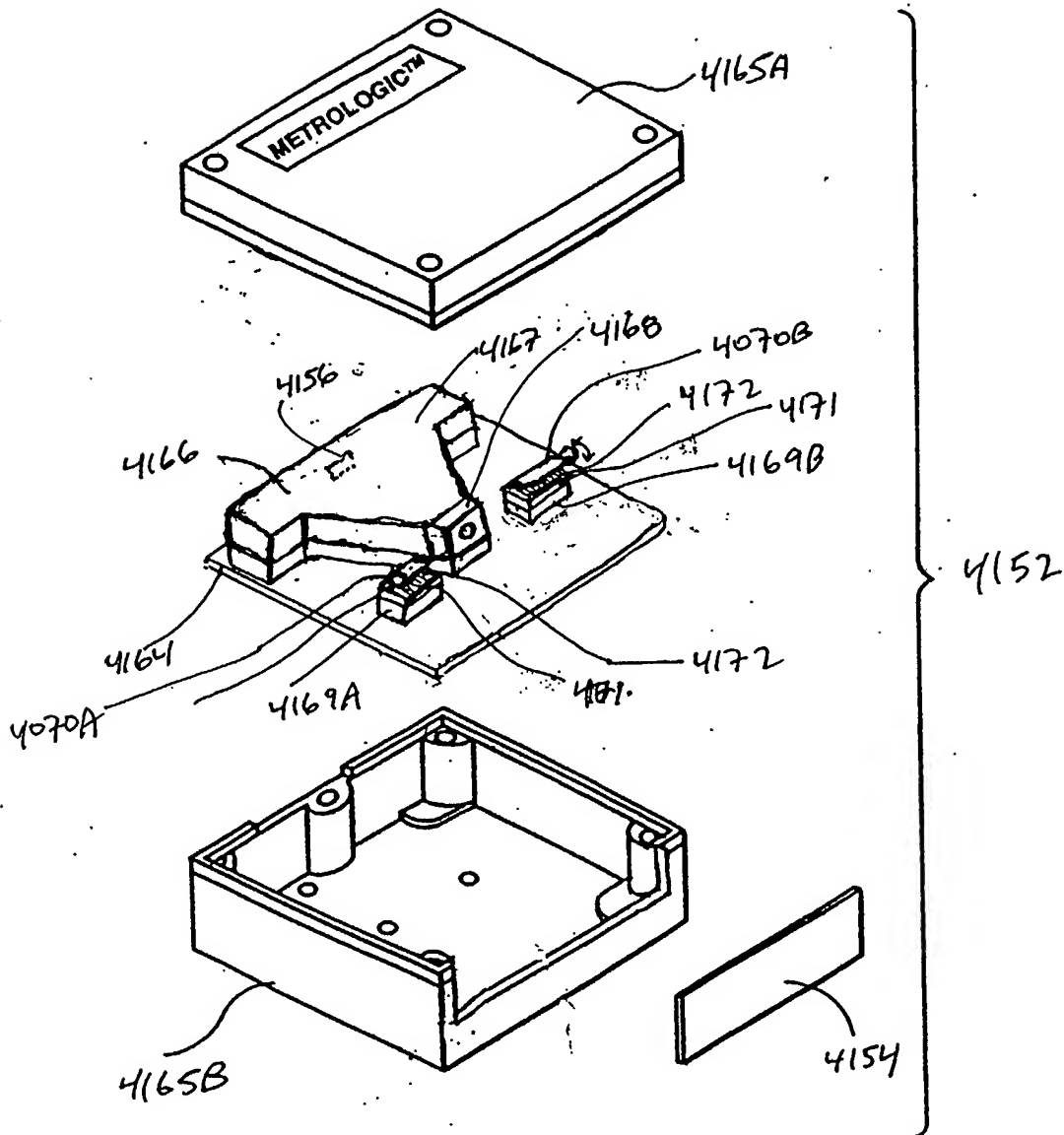
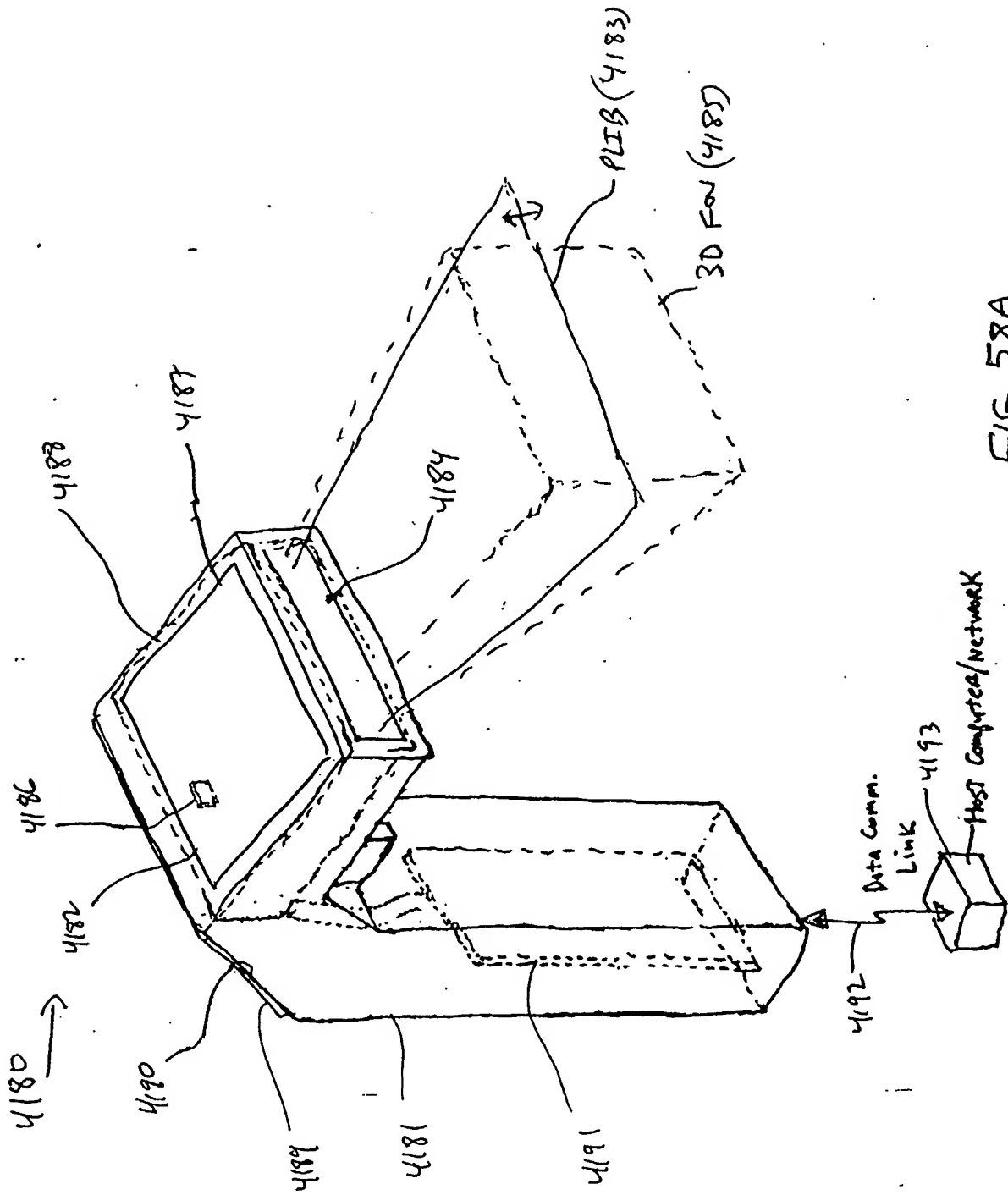


FIG. 57B

Phase only LCR
PM panel

Fig 1F8F-86

344/385



345/385

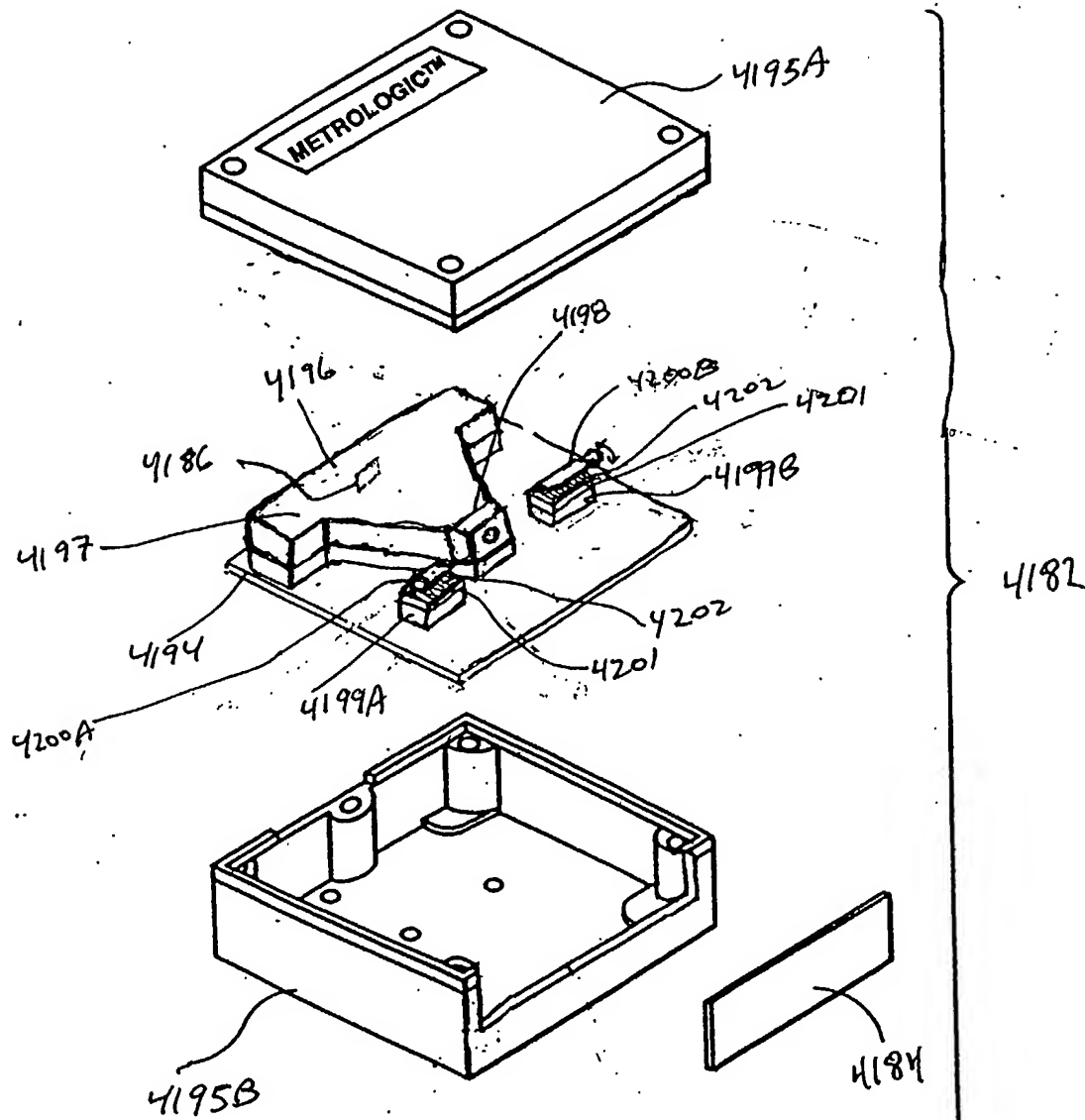


FIG. 58B

115 optical shield
Fig. 1714A-14B

346/385

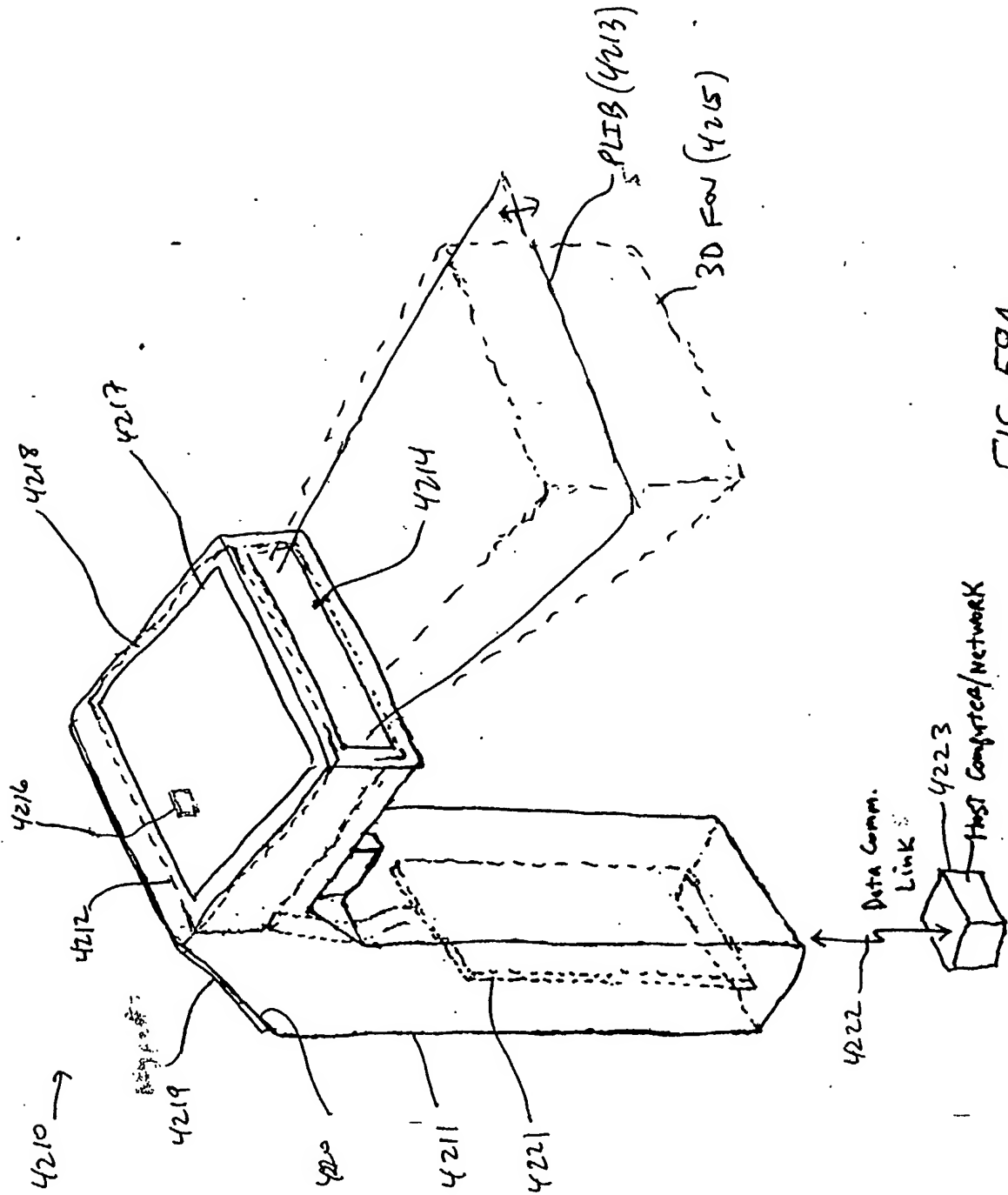


FIG. 59A

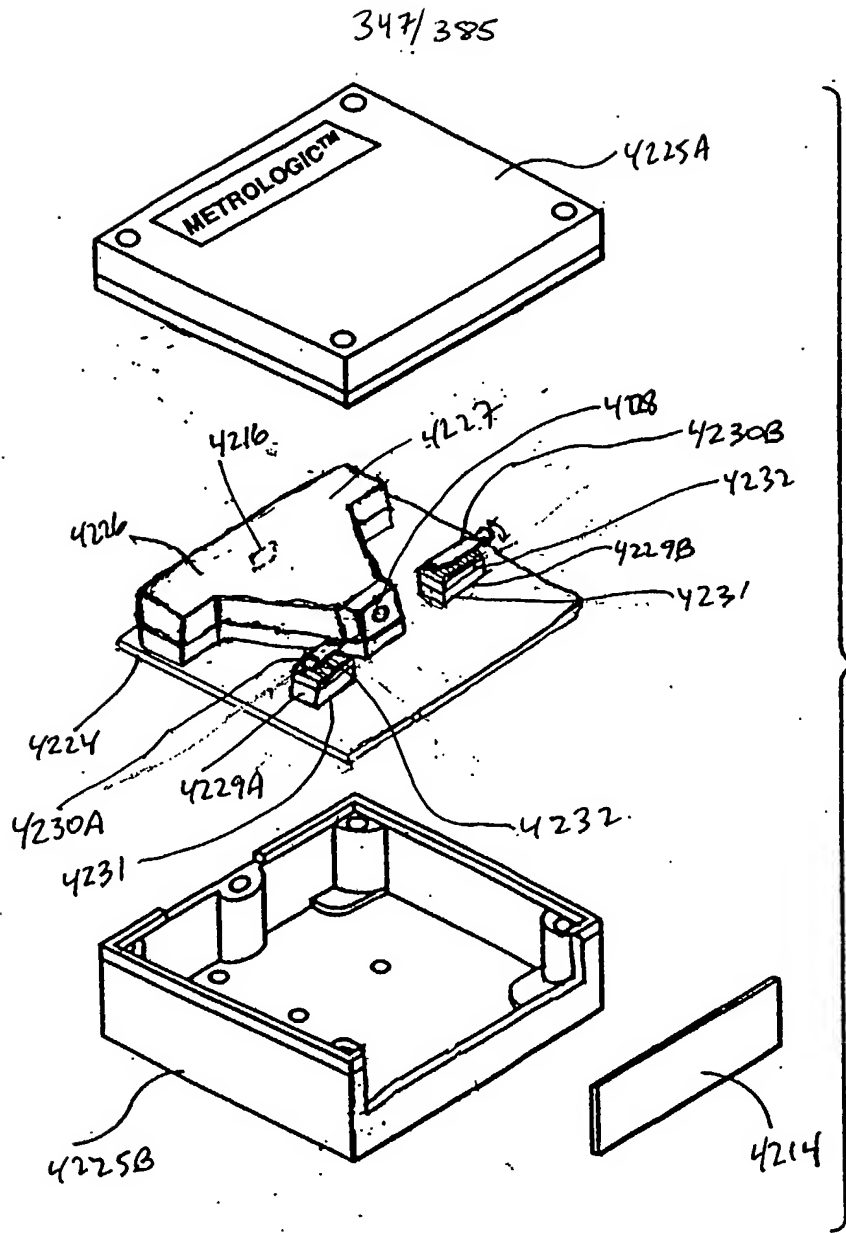


FIG. 59B

MLL
Fig. 15A-15B

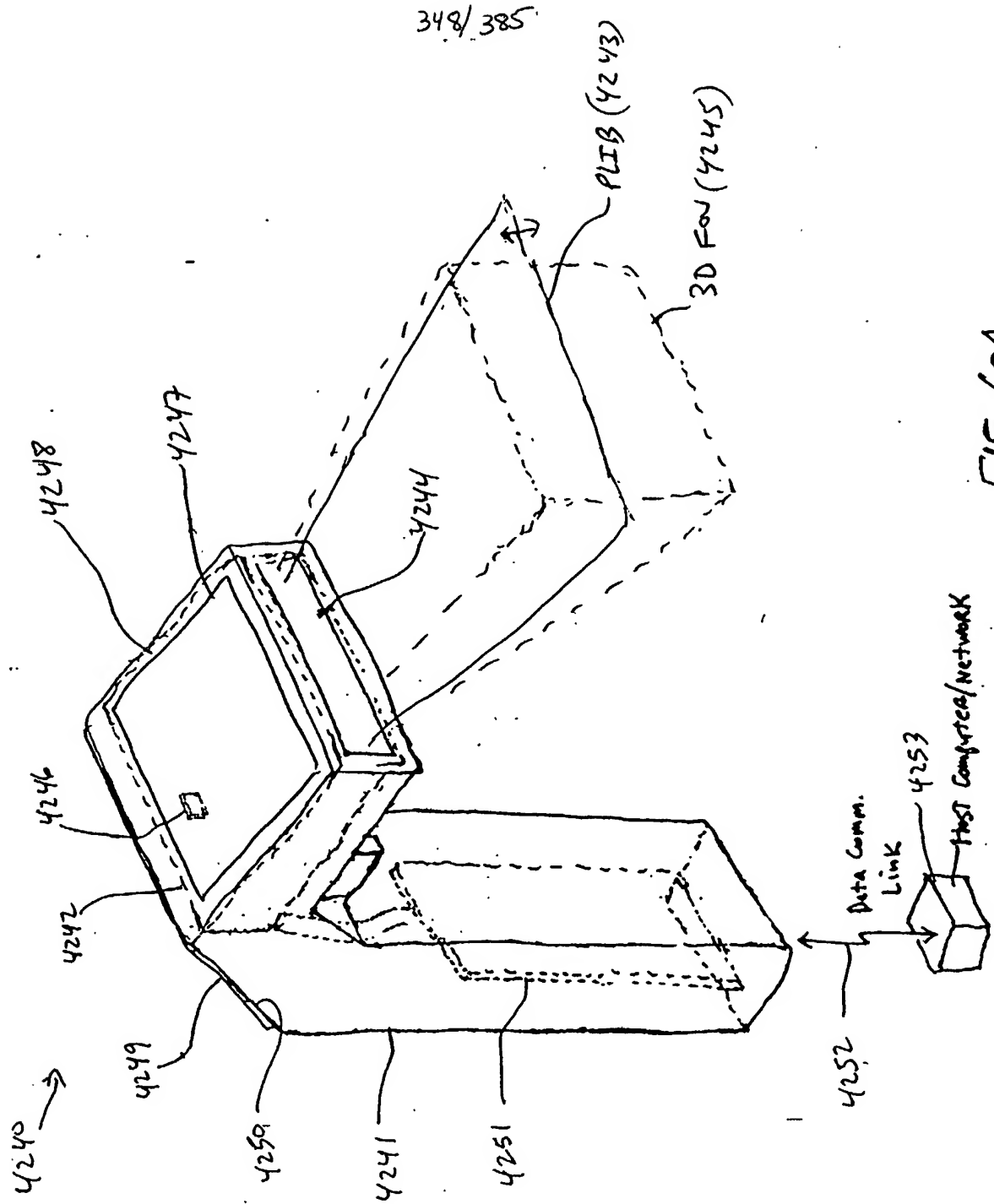


FIG. 60A

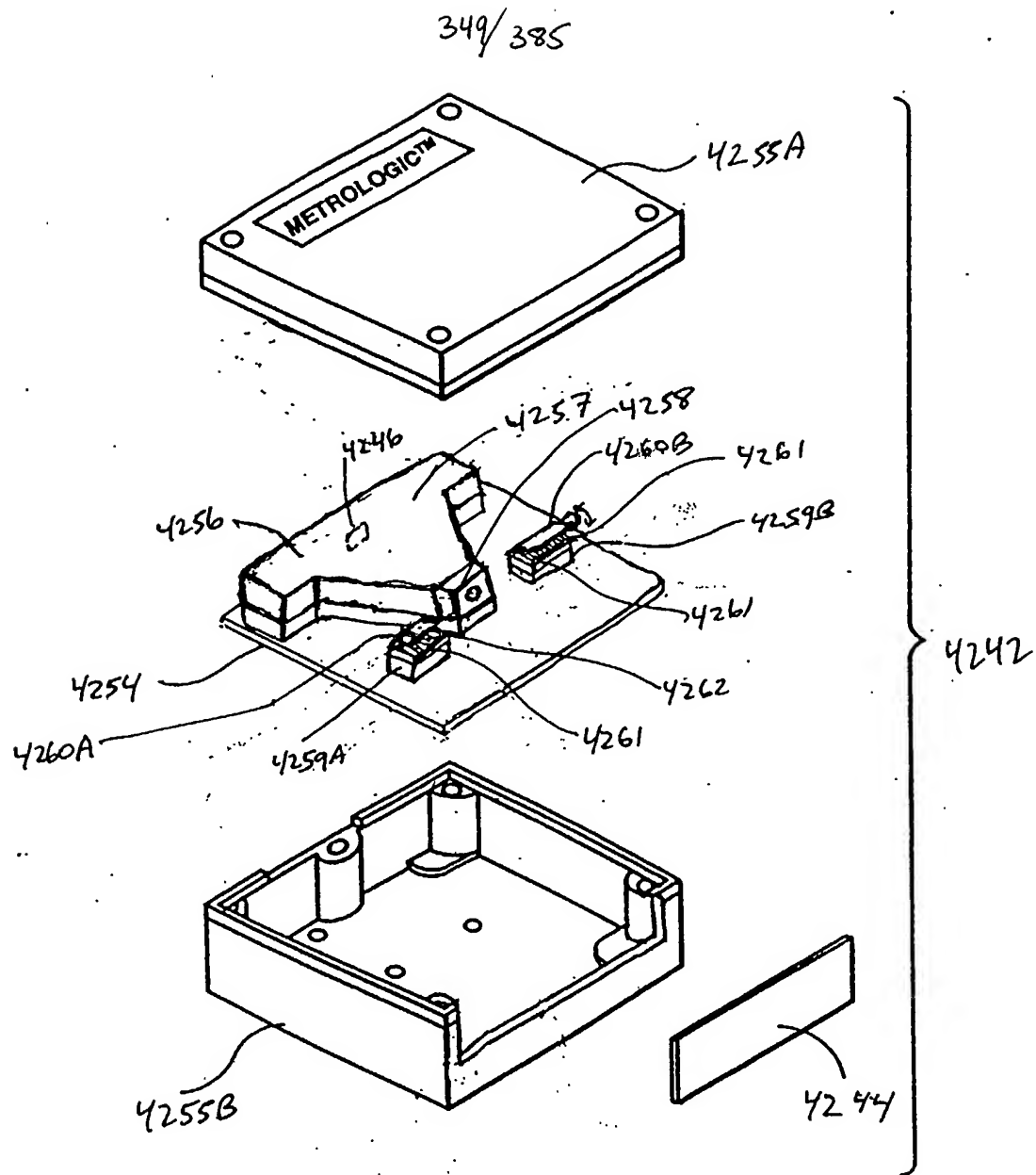


FIG. 60B

Bthalon (Tang. phase mod.)
Fig. 1 I 17A-17B

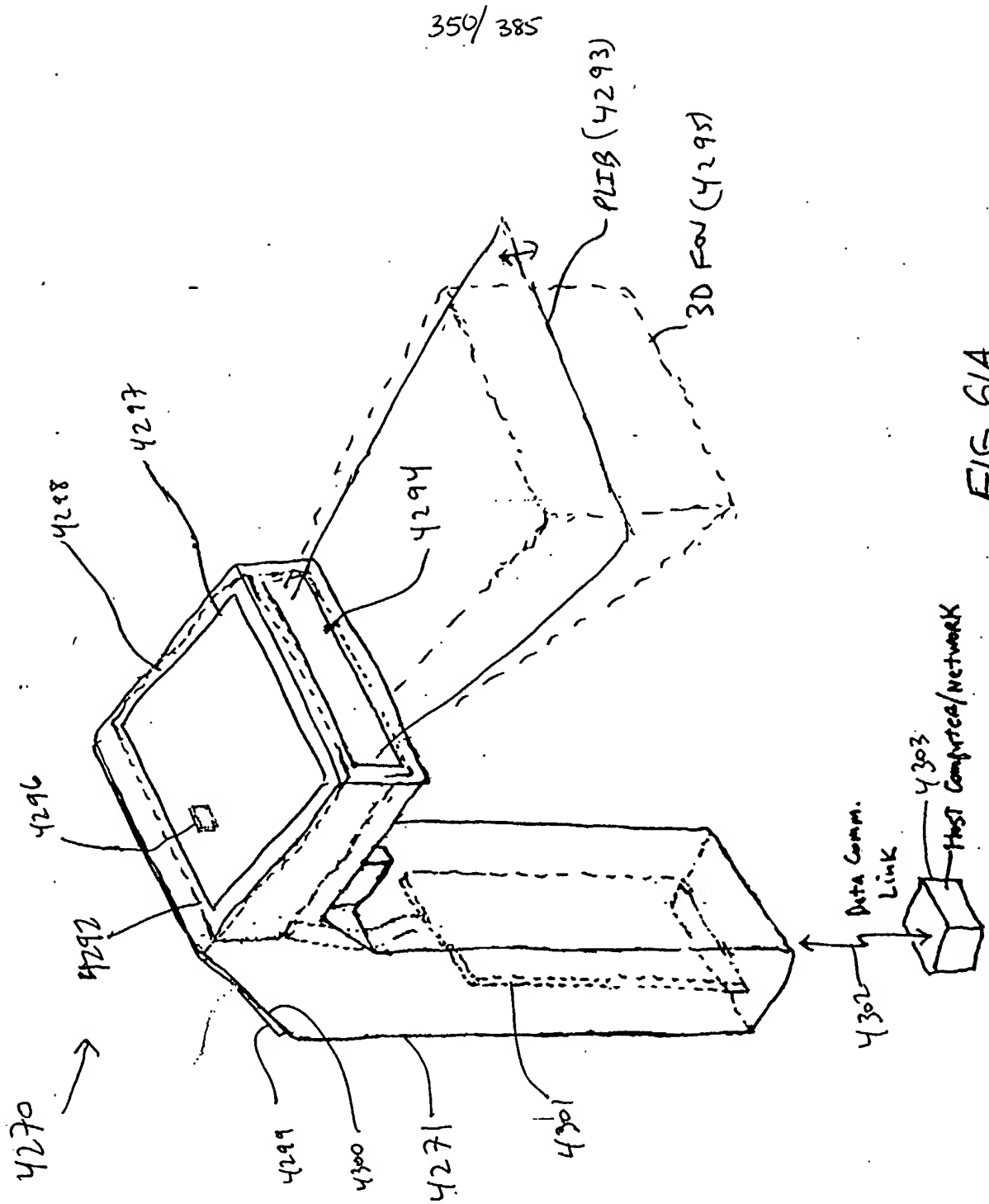


FIG. 61A

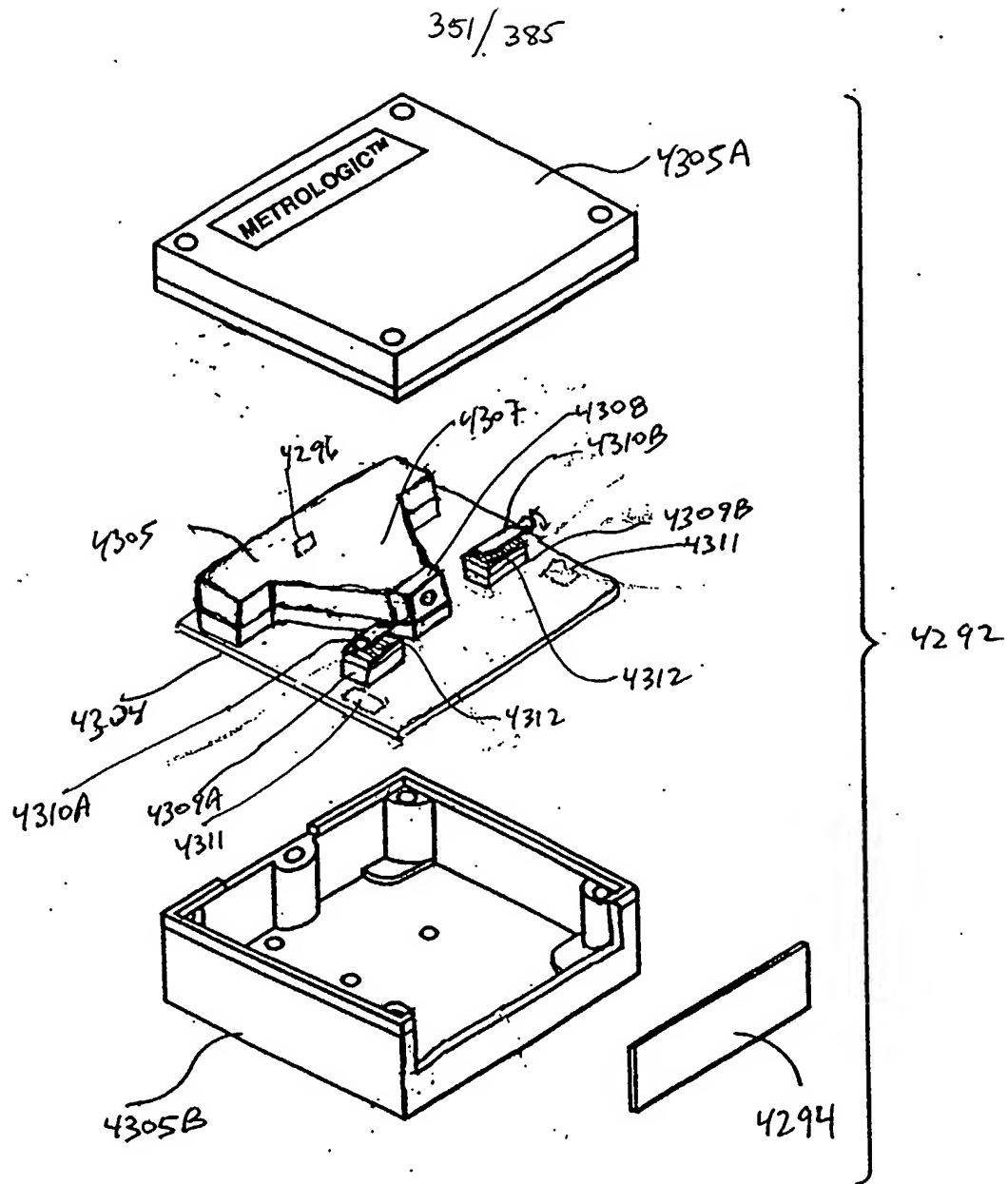


FIG. 61B

mod. hugging

Fig. 1A-19B

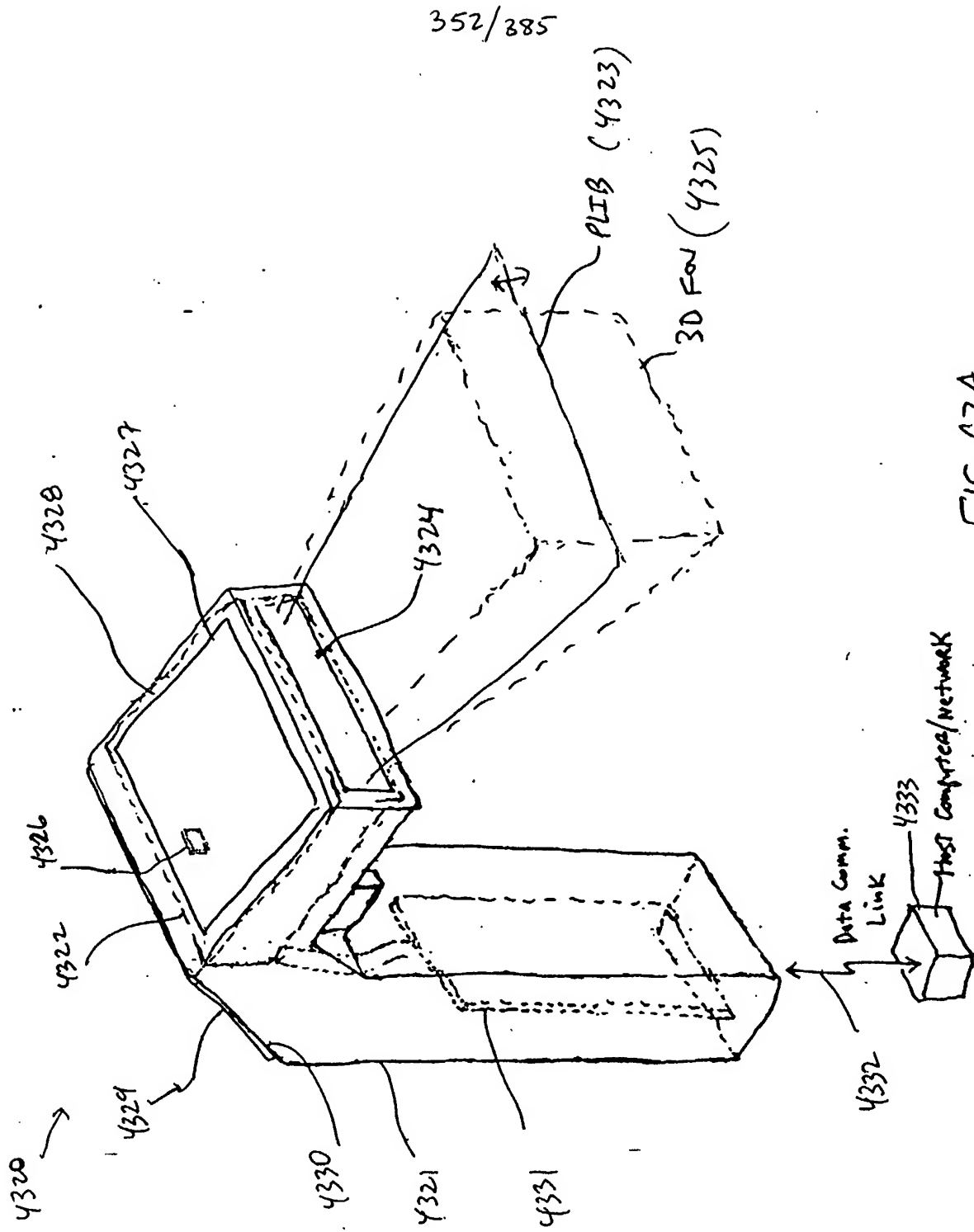


FIG. 62A

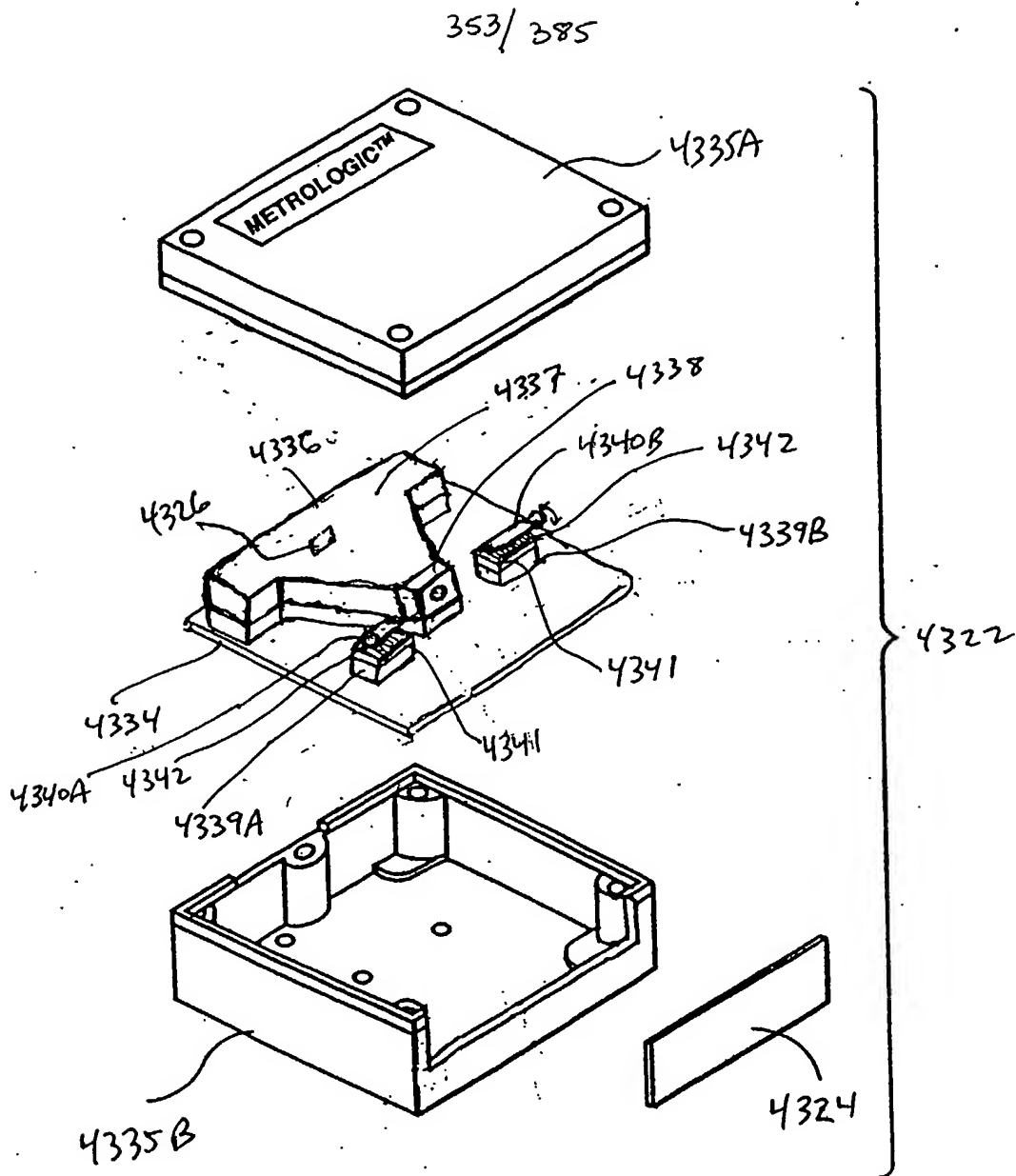
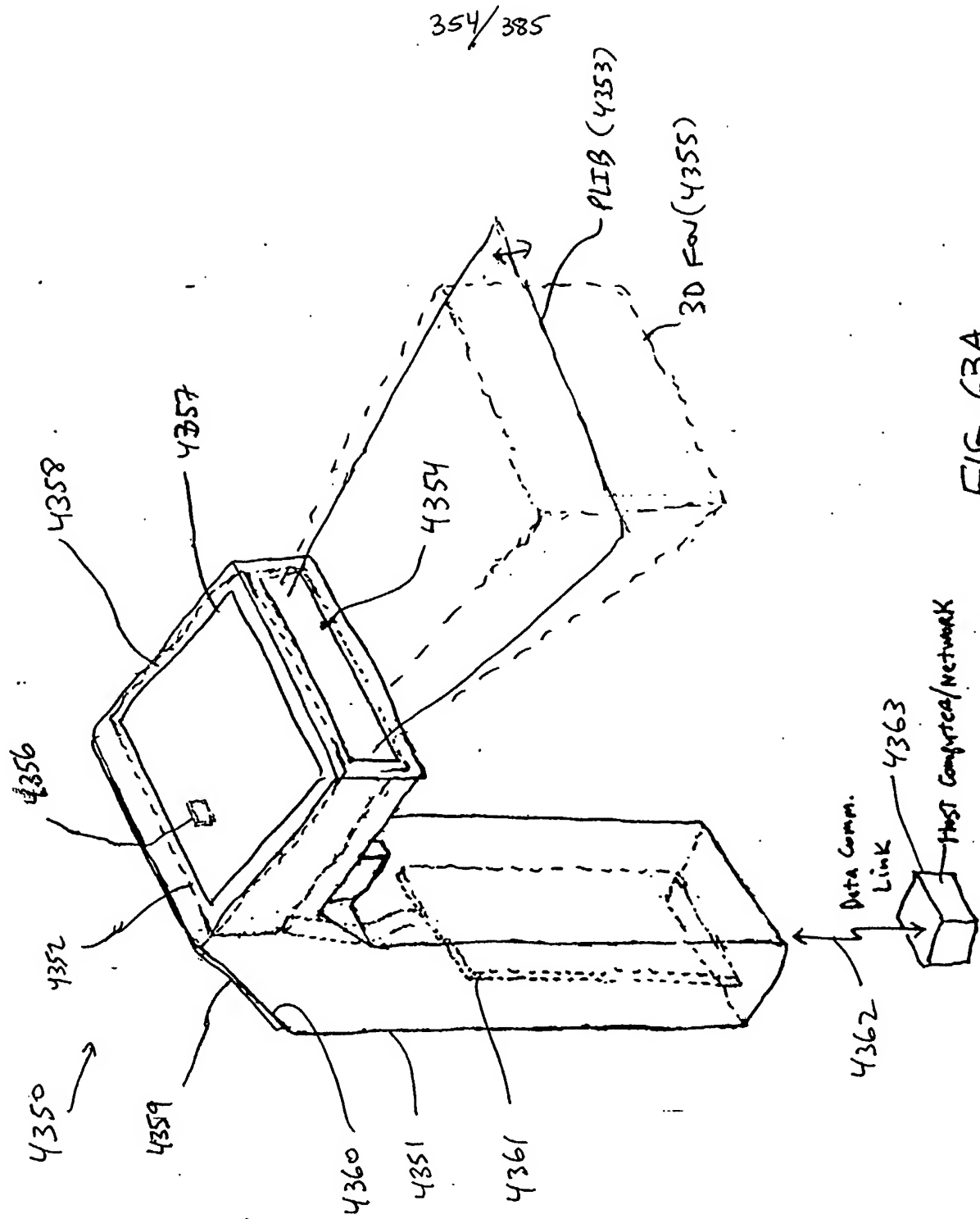


FIG. 62B

measuring
spot intensity
mod. panel

Fig. 1F21A-21D



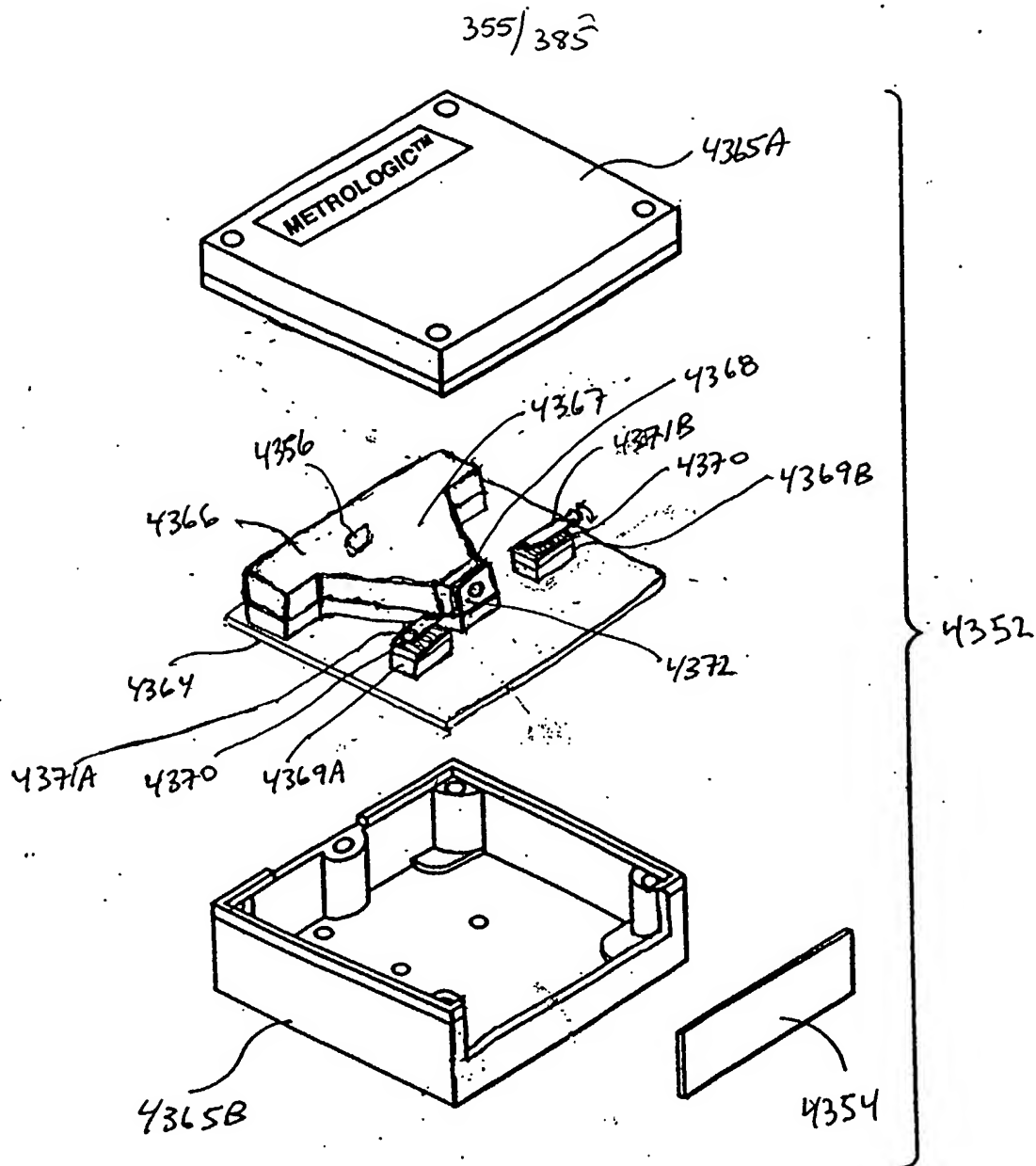


FIG. 63B

ED of.
Mechanical Refitting IPIs
Fig 1E
23A-23B

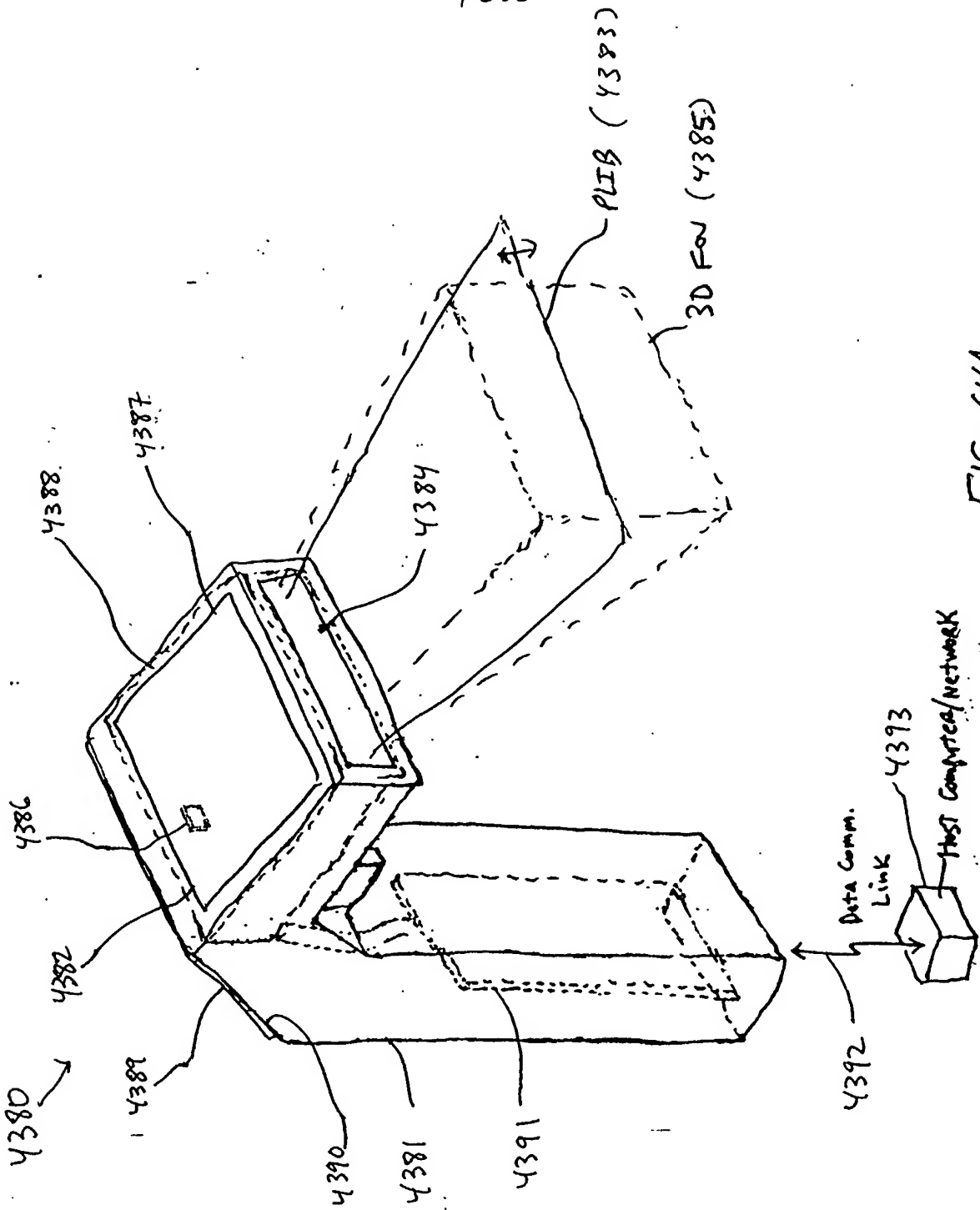


FIG. 64A

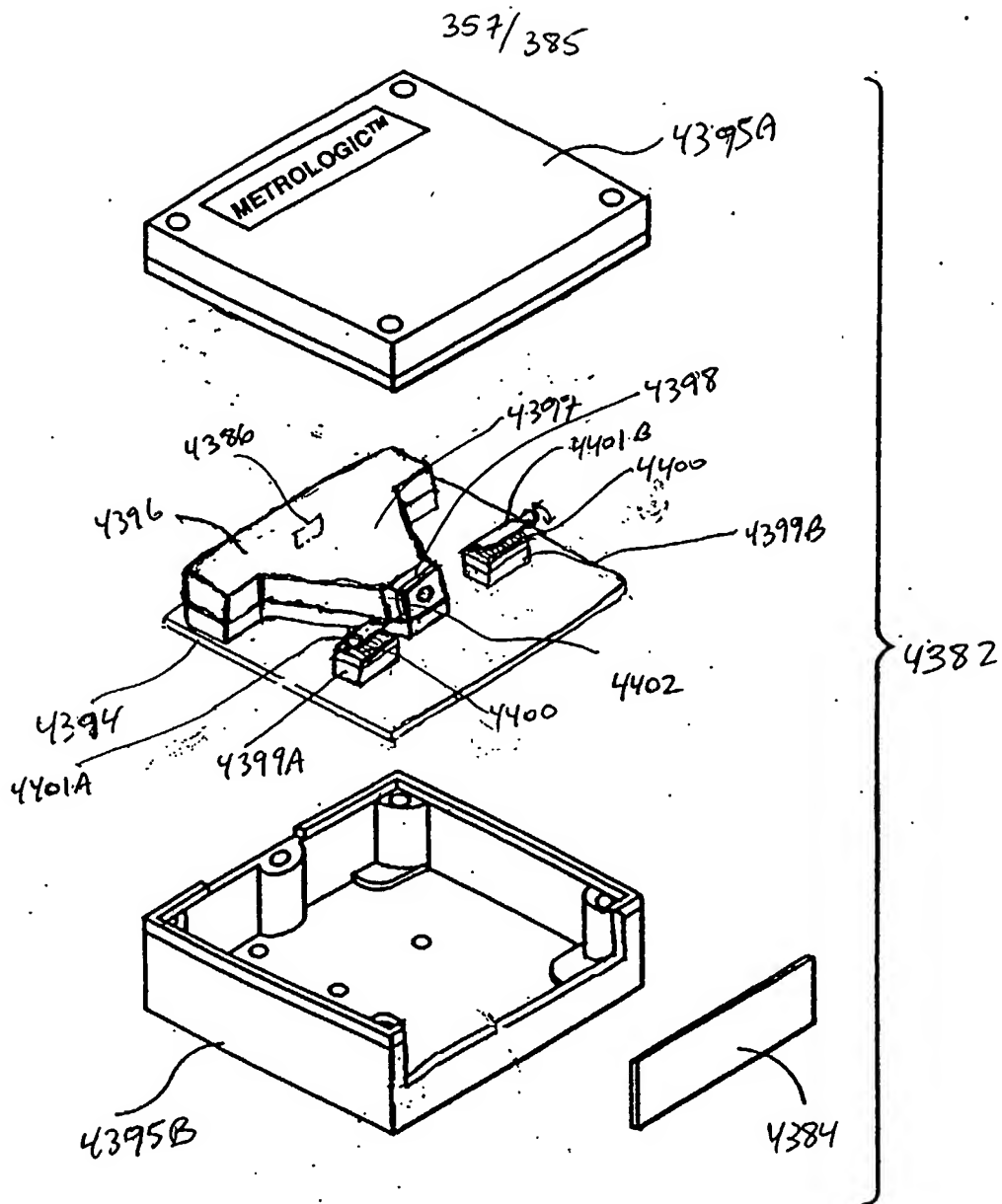


FIG. 64B

* E-optical
Shutter Before
IP Lens
Fig. 1E24A

358/285

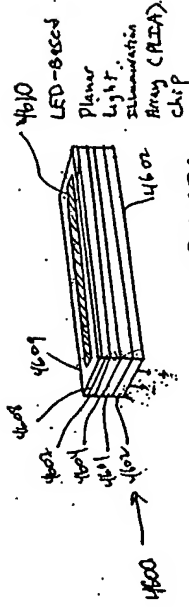


FIG. 67A

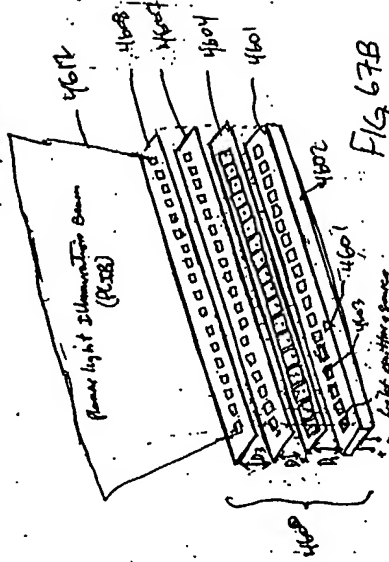


FIG. 67B

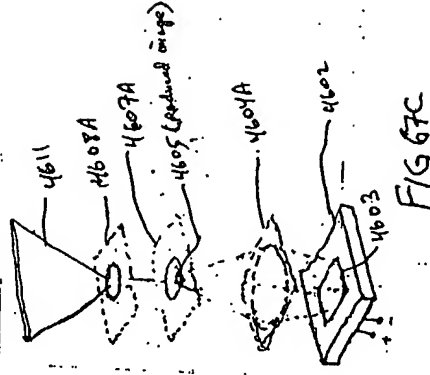


FIG. 67C

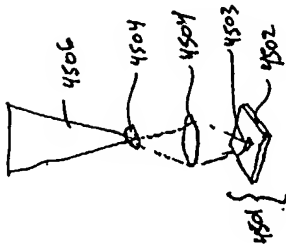


FIG. 65B

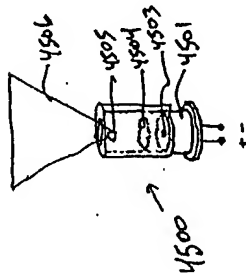


FIG. 65A

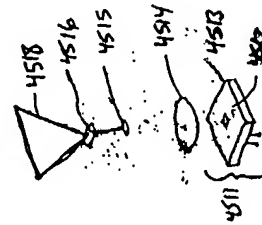


FIG. 66B

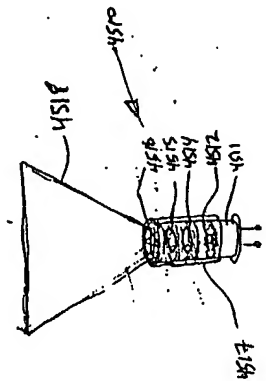


FIG. 66A

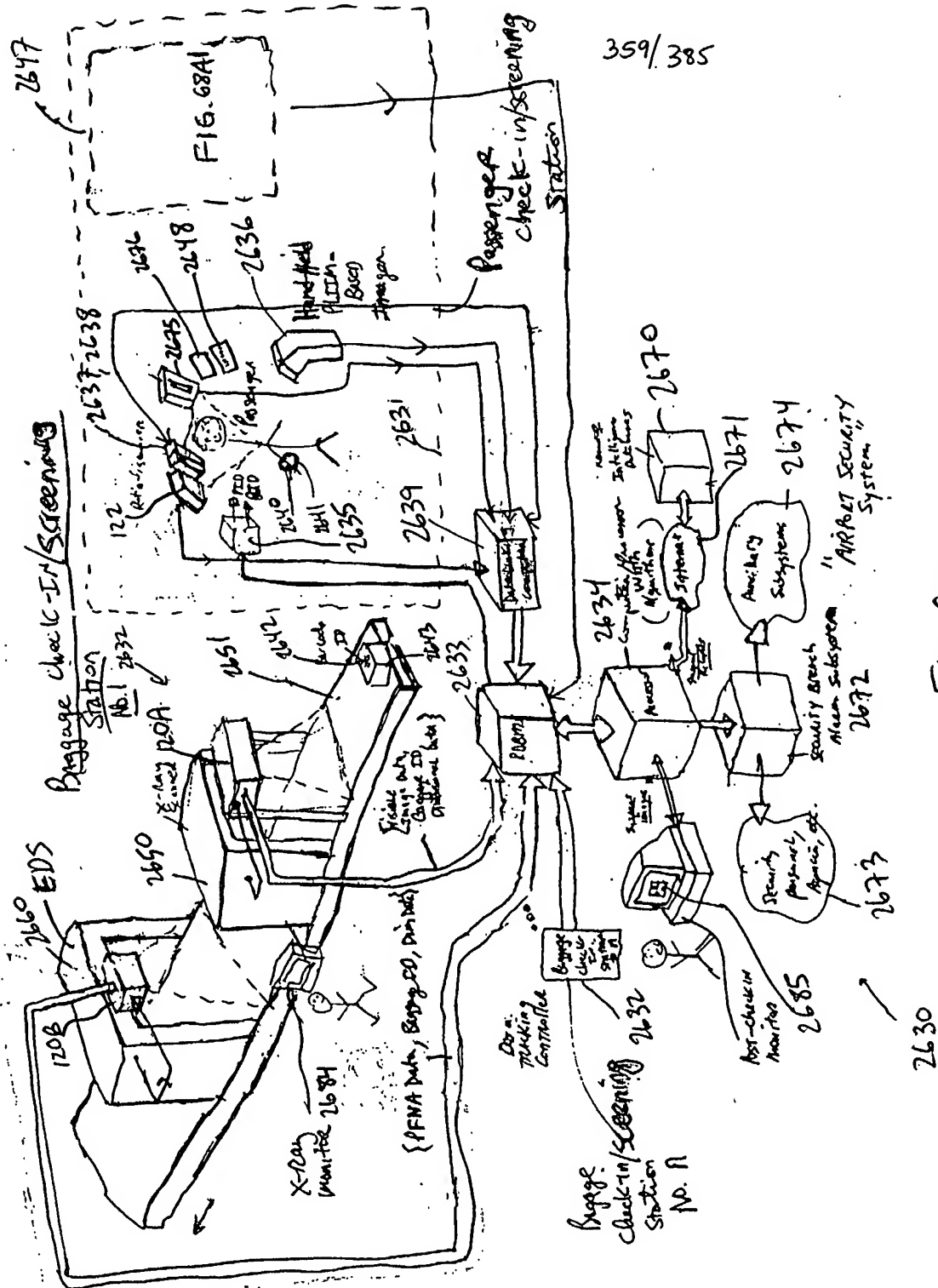


FIG. 68.

360/385

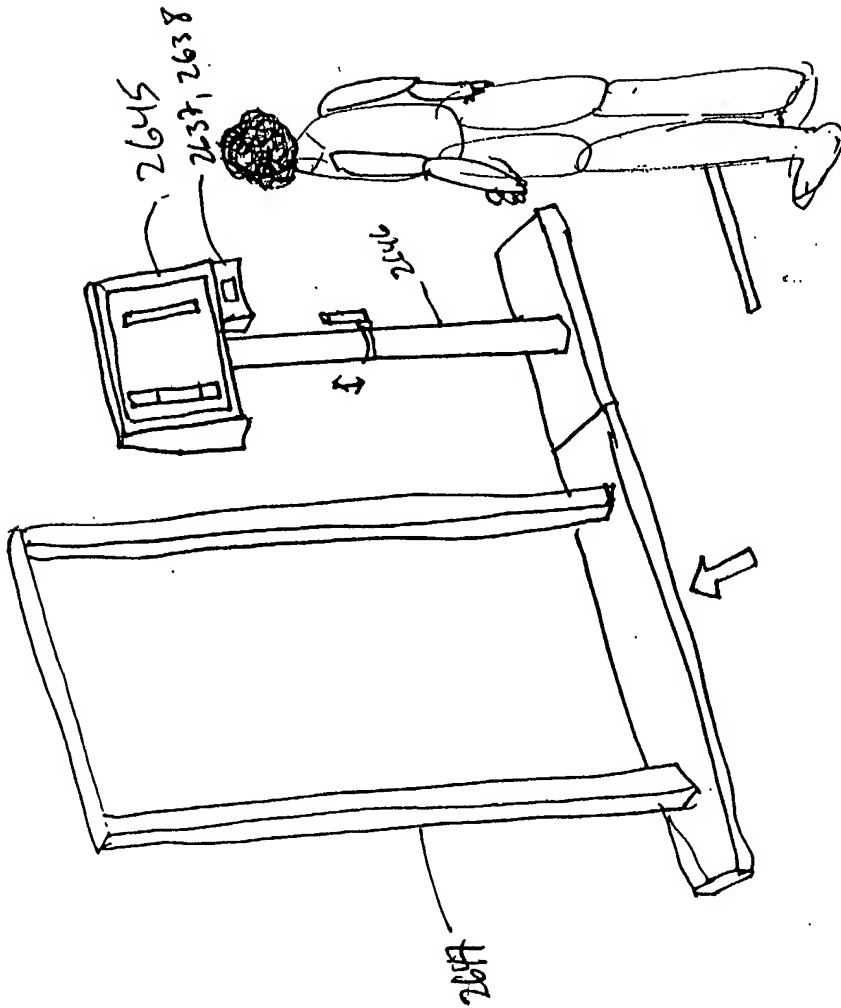


FIG. 68A

361/385

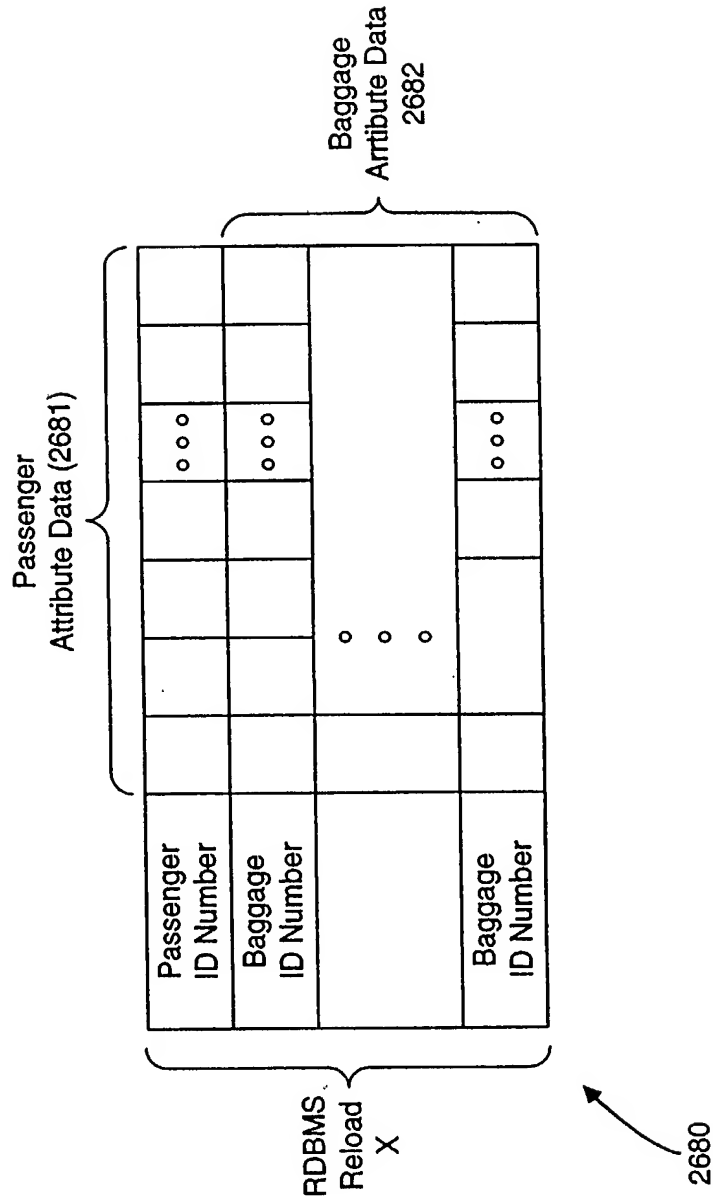


FIG. 68B

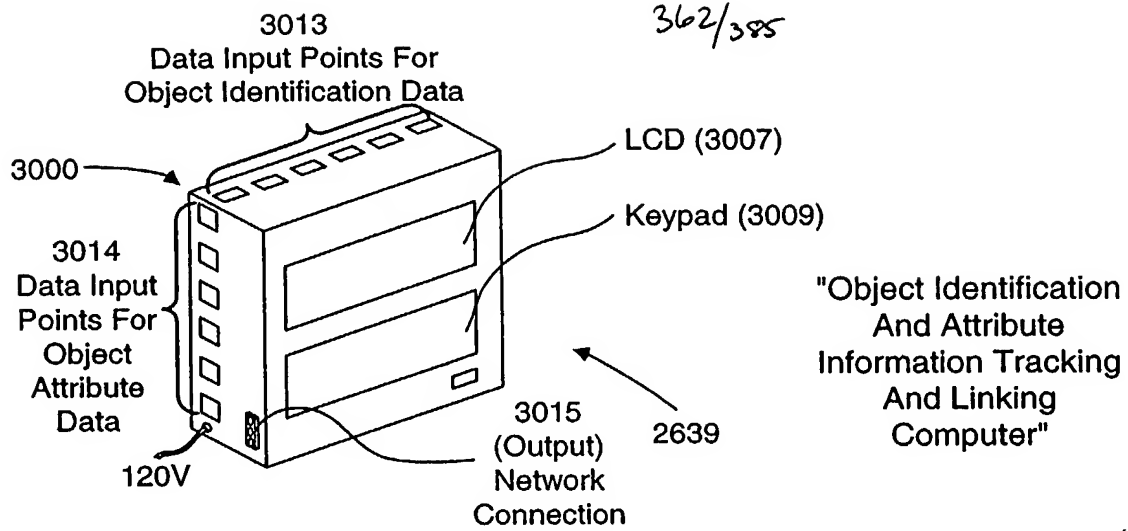


FIG. 68C1

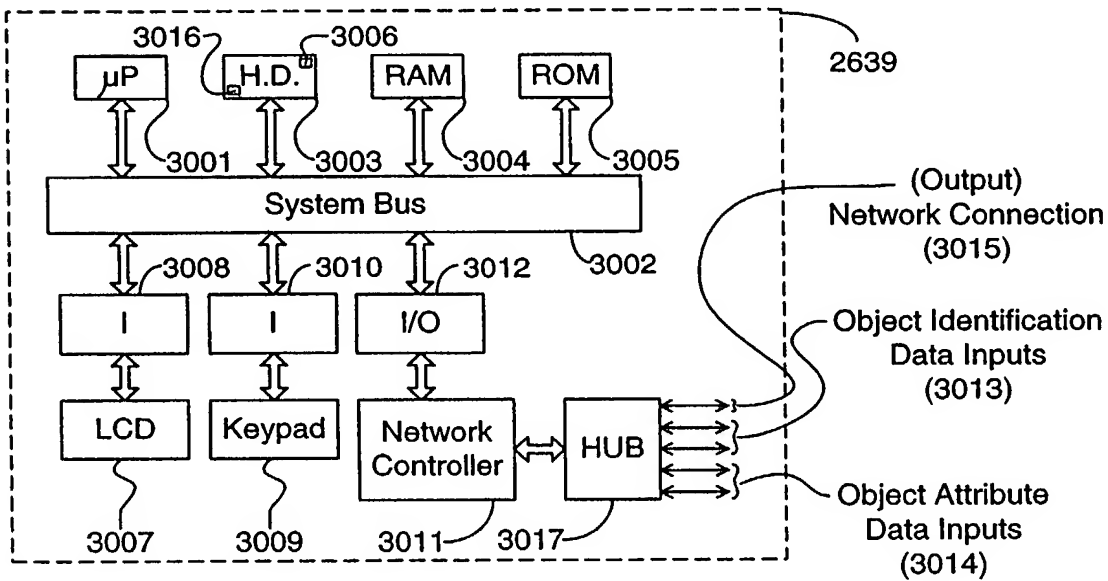


FIG. 68C2

Object Identification And Attribute Information Tracking And Linking Computer System.

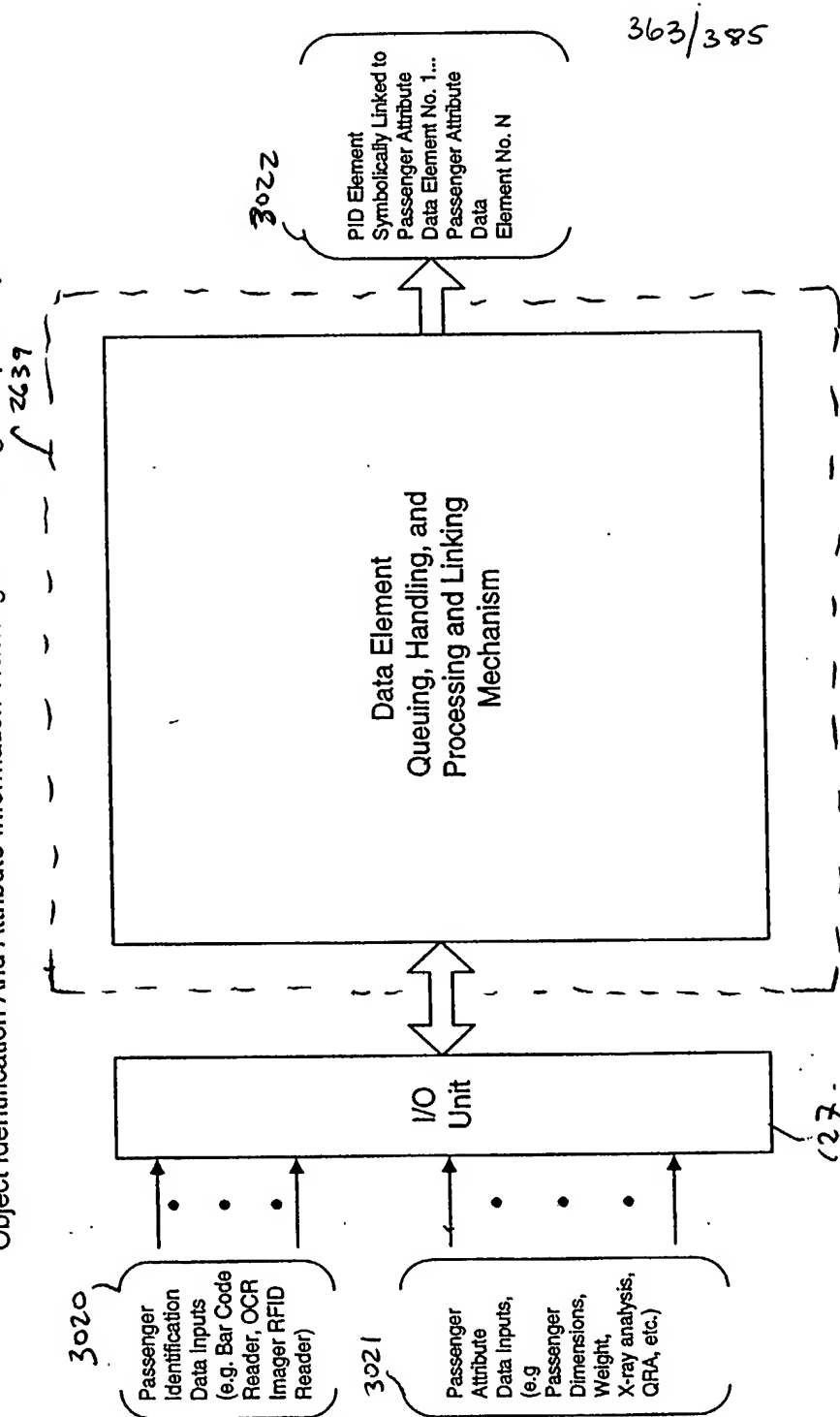


FIG. 68C3

Data Element Queuing, Handling, and Processing Subsystem Employed In The Object Identification And Attribute Acquisition System Of The Present Invention. (131)

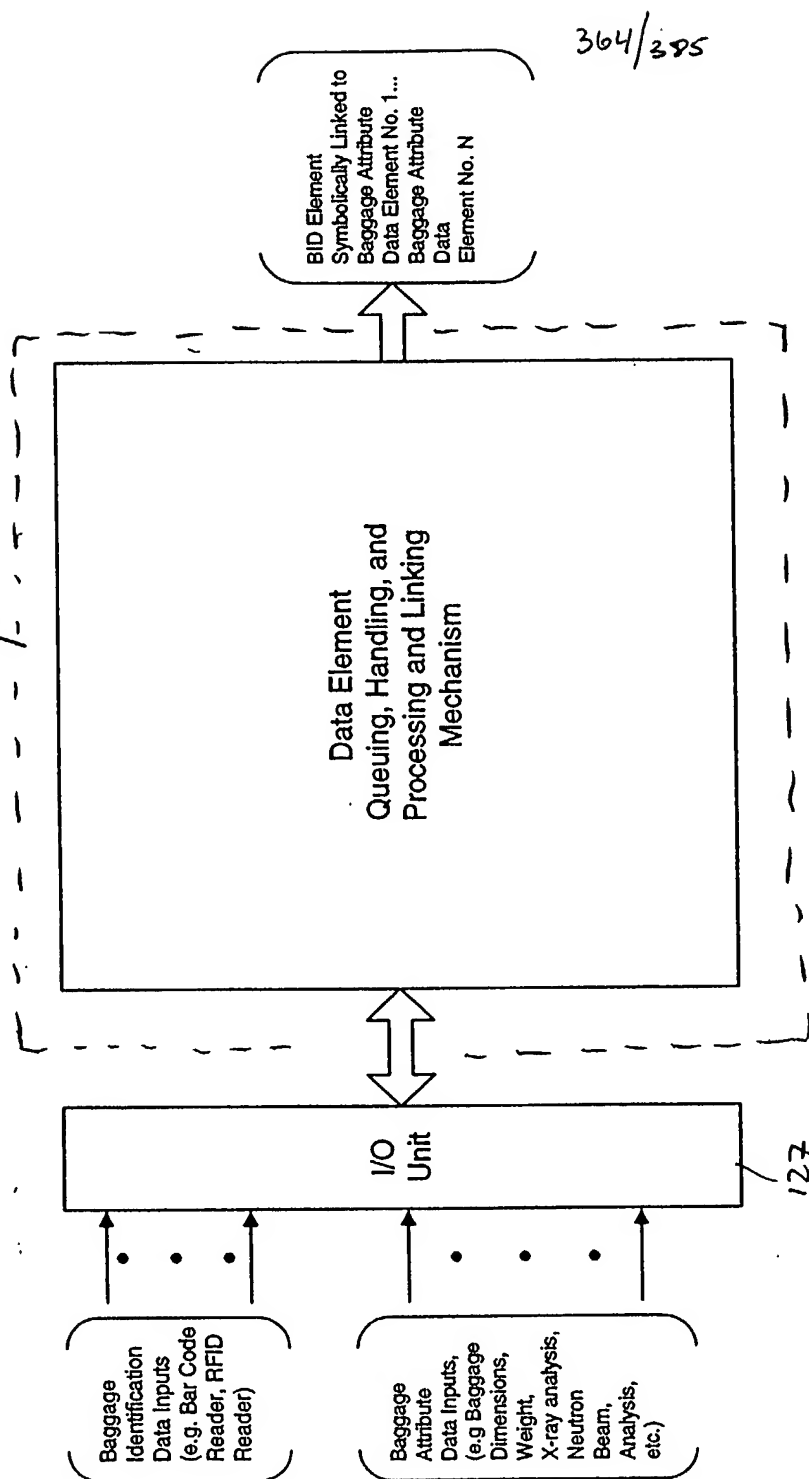


FIG. 68C4

365/385

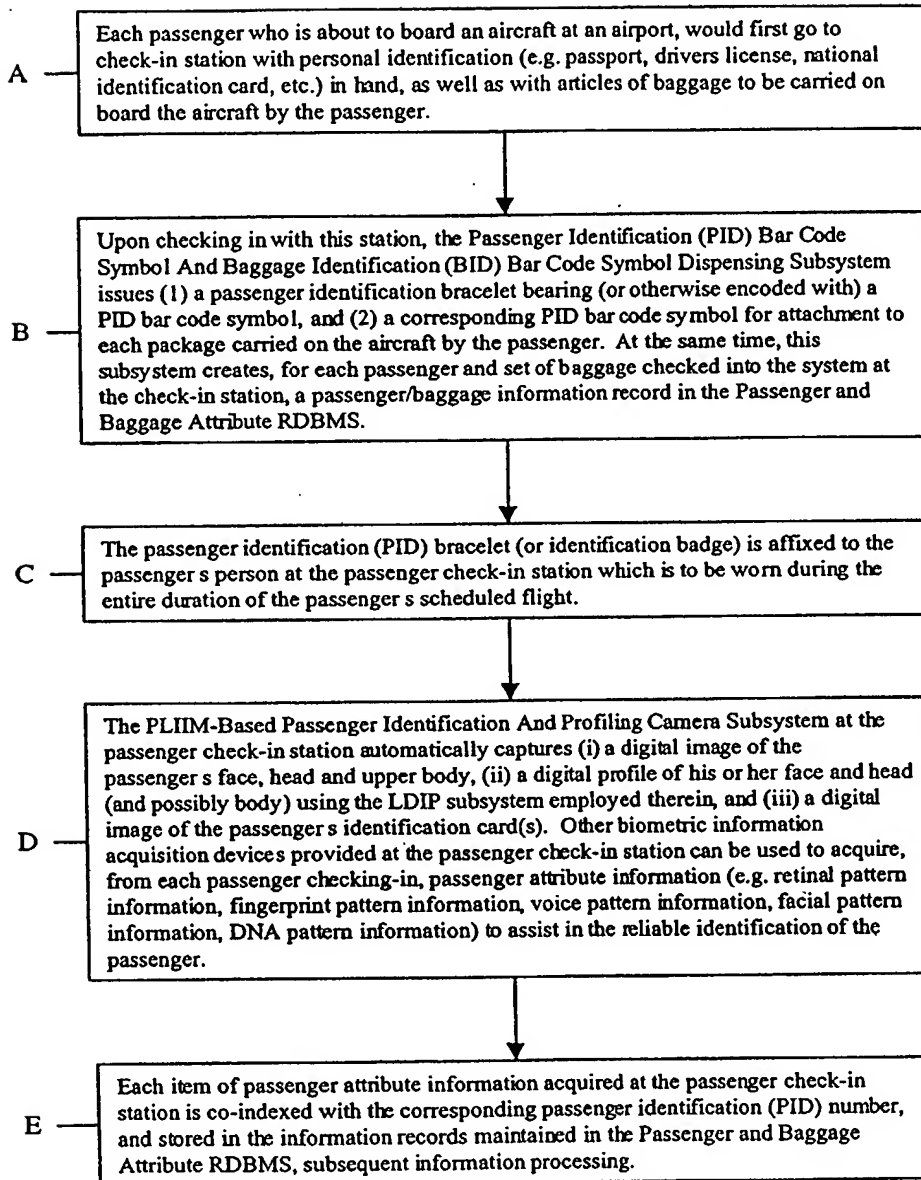


FIG. 68D1

366/385

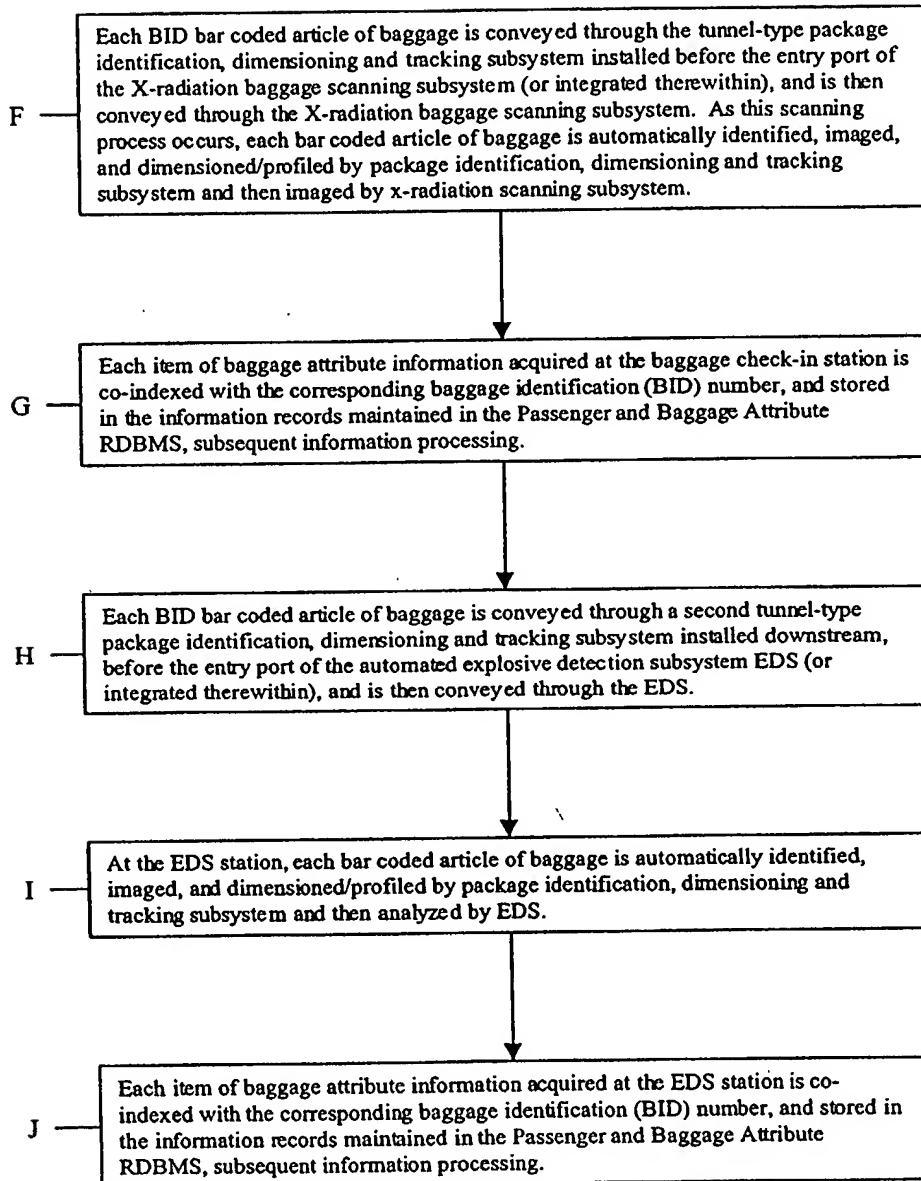


FIG. 68D2

367/385

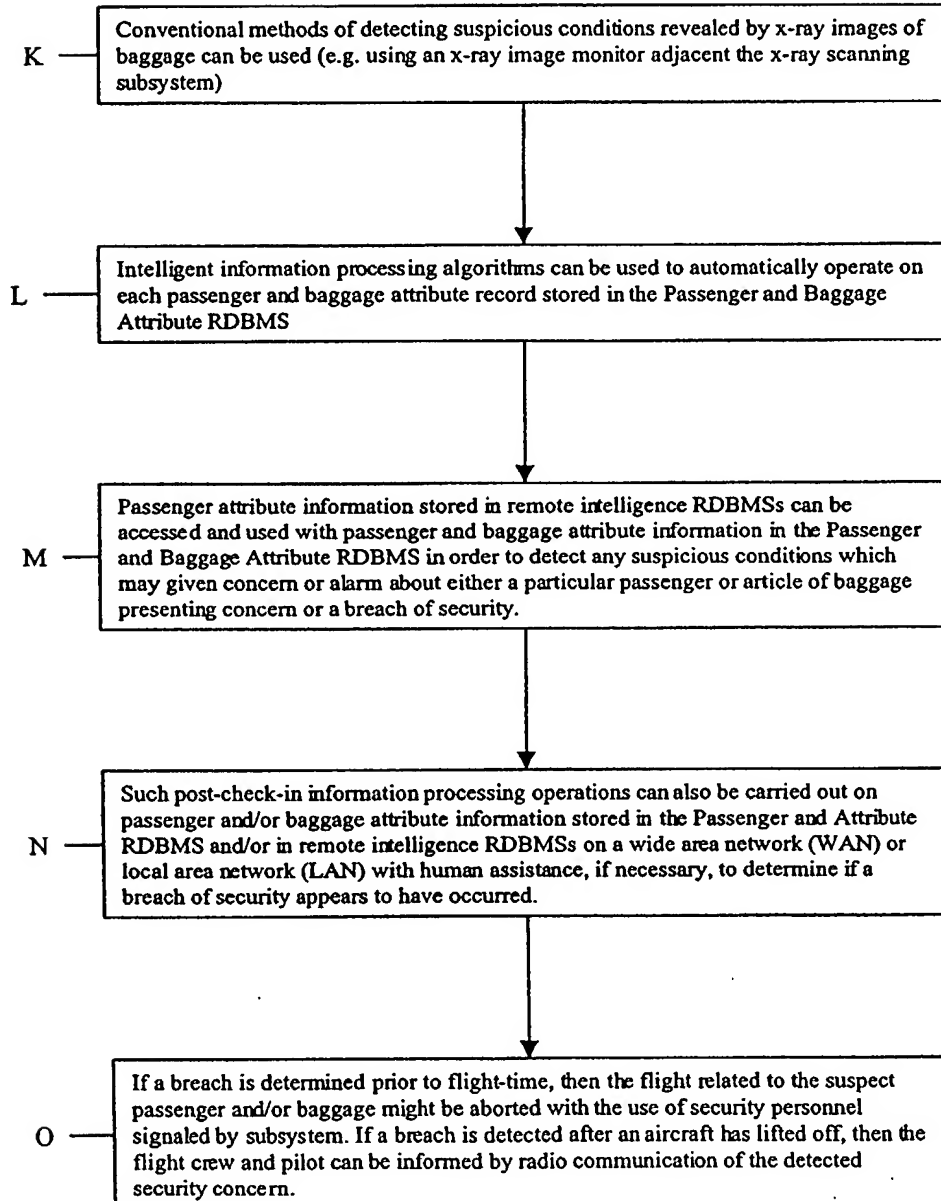


FIG. 68D3

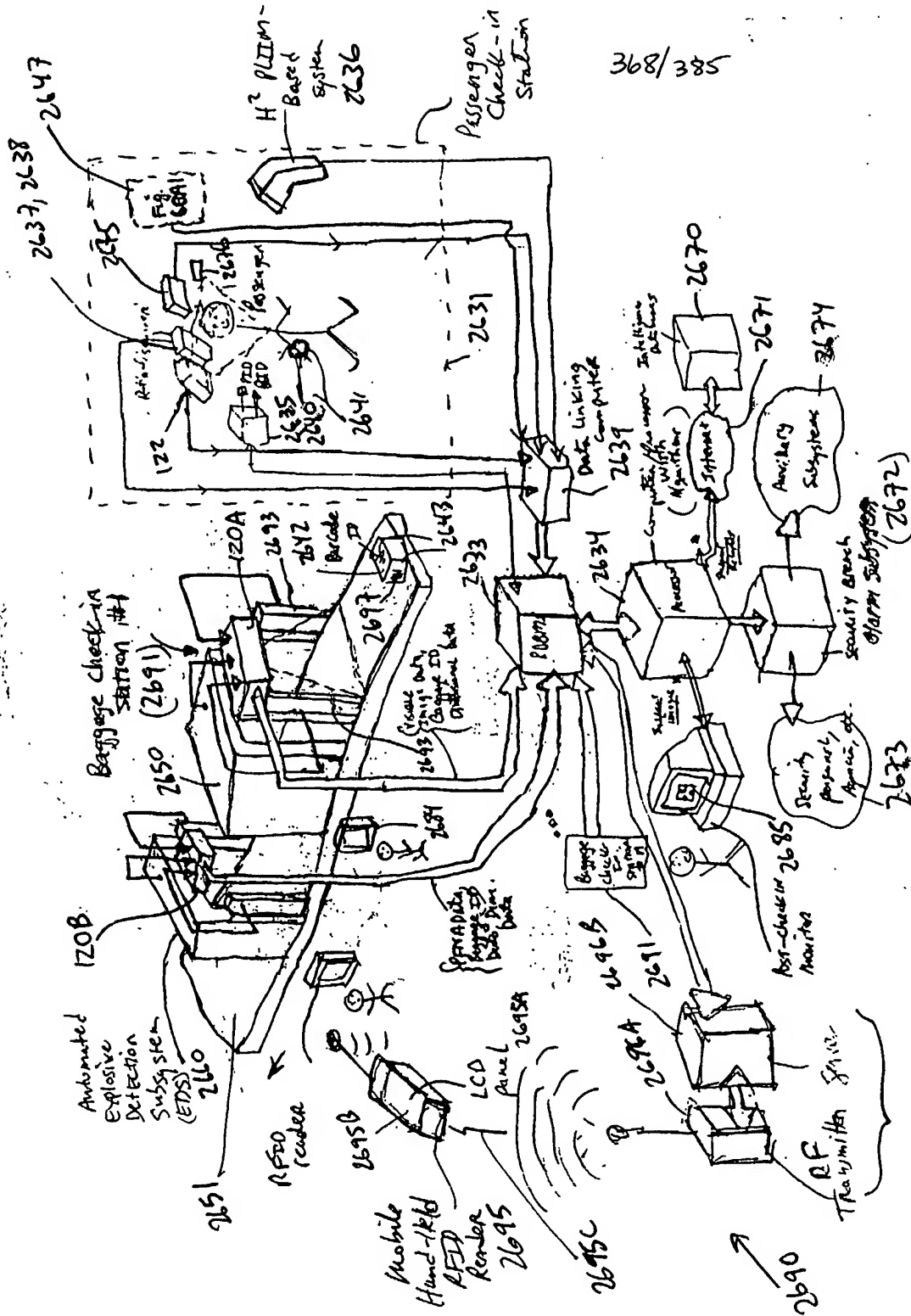


FIG. 69A

2696

369/385

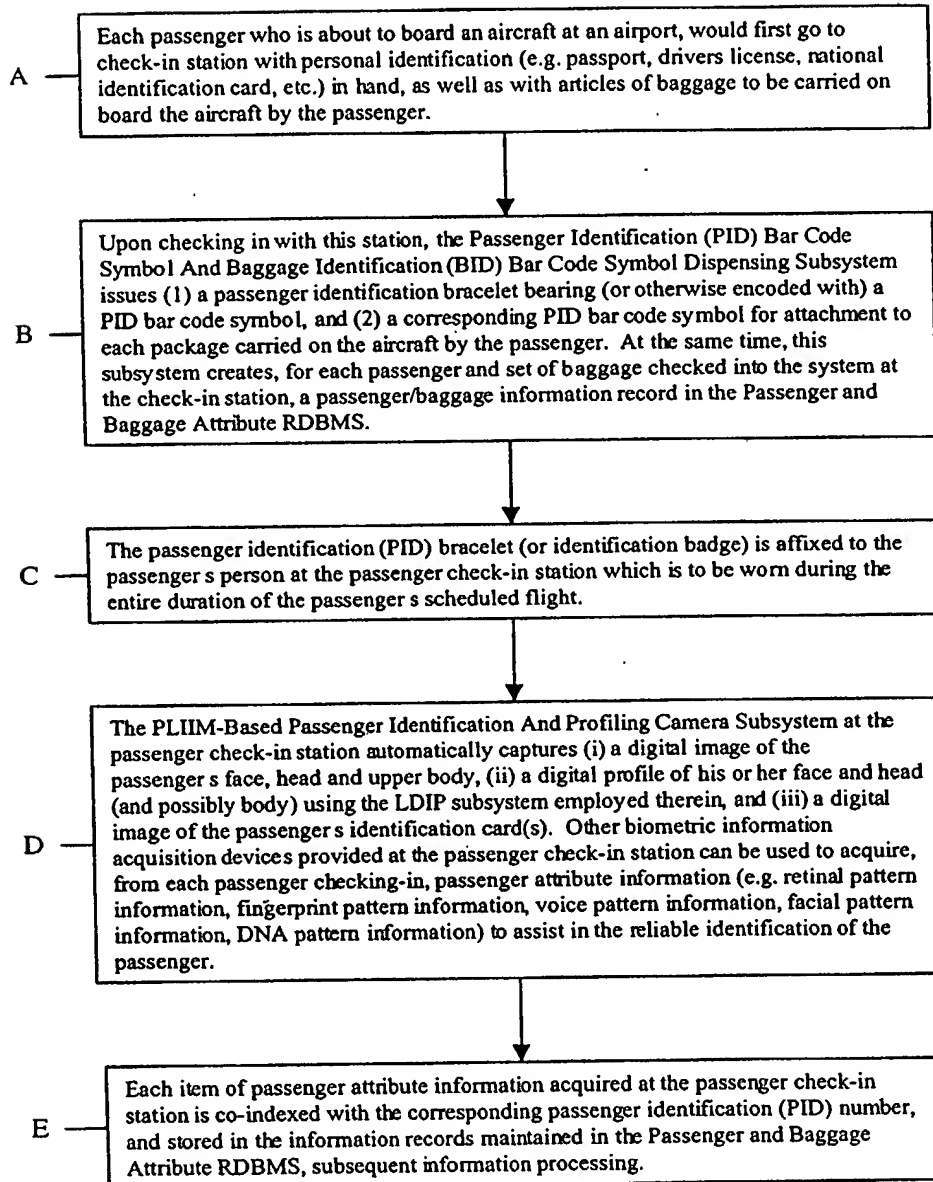


FIG. 69B1

370/395

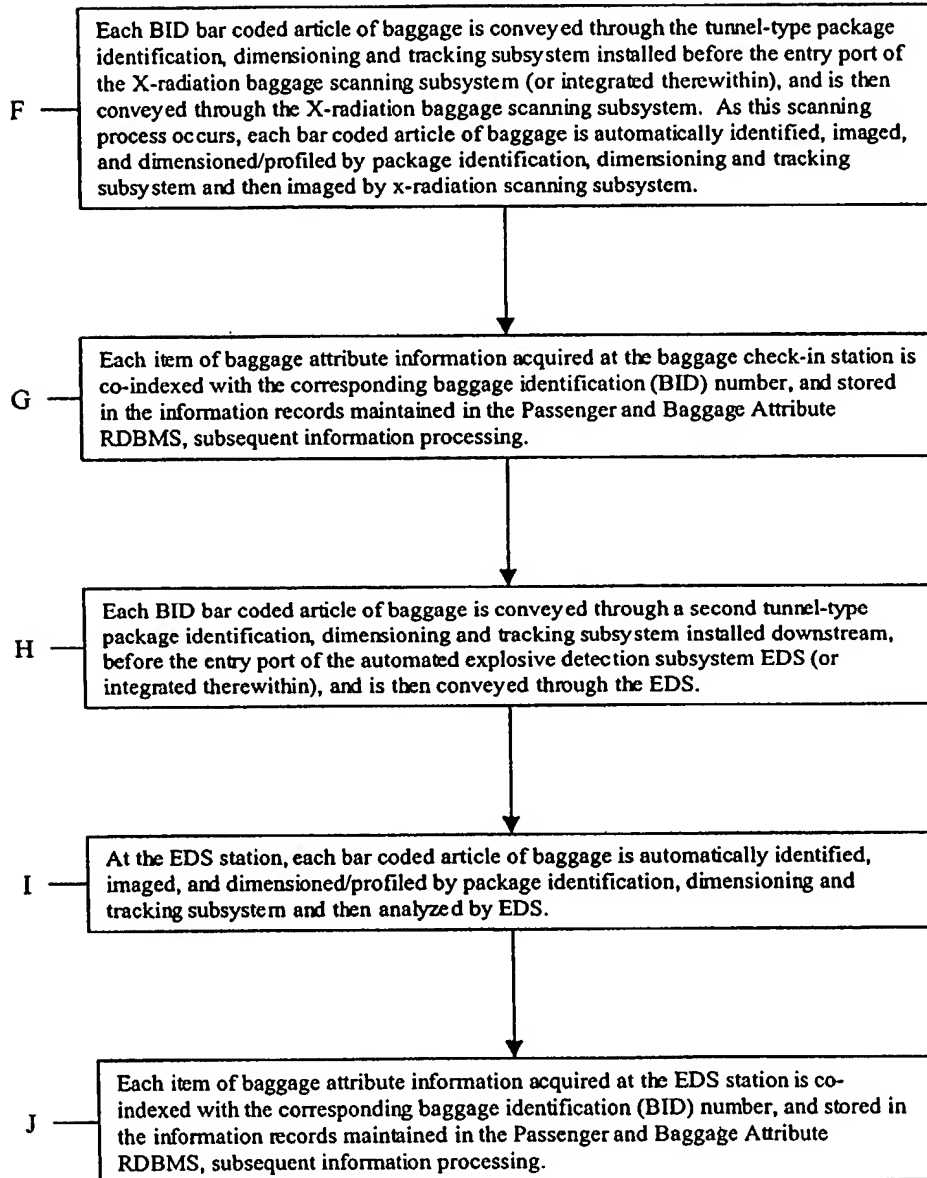


FIG. 69B2

371/385

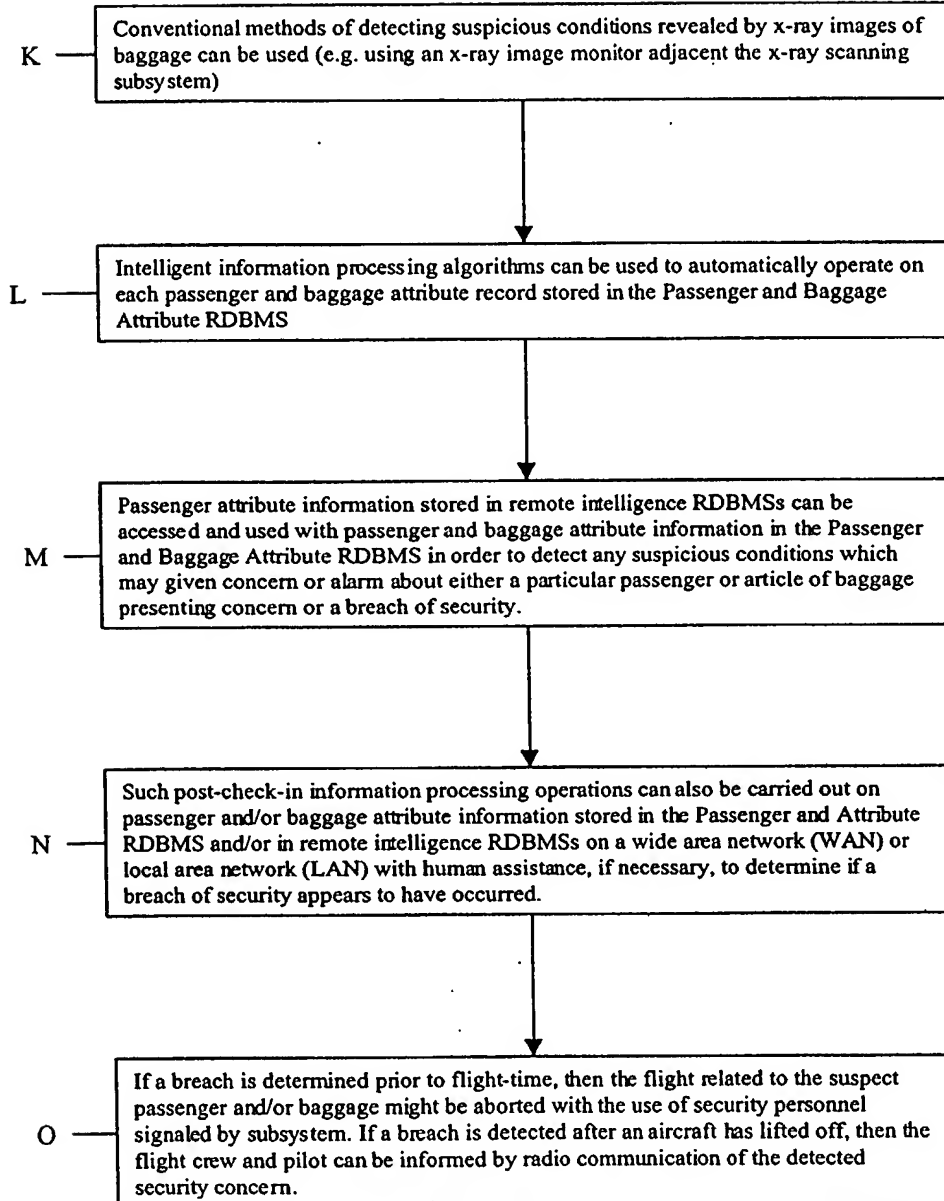


FIG. 69B3

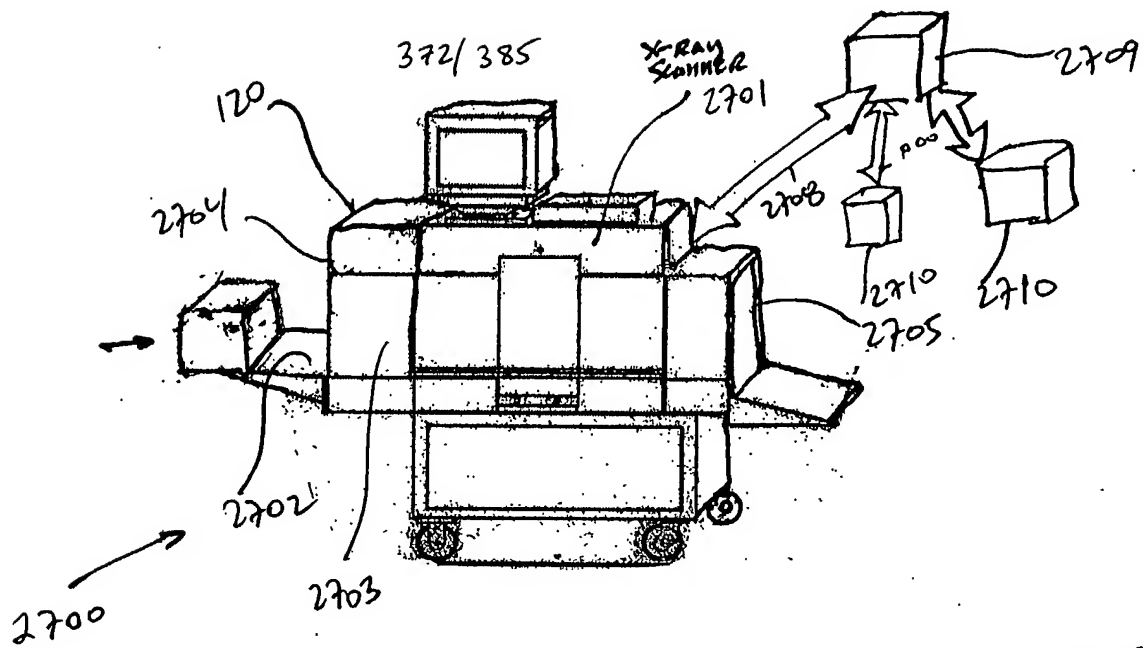
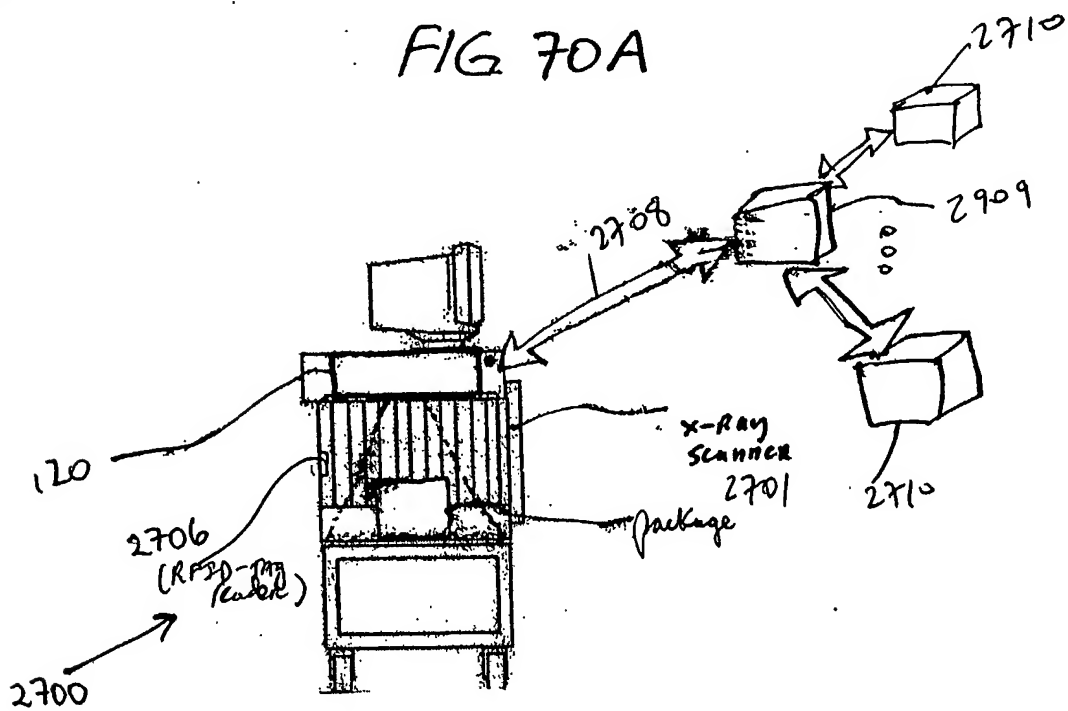


FIG 70A



F/G. 70B

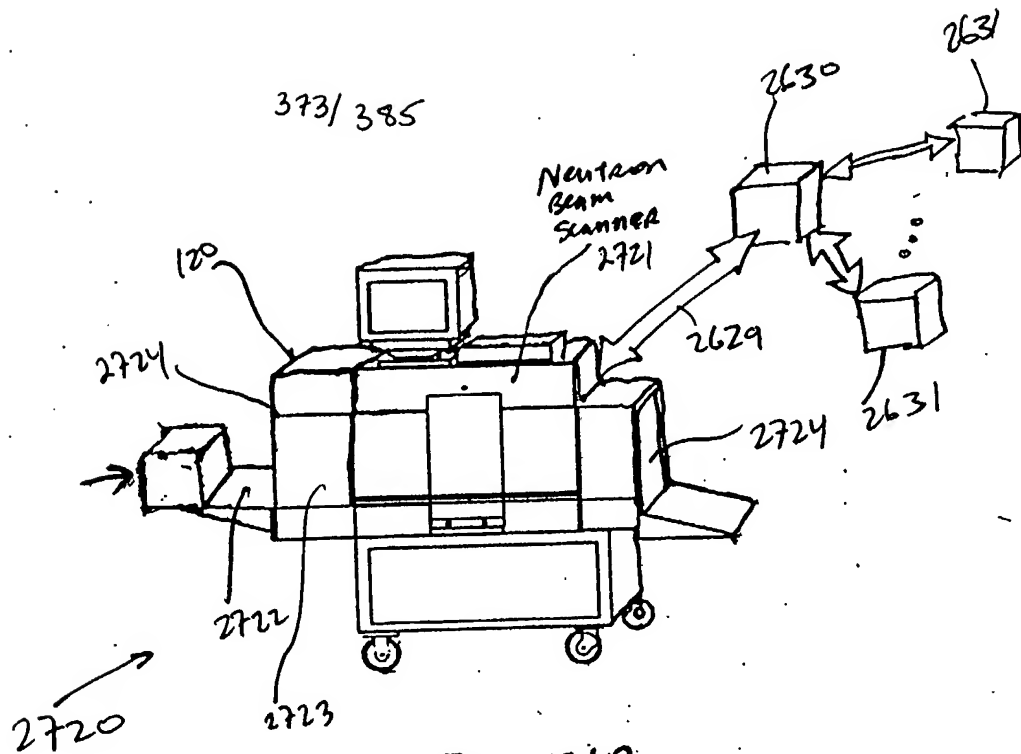


FIG. 7A

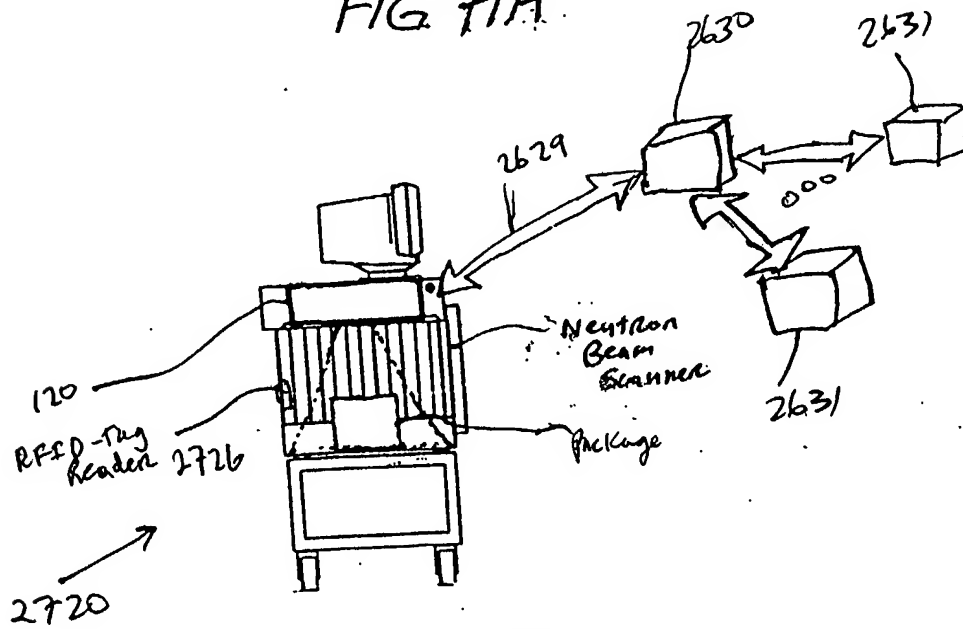


FIG. 7B

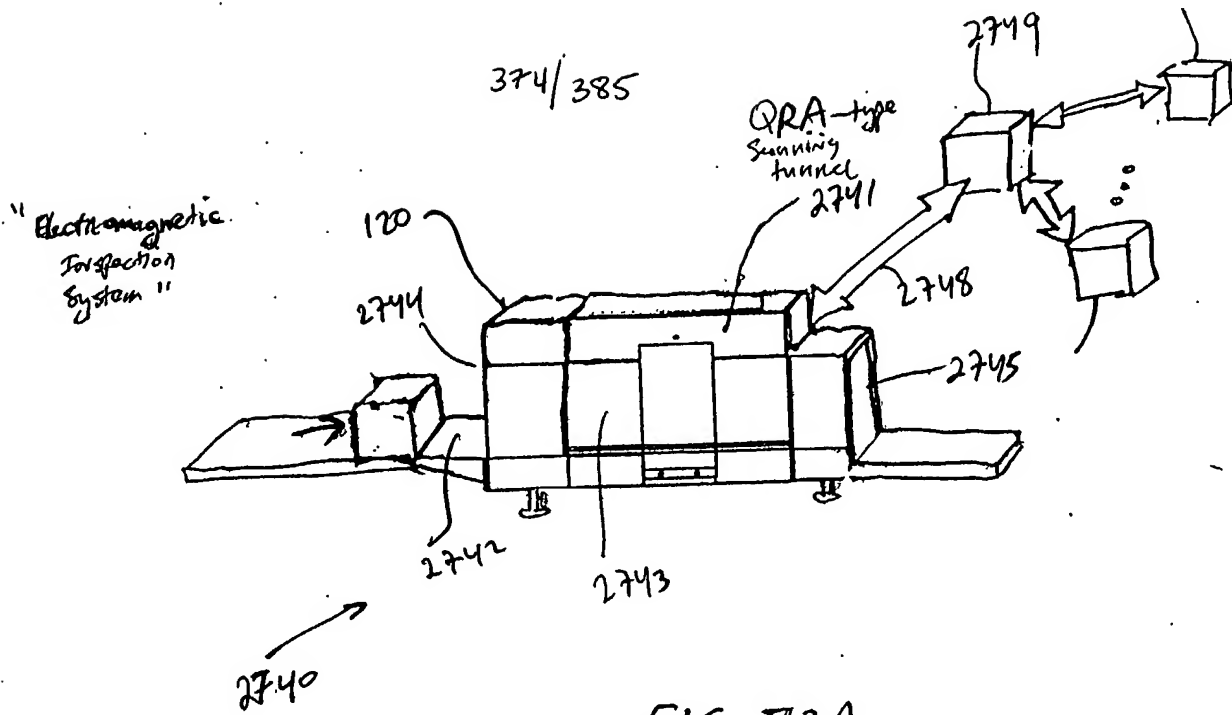


FIG 72A

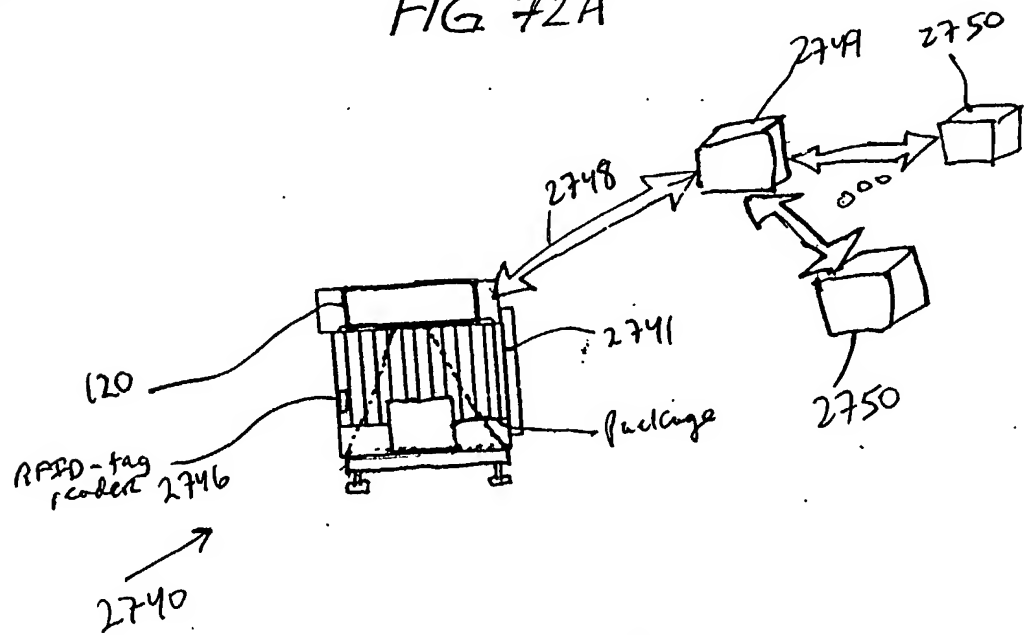
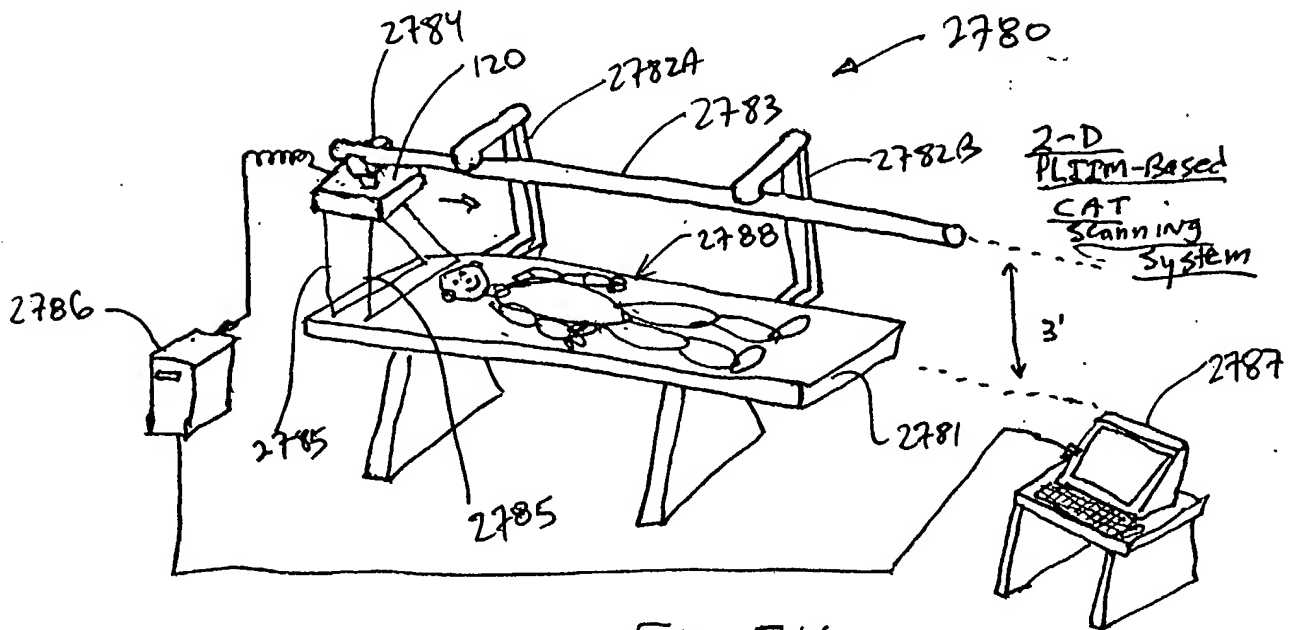
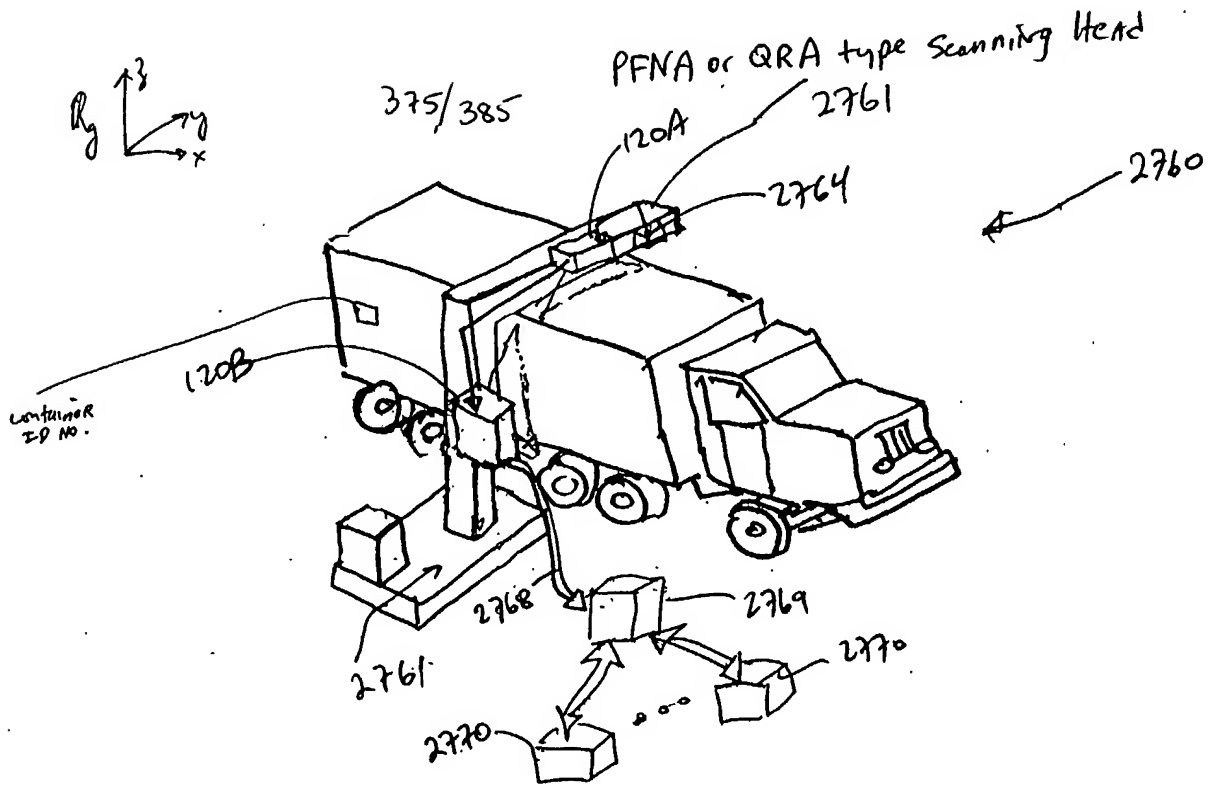
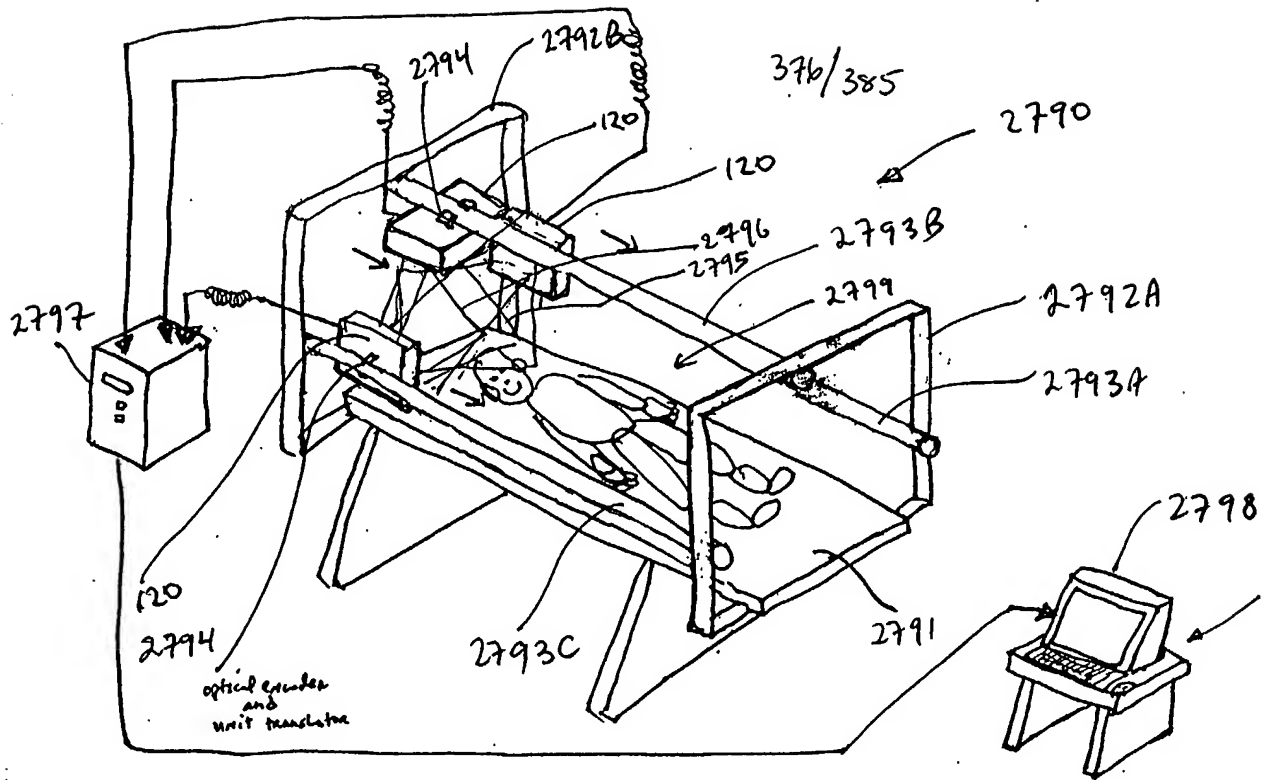


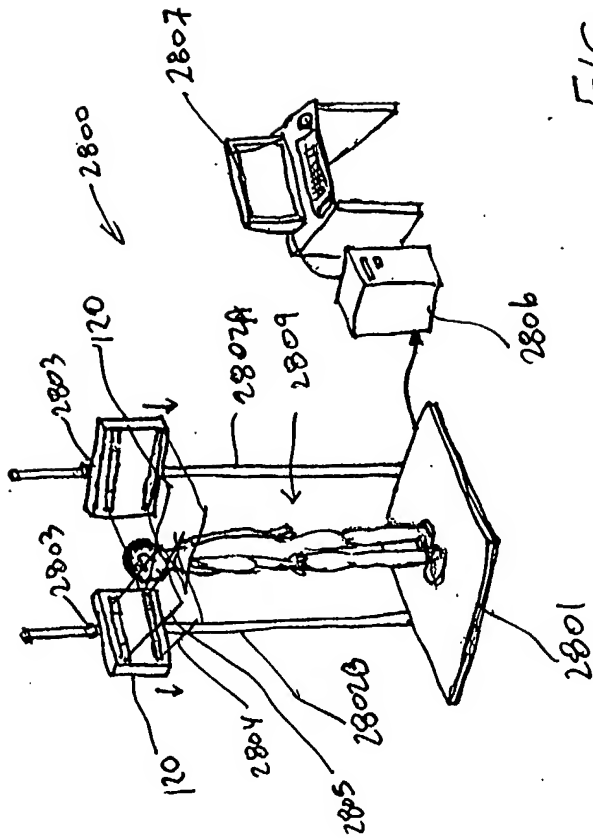
FIG. 72B



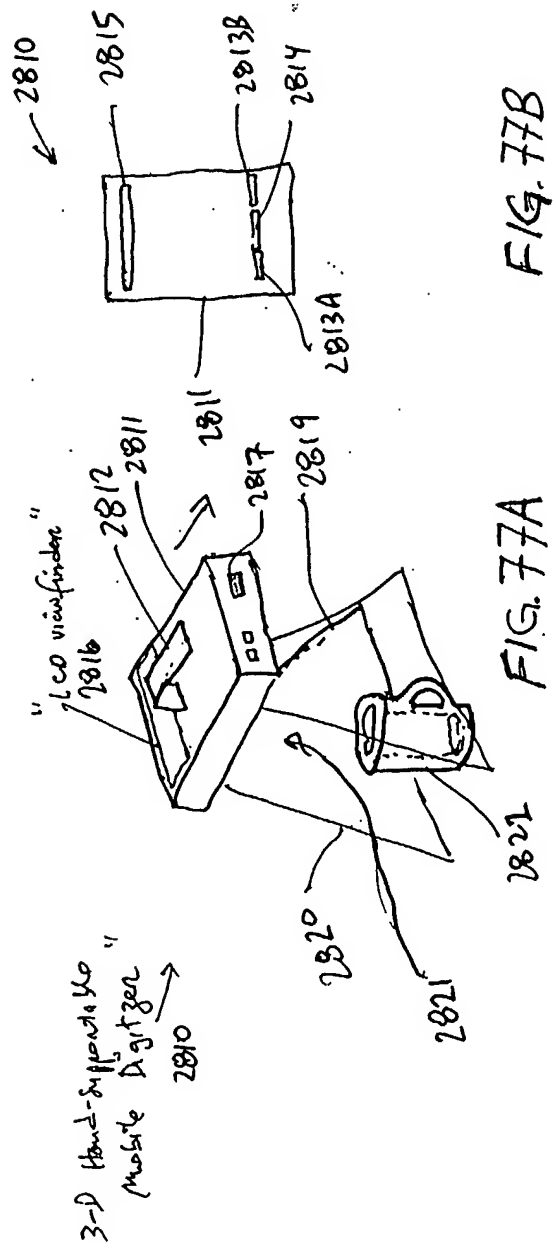


3-D PLT-IM-Based
CAT Medical Scanning
System

FIG. 75



377/385



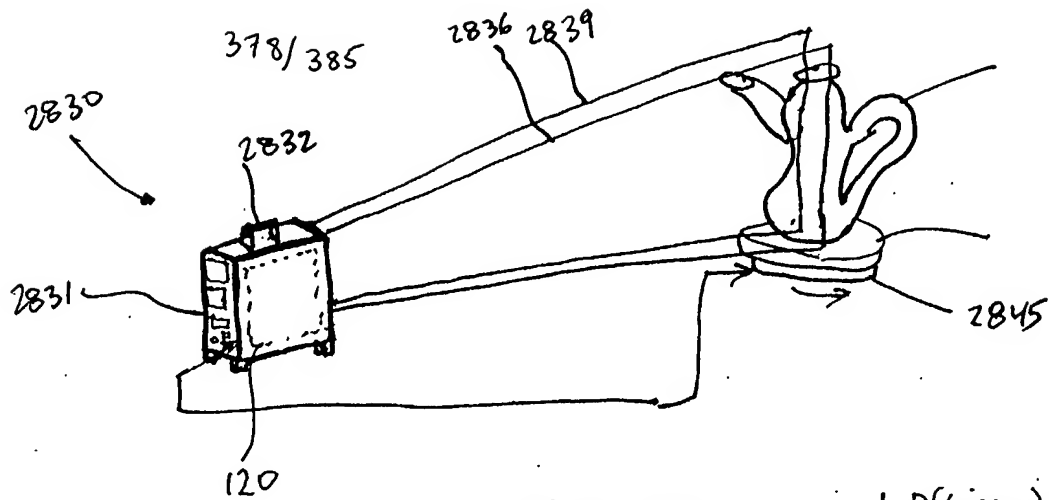


FIG. 78A

1-D(Linear) sensor

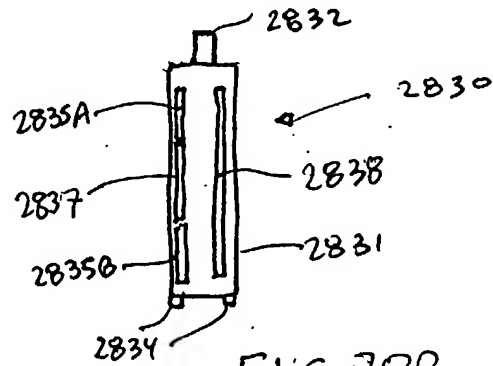


FIG. 78B

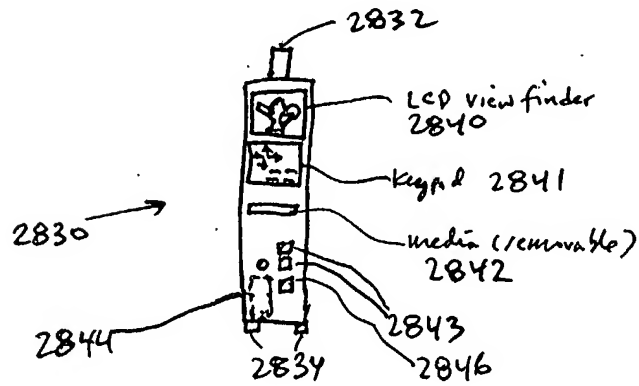
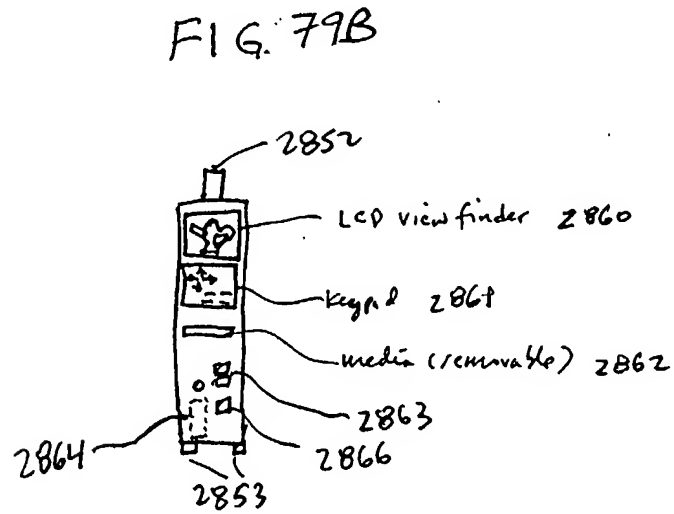
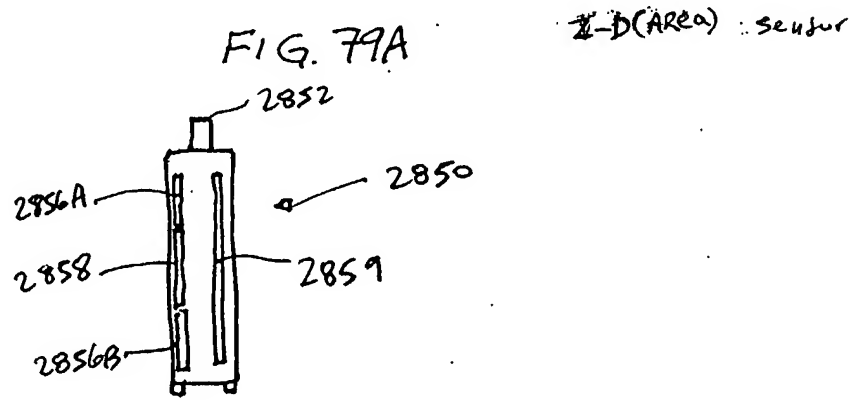
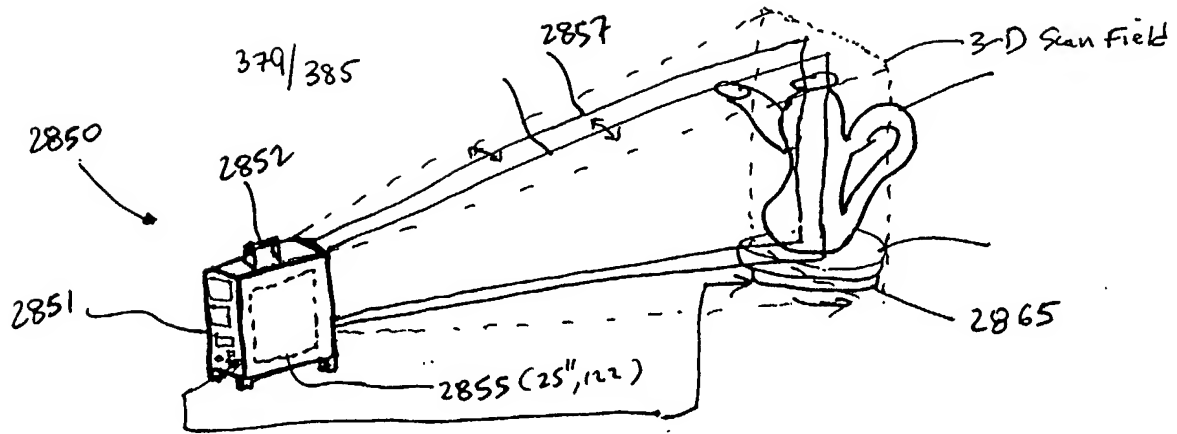
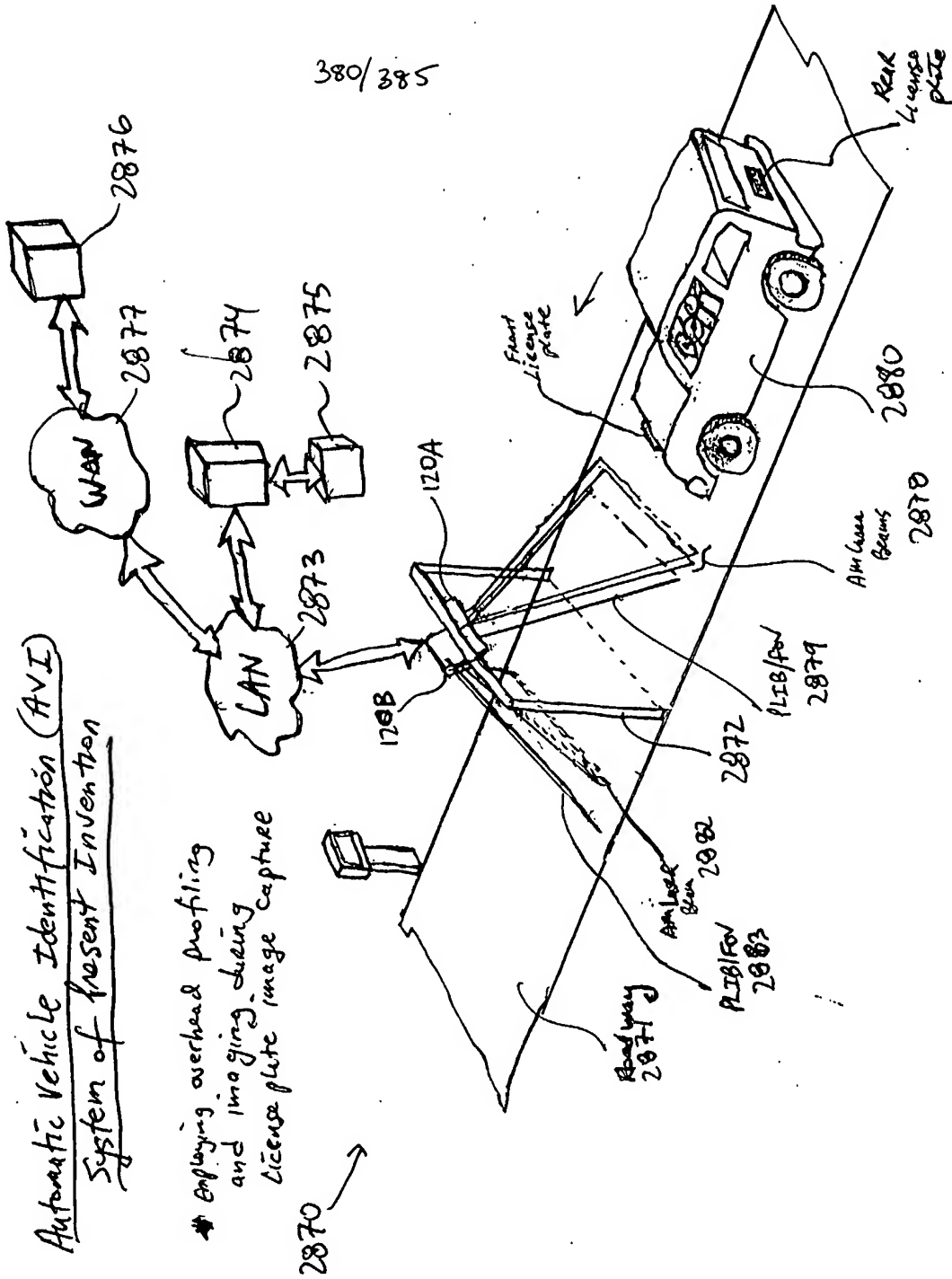


FIG. 78C





Automatic Vehicle Identification (AVI)

- * Employing overhead profiling and imaging techniques during license plate image capture

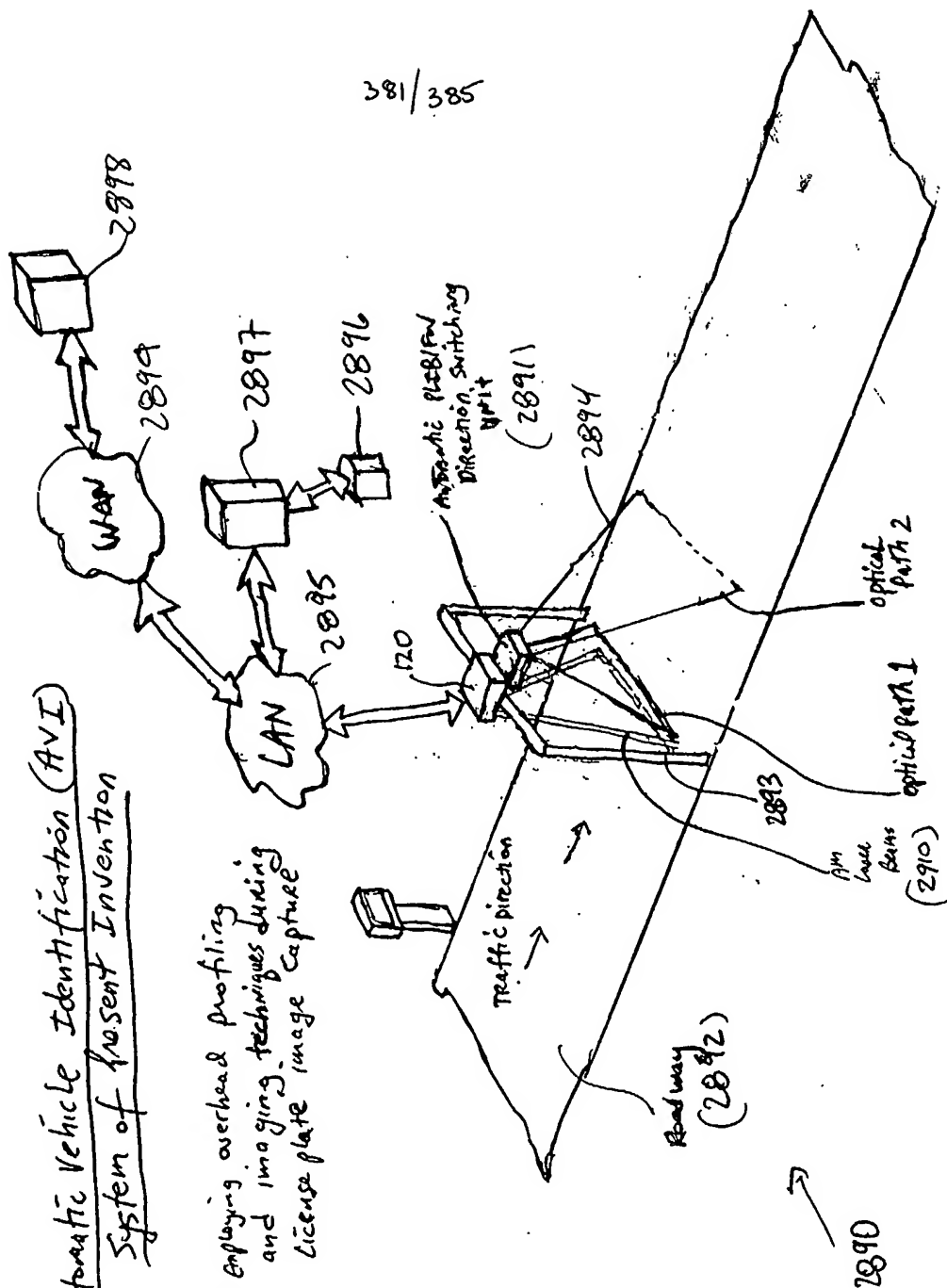


FIG. 81A

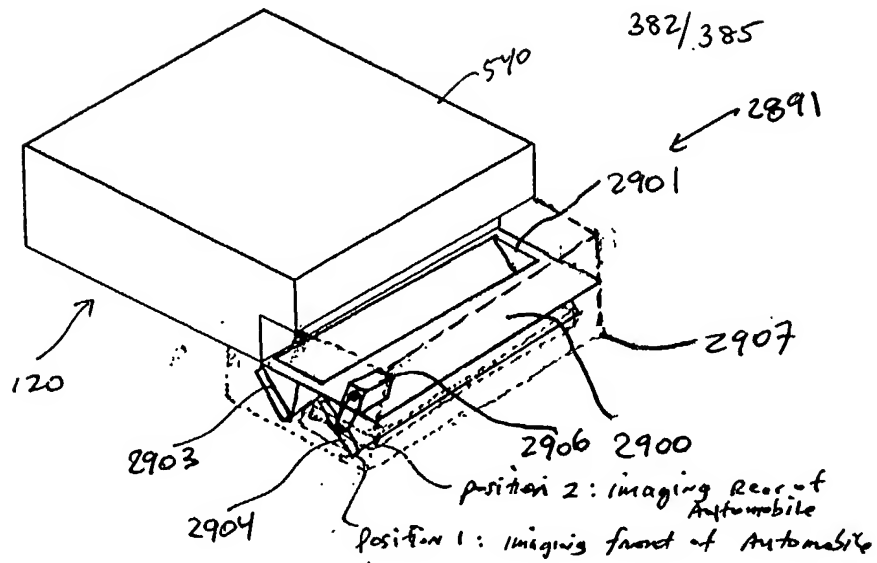


FIG. 81B

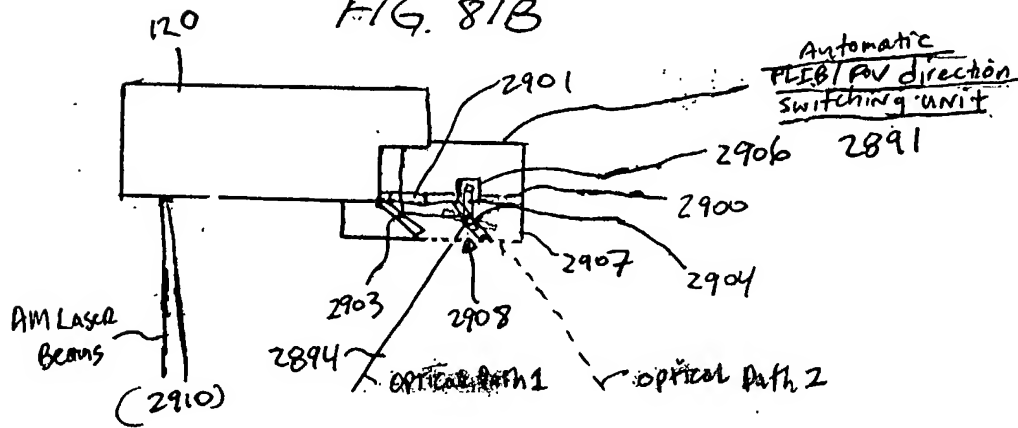


FIG. 81C

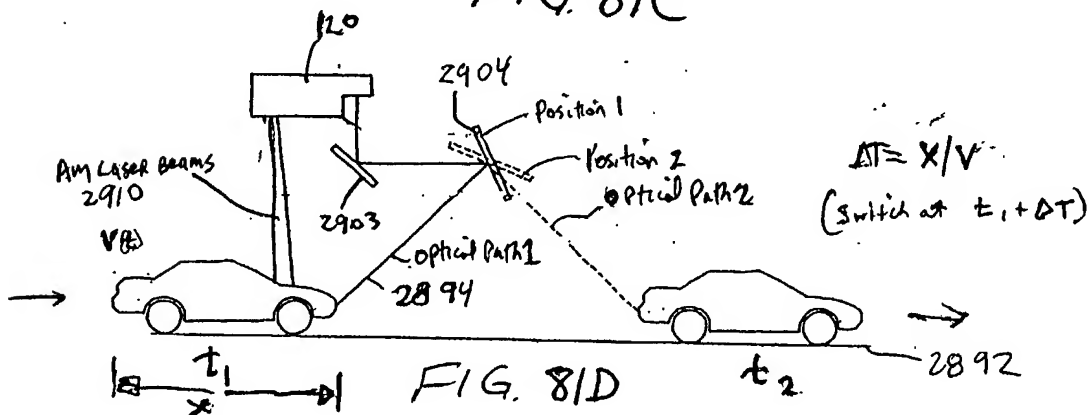
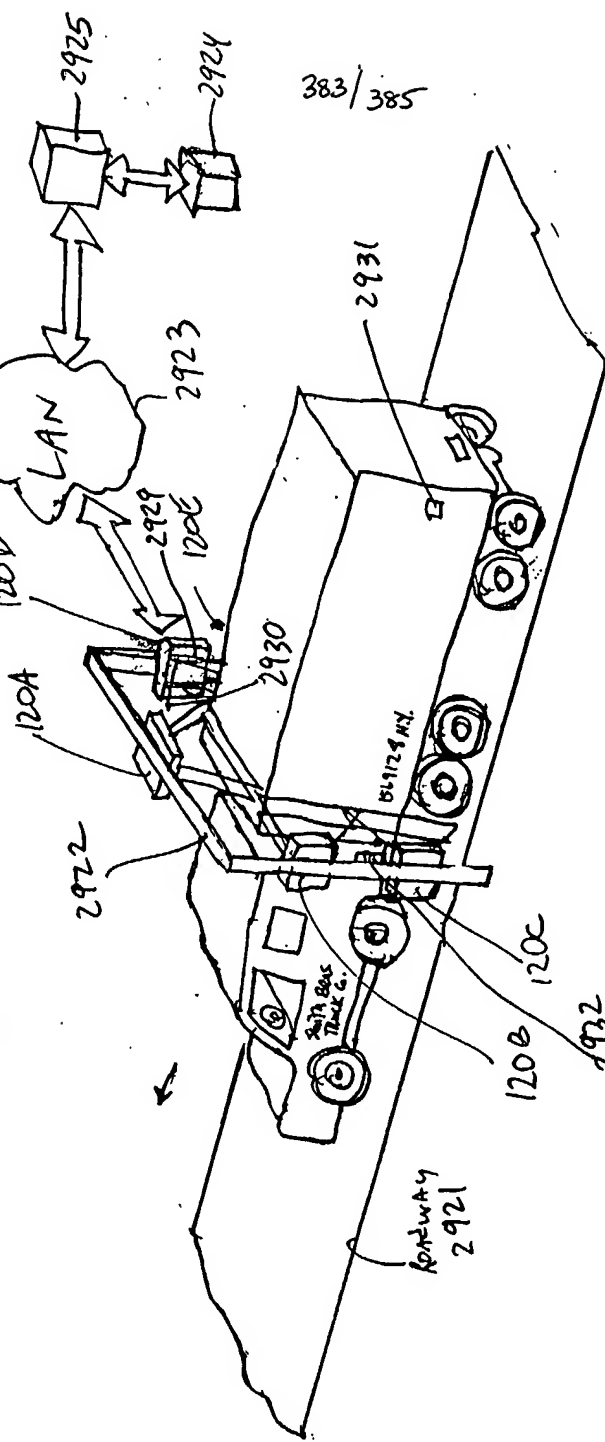


FIG. 81D

Automatic Vehicle Classification (AVC)
System of the Present Invention

2920



* Employing overhead and lateral
Profiling and imaging
Techniques

FIG. 82

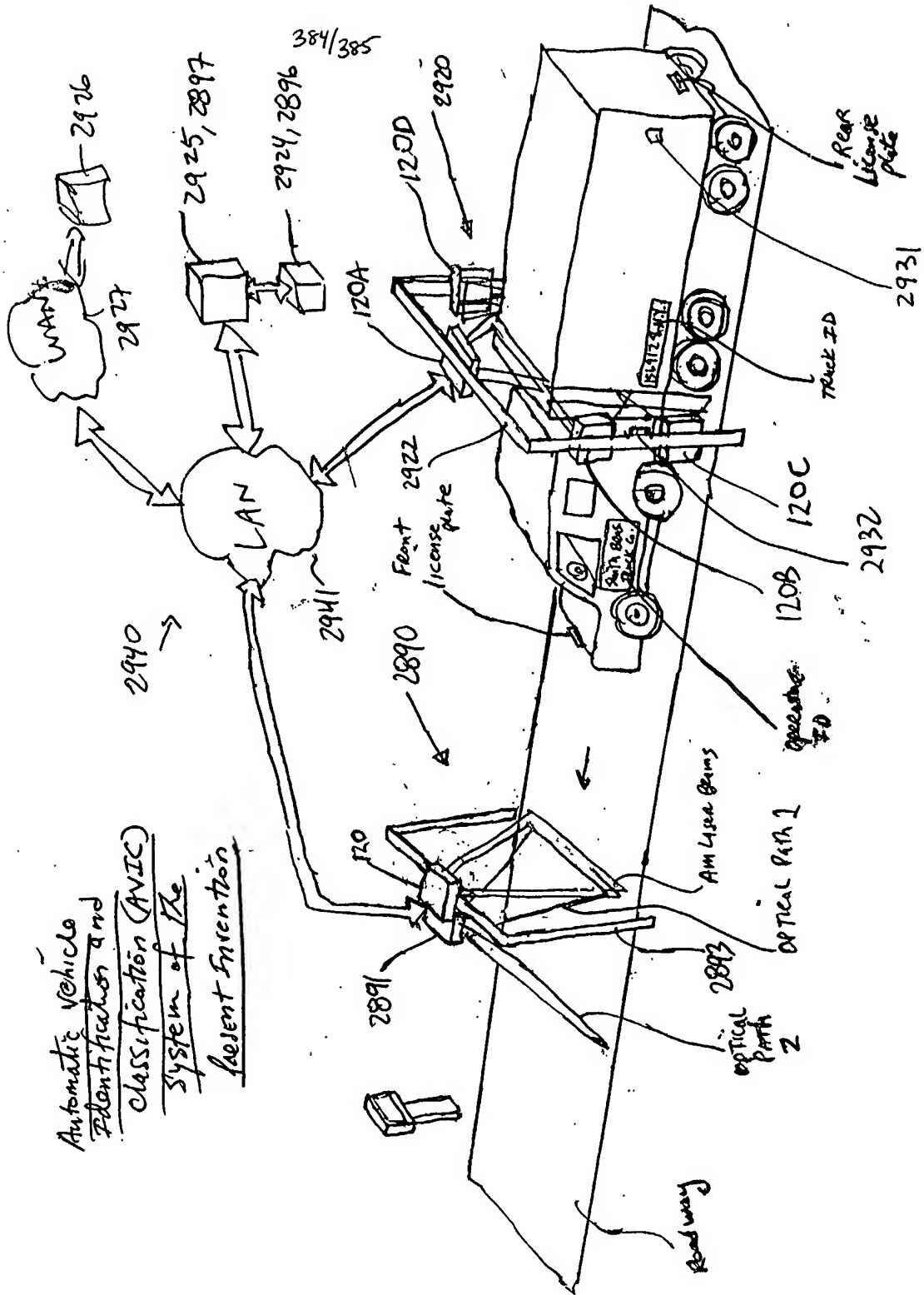


FIG. 83

